MAJOR OIL PLAYS IN UTAH AND VICINITY

Thomas C. Chidsey, Jr., Compiler and Editor

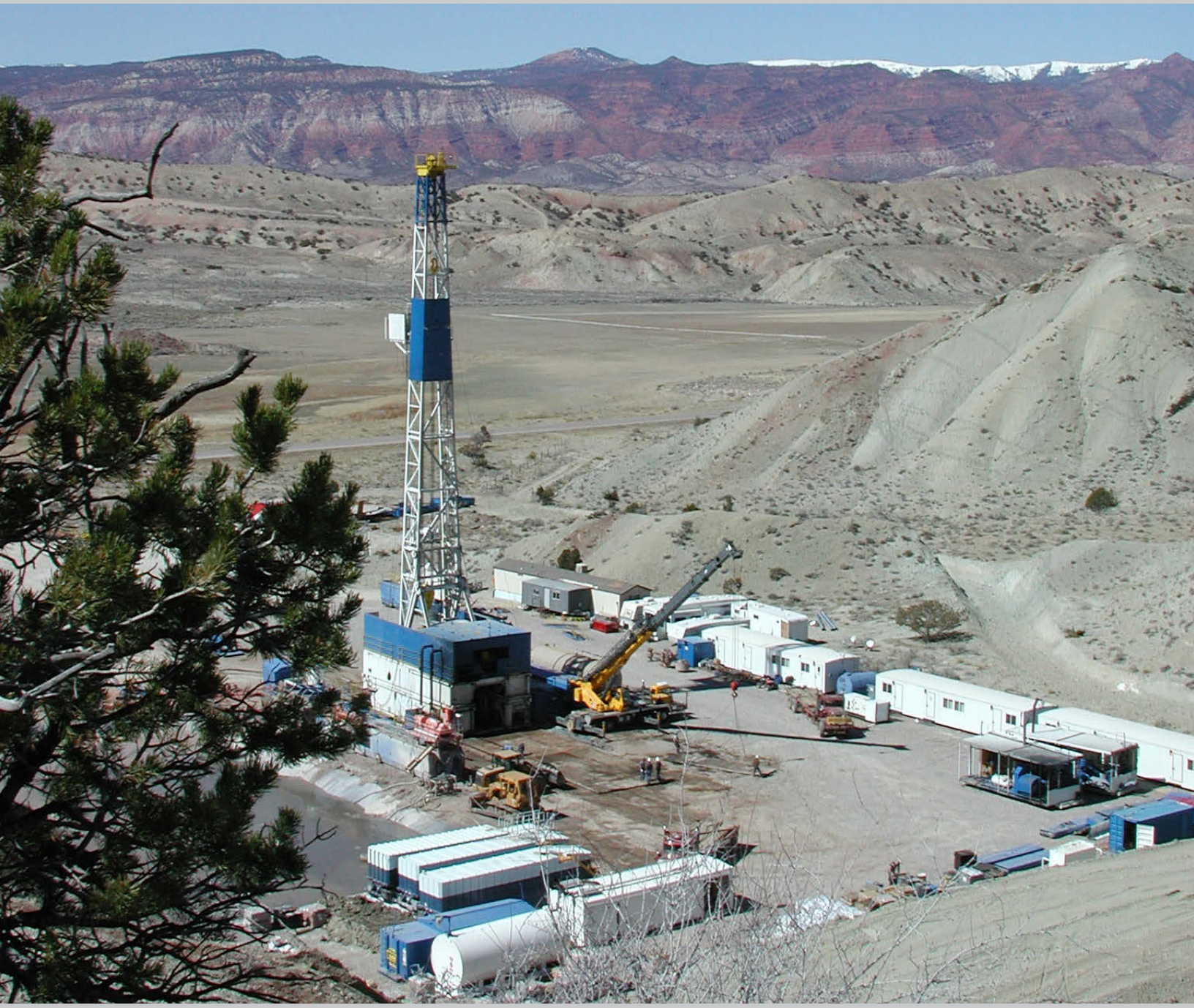

BULLETIN 137
UTAH GEOLOGICAL SURVEY
a division of
UTAH DEPARTMENT OF NATURAL RESOURCES
2016

Blank pages are intentional for printing purposes.

MAJOR OIL PLAYS IN UTAH AND VICINITY

Thomas C. Chidsey, Jr., Compiler and Editor

Cover photo: *The first central Utah thrust belt discovery, Covenant field, Sevier County, Utah, in 2004. The field produces oil from the Jurassic Navajo Sandstone and Temple Cap Formation. View to the west-southwest; Jurassic Arapien Formation in the foreground and Paleocene Flagstaff Limestone in the far distance.*

ISBN: 978-1-55791-922-9

BULLETIN 137
UTAH GEOLOGICAL SURVEY
a division of
UTAH DEPARTMENT OF NATURAL RESOURCES
2016

STATE OF UTAH
Gary R. Herbert, Governor

DEPARTMENT OF NATURAL RESOURCES
Michael Styler, Executive Director

UTAH GEOLOGICAL SURVEY
Richard G. Allis, Director

PUBLICATIONS
contact
Natural Resources Map & Bookstore
1594 W. North Temple
Salt Lake City, UT 84116
telephone: 801-537-3320
toll-free: 1-888-UTAH MAP
website: mapstore.utah.gov
email: geostore@utah.gov

UTAH GEOLOGICAL SURVEY
contact
1594 W. North Temple, Suite 3110
Salt Lake City, UT 84116
telephone: 801-537-3300
website: geology.utah.gov

CONTENTS

FOREWORD

One of the benefits of Utah's diverse geology is a wealth of petroleum resources. Three oil-producing provinces exist in Utah and adjacent parts of Wyoming, Colorado, and Arizona—the thrust belt, Paradox Basin, and Uinta Basin. Utah produces oil from eight major "plays" within these provinces, where a play is defined by the U.S. Geological Survey as a set of known or postulated oil accumulations sharing similar geologic, geographic, and temporal properties such as hydrocarbon-generating source rocks, oil migration pathways, trapping mechanisms, and hydrocarbon types. This Bulletin, funded in part by the U.S. Department of Energy, describes concisely and in new detail each of these major oil plays.

Utah oil fields have produced over 1.57 billion barrels (250 million m^3) since production began in the 1940s. Among oil-producing states, Utah currently ranks eleventh in domestic oil production. There are over 150 active oil fields in Utah. Despite over 40 years of production at rates that have varied by a factor of three, Utah's proven oil reserves have risen to more than 812 million barrels (129 million m^3), indicating significant oil remains to be produced.

This Bulletin will help increase recoverable oil reserves from existing field reservoirs and new discoveries by providing "stand alone" play portfolios for the major oil-producing provinces. The play portfolios include the following descriptions: (1) tectonic setting, (2) reservoir stratigraphy, thickness, and rock types (lithology), (3) type of oil traps, (4) rock properties, (5) oil and gas chemical and physical characteristics, (6) source rocks including timing of generation and migration of oil, (7) exploration and production history, (8) case-study oil field evaluations, (9) descriptions of reservoir outcrop analogs for each play, (10) exploration potential and trends, and (11) maps of the major oil plays and subplays.

The Utah play portfolios in this Bulletin provide a comprehensive geologic and geographic reference to help petroleum companies plan exploration, land-acquisition strategies, and field development. These portfolios can also help pipeline companies plan future facilities and pipelines routes. Other potential users of the portfolios include petroleum engineers, petroleum land specialists, landowners, bankers and investors, economists, utility companies, manufacturers, county planners, and numerous government resource management agencies.

Thomas C. Chidsey, Jr.
Utah Geological Survey

ABSTRACT

Utah oil fields have produced over 1.57 billion barrels (bbls) of oil (250 million m^3) and hold 812 million bbls (129 million m^3) of proved reserves. The 13.7 million bbls (2.2 million m^3) of production in 2002 was the lowest level in over 40 years and continued the steady decline that began in the mid-1980s. However, in late 2005 oil production increased, due, in part, to the discovery of Covenant field in the south-central Utah Navajo Sandstone thrust belt ("Hingeline") play, and to increased development drilling in the south-central Uinta Basin, reversing the decline that began in the mid-1980s. The Utah Geological Survey believes providing play portfolios for the major oil-producing provinces (Paradox Basin, Uinta Basin, and thrust belt) in Utah and adjacent areas in Colorado and Wyoming can continue this new upward production trend. Oil plays are geographic areas with petroleum potential caused by favorable combinations of source rock, migration paths, reservoir rock characteristics, and other factors. The play portfolios include "stand alone" descriptions and maps of the major oil plays by reservoir; production and reservoir data; case-study field evaluations; and descriptions of reservoir outcrop analogs.

The most prolific oil reservoirs in the Utah/Wyoming thrust belt province are the eolian, Triassic-Jurassic Nugget Sandstone and marine Jurassic Twin Creek Limestone. Traps form on discrete subsidiary closures along major ramp anticlines where the depositionally heterogeneous reservoirs are also extensively fractured; hydrocarbons were generated from subthrust Cretaceous source rocks.

The Jurassic Navajo Sandstone/Temple Cap Formation "Hingeline" play is the only petroleum play in the central Utah thrust belt. The 2004 discovery of Covenant field in the Hingeline (central Utah thrust belt) changed the oil development potential in the play from hypothetical to proven. Potential traps include fault-propagation/fault-bend anticlines containing eolian sandstones of the Navajo and White Throne Member of the Temple Cap. Hydrocarbons were likely generated and migrated from Carboniferous source rocks in Late Cretaceous time.

The Uinta Basin represents Utah's greatest petroleum province and has the best potential for adding new reserves. Oil and associated gas production in the Laramide-age Uinta Basin is mostly from stratigraphic traps in fluvial-deltaic sandstones and lacustrine carbonates in the Paleocene and Eocene Green River and Colton/Wasatch Formations, which were deposited in and around ancestral Lake Uinta. The source rocks for the Uinta Basin plays are kerogen-rich shale and marlstone of the Green River.

The Mississippian Leadville Limestone, a shallow, open-marine, carbonate-shelf deposit, is a major oil and gas play in the Utah/Colorado Paradox Basin. Most Leadville production is from the Paradox fold and fault belt in basement-involved structural traps that have closure on both anticlines and faults, and some production potential in hydrothermal dolomite diagenetic traps. The Leadville has heterogeneous reservoir properties due to lithofacies of varying porosity and permeability, diagenetic effects (dolomitization), and fracturing. Hydrocarbons in Leadville reservoirs were likely generated from source rocks in the Pennsylvanian Paradox Formation and migrated into traps, primarily along fault planes and fractures.

The most prolific oil and gas play in the Paradox Basin targets the Pennsylvanian Paradox Formation. The cyclic Paradox Formation was deposited on a shallow-water carbonate shelf (often restricted) that locally contained carbonate buildups, commonly phylloid-algal mounds. Trap types include stratigraphic, stratigraphic with some structural influence, combination stratigraphic/structural, and diagenetic. The Paradox Formation has heterogeneous reservoir properties due to depositional lithofacies of varying porosity and permeability and a variety of positive and negative diagenetic effects. The fractured organic-rich Cane Creek shale zone in the Paradox has the potential to add significant reserves using horizontal drilling. The Cane Creek and other organic-rich shale zones in the Paradox are the source for the hydrocarbons in the formation.

Utah is unique in that there are outcrop analogs for all producing oil and gas reservoirs in the state. Production-scale outcrop analogs provide an excellent view of reservoir petrophysics, facies characteristics, and boundaries contributing to the overall heterogeneity of reservoir rocks. They can be used as a "template" for evaluation of data from conventional core, geophysical and petrophysical logs, and seismic surveys. When combined with subsurface geological and production data, these outcrop analogs can improve (1) development drilling and production strategies such as horizontal drilling, (2) reservoir-simulation models, (3) reserve calculations, and (4) design and implementation of secondary/tertiary oil recovery programs and other best practices used in the oil fields of Utah and vicinity.

CHAPTER 1: INTRODUCTION

by

Thomas C. Chidsey, Jr.

Utah Geological Survey

CONTENTS

FIGURES

CHAPTER 1:
INTRODUCTION

OVERVIEW

Utah oil fields have produced over 1.57 billion barrels (bbls) (250 million m^3) (Utah Division of Oil, Gas, and Mining, 2016a). The 13.7 million bbls (2.2 million m^3) of production in 2002 was the lowest level in over 40 years. However, in 2005 oil production increased (figure 1.1), due, in part, to the discovery of Covenant field in the central Utah Navajo Sandstone/Temple Cap Formation thrust belt ("Hingeline") play, and to increased development drilling in the south-central Uinta Basin, reversing the decline that began in the mid-1980s (Utah Division of Oil, Gas, and Mining, 2016b). Despite over 40 years of production at rates that have varied by a factor of three, proven crude oil reserves during this time have risen above 555 million bbl (88 million m^3), indicating significant oil remains to be produced (Energy Information Administration, 2015). When higher oil prices prevail, secondary and tertiary recovery techniques boost production rates, ultimate recovery, and, of coarse, revenue from known fields.

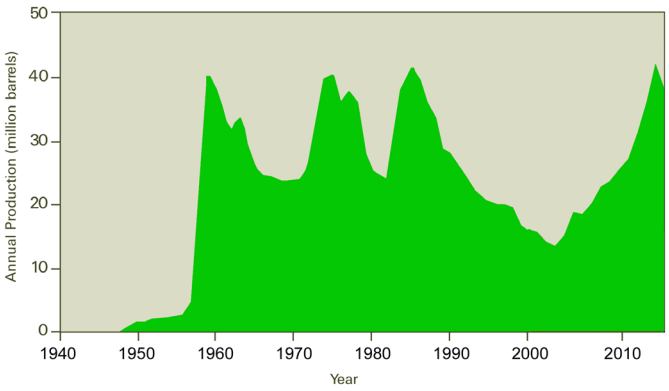

Figure 1.1. *Oil production in Utah as of January 1, 2016, showing an increase due, in part, to the 2004 discovery of Covenant field in the central Utah thrust belt and increased development drilling in the central-south Uinta Basin. Data source: Utah Division of Oil, Gas, and Mining production records.*

While Utah still contains large areas that are virtually unexplored, significant potential for increased recovery from existing fields may be achieved by employing improved reservoir characterization and the latest drilling (horizontal), completion (hydraulic fracturing), and secondary/tertiary recovery technologies. New exploratory targets may be identified from three-dimensional (3-D) seismic acquisition, surface geochemical surveys, and remote sensing techniques. Development of potential prospects is within the economic and technical capabilities of both major and independent operators.

The primary goal of this bulletin is to increase recoverable oil reserves from existing field reservoirs and new discoveries by providing play portfolios for the major oil-producing provinces (thrust belt, Uinta Basin, and Paradox Basin) in Utah and adjacent areas in Wyoming, Colorado, and Arizona (figures 1.2 and 1.3). The U.S. Geological Survey defines "a play" as a set of known or postulated oil accumulations sharing similar geologic, geographic, and temporal properties such as source rock, migration pathway, timing, trapping mechanism, and hydrocarbon type (Gautier and others, 1996). This definition was the basis for the plays determined in this study. Analysis of the plays required evaluation of regional cross sections, correlation and mapping of reservoir facies, identification of wells with hydrocarbon "shows," use of geologic and engineering characteristics of each reservoir, and gathering field and production data from each reservoir. We also used current technology, primarily data from well logs, sample descriptions, tests, well completions, cores, publications, and outcrops.

The play portfolios include the following descriptions: (1) tectonic setting; (2) reservoir stratigraphy, thickness, and lithology; (3) type of traps; (4) seals; (5) petrophysical properties; (6) diagenetic analysis; (7) oil and gas characteristics; (8) source rocks including timing, generation, and migration of oil; (9) exploration and production history; (10) case-study field evaluations; (11) descriptions of reservoir outcrop analogs for each play; (12) exploration potential and trends; and (13) maps of the major oil plays and subplays. Each play portfolio is designed as a "stand alone" description and thus may contain information, recommendations, etc., found in related plays.

EXPLORATION HISTORY

Oil and gas drilling has fluctuated greatly over Utah's 100-year exploration history due to discoveries, oil and gas price trends, and changing exploration targets (figure 1.4). In 1891, natural gas was accidentally discovered at a depth of 1000 feet (300 m) in Farmington Bay on the eastern shore of Great Salt Lake during the drilling of a water well. Between 1895 and 1896, gas from several wells near this location was transported to Salt Lake City in a wooden pipe, marking Utah's first use of local oil or gas. During the early 1900s, the first drilling targets were based on naturally occurring oil seeps at Rozel Point (northern Great Salt Lake), Mexican Hat (near Monument Valley, southeastern Utah), and near the town of Virgin (near Zion National Park) (figures 1.5 through 1.7). Surface anticlines were also the sites of early exploration (figures 1.8 and 1.9). Although oil shows were also found at several other eastern Utah locations in later

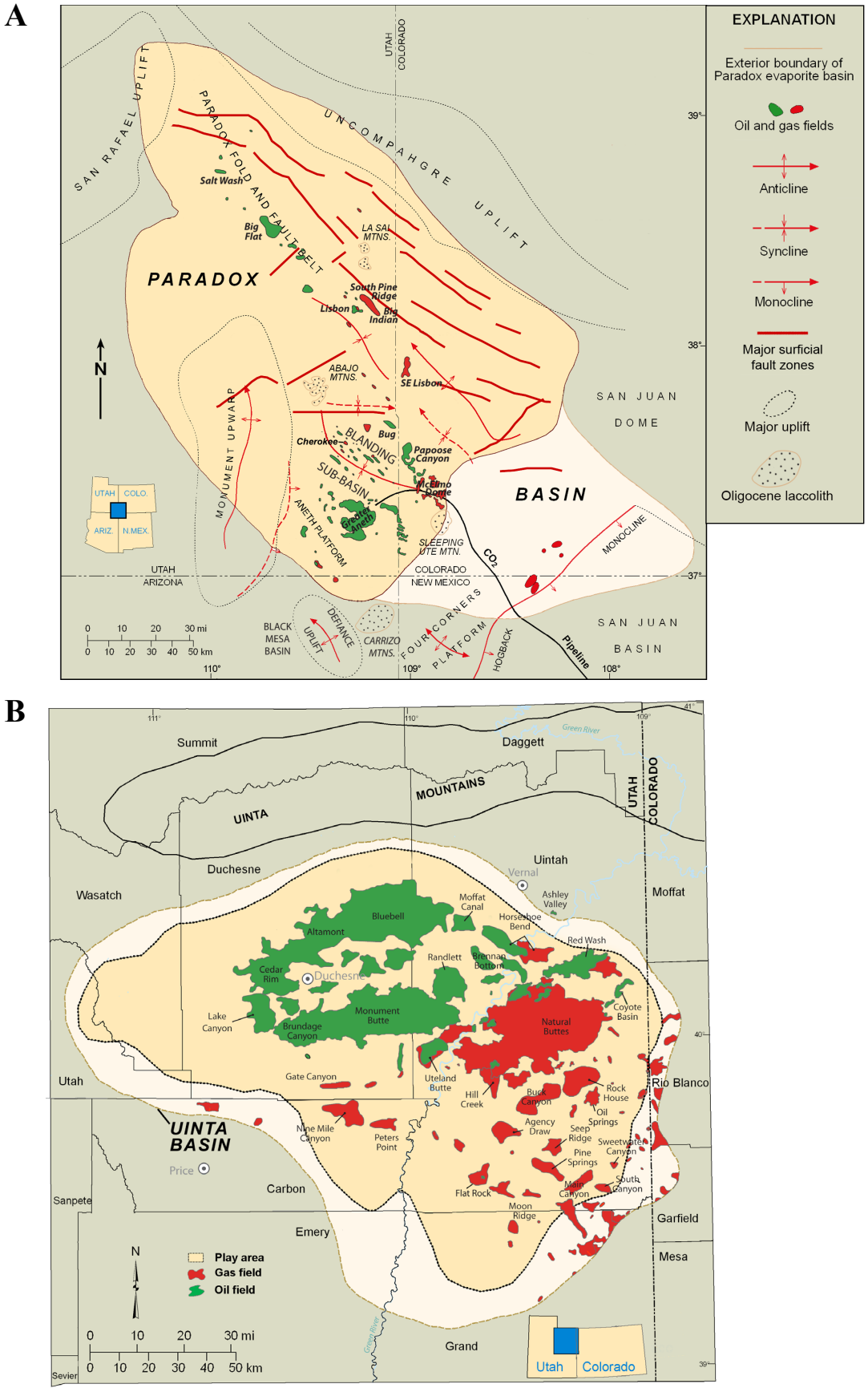

Figure 1.2. A. *Oil and gas fields in the Paradox Basin of Utah, Colorado, and Arizona. Modified from Harr (1996).* ***B.*** *Oil and gas fields in the Uinta Basin of Utah and Colorado. Modified from Wood and Chidsey (2015). Play areas in the Paradox and Uinta Basins colored light orange.*

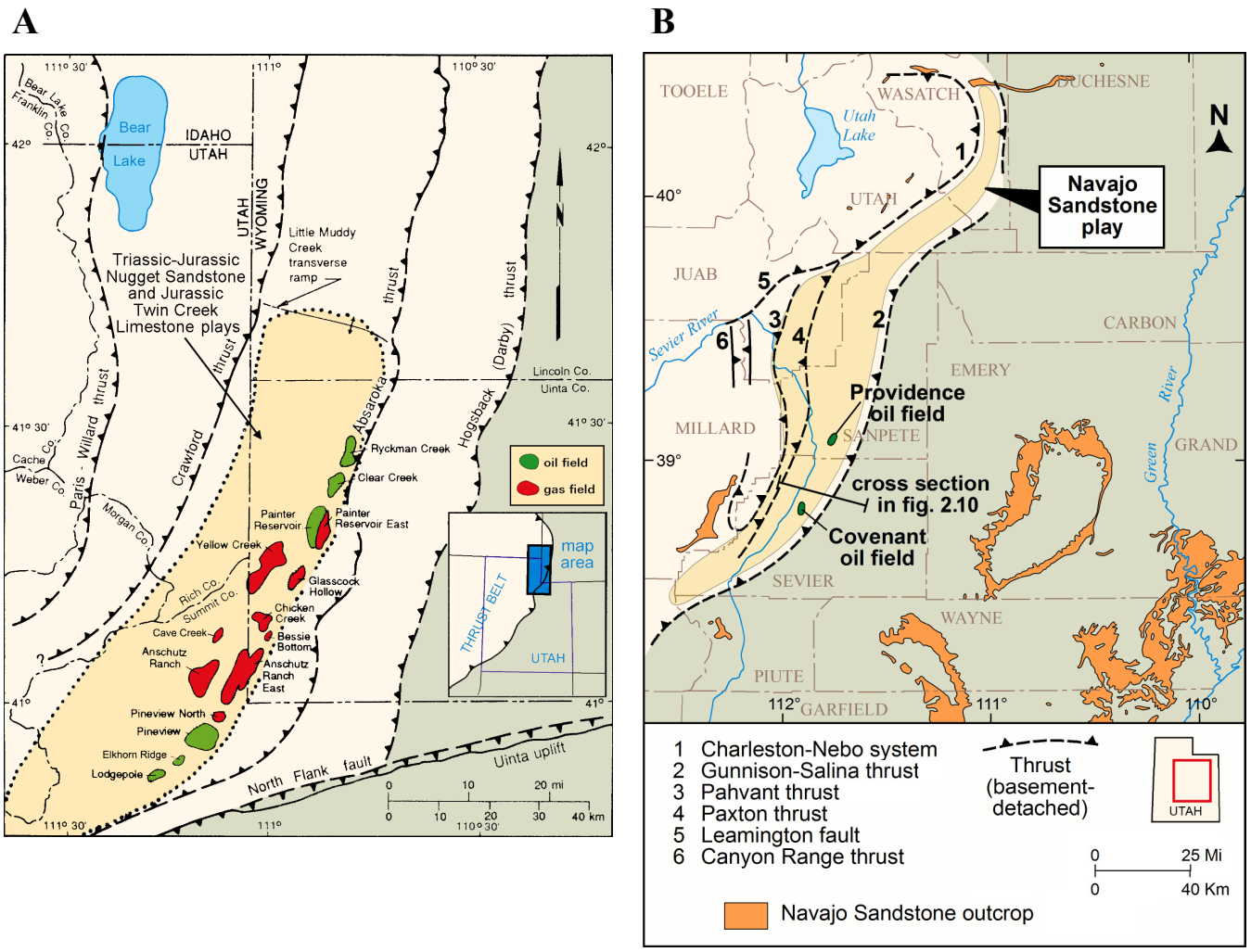

Figure 1.3. *A. Oil and gas fields, uplifts, and major thrust faults in the Utah-Wyoming thrust belt.* ***B.*** *Location of Covenant and Providence oil fields, uplifts, and selected thrust systems in the central Utah thrust belt province. Numbers and sawteeth are on the hanging wall of the corresponding thrust system. Modified from Hintze (1980), Sprinkel and Chidsey (1993), and Peterson (2001). Play area in the thrust belt colored light orange.*

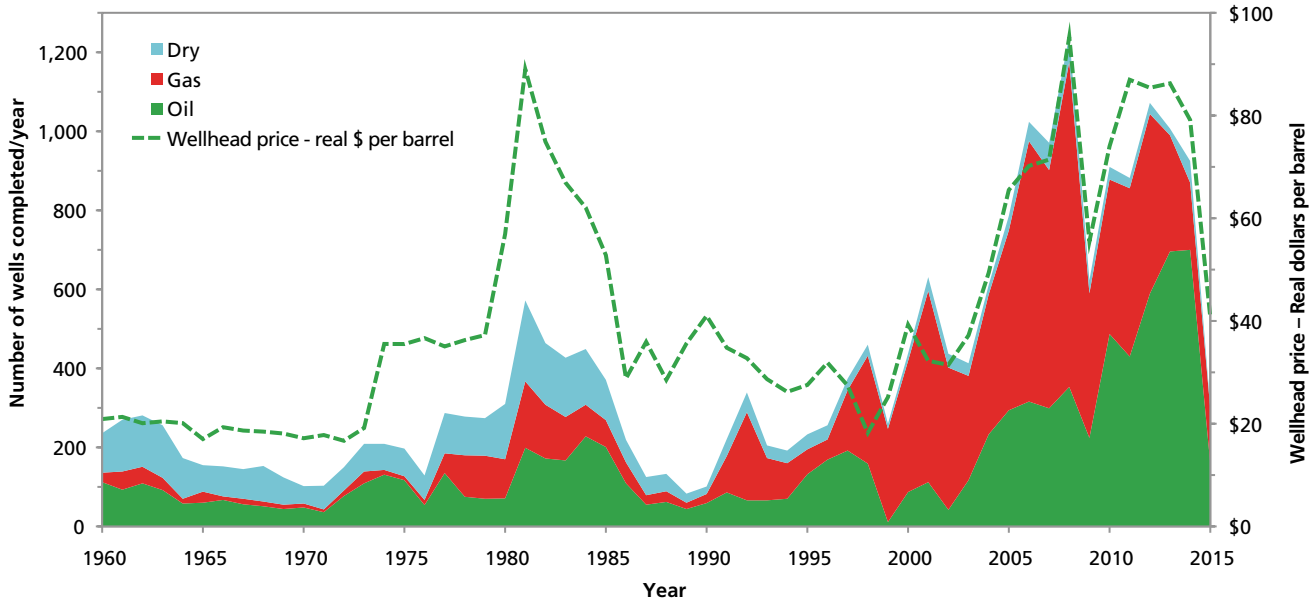

Figure 1.4. *Utah oil and gas drilling history. Data source: Utah Division of Oil, Gas, and Mining production records; after Vanden Berg (2016).*

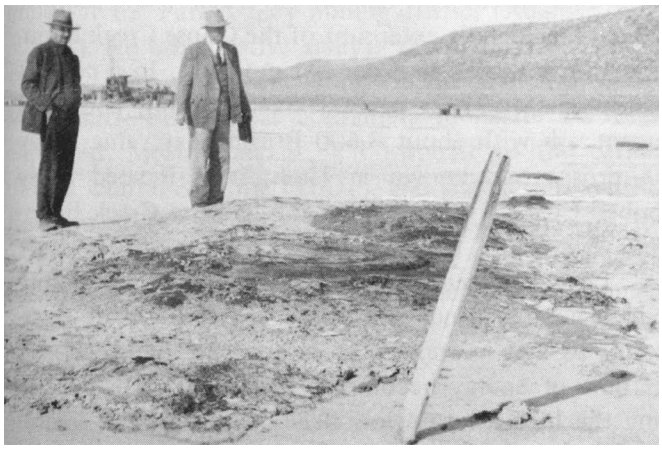

Figure 1.5. *Oil seeps at Rozel Point, Utah, exposed during low lake level. Photograph circa 1937 (contributed by Jack N. Conley, Petroleum Geologist [from Doelling, 1980]).*

Figure 1.6. *Cable-tool drilling near Mexican Hat, San Juan County, Utah, circa 1920. Used by permission, Utah State Historical Society, all rights reserved.*

Figure 1.7. *Townspeople visiting Virgin Dome Oil Company drilling operations at Virgin oil field (non-commercial), Washington County, Utah, in 1919. Used by permission, Utah State Historical Society, all rights reserved.*

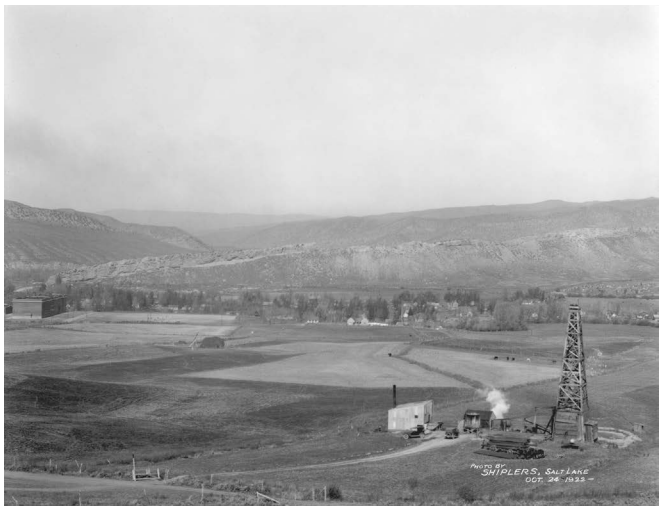

Figure 1.8. *Wildcat well by the Western Empire Petroleum Company on the Coalville anticline of the Utah thrust belt, Summit County, drilled in 1922; view to the northwest. Used by permission, Utah State Historical Society, all rights reserved.*

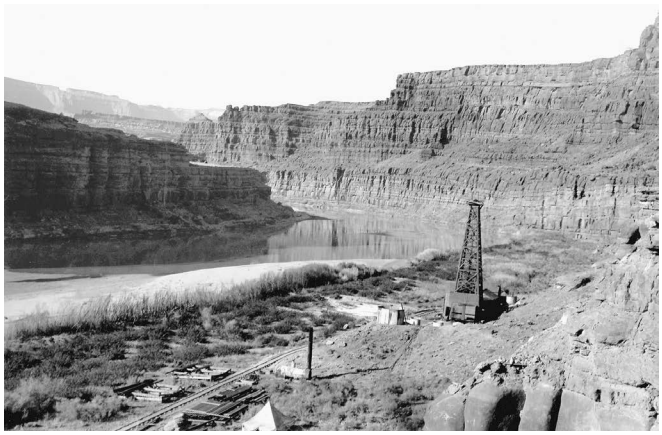

Figure 1.9. *The Midwest Exploration and Utah Southern No. 1 Shafer wildcat well (section 31, T. 26 S., R. 21 E., Salt Lake Base Line and Meridian [SLBL&M]) on the Cane Creek anticline, northern Paradox Basin, Grand County, Utah, drilled in 1924; view down the Colorado River to the southwest. Used by permission, Utah State Historical Society, all rights reserved.*

decades, Utah's first large-scale commercial oil well, Ashley Valley No. 1, was drilled in 1948 near the town Vernal along the northeast boundary of the Uinta Basin. By 1960, Utah was the 10th largest oil-producing state in the country and has remained in the top 15 since then.

During the boom period of the early 1980s, activity peaked at over 500 wells drilled per year. After slowing in the 1990s, Utah entered another boom period rivaling the early 1980s. In 2012, the Utah Division of Oil, Gas, and Mining issued a record 2105 drilling permits and 1105 wells were spudded (Utah Division of Oil, Gas, and Mining, 2016b, 2016c). This increase in activity was spurred by overall high prices for oil, improved drilling and completions techniques for natural gas, and perceptions that Utah is highly prospective and under-

explored. The success rate of exploration drilling for both oil and gas has also improved, with very few dry holes being reported compared to the 1980s drilling boom. However, the 2015 drop in oil prices resulted in a significant decrease in drilling activity proving once again the cyclic nature of the petroleum industry.

Horizontal drilling technology, more elaborate completion techniques (such as hydraulic fracturing), and secondary and tertiary enhanced oil recovery programs should collectively result in a boost in statewide production rates and ultimate recovery from both known fields and new discoveries when oil prices are high. Also a return to high petroleum prices, coupled with lower natural gas prices, will provide the economic climate needed to entice more high-risk exploration investments (more wildcats), resulting in new discoveries and development of liquid hydrocarbon reserves in Utah. In 2015, Utah had nearly 12,000 producing oil and gas wells. Interest also resurgenced in Utah's substantial oil shale and tar sand resources, which received brief attention during the 1970s oil supply crisis.

BENEFITS

The overall goal of this bulletin is enhanced petroleum production in Utah. Specific benefits expected to result from this publication include the following:

1. improved reservoir characterization to prevent premature abandonment of numerous small fields in the Paradox and Uinta Basins,
2. identification of the type of untapped compartments created by reservoir heterogeneity (for example, diagenesis and abrupt facies changes) to increase recoverable reserves,
3. documentation of reservoir trends to stimulate field extension and exploration drilling in undeveloped parts of producing fairways,
4. provide information to determine optimal well spacing/location to reduce the number of wells needed to successfully drain a reservoir, thus reducing development costs and risk, and allowing more productive use of limited energy investment dollars, and
5. communication of the above findings to encourage new development and exploration efforts, and increase petroleum supply and royalty income for the federal, state, local, Native American, and fee owners.

The Utah play portfolios in this bulletin provide a comprehensive geologic and geographic reference to help petroleum companies plan exploration, land-acquisition strategies, and field development. These portfolios can also help pipeline companies plan future facilities and pipelines. Other potential users of the portfolios include petroleum engineers, petroleum land specialists, landowners, bankers and investors, economists, utility companies, manufacturers, county planners, and numerous government resource management agencies.

CHAPTER 2:
MAJOR OIL-PRODUCING PROVINCES IN UTAH AND VICINITY

by

Thomas C. Chidsey, Jr., and Craig D. Morgan
Utah Geological Survey

CONTENTS

FIGURES

CHAPTER 2:
MAJOR OIL-PRODUCING PROVINCES IN UTAH AND VICINITY

GEOLOGIC SETTING

A combination of depositional and structural events created the major oil-producing provinces in Utah: Paradox Basin, Uinta Basin, and thrust belt (figures 1.2 and 1.3; for specific field locations and detailed information on each field, see "Oil and Gas Fields Map of Utah" by Wood and Chidsey, 2015). Oil production in the thrust belt and Paradox Basin extends into Wyoming and Colorado, respectively, but the bulk of the production is from Utah.

The ages of the rocks exposed in Utah include every geologic eon, era, period, and epoch. Many of these rocks have the qualities necessary to create the oil reservoirs, sources, and seals that make Utah a petroleum-producing state with large, relatively unexplored areas of hydrocarbon potential.

Utah Mississippian rocks represent widespread shallow-marine carbonate deposition (figure 2.1A). These rocks contain one of the most complete Mississippian sequences in North America (Hintze and Kowallis, 2009). The Mississippian includes the Leadville Limestone reservoir in southeastern Utah. During the Pennsylvanian (figure 2.1B), the Paradox Basin developed in southeastern Utah where cyclic organic-rich shales, carbonates, and evaporites of the Paradox Formation accumulated under restricted marine conditions in the rapidly subsiding basin. The Paradox Basin contains Utah's largest oil field, Greater Aneth. Renewed movement on deep, older basement faults in the basin formed structures, which are oil productive in Mississippian-age carbonates.

In Early Jurassic time, Utah had an arid climate and lay 15 degrees north of the equator. During this time the most prolific oil reservoir in the two thrust belt areas, the Nugget/Navajo Sandstone, was deposited in an extensive dune field comparable to the present Sahara (figure 2.1C). A shallow seaway extended from Canada to southern Utah during the Middle Jurassic that produced coastal dunes of the Temple Cap Formation (figure 2.1D) and marine and marginal marine deposits of the Twin Creek Limestone, etc. (figure 2.1E) (Hintze and Kowallis, 2009). Correlative rocks form many of the spectacular canyons in the parks of southern Utah.

During the Cretaceous, compressional forces of the Sevier orogeny produced highlands in western Utah and the Western Interior Seaway covered most of eastern Utah (figure 2.1F). Extensive coal swamps formed near the coastline of fluvial- and wave-dominated deltas that migrated eastward across the state as the sea eventually retreated. The Sevier orogeny continued into the Paleocene producing the "thin-skinned" folds and faults of the thrust belt that have been such prolific oil producers in northern Utah (figure 2.1G). Concealed, deep exploration targets beneath the Sevier thrusts offer frontier-drilling opportunities in the poorly explored western half of Utah.

The Laramide orogeny, between latest Cretaceous and Eocene time, produced numerous basins and basement-cored uplifts in the Rocky Mountain states. In Utah, the Uinta Basin is one such basin, and a major oil contributor. During the Paleocene and Eocene (figure 2.1G and 2.1H), lakes Flagstaff and Uinta formed in the Uinta Basin where over 11,000 feet (3350 m) of alluvial, marginal lacustrine (fluvial, deltaic, beach), and open lacustrine sediments accumulated in an intertonguing relationship. Waterflood projects and horizontal drilling have been very successful in increasing oil production in the south-central part of the basin.

The principal source rocks for these three provinces were deposited during the Mississippian, Pennsylvanian, Permian, Cretaceous, and Tertiary as marine and lacustrine shale. The reservoir rocks were deposited in a variety of environments including deltaic, shallow-shelf marine, eolian-dune, coastal-plain, and river-floodplain settings.

DEFINITION OF MAJOR OIL PLAYS

Oil plays are geographic areas with petroleum potential caused by favorable combinations of source rock, migration paths, reservoir rock characteristics, and other factors. Numerous plays (and subplays), delineated and described in the following sections and listed below, are found in the Utah/Wyoming thrust belt, central Utah thrust belt or "Hingeline," Uinta Basin, and Paradox Basin oil-producing provinces of Utah and vicinity (figures 1.2 and 1.3). For this study, we describe those oil plays as being major because they have produced over 4.0 million bbls of oil (BO) (0.6 million m^3) as of January 1, 2016. Also included are geologic, reservoir, and production data for individual fields within those plays that have produced over 500,000 BO (80,000 m^3) as of January 1, 2016.

This publication includes play portfolios for the following four major oil provinces in Utah and vicinity (southwestern Wyoming, southwestern Colorado, and northeastern Arizona): (1) the Triassic-Jurassic Nugget Sandstone and Jurassic Twin Creek Limestone thrust belt plays (including five subplays) in Utah and Wyoming, (2) the Jurassic Navajo Sandstone/Tem-

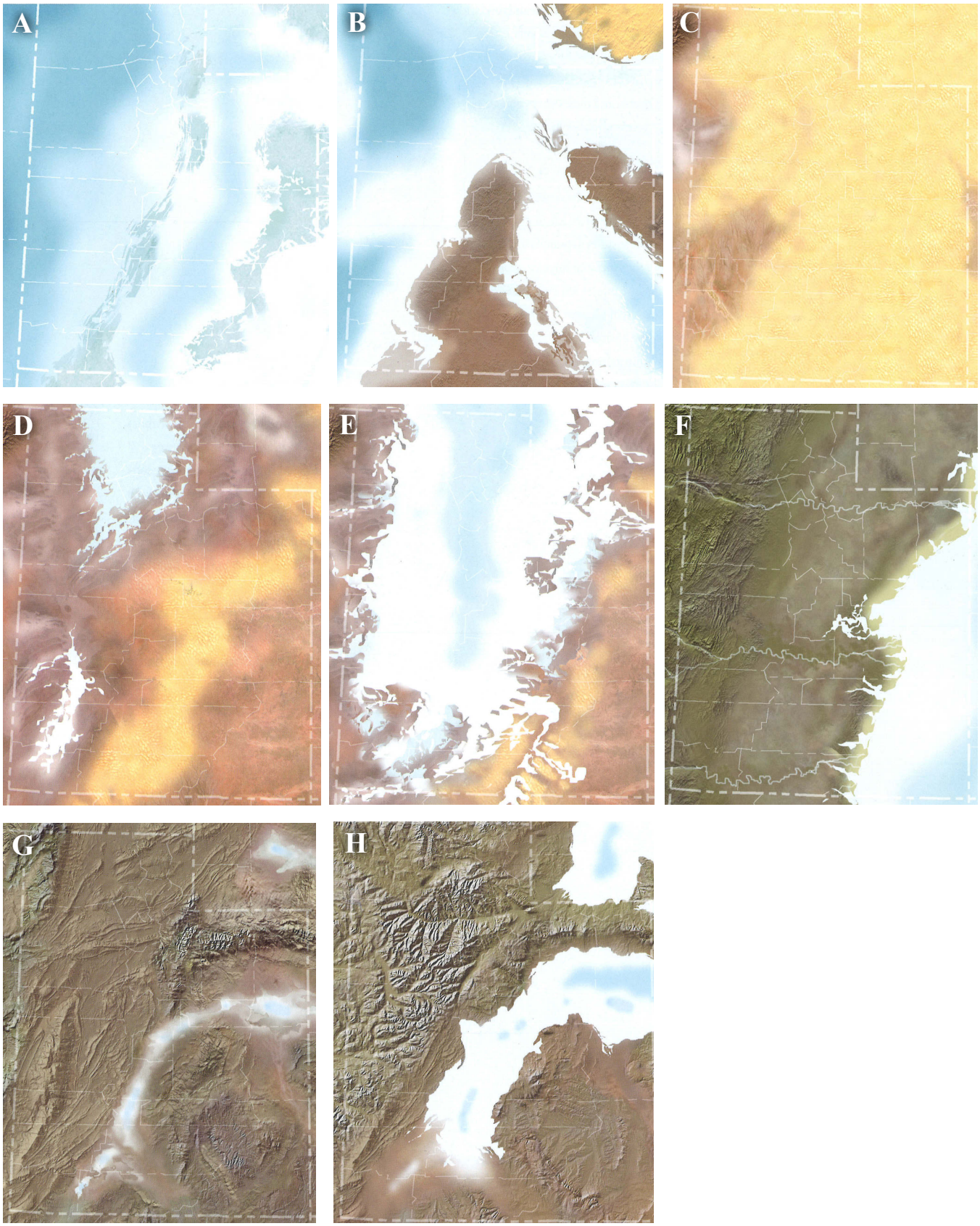

Figure 2.1. *Paleogeographic maps of Utah during the Mississippian (A), Pennsylvanian (B), Early Jurassic (C), early Middle Jurassic (D), Middle Jurassic (E), Late Cretaceous (F), Paleocene (G), and Eocene (H) representing deposition of Utah oil reservoirs or major structural events that created the right conditions to generate and trap hydrocarbons. See text for detailed discussion of the paleogeographic setting for each map. Modified from Blakey and Ranney (2008).*

ple Cap Formation Hingeline play in the central Utah thrust belt, (3) the Conventional Southern Uinta Basin (including six subplays), the Conventional Northern Uinta Basin (including two subplays) and the Deep Uinta Basin Overpressured Continuous plays in Utah, and (4) the Mississippian Leadville Limestone and Pennsylvanian Paradox Formation plays (including four subplays) in the Paradox Basin of Utah, Colorado, and Arizona.

Two oil plays are not included in this publication even though they both have yielded over 20 million BO (3.1 million m^3): the Permian Kaibab Limestone/Triassic Moenkopi Formation (Timpoweap Member) Kaiparowits Basin play in south-central Utah and the Pennyslvanian Weber Sandstone Uinta uplift play in eastern Utah. Only one field exists in each of these plays—Upper Valley (discovered in 1964 and has produced nearly 28.8 million bbls [4.6 million m^3], Utah Division of Oil, Gas, and Mining, 2016a) and Ashley Valley (discovered in 1948 and has produced nearly 21 million bbls [3.3 million m^3], Utah Division of Oil, Gas, and Mining, 2016a) in the Kaiparowits Basin and the Uinta uplift, respectively.

Upper Valley field (figure 2.2) and the potential of the Kaiparowits Basin area have been described in detail by Campbell (1969), Peterson (1973), Sharp (1976, 1978), Montgomery (1984), Goolsby and others (1988), Doelling and Davis (1989), Allin (1990, 1993), Gautier and others (1996), and Allison (1997). Production at Upper Valley is from carbonate zones in the Beta Member of the Permian Kaibab Limestone and the Timpoweap Member of the Triassic Moenkopi Formation. The field is located on the flank of an elongate, north-northwest to south-southeast-trending surface anticline. However, the oil has been hydrodynamically displaced to the west flank of the structure (figure 2.2). Many wells were drilled both prior to and since the discovery of Upper Valley targeting the crests of numerous surface structures in the Kaiparowits Basin rather than the more risky flanks. Therefore, remaining potential may be significant along those flanks, but with the designation of a major part of the region as the Grand Staircase–Escalante National Monument in 1996, further exploration is unlikely and thus we elected to omit the Kaiparowits Basin play from this report (the reader should refer to the studies listed above when evaluating the Permian Kaibab Limestone/Triassic Moenkopi Formation Kaiparowits Basin play).

Ashley Valley field and the potential of the Pennyslvanian Weber Sandstone north of the Uinta Basin–Mountain boundary fault along the south flank of the Uinta Mountains (figure 2.3) have been described in detail by Peterson (1950, 1957, 1961), Johnson (1964), Hefner and Barrow (1992), Hemborg (1993), Larson (1993), Gautier and others (1996), Johnson (2003), and Chidsey and Sprinkel (2005). The Weber Sandstone also serves as a groundwater aquifer for the region. Recharge occurs in high-elevation areas where the Weber crops out. These hydrodynamic conditions suggest that Permian-sourced oil in the Weber may have been flushed to the south by fresh groundwater moving from the north and northwest, thus leaving the best but limited oil potential closest to the Uinta Basin–Mountain boundary fault where Cretaceous-sourced oil contributed to the hydrocarbon system. Oil remains in the Ashley Valley structure possibly because faulting acted as barriers or baffles to groundwater flow. Potential drilling targets require the same general structural configuration (Chidsey and Sprinkel, 2005). Since 1948, over 60 Weber exploratory wells have been drilled in the region to find additional fields like Ashley Valley field (figure 2.3). Targets include subtle anticlines on trend with Ashley Valley and major surface structures. Other wells have also tested the Weber potential beneath basement-involved thrusts. None have been successful. Thus, with little industry success or interest in the Weber Sandstone based on the drilling history and relatively limited potential, we also elected to omit the play from this report (the reader should refer to the studies listed above when evaluating the Weber Sandstone Uinta uplift play).

OVERVIEW OF MAJOR OIL-PRODUCING PROVINCES

The following are general descriptions of the major oil-producing provinces for Utah and vicinity (data sources [monthly and cumulative production, number of active wells, and number of active fields]: Conlon, 1978; Matheny, 1978; Riggs, 1978a, 1978b, 1978c; Wyoming Oil and Gas Conservation Commission, 2016; Colorado Oil and Gas Conservation Commission, 2016; Arizona Oil and Gas Conservation Commission, 2016; Utah Division of Oil, Gas, and Mining, 2016a).

Utah-Wyoming Thrust Belt

The Utah-Wyoming-Idaho salient of the Cordilleran thrust belt is defined as the region north of the Uinta Mountains of northeastern Utah and south of the Snake River Plain of Idaho, with the Green River basin of Wyoming forming the eastern boundary (figure 2.4). Thrusting extends westward into the Great Basin for more than 100 miles (160 km). The thrust belt formed during the Sevier orogeny (Armstrong, 1968); in northwestern Utah, thrusting began in latest Jurassic or earliest Cretaceous time. The Sevier thrust system consisted of, from west to east, the thrust belt, a foredeep basin, a forebulge high, and a back-bulge basin (figure 2.5) (Willis, 1999).

The Sevier orogeny was the result of crustal shortening caused by tectonic convergence from subduction of the Farallon plate along western North America. Shortening in basement and igneous rocks to the west was transferred along weak bedding planes in the shale and evaporate beds in the thick Paleozoic and Mesozoic section to the east (Peyton and others, 2011). The result was a detached (not involving basement rock) or "thin-skinned" style of compressional deformation involving mainly sedimentary rocks in the Utah-Wyoming-Idaho thrust belt (figure 2.6) (Royse and others, 1975; Willis, 1999). The

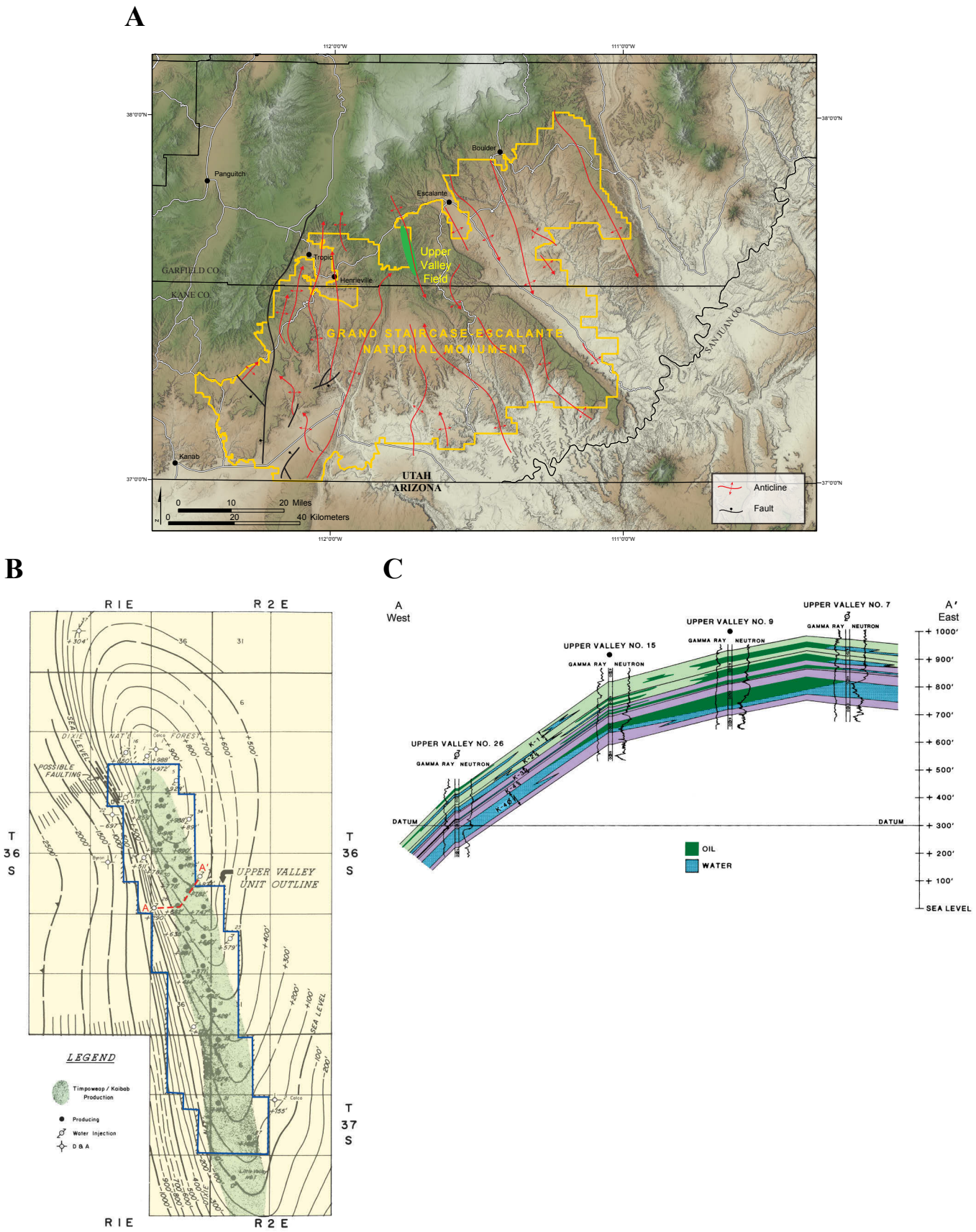

Figure 2.2. *Geology of Upper Valley field, Kaiparowits Basin, Garfield County, Utah.* ***A.*** *Location of Upper Valley field, structures in the Laramide-age Kaiparowits Basin and Grand Staircase–Escalante National Monument.* ***B.*** *Structure contour map on top of the K-4 porosity zone, Permian Kaibab Limestone.* ***C.*** *East-west structural cross section showing hydrodynamically displaced oil/water contact. After Sharp (1976).*

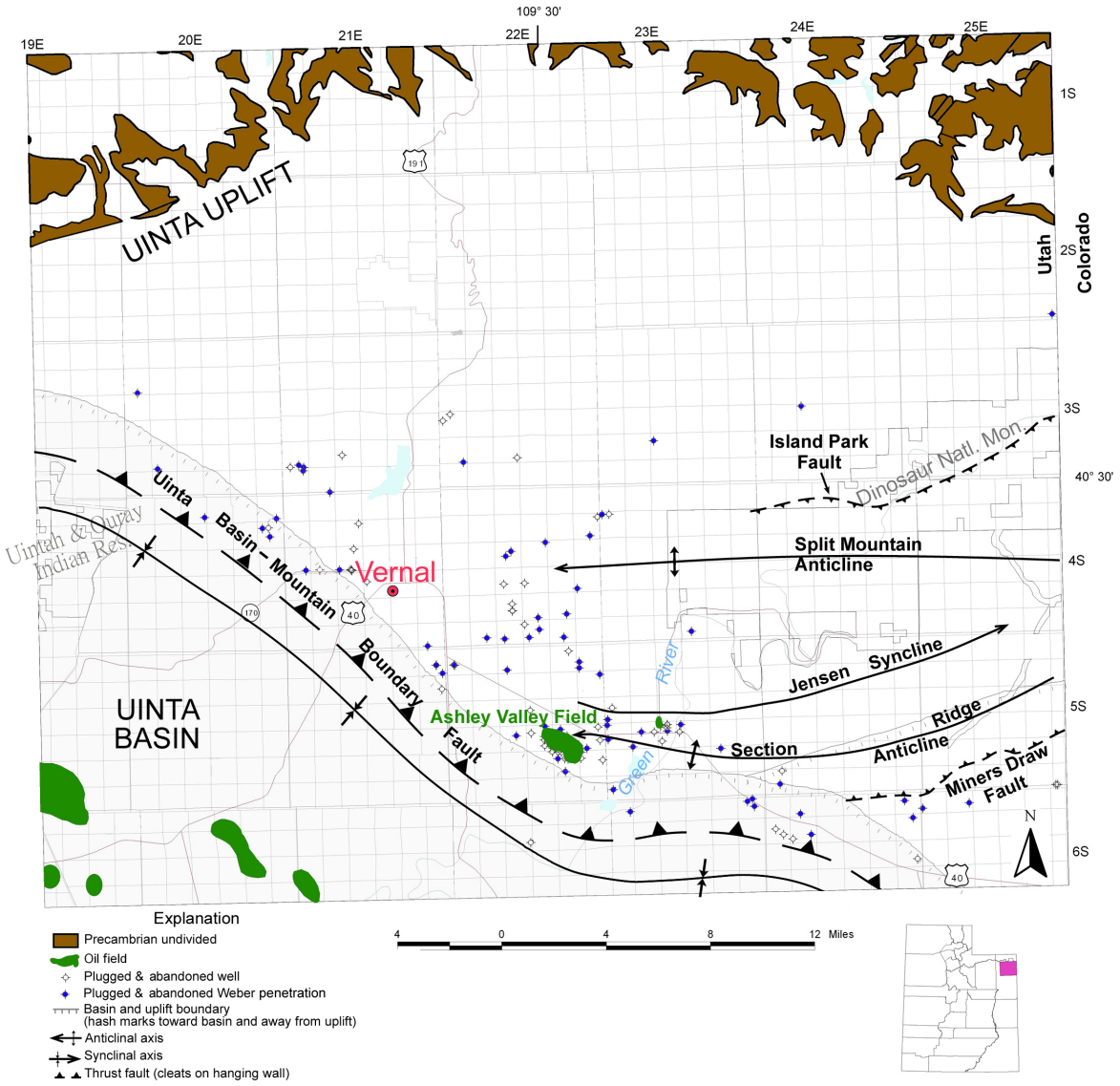

Figure 2.3. *Location of Ashley Valley field and Pennsylvanian Weber exploratory wells, Ashley Valley area, Uintah County, Utah.*

Sevier orogeny overlaps with the Late Cretaceous to Oligocene Laramide orogeny which produced basement-cored uplifts reflecting an eastward extension of the west coast subduction zone (Hintze, 2005).

The eastward-directed compression migrated from west to east and, thus the stacked thrust plates are oldest in the west and youngest in the east (figure 2.6). When the wedge of rock within a thrust plate became too thick during eastward migration, movement along the thrust fault ended and stepped forward to create a new, younger thrust. These younger, eastern thrusts tended to move less than the older, western thrusts. They also are thinner, closer spaced, and form smaller amplitude folds (Willis, 1999; Yonkee and Weil, 2011).

Four major thrust faults are in the region (from west to east and oldest to youngest): the Paris-Willard, Crawford, Absaroka, and Hogsback (Darby) (figures 1.3A and 2.7). At the time of their emplacement the accompanying forebulge was east of Utah. These thrust plates may be up to 50,000 feet (15,000 m) thick and transported as much 60 miles (100 km) east (Willis, 1999; Hintze, 2005). The thrusts generally trend in a north-northeast direction. Major thrusts have ramp-flat geometries with the leading edges listric in form and structurally complex—numerous large-scale fault-bend and fault-propogation folds and thrust splays (Yonkee and Weil, 2011) (figure 2.8). The stacked thrust plates near the leading edge of the thrust belt overlie younger organic-rich Cretaceous marine shale which is the source for the hydrocarbons in Utah and Wyoming fields.

During later Miocene to Holocene regional extension, some thrust faults experienced “relaxation” and became listric normal faults along previous thrust fault planes. Many of these later listric normal faults became bedding plane faults within the Jurassic Preuss salt or shale above thrust-induced structures below. Thus, the surface geology often does not reflect the deeper structural configuration.

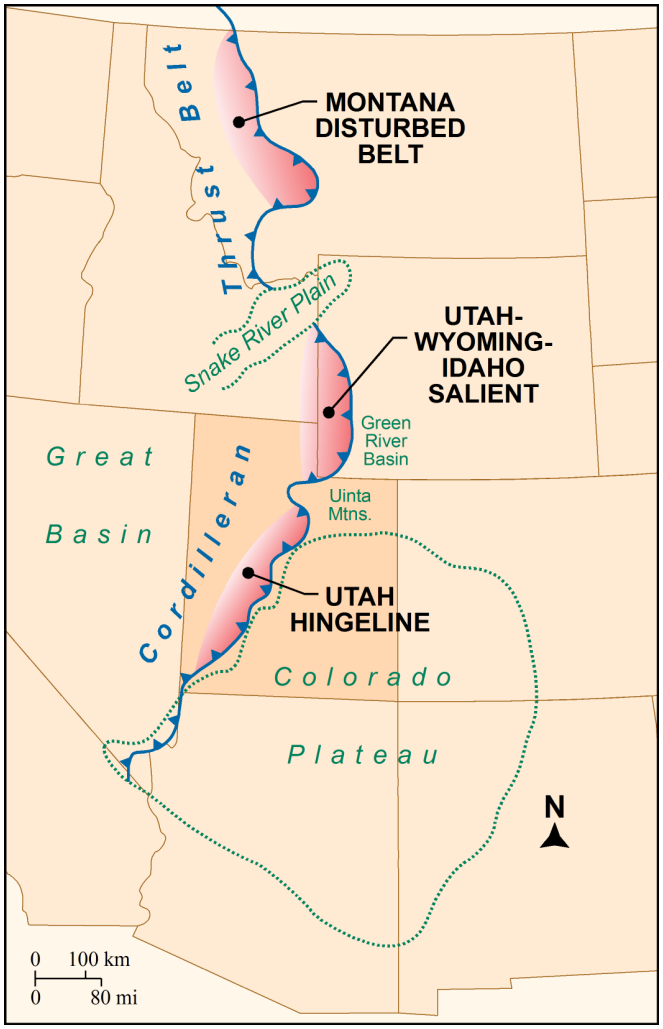

Figure 2.4. *Location of the Cordilleran thrust belt including the Montana "Disturbed" belt, Utah-Wyoming-Idaho salient, and Utah "Hingeline." Modified from Gibson (1987).*

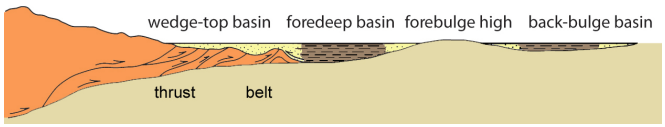

Figure 2.5. *Typical parts of a thrust system. From Willis (1999).*

Associated with thrusting was synorogenic deposition which is used to determine the age of thrust emplacement (figures 2.7 through 2.9). Synorogenic deposits are represented by thick conglomerates, such as the middle Cretaceous (Santonian\Coniacian) Echo Canyon and Weber Canyon Conglomerates that record movement on the Crawford thrust and regional subsidence (Yonkee and Weil, 2011). They grade eastward into fluvial, coastal-plain, and deltaic deposits (Willis, 1999). The Absaroka thrust moved in Late Cretaceous (mid-Campanian-Maastrichtian) to Paleocene time (Yonkee and Weil, 2011). Most thrust belt oil fields are on the Absaroka thrust plate (figure 1.3A). Traps form on discrete, seismically defined, subsidiary closures along strike on major ramp anticlines (Lamerson, 1982).

The oil plays (and subplays), and their reservoirs, trapping mechanisms, source rocks, production data, and other general information pertaining to the Utah/Wyoming thrust belt province are outlined below:

- Major oil plays (and subplays):
  - Triassic-Jurassic Nugget Sandstone thrust belt play

    Subplays – Nugget Sandstone Absaroka thrust – Mesozoic-cored shallow structures subplay

    Nugget Sandstone Absaroka thrust – Mesozoic-cored deep structures subplay

    Nugget Sandstone Absaroka thrust – Paleozoic-cored shallow structures subplay
  - Jurassic Twin Creek Limestone thrust belt play

    Subplays – Twin Creek Limestone Absaroka thrust – Mesozoic-cored shallow structures subplay

    Twin Creek Limestone Absaroka thrust – Paleozoic-cored shallow structures subplay
- Major oil reservoirs: Upper Triassic–Lower Jurassic Nugget Sandstone, eolian dune sandstone; Middle Jurassic Twin Creek Limestone, shallow marine limestone.
- Trapping mechanisms: anticlines in the hanging walls of detached (not involving basement rocks) thrust systems, and untested subthrust structures (beneath detached and basement-cored faults).
- Source rocks: Cretaceous Mowry Shale; possibly Permian Phosphoria Formation.
- Timing of generation and migration of oil: hydrocarbon generation occurred since early Oligocene.
- First commercial discovery: Pineview field, 1975.
- Number of active oil fields/wells: 13 fields/188 wells.
- Average 2015 monthly production: 43,000 BO (6900 m^3), 5.3 billion cubic feet of gas (BCFG [0.15 BCMG]).
- Cumulative production as of January 1, 2016: 305 million BO (48.5 million m^3), 6.03 trillion cubic feet of gas (TCFG) (0.17 TCMG).
- Types of enhanced oil recovery techniques: gas re-injection to maintain pressure, horizontal drilling.
- Outcrop analogs in Utah: structural—northern Wasatch Range and Crawford Mountains; reservoirs—northern Wasatch Range, west end of the Uinta Mountains, central and southern Utah.

Central Utah Thrust Belt – Hingeline

The central Utah thrust belt is part of the Sevier (Cordilleran) thrust belt (figure 2.4) that trends through the entire state, also referred to by many geologists as "the Hingeline" and is loosely defined as the portion of the thrust belt south of the Uinta Mountains of northeastern Utah, trending through central Utah to the Marysvale–Wah Wah volcanic complex of

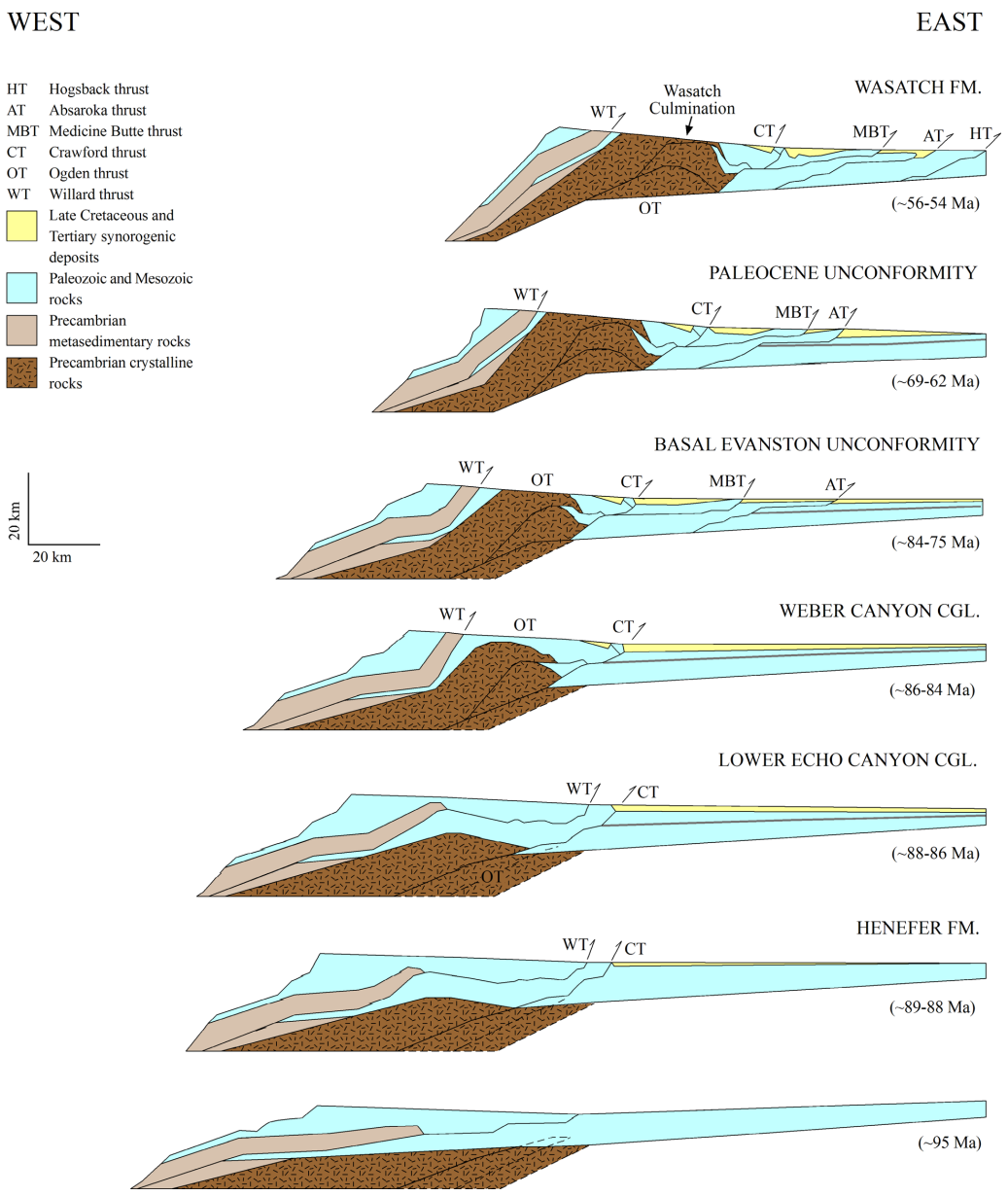

Figure 2.6. *Sequential restored cross section across the Sevier thrust belt at the approximate latitude of Ogden in northern Utah showing the development of thrust faults, the eastward progression of the thrust front, and the deposition and subsequent deformation of synorogenic deposits. Modified from Coogan (1992), Yonkee (1992), DeCelles (1994), and Willis (1999).*

south-central Utah. Classic papers describing and interpreting the geology of the Hingeline region include those of Eardley (1939), Kay (1951), Armstrong (1968), and Stokes (1976). Throughout this area's geologic history, the Hingeline has marked a pronounced boundary between different geologic terranes and processes.

1. From Late Proterozoic to Triassic time, the Hingeline marked the boundary between a very thick succession of sediments deposited in western Utah and a thin succession deposited in eastern Utah.
2. During Cretaceous and early Tertiary time, the Hingeline coincided with and influenced thrusts at the eastern edge of the Sevier orogenic belt.
3. Today in central Utah, the Hingeline marks the general boundary between the Basin and Range and Colorado Plateau physiographic provinces.

In reality, the Hingeline is an area rather than a line, and includes geologic features common in both the Basin and Range and Colorado Plateau physiographic provinces: Sevier orogenic thrust faults, basement-cored Late Cretaceous–Oligocene Laramide uplifts (plateaus and the Wasatch monocline), and Miocene to Holocene normal faults. Paleozoic rocks thicken westward across the Hingeline area from thin cratonic deposits, whereas the Upper Cretaceous section includes thick synorogenic deposits reflecting proximity of the Sevier orogenic belt to the west.

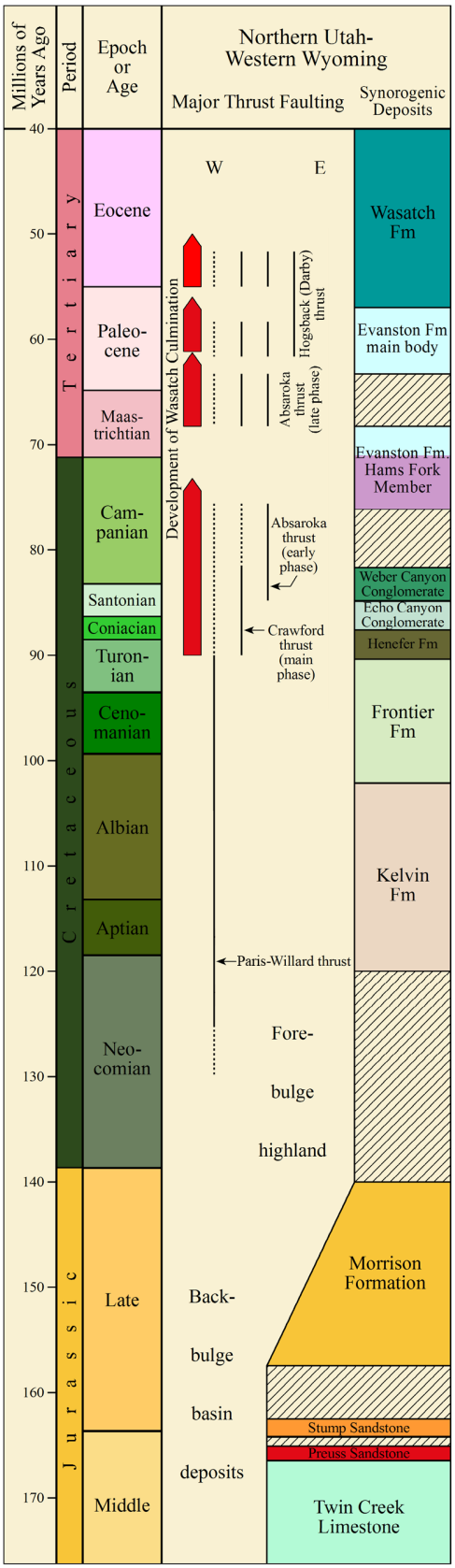

Figure 2.7. *Middle Jurassic through early Eocene thrust development and related synorogenic deposits in northern Utah. Figure is generalized and several minor formations are not shown. Data from Coogan (1992), Yonkee (1992), DeCelles (1994), DeCelles and others (1995), Coogan and DeCelles (1998). Modified from Willis (1999).*

An extensional fault system, including the high-angle, basement-involved "Ephraim fault," was active in central Utah during the Middle Jurassic (Moulton, 1976; Schelling and others, 2005). In the Late Jurassic, Utah was mostly a forebulge high (Willis, 1999). In central Utah, large-scale thrust sheets were emplaced during latest Jurassic through early Tertiary time by compression of the actively evolving foreland basin (Schelling and others, 2005; DeCelles and Coogan, 2006). The youngest evidence of thrust faulting is 40 million years old in central Utah (Lawton, 1985; Decelles and others, 1995; Lawton and others, 1997; Willis, 1999; Constenius and others, 2003; Decelles, 2004; DeCelles and Coogan, 2006). Thrusting extended westward for more than 100 miles (160 km).

Major thrust faults in central Utah (from west to east) include the Canyon Range, Leamington, Pahvant (Royse, 1993), Paxton, Charleston-Nebo, and the Gunnison-Salina (Villien and Kligfield, 1986; Schelling and others, 2007) (figure 1.3). These thrust faults represent detached, thin-skinned, compressional styles of deformation, with eastward combined movement of greater than 90 miles (140 km) for the Canyon Range and Pahvant thrusts (DeCelles and Coogan, 2006). Easternmost thrust systems moved less than western thrust systems and are generally younger; the Canyon Range thrust was emplaced during latest Jurassic–Early Cretaceous time, the Pahvant thrust was emplaced in Albian time, the Paxton thrust was emplaced in Santonian time, and the Gunnison-Salina thrust was active from late Campanian through early Paleocene time (DeCelles and Coogan, 2006). The Ephraim fault and other Middle Jurassic faults may have also experienced additional Laramide-age (Maastrichtian through Eocene) movement.

Surface traces of the thrust faults generally trend in a north-northeast direction. Some of the thrust faults do not extend to the surface, and the term "blind" thrust is applied to buried faults like the Gunnison-Salina thrust. The Pahvant, Paxton, and Gunnison-Salina thrust systems contain Lower Cambrian through Cretaceous strata. Jurassic shale, mudstone, and evaporite beds serve as the main glide planes along the hanging-wall flats of these thrust systems.

The leading edges of the thrust faults are listric in form and structurally complex. They include numerous thrust splays, back thrusts, duplex systems (particularly in the younger eastern thrusts), fault-propagation folds (fault-bend folds), and ramp anticlines such as the huge fold that makes up most of Mount Nebo (near the city of Nephi) along the Charleston-Nebo thrust system where overturned upper Paleozoic and attenuated Triassic and Jurassic rocks are spectacularly displayed. The duplex systems are similar to those found in the Alberta Foothills in the eastern Canadian Rocky Mountains (Dahlstrom, 1970); these types of features are not present in the Utah-Wyoming-Idaho salient of the thrust belt to the north.

Central Utah thrust plates, like the Canyon Range thrust plate, are as much as 36,000 feet (12,000 m) thick (DeCelles and Coogan, 2006), although younger eastern plates tend to be

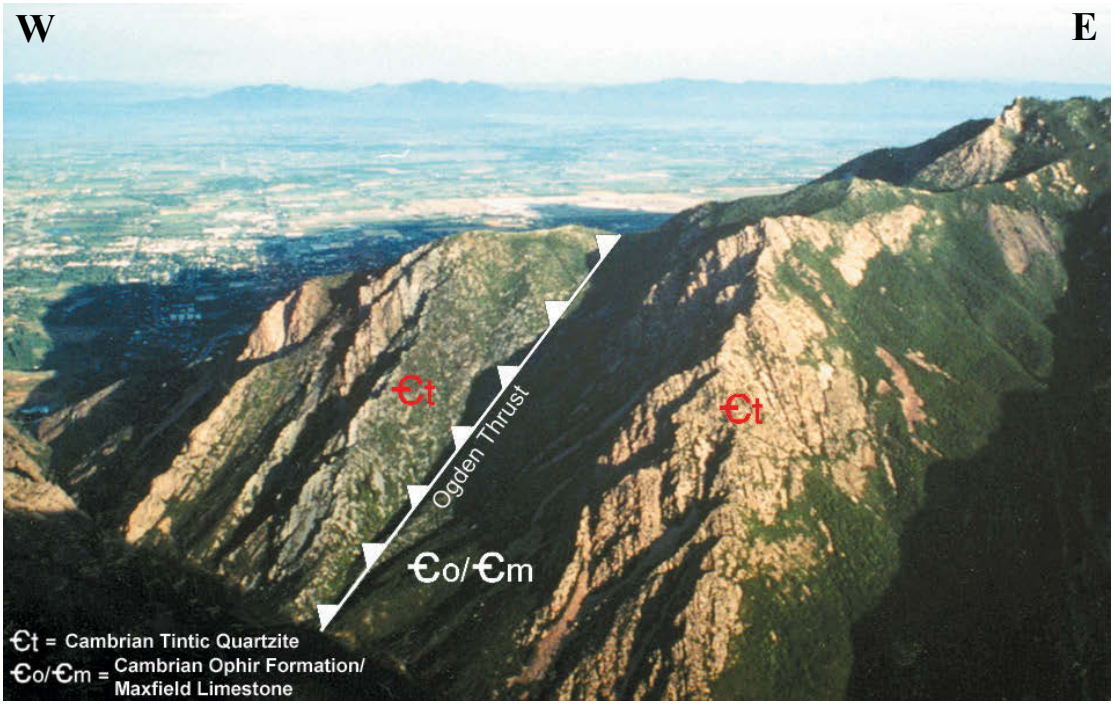

Figure 2.8. *Steeply dipping, Cambrian-age Tintic Quartzite (repeated) with intervening Ophir Formation and Maxfield Limestone along the Ogden thrust, east of Ogden, Utah.*

Figure 2.9. *Gently dipping synorogenic Coniacian-Santonian Echo Canyon Conglomerate, near the junction of Weber and Echo Canyons, northern Utah. Inset: Close up of interbedded conglomerate and sandstone. Photo by Hugh Hurlow, UGS.*

thinner. The eastern plates also deformed into smaller-amplitude fault-propagation folds and ramp anticlines than did western plates (Willis, 1999). Middle Jurassic extensional faults, such as the Ephraim and similar faults in the region, determined the position of these ramp anticlines and associated duplexes along thrust systems by acting as buttresses to plate movement (Schelling and others, 2005). However, a blind, low-angle thrust fault continues east of the Ephraim fault within the Jurassic Arapien Shale–Carmel Formation under the Wasatch Plateau (Neuhauser, 1988). Smaller imbricate faults from the décollement form fault-propagation/fault-bend folds, which are some of the producing anticlines along the Wasatch Plateau.

Neogene reactivated movement along many thrust ramps, splays, and associated back thrusts formed listric normal faults. Other normal faults related to Basin-and-Range extension dissected thrust plates into additional, compartmentalized blocks (Schelling and others, 2005). The Wasatch monocline and other monoclinal structures formed at this time. Some local ductile deformation of Jurassic evaporites further complicated the structural picture of the region (Witkind, 1982). Potential hydrocarbon traps form on discrete, seismically defined, subsidiary closures along strike on major ramp anticlines and fault-propagation/fault-bend folds.

The oil play, reservoir, trapping mechanisms, source rocks, production data, and other general information pertaining to the central Utah thrust belt–Hingeline province are outlined below:

- Major oil play: Jurassic Navajo Sandstone/Temple Cap Formation central Utah thrust belt–Hingeline play.
- Major oil reservoirs: Early Jurassic Navajo Sandstone, eolian dune sandstone; Middle Jurassic White Throne Member of the Temple Cap Formation, coastal eolian dune sandstone.
- Trapping mechanisms: anticlines in the hanging walls of detached (not involving basement rocks) thrust systems created by thrust imbricates, or imbricate fans above, and antiformal stacks of horses forming duplexes below the major thrusts (figure 2.10).
- Source rocks: organic-rich marine shale within the Mississippian Manning Canyon Shale, Delle Phosphatic Member of the Deseret Limestone, Doughnut Formation, or Chainman Shale; possibly Permian Park City/Phosphoria Formation (figure 2.10).
- Timing of generation and migration of oil: most of the hydrocarbon generation and migration probably occurred during Cretaceous to early Tertiary. However, some hydrocarbon generation and migration probably began as early as Permian or Triassic time in the older Paleozoic rocks and as late as Tertiary time in Mesozoic rocks.
- First commercial oil discovery: Covenant field, 2004.
- Number of active oil fields/wells: two fields/26 wells.
- Average 2015 monthly production: 126,000 BO (20,000 m^3).
- Cumulative production as of January 1, 2016: 22,500,000 BO (3,600,000 m^3).
- Types of enhanced oil recovery techniques: possible future carbon dioxide/nitrogen injection.
- Outcrop analogs in Utah: San Rafael Swell, Pahvant Range, southern Wasatch Range, and throughout the Colorado Plateau of southern Utah.

Uinta Basin

The Uinta-Piceance Province in northeastern Utah and northwestern Colorado, as defined by the U.S. Geological Survey (USGS), contains the contiguous outcrops of Maastrichtian and Tertiary rocks, and also includes the southwest- to northeast-trending Wasatch Plateau and Castle Valley (Dubiel, 2003). Our discussion will be restricted to the Uinta Basin portion of the province (figure 2.11), which incorporates a small portion of the western flank of the Douglas Creek Arch that separates the Uinta and Piceance Basins. The Uinta Basin covers nearly 16,000 square miles (41,000 km^2). The Uinta Basin (excluding the Wasatch Plateau and Castle Valley) is a topographic and structural trough that is sharply asymmetrical, with a steep north flank bounded by the east-west-trending Uinta Mountains and a gently dipping south flank (figure 2.12) bounded by the San Rafael and Uncompahgre uplifts.

The Uinta Basin formed in Late Cretaceous (Maastrichtian) time when a large structural sag with internal drainage was created. The earliest deposits in the intermontane basin were predominantly alluvial (Ryder and others, 1976) with some shallow lacustrine and paludal deposits that compose the North Horn Formation. In early late Paleocene time, a large lake known as ancestral Lake Uinta developed in the basin (Franczyk and others, 1992) (includes Lake Flagstaff of some workers). Deposition in and around Lake Uinta consisted of open- to marginal-lacustrine sediments that make up the Green River Formation. Alluvial redbed and floodplain deposits that are laterally equivalent to, and intertongue with, the Green River form the Colton (Wasatch) Formation (figure 2.13). The Eocene Uinta Formation and the Eocene to lower Oligocene Duchesne River Formation overlie the Green River.

The significant oil plays in the Uinta Basin are part of the Green River Total Petroleum System (TPS). The USGS defines the Green River TPS as a complex of entirely continental rocks (North Horn, Wasatch, Colton, Green River, Uinta, and Duchesne River Formations) that host gilsonite veins, oil shales, tar sands, and oil and gas, all sourced from lacustrine rocks within the Paleocene to Eocene Green River Formation (Dubiel, 2003). Source rocks are: (1) type I kerogen from the open-lacustrine facies, (2) type I, II, and III, kerogen from the marginal-lacustrine facies, and (3) type III kerogen from alluvial facies (Dubiel, 2003).

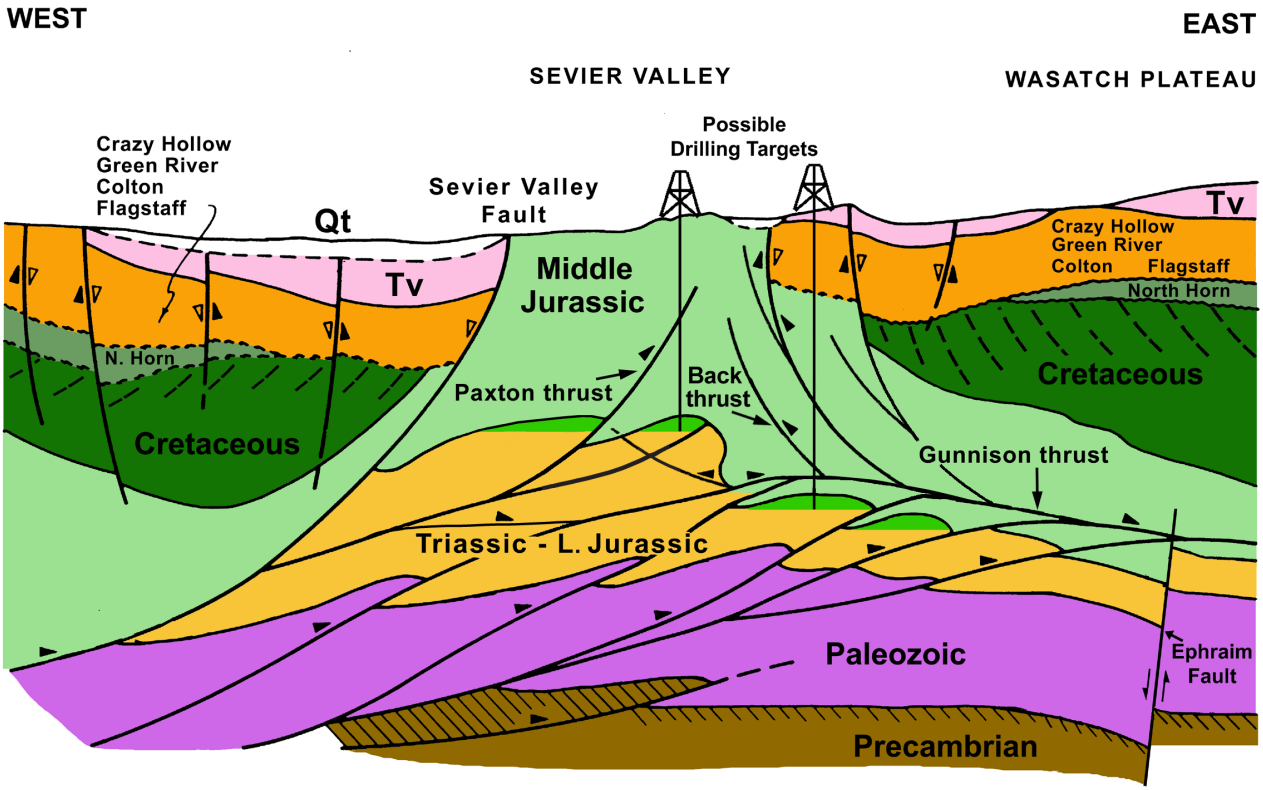

Figure 2.10. *Schematic east-west structural cross section through Sevier Valley, Utah (line of section shown on figure 1.3B), just north of the 2004 Covenant field discovery (Jurassic Navajo Sandstone), showing potential Lower Jurassic exploratory drilling targets in thrust imbricates, fault-propagation folds, and duplexes above and below the Gunnison thrust. Note the presence of the basement-involved Ephraim fault in relationship to the duplex system. Modified from Villien and Kligfield (1986).*

The maximum depth to the base of the Green River TPS is about 20,000 feet (6100 m) along the axis of the Uinta Basin (Fouch and others, 1994). Operators typically assign all strata containing red beds to the Wasatch or Colton Formations; however, oil and gas production is mostly from tongues of the Green River Formation within the alluvial Wasatch and Colton (Fouch and others, 1992; Fouch and others, 1994).

The dominant sediment source for the Green River and Colton Formations in the Cedar Rim, Altamont, Bluebell, and Red Wash fields was from the north, while the sediment source for the greater Monument Butte, Duchesne, Brundage Canyon, Sower Canyon, Antelope Creek, and Uteland Butte fields, was from as far south as Arizona (figure 2.14). As a result, the deposition and the resulting reservoir properties are significantly different between south-sourced and north-sourced depositional systems.

The USGS (Dubiel, 2003) defines two assessment units in the Green River TPS within the Uinta Basin: (1) the Deep Uinta Overpressured Continuous Oil Assessment Unit (AU 50200561) and (2) the Uinta Green River Conventional Oil and Gas Assessment Unit (AU 50200501) (figure 2.15). The Green River Conventional Oil and Gas Assessment Unit extends farther west than the Uinta Basin boundary. The western boundary of the Uinta Basin in Wasatch and Utah Counties is defined by the Charleston-Nebo thrust, and Maastrichtian and Tertiary rocks beneath the thrust define the assessment unit boundary. As a result, the assessment unit boundary extends beyond the basin boundary.

The USGS (Dubiel, 2003) defines the Deep Uinta Overpressured Continuous Oil Assessment Unit by overpressured (gradient >0.5 pounds per square inch per foot [psi/ft]; 11.3 kPa/m) source and reservoir rocks in the Green River Formation (figure 2.16). The overpressured area is located near the basin center mostly in the Colton Formation and Flagstaff Member of the Green River in the Altamont, Bluebell, and Cedar Rim fields. The 0.5 psi/ft (11.3 kPa/m) gradient is encountered as shallow as 8500 feet (2600 m). However, most of the high-volume, overpressured oil production is typically from 12,000 to 14,000 feet (3600–4300 m) in the Flagstaff Member.

The USGS defines the Uinta Green River Conventional Oil and Gas Assessment Unit by the distribution of normally pressured (<0.5 psi/ft [11.3 kPa/m]) oil and gas accumulations in the Green River Formation, typically at depths less than 8500 feet (2600 m) (Dubiel, 2003). The unit overlies the entire area of the Deep Uinta Overpressured Continuous Oil Assessment Unit. The Uinta Green River Conventional Oil and Gas Assessment Unit consists entirely of the part of the Green River that overlies the Colton and Wasatch formations. A transitional interval from about 8500 to 11,000 feet (2600–3400 m) is slightly overpressured (0.50 to 0.55 psi/ft [11.3–12.4 kPa/m])

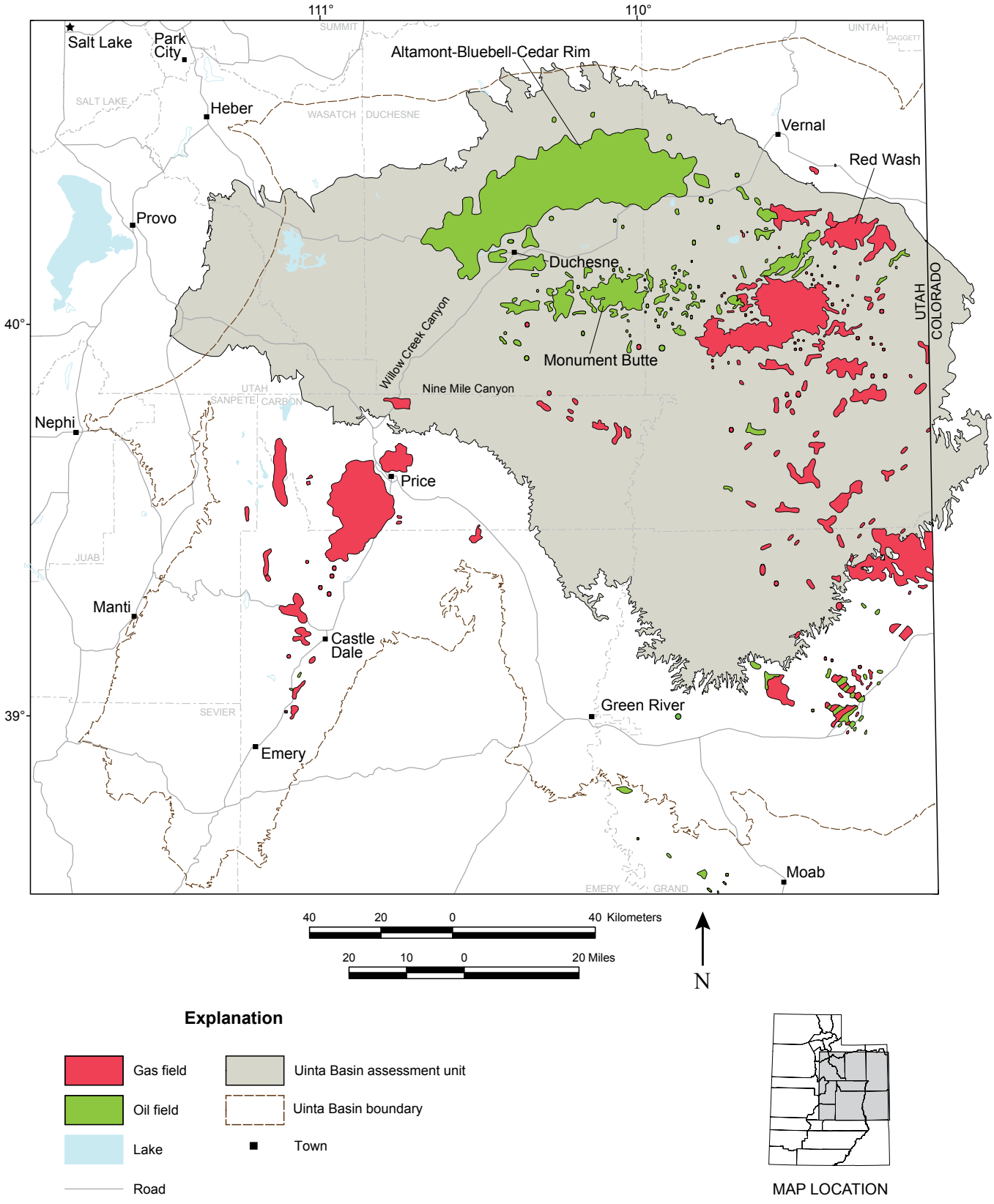

Figure 2.11. *Map showing the location of the Uinta Basin and some of the major oil and gas fields.*

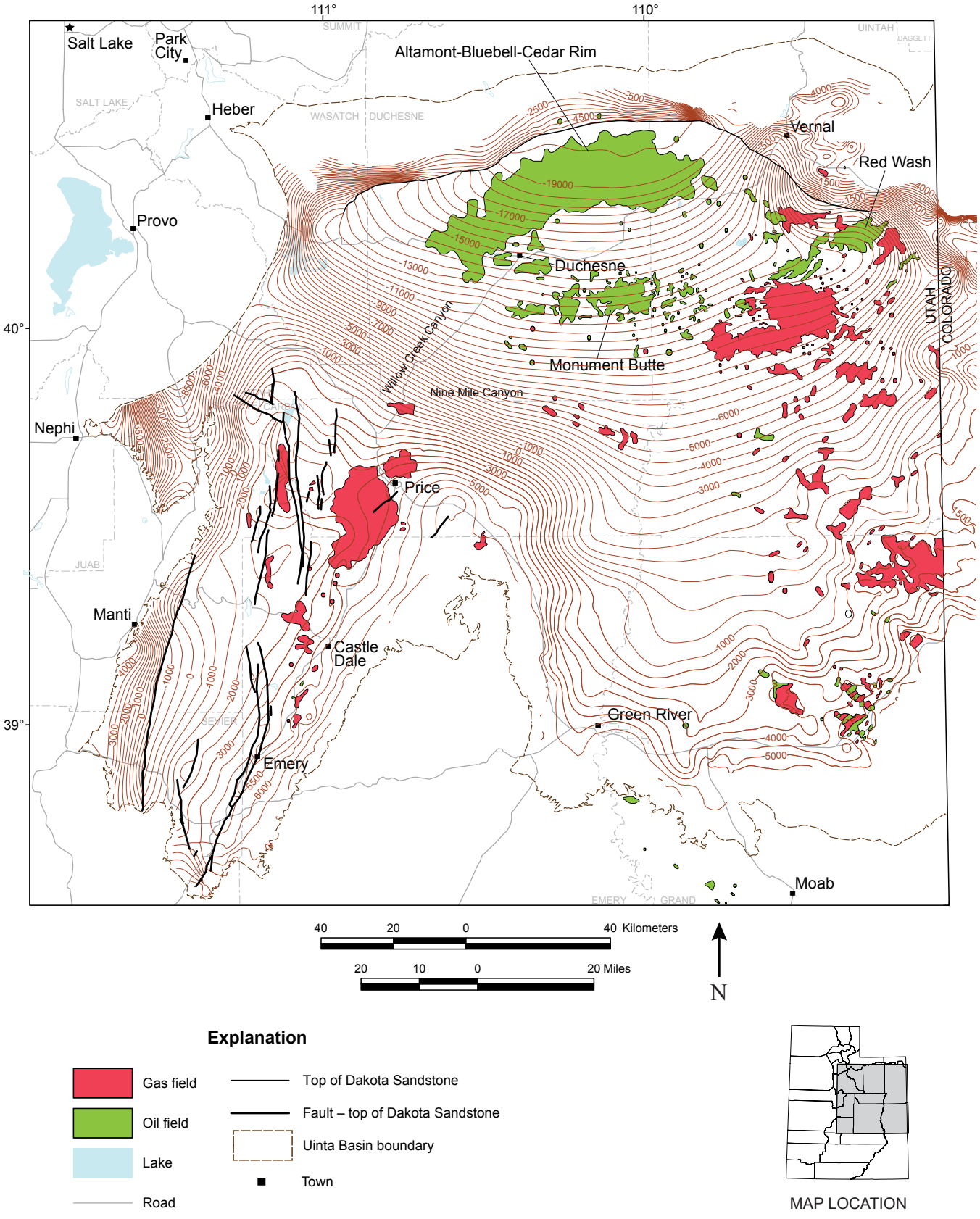

Figure 2.12. *Structure contour map on top of the Cretaceous Dakota Sandstone, Uinta Basin. Contour interval is 500 feet sea-level elevation. Contours from Roberts (2003).*

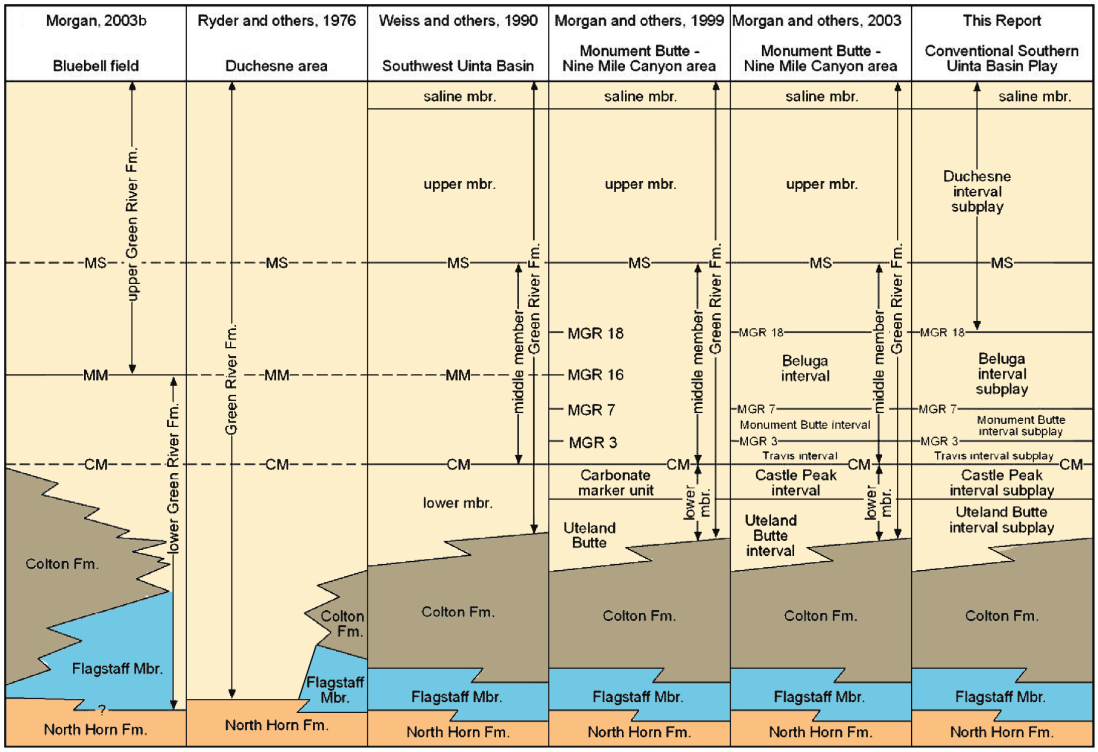

Figure 2.13. *Generalized Uinta Basin nomenclature chart used in this report for the Green River through North Horn Formations. MS = Mahogany Shale, MM = middle marker, CM = carbonate marker, and MGR = middle Green River.*

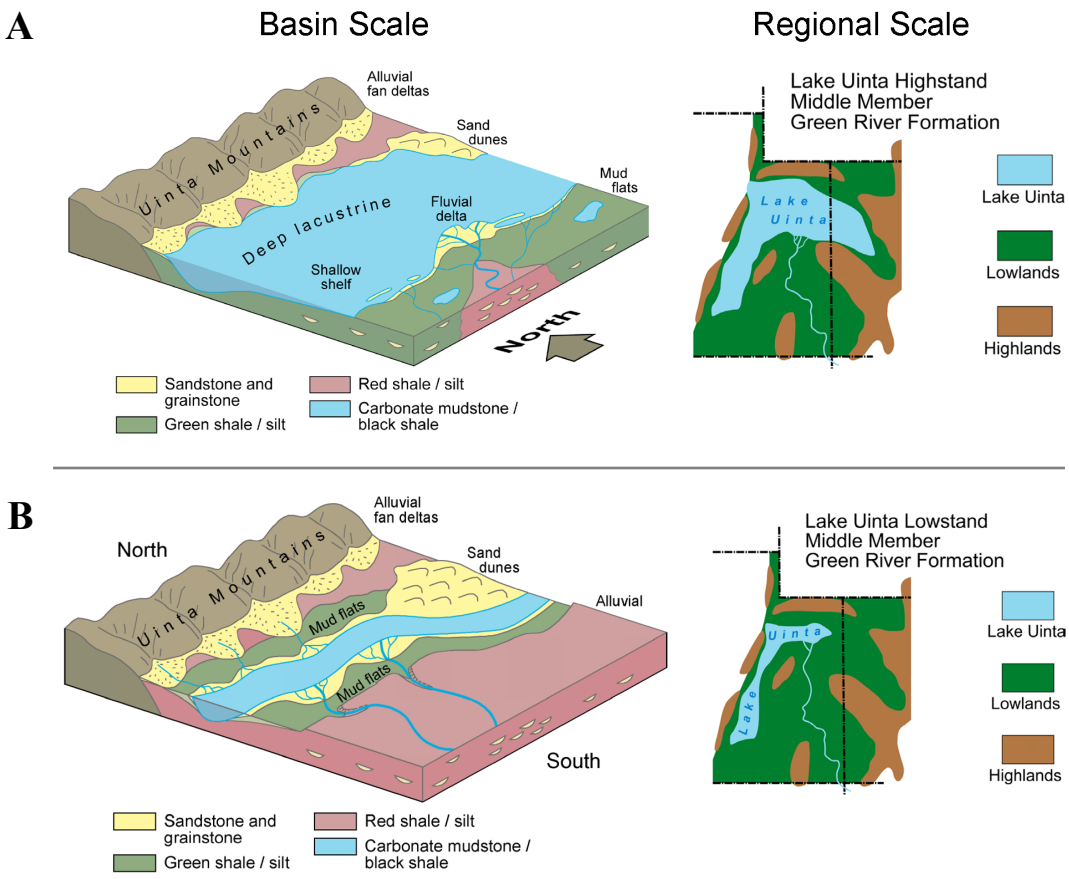

Figure 2.14. *Diagrams showing the generalized basin and regional scale depositional setting for Lake Uinta during high-lake levels (A) and low-lake levels (B). The Uinta Mountains were the source for the sediments in the northern portion of the lake while sediments in the southern portion of the lake were sourced from the much larger Four Corners area. From Morgan and others (2003).*

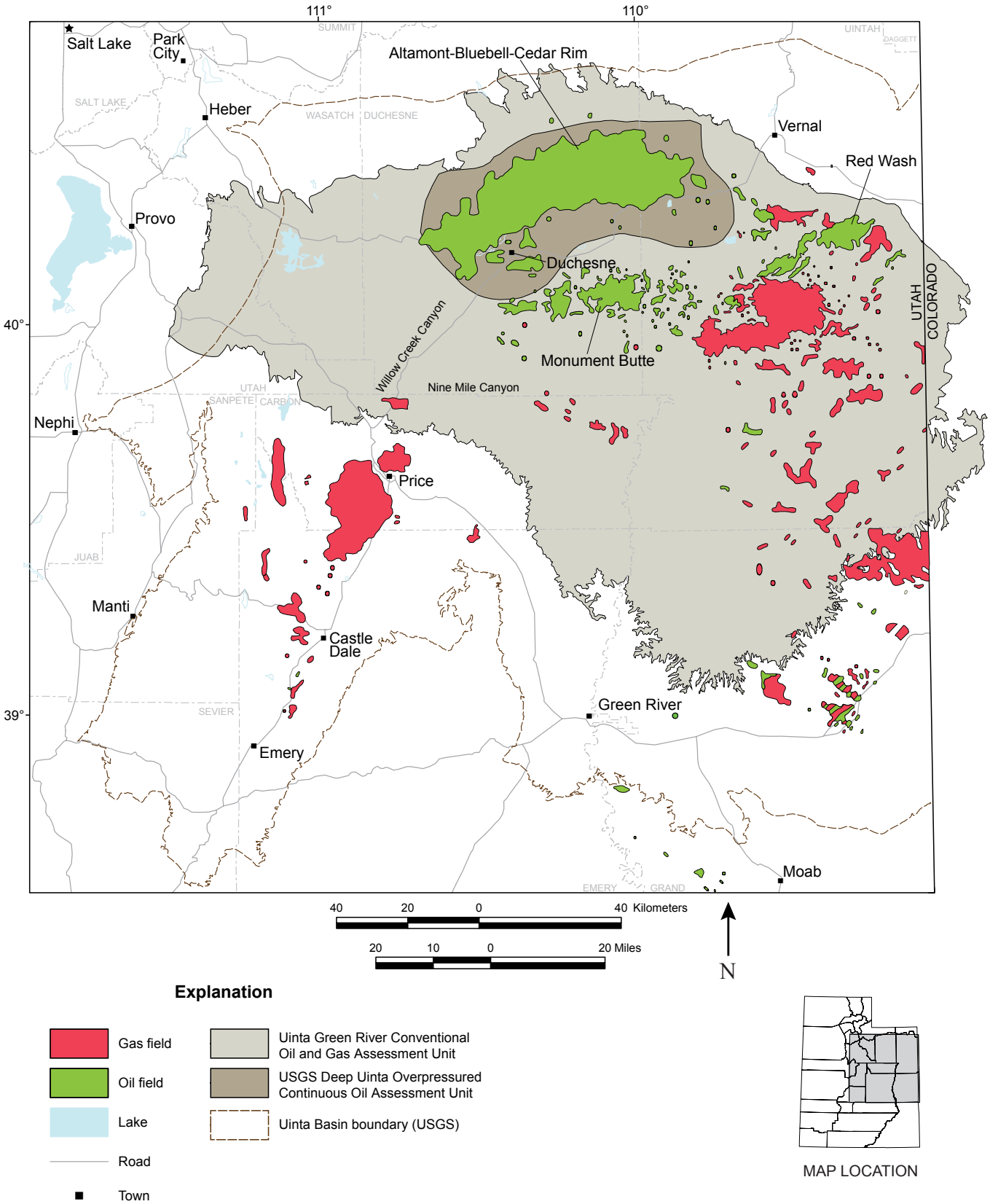

Figure 2.15. *Map showing the USGS Deep Uinta Overpressured Continuous Oil Assessment Unit and the Uinta Green River Conventional Oil and Gas Assessment Unit of Dubiel (2003).*

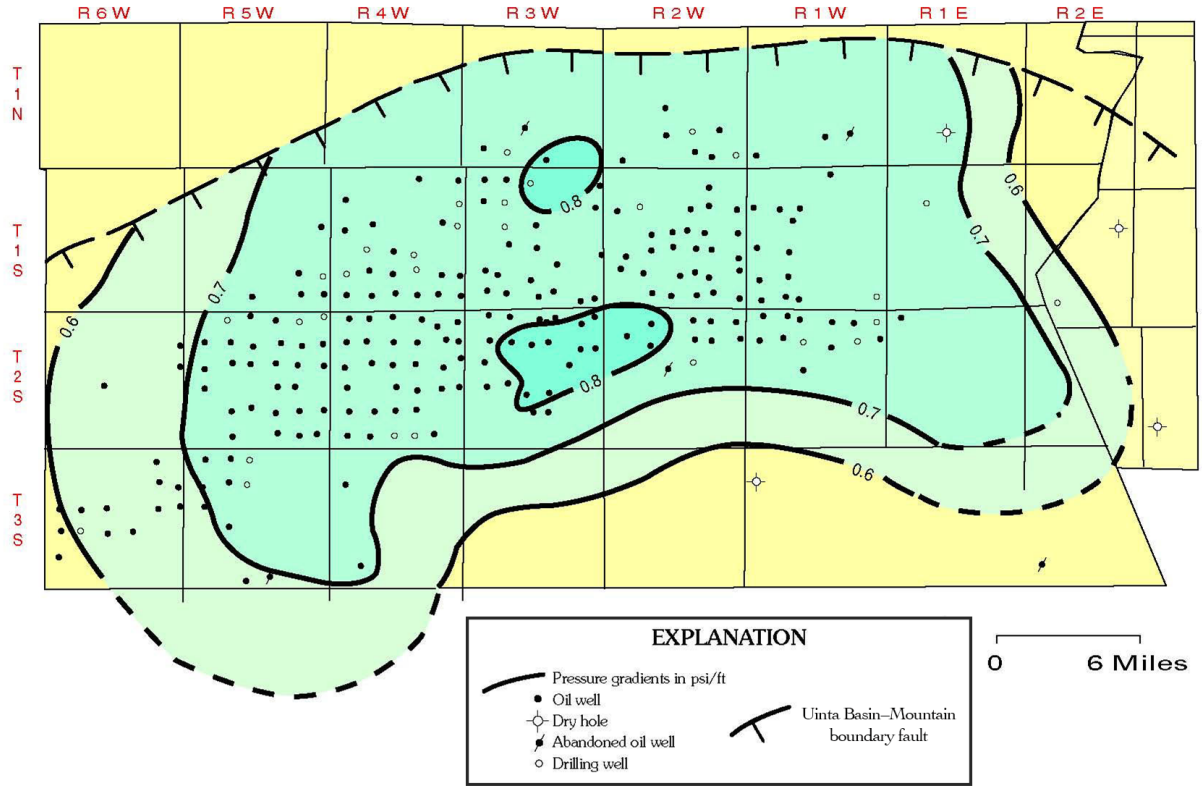

Figure 2.16. *Distribution of wells and contours of pressure-gradient data in the Altamont-Bluebell field area. From Dubiel (2003).*

but many of the reservoir characteristics are more like the overlying Conventional Northern Uinta Basin play (CNUBP) and is discussed in that play description.

The Deep Uinta Overpressured Continuous Oil Assessment Unit and the Deep Uinta Basin Overpressured Continuous play (DUBOCP) have the same boundaries. We divide the Uinta Green River Conventional Oil and Gas Assessment Unit into a Conventional Southern Uinta Basin play (CSUBP) and a CNUBP, which have some overlap (figures 2.17 and 2.18); each are further divided into subplays. The subplays are based on depositional environments of the reservoir rocks which were strongly influenced by the: (1) sediment source, (2) gradient of the depositional slope, and (3) energy regime of the environment which affected the amount of sediment reworking (figure 2.19).

Most of the crude oils produced from the Green River TPS in the Uinta Basin are characterized as yellow or black wax. Production from the DUBOCP is dominantly yellow wax while most of the oil production from the CNUBP and CSUBP is black wax. Asphaltine oil has been produced from a few shallow wells in the Duchesne interval of fractured shale/marlstone subplay in the CSUBP. Associated gas is produced from the Green River TPS and typically has a high heat value—greater than 1000 British thermal units per cubic feet (Btu/ft^3).

The oil plays (and subplays), reservoirs, trapping mechanisms, source rocks, production data, and other general information pertaining to the Uinta Basin province are outlined below:

- Major oil plays (and subplays):
  - Conventional Northern Uinta Basin play
    - Subplays – Conventional Bluebell subplay
    - Conventional Red Wash subplay
  - Conventional Southern Uinta Basin play
    - Subplays – Conventional (and unconventional [horizontal drilling]) Uteland Butte interval subplay
    - Conventional Castle Peak interval subplay
    - Conventional Travis interval subplay
    - Conventional Monument Butte interval subplay
    - Conventional Beluga interval subplay
    - Conventional Duchesne interval fractured shale/marlstone subplay
  - Deep Uinta Basin Overpressured Continuous play
- Major oil reservoirs: Eocene Green River and Wasatch (Colton) Formations, lacustrine (carbonates) to alluvial channel and bar sandstone.
- Trapping mechanisms: stratigraphic conventional, basin centered, and tight oil (Uteland Butte Member of the Green River Formation).
- Source rocks: Eocene lacustrine shale.

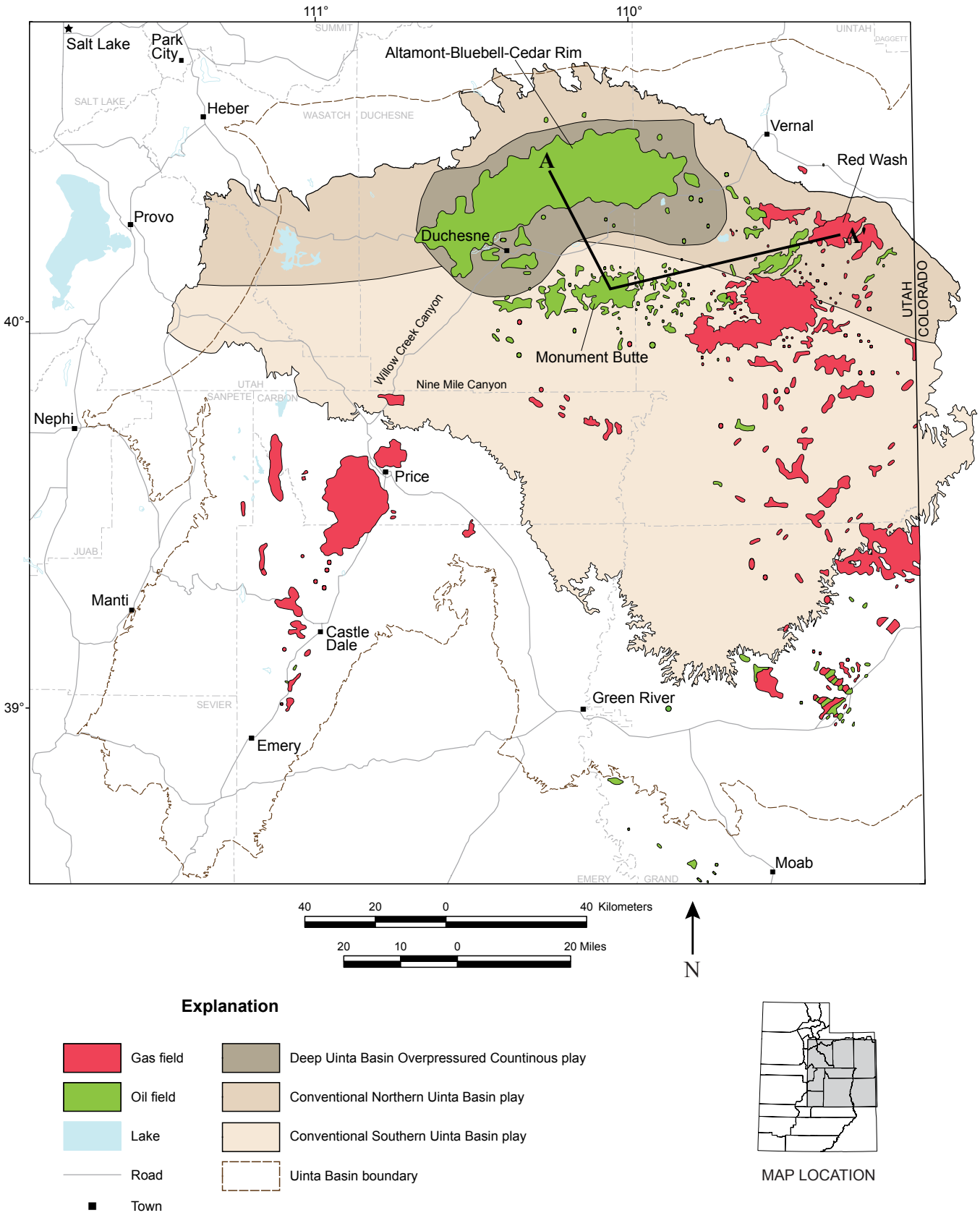

Figure 2.17. *Map showing the Deep Uinta Basin Overpressured Continuous play which underlies the Conventional Northern and Conventional Southern Uinta Basin plays; these plays overlap. Cross section A–A' shown on figure 2.18.*

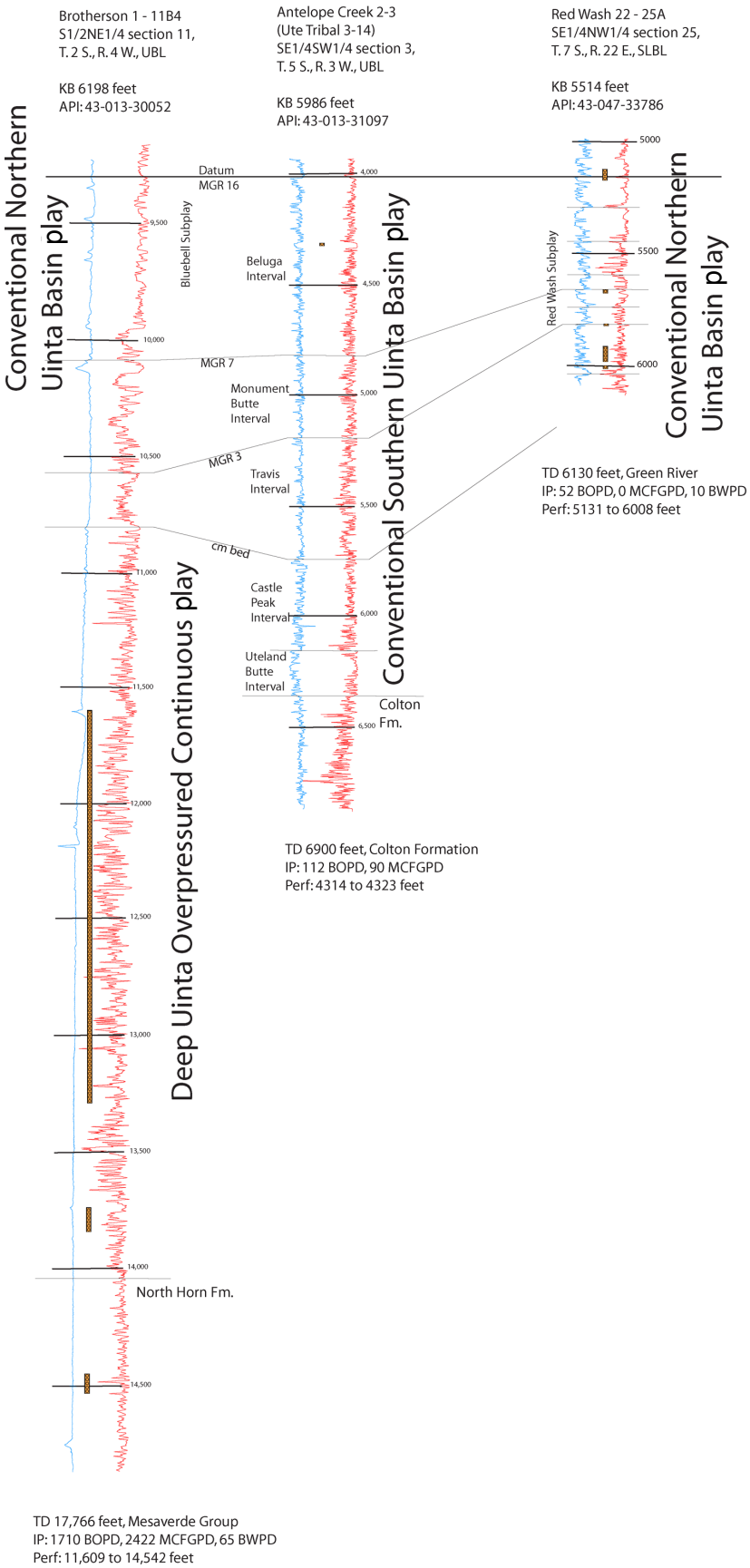

Figure 2.18. *Well-log cross section showing correlation of the Uinta Basin plays. Line of section shown on figure 2.17. Perforations are shown as solid orange lines in the depth column. The Brotherson No. 1-11 B4 well displays spontaneous potential and sonic logs. The Antelope Creek No. 2-3 and Red Wash No. 22-25A wells display gamma-ray and sonic logs.*

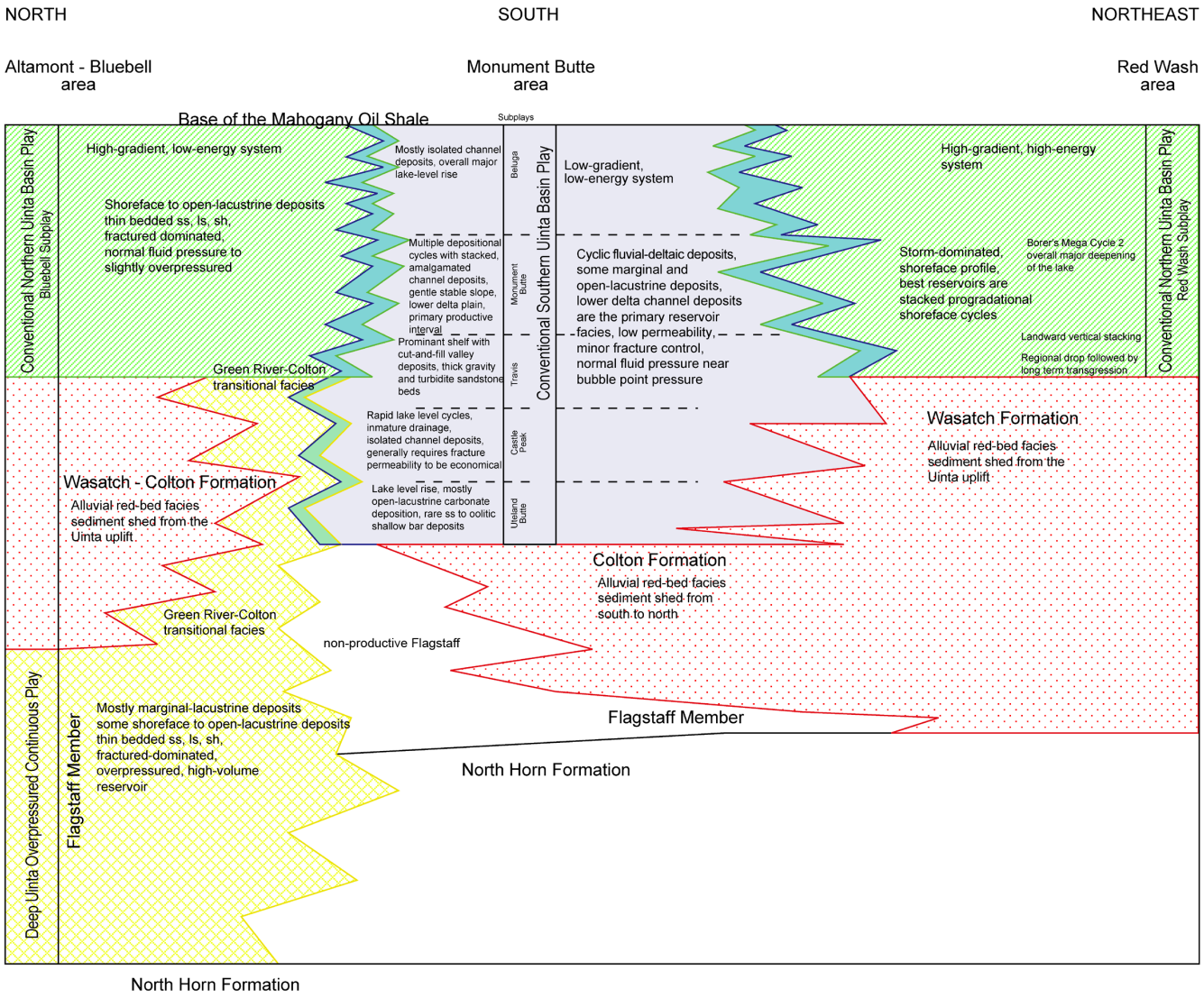

Figure 2.19. *Diagrammatic correlation of the Green River plays in Uinta Basin. Sediment source and depositional energy systems resulted in varying reservoir characteristics in each of the plays and subplays.*

- Timing of oil generation and migration: peak generation occurred during maximum burial between 30 to 40 million years ago (Ma) and continues today in the deepest part of the basin. Vertical and lateral migration began prior to peak generation.
- First commercial oil discovery: Roosevelt field, 1949.
- Number of active oil fields/wells: 84 fields/ 11,633 wells.
- Average 2015 monthly production: 2,447,000 BO (389,000 m^3), 30 BCFG (0.84 BCMG).
- Cumulative production as of January 1, 2016: 717 million BO (114 million m^3), 6.1 TCFG (0.2 TCMG) of gas.
- Types of enhanced oil recovery techniques: waterflood and horizontal drilling in the Green River Formation.
- Outcrop analogs in Utah: Roan and Badlands Cliffs, and Raven Ridge, central Utah plateaus.

Paradox Basin

The Paradox Basin is located principally in southeastern Utah and southwestern Colorado and has small portions in northeastern Arizona and the northwestern corner of New Mexico (figure 1.2A). The Paradox Basin is an elongate, northwest-southeast-trending, evaporite-rich basin that predominately developed during the Pennsylvanian, about 330 to 310 Ma. The most obvious structural features in the basin are the spectacular anticlines that extend for miles in the northwesterly trending fold and fault belt. The events that caused these and many other structural features began in the Proterozoic, when movement initiated on high-angle basement faults and fractures 1700 to 1600 Ma (Stevenson and Baars, 1986, 1987). During Cambrian through Mississippian time, this region, as well as most of eastern Utah, was the site of typical thin, marine deposition on a craton, whereas thicker deposits accumulated in a miogeocline to the west (Hintze and Kowallis,

2009). However, major changes began in the Pennsylvanian when a pattern of basins and fault-bounded uplifts developed from Utah to Oklahoma as a consequence of the collision of South America, Africa, and southeastern North America (Kluth and Coney, 1981; Kluth, 1986), or from a smaller-scale collision of a microcontinent with south-central North America (Harry and Mickus, 1998). One result of this tectonic event was the uplift of the Ancestral Rockies in the western United States. The Uncompahgre Highlands (uplift) in eastern Utah and western Colorado initially formed as the westernmost range of the Ancestral Rockies during this ancient mountain orogenic period.

The Uncompahgre Highlands are bounded along their southwestern flank by a large basement-involved, high-angle, reverse fault identified from seismic surveys and exploration drilling (Frahme and Vaughn, 1983). As the highlands rose, an accompanying depression, or foreland basin, formed to the southwest—the Paradox Basin. The formation of the Paradox Basin was strongly influenced by rejuvenation of pre-existing (late Precambrian), northwesterly trending structures (Baars and Stevenson, 1981). Rapid basin subsidence, particularly during the Pennsylvanian and continuing into the Permian, accommodated large volumes of evaporitic and marine sediments that intertongue with non-marine arkosic material shed from the highland area to the northeast (figures 2.20 and 2.21) (Hintze and Kowallis, 2009). Deposition in the basin produced a thick cyclical sequence of carbonates, evaporites, and organic-rich shale (Peterson and Hite, 1969; Hite and others, 1984; Rasmussen, 2010). The Paradox Basin is defined for the purposes of this study by the maximum extent of an¬hydrite beds in the Pennsylvanian Paradox Formation.

The present Paradox Basin includes or is surrounded by other uplifts that formed during the Late Cretaceous–early Tertiary Laramide orogeny, such as the Monument upwarp in the west-southwest, and the Uncompahgre uplift, corresponding to the earlier Uncompahgre Highlands, forming the northeast boundary (figure 1.2A). Oligocene laccolithic intrusions form the La Sal and Abajo Mountains in the north and central parts of the basin in Utah, whereas the Carrizo Mountains in Arizona, and the Ute, La Plata, and San Miguel Mountains in Colorado were intruded along the southeastern boundary of the basin (figure 1.2A).

The Paradox Basin can generally be divided into three areas: the Paradox fold and fault belt in the north, the Blanding sub-basin in the south-southwest, and the Aneth platform in the southernmost part in Utah (figure 1.2A). The area now occupied by the Paradox fold and fault belt was also the site of greatest Pennsylvanian/Permian subsidence and salt deposition. Folding in this area began as early as the Late Pennsylvanian as sediments were laid down thinly over, and thickly in areas between, rising salt (Doelling, 2003). The Paradox fold and fault belt was created during the Late Cretaceous through Quaternary by a combination of (1) reactivation of basement normal faults, (2) additional salt flowage followed by dissolution and collapse, and (3) regional uplift (Doelling, 2003). The relatively undeformed Blanding sub-basin and Aneth platform developed on a subsiding shallow-marine shelf. Each area contains oil and gas fields with structural, stratigraphic, or combination traps formed on discrete, often seismically defined, closures.

Most oil and gas produced from the Mississippian Leadville Limestone is in basement-involved, northwest-trending structural traps with closure on both anticlines and faults (figure 2.22). Most Paradox Formation petroleum production comes from stratigraphic traps in the Blanding sub-basin and Aneth platform that locally contain phylloid algal-mound and other carbonate lithofacies buildups (figure 2.22). The sources of the petroleum are several black, organic-rich shales (the Gothic and Chimney Rock, for example) within the Paradox Formation (Hite and others, 1984; Nuccio and Condon, 1996).

The oil plays (and subplays), reservoirs, trapping mechanisms, source rocks, production data, and other general information pertaining to the Paradox Basin province are outlined below:

- Major oil plays (and subplays):
  - Mississippian Leadville Limestone, Paradox Basin play
  - Pennsylvanian Paradox Formation, Paradox Basin play

    Subplays – fractured shale subplay

    Blanding sub-basin Desert Creek zone subplay

    Blanding sub-basin Ismay zone subplay

    Aneth platform Desert Creek zone subplay
- Major oil reservoirs: Mississippian Leadville Limestone, shallow-shelf marine limestone and dolomite; Pennsylvanian Paradox Formation, shallow-shelf marine limestone and dolomite in the Desert Creek and Ismay zones, and fractured units in the Cane Creek shale.
- Trapping mechanisms: stratigraphic—carbonate buildups (algal mounds, shoals, islands) sealed by anhydrite, salt, or organic-rich shale; structural—fracture zones and faulted and asymmetrical anticlines; diagenetic—dolomitization and dissolution.
- Source rocks: black, organic-rich marine shale within the Pennsylvanian Paradox Formation.
- Timing of oil generation and migration: hydrocarbon generation occurred during maximum burial in the Late Cretaceous and early Tertiary with migration beginning at that time.
- First commercial discovery: Boundary Butte field, 1947.
- Number of active oil fields/wells: 71 fields/771 wells.
- Average 2015 monthly production: 448,000 BO (71,200 m^3), 919 MCFG (26 MCMG).

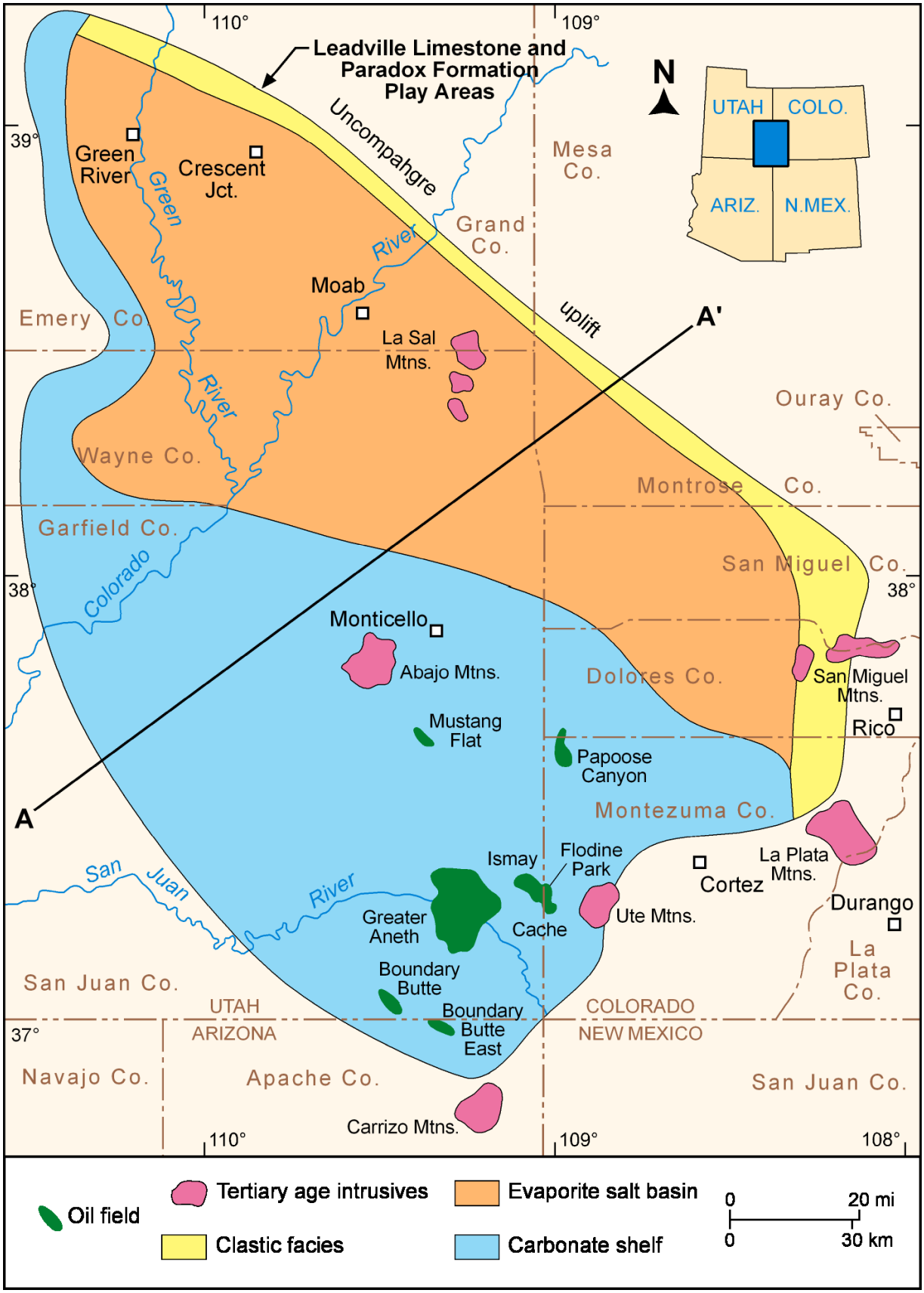

Figure 2.20. *Generalized map of Paradox Formation facies with clastic wedge, evaporite salt basin, and carbonate shelf. Modified from Wilson (1975). Cross section A–A' shown on figure 2.21.*

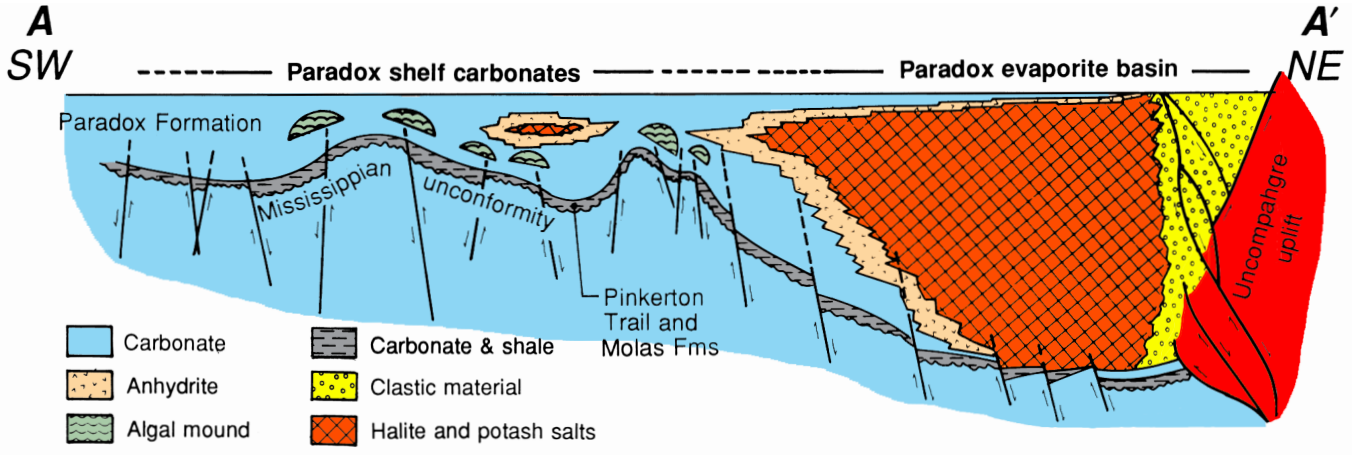

Figure 2.21. *Generalized cross section across the Paradox Basin with gross facies relations between Middle Pennsylvanian shelf carbonates, restricted basin evaporites, and coarse clastics proximal to the Uncompahgre uplift. Modified from Baars and Stevenson (1981). Maximum extent of anhydrite beds in the Paradox Formation that define the basin is not shown. Location of cross section shown on figure 2.20.*

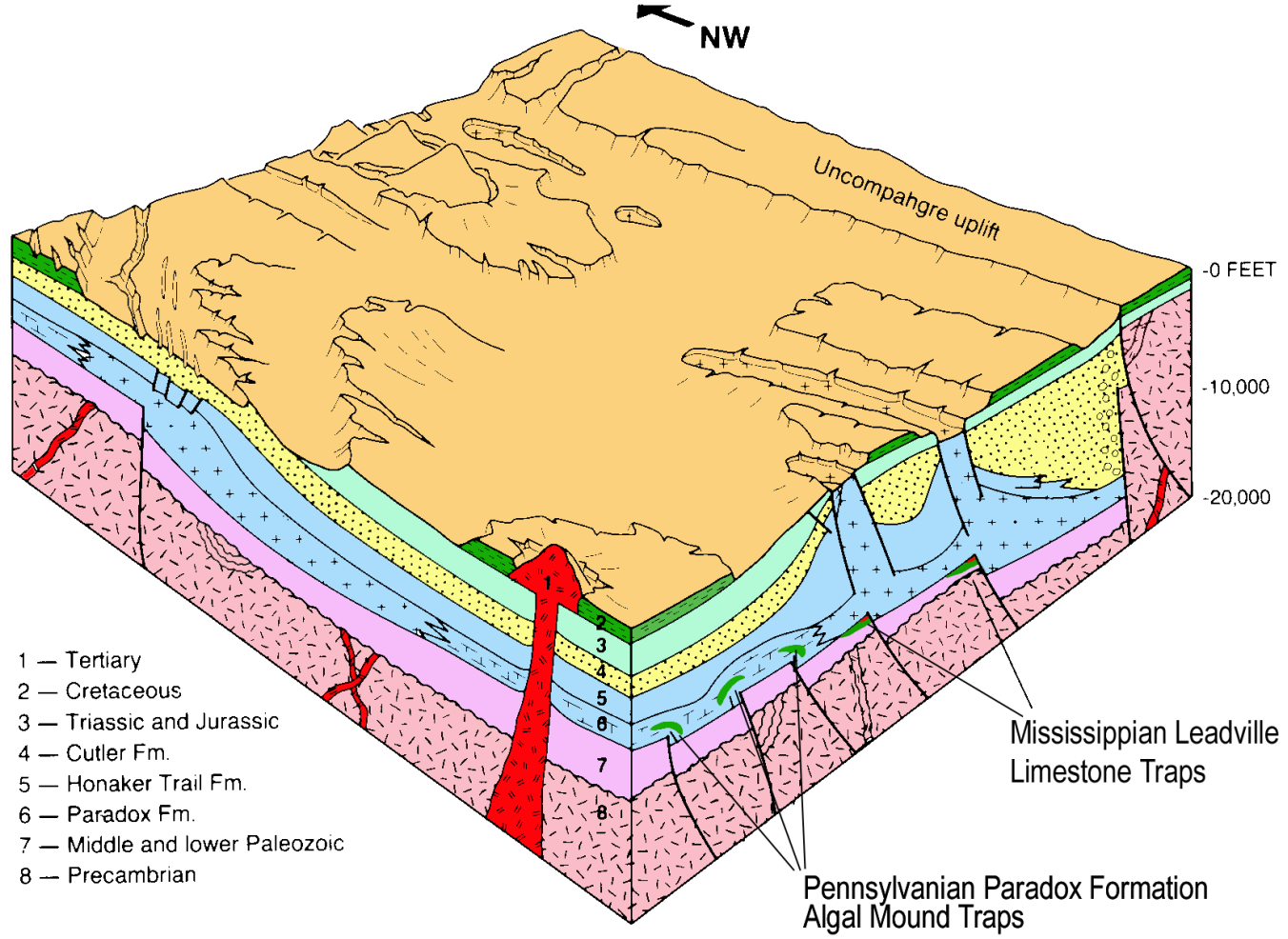

Figure 2.22. *Schematic block diagram of the Paradox Basin displaying basement-involved structural trapping mechanisms for the Leadville Limestone fields and carbonate buildups for Paradox Formation fields. Modified from Petroleum Information (1984a); original drawing by J.A. Fallin.*

- Cumulative production as of January 1, 2016: 627 million BO (99.7 million m^3), 1.6 TCFG (0.04 TCMG).
- Types of enhanced oil recovery projects: waterflood, CO_2 flood (CO_2 provided by pipeline from McElmo Dome in Colorado from the Mississippian Leadville Limestone), gas injection using horizontal wellbores.
- Outcrop analogs in Utah: shallow-shelf carbonates and karst features, Mississippian Madison and Deseret Limestones, south flank of the Uinta Mountains; Ismay and Desert Creek algal mounds, Pennsylvanian Paradox Formation, exposed along the San Juan River in southeastern Utah.

CHAPTER 3:
TRIASSIC-JURASSIC NUGGET SANDSTONE THRUST BELT PLAY

by

Thomas C. Chidsey, Jr., and Douglas A. Sprinkel
Utah Geological Survey

CONTENTS

FIGURES

TABLE

CHAPTER 3:
TRIASSIC-JURASSIC NUGGET SANDSTONE THRUST BELT PLAY

INTRODUCTION

The most prolific oil and gas play confined to the hanging wall of the Absaroka thrust system is the Triassic-Jurassic Nugget Sandstone thrust belt play (figure 3.1). The Nugget has produced nearly 292 million BO (46 million m^3) and 6.0 TCFG (0.17 TCMG); however, much of the gas included in the production figures is cycled gas, including nitrogen gas (N_2), for pressure maintenance (Utah Division of Oil, Gas, and Mining, 2016a; Wyoming Oil and Gas Conservation Commission, 2016). Pineview field, Summit County, Utah, was the first to produce oil and gas from the Nugget in 1975 (Conner and Covlin, 1977; Petroleum Information, 1981) and led the way for additional discoveries over the next eight years. Thirteen Nugget fields currently exist: eight entirely in Wyoming, four entirely in Utah, and one (Anschutz Ranch East) in both Utah and Wyoming. Geologic data for individual fields in the play are summarized in table 3.1.

The play outline represents the maximum extent of petroleum potential in the geographical area as defined by producing reservoirs, hydrocarbon shows, and untested hypotheses. The attractiveness of the Nugget Sandstone thrust belt play (and other thrust belt plays) to the petroleum industry depends on the likelihood of successful development, reserve potential, pipeline access, drilling costs, oil and gas prices, and environmental concerns. When evaluating these criteria, certain aspects of the Nugget play may meet the exploration guidelines of major oil companies while other aspects meet the development guidelines of small, independent companies.

Prospective drilling targets in the Nugget Sandstone thrust belt play are delineated using high-quality two-dimensional (2-D) and three-dimensional (3-D) seismic data, 2-D and 3-D forward modeling/visualization tools, well control, dipmeter information, high-quality surface geologic maps, and detailed analyses of structural geometry (Chidsey, 1999; Meneses-Rocha and Yurewicz, 1999). Incremental restoration of balanced cross sections is one of the best methods to assess trap geometry (Meneses-Rocha and Yurewicz, 1999). Several techniques can be used to determine the timing of structural development, petroleum migration, and entrapment, and to decipher fill and spill histories. These techniques include illite age analysis, apatite fission track analysis; use of fluid inclusions (Meneses-Rocha and Yurewicz, 1999); and surface geochemical surveys.

The Triassic-Jurassic Nugget Sandstone thrust belt play is in the southwest Wyoming and northern Utah thrust belt (figure 3.1). The play area is bounded by truncations of the Nugget against the leading edge of the Absaroka thrust on the east, the Crawford thrust on the west, the North Flank fault of the Uinta uplift on the south, and the Little Muddy Creek transverse ramp on the north where the Nugget is exposed (figures 3.1 and 3.2). The Nugget Sandstone thrust belt play is productive along three principal anticlinal trends, and thus divided into three subplays (figure 3.2): (1) Absaroka thrust–Mesozoic-cored shallow structures, (2) Absaroka thrust–Mesozoic-cored deep structures, and (3) Absaroka thrust–Paleozoic-cored shallow structures (Lamerson, 1982). Each subplay has its own unique structural characteristics, average depth, and type and nature of petroleum. Each requires different engineering and completion techniques. Depths to individual reservoirs are related to their position with respect to (1) the northeast-trending leading edge of the Absaroka thrust and associated imbricate thrusts (fields shallower to the west), and (2) two east-trending transverse ramps (fields deeper in the center, shallower to the north and south). Nugget thickness, lithology, lithofacies, reservoir properties, and diagenetic effects are generally the same for all three subplays.

DEPOSITIONAL ENVIRONMENT

In Early (Pleinsbachian/Toarcian) Jurassic time, Utah had an arid climate and lay 15° north of the equator (Smith and others, 1981). The Nugget Sandstone and age-equivalent rocks, such as the Navajo Sandstone (note: the Navajo is equivalent to the upper part of the Nugget), were deposited in an extensive erg, which extended from present-day Wyoming to Arizona (figure 3.3), and was comparable to the present Sahara desert in North Africa or the Alashan area of the Gobi desert in northern China. Nugget/Navajo dunes were large to small, straight-crested to sinuous, coalescing, transverse barchanoid ridges (Picard, 1975). Regional analyses of the mean dip of dune foreset beds indicate the paleowind direction was dominantly from the north and northwest (figure 3.3) (Kocurek and Dott, 1983; Peterson, 1988). The Nugget/Navajo erg system included interdune playas and oases.

Research on the geochronology of detrital zircon grains in the Nugget/Navajo Sandstone suggests that most of the sand was eroded from the ancestral Appalachian Mountains, transported to the west by a continental-scale river system to the western shore of North America during the Jurassic, and then blown southward into the Nugget/Navajo dune field (Dickinson and Gehrels, 2003, 2010; Rahl and others, 2003; Biek and

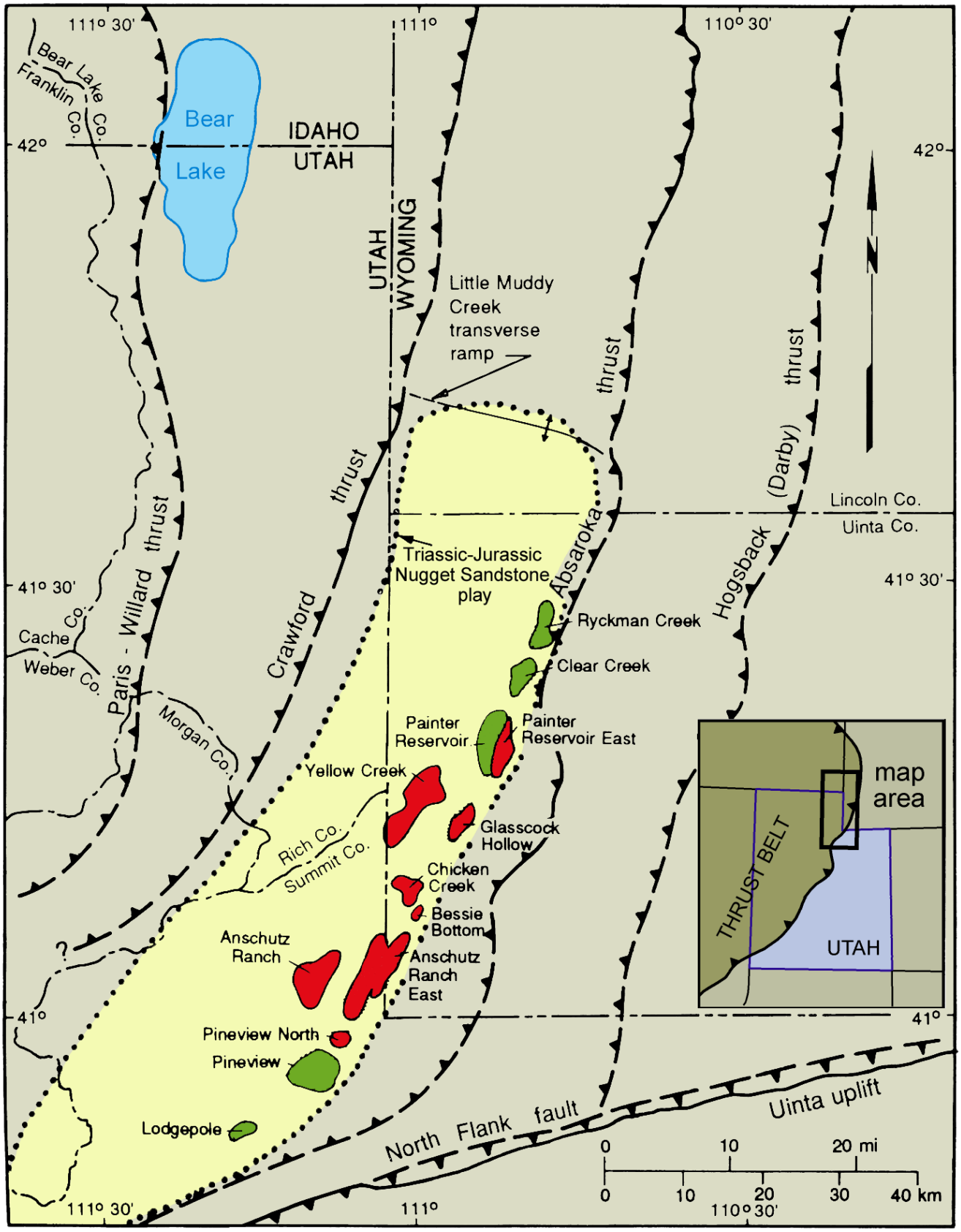

Figure 3.1. *Location of reservoirs that produce oil (green) and gas and condensate (red) from the Triassic-Jurassic Nugget Sandstone, Utah and Wyoming; major thrust faults are dashed where approximate (teeth indicate hanging wall). The Nugget Sandstone thrust belt play area is dotted. Modified from Chidsey (1993).*

Table 3.1. *Geologic, reservoir, and production data for fields in the Triassic-Jurassic Nugget Sandstone thrust belt play. Data compiled from Loucks (1975), Maher (1976), Conner and Covlin (1977), Kelly and Hine (1977), Blazzard (1979a, 1979b), Jones (1979), Moklestad (1979), Lamb (1980), Petroleum Information (1981, 1984b), Frank and Gavlin (1981), Bergosh and others (1982), Frank and others (1982), Lelek (1982), Lindquist (1983, 1988), Sercombe (1989), Tillman (1989), White and others (1990), Chase and others (1992a, 1992b), Holm (1992), Mullen (1992a, 1992b), Powers (1992), Benson (1993a), Cook and Dunleavy (1996), Chidsey (1993), Lindquist and Ross (1993), Utah Division of Oil, Gas, and Mining (2016a, and well records), and Wyoming Oil and Gas Conservation Commission (2016).*

State	County	Field	Discovery Date	Active Producers	Abandoned Producers	Acres	Spacing (acres)	Pay (feet)	Porosity (%)	Perm. (mD)	Temp. (°F)	Initial Reservoir Pressure (psi)	Average Monthly Production		Cumulative Production	
													Oil (bbl)	Gas (MCF)	Oil (bbl)	Gas (BCF)
Utah	Summit	Pineview	1975	6	8	2180	80	135	11	50	200	4200	9568	19,183	16,214,752	22.1
Utah	Summit	Pineview North	1982	2	2	1200	80	400	12	1.3	205	2000	440	5329	875,095	10.1
Utah	Summit	Lodgepole	1976	0	2	640	160	43	10	229	188	4474	0	0	338,415	0.2
Utah	Summit	Anschutz Ranch	1979	2	2	1680	160	300	11	16	146	2915	236	23,768	535,775	30.5
Utah/ Wyoming	Summit/ Uinta	Anschutz Ranch East	1979	40	19	4500	80	W-300 E-501	W-10.1 E-9	W-3 E-2	W-215 E-230	W-5310 E-5902	2010	283,386*	130,846,117	3034.6*
Wyoming	Uinta	Ryckman Creek	1976	30	5	1200	40	22	15	34	129	2900	0	0	18,970,638	266.7
Wyoming	Uinta	Clear Creek	1979	14	0	1200	80	30	13	5.4	138	3443	760	0	5,941,959	142.3
Wyoming	Uinta	Painter Reservoir	1977	42	1	1666	40	450	12	7.1	164	4020	327	349,131	38,358,174	795.8
Wyoming	Uinta	East Painter Reservoir	1987	30	0	1200	80	900	12	5.4	170	NA	27,006	4,632,824	75,522,799	1617.8
Wyoming	Uinta	Yellow Creek	1976	1	1	480	160	300	NA	NA	117	NA	0	0	62,867	0.2
Wyoming	Uinta	Glasscock Hollow	1980	4	2	915	none	110	11	65	220	5620	642	14,312	3,025,805	24.2
Wyoming	Uinta	Chicken Creek	1983	3	2	430	160	200	11	NA	219	6021	468	112	1,044,386	6.3
Wyoming	Uinta	Bessie Bottom	1983	1	0	160	160	170	8.5	0.6	242	6227	39	0	208,534	1.8

NA = Not Available

For Anshcutz Ranch East field, W = West Lobe and E = East Lobe

*Includes cycled gas

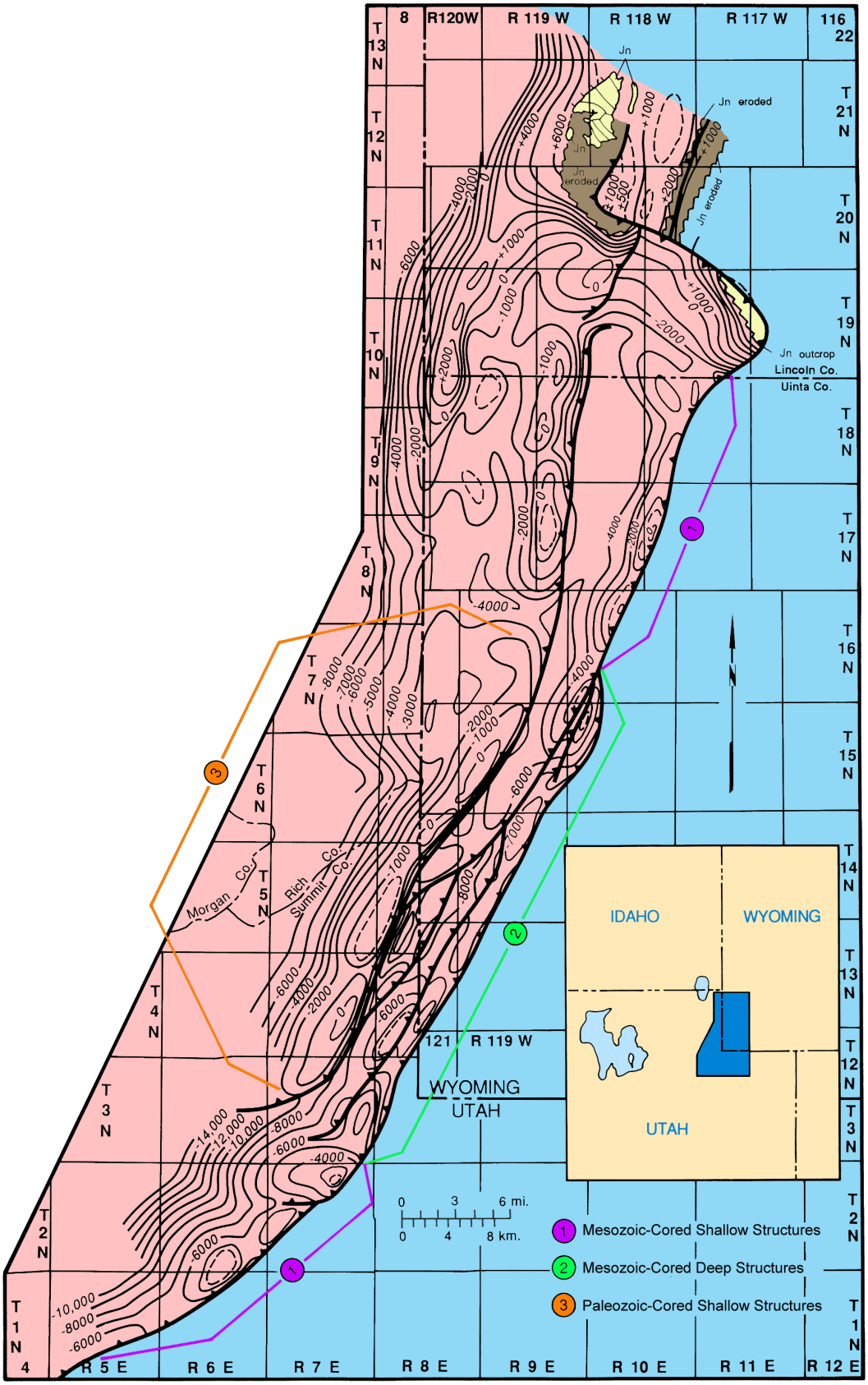

Figure 3.2. *Generalized structure contour map of the top of the Triassic-Jurassic Nugget Sandstone on the southern Absaroka thrust plate, Utah-Wyoming thrust belt. The three principal anticlinal trends, which define the subplays, are indicated based on their location with respect to the leading edge of the Absaroka thrust, the presence of imbricate thrusts which separate the trends, and the depth to the Nugget. Datum mean sea level, contour interval 1000 feet, dashed where approximate. Modified from Lamerson (1982).*

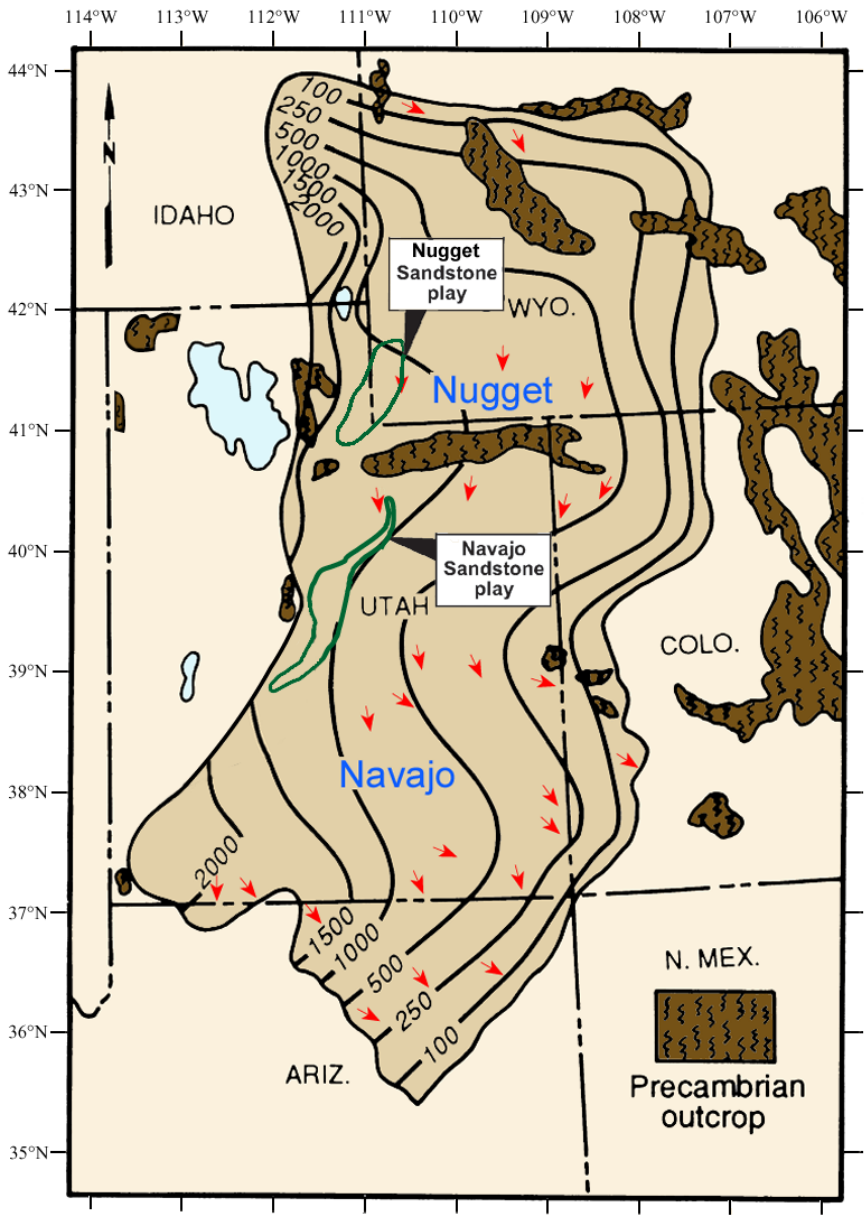

Figure 3.3. *Regional isopach map of the Nugget/Navajo Sandstone based on measured sections and well data. Paleowind, generally from the north and northwest, is shown by arrows. Contours are in feet. Modified from Picard (1975), Kocurek and Dott (1983).*

others, 2010). The massive thickness of Nugget/Navajo sand was preserved because of basin subsidence associated with Early Jurassic compressional deformation near the west margin of North America (Allen and others, 2000; Biek and others, 2010). This deformation caused the continental interior to flex downward, creating accommodation space for sand and other sedimentary accumulations (Biek and others, 2010).

STRATIGRAPHY AND THICKNESS

The Nugget Sandstone is typically 1100 feet (340 m) thick in the play area (Hintze and Kowallis, 2009) and has a characteristic geophysical log response (figure 3.4). Lindquist (1988) identified lower, middle, and upper units in the Nugget from core and geophysical log analysis of wells in Anschutz Ranch East field (figures 3.1 and 3.5). Each unit has a subtle but distinct characteristic geophysical log response.

In outcrops and wells of the southwest Wyoming and northern Utah thrust belt, the Upper Triassic–Lower Jurassic Wingate and Lower Jurassic Kayenta Formations of the Glen Canyon Group are not present. Thus, the Nugget Sandstone is used for the equivalent Triassic-Jurassic section which is dominated by eolian sandstone (Sprinkel and others, 2011). The Nugget Sandstone is overlain by the Middle Jurassic Twin Creek Limestone and underlain by the Triassic Ankareh Formation (figure 3.4). Average depth to the Nugget for all the thrust belt fields is 10,630 feet (3240 m).

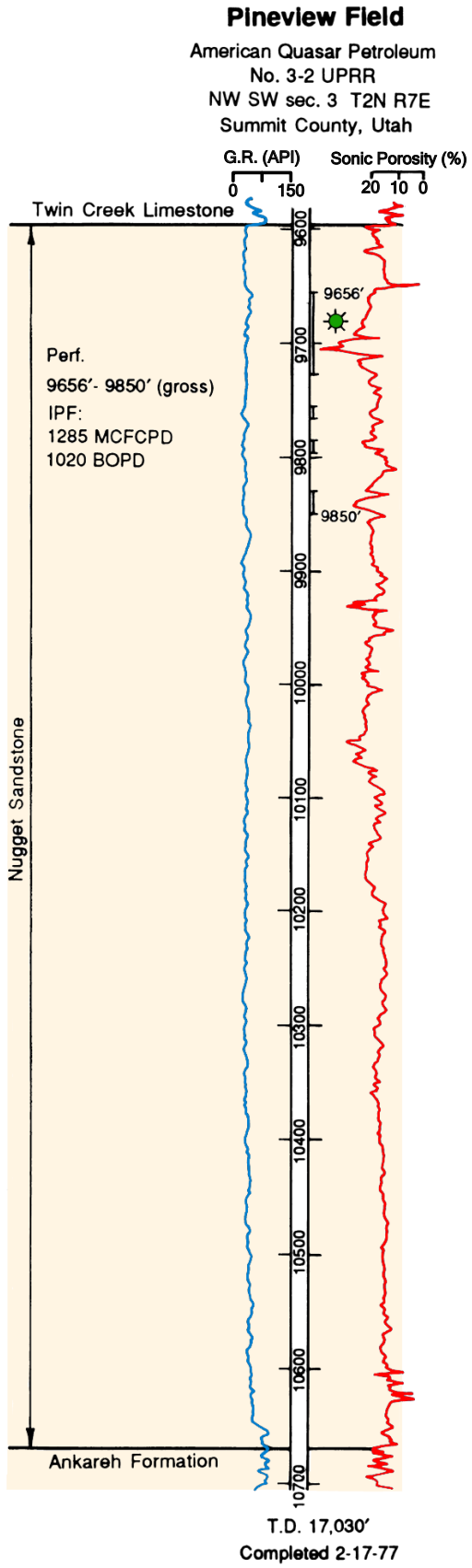

Figure 3.4. *Typical gamma ray-sonic log of the Nugget Sandstone. Example from a development well in the Pineview field, Summit County, Utah. The vertical lines between depths of 9656 and 9850 feet on the log indicate producing (perforated) intervals.*

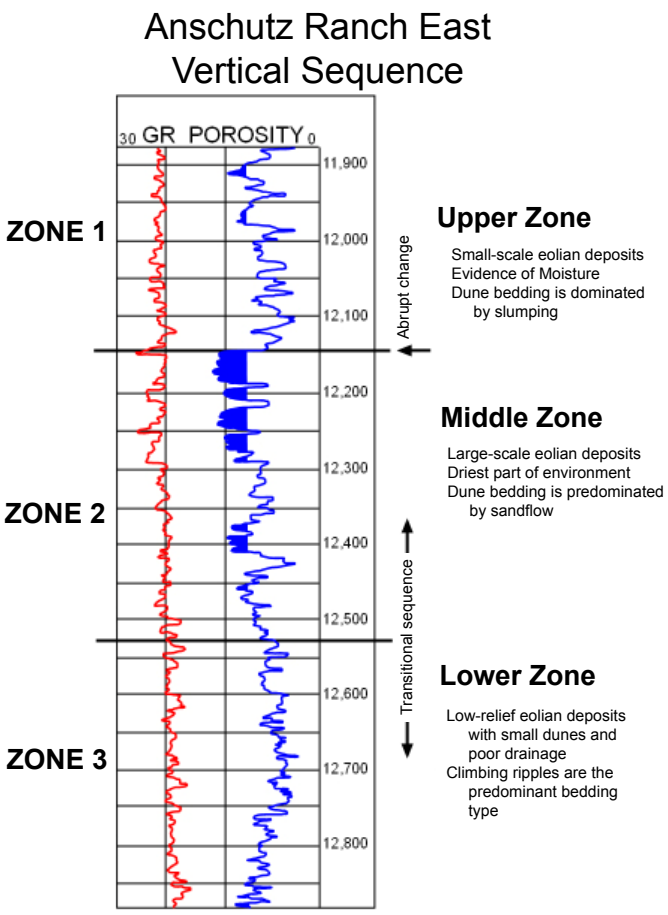

Figure 3.5. *Reservoir quality of the Nugget Sandstone based on porosity and gamma ray characteristics, ARE No. W29-12 well (section 29, T. 4 N., R. 8 E., SLBL&M), Anschutz Ranch East field, Summit County, Utah. Modified from White and others (1990), Keele and Evans (2008).*

LITHOLOGY AND FRACTURING

The lower Nugget Sandstone is composed of (1) a basal, thin-bedded unit about 140 feet (47 m) thick, characterized by horizontal stratification and ripple marks, and (2) an overlying 220-foot-thick (67 m) section dominated by climbing ripple laminae and small-scale cross-beds (Picard, 1975; Lindquist, 1988). The middle and upper units consist of a cyclic dune/interdune sequence (the principal petroleum-bearing section) more than 740 feet (250 m) thick, characterized by cross-stratification (figure 3.6). The middle unit is dominated by large-scale, planar or wedge-planar cross-beds (up to 35°) (Conner and Covlin, 1977), and is about 390 feet thick (130 m). The upper unit is dominated by wind ripples and small-scale cross-beds and is about 350 feet thick (115 m). The boundary between the lower and middle units is transitional but is abrupt between the middle and upper units (figure 3.5) (Lindquist, 1988).

The dune/interdune sequence generally consists of fine- to coarse-grained, subangular to subrounded sand or silt grains cemented by calcite (Picard, 1975). Dune deposits consist al-

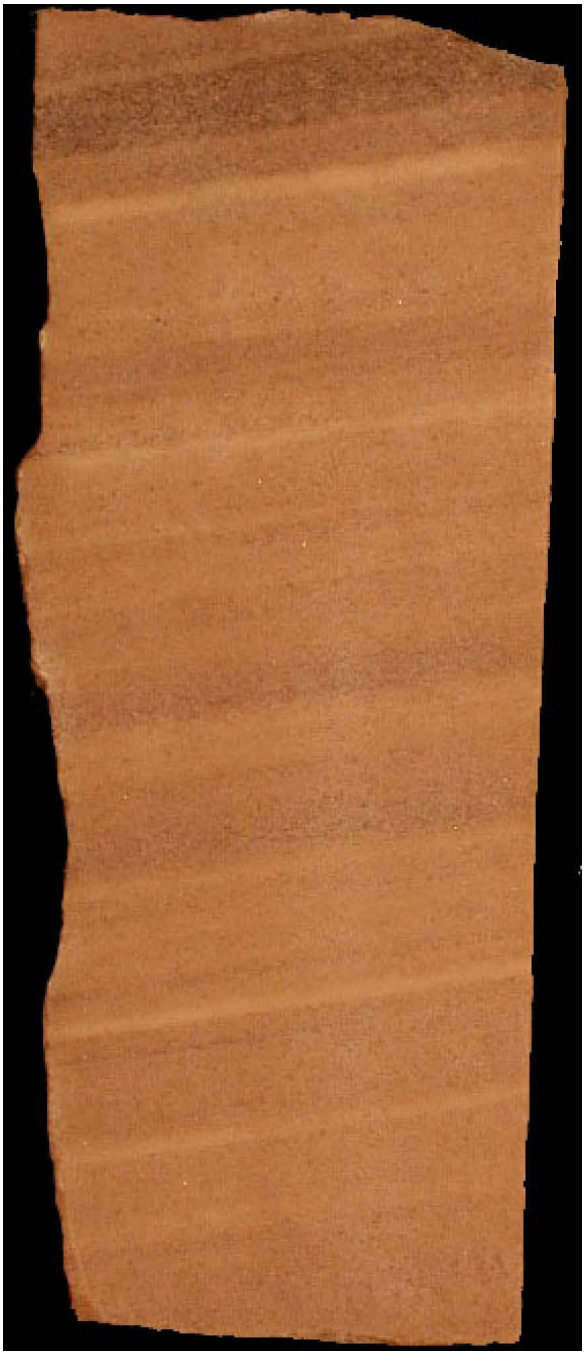

Figure 3.6. *Typical Nugget Sandstone, from the Champlin No. 1 McDonald 31-3 well (section 3, T. 2 N., R. 7 E., SLBL&M, slabbed core from 9872 feet), Pineview field (figure 3.1), showing cross-bedding in fine-grained sandstone deposited in a dune environment.*

most entirely of sandstone, whereas interdune deposits consist of both sandstone and siltstone with some carbonate and evaporite lithologies. Dune lithofacies from the brink to the toe of the dune slipface consist of (1) thin, graded, tabular grainfall laminae (rarely preserved), (2) thick, subgraded avalanche laminae, and (3) thin, tightly packed, reworked ripple strata at the dune toe (Lindquist, 1983). Interdune lithofacies consist of fine-grained, thin, low-angle to horizontal laminae with zones of bioturbation (Lindquist, 1983).

Framework and matrix grains in sandstone (>1/16 mm and <1/16 mm, respectively) and siltstone (1/16 to 1/256 mm and <1/256 mm, respectively) are commonly composed of more than 90% quartz (usually frosted) with varying amounts of K-feldspar, plagioclase, and rock fragments (figure 3.7A). The typical sandstone contains 11% authigenic cement and 2% matrix grains; the typical siltstone contains 18% authigenic cement and 11% matrix grains (figure 3.7B) (Picard, 1975).

Fractures in the Nugget Sandstone consist of two types: (1) early, gouge-filled, silica cemented, impermeable fractures (figure 3.8), and (2) later, typically open (little gouge or cement), permeable fractures (Conner and Covlin, 1977). The later fractures are related to fault-propagation folding during the Sevier orogeny after deep burial (Royce and others, 1975; Conner and Covlin, 1977; Dixon, 1982; Lamerson, 1982).

HYDROCARBON SOURCE AND SEALS

Hydrocarbons in Nugget Sandstone reservoirs were generated from subthrust Cretaceous source rocks (Warner, 1982). These rocks include organic-rich units in the Bear River, Aspen (Mowry equivalent [Nixon, 1973]), and Frontier Formations. The source rocks began to mature after being overridden by thrust plates. Hydrocarbons were then generated, expelled, and subsequently migrated, primarily along fault planes, into overlying traps during the last 55 million years (Warner, 1982). Many structures in the hanging wall have juxtaposed the Nugget directly over these source rocks. Fracture systems developed along thrust imbrications may have provided secondary migration routes (Lamerson, 1982).

Burtner and Warner (1984) evaluated the hydrocarbon generation from the Mowry Shale in the Green River Basin (overridden in the western part by the thrust belt) and other northern Rocky Mountain basins. Their study showed that the Mowry ranges from 0.7 to 4.1 weight percent total organic content (TOC) and contains a mixture of type II (marine) and type III (terrestrial) organic matter. In the Green River Basin, Mowry areas having T_{max} values (the temperature during pyrolysis of peak hydrocarbon generation) greater than 435°C coincide with areas anomalously low in TOC, indicating that hydrocarbons and CO_2 were generated and subsequently migrated out of the source beds (Burtner and Warner, 1984).

The seals for the Nugget producing zones are the overlying argillaceous and gypsiferous beds of the Gypsum Spring Member of the Jurassic Twin Creek Limestone, or a 10- to 60-foot-thick (3–30 m), low-permeability zone on top of the Nugget Sandstone. Hydrocarbons in the Nugget/Twin Creek system are further sealed by salt beds within the overlying Jurassic Preuss Formation.

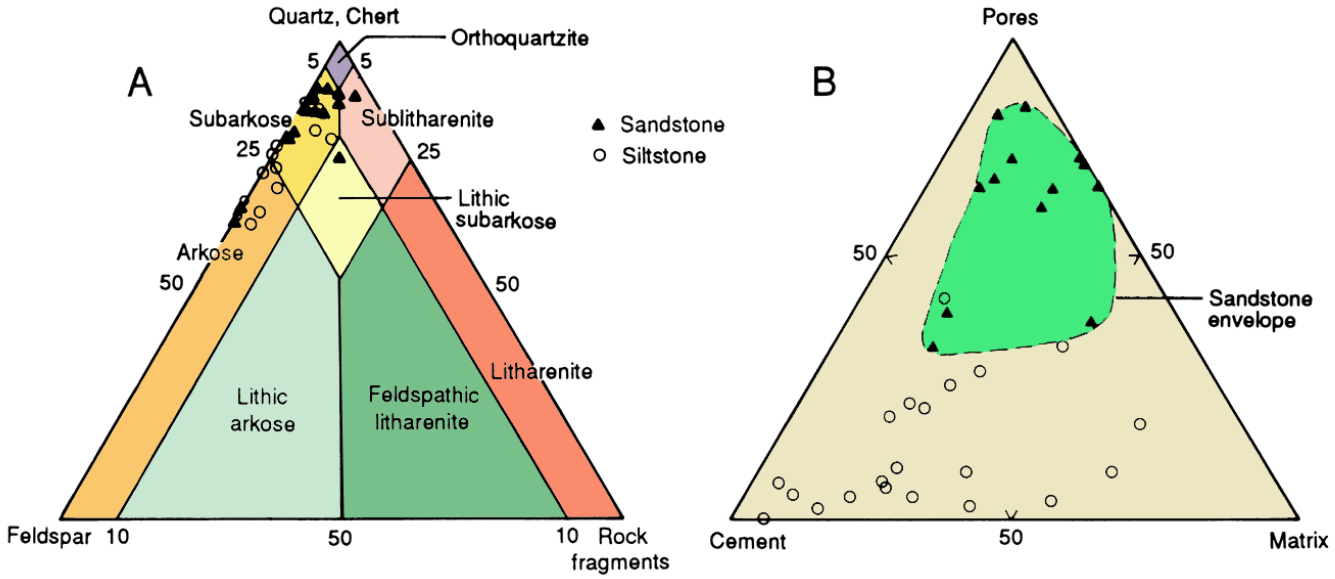

Figure 3.7. *Trilinear plots of (A) quartz, feldspar, and rock fragments and (B) pores, cement, and matrix of sandstone and siltstone in the Nugget Sandstone. Matrix grains are <1/16 mm for sandstone and <1/256 mm for siltstone. After Picard (1975).*

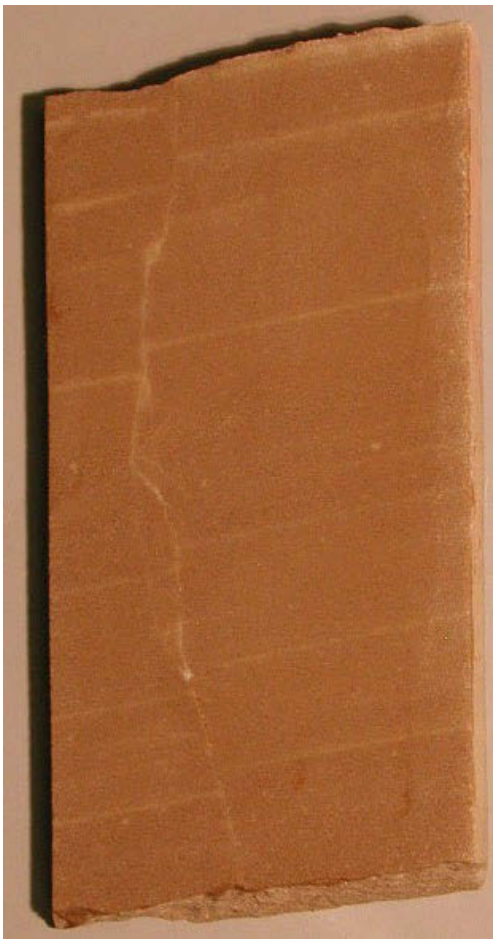

Figure 3.8. *Early, gouge-filled and cemented fractures, with slight offsets, in the Nugget Sandstone, from the Champlin No. 1 McDonald 31-3 well (section 3, T. 2 N., R. 7 E., SLBL&M, slabbed core from 9898.5 feet), Pineview field (figure 3.1).*

STRUCTURE AND TRAPPING MECHANISMS

Absaroka Thrust–Mesozoic-Cored Shallow Structures Subplay

The Nugget Sandstone Absaroka thrust–Mesozoic-cored shallow structures subplay is located in the western part of Summit County, Utah, and Uinta County, Wyoming (figure 3.9). The subplay represents a linear, hanging-wall, Mesozoic-cored, ramp anticline parallel to the leading edge of the Absaroka thrust (figure 3.10). Average depth to the Nugget in the shallow subplay is 9300 feet (3100 m). Two broad structural highs (culminations), separated by a structural low (depression), are present along the ramp anticline (Lamerson, 1982; Chidsey, 1993) where individual traps are formed by closure on subsidiary anticlines (figure 3.2). These culminations may be due to proximity to transverse ramp features. The north culmination is related to the Little Muddy Creek transverse ramp along the north border of the Nugget play area and contains Painter Reservoir (figure 3.11), Clear Creek, and Ryckman Creek fields (figures 3.1 and 3.9). The south culmination is related to a transverse ramp associated with the Uinta uplift along the south border of the play area and contains Pineview and Lodgepole fields (figures 3.1 and 3.9). The eastern boundary of the subplay is defined by the truncation of the Nugget against the leading edge of the Absaroka thrust. The western boundary is defined by a branch line representing the intersection of the thrust planes of the Absaroka thrust and a large imbricate thrust (Boyer and Elliott, 1982). The southern part of the Absaroka thrust plate trends southwest toward the Wasatch Range where the Nugget Sandstone play area terminates. The subplay is mapped as two 5-mile-wide (8 km) bands (figure 3.9).

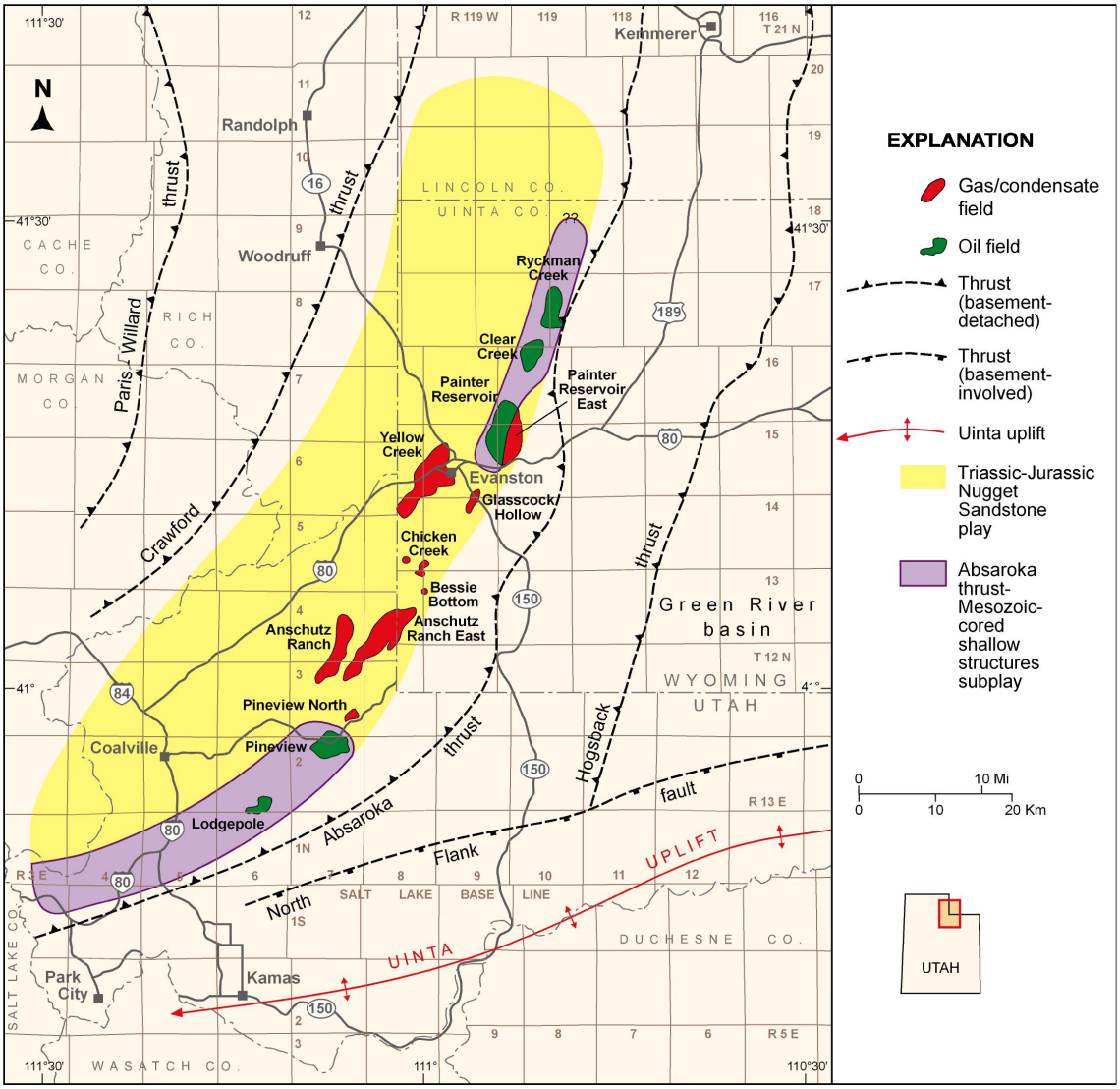

Figure 3.9. *Location of the Nugget Sandstone Absaroka thrust–Mesozoic-cored shallow structures subplay, Summit County, Utah, and Uinta County, Wyoming. Northern extent of the subplay is unknown.*

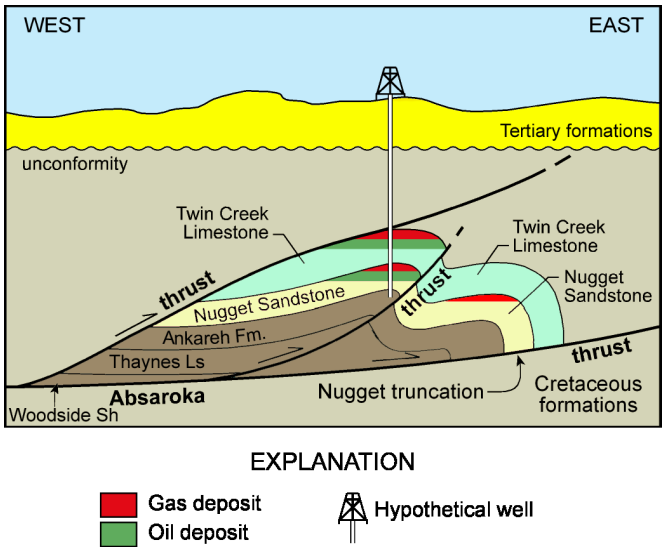

Figure 3.10. *Schematic cross section of traps in the Nugget Sandstone Absaroka thrust–Mesozoic-cored shallow and deep structures subplays.*

Potential petroleum-trapping mechanisms in the Nugget Sandstone Absaroka thrust–Mesozoic-cored shallow structures subplay consist of long, narrow, doubly plunging anticlines (figure 3.12) (Royce and others, 1975; Conner and Covlin, 1977; Dixon, 1982; Lamerson, 1982). These anticlines are asymmetric and overturned to the east along the leading edge of the Absaroka thrust (West and Lewis, 1982). Pineview field, Summit County, Utah, exemplifies the traps in the subplay (figures 3.9, 3.12, and 3.13). The Nugget reservoir covers approximately 1280 acres (572 ha) and has more than 1000 feet (300 m) of structural closure.

Absaroka Thrust–Mesozoic-Cored Deep Structures Subplay

The Nugget Sandstone Absaroka thrust–Mesozoic-cored deep structures subplay is also located in the western part of Summit County, Utah, and Uinta County, Wyoming (figure 3.14). The subplay represents a linear, Mesozoic-cored ramp

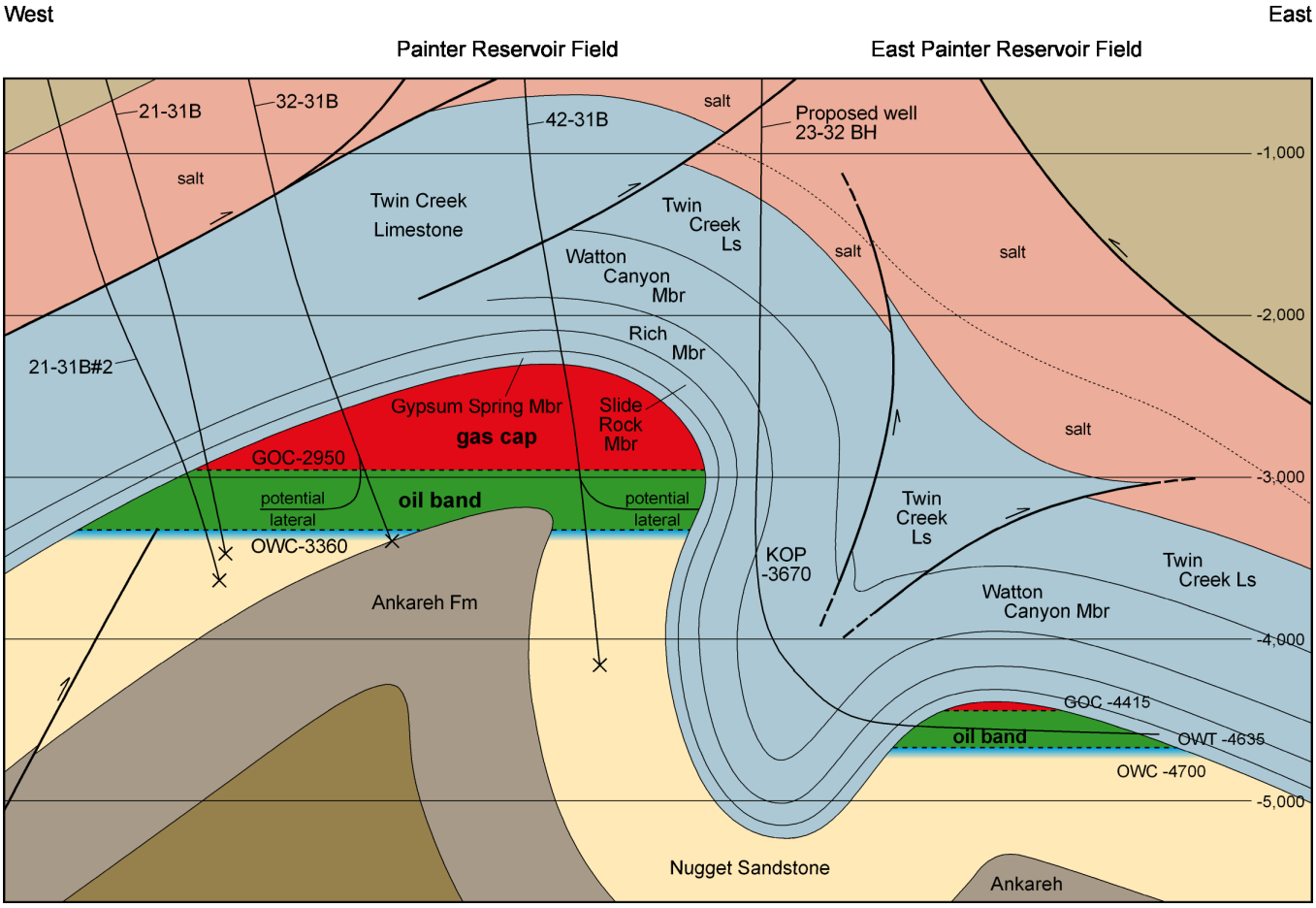

Figure 3.11. *East-west structural cross section through the Painter Reservoir and East Painter Reservoir fields, Uinta County, Wyoming, showing typical traps for Nugget Sandstone fields. The cross section also shows the geometry of the structure in the shallow (Painter Reservoir) and deep (Painter Reservoir East) Absaroka thrust–Mesozoic-cored structures subplays. Depth in feet, datum = mean sea level. Modified from Wyoming Oil and Gas Conservation Commission (1998).*

anticline developed in the structural depression between the north and south culminations of the shallow structures subplay and along the truncation of the Nugget against the Absaroka thrust (figures 3.2 and 3.10) (Lamerson, 1982). The Mesozoic-cored shallow and deep structures subplays are also separated by imbricate thrusts along strike, and backlimb thrust faults are present locally. Average depth to the Nugget in the deep subplay is 12,800 feet (3900 m). Discrete anticlinal closures form Pineview North, Anschutz Ranch East, Bessie Bottom, Chicken Creek, Glasscock Hollow, and Painter Reservoir East fields (figures 3.1 and 3.14). The subplay extends north as a 5-mile-wide (8 km) band into Uinta County, Wyoming (figure 3.14).

Similar to the Absaroka thrust–Mesozoic-cored shallow structures subplay, potential petroleum-trapping mechanisms in the Nugget Sandstone Absaroka thrust–Mesozoic-cored deep structures subplay also consist of long, narrow, doubly plunging anticlines (figures 3.15 and 3.16) (Royce and others, 1975; Conner and Covlin, 1977; Dixon, 1982; Lamerson, 1982). These anticlines are asymmetric and overturned to the east as well. Splay faults and salt near the anticlinal axes are common, complicating drilling operations and compartmentalizing productive zones (figure 3.16).

Anschutz Ranch East field is an excellent example of Mesozoic-cored deep structures (figure 3.1). The field is the largest in the subplay in terms of hydrocarbon column thickness, cumulative production and reserves, and areal extent (figures 3.15 and 3.16). The reservoir covers approximately 4620 acres (1870 ha) and is divided into two structural lobes. The larger west lobe is a narrow, elongate anticline overturned to the east (Lelek, 1982). Average depth to the Nugget Sandstone in the west lobe is 12,900 feet (4300 m) and the lobe has more than 2100 feet (700 m) of closure. When the west lobe reservoir was discovered in 1979, the hydrocarbon column was near the spill point. The smaller east lobe has the same general configuration as the west lobe and is separated from it by an overturned syncline (Lelek, 1982). Average depth to the Nugget Sandstone in the east lobe is 14,325 feet (4775 m) and the lobe has more than 1000 feet (330 m) of closure. When the east lobe reservoir was discovered in 1981, the hydrocarbon column was also near the spill point (Petroleum Information, 1984b).

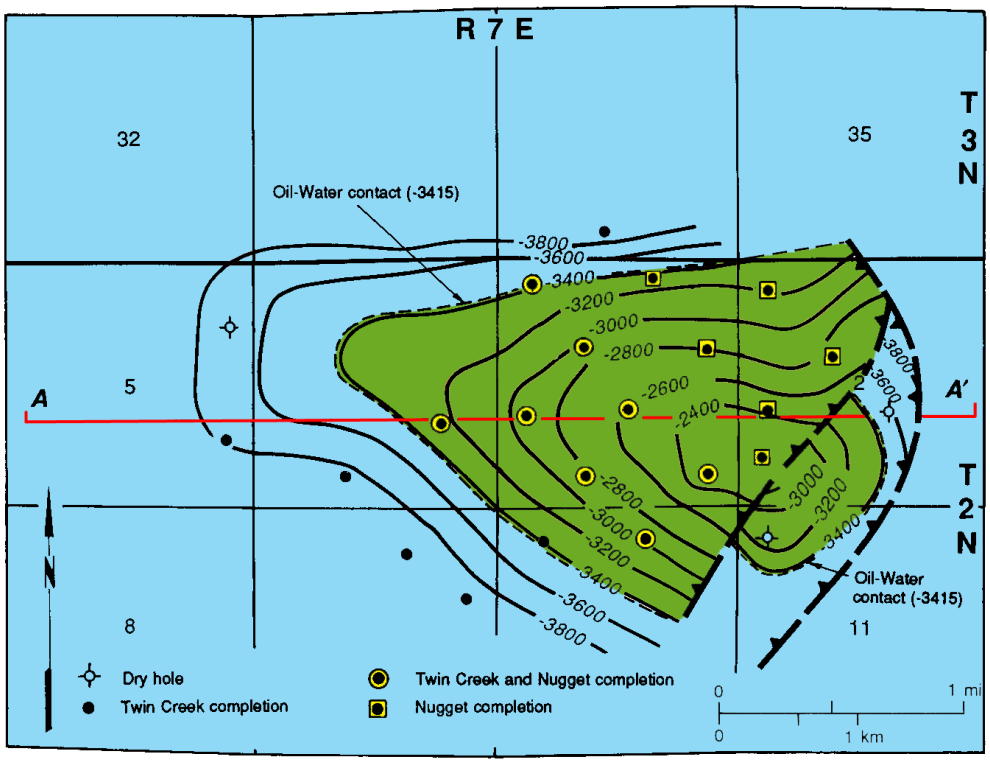

Figure 3.12. *Structure contour map of the top of the Nugget Sandstone, Pineview field, Summit County, Utah, typical of the geometry of Mesozoic-cored shallow structures on the southern culmination, Triassic-Jurassic Nugget Sandstone and Jurassic Twin Creek Limestone thrust belt plays. Oil is trapped in an asymmetrical thrusted anticline in the hanging wall of the Absaroka thrust system. Contour interval = 200 feet, datum = mean sea level. After Utah Division of Oil, Gas, and Mining (1978). Cross section A–A′ shown on figure 3.13.*

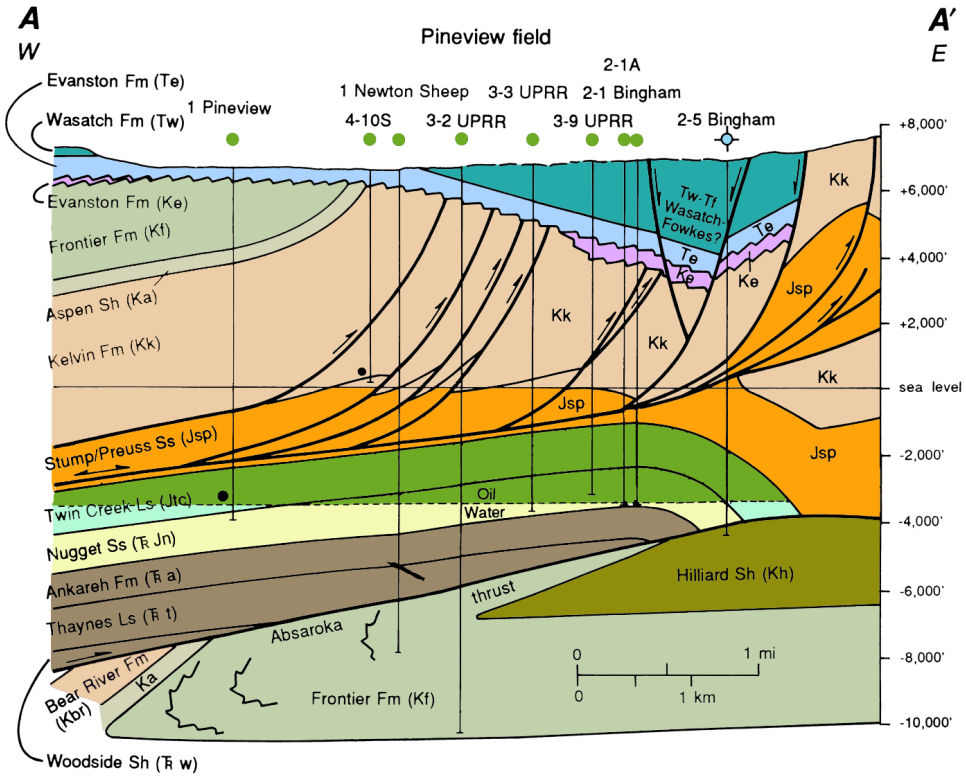

Figure 3.13. *East-west cross section through the Pineview structure. Line of section shown on figure 3.12. Note that the field also produces oil from the Jurassic Twin Creek Limestone that has a common oil/water contact with the Nugget. Reservoir zones are juxtaposed against Cretaceous source rocks in the subthrust along the east flank of the structure. After Lamerson (1982).*

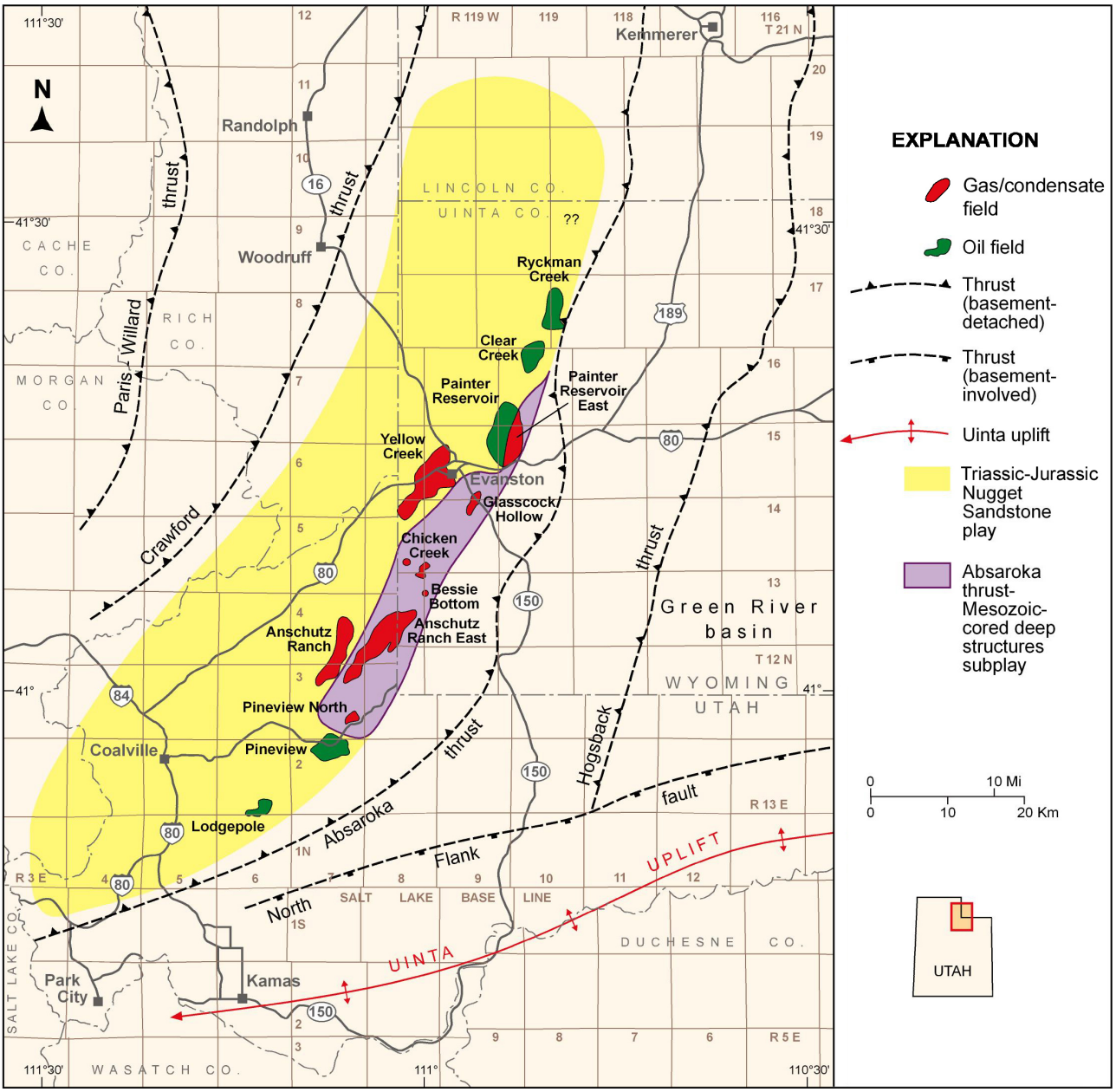

Figure 3.14. *Location of the Nugget Sandstone Absaroka thrust–Mesozoic-cored deep structures subplay, Summit County, Utah, and Uinta County, Wyoming. Northern extent of the subplay is unknown.*

Absaroka Thrust–Paleozoic-Cored Shallow Structures Subplay

The Nugget Sandstone Absaroka thrust–Paleozoic-cored shallow structures subplay is located immediately west of the Mesozoic-cored structures subplays (figure 3.17). The subplay represents a very continuous and linear, hanging-wall, Paleozoic-cored, ramp anticline parallel to the leading edge of the Absaroka thrust (figure 3.18). The eastern boundary of the subplay is defined by the truncation of the Nugget against a thrust splay. The western boundary is defined as the point at which the dips of bedding in the Nugget on the west flank of the ramp anticline begins to flatten out. The southern part of this ramp anticline trends southwest toward the Wasatch Range where the Nugget Sandstone play area terminates. The play extends north as a 3-mile-wide (4.8 km) band through Summit County, Utah, and into western Uinta County, Wyoming (figure 3.17).

Potential petroleum-trapping mechanisms in the Nugget Sandstone Absaroka thrust–Paleozoic-cored shallow structures subplay also consist of long, narrow, doubly plunging anticlines that trend north to northeast (figures 3.19 and 3.20) (Royce and others, 1975; Conner and Covlin, 1977; Petroleum Information, 1981; Dixon, 1982; Lamerson, 1982). These anticlines are also asymmetric and overturned to the east. Two fields exist in the Nugget Sandstone Absaroka thrust–Paleozoic-cored shallow structures subplay: Anschutz Ranch in Summit County, Utah, and Yellow Creek in Uinta County, Wyoming (figure

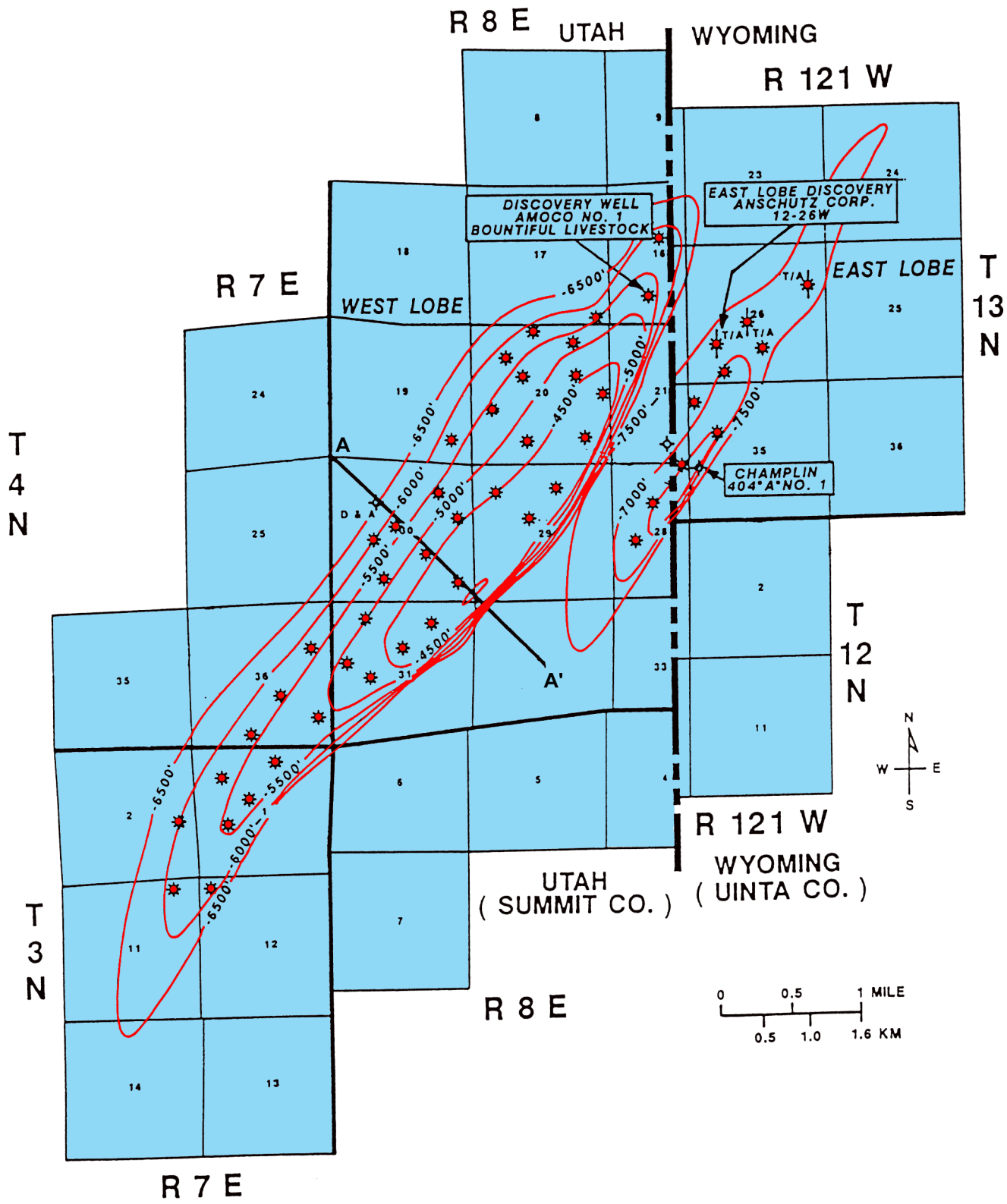

Figure 3.15. *Structure contour map of the top of the Nugget Sandstone, Anschutz Ranch East field, Summit County, Utah, and Uinta County, Wyoming, typical of the geometry of Mesozoic-cored deep structures, Triassic-Jurassic Nugget Sandstone thrust belt play. Retrograde condensate and gas are trapped in east and west lobes of a large northeast-southwest-trending, thrusted anticline in the hanging wall of the Absaroka thrust system. Contour interval = 500 feet, datum = mean sea level. After Lelek (1982). Cross section A–A' shown on figure 3.16.*

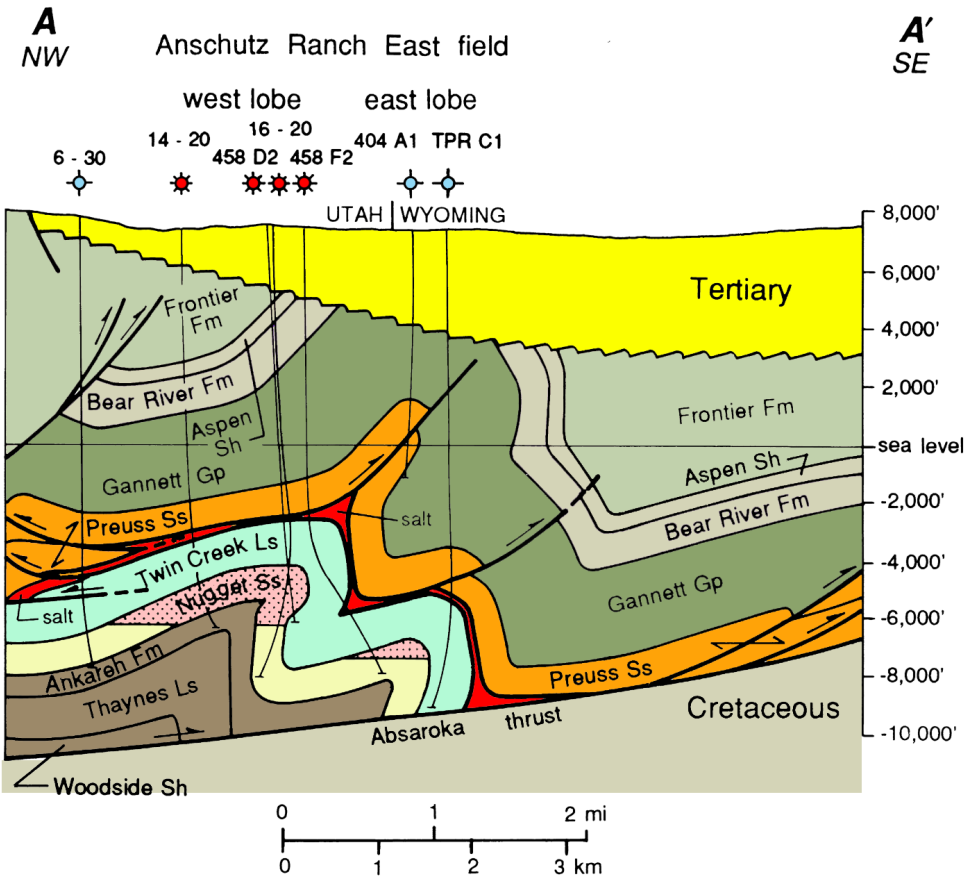

Figure 3.16. *Northwest-southeast cross section through the Anschutz Ranch East structure showing the large west lobe and the deeper, smaller east lobe (base of pink stippled area represents the gas-water contact). Line of section shown on figure 3.15. After West and Lewis (1982).*

3.17). Anschutz Ranch field consists of a large, elongate anticline that has more than 7100 feet (2164 m) of structural closure involving Upper Triassic through Ordovician rocks; the reservoir covers approximately 2880 acres (1170 ha). However, hydrocarbons are trapped only on the very crest of the structure, as is the case at Yellow Creek field.

RESERVOIR PROPERTIES

The Nugget Sandstone has heterogeneous reservoir properties because of (1) cyclic dune/interdune lithofacies with better porosity and permeability that developed in certain dune morphologies, (2) diagenetic effects, and (3) fracturing. The typical sandstone has an average porosity of 14%; the typical siltstone has an average porosity of 7% (figure 3.7B; Picard, 1975). They exhibit significant secondary porosity in the form of fracturing. Permeabilities in the Nugget range from 1 to more than 200 mD. The best permeability within Nugget dune deposits is along bounding surfaces (bedding planes); preferred directions are along the dip and strike of the individual slipfaces (cross-beds) (figure 3.21A; Lindquist, 1983). Porosity and permeability are greatest in thickly laminated avalanche deposits (Hunter, 1977; Schenk, 1981). Nugget interdunes, however, have significantly poorer reservoir characteristics than the dune lithofacies (figure 3.21B). In Painter Reservoir, for example, the average porosity and permeability is only 9.7% and 1.5 mD, respectively, in interdune lithofacies, but 13.6% and 16.5 mD in dune lithofacies (Tillman, 1989). The low-permeability interdune lithofacies is a potential barrier to flow (figure 3.21B). Identification and correlation of dune/interdune lithofacies in individual Nugget reservoirs are critical to understanding the effects on production rates and paths of petroleum movement. Natural fractures also affect permeability and control hydrocarbon production and injection fluid-pathways (Parra and Collier, 2000).

Diagenetic effects and fracturing have both reduced and enhanced the reservoir permeability of the Nugget Sandstone. Overgrowths of quartz and feldspar, authigenic clay mineralization (illite and chlorite), ferroan dolomitization, emplacement of asphaltenes, and the development of gouge and calcite-filled fractures locally have reduced reservoir permeability (Lindquist, 1983). Dissolution of silicate minerals and the development of open fractures have increased reservoir permeability (Lindquist, 1983).

Nugget net-pay thickness is variable, depending on fracturing, and ranges from 22 to 900 feet (7–300 m). The average Nugget reservoir temperature is 185°F (85°C). Water saturations

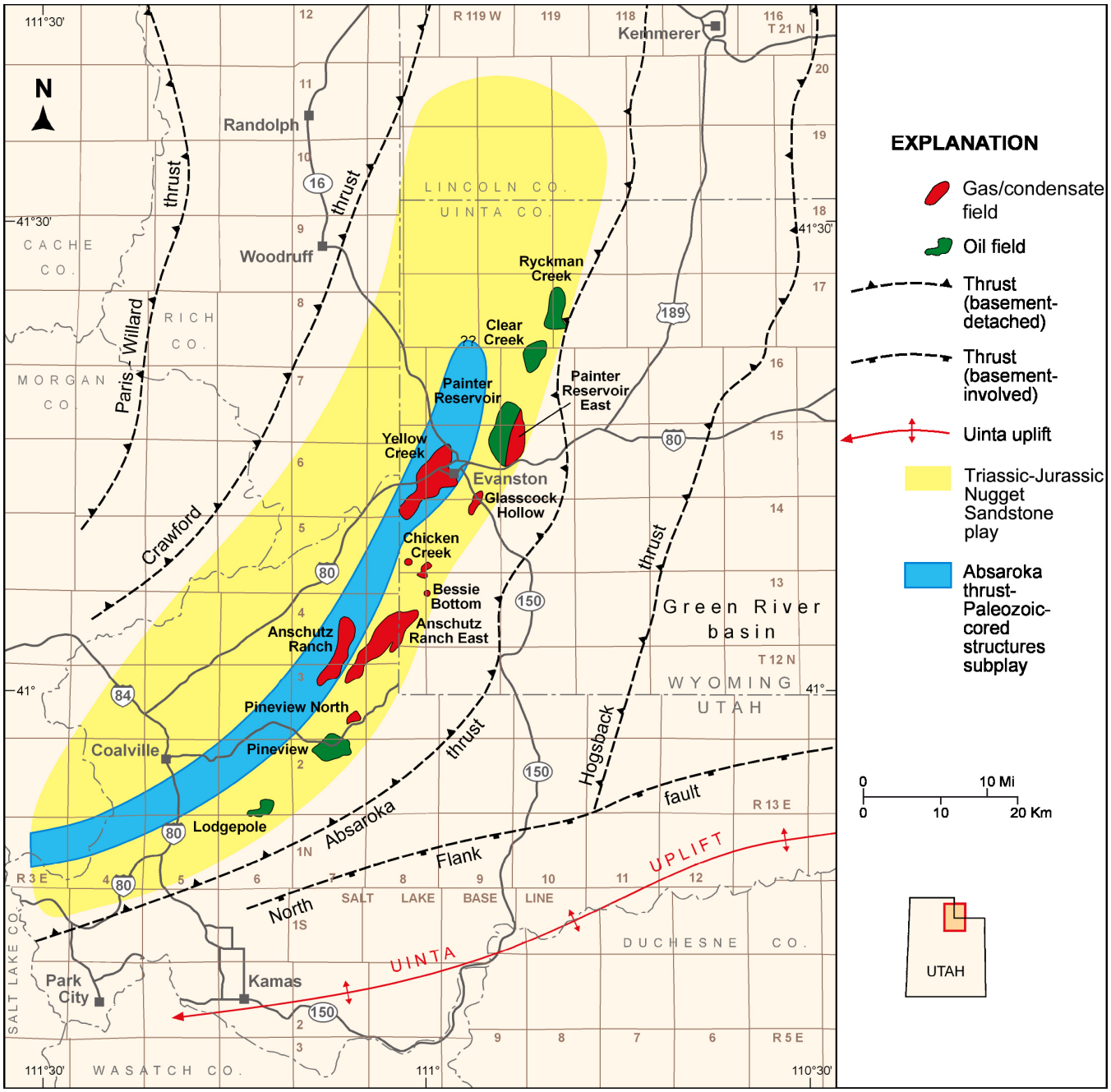

Figure 3.17. *Location of the Nugget Sandstone Absaroka thrust–Paleozoic-cored shallow structures subplay, Summit County, Utah, and Uinta County, Wyoming. Northern extent of the subplay is unknown.*

range from 22 to 45%, and average resistivity (R_w) is 0.284 ohm-m at 68°F (20°C). Initial reservoir pressures average about 3900 pounds per square inch (psi [26,890 kPa]). The reservoir drive mechanisms include pressure depletion, active water drive, and solution gas.

Reservoir data for individual fields in the Triassic-Jurassic Nugget Sandstone thrust belt play are summarized in table 3.1. For details see Loucks (1975), Maher (1976), Conner and Covlin (1977), Blazzard (1979a, 1979b), Kelly and Hine (1977), Jones (1979), Moklestad (1979), Lamb (1980), Petroleum Information (1981, 1984b), Frank and Gavlin (1981), Bergosh and others (1982), Frank and others (1982), Lelek (1982), Lindquist (1983, 1988), Sercombe (1989), White and others (1990), Chase and others (1992a, 1992b), Holm (1992), Mullen (1992a, 1992b), Powers (1992), Benson (1993a), Cook and Dunleavy (1996), Chidsey (1993), and Lindquist and Ross (1993).

OIL AND GAS CHARACTERISTICS

In major reservoirs, the produced Nugget oil and retrograde condensate are rich, volatile crudes. The API gravity of the oil

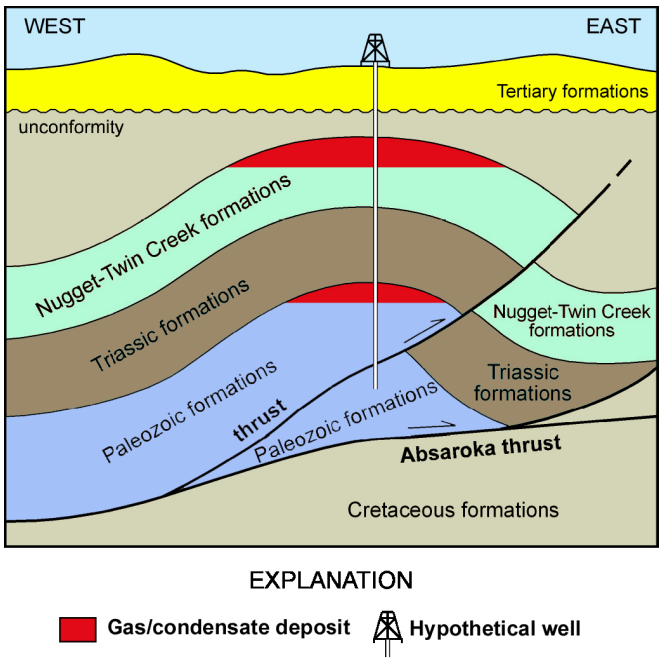

Figure 3.18. *Schematic cross section of traps in the Nugget Sandstone and Twin Creek Limestone Absaroka thrust–Paleozoic-cored shallow structures subplays.*

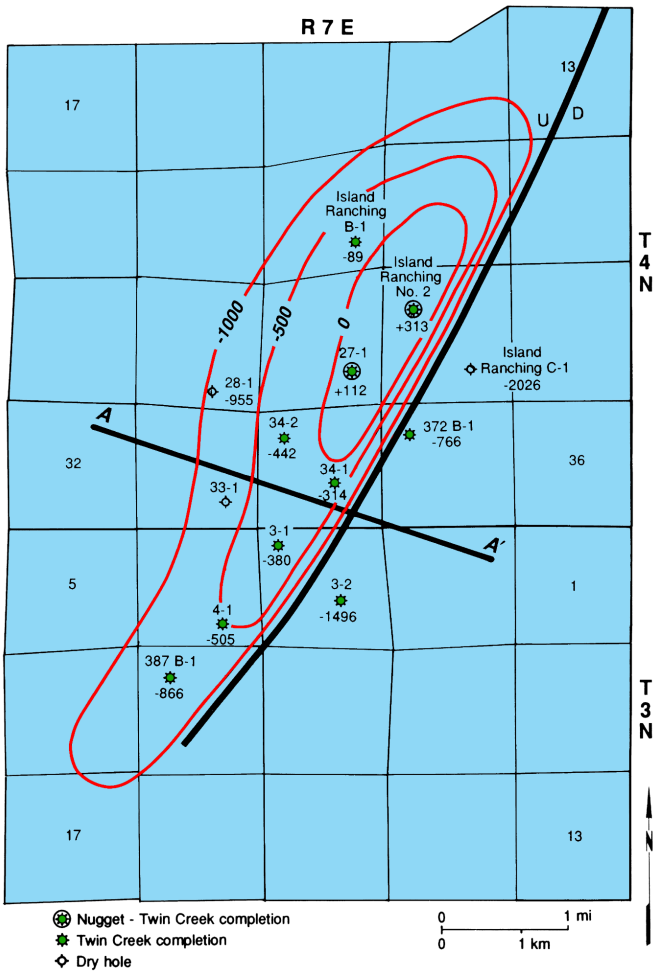

Figure 3.19. *Structure contour map of the top of the Nugget Sandstone, Anschutz Ranch field, Summit County, Utah, typical of the geometry of Paleozoic-cored shallow structures in the Triassic-Jurassic Nugget Sandstone thrust belt play. Gas and condensate are trapped only on the very crest of a large northeast-southwest-trending, doubly plunging, asymmetric, thrusted anticline in the hanging wall of the Absaroka thrust system. Contour interval = 500 feet, datum = mean sea level. Modified from Utah Division of Oil, Gas, and Mining (1980a). Cross section A–A' shown on figure 3.20.*

ranges from 43° to 48°; the gas-oil ratio (GOR) ranges between 300 and 640 cubic feet/bbl. The API gravity of the condensate ranges from 47° to 63°; the GOR ranges from 3800 and 7750 cubic feet/bbl. Oil colors vary from light to dark brown, and condensate can be clear to various shades of yellow, orange, and brown. In some cases, color can change with location or structural position within a single field. In Anschutz Ranch East field (figure 3.1), for example, the color of the condensate oil changes with the structural position of the producing wells. Condensate on the crest is pale yellow, turning darker shades (yellow through brown) with increasing depth (figure 3.22). The color change is likely the result of gravity segregation within the reservoir where condensate at the top of structure contains more dissolved gas than at the bottom. The viscosity of the crude oil is 2.18 centistokes (cst) at 104°F (40°C); in Saybolt Universal Seconds (sus) the viscosity averages 33.2 at 104°F (40°C). The viscosity of the condensate averages 1.09 cst and 29.4 sus at 104°F (40°C). The pour point of the crude oil is 15°F (9.4°C). The average weight percent sulfur and nitrogen of produced Nugget hydrocarbon liquids are 0.04 and 0.004, respectively.

In the Mesozoic-cored shallow structures subplay, the three Wyoming fields on the northern culmination produce associated gas that is very uniform in composition: 74 to 80% methane, 11 to 15% ethane, 5 to 7% propane, 2% butane, 0.4% pentane, and 2% N_2 (Frank and Gavlin, 1981). Heating values average 1252 Btu/ft^3. Pineview field on the south culmination produces associated gas that is significantly different in composition: 35% methane, 10% ethane, 9% propane, 8% butane, 4% pentane, 2% hexane, 31% heptanes (and higher hydrocarbon fractions), 0.6% N_2, and 0.7% CO_2 (Petroleum Information, 1984b). The heating value is 2964 Btu/ft^3. Fields on the Mesozoic-cored deep structures subplay produce nonassociated gas that is remarkably uniform in composition: 74 to 79% methane, 12 to 15% ethane, 5% propane, 2% butane, <1% pentane, and 2% N_2 (Frank and Gavlin, 1981; Moore and Sigler, 1987). Heating values average 1216 Btu/ft^3. The Nugget reservoir in Anschutz Ranch field (figure 3.1) on the Paleozoic-cored shallow structures subplay produces nonassociated gas (with condensate) that is somewhat different in composition than gas produced on the Mesozoic-cored shallow and deep structures subplays. The gas contains 81% methane, 8% ethane, 3% propane, 1.5% butane, 0.6% pentane, and 6% N_2, making it a low-quality gas (UGS field files). The heating value is 1101 Btu/ft^3. Gas produced from the reservoirs in the Nugget Sandstone thrust belt play contains no H_2S.

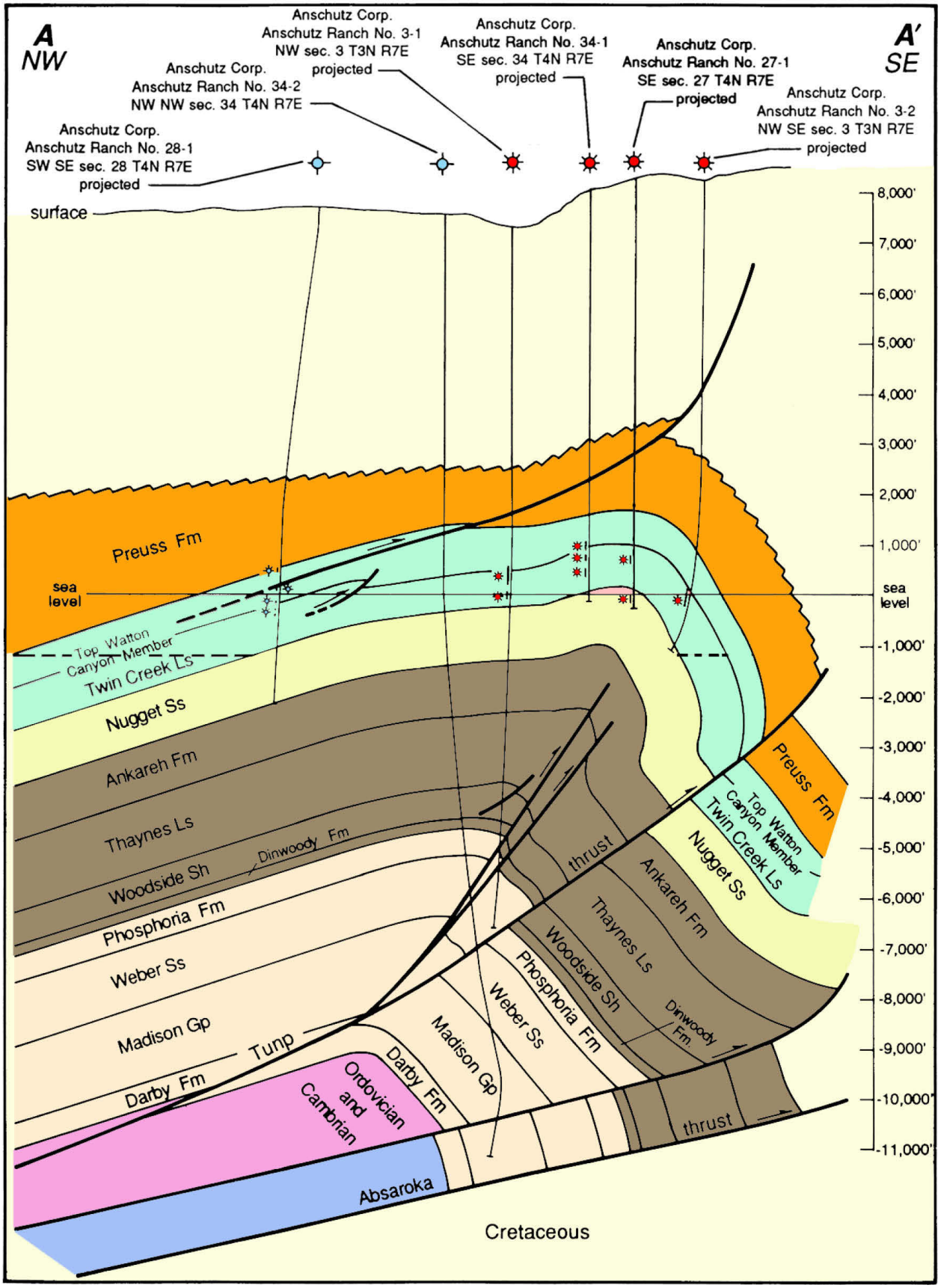

Figure 3.20. *Northwest-southeast cross section through the Anschutz Ranch structure. Line of section shown on figure 3.19. Cretaceous formations in the footwall of the Absaroka thrust system charge the overlying, fractured sandstone units of the Nugget Sandstone with gas and condensate. Modified from Utah Division of Oil, Gas, and Mining (1980c).*

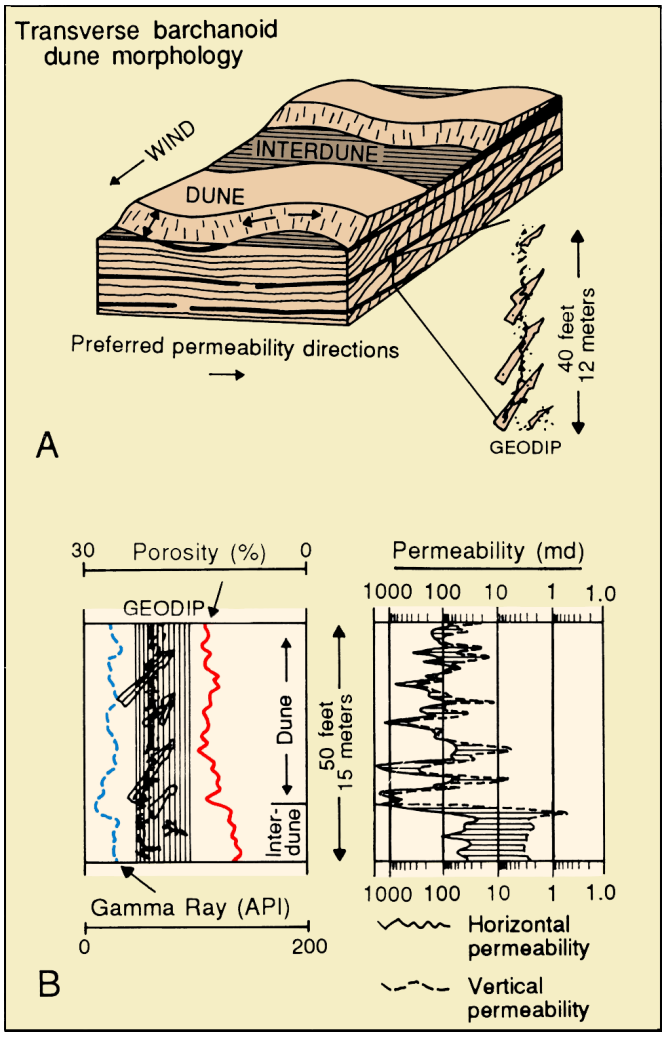

Figure 3.21. *Transverse barchanoid dune morphology.* ***A.*** *Schematic dune/interdune sequence in the Nugget Sandstone correlating transverse barchanoid dune morphology to structurally corrected stratigraphic dipmeter data (Geodip). The slipface of a dune (surface between the dune brink and toe), on which deposits form cross-beds, dips in the downwind, dune-migrating direction. Arrows indicate preferred permeability directions along the dip and strike of dune slipfaces (cross-beds).* ***B.*** *Geophysical logs demonstrate the differences in porosity and directional permeability between the dune and interdune lithofacies. Lined area indicates vertical and horizontal permeability contrasts particularly within the interdune lithofacies. After Lindquist (1983), Chidsey (1993).*

Figure 3.22. *Color changes in retrograde condensate from Anschutz Ranch East field, Summit County, Utah. Sample bottles are labeled with subsea structural elevation.*

PRODUCTION

Five fields in the Triassic-Jurassic Nugget Sandstone Absaroka thrust–Mesozoic-cored shallow structures subplay have produced crude oil and associated gas. Pineview, Lodgepole, Painter Reservoir, Clear Creek, and Ryckman Creek fields (figure 3.1) in combination have produced 80 million BO (12.7 million m^3) and 1.23 TCFG (34.7 BCMG) from the Nugget as of January 1, 2016 (Utah Division of Oil, Gas, and Mining, 2016a; Wyoming Oil and Gas Conservation Commission, 2016) (table 3.1). This subplay currently has 92 active producers and 16 abandoned Nugget producers (table 3.1).

Six fields in the Triassic-Jurassic Nugget Sandstone Absaroka thrust–Mesozoic-cored deep structures subplay have produced retrograde condensate and nonassociated gas. Pineview North, Anschutz Ranch East, Bessie Bottom, Chicken Creek, Glasscock Hollow, and East Painter Reservoir fields (figure 3.1) in combination have produced 211 million bbls of condensate (BC [33.6 million m^3) and 4.7 TCFG (133 BCMG) from the Nugget as of January 1, 2016 (Utah Division of Oil, Gas, and Mining, 2016a; Wyoming Oil and Gas Conservation Commission, 2016) (table 3.1). This subplay currently has 80 active producers and 25 abandoned producers (table 3.1). A major nitrogen injection pressure maintenance program is used to prevent retrograde condensate loss at Anschutz Ranch East field.

Two fields in the Triassic-Jurassic Nugget Sandstone Absaroka thrust–Paleozoic-cored shallow structures subplay have produced nonassociated gas and condensate. Anschutz Ranch and Yellow Creek fields (figure 3.1) have combined to produce 598,642 BC (95,176 m^3) and 31 BCFG (0.9 BCMG) from the Nugget as of January 1, 2016 (Utah Division of Oil, Gas, and Mining, 2016a; Wyoming Oil and Gas Conservation Commission, 2016) (table 3.1). This subplay has three active and three abandoned Nugget producers (table 3.1).

In 2015, the monthly production from the Nugget Sandstone averaged 41,495 BO (and condensate) (6597 m^3) and 5.3 BCFG (0.2 BCMG) (Utah Division of Oil, Gas, and Mining, 2016a; Wyoming Oil and Gas Conservation Commission, 2016). Monthly production peaked in 1979 and has generally declined since then. However, in the 1990s, the intensely fractured and depositionally heterogeneous zones of the Nugget in Lodgepole, Pineview, and Painter Reservoir fields were exploited using horizontal-drilling techniques with moderate success. Lodgepole field was sub-commercial prior to the horizontal-drilling program.

EXPLORATION POTENTIAL AND TRENDS

Future exploration in the Nugget Sandstone thrust belt play could focus on more structurally complex and subtle, thrust-related traps that overlie organic-rich Cretaceous strata. Possible structural targets include complex traps formed by true duplexes, overlapping ramp anticlines, and hybrid duplexes (Mitra, 1986). In these structures, naturally fractured sandstone beds and the overlying seals of the Twin Creek Limestone are repeated many times. Other thrust-related structural traps include subtle fault-propagation folds formed by imbricate thrust faults or stacked imbricate faults. These traps may be developed along secondary fault-propagation folds, along backlimb thrust faults, or between imbricate splays on the forelimb of anticlines (Mitra, 1986, 1990). Nugget structures may be present beneath the leading edge of the Hogsback thrust and North Flank fault of the Uinta uplift (Chidsey, 1999). Minor irregularities along the Nugget truncation against major thrusts may also be the locations for untested structures, particularly in the Mesozoic-cored shallow and deep structures subplays on the Absaroka thrust system.

CHAPTER 4:
JURASSIC TWIN CREEK LIMESTONE THRUST BELT PLAY

by

Thomas C. Chidsey, Jr., and Douglas A. Sprinkel
Utah Geological Survey

CONTENTS

FIGURES

TABLE

CHAPTER 4:
JURASSIC TWIN CREEK LIMESTONE THRUST BELT PLAY

INTRODUCTION

The Jurassic Twin Creek Limestone thrust belt play (figure 4.1), like the Triassic-Jurassic Nugget Sandstone play, is confined to the hanging wall of the Absaroka thrust system. The Twin Creek has produced over 20 million BO (3.2 million m^3) and 186 BCFG (5.3 BCMG) (Utah Division of Oil, Gas, and Mining, 2016a; Wyoming Oil and Gas Conservation Commission, 2016). The play outline closely matches that of the Nugget Sandstone play and also represents the maximum extent of petroleum potential in the geographical area as defined by producing reservoirs, hydrocarbon shows, and untested hypotheses. Prospective drilling targets in the Twin Creek Limestone thrust belt play are also delineated using the same methods as the underlying Nugget Sandstone play.

The Jurassic Twin Creek Limestone thrust belt play is also in the southwest Wyoming and northern Utah thrust belt (figure 4.1). Pineview field was the first to produce oil and gas from the Twin Creek in 1975 (Conner and Covlin, 1977; Petroleum Information, 1981). Currently seven Twin Creek fields exist, with only one in Wyoming (Yellow Creek). Geologic data for individual fields in the play are summarized in table 4.1. The Twin Creek Limestone play is divided into two subplays (1) Absaroka thrust–Mesozoic-cored structures and (2) Absaroka thrust–Paleozoic-cored structures.

DEPOSITIONAL ENVIRONMENT

The Twin Creek Limestone and equivalent rocks were deposited in a shallow-water embayment south of the main body of a Middle Jurassic sea that extended from Canada to southern Utah (figure 4.2) (Imlay, 1980; Kocurek and Dott, 1983; Hintze and Kowallis, 2009). Eustatic fluctuations caused numerous transgressions and regressions resulting in deposition of shallow-water carbonates, fine-grained clastic redbeds, and sabkha evaporites (Imlay, 1967, 1980; Kocurek and Dott, 1983). Microbial carbonate mudstone (figure 4.3) was deposited in backbank, low-energy brackish water environments. Sporadic oolitic- and peloid-bearing beds represent higher energy environments; a few zones contain fossils and fossil hash. Analysis of core from Pineview field indicates the following lithofacies: open marine, low- to high-energy middle shelf, microbial mats/tidal flat, marine sabkha, inner shelf microbial lagoon, oolitic shoals, tubular tempestites, and terrestrial.

STRATIGRAPHY AND THICKNESS

Seven formal members are recognized in both nearby outcrops and the subsurface within the Twin Creek Limestone thrust belt play area (Imlay, 1967) and each member has a characteristic geophysical log response (figure 4.4). Thickness of the Twin Creek ranges from approximately 1400 feet to nearly 1900 feet (470–630 m) (Imlay, 1967; Sprinkel and Chidsey, 1993) on the Absaroka thrust plate, where it is overlain by the Middle Jurassic Preuss Formation and underlain by the Triassic-Jurassic Nugget Sandstone. The average depth to the Twin Creek for these reservoirs is 6600 feet (2200 m).

LITHOLOGY AND FRACTURING

The Twin Creek Limestone is composed of a variety of lithologies including micritic to argillaceous limestone, evaporites, and siltstone and claystone. Carbonate fabrics consist of microbially laminated mudstone (figure 4.3), wackestone, packstone, grainstone/rudstone, and thrombolite boundstone with beds of siltstone and shale. These units may contain variable amounts of peloids, hypersaline oolites/oncolites (figure 4.5), soft pellets, and skeletal grains (crinoids, bryozoans, brachiopods, benthic forams, and bivalves) and structures such as mud cracks, ripples, cross-beds, burrows, anhydrite nodules, and numerous stylolites and fractures. Tightly cemented oolitic grainstone, dolomitized zones, and thin shaly intervals are also present (Bruce, 1988; Parra and Collier, 2000).

Post-burial diagenesis includes cementation, compaction, and fracturing. Oil and gas production comes from zones in the denser, naturally fractured carbonate beds in the middle to lower part of the formation (figures 4.5 and 4.6). Fracturing is related to fault-propagation folding during the Sevier orogeny (Royce and others, 1975; Conner and Covlin, 1977; Dixon, 1982; Lamerson, 1982; Bruce, 1988). In Lodgepole field (figure 4.1) and elsewhere, the fracture intensity is controlled by lithology (Parra and Collier, 2000). Dolomitized mudstone has considerable fracturing; for example, significant fracturing occurs near the base of the Watton Canyon Member. Fracture intensity decreases as silt content increases and dolomitization decreases; for example, only rare fractures are found in the Giraffe Creek and upper Leeds Creek Members (Parra and Collier, 2000). Fractures display a complex history of opening, calcite filling (mineralization), and dissolution. Representative thin sections show nearly parallel, sub-vertical and sub-horizontal swarms of calcite- or anhydrite-filled microfractures. Visible

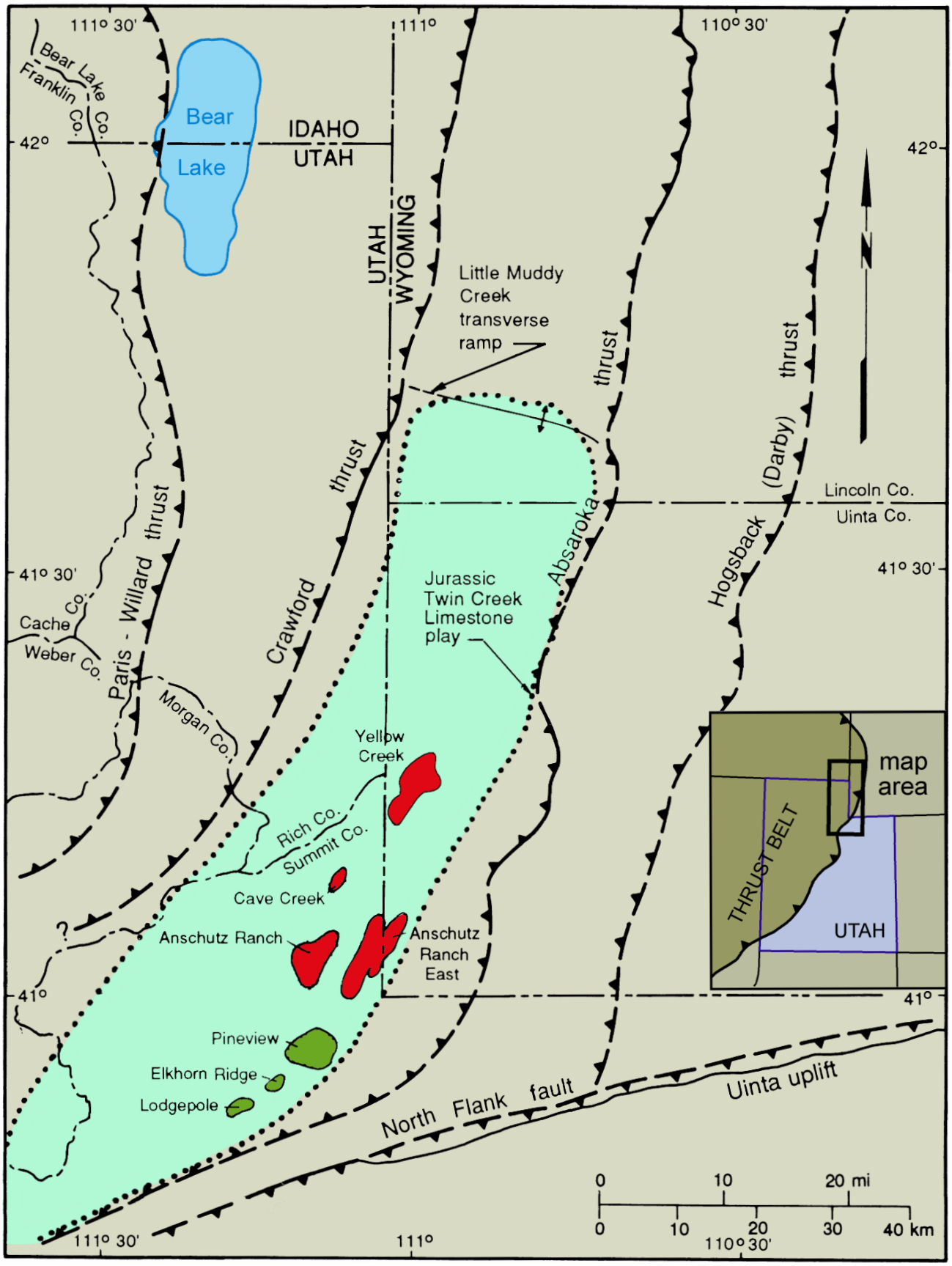

Figure 4.1. *Location of reservoirs that produce oil (green) and gas and condensate (red) from the Jurassic Twin Creek Limestone, Utah and Wyoming; major thrust faults are dashed where approximate (teeth indicate hanging wall). The Twin Creek Limestone thrust belt play area is dotted. Modified from Sprinkel and Chidsey (1993).*

Table 4.1. *Geologic, reservoir, and production data for fields in the Jurassic Twin Creek Limestone thrust belt play. Data from Blazzard (1979a, 1979b, 1979c), Moklestad (1979), Petroleum Information (1981), Ver Ploeg and De Bruin (1982), Bruce (1988), Walters (1992), Benson (1993a, 1993b), Sprinkel and Chidsey (1993), Cook and Dunleavy (1996), Utah Division of Oil, Gas and Mining (2016a, and well records), and Wyoming Oil and Gas Conservation Commission (2016).*

State	County	Field	Discovery Date	Active Producers	Abandoned Producers	Acres	Spacing (acres)	Pay (feet)	Porosity (%)	Perm. (mD)	Temp. (°F)	Initial Reservoir Pressure (psi)	Average Monthly Production		Cumulative Production	
													Oil (bbl)	Gas (MCF)	Oil (bbl)	Gas (BCF)
Utah	Summit	Anschutz Ranch	1978	4	6	2880	320	520	3	30	124	2660	236	24,448	955,380	62.9
Utah	Summit	Anschutz Ranch East	1991	0	1	80	80	322	4	NA	188	NA	0	0	114,067	1.1
Utah	Summit	Cave Creek	1983	0	2	1600	640	20	4	NA	125	2396	0	0	133,208	9.7
Utah	Summit	Elkhorn Ridge	1977	0	6	480	40	90	3	7	168	3854	0	0	1,837,203	0.8
Utah	Summit	Lodgepole	1976	2	6	640	160	75	3	7	168	4474	288	0	1,799,655	0.5
Utah	Summit	Pineview	1975	4	12	2080	80	200	2	3.8	210	4200	4538	12,121	8,115,064	10.6
Wyoming	Uinta	Yellow Creek	1976	7	18	7840	160	170	2	NA	117	2555	0	0	2,029,877	24.8

NA = Not Available

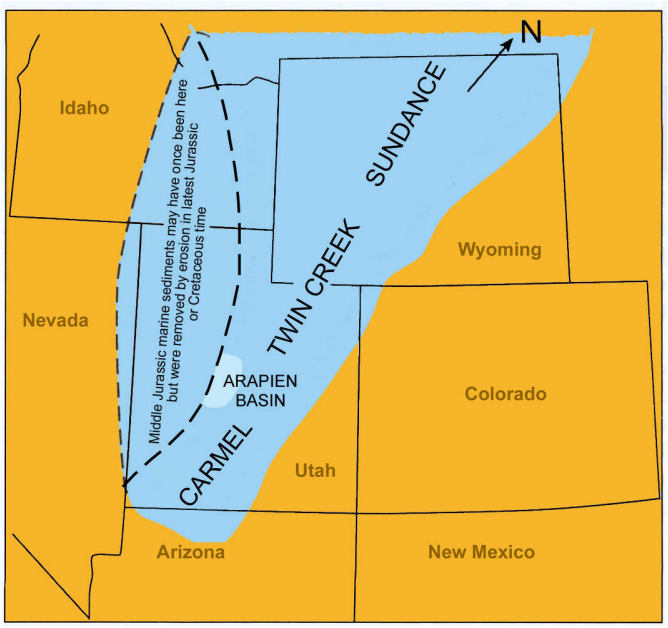

Figure 4.2. *Generalized map of the Middle Jurassic marine invasion of the Sundance-Twin Creek-Arapien-Carmel seas from the north (Utah's position during the Middle Jurassic). Modified from Kocurek and Dott (1983), Hintze and Kowallis (2009).*

Figure 4.3. *Typical Twin Creek Limestone, Watton Canyon Member, from the UPRR No. 3-3 well (section 3, T. 2 N., R. 7 E., SLBL&M, slabbed core from 8749 feet) showing mm-scale microbially laminated, carbonate mudstone deposited in backbank, low-energy brackish water environment. Note that essentially no porosity is present.*

porosity occurs as isolated dissolution pores and partially open microfractures. Both bed parallel (horizontal) and bed normal (vertical) stylolites are common. Replacement dolomite, microporosity, pyrite, and late calcite, and possibly emplacement of bitumen were controlled by fractures or stylolites.

HYDROCARBON SOURCE AND SEALS

Hydrocarbons in Twin Creek Limestone reservoirs were generated from the same subthrust Cretaceous source rocks as those that sourced the Nugget Sandstone (Warner, 1982; Bruce, 1988). Fracture systems in the brittle carbonate beds have provided hydrocarbon migration paths in addition to fault planes

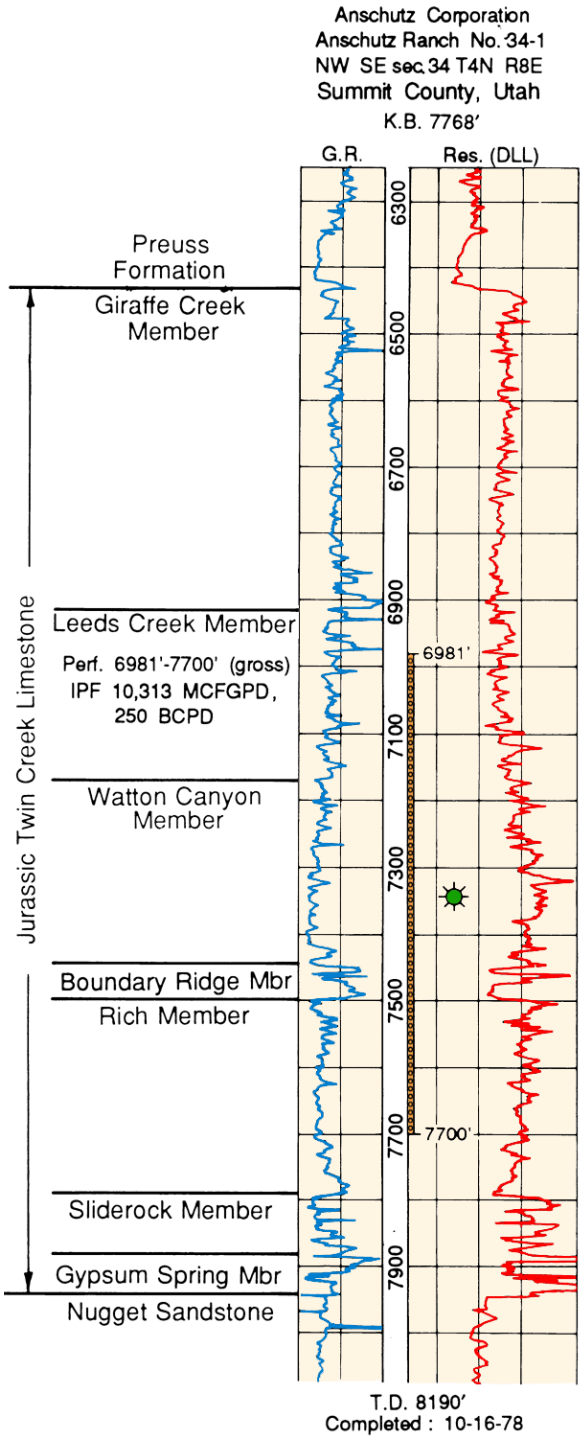

Figure 4.4. *Typical gamma ray-resistivity log of the members of the Twin Creek Limestone, Anschutz Ranch field discovery well, Summit County, Utah.*

that are in contact with source rocks. For additional details, see the Hydrocarbon Source and Seal section in chapter 3.

The seals for the producing horizons are overlying argillaceous and clastic beds, and non-fractured units within the Twin Creek Limestone. Hydrocarbons in the Twin Creek, like the Nugget Sandstone, are further sealed by salt beds within the overlying Preuss Formation.

STRUCTURE AND TRAPPING MECHANISMS

Absaroka Thrust–Mesozoic-Cored Structures Subplay

The Twin Creek Limestone Absaroka thrust–Mesozoic-cored structures subplay is located in the western part of Summit County, Utah, and Uinta County, Wyoming (figure 4.7). The subplay represents a linear, hanging wall, Mesozoic-cored, ramp anticline parallel to the leading edge of the Absaroka thrust (figure 3.10). This ramp anticline can be divided into a broad structural culmination and a structural depression within the subplay area. The culmination is present in the southern part of the subplay and related to the proximity of a transverse ramp associated with the Uinta uplift (Lamerson, 1982; Chidsey, 1993). The depression is located in the northernmost part of the subplay area in Summit County, Utah, and southwestern Uinta County, Wyoming, between the culmination to the south and another culmination related to the Muddy Creek transverse ramp to the north in Lincoln County, Wyoming (figure 4.1) (Lamerson, 1982; Chidsey, 1993). The eastern boundary of the subplay is defined by the truncation of the Twin Creek Limestone against the leading edge of the Absaroka thrust. As is the case with other thrust belt plays and subplays, the western boundary is defined by a branch line representing the intersection of the thrust planes of the Absaroka thrust and a large imbricate thrust (Boyer and Elliott, 1982). Like the Nugget Sandstone play, the Twin Creek Limestone play area terminates where the southern part of the Absaroka thrust plate trends southwest toward the Wasatch Range. The subplay extends north as a 5-mile- (8 km) wide band into Uinta County, Wyoming (figure 4.7).

Potential petroleum-trapping mechanisms in the Twin Creek Limestone Absaroka thrust–Mesozoic-cored structures subplay consist of long, slightly broader, doubly plunging anticlines—the same structures that often produce from the underlying Nugget Sansdstone (Royce and others, 1975; Conner and Covlin, 1977; Dixon, 1982; Lamerson, 1982). These anticlines are asymmetric, overturned to the east, and often develop faulted en echelon structures along the leading edge of the Absaroka thrust because of variations in the competence and thickness of the carbonate stratigraphic sequence (West and Lewis, 1982). Traps on the culmination typically produce oil and associated gas; traps on the depression produce nonassociated gas and retrograde condensate. All fields in the Twin Creek Limestone Absaroka thrust–Mesozoic-cored structures subplay are located on subsidiary closures associated with the southern culmination in Utah. Pineview field, Summit County, Utah, exemplifies the traps in the subplay (figures 4.7, 3.12, and 3.13). The reservoir covers approximately 1280 acres (572 ha) with more than 1000 feet (300 m) of structural closure. However, to date, no Twin Creek production has been discovered on traps in the structural depression.

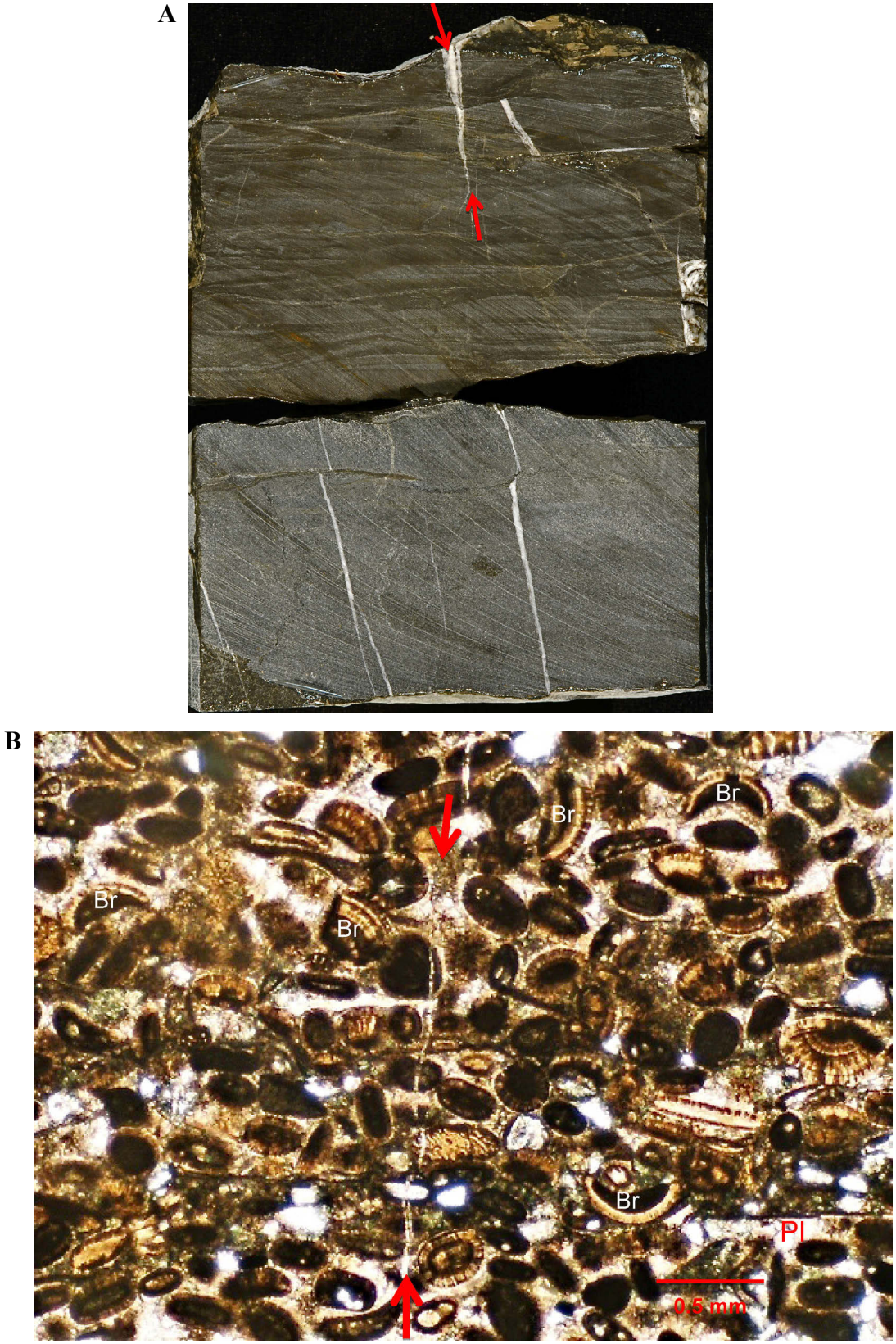

Figure 4.5. *Typical Twin Creek Limestone, Rich Member, from the UPRR No. 3-3 well (section 3, T. 2 N., R. 7 E., SLBL&M, slabbed core from 9008 feet).* ***A.*** *Oolitic skeletal grainstone bound and laminated by microbial structures. Note the two types of vertical fractures: (1) a tension gash (between red arrows), and (2) vertical tectonic fractures healed with white calcite.* ***B.*** *Photomicrograph of the core showing oolitic/skeletal grainstone diluted with quartz silt grains. Note the abundance of syndepositionally broken ooids (Br) with "cerebroid" margins, as well as the complex cementation that occluded all matrix pores. A microfracture (between red arrows) is healed with calcite. Courtesy of David E. Eby, Eby Petrography & Consulting, Inc.*

Figure 4.6. *Twin Creek Limestone reservoir rock, Watton Canyon Member, from the UPRR No. 3-3 well (section 3, T. 2 N., R. 7 E., SLBL&M, slabbed core from 8747 feet) showing highly fractured carbonate mudstone with open, bitumen-lined and calcite-filled fractures. Note zone of fossil hash at the base of the core.*

Absaroka Thrust–Paleozoic-Cored Structures Subplay

The Twin Creek Limestone Absaroka thrust–Paleozoic-cored structures subplay is located immediately west of the Mesozoic-cored structures subplay (figure 4.8). The structural characteristics of this subplay are essentially the same as the Absaroka thrust–Paleozoic-cored structures subplay in the Nugget Sandstone described in chapter 3. Thus, this subplay is also a very continuous and linear, hanging wall, Paleozoic-cored, ramp anticline along the leading edge of the Absaroka thrust (figure 3.18). The eastern boundary of the subplay is defined by the truncation of the Twin Creek against a thrust splay. The western boundary is defined as the point at which the dips in the Twin Creek on the west flank of the ramp anticline begin to flatten out. Again, the southern part of this ramp anticline trends southwest toward the Wasatch Range where the Twin Creek Limestone play area terminates. The play extends north as a 3-mile- (4.8 km) wide band through Summit County, Utah, and into Uinta County, Wyoming (figure 4.8).

Potential petroleum-trapping mechanisms in the Twin Creek Limestone Absaroka thrust–Paleozoic-cored structures play also consist of long, relatively narrow, doubly plunging anticlines that trend north to northeast (figures 4.9 and 4.10) (Royce and others, 1975; Conner and Covlin, 1977; Petroleum Information, 1981; Dixon, 1982; Lamerson, 1982; Bruce, 1988). These anticlines are also asymmetric and overturned to the east. Splay faults and salt near the anticlinal axes are common, complicating drilling operations and compartmentalizing productive zones. Three fields are in the Twin Creek Limestone Absaroka thrust–Paleozoic-cored structures subplay (figure 4.8). For example, the Anschutz Ranch field, Summit County, Utah, consists of a large, elongate anticline with more than 7100 feet (2164 m) of structural closure involving Jurassic through Ordovician rocks; the reservoir covers approximately 2880 acres (1170 ha).

RESERVOIR PROPERTIES

Most oil and gas production is from perforated intervals in the Watton Canyon, upper Rich, and Sliderock Members (figure 4.4). These members have primary porosity ranging from 2 to 4%, when present, in the producing horizons, but exhibit significant secondary porosity in the form of fracturing. Permeabilities in these members range from 4 to more than 30 mD (Blazzard, 1979a, 1979b, 1979c; Moklestad, 1979; Ver Ploeg and De Bruin, 1982; Bruce, 1988; Walters, 1992; Benson, 1993a, 1993b; Cook and Dunleavy, 1996; Sprinkel and Chidsey, 1993). The permeability is also formed by natural fractures and controls hydrocarbon production and injection fluid pathways (Parra and Collier, 2000). Other members produce hydrocarbons, but the volume is typically small, and the production zones generally require acidizing or other stimulation. The net pay thickness is variable, depending on fracturing, and ranges from 30 to 150 feet (10–50 m).

Closely spaced fractures are developed on bedding planes and within dense, homogeneous, non-porous (in terms of primary porosity) limestone beds of the Rich and Watton Canyon Members. The contact with the basal siltstone units (where fractures are sealed) of the overlying members set up the Rich and Watton Canyon for hydrocarbon trapping and production. Thin-bedded siltstone within the Rich and Watton Canyon Members creates additional reservoir heterogeneity.

The average Twin Creek reservoir temperature is 150°F (65°C). Water saturations range from 15 to 37%, with a salinity of 25,000 parts per million (ppm) NaCl for Pineview field and a R_w of 0.160 ohm-m at 68°F (20°C) for Elhorn Ridge field (Benson, 1993a, 1993b; Cook and Dunleavy, 1996). Initial reservoir pressures average about 4200 psi (29,000 kPa). The reservoir drive mechanisms include pressure depletion, active drive, and solution gas.

Reservoir data for individual fields in the Jurassic Twin Creek Limestone thrust belt play are summarized in table 4.1.

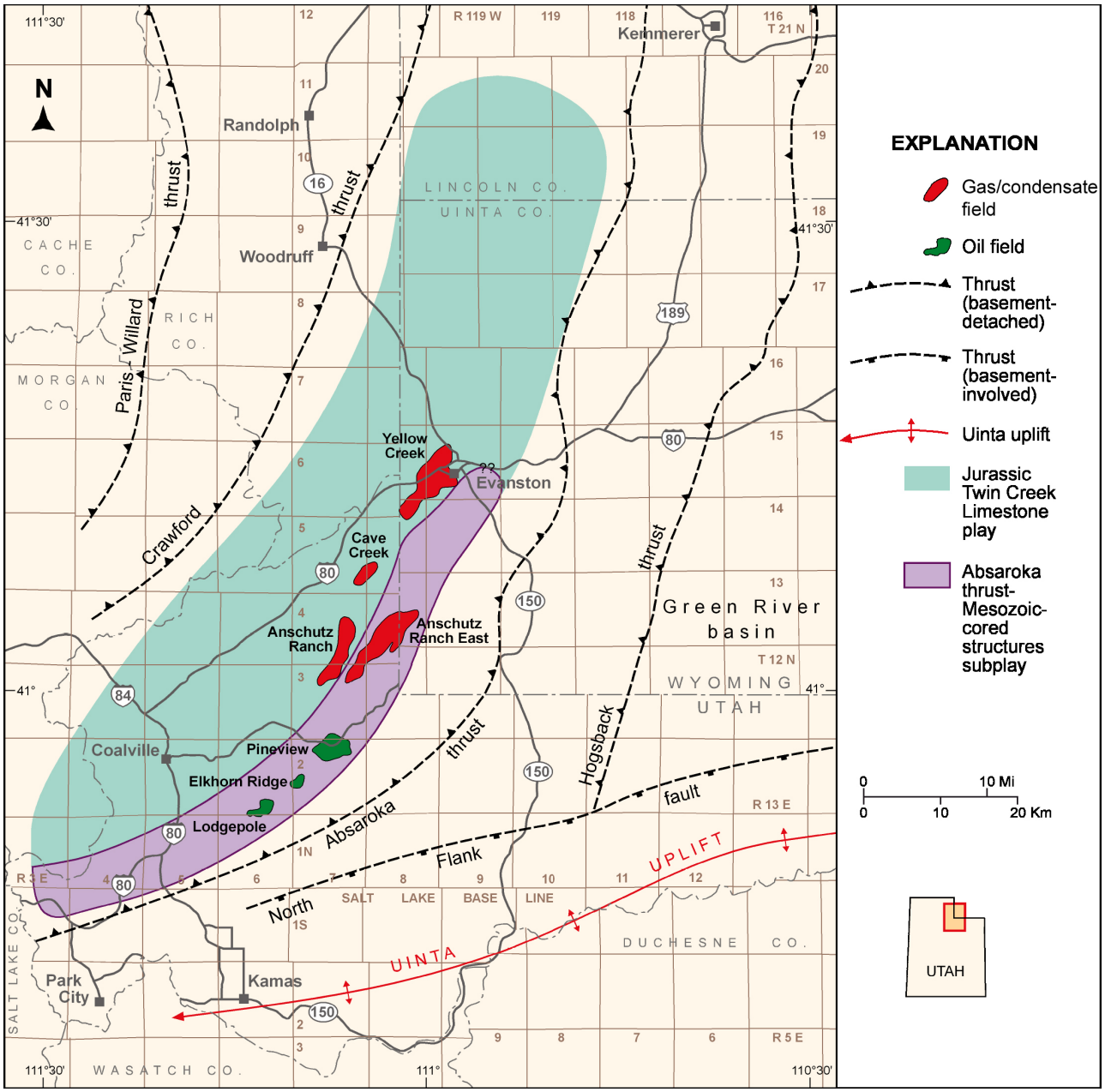

Figure 4.7. *Location of the Twin Creek Limestone Absaroka thrust–Mesozoic-cored structures subplay, Summit County, Utah, and Uinta County, Wyoming. Northern extent of the subplay is unknown.*

OIL AND GAS CHARACTERISTICS

In major reservoirs, the produced Twin Creek oil is a volatile crude (GOR between 1035 and 1198 cubic feet/bbl) (Sprinkel and Chidsey, 1993). The API gravity of the oil ranges from 24.1° to 45.7°; condensate API gravity ranges from 67.5° to 73.5°. Oil colors vary from amber to dark brown, and condensate is clear. The viscosity of the crude oil averages 2.0 cst at 104°F (40°C), but can be as high as 7.9 cst at 122°F (50°C); in Saybolt Universal Seconds the viscosity averages 32.6 sus at 104°F (40°C), but can be as high as 51.7 sus at 122°F (50°C). The viscosity of the condensate is 0.51 cst and 27.4 sus at 104°F (40°C). The pore point of the crude oil ranges from 20 to 70°F (-7 to 21°C). The average weight percent sulfur and nitrogen of produced Twin Creek hydrocarbon liquids are 0.07 and 0.008, respectively.

Composition of associated gas from the Pineview Twin Creek Limestone reservoir contains 17% methane, 27% ethane, 35% propane, 16% butane, 4% pentane, and 1% other components (Moore and Sigler, 1987). The gas has a heating value of 2321 Btu/ft^3. Composition of nonassociated gas from Anschutz Ranch, Cave Creek, and Yellow Creek reservoirs is remarkably uniform and significantly different from the associated gas. Gas from these reservoirs contains 75 to 80% methane, 7 to 9% ethane, 4% propane, 3% butane, 1% pentane, 6 to 7%

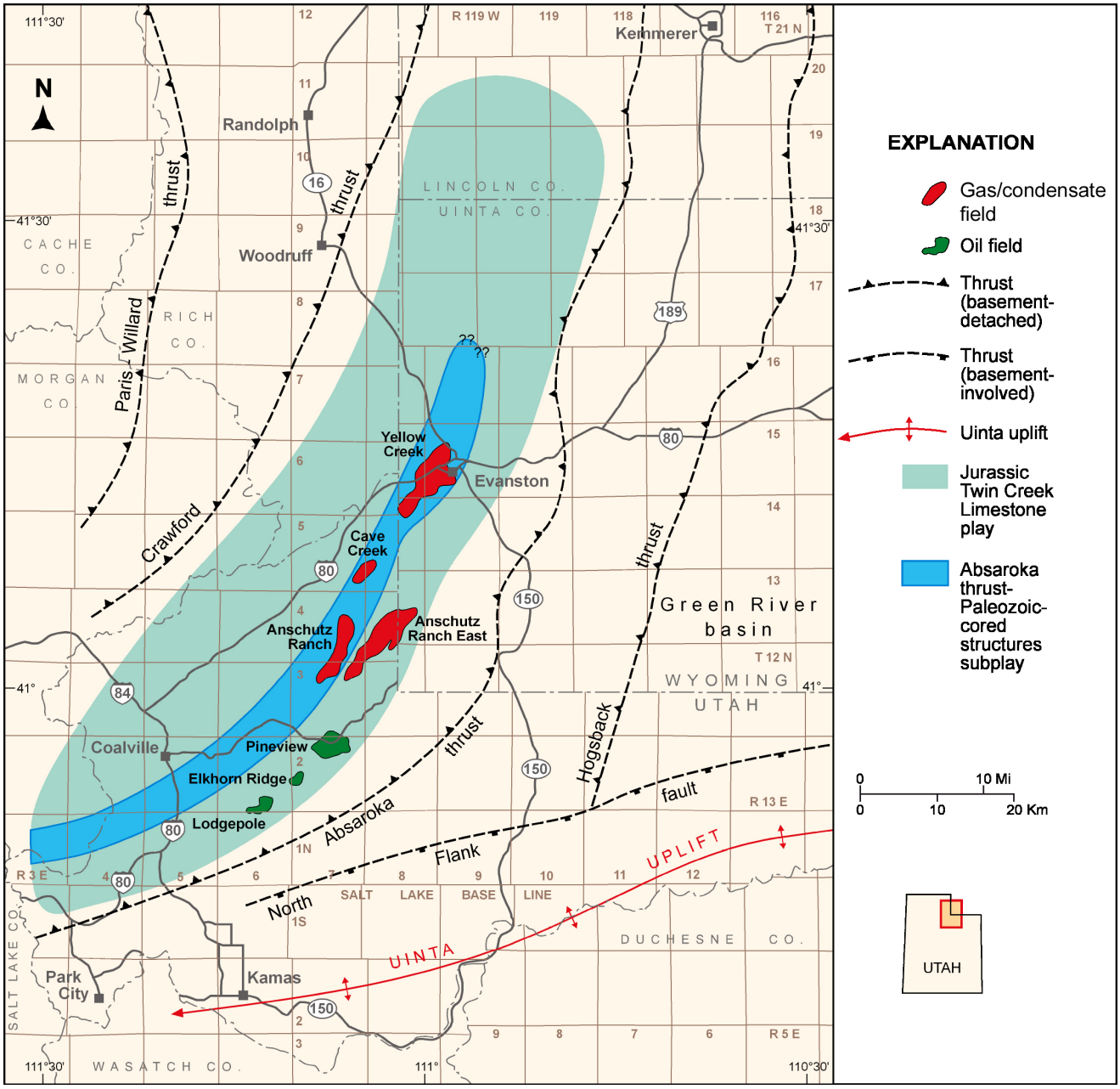

Figure 4.8. *Location of the Twin Creek Limestone Absaroka thrust–Paleozoic-cored structures subplay, Summit County, Utah, and Uinta County, Wyoming. Northern extent of the subplay is unknown.*

N_2, and 1% other components (Petroleum Information, 1981; Moore and Sigler, 1987). Heating values average 1170 Btu/ft^3. Gas produced from the reservoirs in the Twin Creek play contains no H_2S.

PRODUCTION

Fields in the Jurassic Twin Creek Limestone Absaroka thrust–Mesozoic-cored structures subplay produce crude oil and associated gas. Pineview, Elkhorn Ridge, and Lodgepole fields (figure 4.1) are located on the culmination part of the subplay, and combined, have produced 11.8 million BO (1.9 million m^3) and 12 BCFG (0.34 BCMG) from the Twin Creek as of January 1, 2016 (Utah Division of Oil, Gas, and Mining, 2016a) (table 4.1). In the depression part of the subplay, only one well, within Anschutz Ranch East field, is productive from the Twin Creek. There are currently six active producers and 18 abandoned wells in the Twin Creek Mesozoic-cored structures subplay (table 4.1).

Current Twin Creek production in the Jurassic Twin Creek Limestone Absaroka thrust–Paleozoic-cored structures subplay consists of nonassociated gas and condensate. Anschutz Ranch, Cave Creek, and Yellow Creek fields (figure 4.1) are located in this subplay and combined have produced 3.1 million BC (0.5 million m^3) and 97.3 BCFG (2.8 BCMG) from

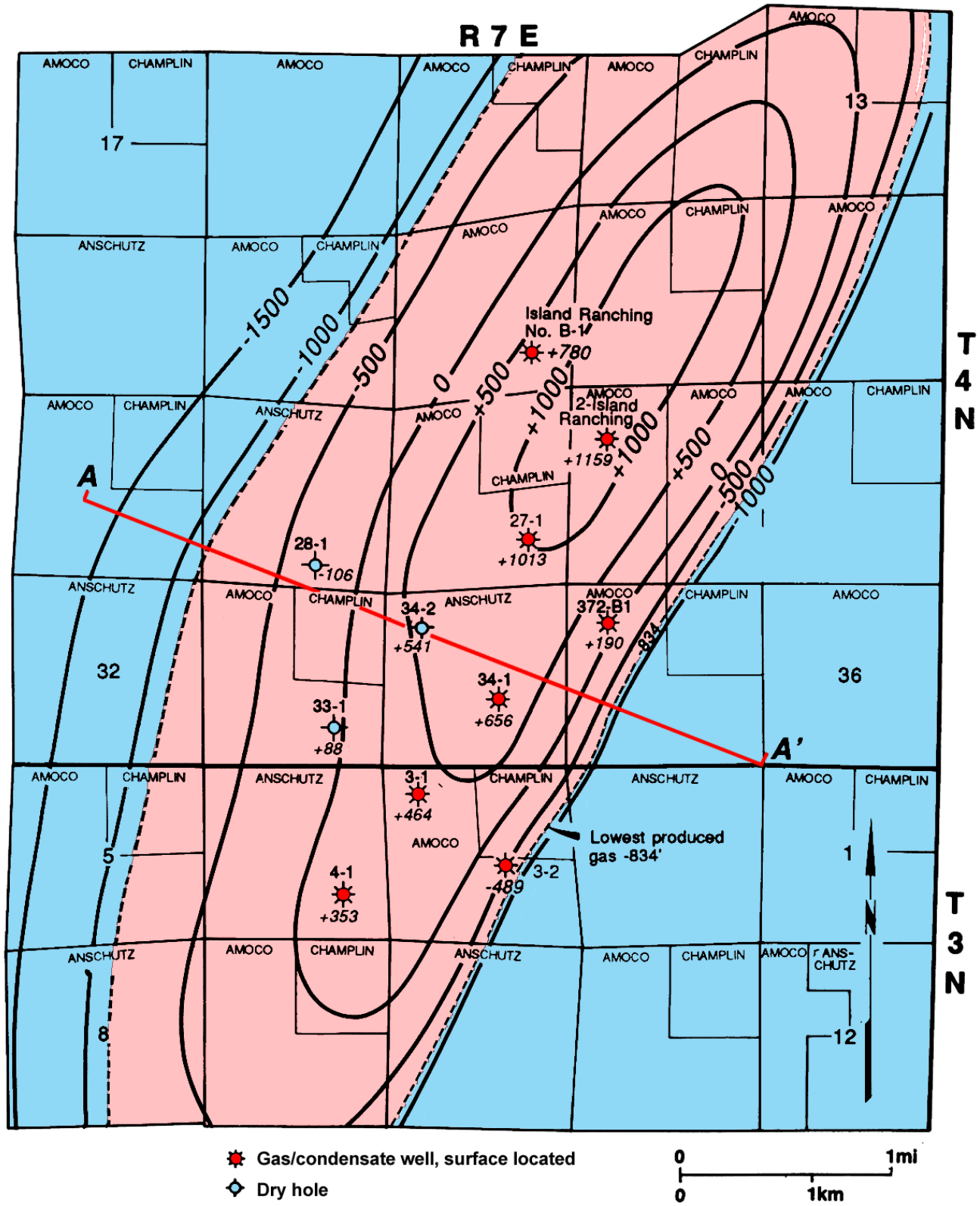

Figure 4.9. *Structure contour map of the top of the Twin Creek Limestone, Anschutz Ranch field, Summit County, Utah, typical of the geometry of Paleozoic-cored structures in the Jurassic Twin Creek Limestone thrust belt play. Gas and condensate are trapped by the doubly plunging, asymmetric anticline in the hanging wall of the Absaroka thrust system. Modified from Utah Division of Oil, Gas, and Mining (1980b). Cross section A–A' shown on figure 4.10.*

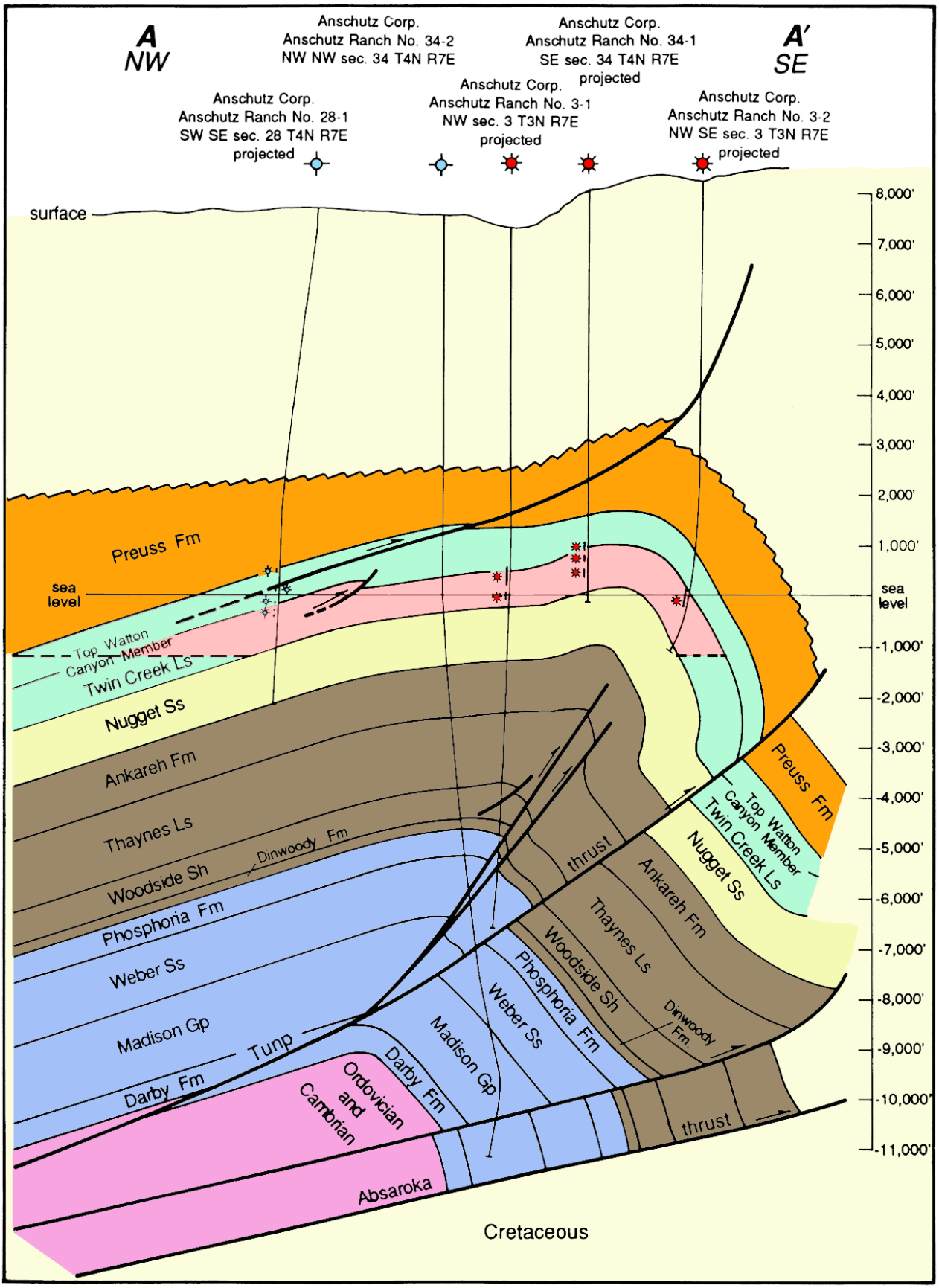

Figure 4.10. *Northwest-southeast cross section through the Anschutz Ranch structure. Line of section shown on figure 4.9. Cretaceous formations in the footwall of the Absaroka thrust system charge the overlying, highly fractured limestone beds of the Twin Creek Limestone with gas, condensate, and oil. Modified from Utah Division of Oil, Gas, and Mining (1980c).*

the Twin Creek as of January 1, 2016 (Utah Division of Oil, Gas, and Mining, 2016a; Wyoming Oil and Gas Conservation Commission, 2016) (table 4.1). Currently 11 active and 18 abandoned Twin Creek producers are in the Paleozoic-cored structures subplay (table 4.1).

In 2015, the monthly production from the Twin Creek Limestone averaged 5061 BO (and condensate) (805 m^3) and 38,148 MCFG (1080 MCMG) (Utah Division of Oil, Gas, and Mining, 2016a; Wyoming Oil and Gas Conservation Commission, 2016). Monthly production peaked in 1979, and has generally declined since then. However, in the 1990s, the intensely fractured and depositionally heterogeneous Watton Canyon and Rich reservoirs of the Twin Creek in the Elkhorn Ridge, Lodgepole, and Pineview fields were exploited using horizontal-drilling techniques. Elkhorn Ridge and Lodgepole fields were sub-commercial prior to the horizontal-drilling programs. A horizontal-drilling program also revitalized production from the Twin Creek in Cave Creek field.

EXPLORATION POTENTIAL AND TRENDS

Future exploration could target the structurally complex, thrust-related traps that include complex traps that may be drilled for Nugget reservoirs. In these structures, the dense, naturally fractured limestone beds and the overlying seals of the Twin Creek Limestone are repeated many times. The key to new discoveries will be the: (1) determination of fracture types and orientation for the application of horizontal drilling, and (2) recognition of microbial carbonates and any associated porosity development.

CHAPTER 5:
JURASSIC NAVAJO SANDSTONE/TEMPLE CAP FORMATION HINGELINE PLAY

by

Thomas C. Chidsey, Jr., and Douglas A. Sprinkel
Utah Geological Survey

CONTENTS

FIGURES

TABLE

CHAPTER 5:
JURASSIC NAVAJO SANDSTONE/TEMPLE CAP FORMATION HINGELINE PLAY

INTRODUCTION

Central Utah has had petroleum exploration for over 50 years because explorationists viewed the geology as a natural extension of successful plays in the Utah-Wyoming-Idaho salient of the Sevier (Cordilleran) thrust belt to the north (figures 1.3 and 2.2). Early efforts tested anticlines identified from surface mapping and seismic reflection data. The map on figure 5.1 represents about 276 square townships. Since 1918, the area had fewer than 120 wells drilled, which means only one well was drilled per every two townships, or one well per about 72 square miles (186 km^2). The first well in the region was drilled in 1918. No wells were drilled during the Great Depression years of the 1930s, but increases followed each decade through the 1980s (figure 5.2). During the late 1970s to early 1980s, companies drilled thrust belt-style structures in the wake of the 1975 Pineview discovery in northern Utah (figure 1.3A), and because of a significant increase in oil prices from the Arab oil embargo and the Iranian revolution. Drilling peaked in 1985 but decreased thereafter due to a drop in oil prices and the high risk and costs associated with exploration in the Hingeline area. Although early efforts failed to find commercial hydrocarbon deposits, companies confirmed the area was similar in structural style, reservoir types, and timing to the productive thrust belt to the north. The lack of Cretaceous hydrocarbon source beds below the thrust structures seemingly was to blame for the early exploration failures; however, oil and gas shows were commonly noted in Mississippian, Permian, Triassic, and Jurassic rocks. The 2004 discovery of Covenant field (figures 1.3B and 5.1) by Wolverine Gas and Oil Company in the Early Jurassic Navajo Sandstone and White Throne Member of the Middle Jurassic Temple Cap Formation (figure 5.3) (Sprinkel and others, 2009) along the Sanpete-Sevier Valley antiform changed the oil development potential in the central Utah thrust belt from hypothetical to proven. In 2008 Wolverine added a second Navajo discovery in the trend to the north in Sanpete County—Providence field (figures 1.3B and 5.1); the Temple Cap is not productive in Providence.

The Jurassic Navajo Sandstone/Temple Cap Formation Hingeline play extends 200 miles (320 km) south-southwest starting 20 miles (30 km) north of Provo, Utah, and extending to southwestern Sevier County; it thins from 25 miles (40 km) wide in the north to zero in the south (figure 1.3B). The play lies due south of the Utah-Wyoming-Idaho salient and straddles the boundary between the eastern Basin and Range (eastern Millard, Juab, and Utah Counties) and High Plateaus (central Sevier and Sanpete Counties) physiographic provinces. The Jurassic Navajo Sandstone/Temple Cap Formation Hingeline play area represents the maximum extent of petroleum potential in the geographical area as defined by the two producing reservoirs, limited well data, potential hydrocarbon sources and migration history, and regional structural interpretations. The attractiveness of the Jurassic Navajo Sandstone/Temple Cap Formation Hingeline play (and other thrust belt plays) to the petroleum industry depends on the successful development of Covenant and Providence fields, the quality of seismic data, reserve potential, drilling costs, and oil and gas prices. Since the discovery of Covenant field, these criteria in the Navajo/Temple Cap Hingeline play have met only the exploration guidelines of small, independent companies.

Like the thrust belt to the north, prospective drilling targets in the Jurassic Navajo/Temple Cap Sandstone Hingeline play are delineated using high-quality 2-D and, possibly in the near-future, 3-D seismic data, 2-D forward modeling/visualization tools, well control, dipmeter information, high-quality surface geologic maps, and detailed analyses of structural geometry (Schelling and others, 2007). Determining the time of structural development, petroleum migration, and entrapment are critical to identify prospects. Surface geochemical surveys and remote sensing techniques have been employed to high-grade areas for further evaluation, especially where high quality seismic data is difficult to obtain.

DEPOSITIONAL ENVIRONMENTS

Navajo Sandstone

The Navajo Sandstone was deposited during Early (Pliensbachian/Toarcian) Jurassic time, in the extensive dune field (erg) that included the equivalent upper part of the Nugget Sandstone (see chapter 3). This erg extended from present-day Wyoming to Arizona (figure 3.3). The eolian deposits included dunes, interdunes, and sand sheets. Navajo dunes, in what is now central and southern Utah, were often large (widths up to 2200 feet [670 m]) transverse barchanoid ridges as suggested by large-scale cross-bedding that indicated paleowind directions were dominantly from the north and northwest (figure 3.3) (Picard, 1975; Kocurek and Dott, 1983; Fryberger, 1990; Hartwick, 2010). For the discussion of the provenance of the Navajo Sandstone and equivalent rocks, see chapter 3.

In addition to a "sea" of wind-blown sand dunes, the Navajo erg system included interdune playas and oases. A high water table produced oases; deposition occurred when springs and

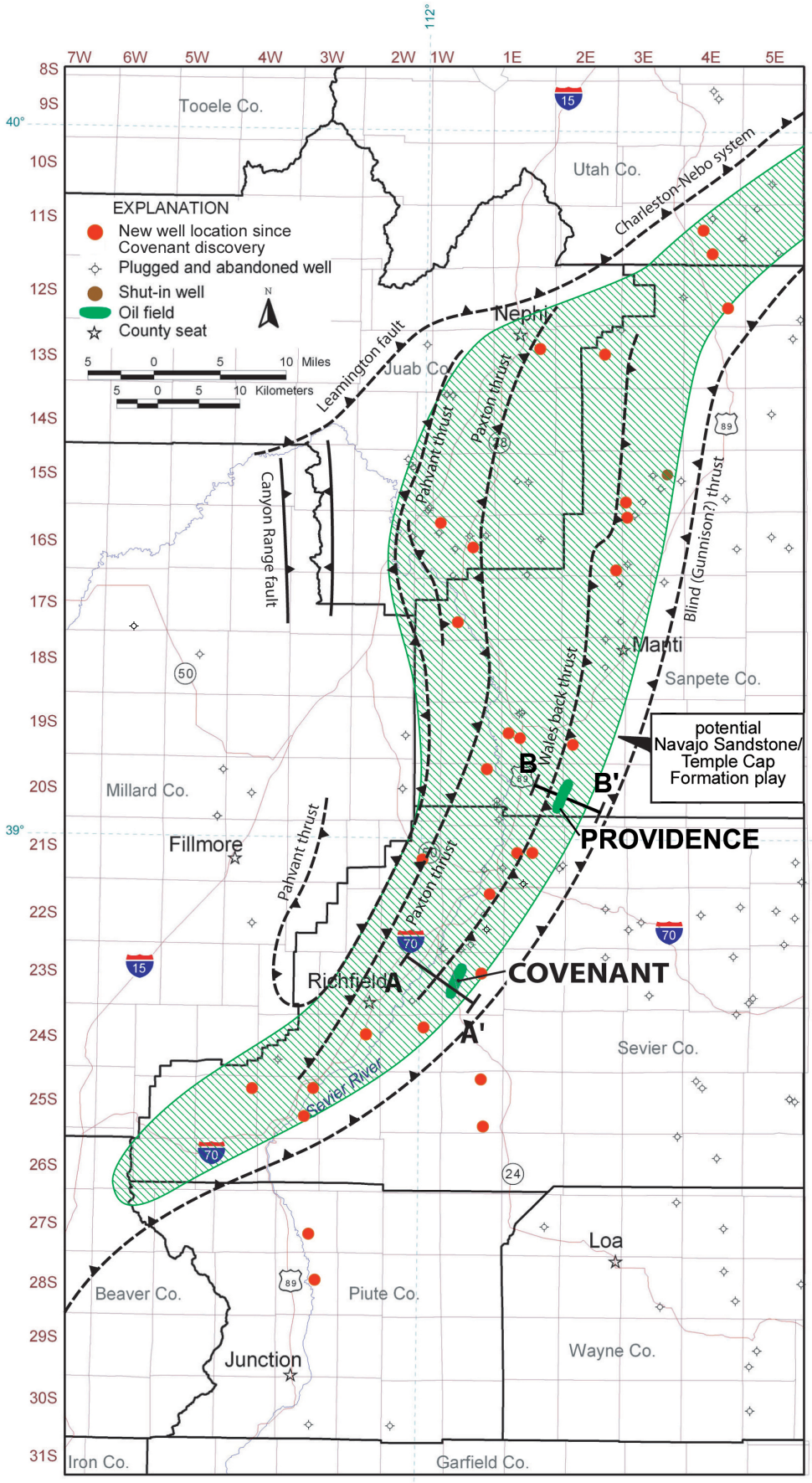

Figure 5.1. *Jurassic Navajo Sandstone/Temple Cap Formation Hingeline play area showing regional exploratory well locations through 2016.*

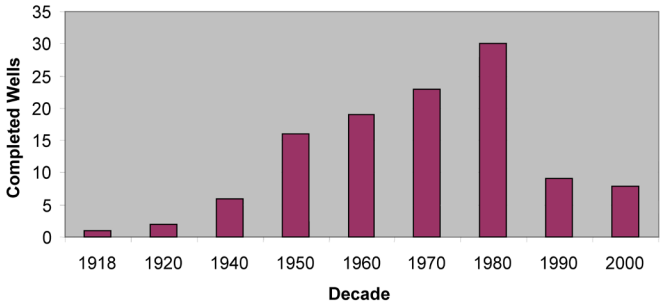

Figure 5.2. *Exploration history of central Utah (Utah Division of Oil, Gas, and Mining well files, http://www.ogm.utah.gov/).*

lakes existed for relatively long periods of time. The high water table also resulted in early soft-sediment deformation in overlying dune sands (Sanderson, 1974; Doe and Dott, 1980). Some Navajo interdunes were erosional (deflation) areas associated with running water, such as a wadi (desert wash). A wadi is a usually dry streambed or channel in a desert region. Sand sheets, represented by low-relief, poorly drained, vegetated or gravel pavement deposits, were also common (Lindquist, 1988). These areas acted as sand transport surfaces.

Temple Cap Formation

The Temple Cap Formation is divided into the three members: the Sinawava (basal), White Throne, and Esplin Point (figure 5.3) (Biek and others, 2010; Sprinkel and others, 2011). In Middle Jurassic (Bajocian) time, a shallow seaway spread south from Canada to south-central and southwestern Utah (figure 4.2) (Blakey, 1994; Peterson, 1994; Hintze and Kowallis, 2009; Biek and others, 2010). The Sinawava Member represents a brief time of coastal sabkha and tidal flat environments. Wind-blown sand dunes of the White Throne Member signify a return to eolian conditions of a coastal dune field (Blakey, 1994; Peterson, 1994). White Throne dunes were smaller than Navajo dunes (widths up to 1650 feet [500 m]) (Hartwick, 2010). Regional outcrop and Covenant core analyses of the mean dip of dune foreset beds indicate paleocurrent and paleowind directions were dominantly from the northeast (Peterson, 1988; Hartwick, 2010). The close proximity to the coast is indicated by a few thin interbedded marine dolomitic limestone beds within the White Throne in Covenant core, which indicate relatively short-lived, and perhaps local marine incursions into the coastal dune field. These limestone units appear as high gamma-ray zones (figure 5.3) and contain Bajocian-age (Middle Jurassic) marine palynomorphs (dinoflagellate cysts) (figure 5.4). The uppermost Esplin Point Member documents a rise in sea level and a return to coastal sabkha, tidal flat, and nearshore marine conditions that continued with deposition of the Arapien Formation above.

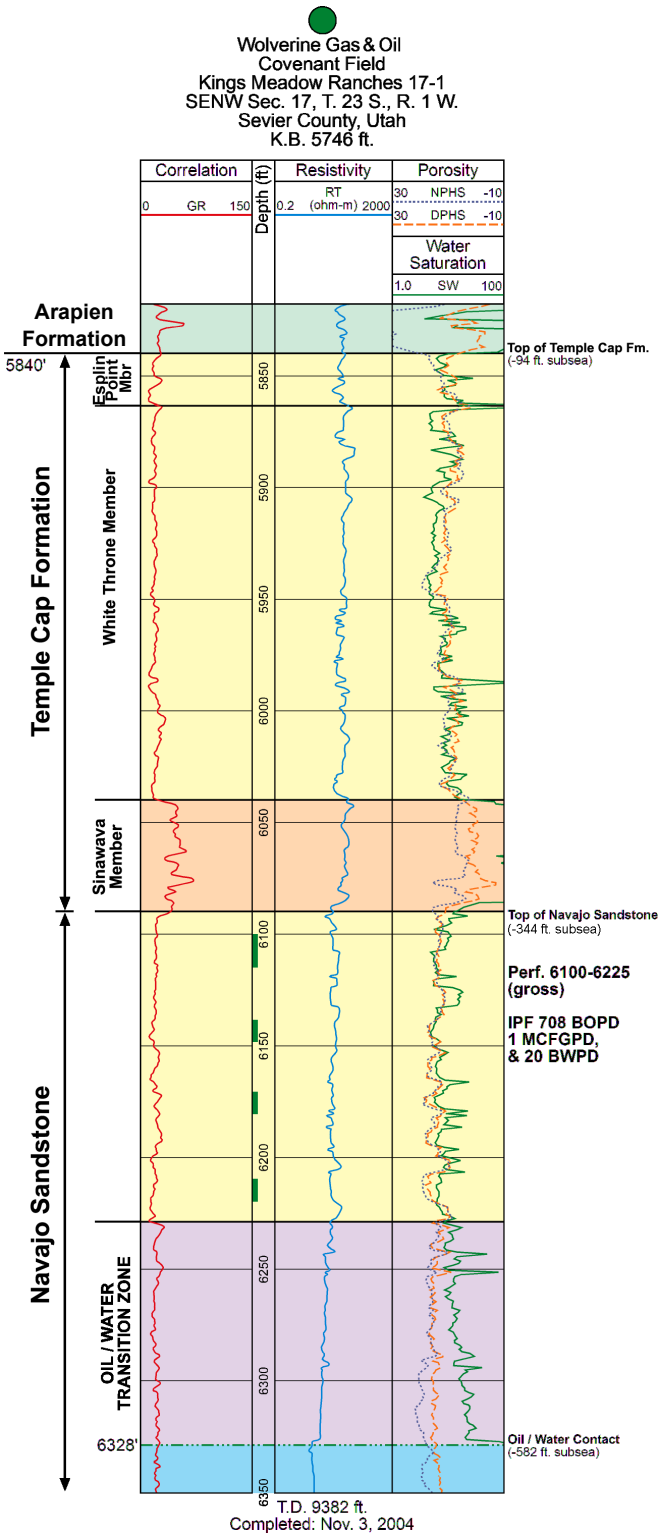

Figure 5.3. *Typical combined gamma ray, resistivity, and neutron-density log of the Navajo Sandstone and Temple Cap Formation from the Kings Meadow Ranches No. 17-1 discovery well of Covenant field, Sevier County, Utah. The vertical green bars between depths of 6100 and 6225 feet on the log indicate producing (perforated) intervals.*

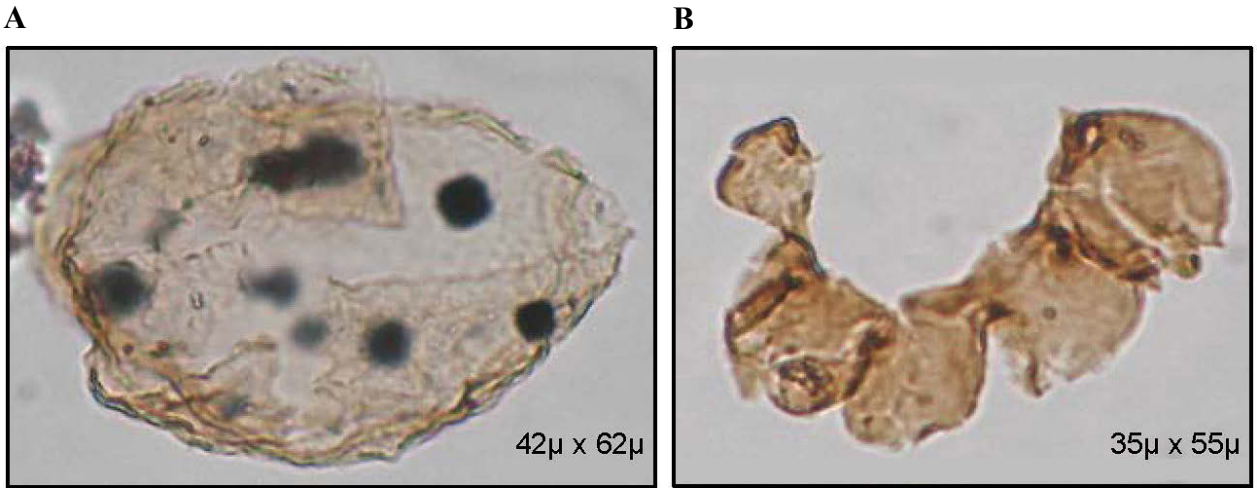

Figure 5.4. *Close-up images of marine palynomorphs (dinoflagellate cysts)* Gongylodinium hocneratum *(A) and microforam test lining (B), recovered from the White Throne Member of the Temple Cap Formation, Kings Meadow Ranches No. 17-3 well, 6634.7 feet. Courtesy of Oolithica.*

STRATIGRAPHY AND THICKNESS

The Navajo Sandstone is 610 to 1620 feet (190–590 m) thick (Hintze and Kowallis, 2009) and the Temple Cap Formation is about 320 feet (98 m) thick in the play area. The depth to the Navajo in Covenant field is 6090 feet (1860 m); 5840 feet (1780 m) to the Temple Cap. The Sinawava, White Throne, and Esplin Point Members of the Temple Cap are 48 feet (15 m), 211 feet (64 m), and 57 feet (17 m) thick, respectively. The Temple Cap is separated from the underlying Navajo by the J-1 unconformity (Pipiringos and O'Sullivan, 1978). At Covenant field, all three members are present based on core and geophysical log analysis (Sprinkel and others, 2009) (they are also present at Providence field). Air-fall ash beds containing sanidine, biotite, and zircon indicate the Temple Cap is 177.8 to 171.4 Ma (2σ) (Sprinkel and others, 2009). Navajo and White Throne have subtle but distinct characteristic geophysical log responses (figure 5.3); the Sinawava has a high gamma-ray profile recognized on other logs regionally.

The central Utah thrust belt is divided into eastern, central, and western areas based on Temple Cap and equivalent stratigraphy (figures 5.5 and 5.6). In Covenant and Providence fields (central area) the Temple Cap Formation is overlain by the Sliderock Member of the Middle Jurassic Arapien Formation and the Navajo Sandstone is underlain by the Triassic Chinle Formation. The Temple Cap and its members grade and intertongue from marine in the west and thin east becoming all eolian (White Throne Member) as shown on figure 5.7 (Sprinkel and others, 2011; Doelling and others, 2013).

LITHOLOGY AND FRACTURING

The productive part of the Navajo Sandstone at Covenant field is about 240 feet (80 m) thick; the White Throne Member of the Temple Cap Formation is about 200 feet (70 m) thick. These units are characterized by thick, large-scale, trough, planar, or wedge-planar cross-beds (35 to 40°) commonly recognized as classic eolian dune features (figures 5.8 and 5.9); contorted bedding, wind ripples, and small-scale cross-beds are also common (Sanderson, 1974; Dalrymple and Morris, 2007). Dune lithofacies from the brink to the toe of the dune slipface consist of (1) thin, graded, tabular grainfall laminae (rarely preserved), (2) thick, subgraded avalanche laminae, and (3) thin, tightly packed, reworked ripple strata at the dune toe (Lindquist, 1983). Massive, homogenous beds with no distinct sedimentary structures or laminations are also recognized in the Navajo and were probably formed by water-saturated sand (Sanderson, 1974).

In general, the Navajo Sandstone and White Throne Member consist of very well to well-sorted, very fine to medium-grained (1/16 mm to 1/2 mm), subangular to subrounded, light-yellow-gray sand or silt grains cemented by carbonate cement. However, some intervals show a bimodal grain-size distribution representing silty laminae between sand beds (figure 5.10A). The typical sandstone is 97% white or clear quartz grains (usually frosted) with varying amounts of K-feldspar. Feldspar is more common in the Navajo than White Throne, further indicating a slight variation in depositional environment (figure 5.10B) (Hartwick, 2010). Very little clay is present in the Navajo (Strickland and others, 2005) and White Throne. Glauconite near the base of the White Throne (figure 5.11) suggests a transition to marginal marine conditions.

The Sinawava Member of the Temple Cap Formation is a heterogeneous, 50-foot-thick (17 m) section. This unit is characterized by low-angle to horizontal laminae or distorted bedding consisting of red-brown, very fine to fine-grained, thin, poorly sorted sandstone to mudstone, limestone, and gypsum (figure 5.12) (Sprinkel and others, 2011). Horizontal stratification often contains silty laminae between beds. These beds

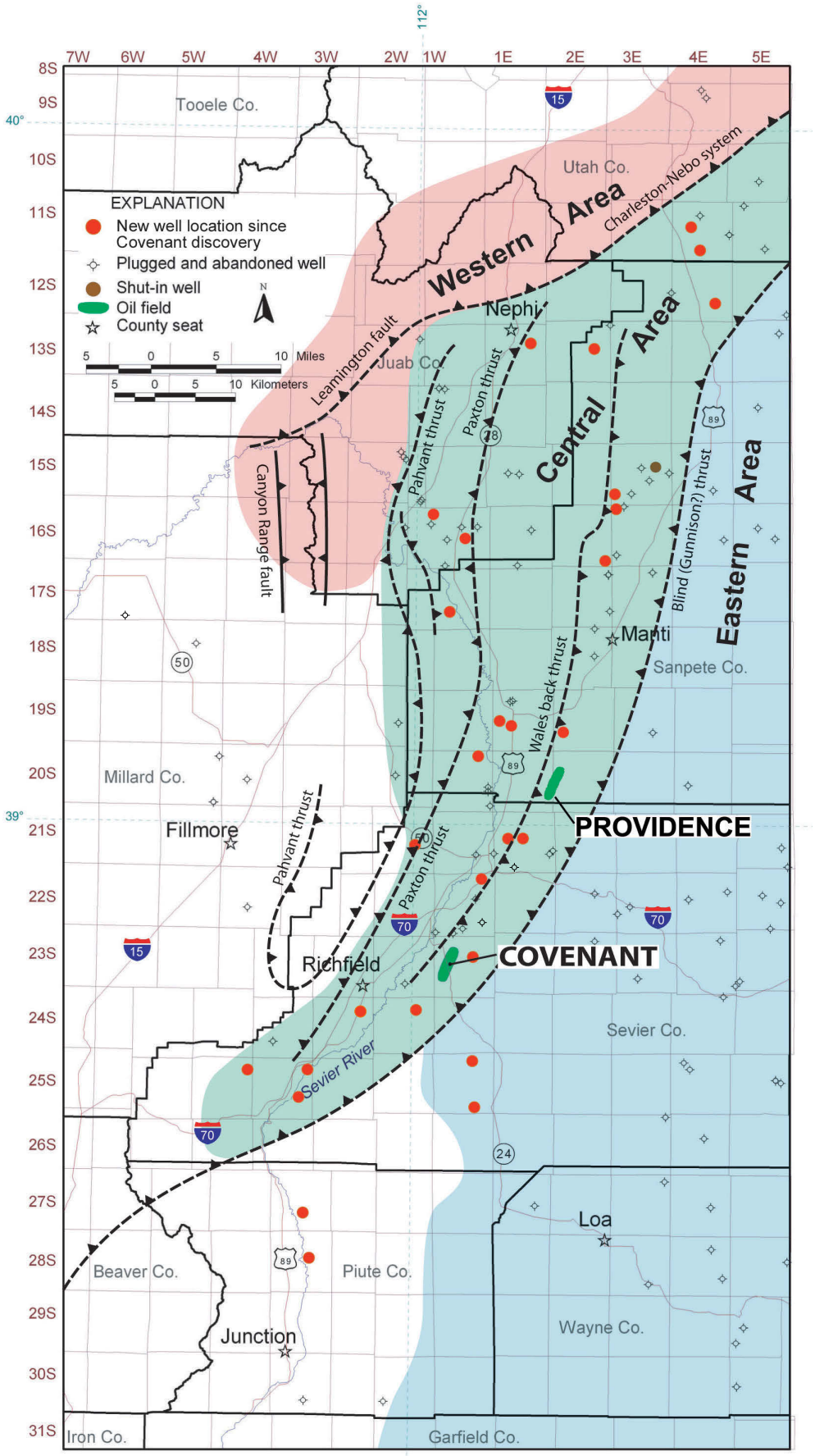

Figure 5.5. *Eastern, central, and western areas of the central Utah thrust belt based on stratigraphy.*

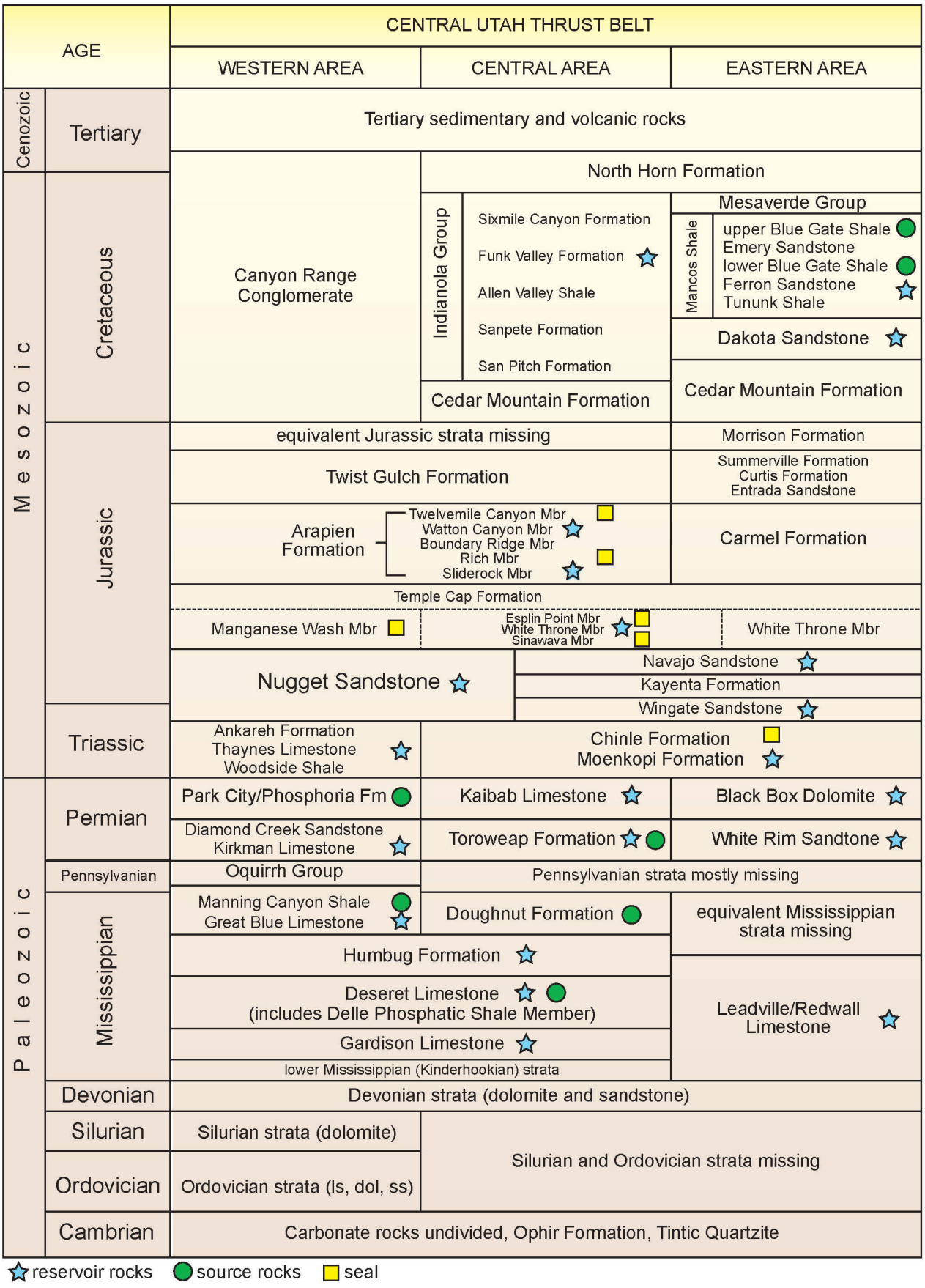

Figure 5.6. *Detailed stratigraphic correlation chart showing Navajo Sandstone, Temple Cap Formation, and other potential reservoir rocks as well as source rocks and seals in central Utah (see figure 5.5 for location of eastern, central, and western areas).*

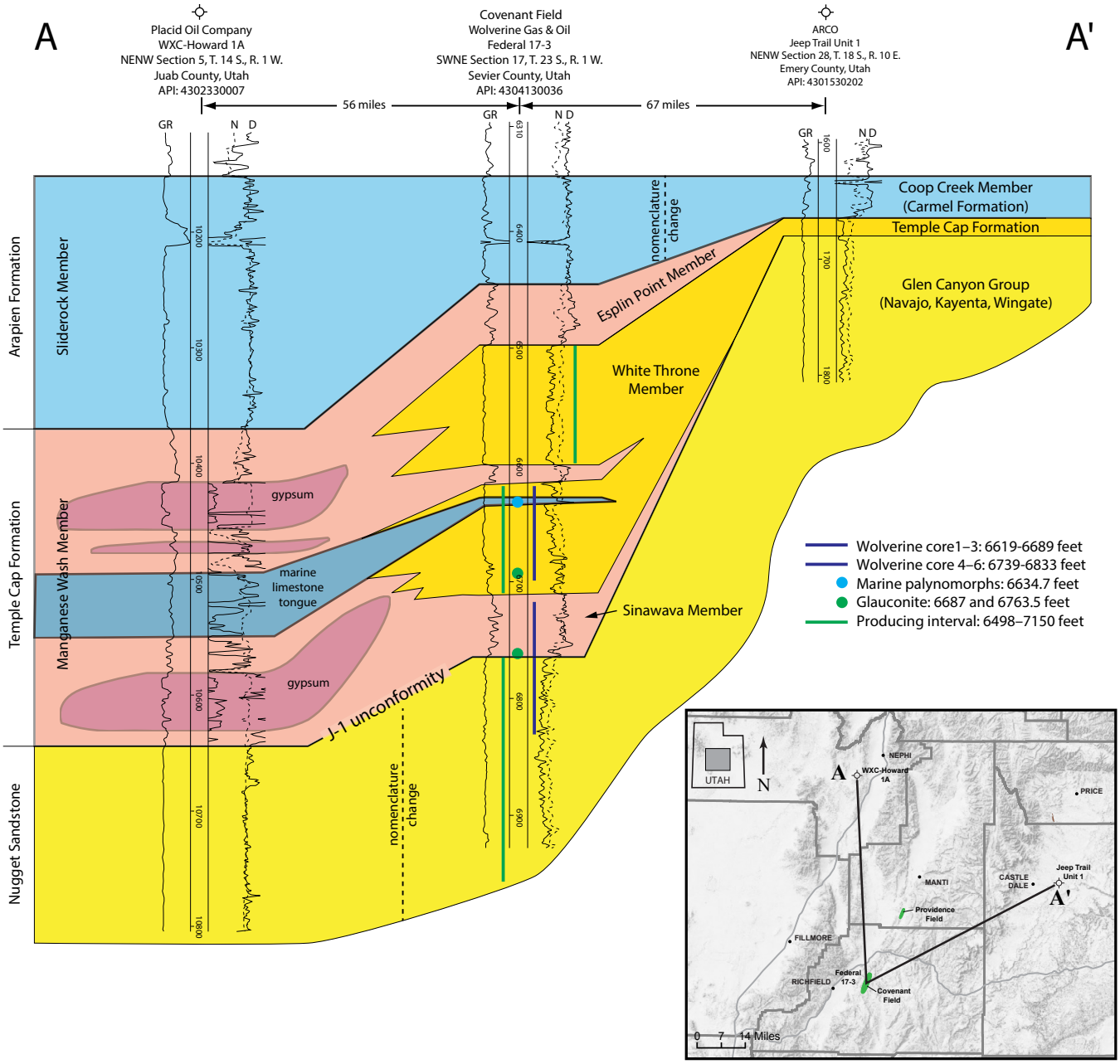

Figure 5.7. *Correlation of the members of the Temple Cap Formation in central Utah. The interpretation suggests the marine to marginal marine beds of sandstone, siltsone, mudstone, gypsum, and some limestone in the west (Manganese Wash Member) intertongues eastward with eolian beds (White Throne Member). Some marine intertonguing (basal Sinawava and capping Esplin Point Members) in the predominantly eolian section is noted by marine palynomorphs and glauconite. East of Covenant field the section thins and becomes exclusively sandstone of the White Throne Member (Sprinkel and others, 2011; Doelling and others, 2013).*

may also display ripples or channel characteristics (scour) suggesting tidal flow or flooding events. Again, the presence of glauconite in sandstone indicates marine to marginal marine conditions. The upper Esplin Point Member capping the Temple Cap has lithofacies similar to the Sinawava.

Fractures in the Navajo Sandstone and Temple Cap Formation consist of two types: (1) early, bitumen and gouge-filled, silica-cemented, impermeable fractures (figure 5.8), and (2) later, typically open (little gouge or cement), permeable fractures. The later fractures are related to fault-propagation folding during the Sevier orogeny after deep burial (Royce and others, 1975).

HYDROCARBON SOURCE AND SEALS

The lack of good Cretaceous source rocks was blamed for early exploration failures in the central Utah thrust belt; however, oil and gas shows were common in Mississippian, Permian, Triassic, and Jurassic rocks. Although minor coaly beds are present in the Upper Cretaceous rocks in the eastern part of central Utah, the Cretaceous strata are more fluvial and nonmarine to the west and probably are only gas-prone. Therefore, unlike the producing structures of the thrust belt in northern Utah and southwestern Wyoming, the structures and faults of central Utah are not in contact with high-quality marine Cretaceous source rocks.

Figure 5.8. *Cross-bedding in fine-grained sandstone deposited in an eolian dune environment of the Navajo Sandstone, from the Kings Meadow Ranches No. 17-3 well (slabbed core from 6776 feet), Covenant field. Also shown are early, bitumen and gouge-filled, silica-cemented, impermeable fractures that have slight offsets.*

Figure 5.9. *Typical White Throne Member of the Temple Cap Formation, from the Kings Meadow Ranches No. 17-3 well (slabbed core from 6669 feet), Covenant field, showing cross-bedding in fine-grained sandstone deposited in a coastal dune environment.*

A

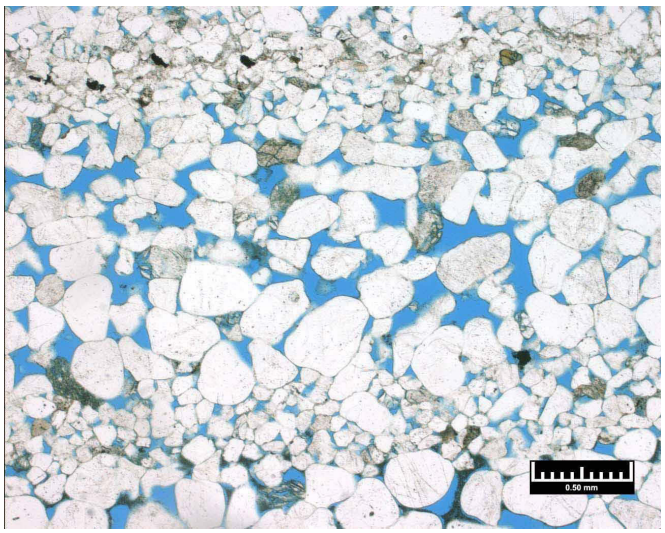

B

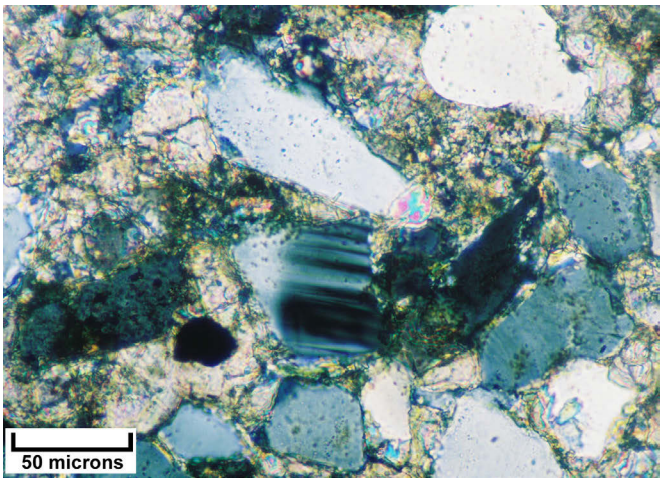

Figure 5.10. *Representative photomicrographs from the Navajo Sandstone in the Kings Meadow Ranches No. 17-3 well.* ***A.*** *Bimodal distribution of subangular to subrounded quartz sand and silt (plane light) deposited in a vast eolian desert dune field. Note a few fractured and corroded K-feldspar grains are present. Blue space is intergranular porosity. Porosity = 14.8%, permeability = 149 mD based on core-plug analysis, 6773 feet. Courtesy of Wolverine Gas & Oil Corporation.* ***B.*** *Dolomite cement around a subangular microcline (striped gray) feldspar among bimodally distributed quartz grains (crossed nicols). Kings Meadow Ranches No. 17-3 well, 6757 feet. Courtesy of David E. Eby, Eby Petrography & Consulting, Inc.*

With the discovery of Covenant and Providence fields, a viable source rock is proven in the central Utah thrust belt; however, the exact geochemical correlation between the oil produced at Covenant and Providence and the formation acting as the source rock has not been demonstrated. Several source candidates are present in the region (figure 5.6) and include the Mississippian Delle Phosphatic Member of the Deseret Limestone and equivalent formations (figure 5.13) (Sandberg and Gutschick, 1984), the Mississippian Chainman Shale (Poole and Claypool, 1984; Sandberg and Gutschick, 1984; Wavrek and others, 2005, 2007) (figures 5.13 and 5.14), the Mississippian Long Trail Shale of the Great Blue Limestone (Poole and Clay-

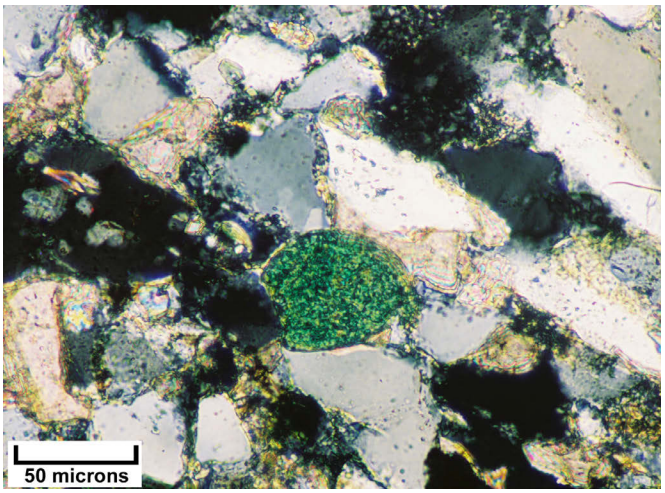

Figure 5.11. *Photomicrograph (crossed nicols) of a single, well-rounded glauconite grain (green) within a matrix of angular to subangular quartz grains surrounded by dolomite cement, near the top of the Sinawava Member of the Temple Cap Formation, Kings Meadow Ranches No. 17-3 well, 6687 feet. Courtesy of David E. Eby, Eby Petrography & Consulting, Inc.*

Figure 5.12. *Representative Sinawava Member of the Temple Cap Formation, from the Kings Meadow Ranches No. 17-3 well (slabbed core from 6752 feet), Covenant field, showing siltstone laminae and shale deposited in a coastal sabkha to tidal flat environment.*

pool, 1984), the Mississippian Doughnut Formation (Swetland and others, 1978), the Mississippian-Pennsylvanian Manning Canyon Shale (Swetland and others, 1978; Poole and Claypool, 1984; Chidsey and others, 2007), and the Permian Park City/Phosphoria Formation (Claypool and others, 1978; Sprinkel and others, 1997; Peterson, 2000, 2001). Total organic carbon for some units within these rocks is 15%. The regional distribution of these formations is shown by Peterson (2001).

What we do know about the possible correlation between the Covenant field oil and its source is based on limited or negative evidence. A graph (figure 5.15) plotting stable carbon-13 isotopes of saturated versus aromatic hydrocarbons from the Covenant field oil with other well-documented Mississippian and Permian oils shows the Covenant oil was derived from marine source beds. This conclusion is based on its canonical variable (CV) of less than 0.47 (Sofer, 1984). Marine Cretaceous source beds are not found in central Utah whereas the geochemistry of the Covenant oil is similar to known Paleozoic oils that have been correlated to source beds in the region (table 5.1). Furthermore, we believe we can eliminate the Mississippian Chainman Shale and the Permian Phosphoria Formation as possible sources based on a graph plotting CV versus pristane/phytane values (figure 5.16). Thus, the Covenant field oil is likely derived from a local Carboniferous source within the central Utah thrust belt (see Wavrek and others, 2005, 2007).

As stated earlier, thrusting in this area is Cretaceous to early Tertiary in age. Most of the hydrocarbon generation and migration probably occurred during this period; however, some could have started as early as Permian or Triassic time in the older Paleozoic rocks and as late as Tertiary time in Mesozoic rocks. Hydrocarbons were then expelled and subsequently migrated into the overlying traps, primarily along fault planes or through porous Paleozoic and Mesozoic carrier beds. Late Tertiary extension in this area may have disrupted the traps more than in the productive thrust belt of northern Utah and southwestern Wyoming.

Oil migrating from the Mississippian Chainman Shale in western Utah requires a post-Sevier-orogeny, long-distance migration, and must have circumvented the Sevier arch where no Mississippian rocks are present. Potential hydrocarbon sources in the Mississippian Delle Phosphatic Member and Mississippian-Pennsylvanian Manning Canyon Shale (containing 2 to 15% TOC) would have to have been generated outside the Pennsylvanian-Permian Oquirrh basin to the north where they would have been deeply buried and too highly "cooked," resulting in the migration of hydrocarbons prior to the formation of the thrust belt traps. In central Utah, the question remains whether these rocks have been buried deep enough on the western parts of the hanging walls of the thrust faults to generate hydrocarbons. However, at least as far east as the Paxton thrust (figure 1.3B), the Mississippian section lies just below the basal décollement in the footwall where thrust loading could have generated hydrocarbons.

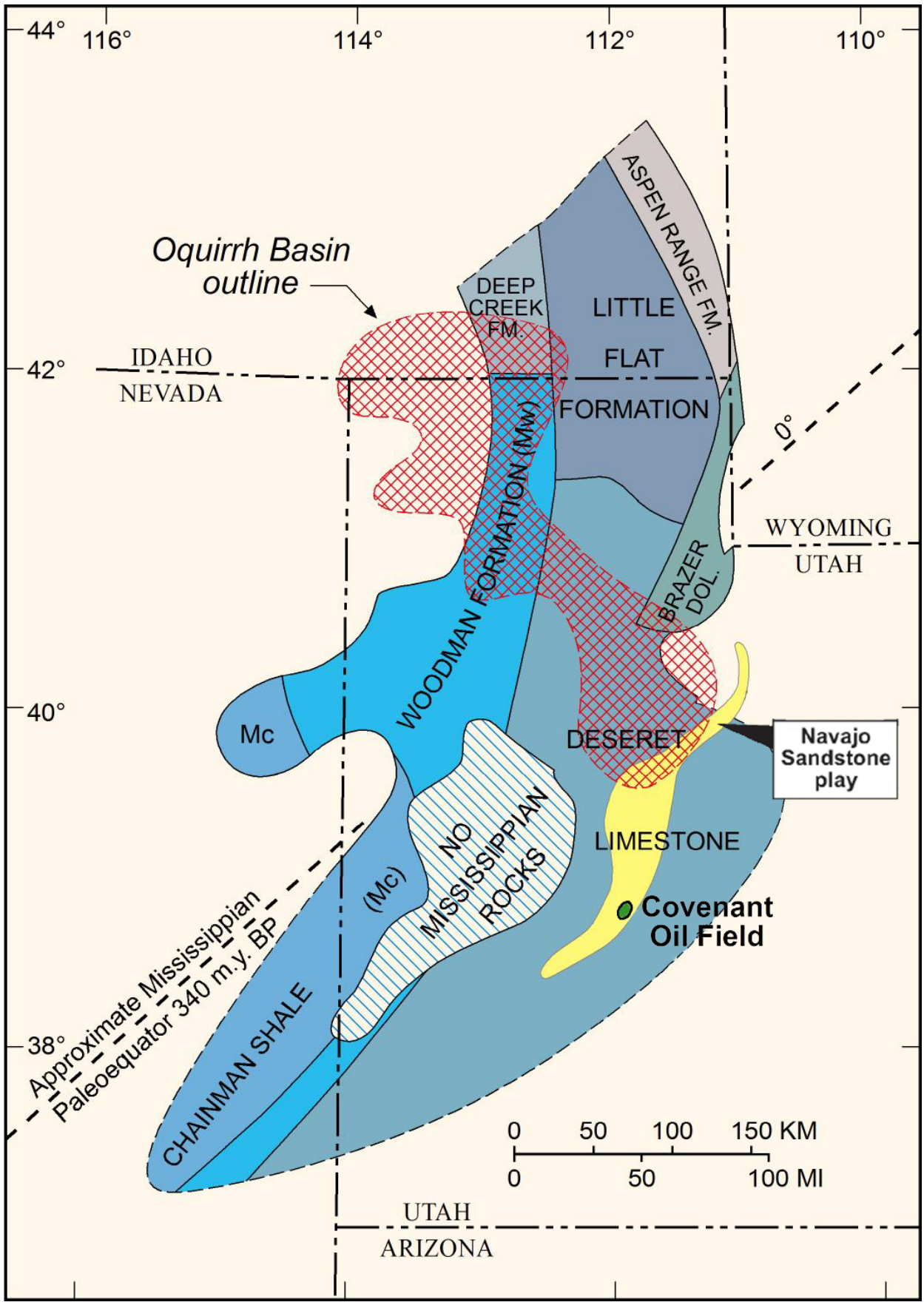

Figure 5.13. *Location of the Mississippian Delle Phosphatic Member present in the Deseret Limestone and other Mississippian formations. Modified from Sandberg and Gutschick (1984).*

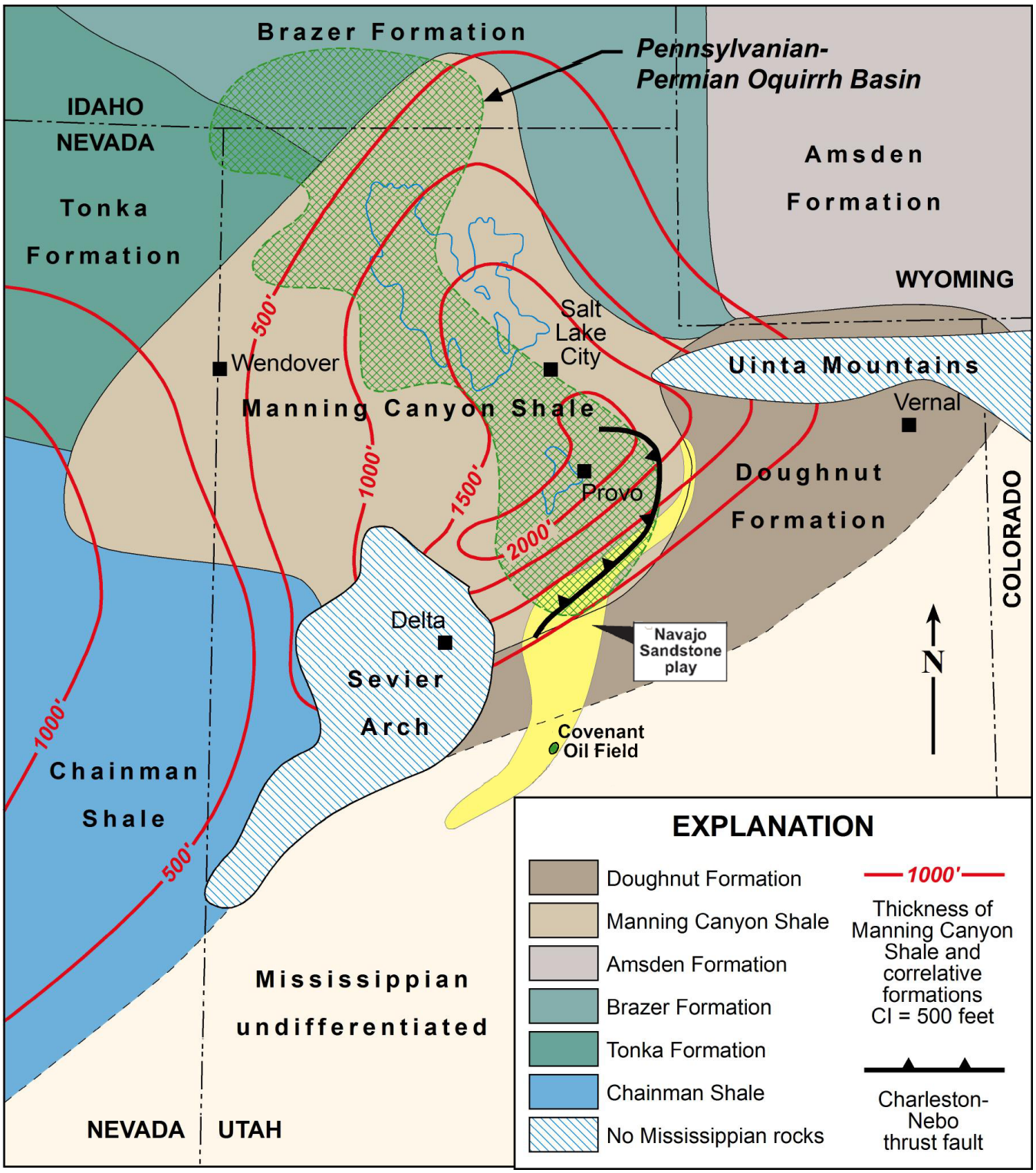

Figure 5.14. *Location and thickness of the Manning Canyon Shale and correlative formations. Modified from Moyle (1958).*

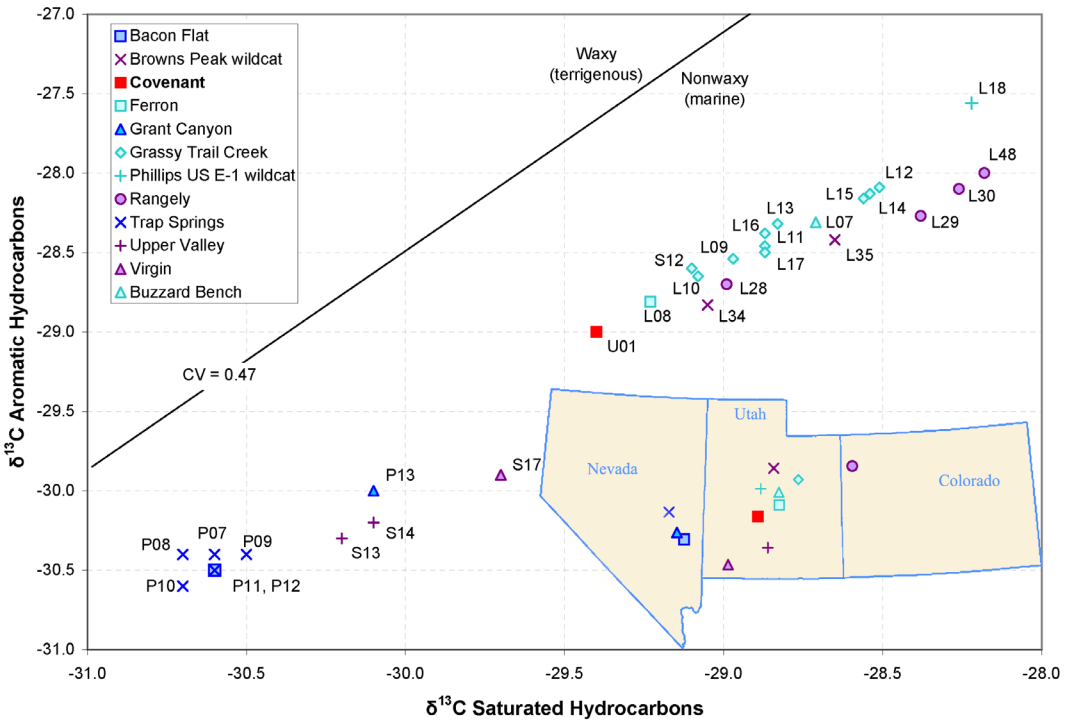

Figure 5.15. *Stable carbon-13 isotope of saturated versus aromatic hydrocarbons from the Covenant field oil and other key oils from Utah, Colorado, and Nevada (see inset for field locations). Units on both axes of the graph depict the carbon isotopes measured in the oil versus the Pee Dee Belemnite (PDB) standard in parts per thousand; a negative value implies the oil sample is depleted in the heavy isotope relative to the standard. The line labeled CV = 0.47 (CV = canonical variable) divides waxy (terrigenous) and nonwaxy (marine) sources (Sofer, 1984), and shows that oils in this region are derived from marine sources.*

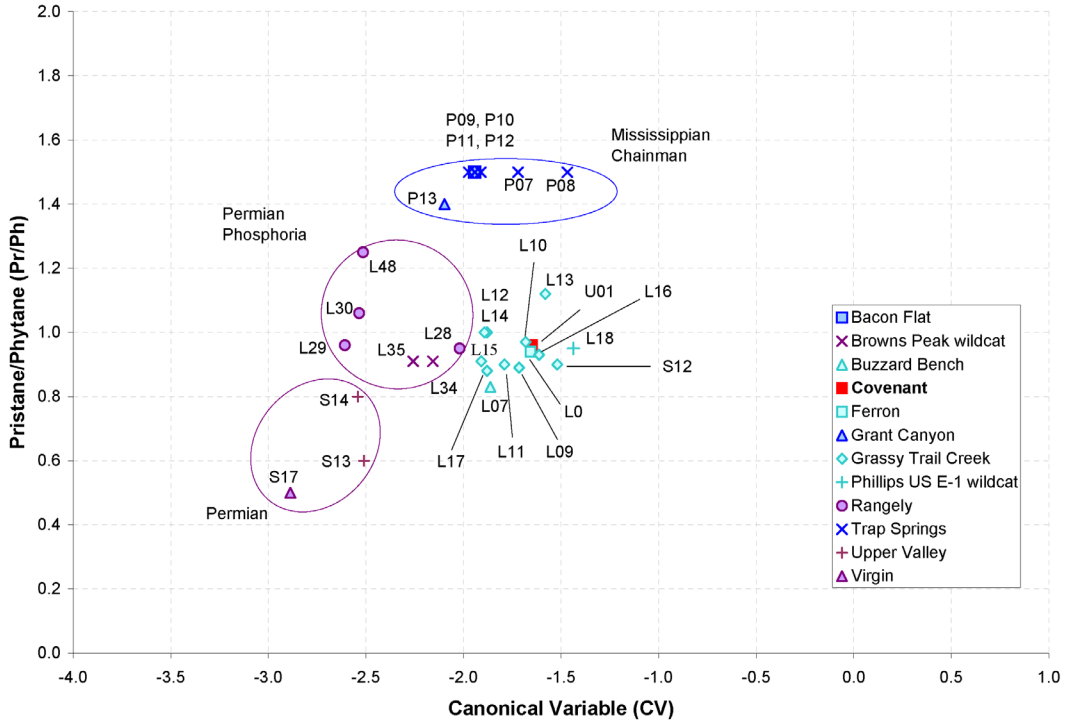

Figure 5.16. *Canonical variable (CV) versus pristane/phytane values from the Covenant field oil and other key oils from Utah, Colorado, and Nevada (see figure 5.15 for field locations). The plot suggests the Covenant field oil is not likely derived from the Mississippian Chainman Shale, a major source of oil in Nevada, or the Permian Phosphoria Formation, a source of oil in Wyoming, northwestern Colorado, and northeastern Utah. This conclusion does not preclude the source of oil in the Covenant field from being a local Carboniferous organic-rich source bed. Correlation presented here is based on this plot only; other geochemical parameters should be used to fully evaluate the correlation of oils.*

Table 5.1. *Geochemistry of oils from Utah, Colorado, and Nevada (see figure 5.15 for field locations).*

ID	Field	Reservoir	Reservoir Age	Oil Type	API[1]	Sulfur[2]	δ13C Sat[3]	δ13C Aro[4]	CV[5]	Pr/Ph[6]	CPI[7]	Well Name	County	State	Depth (ft)
P12[8]	Bacon Flat	Guilmette Formation	D	Mississippian Chainman	24	0.5	-30.6	-30.5	-1.94	1.5	1.5	Bacon Flat 1	Nye	Nevada	5316–5333
L34[9]	Browns Peak wildcat	Entrada Sandstone?	J	Permian Phosphoria	30.8	0.74	-29.05	-28.83	-2.16	0.91	1	Browns Peak Unit 1-G24	Utah	Utah	5788–5812
L35[9]	Browns Peak wildcat	Entrada Sandstone?	J	Permian Phosphoria	35.5	0.74	-28.65	-28.42	-2.26	0.91	0.97	Browns Peak Unit 1-G24	Utah	Utah	5788–5812
L07[9]	Buzzard Bench	Moenkopi Formation	Tr	Uncertain Paleozoic	n.d.	n.d.	-28.71	-28.31	-1.86	0.83	0.99	Federal 41-33	Emery	Utah	9462–9472
U01[10]	Covenant	Navajo Sandstone	J	Carboniferous	40.5	0.48	-29.4	-29	-1.65	0.96	1	Kings Meadow Ranches 17-1	Sevier	Utah	6215–6225
L08[9]	Ferron	Kaibab Limestone	P	Uncertain Paleozoic	35	n.d.	-29.23	-28.81	-1.66	0.94	0.97	Pan Am 3 (Ferron Unit 42-21)	Emery	Utah	7154–7176
P13[8]	Grant Canyon	Guilmette Formation	D	Mississippian Chainman	27	0.5	-30.1	-30	-2.1	1.4	1	Grant Canyon 1	Nye	Nevada	4374–4426
LO9[9]	Grassy Trail Creek	Moenkopi Formation	Tr	Uncertain Paleozoic	n.d.	n.d.	-28.97	-28.54	-1.71	0.89	0.98	Federal 11-23	Emery	Utah	3910–3940
L10[9]	Grassy Trail Creek	Moenkopi Formation	Tr	Uncertain Paleozoic	n.d.	n.d.	-29.08	-28.65	-1.68	0.97	1.01	Federal 11-33	Emery	Utah	3420–3906
L11[9]	Grassy Trail Creek	Moenkopi Formation	Tr	Uncertain Paleozoic	n.d.	n.d.	-28.87	-28.46	-1.79	0.9	0.98	Federal 1-14	Emery	Utah	3687–4010
L12[9]	Grassy Trail Creek	Moenkopi Formation	Tr	Uncertain Paleozoic	n d.	n d.	-28.51	-28.09	-1.88	1	1	Federal 11-41	Emery	Utah	3540–3911
L13[9]	Grassy Trail Creek	Moenkopi Formation	Tr	Uncertain Paleozoic	36.5	0.33	-28.83	-28.32	-1.58	1.12	0.97	Federal 11-41	Emery	Utah	3540–3911
L14[9]	Grassy Trail Creek	Moenkopi Formation	Tr	Uncertain Paleozoic	n.d.	n.d.	-28.54	-28.13	-1.89	1	0.99	Federal 11-42	Emery	Utah	3453–3654
L15[9]	Grassy Trail Creek	Moenkopi Formation	Tr	Uncertain Paleozoic	n d.	n.d.	-28.56	-28 16	-1.91	0.91	0.99	Federal 11-43	Emery	Utah	3382–3966
L16[9]	Grassy Trail Creek	Moenkopi Formation	Tr	Uncertain Paleozoic	n.d.	n.d.	-28.87	-28.38	-1.61	0.93	0.98	Federal 12-32	Emery	Utah	3627–3970
L17[9]	Grassy Trail Creek	Moenkopi Formation	Tr	Uncertain Paleozoic	n d.	n.d.	-28.87	-28.5	-1.88	0.88	0.99	State 2-43X	Emery	Utah	3669–4162
S12[11]	Grassy Trail Creek	Moenkopi Formation	Tr	Uncertain Paleozoic	42.5	n.d.	-29.1	-28.6	-1.52	0.9	n.d.	Grassy Trail 1-33 Federal	Emery	Utah	3420–3906
L18[9]	Phillips US E-1 wildcat	Sinbad Mbr. of Moenkopi Fm.	Tr	Uncertain Paleozoic	n.d.	n.d.	-28.22	-27.56	-1.44	0.95	0.98	United States E-1	Sanpete	Utah	16,115–16,425
L28[9]	Rangely	Weber Sandstone	IP	Permian Phosphoria	33.1	0.73	-28.99	-28.7	-2.02	0.95	1.02	Equity Federal 1-7	Rio Blanco	Colorado	6505–6535
L29[9]	Rangely	Weber Sandstone	IP	Permian Phosphoria	32.8	n.d.	-28.38	-28.27	-2.61	0.96	1	Equity Federal 1-7	Rio Blanco	Colorado	6505–6535
L30[9]	Rangely	Weber Sandstone	IP	Permian Phosphoria	34.5	n d.	-28.26	-28.1	-2.53	1.06	1	Pennell-Hayes 1-31	Rio Blanco	Colorado	6175–6345
L48[9]	Rangely	Morrison Formation	J	Permian Phosphoria-Cretaceous Mancos mix	33.3	n d.	-28.18	-28	-2.51	1.25	1.01	McLaughlin Stuart 2	Rio Blanco	Colorado	3225–3237
P07[8]	Trap Springs	Garrett Ranch Group	T	Mississippian Chainman	30	0.6	-30.6	-30.4	-1.72	1.5	1	Britton 13-21	Nye	Nevada	3976–4140
P08[8]	Trap Springs	Garrett Ranch Group	T	Mississippian Chainman	29	0.6	-30.7	-30.4	-1.47	1.5	1	Trap Springs 19	Nye	Nevada	3374–4100
P09[8]	Trap Springs	Garrett Ranch Group	T	Mississippian Chainman	21	0.6	-30.5	-30.4	-1.97	1.5	1	Zusspan 24-1	Nye	Nevada	4910–4944
P10[8]	Trap Springs	Garrett Ranch Group	T	Mississippian Chainman	19	0.6	-30.7	-30.6	-1.91	1.5	1.00	Trap Springs 1	Nye	Nevada	4220–4853
P11[8]	Trap Springs	Garrett Ranch Group	T	Mississippian Chainman	24	0.5	-30.6	-30.5	-1.94	1.5	1	Trap Springs 3	Nye	Nevada	3269–4083
S13[11]	Upper Valley	Kaibab Limestone	P	Permian	26.8	2.71	-30.2	-30.3	-2.51	0.6	n.d.	Upper Valley Unit 31	Garfield	Utah	6895–7020
S14[11]	Upper Valley	Kaibab Limestone	P	Permian	19.9	2.94	-30.1	-30.2	-2.54	0.8	n.d.	Little Valley 1	Garfield	Utah	7606–7630
S17[11]	Virgin	Kaibab Limestone	P	Permian	n.d.	n.d.	-29.7	-29.9	-2.89	0.5	n.d.	tank battery	Washington	Utah	surface

[1] oil gravity in degrees API
[2] weight percent sulfur
[3] δ13C saturates in Pee Dee Belemnite (PDB) standard in parts per thousand
[4] δ13C aromatics in Pee Dee Belemnite (PDB) standard in parts per thousand
[5] canonical variable (Sofer, 1984)
[6] pristane/phytane
[7] carbon preferential index (Hunt, 1979)
[8] Poole and Claypool, 1984
[9] Lillis and others, 2003
[10] Baseline DGSI, 2005
[11] Sprinkel and others, 1997
n.d. = no data

T - Tertiary
J - Jurassic
Tr - Triassic
P - Permian
IP - Pennsylvanian
D - Devonian

Wavrek and others (2010) conducted a detailed analysis of the hydrocarbon charge at Covenant and Providence fields. Their work indicates differential thermal stress and secondary alteration processes explain the differences in hydrocarbon constituents between the fields (Wavrek and others, 2010). The Covenant source was on the Aurora/Valley Mountain thrust plate of Schelling and others (2007). Primary migration occurred 90 to 100 Ma into a paleotrap. When the current Covenant trap formed 70 to 80 Ma, remigration stripped the original gas-saturated oil of volatiles (Wavrek and others, 2010). The potential Providence source was more proximal, within the Salina thrust plate, and hydrocarbon migration occurred 70 to 80 Ma, concurrent with the creation of the Providence structure (Wavrek and others, 2010). No stripping of volatiles occurred. Finally, the presence of significant amounts of carbon dioxide and nitrogen with hydrocarbon gases at Providence field likely represents a mixing event from sources separate from those responsible for the hydrocarbon charge (Wavrek and others, 2010). These inorganic components could have been generated and migrated from the Tertiary (Oligocene) volcanic activity that occurred in the region south of the Covenant and Providence field areas.

The principal regional seal for the Navajo and White Throne producing zones consists of salt, gypsum, mudstone, and shale in the Rich and Twelvemile Canyon Members of the overlying Jurassic Arapien Formation (figures 5.6 and 5.17). Mudstone and argillaceous limestone intervals within the Sinawava Member (figure 5.12) and interbedded limestone in the White Throne are the principal seals at Providence and secondary seals at Covenant. Hanging-wall/footwall cutoffs along splay and back thrust faults may also act as local seals. Interdunal and other low permeable lithofacies within the Navajo and White Throne, and possible unrecognized splay and back-thrust faults, may act as local seals, barriers, or baffles to fluid flow.

STRUCTURE AND TRAPPING MECHANISMS

Internal deformation within large-scale thrust plates includes frontal and lateral duplex zones. The deformation front along the leading edge of these major thrusts, particularly the Paxton and Gunnison detachment-Salina thrusts, includes com-

Figure 5.17. *Arapien Formation exposed in Salina Canyon north of Covenant field; inset photo of salt core from Redmond quarry in the Arapien north of the town of Salina.*

plex back thrusting, tectonic-wedge formation, triangle zones, and passive-roof duplexing (Schelling and others, 2005, 2007). Fault-propagation/fault-bend folds and low-amplitude anticlines in both the hanging walls and footwalls of thrusts associated with these features may form multiple structural traps—the targets of the Covenant and Providence discoveries. These features are obscured by complex surface geology which includes (1) major folds (figure 5.18), (2) angular unconformities, (3) Oligocene volcanic rocks, (4) Basin and Range-age (Miocene-Holocene) listric(?) normal faulting, and (5) local diapirism. Updip pinchout and isolated stratigraphic traps in the Mesozoic section are also possible.

The Gunnison thrust in the eastern play area is primarily a bedding-plane fault developed in weak mudstone and evaporite beds of the Arapien Shale. Thrust imbricates or imbricate fans above and antiformal stacks of horses (a horse block is generally defined as any block bounded by faults) forming a duplex below the Gunnison, Salina, and other thrusts create multiple, potential drilling targets (figure 2.10) (Villien and Kligfield, 1986). Jurassic extensional faults may be the key to hydrocarbon migration pathways and locating antiformal stacks that may contain traps along thrusts (Schelling and others, 2005; Strickland and others, 2005).

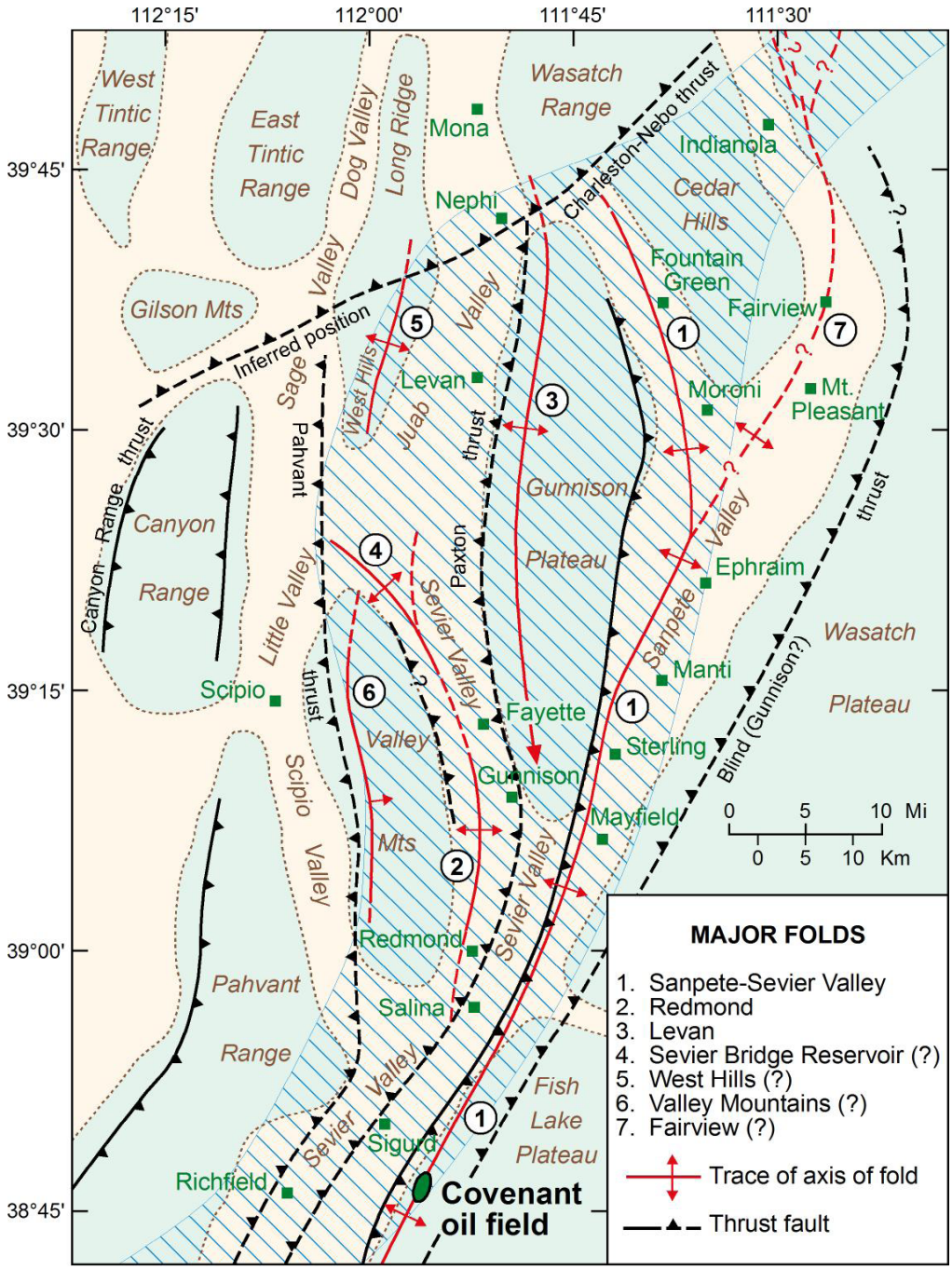

Figure 5.18. *Major folds in central Utah. Modified from Witkind (1982). Play area represented by hachured pattern.*

Covenant field (figures 1.3B and 5.1), Sevier County, is located along the east flank of the Sanpete-Sevier Valley fold (figure 5.18). The Kings Meadow Ranches No. 17-1 discovery well (SE1/4NW1/4 section 17, T. 23 S., R. 1 W., SLBL&M) was drilled updip from two abandoned wells about 2 miles (3 km) to the north: the Standard Oil of California Sigurd Unit No. 1 (NE1/4SE1/4 section 32, T. 22 S., R. 1 W., SLBL&M) drilled in 1957, and the Chevron USA Salina Unit No. 1 (NE1/4NE1/4 section 33, T. 22 S., R. 1 W., SLBL&M) drilled in 1980. The White Throne Member of the Temple Cap Formation was encountered at subsea depths of -3390 feet (-1033 m) and -2973 feet (-906 m), respectively, in these wells. The dipmeter in the Salina Unit No. 1 well showed 16° structural dip to the northwest in the Navajo/Temple Cap. This dip combined with seismic data indicate a structural high to the south. The Kings Meadow Ranches No. 17-1 well penetrated the White Throne at a subsea depth of -94 feet (-29 m).

The Covenant field trap is an elongate, symmetric, northeast-trending fault-propagation/fault-bend anticline (figure 5.19) that has nearly 800 feet (270 m) of structural closure and a 450-foot (150 m) oil column (Strickland and others, 2005; Chidsey and others, 2007). The Navajo/White Throne oil-filled reservoir covers about 960 acres (390 ha). The structure formed above a series of splay thrusts in a passive roof duplex along the Gunnison thrust and west of a frontal triangle zone within the Arapien Formation (figure 5.20). The Navajo, Temple Cap, and Arapien Formations are repeated due to an east-dipping back-thrust detachment within the structure. This back thrust forms a hanging-wall cutoff along the west flank and north-plunging nose of the fold.

Providence field lies on trend with and has a similar trap to that of Covenant field to the southwest—an elongate, symmetric, northeast-trending fault-propagation/fault-bend anticline (figure 5.21). The structure formed above a series of splay thrusts in a passive roof duplex along the Salina thrust and west of a probable frontal triangle zone within the Arapien Formation (figure 5.22), west of the Ephraim fault (not shown on figure 5.22). The Federal Arapien Valley No. 24-1 discovery well (SW1/4NW1/4 section 24, T. 20 S., R. 1 E., SLBL&M) was drilled based on geophysical seismic data combined with structural cross section constructions. The Navajo Sandstone is repeated and each is both oil and gas productive (figure 5.22). The well penetrated a repeated Navajo section at subsea-level depths of -3356 feet (-1023 m) and -6541 feet (-1994 m), respectively (figure 5.22).

The upper Navajo ("First" Navajo) trap is formed by the main fault-bend fold along the Salina thrust (figures 5.21 and 5.22). The amount of structural closure has yet to be fully defined; the height of the hydrocarbon column is about 350 feet (107 m). The lower Navajo ("Second" Navajo) trap is a relatively small, isolated horse block under the main fault-bend fold (Chidsey and others, 2011). The height of the hydrocarbon column is about 280 feet (85 m). Unlike Covenant field, no back thrust is present within the trap by the current interpretation. The dipmeter in the Arapien Valley No. 24-1 well indicates that the First Navajo was encountered on the crest of the structure while the Second Navajo dips steeply east perhaps due to drag along the overlying thrust splay.

RESERVOIR PROPERTIES

The Navajo Sandstone and White Throne Member of the Temple Cap Formation have heterogeneous reservoir properties because of (1) various cyclic dune lithofacies with better porosity and permeability in certain dune morphologies, (2) diagenetic effects, (3) extensive fracturing, and a few interbeds of marine limestone in the case of the White Throne. Most of these characteristics can be observed in outcrops around the play area (figure 1.3B) (Dalrymple and Morris, 2007) and in southwestern Utah. Genetic units of eolian sandstone deposits are separated by 1st-order bounding surfaces formed by interdune deposits or major diastems. Internal bounding surfaces are also found within dune cross-beds (Ahlbrandt and Fryberger, 1982; Fryberger, 1990; Grammer and others, 2004). Stacking surfaces or 2nd-order bounding surfaces (superposition surfaces) within a single genetic unit can divide the cross-strata of two dunes and are formed by migrating dunes superimposed on the slipfaces of the underlying dunes (Fryberger, 1990; Grammer and others, 2004; Morris and others, 2005). Growth surfaces or 3rd-order bounding surfaces are high-angle reactivation surfaces dividing sets of ripple strata related to the advance of a single dune (Fryberger, 1990; Grammer and others, 2004). These bounding surfaces represent possible barriers or baffles to fluid flow, both vertically and horizontally, within the Navajo/White Throne reservoirs. Identification and correlation of the numerous bounding surfaces as well as recognition of fracture set orientations and types in individual Navajo/White Throne reservoirs are critical to understanding their effects on production rates, petroleum movement pathways, directionally drilled well plans, and future pressure maintenance programs.

The average porosity for the Navajo Sandstone and White Throne Member at Covenant field is 12% (Strickland and others, 2005; Chidsey and others, 2007); the average grain density is 2.651 g/cm^3 based on core-plug analysis. The average porosity for the First and Second Navajo Sandstone at Providence field is 10.7% and 5.5%, respectively (Chidsey and others, 2011). Sandstone exhibits significant secondary porosity in the form of fracturing. At Covenant field, permeabilities in the Navajo and White Throne from the core data are upwards of 100 mD (8 mD to less the 4 mD at Providence field [Chidsey and others, 2011]). The best permeability within Navajo and White Throne dune deposits is along bounding surfaces (bedding planes), with preferred directions along the dip and strike of the individual slipfaces or lee faces (cross-beds) (figure 3.21; Lindquist, 1983). Porosity and permeability should be greatest in thickly laminated avalanche deposits (Hunter, 1977; Schenk, 1981). Interdunes,

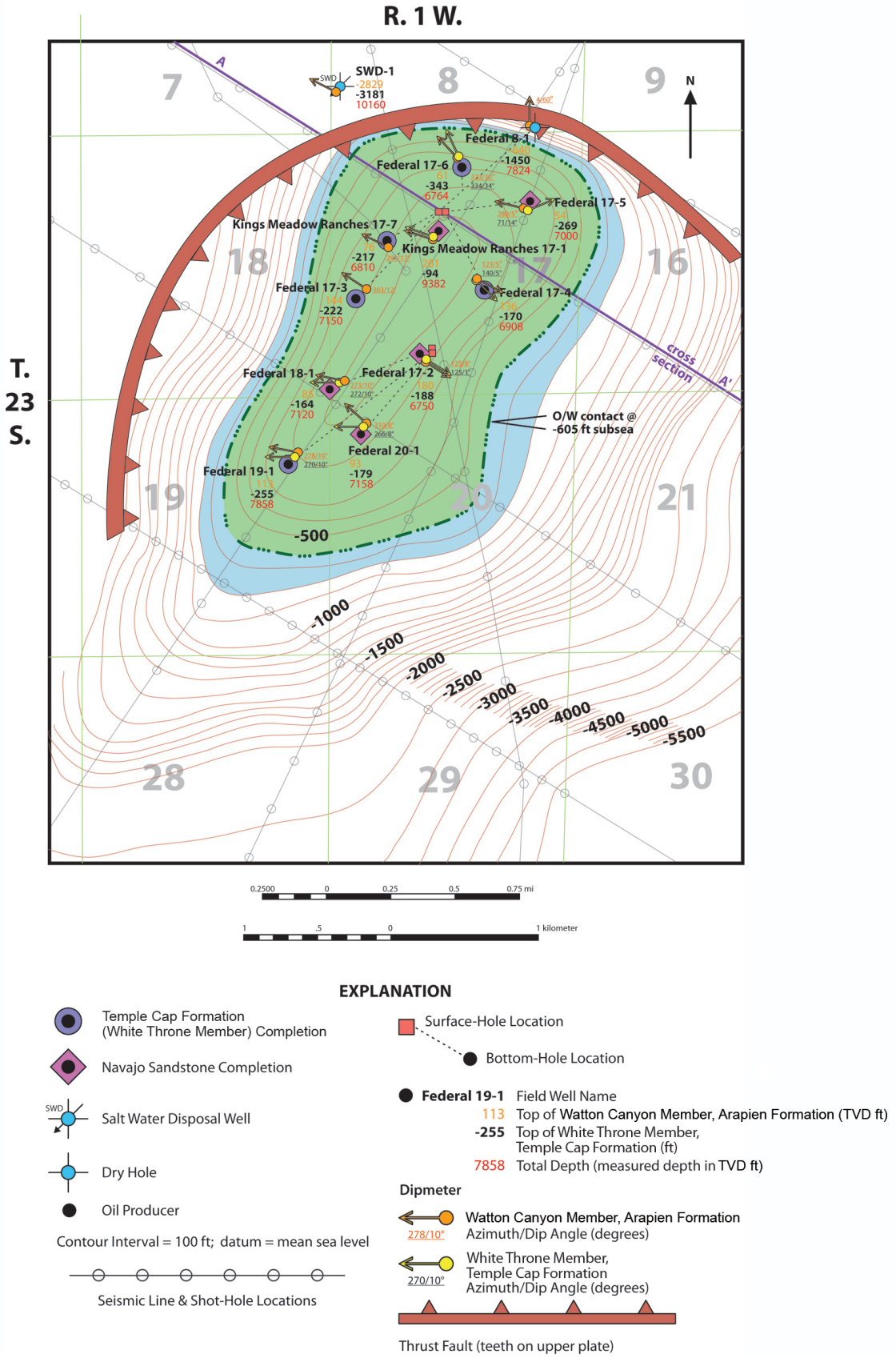

Figure 5.19. *Structure contour map of the top of the White Throne Member of the Temple Cap Formation, Covenant field, based on subsurface well control and seismic data. Original map courtesy of Wolverine Gas & Oil Company; after Chidsey and others (2007). Tops corrected to true vertical depths (TVD). Contour interval = 100 feet, datum = mean sea level. Cross section A–A', which extends beyond the edges of this figure, is shown on figure 5.20.*

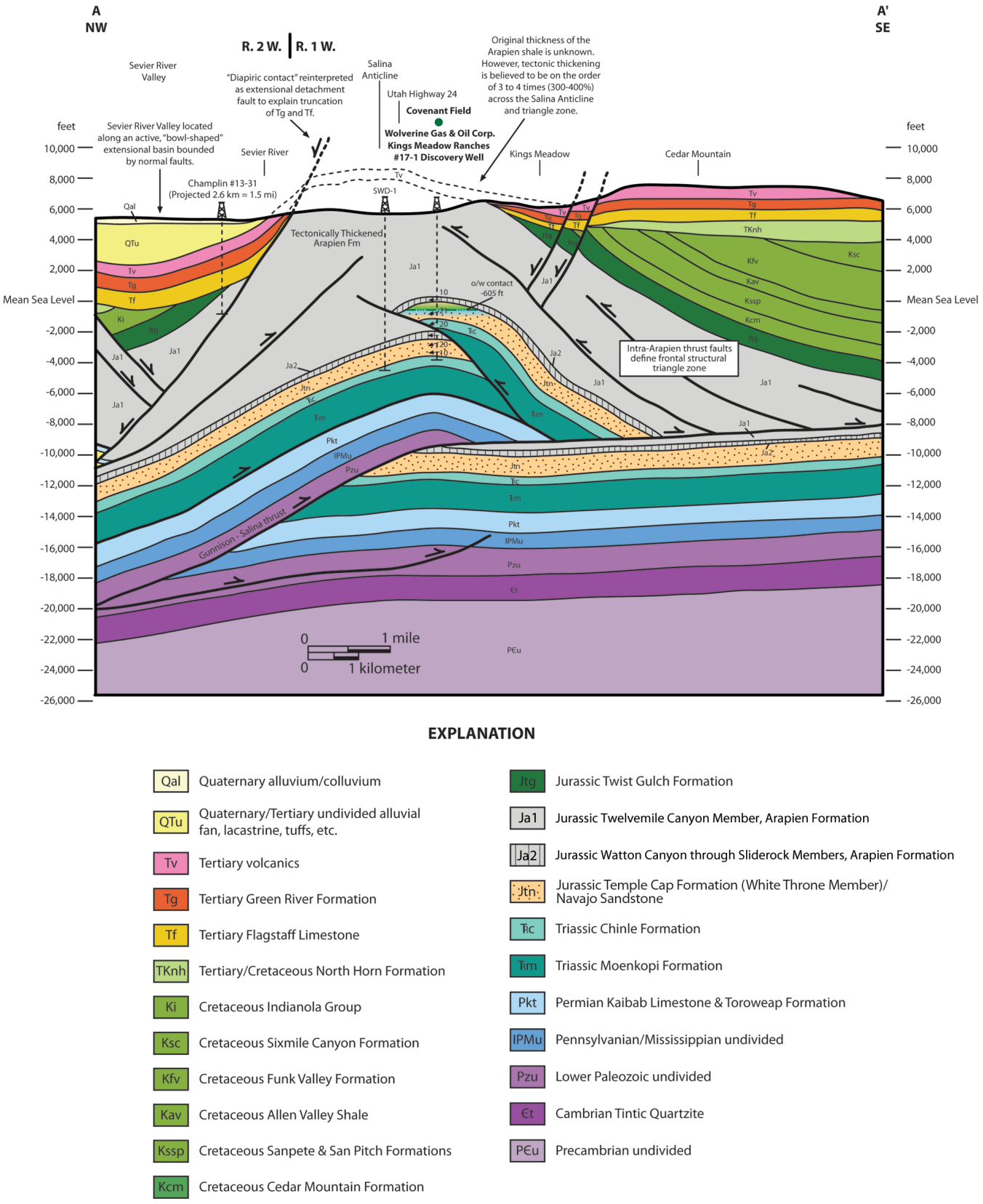

EXPLANATION

Qal	Quaternary alluvium/colluvium
QTu	Quaternary/Tertiary undivided alluvial fan, lacastrine, tuffs, etc.
Tv	Tertiary volcanics
Tg	Tertiary Green River Formation
Tf	Tertiary Flagstaff Limestone
TKnh	Tertiary/Cretaceous North Horn Formation
Ki	Cretaceous Indianola Group
Ksc	Cretaceous Sixmile Canyon Formation
Kfv	Cretaceous Funk Valley Formation
Kav	Cretaceous Allen Valley Shale
Kssp	Cretaceous Sanpete & San Pitch Formations
Kcm	Cretaceous Cedar Mountain Formation
Jtg	Jurassic Twist Gulch Formation
Ja1	Jurassic Twelvemile Canyon Member, Arapien Formation
Ja2	Jurassic Watton Canyon through Sliderock Members, Arapien Formation
Jtn	Jurassic Temple Cap Formation (White Throne Member)/ Navajo Sandstone
Trc	Triassic Chinle Formation
Trm	Triassic Moenkopi Formation
Pkt	Permian Kaibab Limestone & Toroweap Formation
IPMu	Pennsylvanian/Mississippian undivided
Pzu	Lower Paleozoic undivided
Є t	Cambrian Tintic Quartzite
PЄu	Precambrian undivided

Figure 5.20. *Northwest-southeast structural cross section through Covenant field. Modified from Schelling and others (2005), Chidsey and others (2007). Note small back thrust through the anticline that results in a repeated Navajo Sandstone/Temple Cap Formation section. Line of cross section A–A' shown on figures 5.1 and 5.19.*

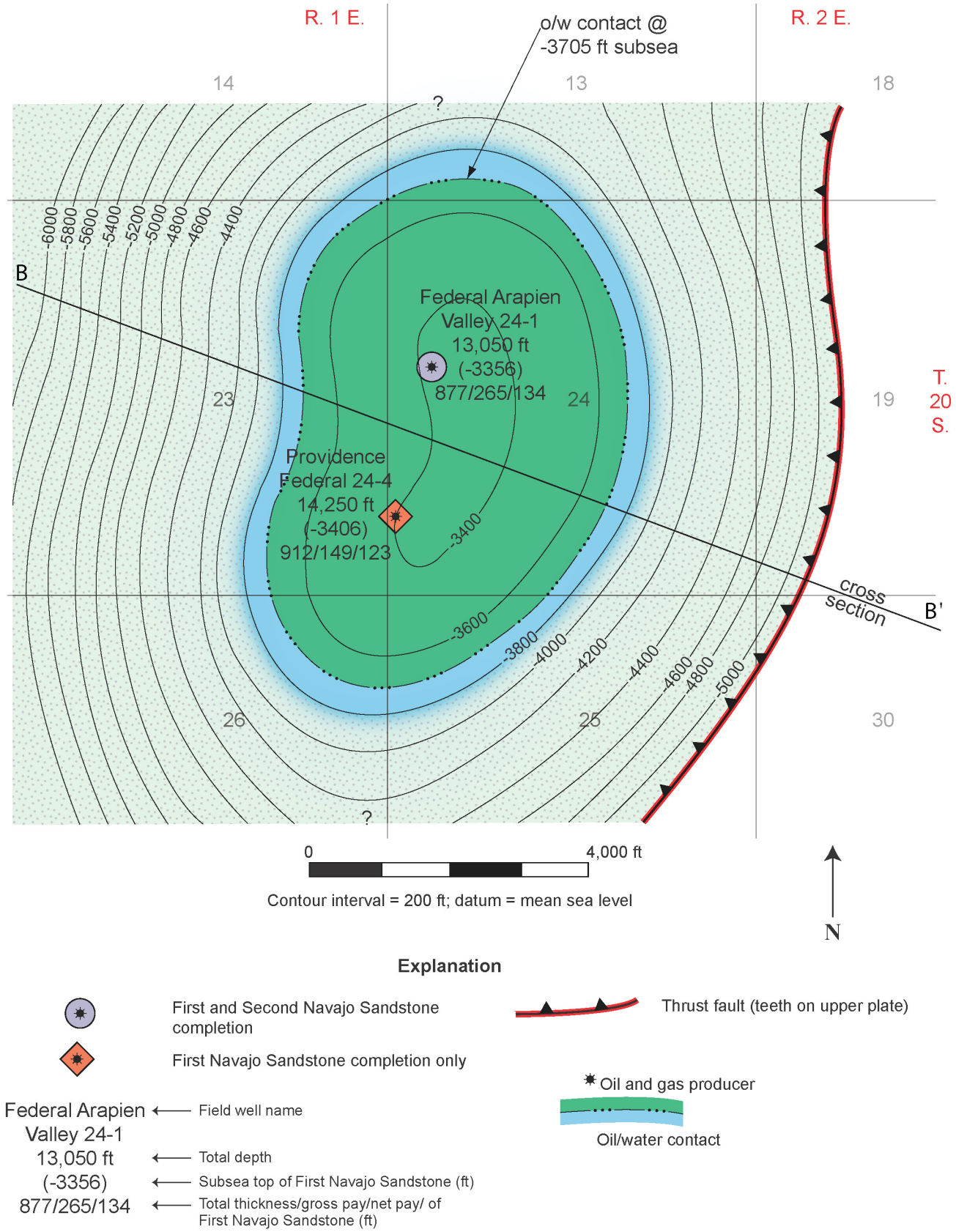

Figure 5.21. *Structure contour map of the top of the First Navajo Sandstone, Providence field, based on subsurface well control and the structural cross section. Contour interval = 200 feet, datum = mean sea level. Cross section B–B', which extends beyond the edges of this figure, is shown on figure 5.22. From Chidsey and others (2011).*

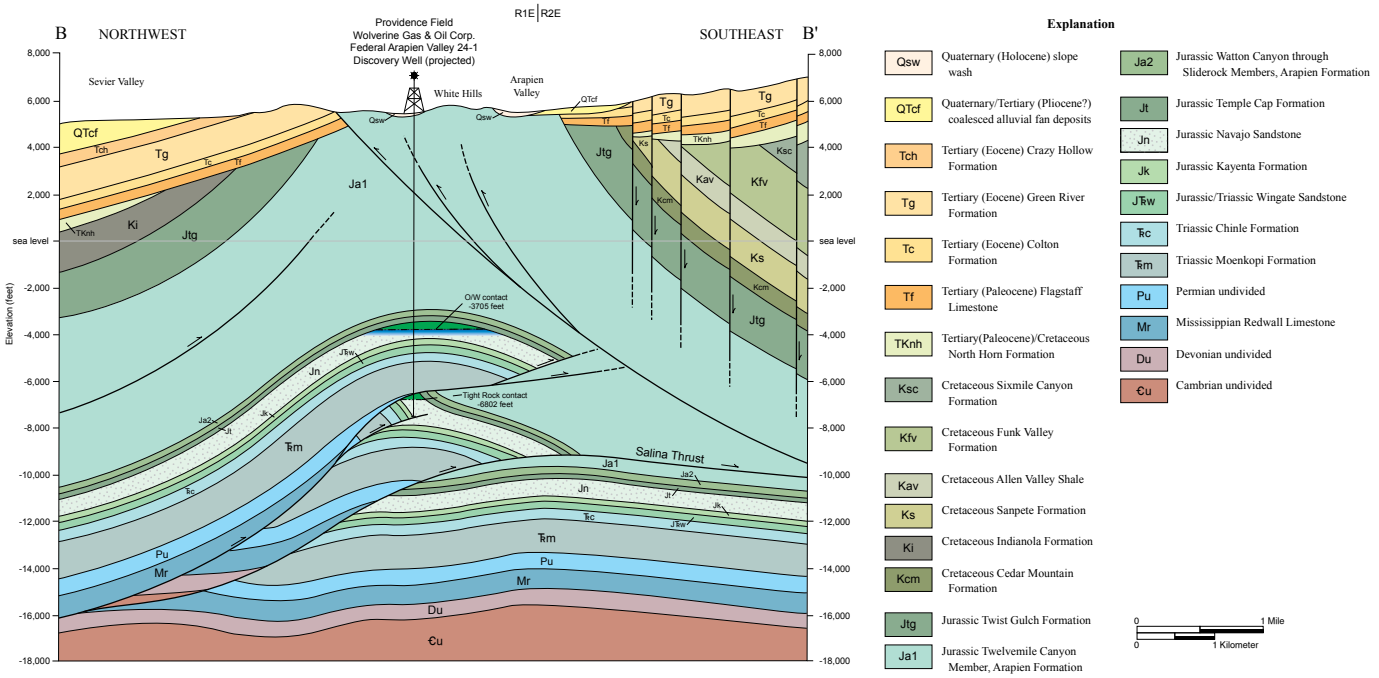

Figure 5.22. *Northwest-southeast structural cross section through Providence field. Note small splay thrust through the anticline that results in a repeated Navajo Sandstone section. Line of cross section B–B' shown on figures 5.1 and 5.21. Modified from Utah Division of Oil, Gas, and Mining (2010); after Chidsey and others (2011).*

as expected, have significantly poorer reservoir characteristics than the dune lithofacies and represent significant barriers to fluid flow. Plotting porosity versus permeability shows gradational changes in reservoir quality within the various dune lithofacies and Sinawava Member coastal sabkha and tidal flat lithofacies (figure 5.23). Mapping dune lithofacies prior to a well completion identifies zones of maximum drainage effects (Strickland and others, 2005).

Diagenetic effects and fracturing can both reduce and enhance the reservoir permeability of the Navajo Sandstone and White Throne Member. At Covenant field, quartz grains have minor overgrowths. Some authigenic clay mineralization has occurred in the form of grain-coating, pore-bridging, and fibrous illite. Some ferroan(?) dolomite and fractured, corroded K-feldspar are also present (Strickland and others, 2005). Development of bitumen and gouge-filled, silica-cemented fractures locally reduce reservoir permeability. Dissolution of silicate minerals and the development of open fractures increase reservoir permeability.

Navajo Sandstone/White Throne Member gross-pay thickness at Covenant field is 487 feet (148 m) and net-pay thickness is 424 feet (129 m), a net-to-gross ratio of 0.87 (Strickland and others, 2005). The Navajo/White Throne reservoir temperature is 188°F (87°C). The average water saturation is 38%, and average produced R_w is 0.279 ohm-m at 77°F (25°C) containing 26,035 total dissolved solids (TDS) measured in milligram/liter (mg/L). Initial reservoir pressures average about 2630 psi (18,134 kPa). The reservoir drive mechanism is a strong active water drive. Geophysical well logs show a transition zone in terms of water saturation above a very sharp oil/water contact within the Navajo (figure 5.3).

The First Navajo Sandstone maximum gross-pay thickness at Providence field is 262 feet (80 m) and net-pay thickness is 134 feet (41 m), a net-to-gross ratio of 0.51. The reservoir temperature is 193°F (89°C). The average water saturation is 49%, and produced R_w is 0.265 ohm-m at 70°F (21°C). The initial reservoir pressure averages about 3545 psi (24,443 kPa). The reservoir drive mechanism is gas expansion with water drive. The Second Navajo Sandstone maximum gross-pay thickness is 279 feet (85 m) and net-pay thickness is 96 feet (29 m), a net-to-gross ratio of 0.34. The reservoir temperature is 244°F (118°C). The average water saturation is 33%, and the R_w of the produced water is the same as the First Navajo (0.265 ohm-m at 70°F [21°C]). The initial reservoir pressure averages about 4930 psi (33,990 kPa). The reservoir drive mechanism is gas expansion with limited (?) water drive (Chidsey and others, 2011).

OIL AND GAS CHARACTERISTICS

Covenant field's oil is a dark brown, low-volatile crude. The API gravity of the oil is 40.5°; the specific gravity is 0.8280 at 60°F (16°C). The viscosity of the crude oil is 4.0 cst at 77°F (25°C) and the pour point is 2.2°F (-16.5°C). The average weight percent sulfur of produced oil is 0.48; nitrogen content is 474 ppm. Stable carbon-13 isotopes are -29.4‰ and -29.0‰ for saturated and aromatic hydrocarbons, respective-

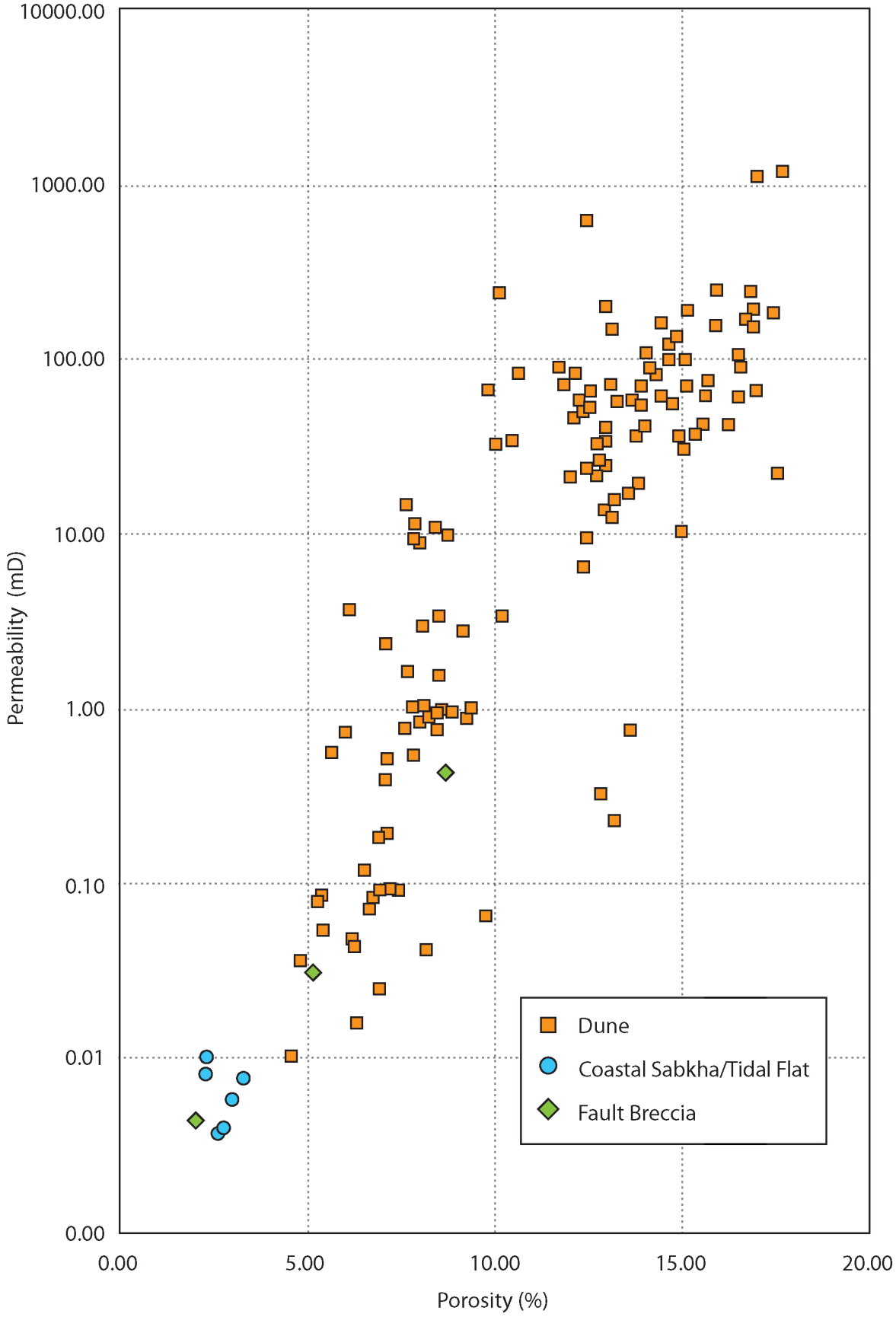

Figure 5.23. *Porosity versus permeability cross plot from the Navajo Sandstone/Temple Cap Formation in Covenant field, based on core-plug analysis, showing gradational changes in reservoir quality within the various dune lithofacies and coastal sabkha/tidal flat lithofacies; zones of brecciation from faulting are also plotted.*

ly. The pristane/phytane ratio is 0.96 (Baseline DGSI, 2005). Covenant field is unusal in that it produces no gas.

At Providence field, the First Navajo oil is a reddish brown, low-volatile crude. The API gravity of the oil is 48.3°; the corresponding specific gravity is 0.7869 at 60°F (16°C). The pour point is -20°F (-29°C). The producing solution gas to oil ratio (GOR) is 10,607 in the First Navajo. The gas is composed of approximately 81% carbon dioxide (CO_2), 6% nitrogen (N_2), 6% methane, 2% ethane, 2% propane, and 3% higher hydrocarbon components; hydrogen sulfide (H_2S) is 32 parts per million (ppm). The Second Navajo oil is a yellow, high-volatile crude. The API gravity of the oil is 54.9°; the corresponding specific gravity is 0.7593 at 60°F (16°C). The producing GOR is 5702. The produced gas is composed of approximately 63% methane, 8% ethane, 4% propane, 5% higher hydrocarbon components, 8% CO_2, and 12% N_2; H_2S is 1000 ppm.

PRODUCTION

Covenant field produces oil and water (about 5 to 10%), and essentially no gas. Cumulative production as of January 1, 2016, was 22,364,596 BO (3,555,687 m³) and 26,743,790 bbls of water (BW) (4,251,923 m³) (Utah Division of Oil, Gas, and Mining, 2016a). Daily oil production averages over 3700 BO (590 m³) and just over 1200 BW (190 m³). Oil production increased through 2009, but has steadily declined ever since while water production has increased to 76% (figure 5.24). The field currently has 24 active wells (12 completed in the Navajo Sandstone and 12 completed in the Temple Cap Formation) and one dry hole, drilled from two pads. The well spacing is about 40 acres (16 ha) within the Covenant unit. Original oil in place (OOIP) reserves are estimated at 100 million bbls (15.9 million m³) (Chidsey and others, 2007). A 40 to 50% recovery of the OOIP may be achieved with efficient operations and completion techniques (Strickland and others, 2005).

Production from Providence field has been sporadic with cumulative production as of January 1, 2016, at 147,565 BO (23,460 m³), 1,330,981 MCFG (37,689 MCMG), and 39,117 BW (6219 m³) (Utah Division of Oil, Gas, and Mining, 2016a). Daily production averaged 251 BO (40 m³), 2415 MCFG (68 MCMG), and 64 BW (10 m³). There are no current well spacing orders for the field. The field currently has one producing oil well and one gas injection well. An extended production test to validate the economic feasibility of the field was conducted during 2010 and concluded in 2011. OOIP reserves are estimated at 10,740,000 bbls (1,708,000 m³). Estimated in place gas reserves are 31.6 BCF (0.89 BCM) based GORs from pressure/volume/temperature analysis.

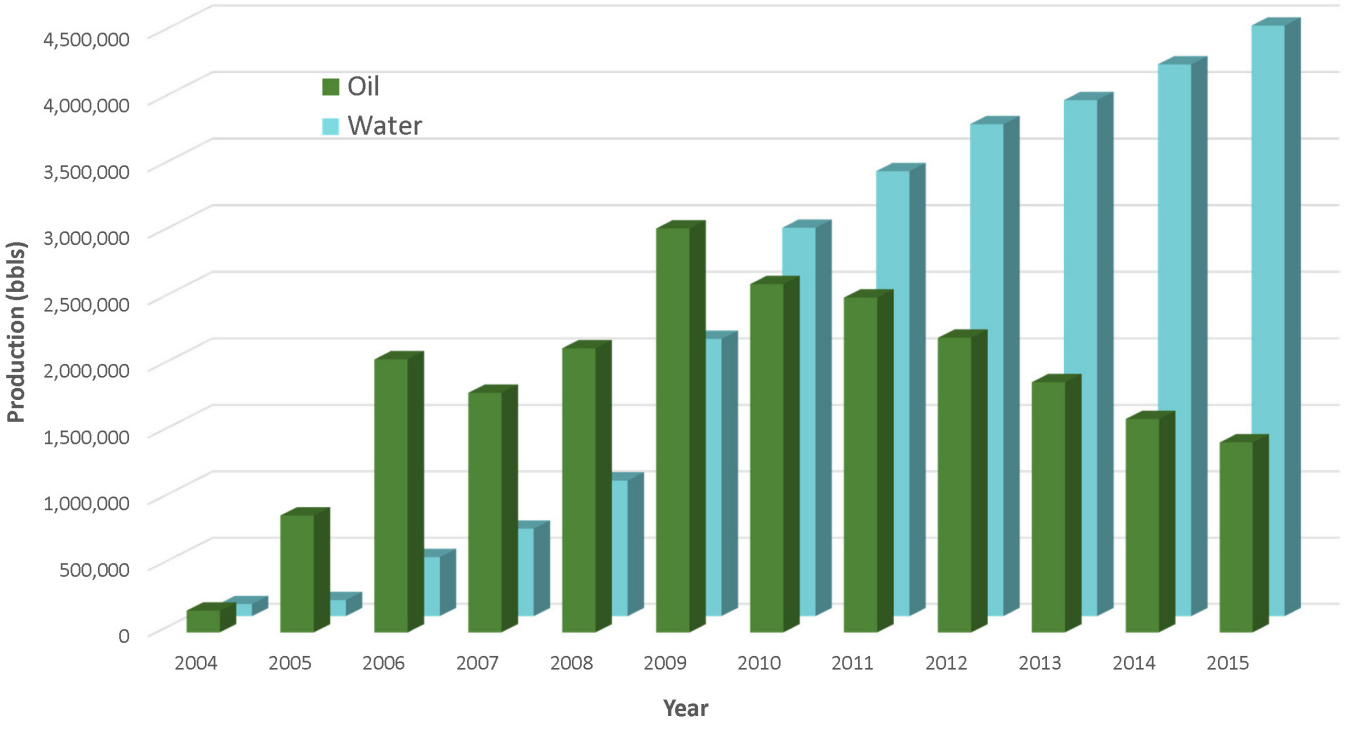

Figure 5.24. *Yearly oil and water production from wells in Covenant field. Data from Utah Division of Oil, Gas, and Mining (2016a).*

EXPLORATION POTENTIAL AND TRENDS

The result of the Covenant discovery was initially high prices and competition for available leases in the play, hundreds of miles of new seismic surveys over much of the play area, and new well permits to test various parts of the play. Extensive 2-D seismic acquisition was permitted and conducted within the play area. Companies turned to 3-D seismic to define the crests of structures identified by 2-D seismic. The potential to discover other major, or even smaller oil fields such as Providence, in this high risk play will be dependent on the price of oil and additional commercially successful drilling effects.

Exploration in the central Utah thrust belt will focus on Paleozoic-cored, blind thrust structures east of the exposed Charleston-Nebo and Pahvant thrusts. Targets include anticlines associated with thrust imbricate and duplex structures, positioned near Jurassic extensional faults, in the Navajo Sandstone, Temple Cap Formation, and other reservoirs such as the Permian Park City–Kaibab Formations, Triassic Moenkopi Formation, and Jurassic Twin Creek Limestone (figure 2.10). The lack of any associated gas at Covenant field suggests the possibility that potential gas-charged traps may be present in the play area.

CHAPTER 6:
DEEP UINTA BASIN OVERPRESSURED CONTINUOUS PLAY

by

Craig D. Morgan
Utah Geological Survey

CONTENTS

FIGURES

TABLES

CHAPTER 6:
DEEP UINTA BASIN OVERPRESSURED CONTINUOUS PLAY

INTRODUCTION

The Deep Uinta Basin Overpressured Continuous play (DUBOCP) is located near the basin center where about the lower 2500 to 3000 feet (750–900 m) of the Green River and intertonguing Colton Formations are overpressured (gradient >0.5 psi/ft [11.3 kPa/m]) (figures 6.1 and 6.2). The most rapid increase in reservoir pressure and most of the high-volume, overpressured oil production is typically from depths of 11,000 to 14,000 feet (3400–4300 m) (figure 6.3). The drill depths given are averages; actual depth to the overpressured interval can vary greatly throughout the fields.

The play has produced nearly 350 million BO (56 million m^3) and 620 billion cubic feet (17 BCM) of associated gas from the three large fields—Altamont, Bluebell, and Cedar Rim (Utah Division of Oil, Gas, and Mining, 2016a). Production is fracture controlled from rocks with typically very low (< 0.1 mD) matrix permeability. The reservoir is fractured lenticular sandstone, shale, and marlstone deposited in the lacustrine and alluvial environments of Lake Uinta (figure 2.14). Well completions typically consist of perforating 40 or more beds in a 1500-foot (450 m), or more, vertical section.

DEPOSITIONAL ENVIRONMENT

The Uinta Basin began developing in middle Paleocene time. Shallow lakes and wetlands (the depositional facies of the Flagstaff Member of the Green River Formation [other publications describe the Flagstaff as a separate formation, i.e., Flagstaff Limestone of Hintze and Kowallis, 2009]) existed in the deep basin area by early Paleocene time. Ancient Lake Flagstaff, followed by Lake Uinta (both lakes will be referred to as Lake Uinta), were dominant features throughout most of the late Paleocene and Eocene in the deep basin area. In most of the basin the Flagstaff is separated from the main portion of the Green River by alluvial deposits of the Colton Formation (figure 2.19). But in the central portion of the basin along the southern limits of Altamont and Bluebell fields, lacustrine deposits of Lake Flagstaff and Lake Uinta are continuous. Ryder and others (1976) defined three major depositional facies in the Colton and Green River Formations: (1) alluvial, (2) marginal lacustrine, and (3) open lacustrine. The depositional environments of the Colton and Green River are described in detail by Fouch (1975, 1976, 1981), Ryder and others (1976), Pitman and others (1982), Franczyk and others (1992), and Fouch and Pitman (1991, 1992).

Abundant detritus was shed from the south flank of the Uinta uplift into the deep basin area from late Paleocene into earliest Eocene time (Franczyk and others, 1992). Alluvial deposits of the Colton Formation were laid down along Lake Uinta's northern margin and intertongue with the deeper-basin, marginal-lacustrine deposits of the Green River Formation. The Colton thins rapidly from north to south in the deep basin play area. Expansion of Lake Uinta resulted in deposition of marginal-lacustrine and open-lacustrine sediments over the Colton (figure 6.4).

STRATIGRAPHY AND THICKNESS

The DUBOCP produces oil and associated gas, in ascending order, from the Flagstaff Member of the Green River Formation, the intertonguing Green River–Colton Formations, and the lower Green River Formation in the deepest portions of the play. The total thickness of the Green River, Colton, and Flagstaff Member strata can be more than 8000 feet (2400 m). The basal contact of the Flagstaff Member with the Paleocene part of the North Horn Formation is poorly defined and is rarely penetrated by wellbores. Typically the lower 2500 to 3000 feet (750–900 m) of the reservoir interval is overpressured and makes up the DUBOCP (figure 2.18). The total depth of most wells in the deep basin play is 12,000 to 14,000 feet (3600–4300 m).

LITHOLOGY AND FRACTURING

Hydrocarbons are produced in the DUBOCP from the Paleocene- and Eocene-age Colton and Green River Formations. Most of the production is from sandstone, but some production comes from shale, limestone, and marlstone beds with open fractures. Factors controlling most of the production in the deep basin play are predominantly the presence of fractures and the abnormally high fluid pressure, and to a lesser extent the facies and porosity distribution. Fractures in the DUBOCP reservoirs are believed to be the result of rapid generation of hydrocarbons within the largely impermeable rock (Lucas and Drexler, 1975; Narr and Currie, 1982; Bredehoeft and others, 1994).

A study of core from the Bluebell field by Wegner (1996) and Wegner and Morris (1996) showed that 78% of the sandstone beds and 43% of the clastic mudstone beds had at least one noticeable fracture. Fracture density, orientation, and fill vary

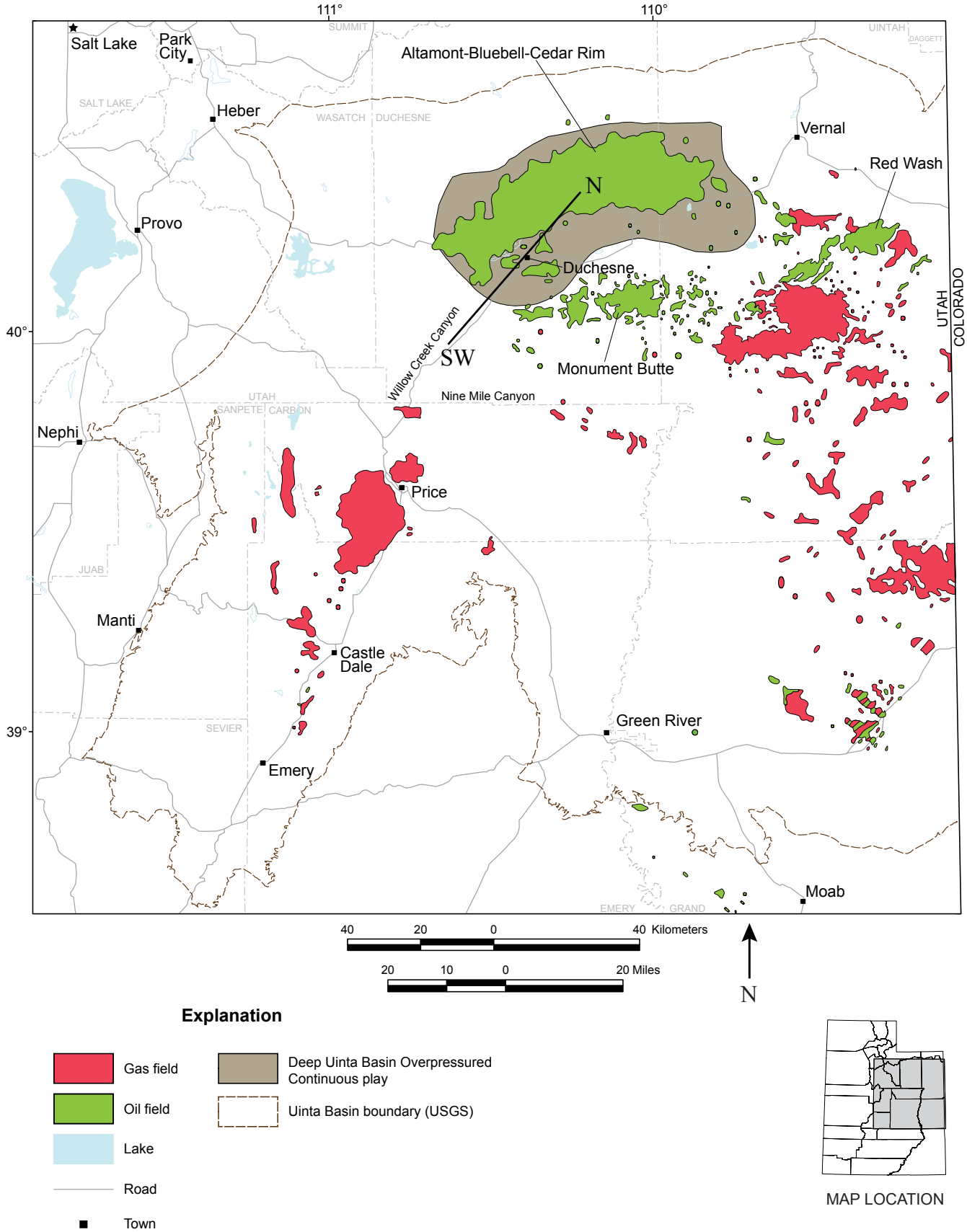

Figure 6.1. *Location of the Deep Uinta Basin Overpressured Continuous play in northern Uinta Basin. The play encompasses the Altamont, Bluebell, and Cedar Rim fields. North-southwest cross section shown on figure 6.2.*

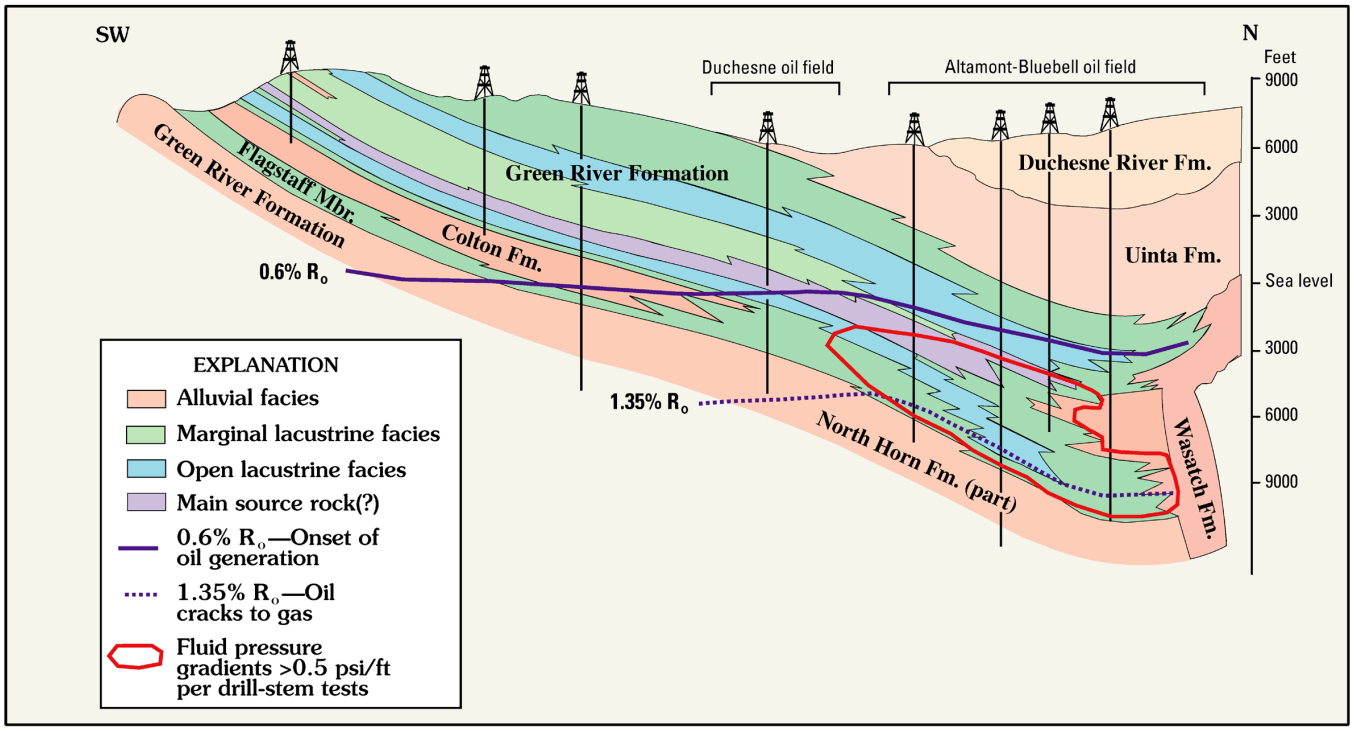

Figure 6.2. *Generalized stratigraphic cross section of the Green River total petroleum system showing the overpressured interval of the Deep Uinta Basin Overpressured Continuous play. Line of section shown on figure 6.1. From Dubiel (2003).*

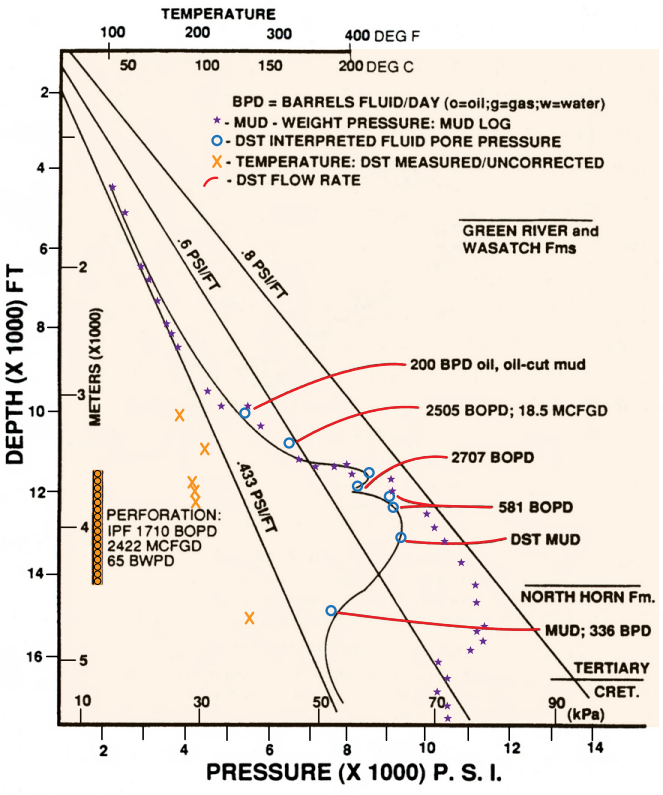

Figure 6.3. *Plot of pressure versus depth for the Brotherson No. 1-11B4 well (section 11, T. 2 S., R. 4 W., UBL&M) at Altamont field. From Bredehoeft and others (1994).*

with differing rock types; sandstone beds tend to have the lowest fracture density but the fractures are longer and generally have more separation than those found in other rock types (Wegner, 1996; Wegner and Morris, 1996). Naturally occurring fractures in the sandstone beds are commonly perpendicular to near-perpendicular to bedding and have a measured vertical length greater than 3.3 feet (1 m) (although many fractures extend out of the sample). Fracture widths range from 0.03 to 0.13 inches (0.5–3.0 mm), and the openings are only partially calcite filled (figure 6.5) (Wegner, 1996; Wegner and Morris, 1996; Morgan, 2003b; Baclawski and others, 2013). The primary fractures in the DUBOCP play generally trend east-west whereas fractures in the shallower Green River reservoirs in the Altamont and Bluebell fields trend northwest-southeast (figure 6.6) based on analysis of 13 other cores by Baclawski and others (2013). The fracture orientations are based on limited borehole imaging logs and borehole breakout analysis (Allison and Morgan, 1996) and seismic data (Harthill and Bates, 1996). More recent borehole imaging logs from the Cedar Rim and western Altamont fields indicate a more north-south fracture trend.

HYDROCARBON SOURCE AND SEALS

The source rocks for the crude oil produced from the DUBOCP are kerogen-rich shale and marlstone of the black shale facies of the Flagstaff Member of the Green River Formation (Dubiel, 2003; Ruble, 1996) and the lower Green River Formation, which were deposited in nearshore and

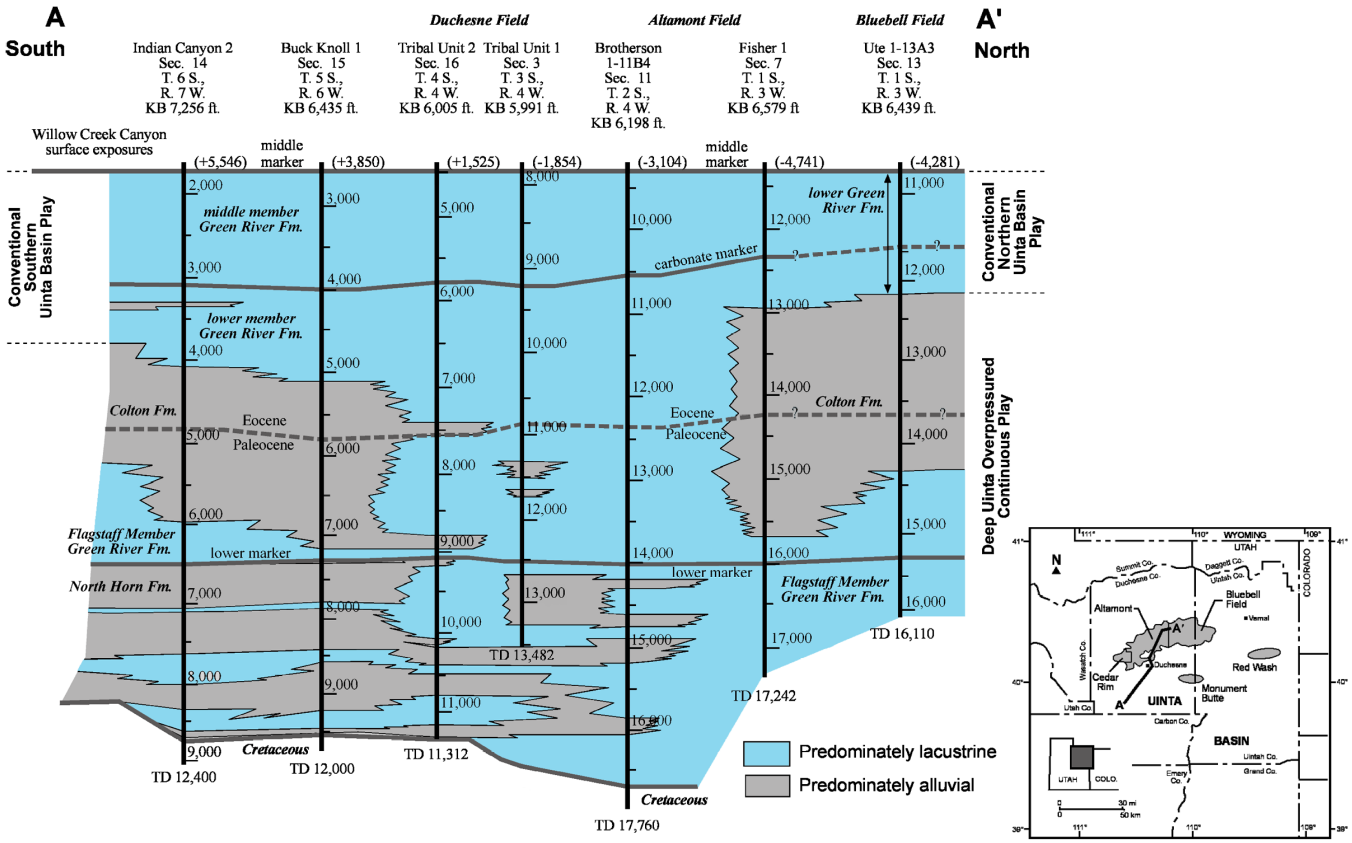

Figure 6.4. *Generalized stratigraphic cross section which extends from outcrops in Willow Creek Canyon through Duchesne, Altamont, and Bluebell fields. Correlations of markers and depositional interpretations for many of the wells are from Fouch (1981). Datum is the middle marker with sea-level elevations in parentheses.*

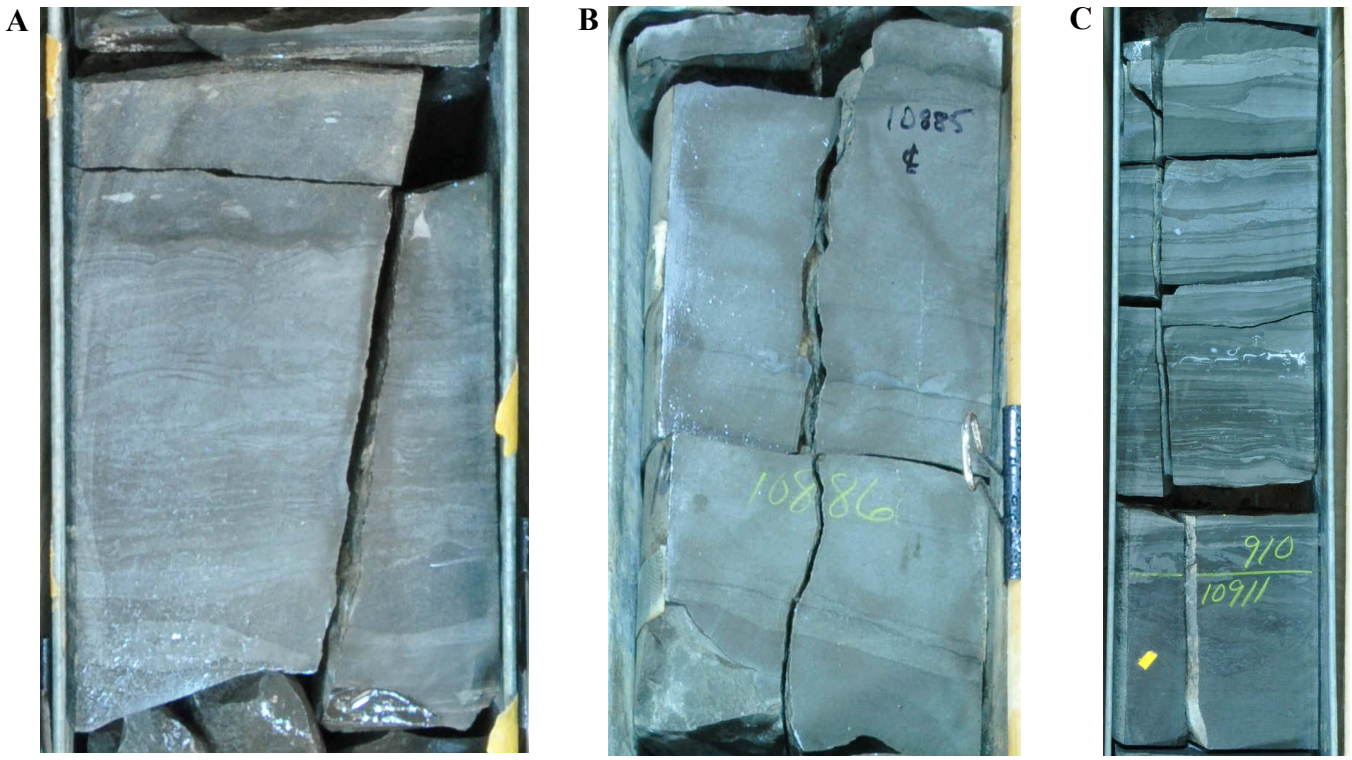

Figure 6.5. *Examples of open fractures in core from the lower Green River Formation, Chevron-Mobil-Lamicq-Urruty No. 1-8A2 (section 8, T. 1 S., R. 2 W., UBL&M, Duchesne County), Bluebell field.* ***A.*** *Slightly inclined, open fracture in fine-grained sandstone and siltstone.* ***B.*** *Open vertical fracture in fine-grained sandstone.* ***C.*** *Open, mineral-lined fracture in siltstone and shale.*

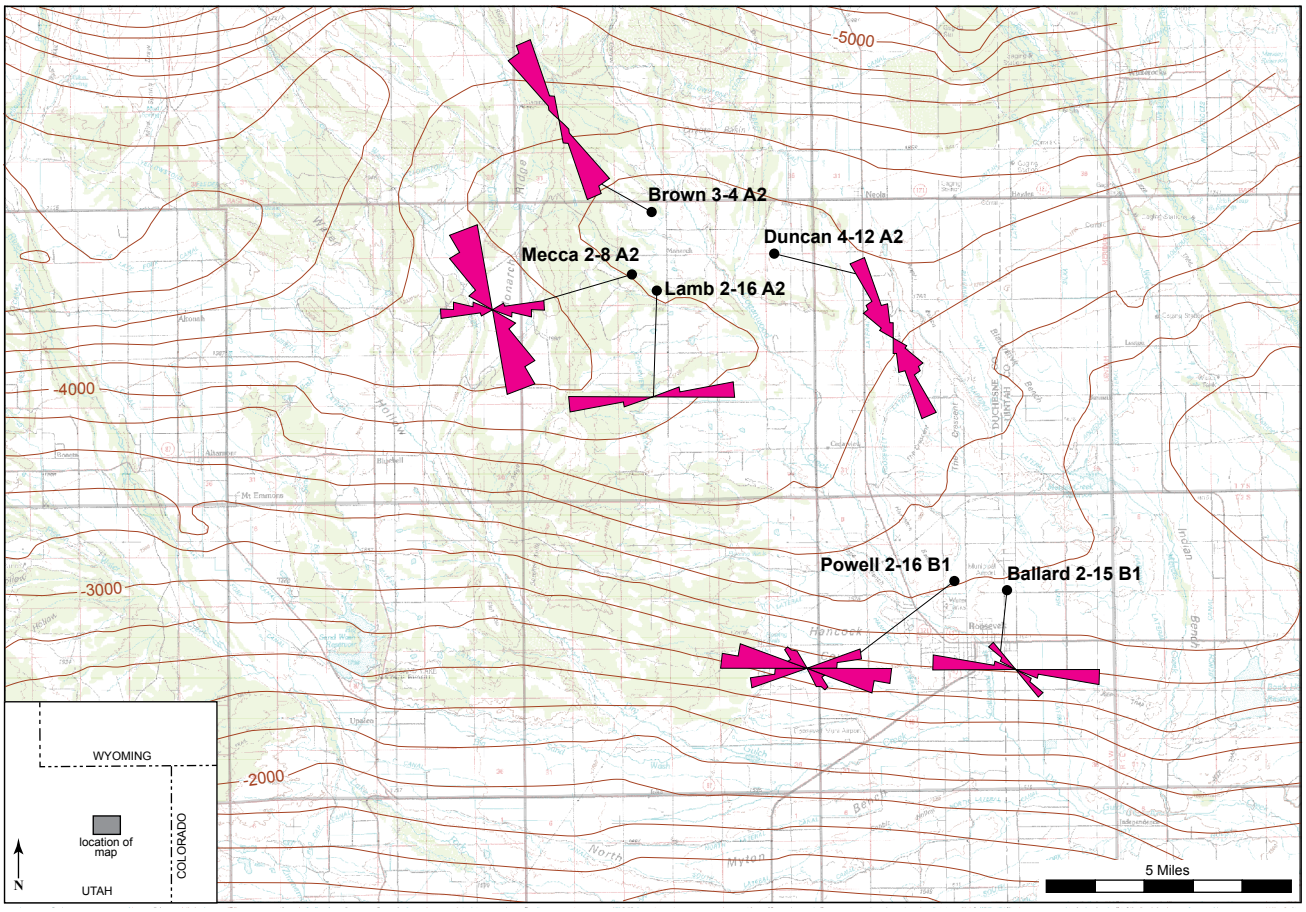

Figure 6.6. *Strike orientation of fractures from selected Green River Formation cores, Bluebell field. Structural contours on top of the middle marker of the Green River; contour interval = 200 feet and datum = mean sea level. Modified from Baclawski and others (2013), courtesy of Devon Energy Company.*

offshore open-lacustrine environments (Tissot and others, 1978; Ruble, 1996; Ruble and others, 1998). Anders and others (1992) showed that the 0.7% vitrinite reflectance level in the center of the Altamont and Bluebell fields is at a present depth of about 8400 feet (2600 m). The 0.7% reflectance level indicates the maturity at which the onset of intense oil generation occurred. In most wells in Altamont and Bluebell fields, the 0.6% reflectance level is at or below the Mahogany oil shale, but above the middle marker of the Green River. As a result, only the lower Green River and the Flagstaff Member are in the oil-generation window.

Lacustrine source rocks in the deepest portion of the basin are presently at or near their maximum burial depth (Dubiel, 2003). Oil and gas are likely currently being generated below about 10,000 feet (3000 m) (Dubiel, 2003). Based on burial history and petroleum-generation modeling of the Shell Brotherson 1-11B4 well in the Altamont field, Dubiel (2003) determined that oil and gas generation began near the base of the Green River Formation around 40 Ma at a depth of 11,000 feet (3300 m). Peak generation occurred during maximum burial between 30 to 40 Ma. The zone of hydrocarbon generation has risen stratigraphically through time (Dubiel, 2003). Much of the oil in the DUBOCP was generated in-situ or has undergone only minor vertical and lateral migration. Dubiel (2003) states that in the deep basin oil has been undergoing thermal cracking to gas and condensate since about 35 Ma contributing to the overpressuring of the reservoir. Vertical and horizontal seals for producing zones are unfractured shale and low-permeable marls within the Green River Formation.

STRUCTURE AND TRAPPING MECHANISMS

The DUBOCP is just south of the structural center of the Uinta Basin. Reservoir structure in the Altamont, Bluebell, and Cedar Rim fields is dominated by north dip into the basin (figures 2.12 and 6.2). Oil is trapped in natural pores and within fractures, which were opened by the high fluid pressures during oil generation (Bredehoeft and others, 1994; McPherson, 1996). Interbedded sandstone, shale, limestone, and marlstone deposited in alluvial to marginal-lacustrine environments pinch out updip into dominantly shale and marlstone deposited in an open-lacustrine environment. Updip facies changes, a reduction of fluid pressure, and associated closing of fractures in the structurally shallower strata combine to form the traps of the DUBOCP.

RESERVOIR PROPERTIES

Oil and gas production in the DUBOCP is from perforated intervals in the Flagstaff Member of the Green River Formation and in the transitional interval where the lower Colton Formation intertongues with the Flagstaff Member. In the Altamont-Bluebell-Cedar Rim field area (figure 6.1), the Colton and Flagstaff contain an oil-bearing overpressured section that is up to 3000 feet (900 m) thick. The upper Colton and lower Green River are productive and locally overpressured, but are included in the Conventional Northern Uinta Basin Play. Sandstone in the DUBOCP has well-log porosities from 1 to 14%, an average of 5%, and core-derived matrix permeabilities of 0.01 mD or less (Morgan, 2003b). Open fractures are the primary reservoir property necessary for oil and gas production from the DUBOCP (figure 6.5).

Oil and gas is produced from fractured sandstone, shale, limestone, and less commonly marlstone. Characterization of the DUBOCP reservoir is very poor due to the:

1. extremely limited amount of core relative to the areal extent and thickness of the reservoir,
2. extremely limited amount of borehole imaging logs from the reservoir,
3. extensive number of perforated beds in the well with little to no knowledge of the contribution each bed makes to the overall production, and
4. low density of wells.

The sandstone beds are typically lenticular channel deposits a few feet thick to rarely a few tens of feet thick, and have very limited lateral extent. Thickness maps of many of the sandstone beds show no relationship to well productivity (Allison, 1995; Morgan, 1997). Shale and limestone beds deposited in the lacustrine environment are often more laterally extensive than the sandstone beds and can be useful correlation markers (Morgan, 2003b). The shale and limestone beds are typically a few feet thick to rarely a few tens of feet thick, but are generally less fractured (Morgan, 2003b).

The fractures, which are critical to oil and gas production in the DUBOCP, like the lithology, are poorly characterized. The fracturing is believed to be extensive, and reduced reservoir pressure in some beds over a large area even with only one well per section is suspected in extensive fracture sets (Morgan, 2003b). Most infill wells have encountered high reservoir pressures from presumably more isolated fracture sets, which often have a more rapid decline than the extensive fracture set (Morgan, 2003b). The orientation, spacing, connectivity, and fluid-flow characteristics of the fractures are virtually unknown. Operators have begun drilling four wells per section which will provide additional information about the reservoir.

Well completions in the DUBOCP typically consist of perforating 40 or more beds in a 1500-foot (450 m), or more, vertical section and hydraulically fracturing them with hydrochloric acid (HCl) or proppant fracture treatment. This technique is commonly referred to as a "shotgun" completion.

Reservoir pressure gradients in the DUBOCP vary from 0.5 to 0.8 psi/ft (11.3–18.1 kPa/m). Representative calculated reservoir pressures are 9600 psi (66,200 kPa) for Bluebell field (assuming 12,000-foot [3600 m] depth and a gradient of 0.8 psi/ft [18.1 kPa/m]), 8400 psi (58,000 kPa) for Altamont field (assuming 12,000-foot [3600 m] depth and a gradient of 0.7 psi/ft [15.8 kPa/m]), and 6000 psi (40,000 kPa) for Cedar Rim field (assuming 10,000-foot [3000 m] depth and a gradient of 0.6 psi/ft [13.5 kPa/m]). Bottom-hole temperature is typically greater than 210°F (99°C). The reservoir drive mechanisms include gas solution and pressure depletion. The wells yield a significant amount of water during the late stages of production but the water is not considered a major drive mechanism. Reservoir data for the individual fields in the DUBOCP are summarized in table 6.1.

OIL AND GAS CHARACTERISTICS

Most of the oil produced from the DUBOCP is characterized as yellow wax (table 6.2). The yellow wax from the John No. 2-7B2 well (section 7, T. 2 S., R. 2 W., Uinta Base Line and Meridian [UBL&M]) is a 39° API gravity crude with a paraffin content of 7.4%. Because of the high paraffin content, the yellow wax has a pour point of 95°F (35°C) and a cloud point of 132°F (56°C). The produced oil is stored on location in heated, insulated stock tanks to keep it above the pour-point temperature. Associated gas from the DUBOCP (table 6.3) contains an average of 73% methane, 14% ethane, 7.5% propane, 5.1% higher fractions, 0.3% CO_2, with an average heating value of 1380 Btu/ft^3 (Moore and Sigler, 1987). For additional information on geochemical analysis and biomarker studies of the Green River oils please refer to Ruble, 1996; Mueller, 1998; Mueller and Philp, 1998; Ruble and Philp, 1998; and Dubiel, 2003.

PRODUCTION

Fields in the DUBOCP produce oil with large amounts associated gas. Altamont-Bluebell-Cedar Rim fields have produced 345 million BO (54.8 million m^3) and 620 BCFG (17.4 BCMG) as of January 1, 2016. The three fields combined produced 636,558 BO (101,205 m^3) and 1544 million cubic feet of gas (MMCFG [43.7 MMCMG]) from 760 active wells during December 2015 (Utah Division of Oil, Gas, and Mining, 2016a). Many of the wells perforated in the deep overpressured interval also have perforations in the overlying Conventional Northern Uinta Basin play interval. As a result, the co-mingled production from the two plays cannot be accurately separated; therefore, all of the production from

Table 6.1. *Geologic, reservoir, and production data for the largest fields in the Deep Uinta Basin Overpressured Continuous play. Production data is from Utah Division of Oil, Gas, and Mining (2016a); other data from Robertson and Broadhead (1993), Smouse (1993a), and Morgan (2003b).*

State	County	Field	Discovery Date	Active Producers	Abandoned Producers	Acres	Spacing (acres)	Pay (feet)	Porosity (%)	Perm. (mD)	Temp. (°F)	Initial Reservoir Pressure (psi)*	Average Monthly Production		Cumulative Production	
													Oil (bbl)	Gas (MCF)	Oil (bbl)	Gas (MCF)
Utah	Duchesne	Altamont	1970	415	254**	139,720	320	40+	5–12	0.1	217	8400	381,469	1,025,436	145,892,946	322,259,047
Utah	Duchesne/ Uintah	Bluebell	1971	293	141**	129,040	320	40+	5–12	0.1	218	9600	264,236	536,150	183,164,913	260,215,003
Utah	Duchesne	Cedar Rim	1969	52	45	21,820	320	40+	5–12	0.1	212	6000	13,369	49,972	15,764,824	37,649,599

* Pressure data estimated based on 12,000 feet and a gradient of 0.8 psi/ft for Bluebell, 12,000 feet and 0.7 psi/ft for Altamont, and 10,000 feet and 0.6 psi/ft for Cedar Rim fields.

** Abandoned producers for the Altamont and Bluebell fields are combined.

Table 6.2. *Comparison of Uinta Basin crude oils. Yellow-wax sample from John No. 2-7B2 well (section 7, T. 2 S., R. 2 W., UBL&M), black-wax sample from Leslie Taylor No. 24-5 well (section 24, T. 1 S., R. 1 W., UBL&M). The Monument Butte black wax is an average from three wells: Monument Butte Nos. 10-35, 8-35, and 12-35 (section 35, T. 8 S., R. 16 E., SLBL&M). From Morgan (2003b).*

Oil Characteristics	Bluebell Yellow Wax (DUBOCP*)	Bluebell Black Wax (CNUBP*)	Monument Butte Black Wax (CSUBP*)
Paraffin Content	7.4% wt.	12.2% wt.	9.6% wt.
Cloud Point	132°F	157°F	122°F
Pour Point	95°F	120°F	95°F
API Gravity	39°	33°	34°

* DUBOCP = Deep Uinta Basin Overpressured Continuous play, CNUBP = Conventional Northern Uinta Basin play, CSUBP = Conventional Southern Uinta Basin play.

Table 6.3. *Comparison of associated gas from Uinta Basin oil plays. From Moore and Sigler (1987).*

Play*	Field	Well	Methane	Ethane	Propane	Higher Fractions	Carbon Dioxide	Hydrogen Sulfide	Btu/ft^3
CNUBP	Red Wash	Unit 1	92.0	2.1	2.1	2.7	1.3	0.0	1096
CNUBP	Red Wash	Unit 32-27C	97.6	0.9	0.2	0.4	0.1	0.0	1026
CNUBP	Bluebell	Unit 2	96.0	1.1	0.9	1.1	0.1	0.0	1057
DUBOCP	Bluebell	Hamblin 1	73.7	14.4	7.2	4.2	0.4	0.0	1347
DUBOCP	Altamont	Brotherson 1	71.4	14.3	7.8	6.0	0.2	0.0	1409
CSUBP	Monument Butte	Unit 10-35	71.8	14.9	9.9	3.3	NA	NA	NA

* CNUBP = Conventional Northern Uinta Basin play, DUBOCP = Deep Uinta Basin Overpressured Continuous play, CSUBP = Conventional Southern Uinta Basin play. NA = data not available.

the Altamont-Bluebell-Cedar Rim fields is attributed to the DUBOCP. All of the production is from primary methods: no enhanced oil recovery techniques are being used in the Altamont-Bluebell-Cedar Rim fields. The OOIP and therefore the percent recovery are highly speculative due to poor understanding of the highly complex, thick (3000 feet [1000 m]), and laterally extensive (500 square miles [1295 km^2]) nature of the reservoir. With a well density of two wells per section, the current production practice will likely recover less than 10% of the OOIP. Infill drilling, improved completion practices, and enhanced-oil-recovery techniques could all increase the ultimate oil recovery.

EXPLORATION POTENTIAL AND TRENDS

The DUBOCP is well defined by drilling in the Altamont-Bluebell-Cedar Rim field area (figure 6.1). New large field discoveries are highly unlikely to be made in the Uinta Basin that produce from the overpressured portion of the Colton and Green River Formations. Drilling may result in some field extensions but even that will be limited by the well-defined overpressured region within the basin.

Infill drilling will continue in portions of the Altamont-Bluebell-Cedar Rim field area where the deep overpressured play has not been developed on two wells per section. Drilling three wells per section has been allowed on a few select sections with the fields. Testimony to allow four wells per section in the Altamont-Bluebell-Cedar Rim fields was presented to the Utah Board of Oil, Gas, and Mining and approved in December 2008. Enhanced oil recovery (EOR) methods have not been attempted in the Altamont-Bluebell-Cedar Rim field area. Several factors have discouraged operators from attempting any EOR pilot projects. Fractures are the dominant reservoir property and could cause early breakthrough of any injected fluid or gas. Fractures can result in injected fluids or gases moving great distances, perhaps even beyond the intended EOR unit. Enhanced-oil-recovery methods generally require a high density of wells to be effective. The Altamont-Bluebell-Cedar Rim field area has been developed with two wells per section and in many areas at least one of those wells has already been plugged and abandoned. As a result, any EOR method would require a significant amount of additional deep drilling. Allowing the production of four wells per section will be a significant step in improving the understanding of the reservoir and potential development of EOR.

The gross productive interval is 1000 to 3000 feet (300–1000 m) thick, with no single bed being a dominant producer, as a result, horizontal drilling has not been attempted in the Altamont-Bluebell-Cedar Rim fields. High-angle wellbores have been drilled in an attempt to encounter thicker productive beds and intersect more fractures. The high angle wells were expensive to drill, more difficult to complete and produce, and did not result in any significant improvement in production.

Seismic data has had limited use in the Altamont-Bluebell-Cedar Rim fields. In the 1990s Pennzoil used seismic to map the thickness of the Green River Formation and drilled what they hoped was the deepest portions of Lake Uinta with the largest volume of source rock. Drilling based on the seismic did not result in better producing wells. Amplitude variation with offset (AVO) seismic analysis and vertical seismic profile (VSP) analysis was used to map fractures in the upper Green River in a portion of the Altamont field (T. 1 S., R. 2 W., UBL&M) where shallow gas was being produced (Lynn and others, 1995; Harthill and Bates, 1996; Harthill and others, 1997; Lynn and others, 1999). The process has not been used to identify specific drilling locations in the upper Green River and is probably not practical for the deeper Green River due to the large offsets that would be necessary. Three-dimensional seismic has been successfully used in many hydrocarbon plays. Since fractures, not structure or stratigraphy, is a dominant control on reservoir performance, 3-D seismic has not been used in the Altamont-Bluebell-Cedar Rim fields.

A large resource potential in the DUBOCP may be recompletions of the current wells. The wells in the Altamont-Bluebell-Cedar Rim field area were completed in a shotgun fashion with perforations in 40 or more beds in a 1500-foot (450 m) or greater vertical interval. Consequently, many of the beds may never have received adequate stimulation. Using cased-hole logs to identify by-passed oil, and selectively stimulating individual beds can recover a significant amount of additional oil. The potential to recomplete wells in the Bluebell field was the subject of a DOE-funded study lead by the UGS (Morgan, 2003b). The Malnar Pike well in the field was recompleted as part of the UGS demonstration and is an example of increased oil production from just two beds (figure 6.7).

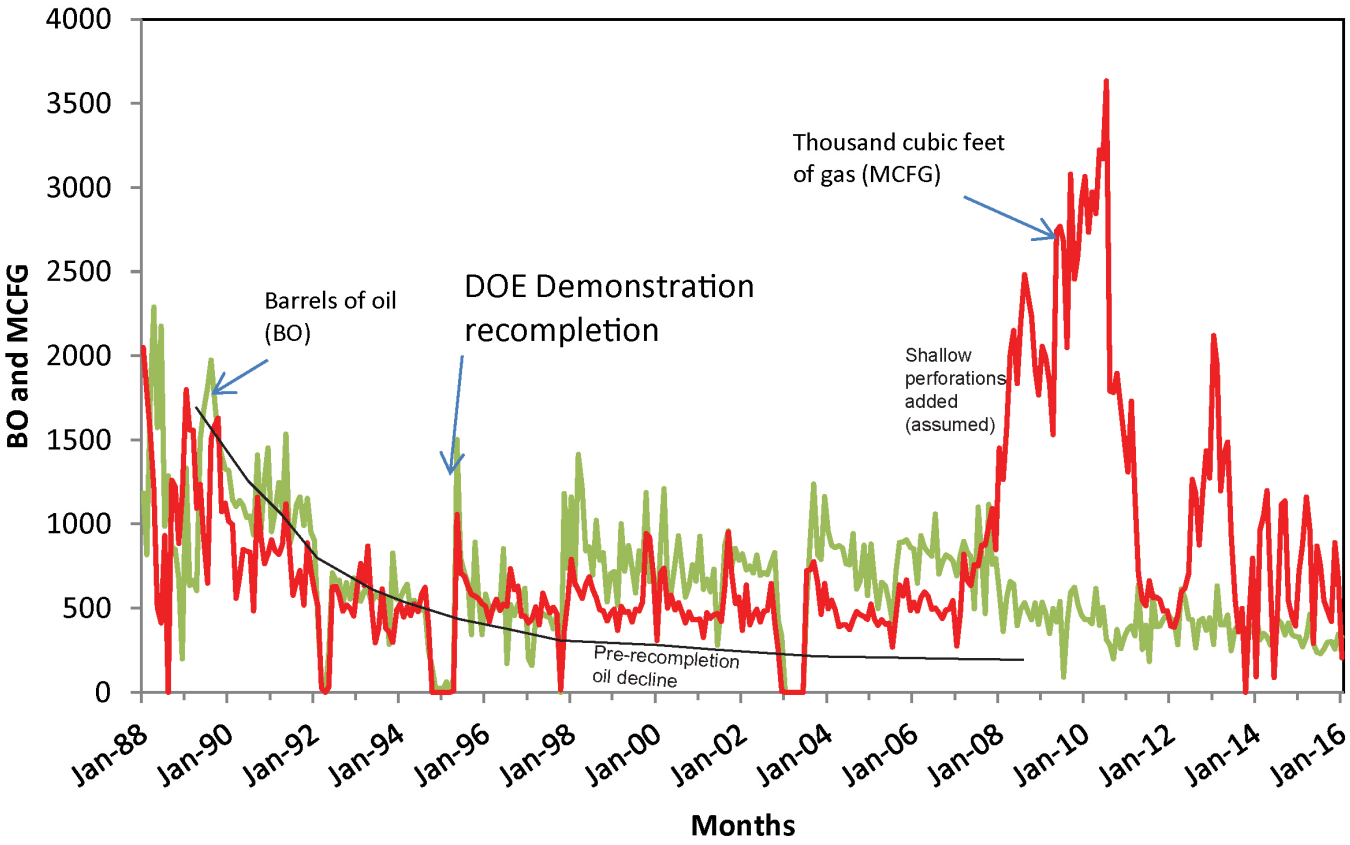

Figure 6.7. *Monthly oil and gas production from the Malnar Pike well (section 17, T. 1 S., R. 1 E., UBL&M), Bluebell field, showing the increased oil production after recompleting in just two beds as part of the U.S. Department of Energy-funded UGS demonstration project (Morgan, 2003b). This example shows potential still exists in a well that has produced for many years in the Deep Uinta Basin Overpressured Continuous play. Based on the production curve the well may have been stimulated again in 2003 and shallow perforations added in 2007 resulting in the significant increase in gas production with continued oil production declining. There are no records in the DOGM well files reporting any activity in 2003 or 2007. Data from Utah Division of Oil, Gas, and Mining (2016a).*

CHAPTER 7: CONVENTIONAL NORTHERN UINTA BASIN PLAY

by

Craig D. Morgan

Utah Geological Survey

CONTENTS

FIGURES

TABLE

CHAPTER 7:
CONVENTIONAL NORTHERN UINTA BASIN PLAY

INTRODUCTION

The Conventional Northern Uinta Basin play (CNUBP) covers the northern Uinta Basin and typically has drill depths ranging from 5000 feet (1500 m) to a maximum of 10,000 feet (3000 m). The play is divided into two subplays (figure 7.1): (1) Conventional Bluebell subplay, and (2) Conventional Red Wash subplay.

DEPOSITIONAL ENVIRONMENT

The CNUBP produces from the Eocene Colton and Green River Formations. Reservoir rocks in the Conventional Bluebell subplay consist of sandstone, shale, limestone, and marlstone deposited in intertonguing alluvial, marginal-lacustrine, to open-lacustrine environments (figures 2.14 and 2.19). Reservoir rocks in the Conventional Red Wash subplay are dominantly sandstone deposited in a shoreface lacustrine environment.

Conventional Bluebell Subplay

The Conventional Bluebell subplay consists of the Altamont-Bluebell-Cedar Rim field area and land north and west of the fields. The Conventional Bluebell subplay overlies the DUBOCP. The subplay produces from the lower Green River Formation and the Green River to Colton transitional facies at drill depths of 8000 to 10,000 feet (2400–3000 m). Most of the production is from sandstone made of clasts shed from the Laramide-age Uinta uplift to the north and deposited in alluvial and marginal-lacustrine environments.

Conventional Red Wash Subplay

The Conventional Red Wash subplay consists of several fields in the northeast portion of the Uinta Basin; the largest is the Red Wash field. The Conventional Red Wash subplay produces from the Douglas Creek Member in the lower portion of the Green River Formation at drill depths of 5000 to 6000 feet (1500–1800 m). Production is from sandstone deposited in shoreface (typically upper shoreface) to shoreline environments (figure 7.2A) and limestone representing nearshore carbonate flats and shoals (figure 7.2B) The Red Wash subplay has the highest average matrix permeability (50–500 mD) of any of the plays in the Green River–Colton Formations.

Borer and McPherson (1998) provide the following description of the depositional environment of the Green River Formation at Red Wash field.

In Red Wash, the overwhelming depositional overprint is that of wave/storm domination. It represents a high sediment supply and high accommodation regime. Middle and upper shoreface regimes are by far the most dominant reservoir facies. Sediment gravity flows, suspension fall out deposits and fluvial deposits are also of reservoir quality and can have a large impact locally on production and waterflood behavior. We consider many sediment gravity flows to be the result of high-energy storm impacts on the shoreline.

STRATIGRAPHIC THICKNESS

The Green River and Colton Formations have a combined thickness of more than 6000 feet (1800 m) in the northern Uinta Basin, but only a portion of the stratigraphic interval is included in the CNUBP. The Bluebell subplay has a 2000-foot-thick (600 m) productive interval in the lower Green River and upper transitional Colton Formations. The Red Wash subplay has a 1000-foot-thick (300 m) productive interval (figure 2.18) in the Douglas Creek Member.

LITHOLOGY AND FRACTURING

The dominant oil-productive lithology is sandstone in both subplays (figure 7.2A); some production is from fractured shale, limestone, and marlstone in the Conventional Bluebell subplay. Grainstones composed of ostracods and ooids (figure 7.2B and figure 7.3) are also productive in the Redwash subplay and are targets using horizontal drilling. Fractures are encountered in both plays and generally enhance the reservoir quality, but are more common in the Bluebell subplay than in the Red Wash subplay.

Fractures are an important part of the Conventional Bluebell subplay reservoir and the underlying DUBOCP in the Altamont, Bluebell, and Cedar Rim fields. The fractures in the Conventional Bluebell subplay generally have a different orientation and possibly a different origin than the fractures in the underlying DUBOCP. Based on limited data, fractures in the DUBOCP reservoirs generally trend east-west, whereas fractures in the overlying Conventional Bluebell subplay reservoirs trend northwest-southeast (Allison and Morgan, 1996; Harthill and Bates, 1996; Morgan, 2003b). In the western Altamont and Cedar Rim fields a north-south fracture set, possibly related to Basin and Range extension, has been identified. Fractures in the DUBOCP reservoirs are believed to be the result of rapid gen-

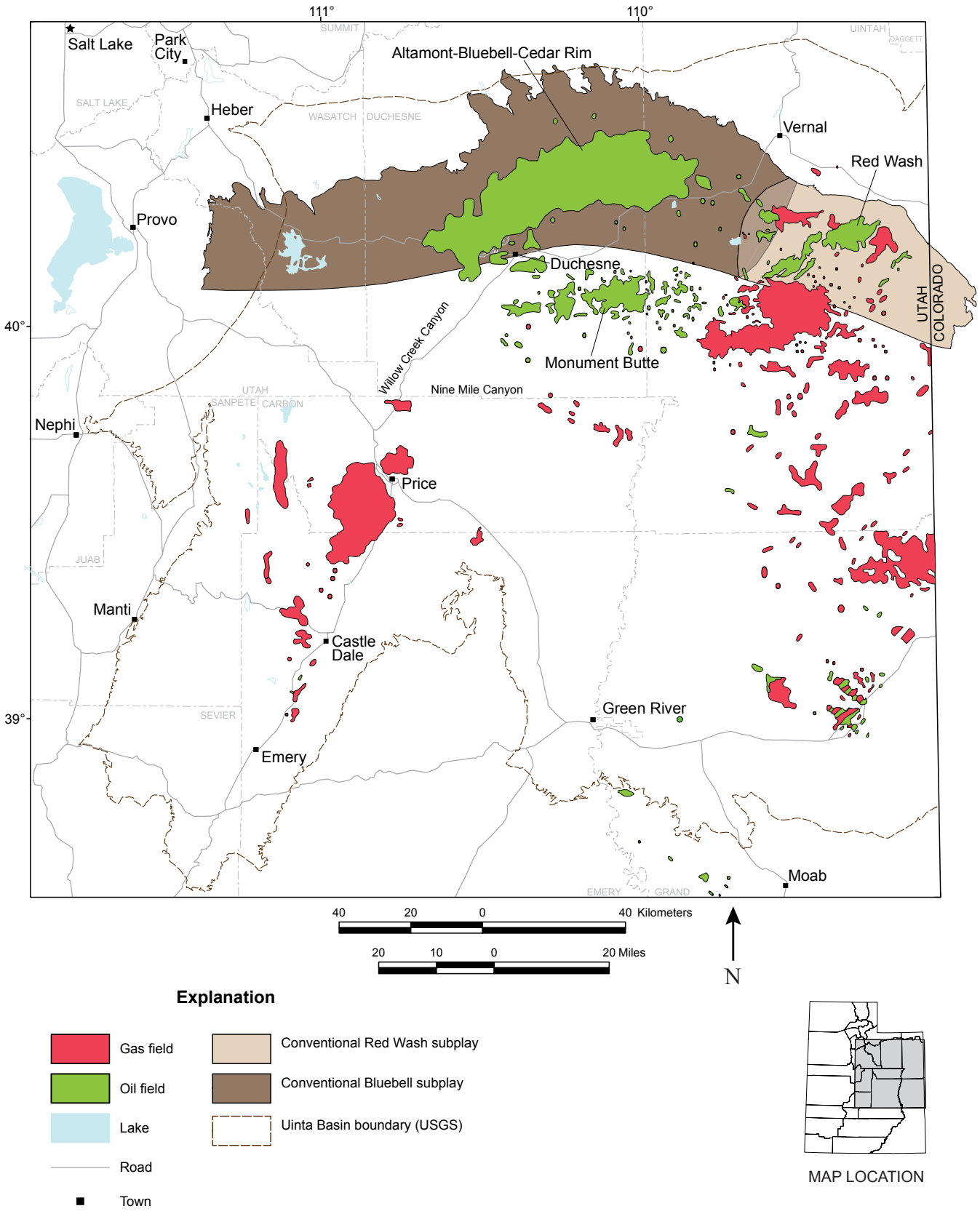

Figure 7.1. *Location map showing the outline of the Uinta Basin and major oil and gas fields. Brown and tan areas are the Conventional Bluebell subplay and the Conventional Red Wash subplay, respectively, that make up the Conventional Northern Uinta Basin play.*

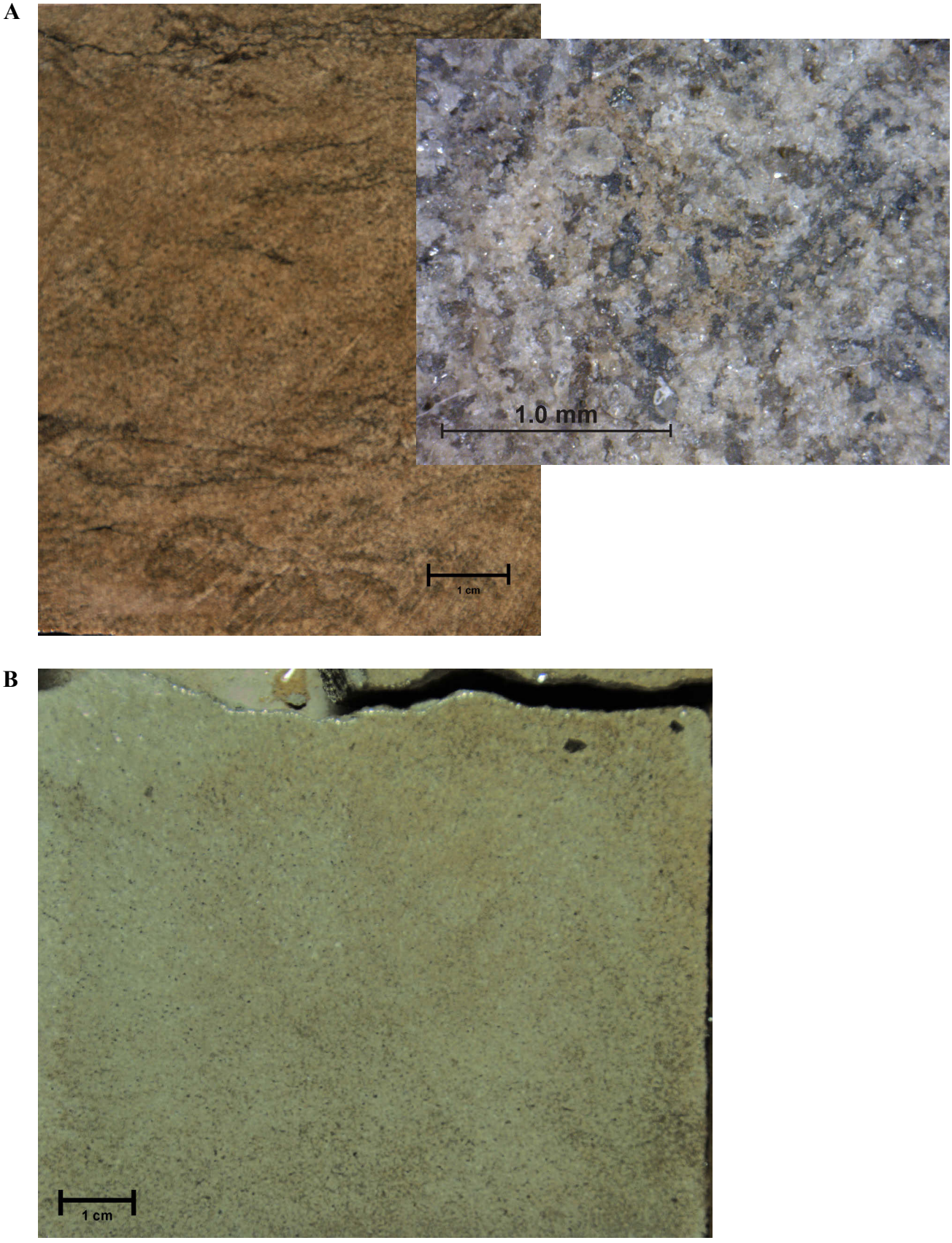

Figure 7.2. *Typical lower Green River Formation reservoirs in the Conventional Red Wash subplay, Wonsits Valley field, northeastern Uinta Basin.* ***A.*** *Upper shoreface, subrounded to subangular, very fine to fine-grained, quartz sandstone (inset showing close-up image) from the WVU No. 101-2 well (section 13, T. 8 S., R. 21 E., SLBL&M, slabbed core from 5414 feet).* ***B.*** *Ostracodal/oolitic grainstone from the WVU No. 128 well (section 10, T. 8 S., R. 21 E., SLBM&M, slabbed core from 5390 feet).*

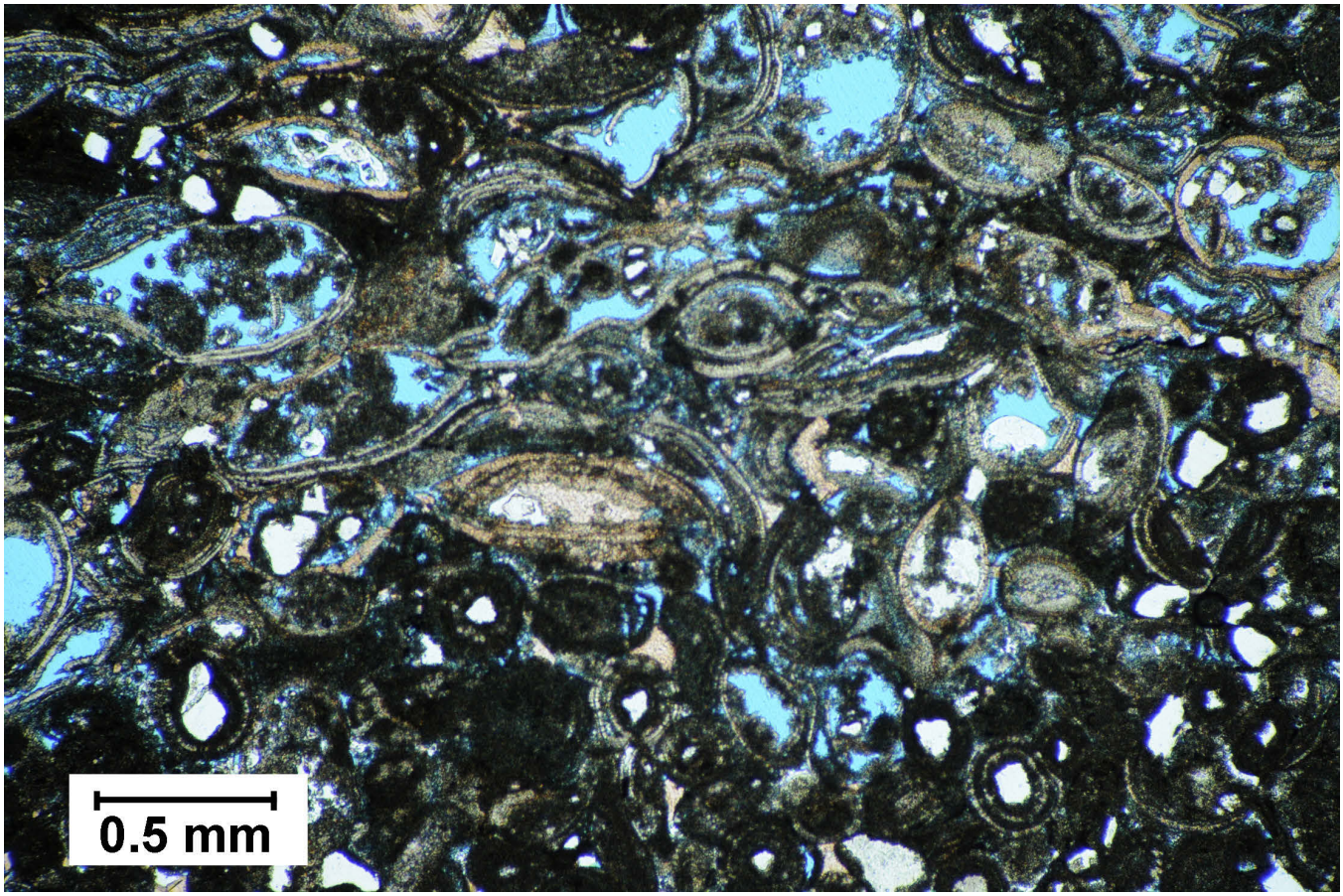

Figure 7.3. *Representative photomicrograph (plane light) of ostracodal grainstone showing both intraparticle and interparticle porosity. Note the presence of a few isolated ooids. From WVU No. 128 well, 5390 feet.*

eration of hydrocarbons within the largely impermeable rock (Lucas and Drexler, 1975; Narr and Currie, 1982; Bredehoeft and others, 1994). The Conventional Bluebell subplay reservoirs are not overpressured (0.5 psi [11.3 kPa/m]) to slightly overpressured, but have open fractures that are probably related to tectonic movement of the basin rather than hydrofracturing during oil generation. As a result, the fractures in the Conventional Bluebell subplay are not controlled by the distribution and thermal maturity of oil-source rock. Fractures in the Conventional Bluebell subplay are typically vertical to near vertical and often have significant calcite filling (Morgan, 2003a).

HYDROCARBON SOURCE AND SEALS

The source rocks for the crude oil produced from the CNUBP are kerogen-rich shale and marlstone of the black shale facies of the Green River Formation and were deposited in nearshore and offshore open-lacustrine environments (Hunt and others, 1954; Forsman and Hunt, 1958; Silverman and Epstein, 1958; Tissot and others, 1978; Ruble, 1996; Ruble and others, 1998). Anders and others (1992) showed that the 0.7% vitrinite reflectance level in the center of the Altamont and Bluebell fields is at about 8400 feet (2600 m) drill depth. The 0.7% reflectance level is the depth at which the onset of intense oil generation occurred. In most wells in Altamont and Bluebell, the 0.6% maturity level is at or below the Mahogany oil shale, but above the middle marker of the Green River. As a result, only the lower Green River and the Flagstaff Member are in the oil-generation window.

Lacustrine source rocks in the deepest portion of the basin are presently at or near their maximum burial depth (Dubiel, 2003). Oil and gas are likely currently being generated below about 10,000 feet (3000 m) (Dubiel, 2003). Based on burial history and petroleum-generation modeling of the Shell Brotherson 1-11B4 well in the Altamont field, Dubiel determined that oil and gas generation began near the base of the Green River Formation around 40 Ma at a depth of 11,000 feet (3300 m). Peak generation occurred during maximum burial between 30 to 40 Ma. The zone of hydrocarbon generation has risen stratigraphically through time (Dubiel, 2003). Much of the oil in the CNUBP was generated in-situ from the black shale facies in the lower Green River and has undergone only minor vertical and lateral migration in the Conventional Bluebell Subplay. Rocks in the Red Wash and neighboring fields have mean random vitrinite reflectance ($R_{o\ [mean]}$) values in the range of 0.40 to 0.55%. The oils from the Red Wash and neighboring fields have thermal maturity geochemical indices equivalent to 0.7 to 0.8% $R_{o\ (mean)}$, indicating migration from

more deeply buried, higher temperature source rocks in the Bluebell-Altamont area. Vertical and horizontal seals for producing zones are unfractured shale and low-permeable marls within the Green River.

STRUCTURE AND TRAPPING MECHANISMS

Stratigraphic traps are the primary trapping mechanism for reservoirs in the CNUBP. Structure is dominantly regional dip northward into the basin with minor flexures or subtle plunging structural anticlinal trends with no four-way closure.

The trap in the Conventional Bluebell subplay is formed by the updip (north to south) pinchout of alluvial and marginal lacustrine sandstone beds into offshore marlstone and shale beds. A subtle west-plunging anticline is mapped at Bluebell field in the middle Green River Formation (figure 7.4), which is not present at deeper horizons. The Altamont and Cedar Rim fields also have a regional northerly dip (figure 2.12).

The trap in the Conventional Red Wash subplay is formed by updip (northwest to southeast) pinchout of wave-dominated marginal lacustrine sandstone and ostracodal/oolitic grainstone beds. A subtle west- to northwest-plunging anticline is mapped in the Red Wash field (figure 7.5).

RESERVOIR PROPERTIES

Oil and gas production in the CNUBP is from the lower Green River Formation and upper Colton Formation (upper Green River/Colton transition). In the Conventional Bluebell subplay the sandstone reservoirs typically have low porosity (8 to 12%) and low matrix permeability (0.01 to 10 mD). The sediment was shed from the Uinta uplift directly north of the play area, deposited as sandstone in alluvial channels and fans, shallow marginal-lacustrine channels and bars in a low-energy environment with very little reworking of the sediment. As a result, the sandstone reservoirs typically are high in clay content and well cemented. Oil and gas is produced from fractured sandstone, shale, limestone, and less commonly marl-

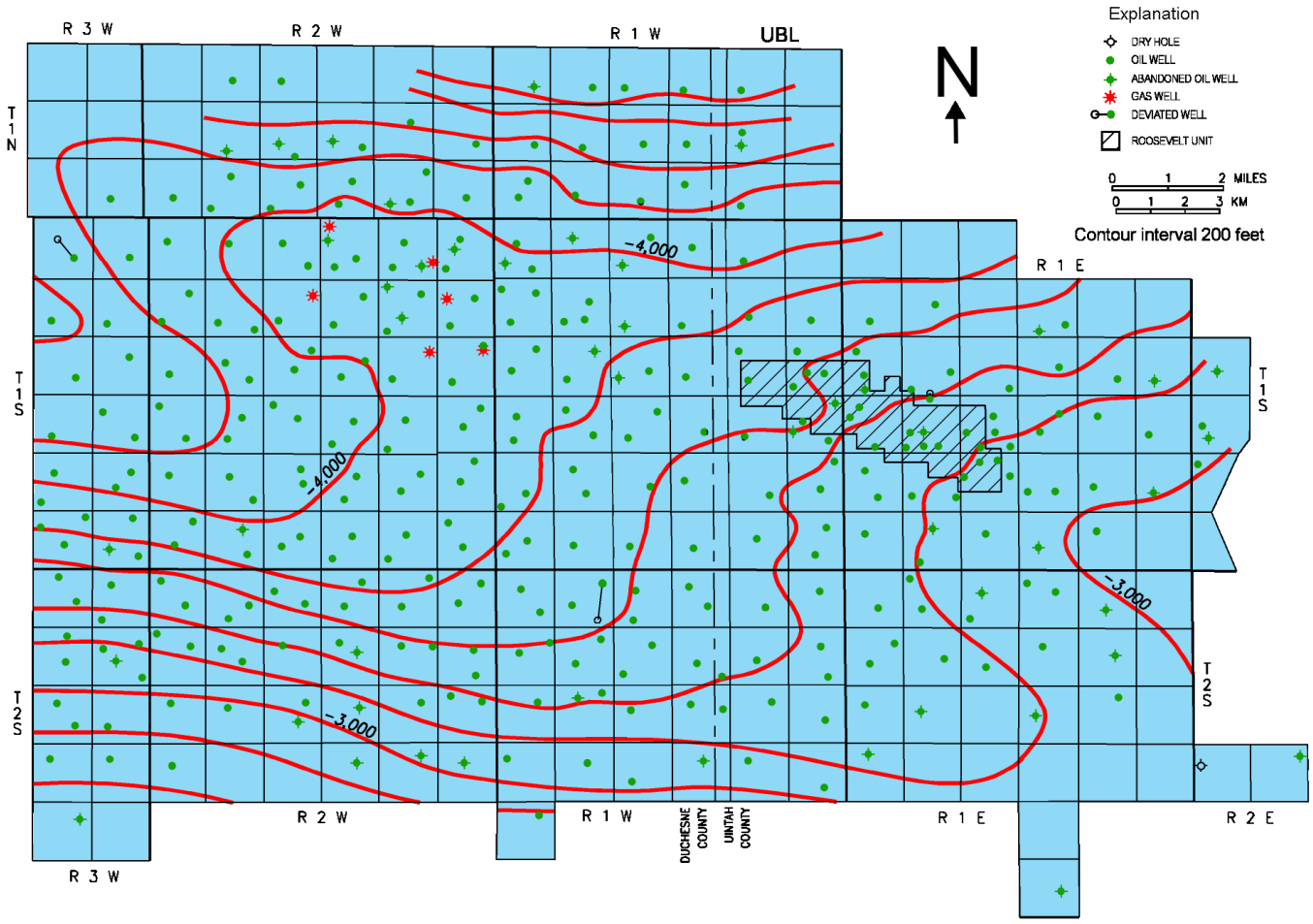

Figure 7.4. *Structure contour map of the top of the middle marker in the middle member of the Green River Formation, Bluebell field, Duchesne and Uintah Counties, Utah. Contour interval is 200 feet; datum = mean sea level. Note the subtle northwest-plunging and west-plunging anticlinal noses in the northern and eastern parts of the field, respectively. From Morgan (2003b).*

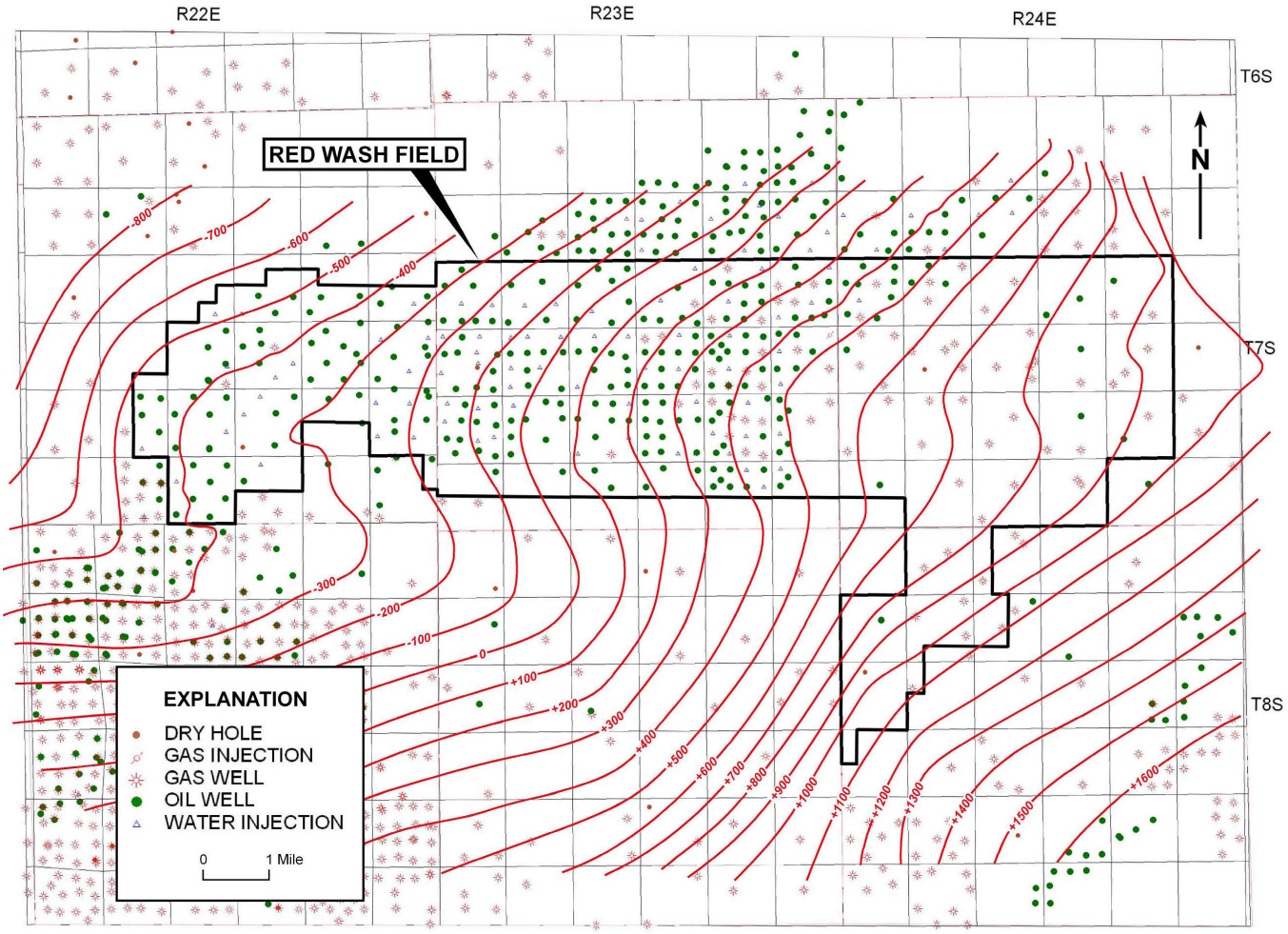

Figure 7.5. *Structure contour map on the top of the Douglas Creek Member of the Green River Formation, Red Wash field. Note the subtle west-plunging anticlinal nose that extends through the field. Contour interval is 100 feet; datum = mean sea level. From Schuh (1993a).*

stone. Characterization of the Conventional Bluebell subplay reservoir is very poor due to the:

1. extremely limited amount of core relative to the areal extent and thickness of the reservoir,
2. extremely limited amount of borehole imaging logs from the reservoir,
3. extensive number of perforated beds in the well with little to no knowledge of the contribution each bed makes to the overall production, and
4. low density of wells.

The sandstone beds are typically lenticular channel and shoreface storm deposits a few feet thick to rarely a few tens of feet thickand have very limited lateral extent. Thickness maps of many of the sandstone beds show no relationship to well productivity (Allison, 1995; Morgan, 1997). Shale and limestone beds deposited in the lacustrine environment, are often more laterally extensive than the sandstone beds and can be useful correlation markers (Morgan, 2003b). The shale and limestone beds are typically a few feet thick to rarely a few tens of feet thick, but are generally less fractured (Morgan, 2003b).

Fractures in the Conventional Bluebell subplay, like the lithology, are poorly characterized. The orientation, spacing, connectivity, and fluid flow characteristics of the fractures are virtually unknown. Drilling four wells per section is providing additional information about the reservoir.

In contrast, the sandstone in the Red Wash field area was derived from wave and storm dominated deposits in a shoreface environment on a steeper, higher energy shelf, and underwent greater reworking during deposition. As a result, the sandstone reservoirs in the Conventional Red Wash subplay have higher porosities (8 to 20%) and significantly higher matrix permeabilities, commonly 50 to 500 mD. Sandstone beds generally range from a few feet to tens of feet thick. Most fields in the Conventional Red Wash subplay produce from multiple beds. The sandstone beds in the Conventional Red Wash subplay are generally more laterally extensive than many of the beds in the Conventional Bluebell subplay. Ostracodal grainstone have been reworked like sandstone reservoirs resulting in reservoir porosities rang-

ing from 10 to 14% (figure 7.3). The grainstone reservoirs range in thickness from a few feet to 20 feet (6 m) and are also laterally extensive. Reservoir data for individual fields in the Conventional Red Wash subplay are summarized in table 7.1.

OIL AND GAS CHARACTERISTICS

Most of the oil produced from the CNUBP is characterized as black wax (table 6.2). The black wax typically has a gravity of 28 to 32°API gravity. The crude at Red Wash field has a lower pour point, 80 to 95°F (27–35°C), than the black wax at Bluebell field, which has a pour point of about 120°F (49°C).

Associated gas from the Red Wash field (table 6.3) contains an average of 95% methane, 1.5% ethane, 1.1% propane, 1.6% higher fractions, 0.7% CO_2, and has an average heating value of 1060 Btu/ft^3 (Moore and Sigler, 1987). Associated gas from the Bluebell field (table 6.3) contains an average of 85% methane, 8% ethane, 3% propane, 2.6% higher fractions, 0.3% CO_2, with an average heating value of 1200 Btu/ft^3 (Moore and Sigler, 1987). For additional information on geochemical analysis and biomarker studies of the Green River oils, please refer to Ruble, 1996; Mueller, 1998; Mueller and Philp, 1998; Ruble and Philp, 1998; and Dubiel, 2003.

PRODUCTION

Fields in the CNUBP produce crude oil and associated gas. Production from the Conventional Bluebell subplay cannot be accurately separated from the DUBOCP and is presented as production for that play. The largest fields (fields with >500,000 BO [79,500 m^3] cumulative production) in the Conventional Red Wash subplay have produced 169.7 million BO (27.0 million m^3) and 605.6 BCFG (17.1 BCMG) as of January 1, 2016. Monthly production from the play in December 2015 was 96,521 BO (15,346 m^3) and 2087 MMCFG (59.1 MMCMG) (Utah Division of Oil, Gas, and Mining, 2016a). The Red Wash field has produced the most oil and continues to be the largest producer in the subplay. The OOIP estimate for Red Wash and Wonsits Valley (the two most productive fields in the Conventional Red Wash subplay) are 550 million BO (87.5 million m^3) and 149 million BO (23.7 million m^3), respectively (Mary McPherson, verbal communication, 1998). The original estimated ultimate recovery (EUR) for Red Wash and Wonsits Valley fields was 106 million BO (16.9 million m^3) and 48 million BO (7.6 million m^3), respectively (Schuh, 1993a, 1993b). As of January 1, 2016, the cumulative production from Red Wash and Wonsits Valley fields was 354 million BO (56.3 million m^3) and 103 million BO (16.4 million m^3), respectively (Utah Division of Oil, Gas, and Mining, 2016a). Both fields have exceeded their original EUR, newer OOIP and EUR calculations for the two fields have not been published. Data on production and number of wells are summarized for the fields in the play in table 7.1.

Table 7.1. *Geologic, reservoir, and production data for the largest fields in the Conventional Red Wash subplay of the Conventional Northern Uinta Basin play (all fields listed are in Uintah County, Utah). Data for the Conventional Bluebell subplay can not be accurately separated from the Deep Uinta Basin Overpressured Continuous play and is presented in that play (see table 6.1). Production data is from Utah Division of Oil, Gas, and Mining (2016a).*

Field	Discovery Date	Active Producers	Abandoned Producers	Acres	Spacing (acres)	Pay (feet)	Porosity (%)	Perm. (mD)	Temp. (°F)	Initial Reservoir Pressure (psi)	Average Monthly Production		Cumulative Production	
											Oil (bbl)	Gas (MCF)	Oil (bbl)	Gas (MCF)
Brennan Bottom	1954	44	5	1760	160	26	12	1.0	162	2580	27,693	18,133	3,818,878	3,587,967
Coyote Basin	1964	20	8	1600	80	8	14	215	120	1559	2384	1223	2,236,169	1,058,377
Red Wash	1951	217	134	31,000	40–80	170	13	42	149	1925	35,308	1,659,654	87,863,301	415,946,337
Walker Hollow	1953	73	24	9040	40		13	42	107	NA	12,862	19,582	20,183,227	34,912,840
White River	1964	28	16	1040	80	16	10	NA	150	2379	1517	25,639	3,102,772	15,439,979
Wonsits Valley	1962	291	111	6240	40	90	12	22	149	2800	18,425	243,411	52,500,635	137,611,054

NA = data not available.

FIELD OVERVIEWS

Greater Altamont-Bluebell-Cedar Rim Field Trend Overview

The greater Altamont-Bluebell-Cedar Rim field trend is located in Duchesne and Uintah Counties, Utah, in the Conventional Bluebell subplay of the Conventional Northern Uinta Basin play (as well as the Deep Uinta Basin Overpressured Continous play). The trend occurs along a generally contiguous, stratigraphic, updip pinchout on the north-dipping flank of the Uinta Basin near the basin axis (figures 2.12, 6.2, and 7.1). The gentle northern regional dip is occasionally interrupted by subtle structural noses (figure 7.4). Oil production is from multiple, stacked, fluvial-deltaic channel and shoreface storm deposit sandstone, and some lacustrine limestone and shale in the upper Green River, lower Green River, and Flagstaff Member of the Green River and Colton (Wasatch) Formations. The Flagstaff Member/Colton reservoir is an overpressured, basin-centered, oil accumulation controlled by fractures (see chapter 6). Typical wells produce from 20 to 50 zones in Altamont and Bluebell reservoirs (Smouse, 1993a). These zones are channel and shoreface sandstone, 3 to 40 feet (1–13 m) thick. The producing Altamont-Bluebell-Cedar Rim field trend extends over a 290,580-acre (117,600 ha) area.

Quartzarenites and litharenites predominate in the north part of the basin. They consist of monocrystalline quartz with chert as the main lithic component (Fouch and others, 1992). Diagenetic effects both reduce and enhance reservoir porosity and permeability. Compaction and authigenic clay formation (illite) have reduced reservoir quality in the Altamont-Bluebell-Cedar Rim field trend (Pitman and others, 1982). Porosity ranges from 2 to 20%, averaging 5%. Permeability is highly variable ranging from 0.1 up to 1000 mD in fractured zones (Fouch and others, 1992; Smouse, 1993a). The drive is solution gas, and the initial water saturation was 10% or greater (Smouse, 1993a).

The first Green River Formation reservoir was discovered in 1949 at Bluebell field (Roosevelt unit) with the completion of the Humble Oil Ute Tribal No. 1 well, NW1/4SW1/4 section 21, T. 1 S., R. 1 E., UBL&M, Uintah County; initial flowing potential (IPF) was 1633 BOPD (260 m^3/d). The first Wasatch Formation reservoir was discovered in 1970 at Altamont field with the completion of the Shell Oil Miles No. 1-36A4 well, SW1/4NE1/4 section 35, T. 1 S., R. 4 W., UBL&M, Duchesne County; IPF was 1004 BOPD (160 m^3/d). The Altamont-Bluebell-Cedar Rim field area currently has 760 producing (or shut-in) wells (Utah Division of Oil, Gas, and Mining, 2016a). Cumulative production as of January 1, 2016, was 344,822,683 BO (54,822,430 m^3), 620 BCFG (17.6 BCMG), and over 763 million BW (121 million m^3) (Utah Division of Oil, Gas, and Mining, 2016a). The original, estimated, primary recovery was 316,000,000 BO (Smouse, 1993a).

Red Wash Field

Red Wash field, Uintah County, Utah, in the Conventional Red Wash subplay, is a stratigraphic pinch-out across a structural nose (figures 7.1 and 7.5) that produces primarily from fluvial-deltaic and shoreface storm/wave sandstone in the Douglas Creek Member of the Green River Formation (Castle, 1990). The net reservoir thickness is 170 feet (50 m), which extends over a 31,000-acre (12,500 ha) area. Porosity ranges from 10 to 22%, along with an average of 42 mD of permeability (Schuh, 1993a).

Red Wash field was discovered in 1951 with the completion of the California Oil Co. (Chevron) Red Wash Unit No. 1 well, NE1/4NE1/4 section 26, T. 7 S., R. 23 E., SLBL&M, Uintah County; IPF was 339 bbls of oil per day (BOPD [54 m^3]) and 698 thousand cubic feet of gas per day (MCFGPD [20 MCMPD]). The field currently has 217 producing (or shut-in) wells (Utah Division of Oil, Gas, and Mining, 2016a). The well spacing is 40 to 80 acres (16–32 ha). The present reservoir field pressure ranges from 400 to 2000 psi (2800–13,800 kpa).

Cumulative production as of January 1, 2016, was 87,863,301 BO (13,969,150 m^3), 416 BCFG (12 BCMG) and over 359 million BW (57 million m^3) (Utah Division of Oil, Gas, and Mining, 2016a). The original estimated primary recovery was 53 million BO (8.4 million m^3) and 300 BCFG (8.5 BCMG) (Schuh, 1993a). The estimated secondary recovery was 53 million BO (8.4 million m^3) using a waterflood program (Schuh, 1993a).

Wonsits Valley Field

Wonsits Valley field, Uintah County, Utah, in the Conventional Red Wash subplay, is a stratigraphic trap due to lateral facies changes (figure 7.6) that produces from medium-grained, quartz sandstone and fine-grained, sandy, ostracodal limestone deposited in a high-energy, barrier-beach complex of the Douglas Creek Member (Castle, 1990). The net reservoir thickness is 90 feet (30 m), which extends over a 6240-acre (2530 ha) area. Porosity and permeability averages 12% and 22 mD, respectively (Schuh, 1993b).

Wonsits Valley field was discovered in 1962 with the completion of the Gulf Oil Co. Stout Federal Unit No. 1 well, NE1/4NE1/4 section 8, T. 8 S., R. 22 E., SLBL&M, Uintah County; IPF was 13 BOPD (2 m^3) and 8 BWPD (1 m^3). The field currently has 291 producing (or shut-in) wells (Utah Division of Oil, Gas, and Mining, 2016a). The well spacing is 40 acres (16 ha). The present reservoir field pressure is 2500 psi (17,200 kpa).

Cumulative production as of January 1, 2016, was 52,500,635 BO (8,346,934 m^3), 137 BCFG (3.9 BCMG), and over 194 million BW (31 million m^3) (Utah Division of Oil, Gas, and Mining, 2016a). The original estimated primary recovery was 21.6 million BO (3.4 million m^3) (Schuh, 1993b). The estimated sec-

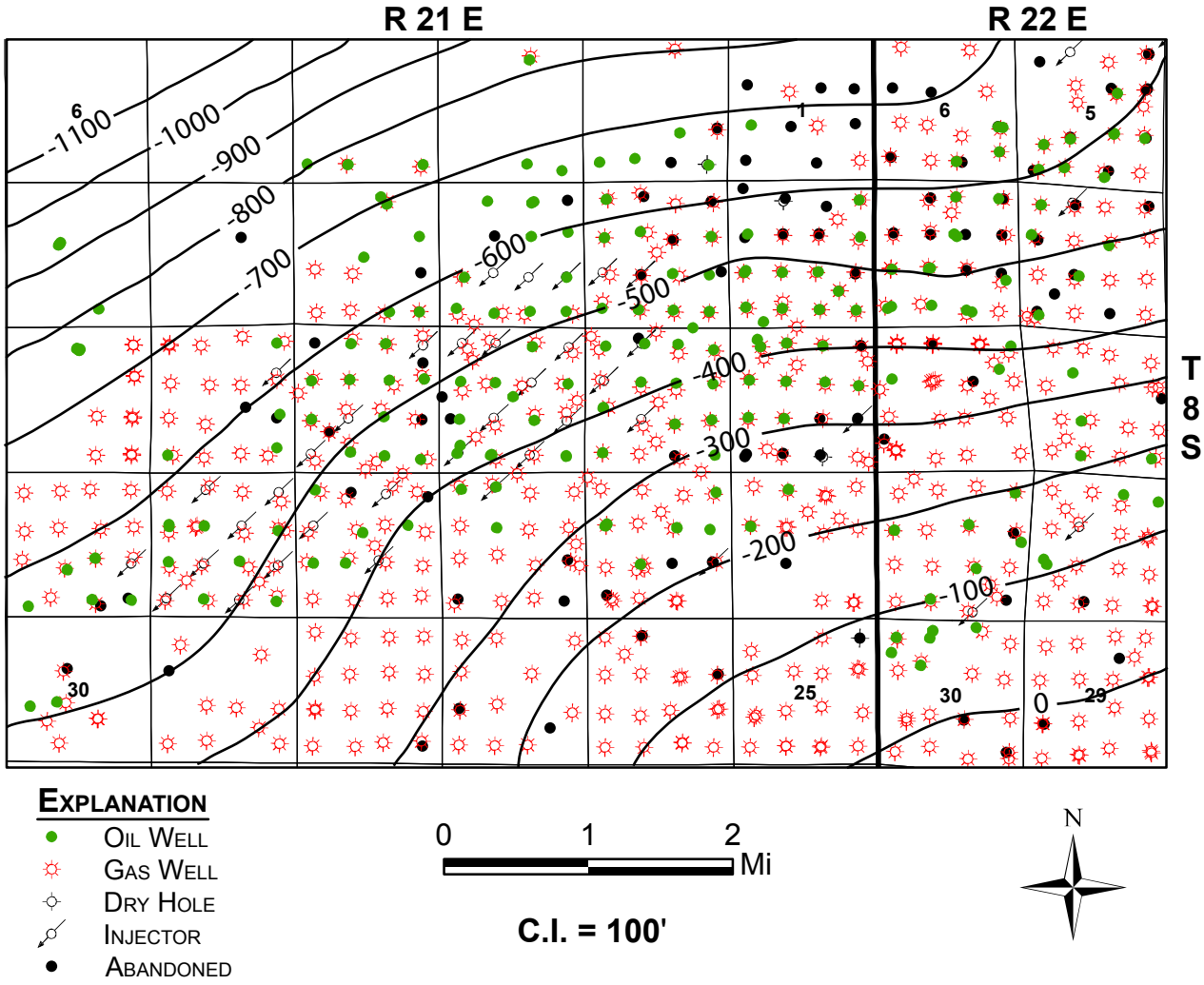

Figure 7.6. *Structure map on top of G1 producing zone of the Green River Formation, Wonsits Valley field, Uintah County, Utah. Modified from Schuh (1993b).*

ondary recovery was 26.4 million BO (4.2 million m^3) using a waterflood program similar to Red Wash field (Schuh, 1993b).

EXPLORATION POTENTIAL AND TRENDS

Conventional Bluebell Subplay

Infill drilling will continue in portions of the Altamont-Bluebell-Cedar Rim field area (figure 7.1) whereas the Conventional Bluebell subplay has not been developed on two wells per section. Down spacing to four producing wells per section was approved by the Utah Board of Oil, Gas, and Mining in December 2008 and could result in hundreds of new wells. The increased well density could eventually lead to EOR in portions of the Altamont-Bluebell-Cedar Rim fields.

The western portion of the Conventional Bluebell subplay is being explored for Mesaverde Group and Mancos Shale gas. The deeper drilling for gas could result in the discovery of new oil fields in the overlying Green River Formation.

Secondary and tertiary recovery methods have not been attempted in the Altamont-Bluebell-Cedar Rim field area. Several factors have discouraged operators from attempting any secondary recovery pilot projects. Fractures in the reservoir rock can cause early breakthrough of any injected fluid or gas. Fractures can result in injected fluids or gases moving great distances, perhaps even beyond the intended secondary recovery unit. Secondary and tertiary recovery methods generally require a high density of wells to be effective. The Altamont-Bluebell-Cedar Rim field area has been developed with two wells per section and in many areas at least one of those wells has already been plugged and abandoned. As a result, any secondary or tertiary recovery method would require a significant amount of additional drilling. Allowing the production of four wells per section is a significant step in improving the understanding of the reservoir and potential development of EOR.

The gross productive interval is 1000+ feet (300 m) thick, no single bed is a dominant producer. As a result, horizontal drilling has not been attempted in the Altamont-Bluebell-Cedar Rim fields. High-angle wellbores have been drilled in an at-

tempt to encounter thicker productive beds and intersect more fractures. The high-angle wells were expensive to drill, more difficult to complete and produce, and did not result in any significant improvement in production.

Seismic data has had limited use in the Altamont-Bluebell-Cedar Rim fields. In the 1990s Pennzoil used seismic to map the thickness of the Green River Formation and drilled what they hoped was the deepest portions of Lake Uinta with the largest volume of source rock. Drilling based on the seismic data did not result in better producing wells. Amplitude variation with offset seismic analysis and VSP analysis was used to map fractures in the upper Green River in a portion of the Altamont field (T. 1 S., R. 2 W.) where shallow gas was being produced (Lynn and others, 1995; Harthill and Bates, 1996; Harthill and others, 1997; Lynn and others, 1999). The process has not been used to identify specific drilling locations in the upper Green River and is probably not practical for the deeper Green River due to the large offsets that would be necessary. Three-dimensional seismic has been successfully used in many hydrocarbon plays. Since fractures, not structure or stratigraphy, is a dominant control on reservoir performance, 3-D seismic has not been used in the Altamont-Bluebell-Cedar Rim fields.

As with the DUBOCP, a large resource potential in the Conventional Bluebell subplay may be exploited by recompleting existing wells. The wells in this shallower subplay were also completed with perforations in 40 or more beds in a 1500-foot (450 m) or greater, vertical interval. As a result, many of the beds may never have received adequate stimulation, like beds in the DUBOCP. Once again, using cased-hole logs to identify by-passed oil and selectively stimulating individual beds can recover a significant amount of additional oil in the Conventional Bluebell subplay. The potential for increased oil recovery from recompletion of older wells has been demonstrated in the Roosevelt federal exploratory unit within Bluebell field (Morgan, 2003b). Before recompletions, production from the unit had dropped to 561 BO (89.2 m^3) by the end of 2002, but a program of recompletions resulted in monthly production averaging over 15,000 BO (2400 m^3). Two new wells were drilled in 2009 and several more wells were completed in 2012 (figure 7.7).

Conventional Red Wash Subplay

Many of the fields in the Conventional Red Wash subplay are currently in secondary recovery waterflood operations and are not actively being drilled. Long-reach horizontal wells in the Wonsits Valley and other nearby fields are being drilled into the G limestone, a major ostracodal/oolitic grainstone, of the lower Green River Formation resulting in increased production from these fields. As a result, for example, annual oil production from the Wonsits Valley field increased in 2006 and

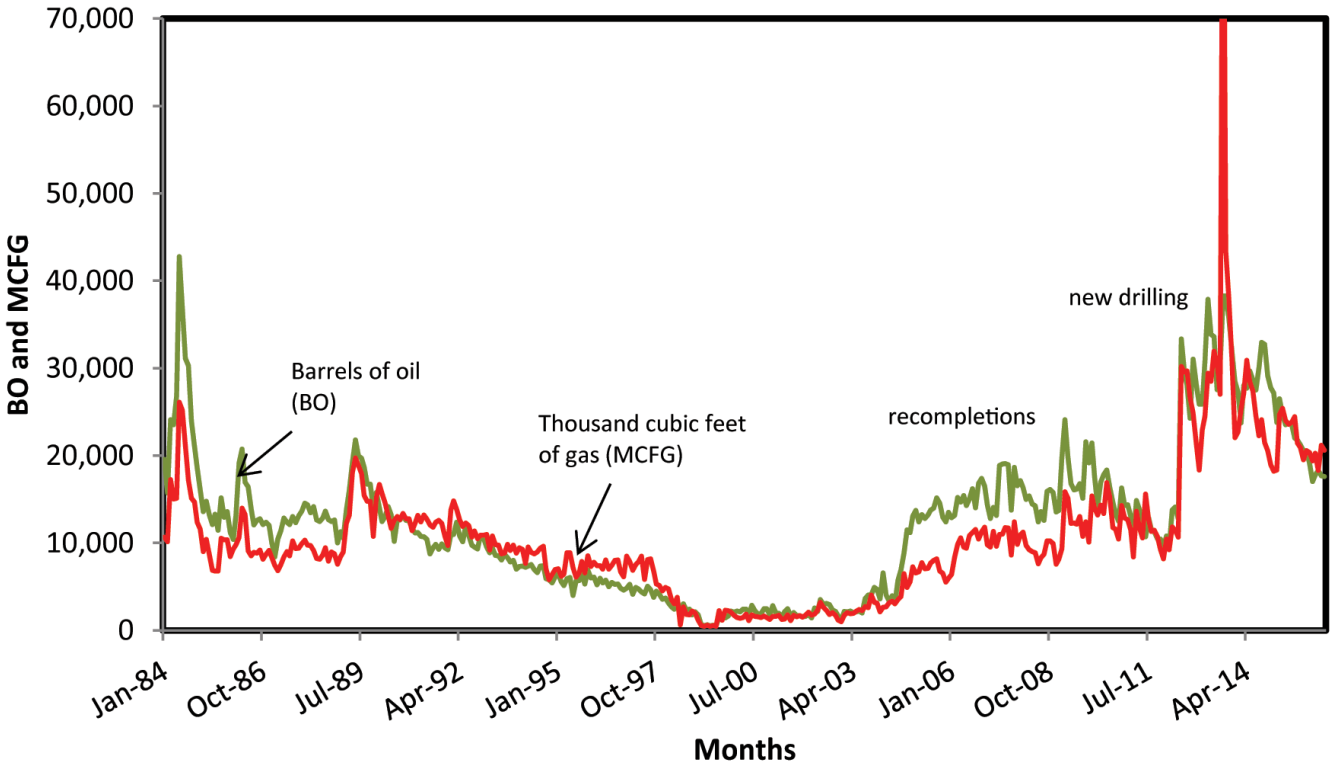

Figure 7.7. *Monthly oil and gas production for the Roosevelt unit in Bluebell field. Production from the unit had dropped to a low of 561 BO/month by the end of 2002, but a program of recompletions begun in 2003 increased production to more than 15,000 BO/month. Many of these recompleteions were in upper Green River Formation and are an example of the potential that still exists in the Conventional Northern Uinta Basin play. Several additional new wells were drilled in the Roosevelt unit in 2012 and were completed in both the deep overpressured beds and shallower conventional beds. Data from Utah Division of Oil, Gas, and Mining (2016a).*

2007 after years of decline. Continued success targeting ostracodal/oolitic grainstones represents significant potential for new oil discoveries in the northeastern Uinta Basin. Tertiary recovery techniques are not currently being tested, but may be considered in the future as production continues to decline. A pilot CO_2 injection test was conducted in the Red Wash and Wonsits Valley fields in the 1980s. The short injection tests had mixed results and no further testing was done. Much of the Conventional Red Wash subplay area is being actively explored for gas in the deeper Wasatch Formation, Mesaverde Group, and Mancos Shale. The deep drilling will likely identify new potential in the shallow Green River Formation that can be exploited in the wells when the deeper reservoirs are depleted or may lead to additional development drilling if the Green River potential is considered significant.

CHAPTER 8: CONVENTIONAL SOUTHERN UINTA BASIN PLAY

by

Craig D. Morgan

Utah Geological Survey

CONTENTS

FIGURES

TABLE

CHAPTER 8:
CONVENTIONAL SOUTHERN UINTA BASIN PLAY

INTRODUCTION

The Conventional Southern Uinta Basin play (CSUBP) covers the central and southern Uinta Basin (figure 8.1) and typically has drill depths ranging from 3000 (900 m) to 6500 feet (2000 m). The play is divided into six subplays: (1) Conventional Uteland Butte Interval subplay, (2) Conventional Castle Peak Interval subplay, (3) Conventional Travis Interval subplay, (4) Conventional Monument Butte Interval subplay, (5) Conventional Beluga Interval subplay (Morgan and Bereskin, 2003), and (6) Conventional Duchesne Interval Fractured Shale/Marlstone subplay (figures 2.13 and 8.2).

The southern shore of Lake Uinta was often very broad and flat, which resulted in laterally extensive transgressions and regressions of the shoreline in response to climatic and tectonic-induced rise and fall of the lake (figures 2.14 and 8.3). The cyclic nature of Green River deposition in the central Uinta Basin resulted in numerous stacked deltaic deposits. Distributary-mouth bars, distributary channels, and nearshore bars are the primary producing reservoirs in the area (figure 2.19).

The changing depositional environments of Eocene Lake Uinta controlled the characteristics of each interval and the reservoir rock contained within (figure 8.3). The Travis reservoir records a time of tectonism that created a steeper slope and a pronounced shelf break where thick cut-and-fill valleys developed during lake-level falls and rises. The Monument Butte reservoir represents a return to a gentle, shallow shelf where channel deposits are stacked in a lowstand delta plain and amalgamated into the most extensive reservoir in the central Uinta Basin. The Beluga reservoir represents a time of major lake expansion with fewer, less pronounced lake-level falls, resulting in isolated single-storied channel and shallow-bar sand deposits. The fractured shale/marlstone rocks in the upper part of the middle member, the upper member, and the saline member of the Green River Formation were deposited during the maximum rise and waning stages of Lake Uinta.

DEPOSITIONAL ENVIRONMENT

The CSUBP produces from the Eocene Green River Formation. The reservoir in the Uteland Butte interval is mainly lacustrine limestone with rare bar sandstone beds, whereas the reservoirs in the overlying four intervals are mainly distributary channel and shallow lacustrine sandstone beds (Morgan and Bereskin, 2003; Morgan and others, 2003).

The Uteland Butte interval was deposited during a major rise in lake level representing the first major transgression of the lake after deposition of the alluvial Colton Formation. The Uteland Butte is distinctive in its abundance of carbonate rocks and lack of sandstone, which could have been caused by one or both of the following situations: (1) the rapid lake-level rise caused siliciclastic sediments to be deposited in proximal alluvial channels, or (2) the main sediment inflow into the lake was far from the central Uinta Basin area, perhaps flowing into the southern arm of the lake south and west of the San Rafael uplift (McDonald, 1972; Vanden Berg and others, 2013). Little (1988), working in the Minnie Maud Creek to Willow Creek Canyon area, described the Uteland Butte environment as shallow-water ostracodal mud flats to muddy offshore lacustrine (figure 8.4). Little (1988) describes 3- to 6-foot (1–2 m) thick beach- or bar-sandstone beds in the Minnie Maud area, but these beds are absent in Willow Creek Canyon (figure 8.1).

The Castle Peak interval in the central Uinta Basin consists of isolated marginal lacustrine channel sandstone beds encased in carbonate that were deposited during a time of numerous and rapid lake-level fluctuations, which developed a simple drainage pattern across the exposed shallow and gentle shelf with each fall and rise cycle (figure 2.19). These channel deposits are typically limited in lateral extent; channel stacking is rare. The lack of channel stacking is attributed to short-duration cycles of lake-level rise and fall. As a result, the drainage system for each cycle never advanced beyond the initial stage. Schumn and Ethridge (1994) show that the initial drainage pattern on an exposed shelf is typically a series of subparallel, unconnected channels.

The Travis interval consists of sand-rich alluvial and deltaic deposits of the Renegade Tongue (Cashion, 1967) in Desolation Canyon, fluvial-deltaic deposits in Nine Mile Canyon, and the green shale facies (Picard, 1955, 1957) in Willow Creek Canyon. These deposits represent a significant basinward shift of facies. In the Monument Butte area, however, the rocks consist of the black shale facies and do not show evidence of a major regression. A significant basinward shift of the shoreline without evidence of shallowing, and perhaps even deepening in the distal reaches, may be the result of tectonic movement in the basin. This tectonic activity may have shifted the regional drainage to the central Uinta Basin area, resulting in the sand-rich deltaic deposits in Desolation and Nine Mile Canyons. Prior to this tectonic activity, channel deposits in the lower member of the Green River Formation in the central Uinta Basin were generally smaller and more isolated, indicating only a local drainage system. Also, a rel-

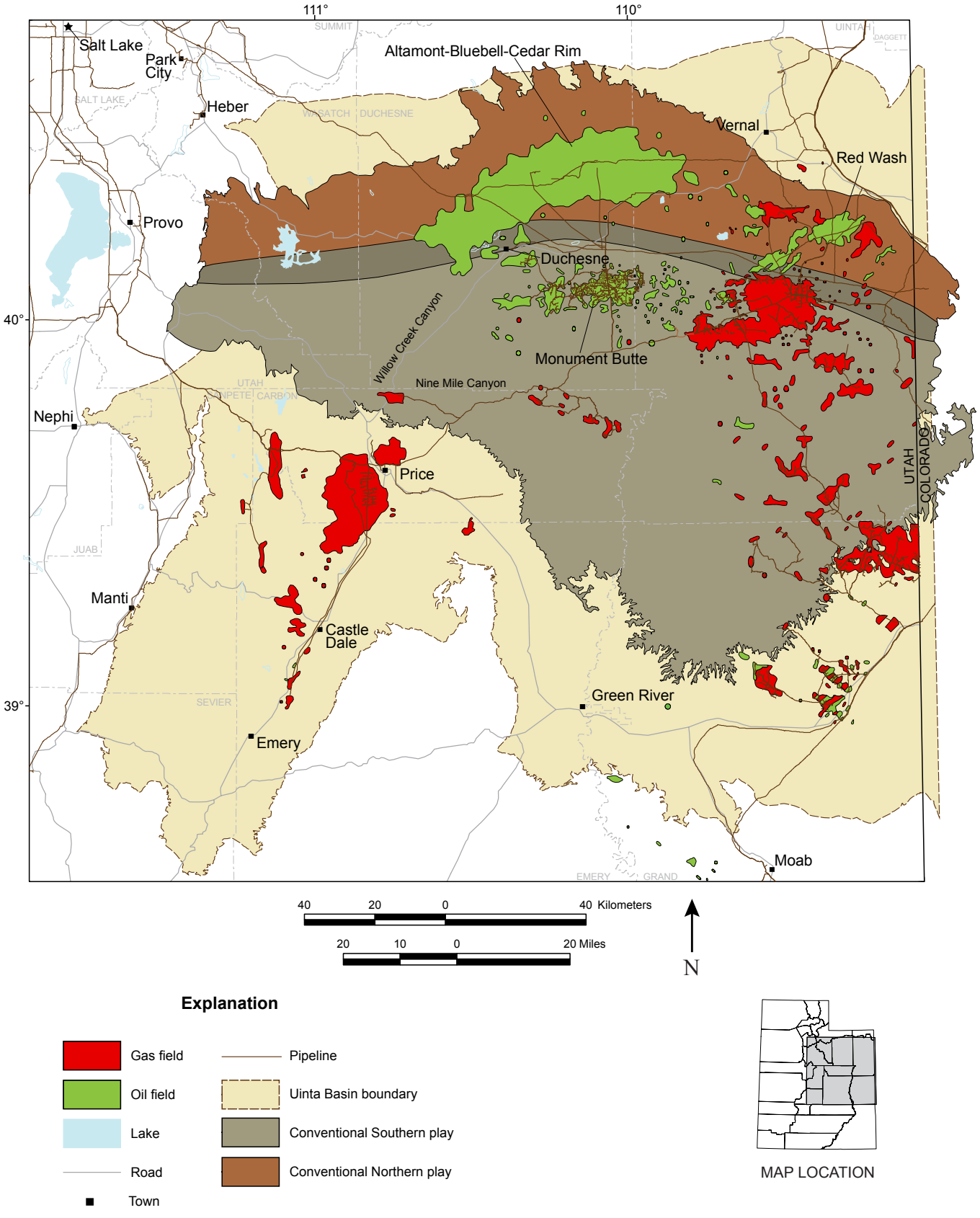

Figure 8.1. *Location map showing the outline of the Uinta Basin, major oil and gas fields, and the Conventional Northern Uinta Basin play and Conventional Southern Uinta Basin play areas. The two plays overlap because the north-sourced deposits and the south-sourced deposits of the Green River Formation intertongue in the central basin.*

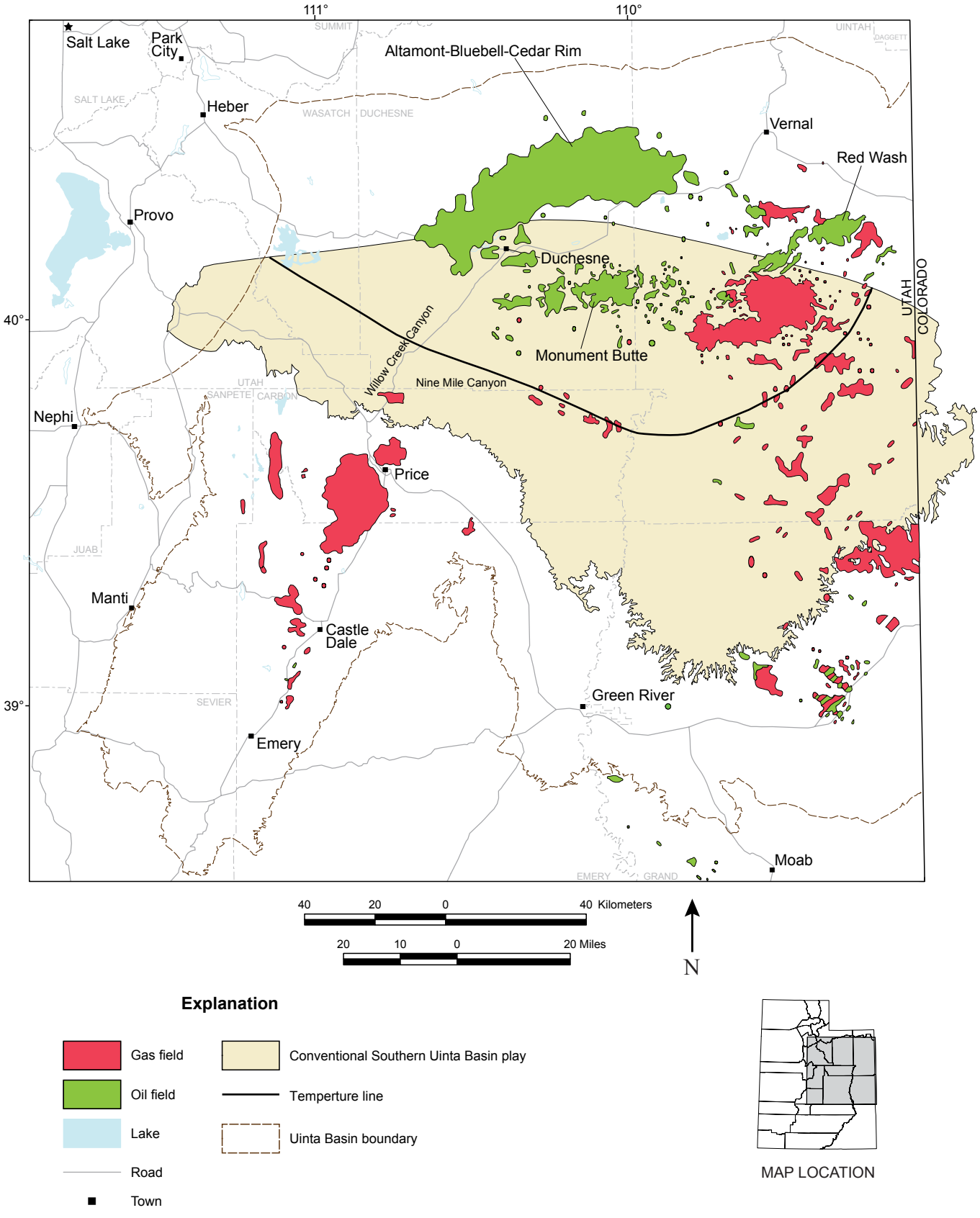

Figure 8.2. *Location map showing the outline of the Uinta Basin, major oil and gas fields, and the Conventional Southern Uinta Basin play area. The subplays encompass the entire Conventional Southern Uinta Basin play area. The solid crescent-shaped line dividing the play into a northern and southern area is the approximate updip boundary where the formation temperature in the CSUBP is near the pour-point temperature of the oil. As a result, the area updip (south) of this line may not have moveable oil in the reservoir.*

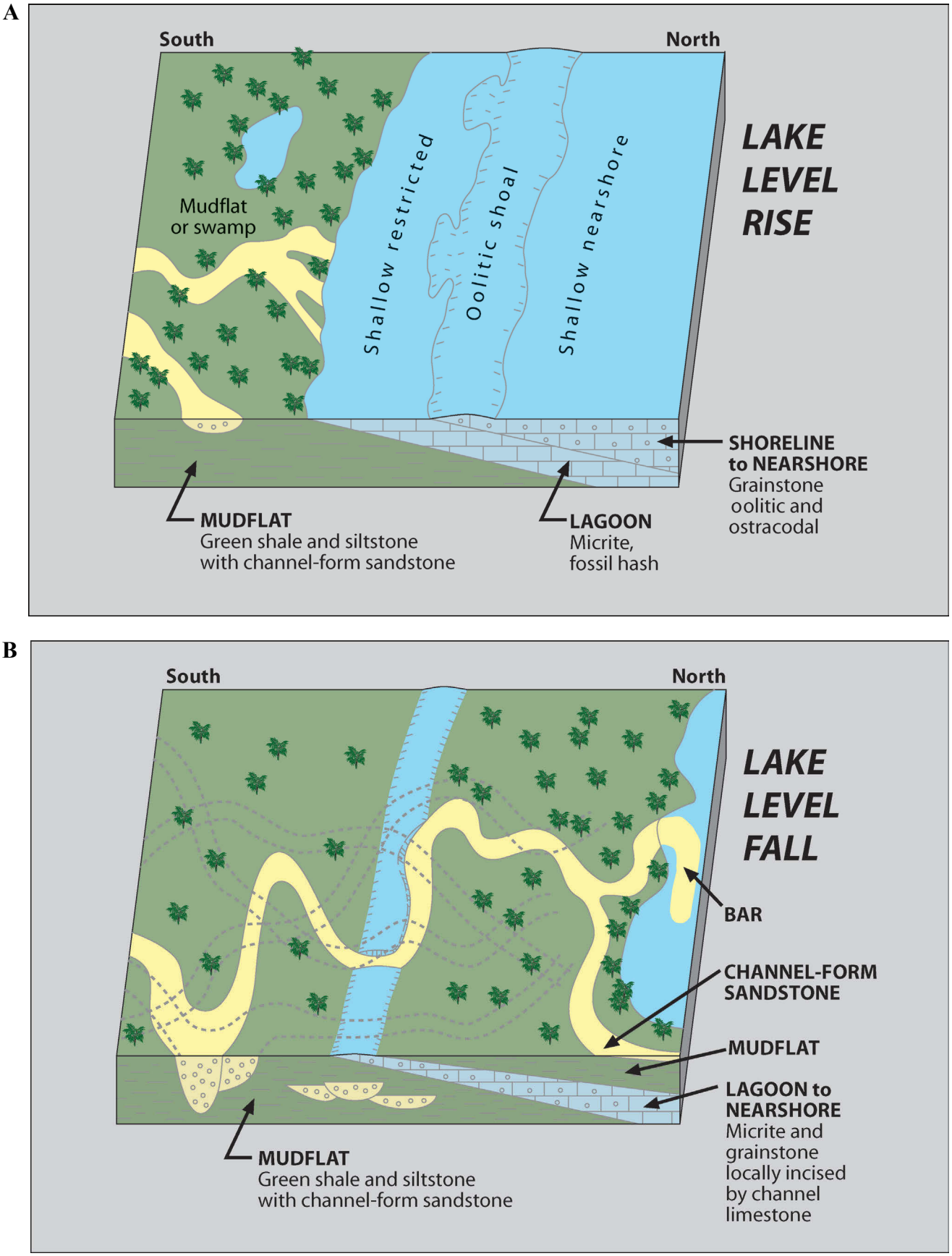

Figure 8.3. *Diagrams showing the generalized shoreline scale depositional setting for Lake Uinta during high-lake levels (A) and low-lake levels (B). From Bereskin and Morgan (2001).*

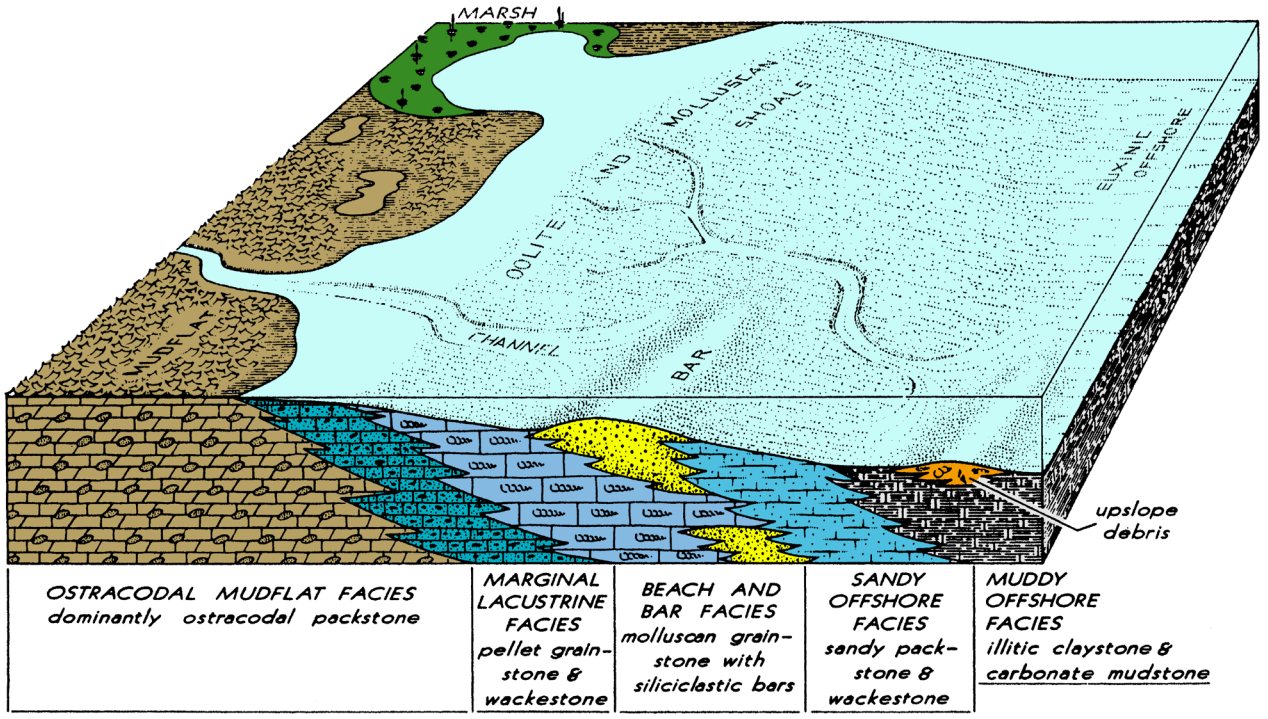

Figure 8.4. *Conceptual 3-D diagram depicting major facies of the Uteland Butte interval of the Green River Formation. From Little (1988).*

atively prominent shelf break developed at this time in the Monument Butte area. Many of the oil-productive sandstone beds in the Travis interval are channel and shallow bar deposits. The primary reservoirs in the Travis are turbidite and shallow lacustrine sandstone beds deposited in narrow cut-and-fill valleys along the shelf break during several lake level fall-and-rise cycles. The Travis is the only stratigraphic interval in the lower or middle members where there is evidence of a sharp shelf break in the central area. Lutz and others (1994) described the Travis reservoir as moderate- to low-density turbidite channel, debris flow, and gravity flow deposits.

The Monument Butte interval is the primary oil-producing section in the central Uinta Basin. The reservoir consists of amalgamated channel and distributary-mouth bar sandstone deposited on the distal, lower delta plain of Lake Uinta when the lake was at a low level and has an area of sediment bypass forming the updip trap (Morgan and others, 2003).

The Beluga interval was deposited during a time of overall lake-level rise and is transitional from the underlying delta facies in the Douglas Creek Member to the overlying deep-lake oil shale deposits of the upper member. This trangressive facies deposition resulted in less total sandstone and more common individual, isolated channel and bar deposits.

STRATIGRAPHY AND THICKNESS

The Green River Formation is generally 4000 feet (1200 m) to 5500 feet (1700 m) thick in the central Uinta Basin. The majority of the production comes from the lower Green River, a 2000-foot-thick (600 m) gross productive interval (figure 2.18), and minor production from a poorly defined interval of fractured shale and marlstone in the upper Green River.

The Uteland Butte interval is defined as the stratigraphic interval from the top of the Colton Formation to the top of LGR 5, a log marker defined by Morgan and others (1999). The Uteland Butte is equivalent to the first lacustrine tongue of Bradley (1931), lower black shale facies of Abbott (1957), basal limestone facies of Little (1988) and Colburn and others (1985), Uteland Butte limestone of Osmond (1992), and basal limestone member of Crouch and others (2000). The black shale facies described by Wiggins and Harris (1994) includes the Uteland Butte and overlying Castle Peak intervals. The Uteland Butte interval ranges in thickness from less than 60 feet (20 m) to more than 200 feet (60 m) in the central Uinta Basin generally from a drill depth range of 4500 feet (1400 m) to 6500 feet (2000 m) (figure 2.18).

The Castle Peak interval (figures 2.13 and 2.18) is defined as the stratigraphic section from the top of the Uteland Butte to the top of the carbonate marker bed of Ryder and others (1976). The interval is equivalent to the Wasatch (Colton) tongue and second lacustrine tongue of Bradley (1931), the Colton tongue and carbonate marker unit of Ryder and others (1976), and is included in Picard's (1955) black shale facies. The alluvial Colton tongue is exposed in Willow Creek and Nine Mile Canyons but extends only a few miles north. Above the Colton tongue, the Castle Peak consists of interbedded black shale, limestone, and limy mudstone, with some sandstone and siltstone.

The Travis interval is defined as the stratigraphic section from the top of the lower member of the Green River Formation (carbonate marker bed) to the top of the MGR 3 marker (figures 2.13 and 2.18). The interval is part of the middle member and ranges in gross thickness from 270 feet (80 m) to 700 feet (200 m) in the central Uinta Basin (Morgan and Bereskin, 2003; Morgan and others, 2003).

The Monument Butte interval is defined as the stratigraphic section from the top of the MGR 3 marker (Travis reservoir) to the top of the MGR 7 marker (figures 2.13 and 2.18). The interval ranges in thickness from 250 feet (75 m) to almost 500 feet (150 m) in the central Uinta Basin (Morgan and Bereskin, 2003; Morgan and others, 2003).

The Beluga interval is defined as the stratigraphic section from the top of the MGR 7 to the top of the MGR 18 (figures 2.13 and 2.18). The interval ranges in thickness from 550 feet (170 m) to more than 1200 feet (370 m) in the central Uinta Basin (Morgan and Bereskin, 2003; Morgan and others, 2003).

The Duchesne interval is defined as the stratigraphic section from the MGR 18 to the top of the Green River Formation. This interval includes part of the middle member and all of the upper and saline members of the Green River (figures 2.13 and 2.18).

LITHOLOGY

The dominant oil-productive lithology is sandstone with lesser amounts produced from carbonates and fractured shales and marlstones. Production is primarily from lower Green River Formation marginal lacustrine distributary channels, including some production from turbidite and slump deposits (Lutz and others, 1994; Bereskin and others, 2004), and minor production from lacustrine carbonate mudstone and grainstone.

The Uteland Butte interval consists of limestone, dolomite, carbonate mudstone, organic-rich shale (that can be correlated throughout the basin), and siltstone, and rare, thin, sandstone (Vanden Berg and others, 2013). Sandstone represents shallow-lacustrine bars deposited during the initial rise of the lake. The Uteland Butte lithologies are dolomitized ostracod and pellet grainstone, packstone and wackestone, and pelecypod-gastropod sandy grainstone interbedded with silty claystone or carbonate mudstone. Grainstone is common near the shallow shoreline of the lake, whereas deeper distal deposits are commonly dolomite and argillaceous limestone. Most of the Uteland Butte interval production is from three, thin (2- to 5-foot thick [0.6–1.5m]) low permeability dolomite beds that contain fractures necessary for reservoir quality (figure 8.5).

The Castle Peak interval is typically medium grained (0.36 to 0.44 mm), poorly to moderately sorted, angular to very well rounded sandstone, mostly lithic arkose or feldspathic litharenite deposited in a fluvial-deltaic distributary system (figures 8.3B, 8.6, and 8.7). Lithics are mostly chert but include metamorphic, granitic, and volcanic rock fragments. Most of the other sandstone beds in the Green River Formation are very fine to fine grained. Framework elements of sandstone in the Castle Peak interval include: (1) monocrystalline and polycrystalline quartz, (2) potassium feldspar (orthoclase and microcline), (3) plagioclase, (4) chert, (5) sheared metaquartz, recrystallized metaquartz, and hydrothermal quartz, (6) intrusive rock fragments, (7) dolomite, siltstone and mudstone clasts, (8) carbonate ooids, (9) isolated mica booklets (biotite, chlorite, and muscovite), (10) some red-brown hematite staining, and (11) assorted heavy minerals such as zircon, epidote, tourmaline, sphene, and rare amphibole. The Castle Peak sandstone is typically highly compacted with extensive quartz and some feldspar cementation (figure 8.7).

Two rock types contain the majority of the sandstone beds in the Travis reservoir. Rock-type T-1 is a very poorly sorted combination of silt and very fine grained sand that commonly contains detrital clay coatings around many of the grains as well as large clasts of highly compacted dolomitic and illitic mudstone (figure 8.8A). This rock type typically has poor porosity and permeability due to tight grain packing, sporadic detrital clay coatings, and pseudomatrix formation of mudstone clasts (figure 8.9). Rock-type T-2 is a laminated assemblage of very fine to fine-grained sandstone that has the appearance of a chaotic breccia of haphazardly distributed carbonate mudstone clasts in a poorly sorted silt to very fine grained matrix with abundant soft-sediment-deformation features (figure 8.8B). Fractures in the Travis reservoir sandstone are rare due to the clay content reducing the overall brittleness of the beds.

Two rock types also contain most of the sandstone beds in the Monument Butte reservoir (figure 8.10). Rock-type MB-1 is the most abundant and is typically very fine to fine grained (median 0.11 to 0.17 mm), moderately well sorted to well sorted, with subangular to subrounded grains (figure 8.11). The framework assemblage is similar in composition and abundance to the medium-grained sandstone in the Castle Peak, except the rock-type MB-1 has more biotite, chlorite, and muscovite. Also, in rock-type MB-1 the mudstone fragments are dolomitic, ankeritic, and carbonate allochems including ankeritic/dolomitic ooids, ankeritic/dolomitic rip-ups, ostracods, or intraclasts. Sandstone units often fine upward and contain low angle cross-bedding (figures 8.10A). Rock-type MB-2 is sandstone consisting of very fine grained sand and coarse silt with increased clay content compared to MB-1. Rock-type MB-2 is a ripple-drift lamination facies found in the upper portion of fining-upward sandstone sequences (figure 8.10B). Compared to MB-1, this rock type is more poorly sorted, angular to subangular, and has more grains coated with illite. MB-2 also contains more mica, especially muscovite, than the rock-type MB-1 sandstone.

Figure 8.5. *Typical Uteland Butte interval from the Bill Barrett No. 14-1-46 well (section 1, T. 4 S., R. 6 W., UBL&M, Duchesne County), Altamont field, slabbed core from 6682 to 6692 feet. The horizontal drilling target is the roughly 5-foot-thick, light brown dolomitic interval. Porosity in this interval ranges from 15 to 30% and permeability averages 0.06 mD. The dolomite is interbedded with organic-rich mudstones and limestones averaging between 1 and 3% TOC. Note the abundant shell fragments indicating deposition in a freshwater lacustrine environment. From Vanden Berg and others (2013).*

Figure 8.6. *Sedimentary structures typical of distributary-channel deposition in the Castle Peak interval showing climbing ripples and/or ripple-drift lamination in upper portion of a channel from the Ute Tribal No. 2-25 well (section 25, T. 5 S., R. 5 W., UBL&M, Duchesne County), Brundage Canyon field, slabbed core from 5549.0 to 5550.6 feet (vertical scales in tenths of a foot). From Bereskin and others (2004).*

The Beluga interval consists of interbedded sandstone, shale, and limestone. The sandstone in the Beluga reservoir is similar in composition to the Monument Butte reservoir sandstone. There are fewer fining-upward sequences and therefore less rock-type MB-2 ripple-drift laminated facies.

The Duchesne interval fractured shale/marlstone subplay consists of shale (including oil shale), marlstone, and rare sandstone. Oil is stored in naturally occurring fractures in the shale and marlstone beds.

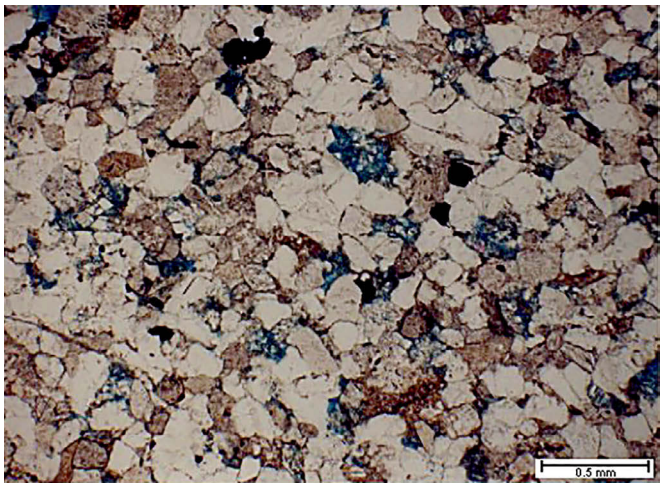

Figure 8.7. *Photomicrograph (plane light) of a typical compacted, subrounded to angular, moderately sorted feldspathic-quartz arenite with silica cement and intergranular porosity (blue). Porosity = 9.7%, permeability = 0.06 mD based on core-plug analysis. From the Castle Peak interval in the Ute Tribal No. 2-25 well, 5536.7 feet. From Bereskin and others (2004).*

HYDROCARBON SOURCE AND SEALS

The source rocks for the crude oil produced from the CSUBP are kerogen-rich shale and marlstone of the Green River Formation, which were deposited in nearshore and offshore open-lacustrine environments (Hunt and others, 1954; Forsman and Hunt, 1958; Silverman and Epstein, 1958; Tissot and others, 1978; Ruble, 1996; Ruble and others, 1998). Based on burial history and petroleum-generation modeling of the Shell Brotherson No. 1-11B4 well in the Altamont field, Dubiel (2003) determined that oil and gas generation began near the base of the Green River around 40 Ma at a depth of 11,000 feet (3300 m). Peak generation occurred during maximum burial between 30 to 40 Ma. The zone of hydrocarbon generation has risen stratigraphically through time (Dubiel, 2003). Mueller (1998) reports that fields in the CSUBP were charged from local unidentified sources with in some cases, a possible contribution from the upper black shale facies. Vertical and horizontal seals for producing zones are unfractured shale and low-permeable marls within the Green River Formation.

STRUCTURE AND TRAPPING MECHANISMS

Stratigraphic traps are the primary trapping mechanism for reservoirs in the CSUBP. Structure is dominantly regional dip northward into the basin with minor flexures or plunging structural anticlinal trends with no four-way closure. The downdip (northern) extent of the CSUBP is not defined. Locations downdip are deeper and encounter a more distal facies of the Green River Formation. As a result, the sand-

Figure 8.8. *Typical Travis interval from the Federal No. 2-33 well (section 33, T. 8 S., R. 16 E., SLBL&M, Duchesne County), Monument Butte field, slabbed core from 5657 to 5677 feet.* ***A.*** *Siltstone to very fine grained sandstone with brown, gray-green, and dark gray clasts; some clasts are deformed. Laminated lithotype is visible in second row from the bottom.* ***B.*** *Chaotic debris flow with irregular breccia clasts and soft-sediment deformation. From Bereskin and others (2004).*

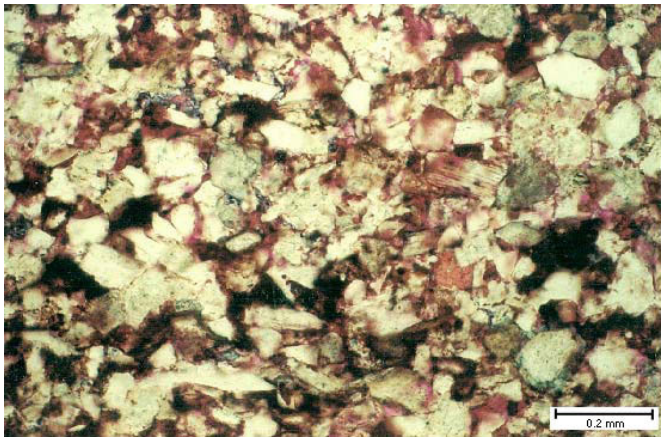

Figure 8.9. *Photomicrograph (plane light) of the laminated sandstone lithotype in the Travis interval from the Federal No. 13-32 well (section 32, T. 8 S., R. 16 E., SLBL&M, Duchesne County), 5397 feet, showing very poor sorting, variable rounding, and detrital and authigenic clays. Porosity is revealed through red-dyed epoxy, however, permeability is impaired by localized compaction. Dark grains are mudstone fragments which have been physically compacted. From Bereskin and others (2004).*

stone beds are often more isolated, thinner and may have reduced reservoir quality due to greater compaction. The updip (southern) extent of the field has been more extensively drilled. As drilling moves updip more of the sandstone beds are water bearing. The updip trapping mechanism is not understood. One possibility is the productive sandstones are pinching out updip and the water-bearing sandstones are deposits of a more proximal marginal-lacustrine facies, representing different parasequences.

RESERVOIR PROPERTIES

Oil and gas production in the CSUBP is mostly from the middle and lower Green River Formation; minor amounts are produced from the upper Green River (Weiss and others, 1990). Reservoir data for individual fields in the CSUBP are summarized in table 8.1. The reservoir rocks are low permeability, 0.1 to 10 mD, rarely 50 mD or more; porosity ranges from 8% to 20% (figures 8.5, 8.7, 8.10, and 8.11). In the thin dolomites

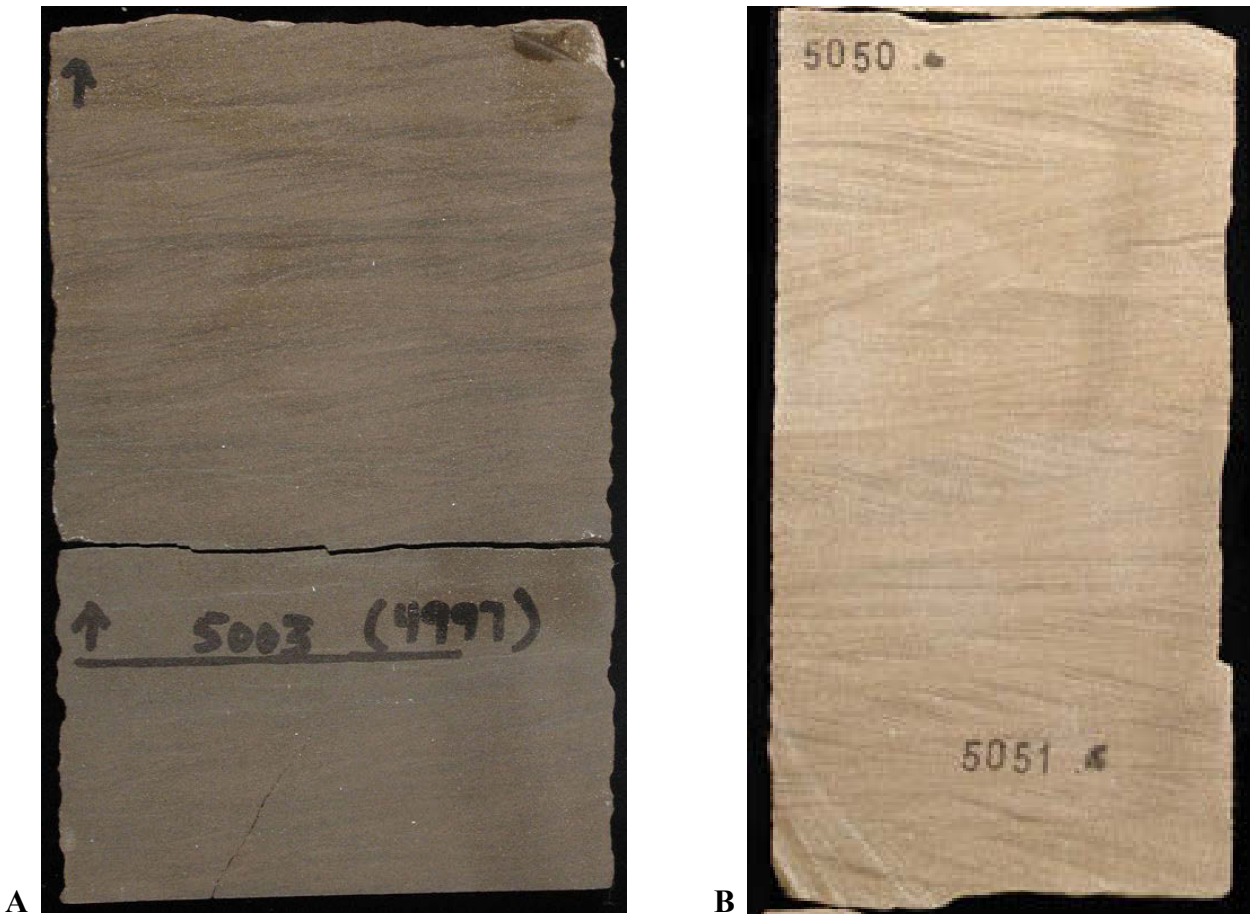

A B

Figure 8.10. *Typical Monument Butte interval core, Monument Butte field.* ***A.*** *Rock-type MB-1 showing oil-stained, fining upward sandstone containing low angle cross-bedding from the Monument Federal No. 3A-35 well (section 35, T. 8 S., R. 16 E., SLBL&M, Duchesne County), slabbed core from 5003 feet. Porosity = 11.6% permeability = 2.02 mD based on core-plug analysis.* ***B.*** *Rock-type MB-2 showing very fined grained sandstone with ripple-drift lamination from the State No. 6-32 well (section 32, T. 8 S., R. 17 E., SLBL&M, Duchesne County), slabbed core from 5050 feet. Porosity = 11.5% permeability = 1.9 mD based on core-plug analysis. From Bereskin and others (2004).*

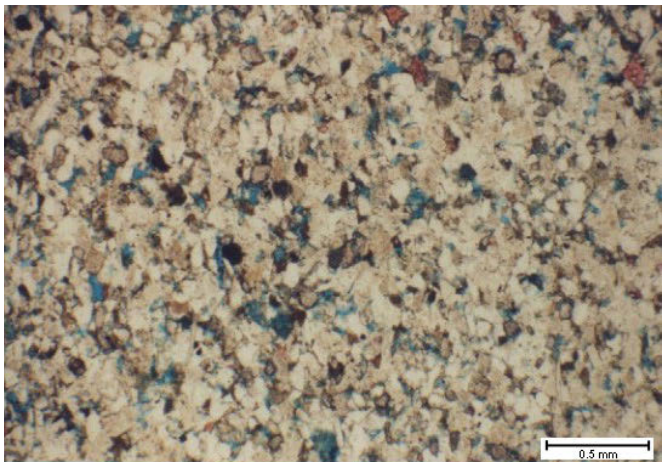

Figure 8.11. *Photomicrograph (plane light) of a typical fine-grained, moderately well sorted sandstone containing subangular to subrounded grains of quartz and feldspar with subordinate biotite and chlorite. Porosity = 9.8% permeability = 0.29 mD based on core-plug analysis. From the State No. 6-32 well, 5052 feet. From Bereskin and others (2004).*

of the Uteland Butte interval porosities are very high, between 15 and 30%, but permeability is very low unless fractures are present (Vanden Berg and others, 2013). Original reservoir pressure is near bubble point, but when pressure drops below the bubble point, gas begins to breakout within the reservoir greatly reducing the oil recovery. As a result, many wells in the greater Monument Butte field area (figure 8.1) are produced for only a year or less before they are converted to waterflood to help maintain reservoir pressure above the bubble point as well as provide a sweep of the oil.

The primary control on reservoir quality is the complex diagensis of individual sandstone beds, which has been described by Bereskin and others (2004). For example, in the Monument Butte reservoir, some of the MB-1 sandstone had early cementation with iron-poor calcite (figure 8.12A), which greatly reduced the effects of compaction. Later dissolution of the iron-poor calcite resulted in some beds with permeabilities in the tens of mD and porosity more than 20% (figures 8.12B). Other sandstone had a later stage of cementation with dolomite, ankerite, siderite, and iron-rich calcite, which greatly reduced the rock pore space (figure 8.12C). Partial dissolution of the late-stage cement restored some of the reservoir potential of the rock, resulting in greater than 10% porosity but less than 20 mD permeability. Examination of rock-type MB-2 sandstone shows that severe compaction occurred soon after deposition, which resulted in abundant microstylolite development. Rarely is early iron-poor calcite cement found in rock-type MB-2. Dissolution of feldspars is minor, resulting in low porosity (<10%) and low permeability (<0.1 mD).

Fractures are important to the economic success of the Castle Peak interval and Uteland Butte interval subplays because of the low matrix permeability typically found in these intervals. Most fractures in the Uteland Butte are near-vertical and often isolated to individual beds (Vanden Berg and others, 2013). Porosity in the Castle Peak interval is typically the result of dissolution of feldspars and some rock fragments. However, fractures in the sandstone are necessary for good hydrocarbon production and are most commonly developed at the base of the bed where the carbonate content is highest, which results in increased brittleness. The Travis interval, Monument Butte Interval, and Beluga Interval subplays are not fracture dependant but production is enhanced when fractures are encountered. The Travis reservoir typically has low porosity and permeability due to tight grain packing, illite coating the grains, and a general lack of secondary intergranular pores. The Duchesne Interval Fractured Shale/Marlstone subplay is entirely dependant on naturally occurring fractures in the upper member of the Green River Formation for economic production. Most of this interval is at shallow drill depths in the basin. As a result, the formation temperatures are often near or below the pour-point temperature of the oil, making it a difficult reservoir to exploit.

The gross productive interval in the CSUBP can be more than 1000 feet (300 m) but the net productive interval is typically tens of feet to more than 100 feet (30 m). Not all of the intervals that make up the subplays are productive in every well. Most of the individual beds that are perforated have a thickness of feet to a few tens of feet.

OIL AND GAS CHARACTERISTICS

Most of the oil produced from the CSUBP is characterized as black wax (table 6.2). The black wax typically has a 28° to 34°API gravity and a pour point from 90°F (32°C) to 120°F (49°C). Associated gas from the CSUBP has a heating value of more than 1100 Btu/ft^3. Associated gas from the Monument Butte No. 10-35 well (table 6.3) contains 71.8% methane, 14.9% ethane, 9.9% propane, and 3.3% higher fractions (Moore and Sigler, 1987).

PRODUCTION

Fields in the CSUBP produce crude oil and associated gas. The nine largest fields in the play (fields with >500,000 BO [79,500 m^3] cumulative production) have produced 124.8 million BO (19.8 million m^3) and 441.1 BCFG (12.5 BCMG) as of January 1, 2016. Monthly production for 2015 from these fields in the play was 681,098 BO (108,286 m^3) and 2.7 BCFG (0.08 BCMG) (Utah Division of Oil, Gas, and Mining, 2016a). The most productive area of the Uteland Butte interval is in the central basin overpressured zone. Production from horizontal wells with lengths over 4000 feet (1220 m) in both the overpressured and normally pressured areas average 500 to 1500 BOPD (80–240 m^3). Data on production and number of wells are summarized for the fields in the play in table 8.1.

A

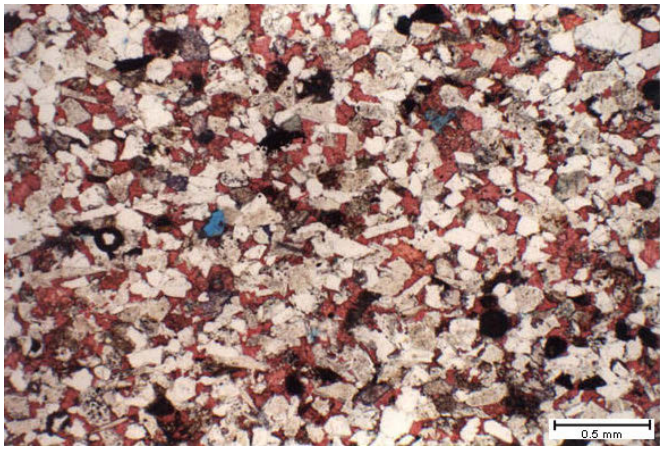

B

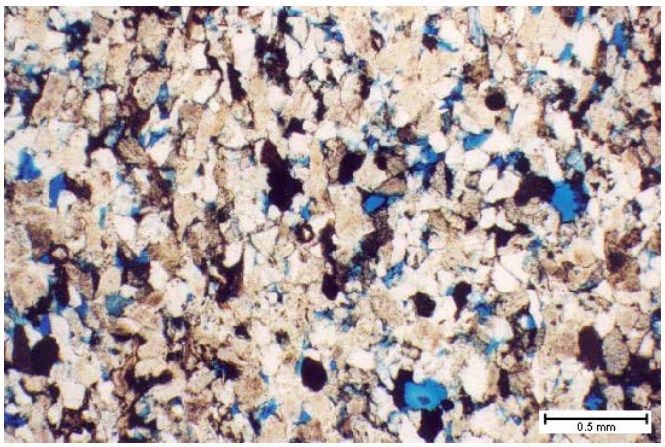

C

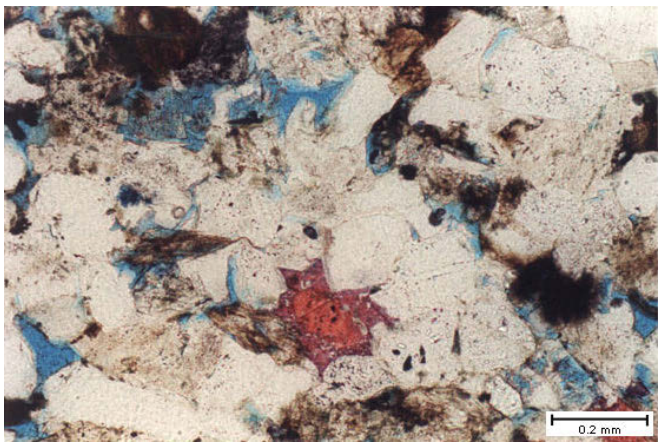

Figure 8.12. *Photomicrographs (plane light) showing diagenetic events in the Monument Butte sandstone reservoirs. From Bereskin and others (2004).* ***A.*** *Pervasive early iron-poor calcite cement (red) prior to leaching. Federal No. 3A-35 well, 5010.6 feet.* ***B.*** *Very fine to fine-grained sandstone showing selective dissolution of rock fragments from Federal No. 10-34 well (section 34, T. 8 S., R. 16 E., SLBL&M, Duchesne County), 5006.0 feet.* ***C.*** *Late stage cementation with iron-rich calcite (rimming iron-poor calcite remnants [red]). Federal No. 3A-35 well, 5002.1 feet.*

MONUMENT BUTTE FIELD OVERVIEW

Monument Butte field (figures 8.1 and 8.2), Duchesne County, Utah, is the most significant field in the Conventional Southern Uinta Basin play in terms of production, wells, and secondary recovery programs. The field is a stratigraphic updip pinchout along the gentle north-dipping flank of the Uinta Basin (figure 8.13). Production is primarily from lower and middle Green River Formation marginal lacustrine stacked, fluvial-deltaic distributary channels, and shoreface wave/storm sands (figure 8.14) (Lomax, 1993; Morgan, 2008). Some minor production occurs in turbidite and slump deposits (Lutz and others, 1994; Bereskin and others, 2004), and from lacustrine carbonate mudstone (microbial) and oolitic grainstone (Osmond, 2000; Chidsey and others, 2015). The productive interval typically ranges from 4500 to 6500 feet (1500–2200 m) in depth (figure 8.15) (Lomax, 1993; Morgan, 2008). The net reservoir thickness is 16 feet (5 m), which extends over a 21,000-acre (8500 ha) area. Porosity and permeability ranges from 10 to 20% and 25 to 30 mD, respectively. The drive is solution gas and the initial water saturation was 30 to 35% (Lomax, 1993).

The majority of the production is from sandstone beds in the Monument Butte interval. The sandstones are generally very fine to fine-grained lithic arkoses to feldspathic litharenites (Bereskin and others, 2004). The channel deposits typically have an erosional base and fine upward with large-scale trough and planar cross-bedding at the base and climbing ripples near the top. The primary control on reservoir quality (porosity and permeability) is the complex diagensis of individual sandstone beds, which has been described by Bereskin and others (2004).

The downdip (northern) extent of Monument Butte field is not well defined. Locations downdip are deeper and encounter a more distal facies of the Green River Formation. As a result, the sandstone beds are commonly more isolated, thinner, and may have reduced reservoir quality due to greater compaction. The updip (southern) extent of the field has been more extensively drilled.

Monument Butte field was discovered in 1981 with the completion of the Lomax Exploration Company Monument Butte Federal No. 1-35 well, SE1/4SE1/4 section 25, T. 8 S., R. 16 E., SLBL&M; IPF was 37 BOPD (6 m^3/d) and 19 MCFGPD (0.5 MCMPD). The field currently has 1181 producing (or shut-in) wells (Utah Division of Oil, Gas, and Mining, 2016a). The original reservoir field pressure was near bubble point at 2150 psi (14,800 kPa). When pressure drops below the bubble point, gas begins to breakout within the reservoir, greatly reducing the oil recovery. As a result, most wells in a unit are produced for only a year or less before the unit is converted to waterflood to help maintain reservoir pressure above the bubble point as well as provide a sweep of the oil.

Cumulative production as of January 1, 2016, was 69,456,994 BO (11,042,780 m^3), 140 BCFG (3.9 BCMG) and over 67

Table 8.1. *Geologic, reservoir, and production data for the largest fields in the Conventional Southern Uinta Basin play. Most of the fields are being actively developed, ever expanding the number of active producers and acres. Most of the data is from Hill and Bereskin (1993); West Willow Creek data is from Osmond (2000). Production data from Utah Division of Oil, Gas, and Mining (2016a).*

State	County	Field	Discovery Date	Active Producer	Abandoned Producers	Acres	Spacing (acres)	Pay (feet)	Porosity (%)	Perm (mD)	Temp (°F)	Initial Reservoir Pressure (psi)	Average Monthly Production		Cumulative Production	
													Oil (bbl)	Gas (MCF)	Oil (bbl)	Gas (MCF)
Utah	Duchesne	Antelope Creek	1963	230	1	1760	40	40	13	8	130	2400	62,120	142,738	9,496,720	19,843,237
Utah	Duchesne	Brundage Canyon	1983	848	7	16,880 +	40	30	11	0.1	120	1700	123,082	1,289,546	22,717,544	147,668,697
Utah	Duchesne	Duchesne	1951	37	16	760	40	Variable	13	8	165	NA	7693	24,563	1,903,247	4,299,475
Utah	Uintah	Eight Mile Flat North	1695	294	12	10,600 +	40	25	15	NA	140	2000	46,692	298,241	11,227,429	44,780,503
Utah	Duchesne and Uintah	Monument Butte	1981	1181	20	100,000	40-20	16	15	25	150	2150	368,768	372,150	69,456,994	140,221,004
Utah	Uintah	Pariette Bench	1962	90	12	2000+	40	NA	NA	NA	NA	NA	6737	394,124	2,037,292	54,130,213
Utah	Uintah	Uteland Butte	1962	53	7	5640	40	20	10	<1.0	NA	NA	5984	68,445	2,123,842	10,880,866
Utah	Uintah	West Willow Creek	1981	5	3	1240	80	100	18	89	NA	NA	544	7359	1,139,839	12,166,894
Utah	Uintah	Windy Ridge	1988	139	3	1720	40	50	NA	NA	NA	NA	59,477	134,874	4,729,593	7,129,044

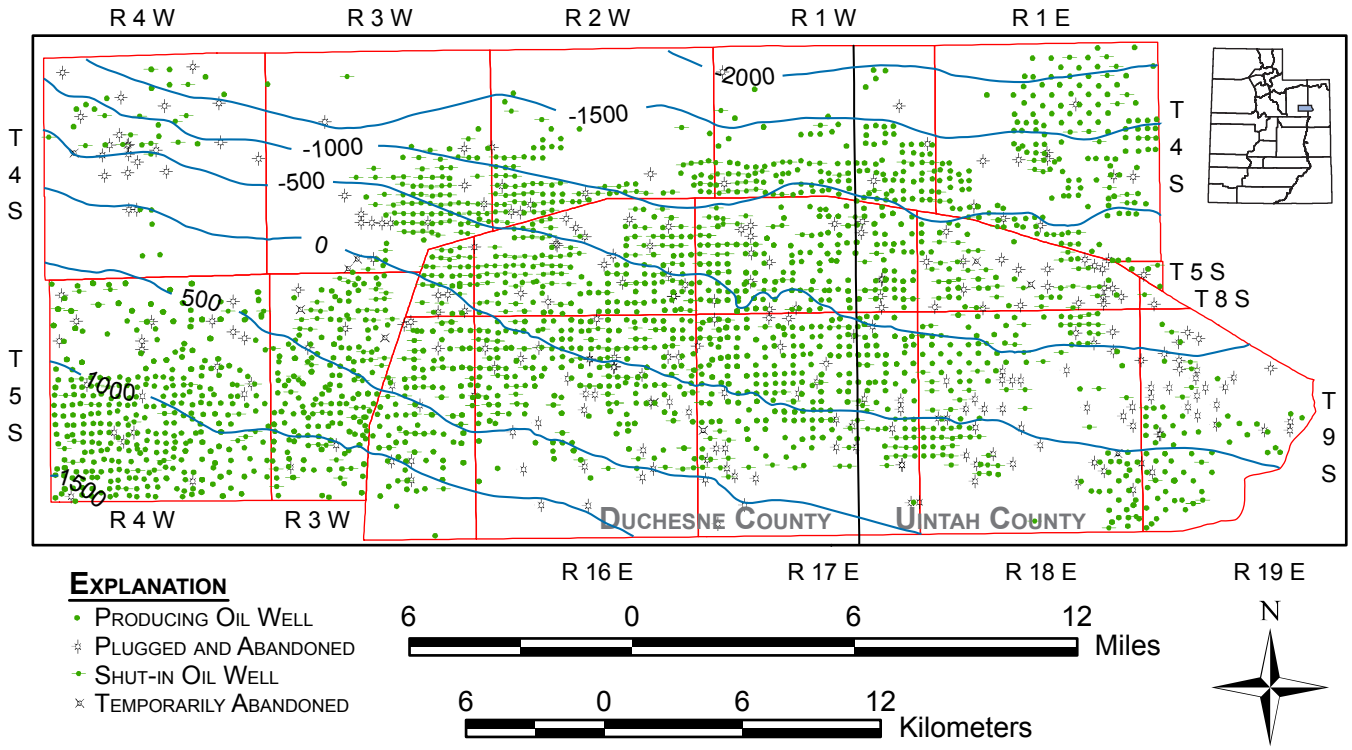

Figure 8.13. *Structure map on top of the lower member of the Green River Formation, greater Monument Butte field area, Duchesne and Uintah Counties, Utah. Contour interval = 500 feet. Modified from Morgan (2008).*

million BW (11 million m³) (Utah Division of Oil, Gas, and Mining, 2016a). The original estimated primary recovery was 5% of the OOIP. With multiple waterflood projects the secondary recovery is expected to be 15 to 25% of the OOIP (Lomax, 1993).

The Monument Butte Green River D unit was the first waterflood in the field and was the focus of a U.S. Department of Energy study from 1992 to 1996. The study concluded that the primary recovery would be 5% of OOIP, but could increase to 20% of OOIP with waterflooding (Pennington and others, 1996). Reservoir quality and recovery potential vary throughout the greater Monument Butte field area. Operators have reported (Utah Board of the Division of Oil, Gas, and Mining hearing files) more conservative recoveries, generally ranging from 12 to 18% of OOIP (primary + waterflood) depending on well spacing. The OOIP and recovery factors are poorly understood due to the large field size combined with the numerous productive beds that are highly complex and laterally discontinuous. Estimates of OOIP typically range from 1 to 2 billion barrels (0.2–0.3 billion m³) (www.newfield.com, March 2008).

EXPLORATION POTENTIAL AND TRENDS

The thin dolomites in the Uteland Butte interval are primary targets using extended reach and super-extended reach lateral wells (greater than 5000 feet [1500 m]). In addition, most operators drilling for the Castle Peak Interval and other overlying subplays can test the Uteland Butte by drilling an additional 100 feet (30 m) to 200 feet (60 m). The typical oil recovery (10s of thousands of bbls) is sufficient to justify the cost to drill the additional depth. The Uteland Butte interval subplay will enlarge with the expansion of the overlying subplays, continued success using targeted horizontal drilling, and of coarse, high oil prices. The subplay represents the greatest potential for new oil discoveries and reserve additions in the Uinta Basin.

The Castle Peak, Travis, Monument Butte, and Beluga intervals are drilled and completed together. Each interval may be the primary reservoir in certain portions of the play, but no interval is completed by itself. As a result, the exploration potential and trend is the same for all of the subplays (figure 8.1). Drilling will expand the Brundage Canyon field to the west, the greater Monument Butte field area (Monument Butte, Eight Mile Flat North, and Pariette Bench fields) to the east, and all fields to the north.

In the southern Uinta Basin the Green River Formation, and all associated subplays, is deeply incised and at shallow depths where the current reservoir temperature is below the pour point of the oil (figure 8.1). As a result, the potential reservoirs will contain heavy oils or tar that require thermal recovery or some other unconventional recovery technique.

The Duchesne Interval Fractured Shale/Marlstone subplay is restricted to the Duchesne field. This subplay is not being explored due to the low volume of oil recovered and the dif-

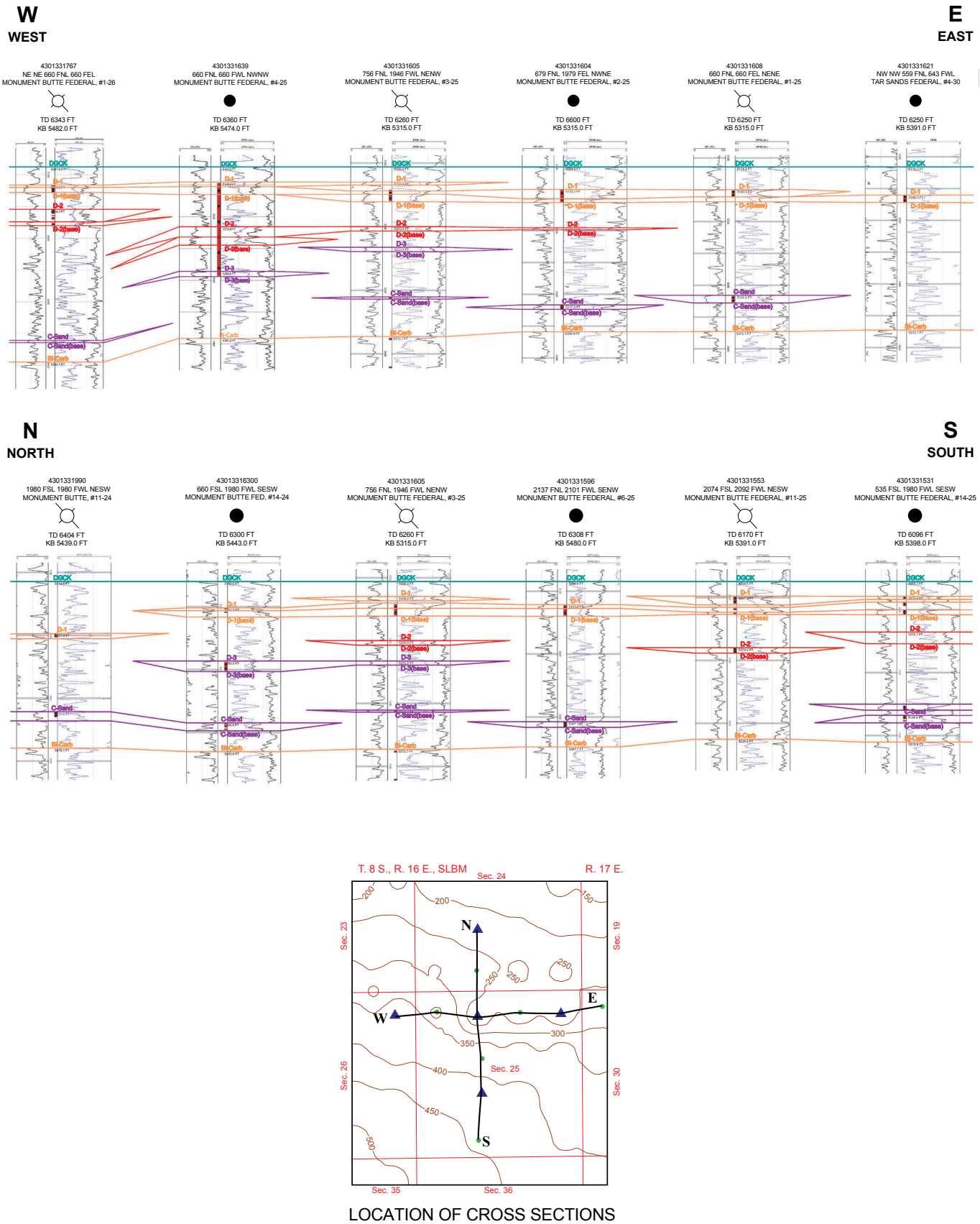

Figure 8.14. *West to east and north to south stratigraphic cross sections showing the stacking nature of the channel sandstone beds that make up the reservoir sandstones, Monument Butte field. Datum is top of the Douglas Creek, wells are about 1400 feet apart. From Morgan (2008).*

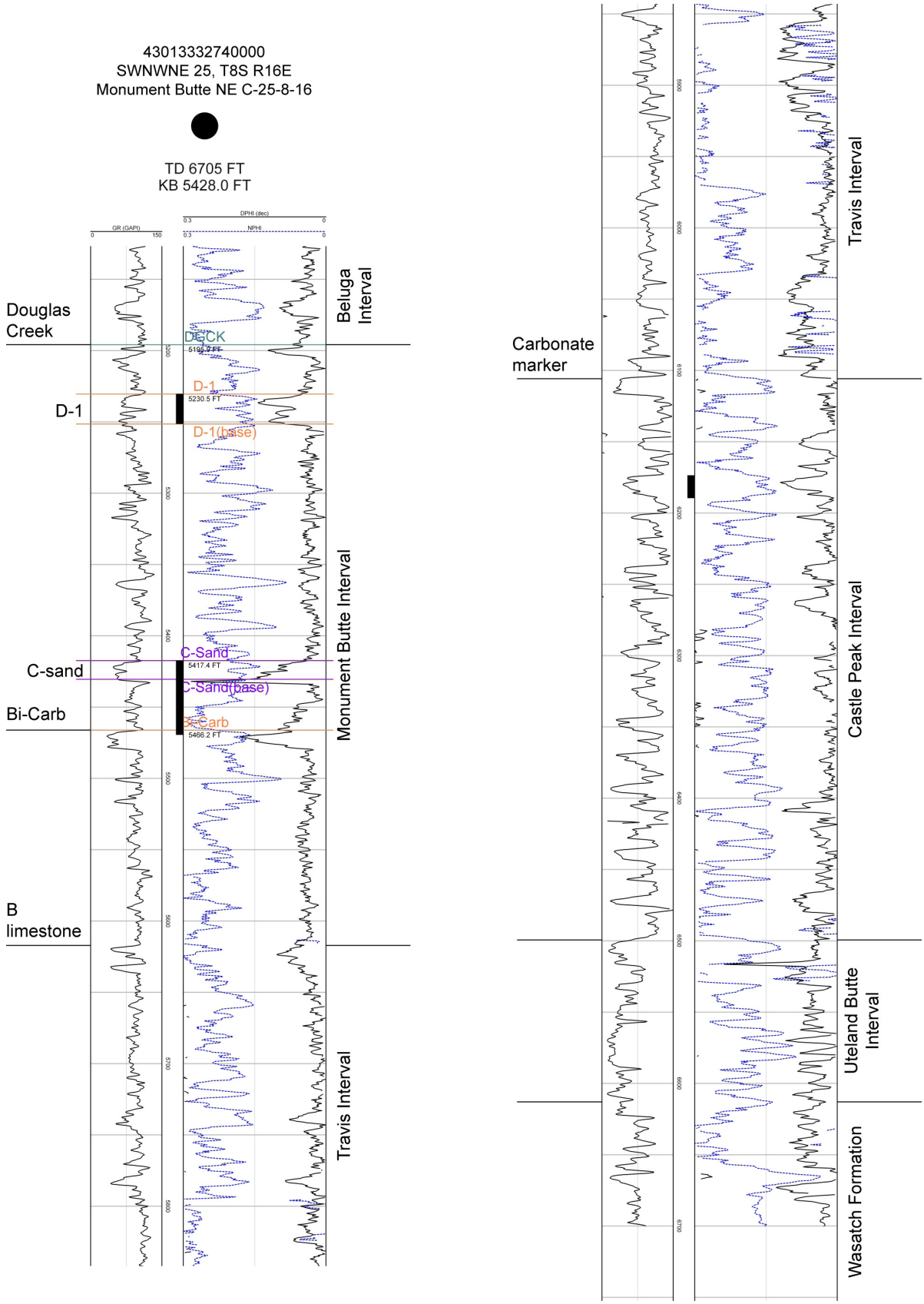

Figure 8.15. *Type log from Monument Butte field. Column one is gamma ray (0–150 API units), column two is density (solid black) and neutron (dashed blue) porosity (0–30%). Perforations are shown as black bars in the depth column. The Monument Butte No. C-25-8-16 well produces from the D-1 sand, C-sand, a bed in the Castle Peak interval, and a bed in the Beluga interval (perforations too shallow to be shown on this log section). From Morgan (2008).*

ficulty in predicting the location of economically productive fractures. Development of the deeper intervals include penetration of the shallower Duchesne interval. As a result, fracture trends or "sweet spots" may be discovered that could lead to exploitation.

Much of the Monument Butte area remains to be developed. About 10 to 15 years are needed to fully develop the field on 40-acre (16.2 ha) spacing at the pre-2015 rate of drilling. Drilling spaced at 20 acres (8.1 ha) per well has successfully tapped banked oil, found new pay, improved sweep efficiency, and accelerated recovery from the Monument Butte waterflood. Infill drilling could result in 1000 more locations extending the drilling to 30 years at pre-2015 levels (Morgan, 2008). The Brundage Canyon field with more than 400 producing wells is not currently under waterflood (Kelso and Ehrenzeller, 2008). Both the Monument Butte area and the Brundage Canyon field may some day be good candidates for tertiary recovery such as CO_2 flooding.

CHAPTER 9:
MISSISSIPPIAN LEADVILLE LIMESTONE PARADOX BASIN PLAY

by

Thomas C. Chidsey, Jr.
Utah Geological Survey

and

David E. Eby
Eby Petrography & Consulting, Inc.

CONTENTS

FIGURES

TABLE

CHAPTER 9:
MISSISSIPPIAN LEADVILLE LIMESTONE PARADOX BASIN PLAY

INTRODUCTION

The Mississippian Leadville Limestone is one of two, major oil and gas plays in the Paradox Basin, the other being the Pennsylvanian Paradox Formation (figure 9.1). Most Leadville production is from the Paradox fold and fault belt (figure 9.2). The Leadville Limestone has produced over 52 million BO (8.3 million m^3) and 867 BCFG (24.6 BCMG) from six fields in the northern Paradox Basin of Utah and Colorado (Utah Division of Oil, Gas, and Mining, 2016a; Colorado Oil and Gas Conservation Commission records). However, much of the gas included in the production figures is cycled gas used in the past for pressure maintenance at Lisbon field, Utah. The 7500-mi^2 (19,400 km^2) play area is relatively unexplored; only about 100 wells penetrate the Leadville (less than one well per township), thus the potential for new discoveries remains great. Geologic data for individual fields in the play are summarized in table 9.1.

The play outline for the Leadville Limestone represents the maximum extent of petroleum potential in the Paradox Basin as defined by producing lithofacies, basement-involved fault trends, hydrocarbon shows and possible migration paths, the likelihood of hydrothermal dolomitization, and untested hypotheses. The attractiveness of the Leadville Limestone Paradox Basin play (and other Paradox Basin plays) to the petroleum industry depends on oil and gas prices, the successful acquisition of high-quality seismic data, reserve potential, pipeline access, drilling costs, and perhaps most significantly in the Paradox Basin, environmental concerns. When evaluating these criteria, most aspects of the Leadville play may meet the exploration and development guidelines of independent companies.

DEPOSITIONAL ENVIRONMENT

The Mississippian (late Kinderhookian through Osagean to early Meramecian time) Leadville Limestone is a shallow, open marine, carbonate-shelf deposit (figure 9.3). Local depositional environments included shallow-marine, subtidal, supratidal, and intertidal (Fouret, 1982, 1996). The western part of the Paradox fold and fault belt includes a regional, reflux-dolomitized, interior bank lithofacies containing Waulsortian mounds (Welsh and Bissell, 1979)—local, mud-supported buildups involving growth of "algae" (Wilson, 1975; Ahr, 1989; Fouret, 1982, 1996).

During Late Mississippian time, the entire carbonate platform in southeastern Utah and southwestern Colorado was subjected to subaerial erosion resulting in formation of a lateritic regolith (Welsh and Bissell, 1979). This regolith and associated carbonate dissolution is an important factor in Leadville reservoir potential (figure 9.4). Solution breccia and karstified surfaces are common, including possible local development of cavernous zones (Fouret, 1982, 1996).

Periodic movement along northwest-trending basement faults affected deposition of the Leadville Limestone. Crinoid banks or mounds, the primary reservoir lithofacies, accumulated in shallow-water environments on upthrown fault blocks or other paleotopographic highs. In areas of greatest paleorelief, the Leadville is completely missing as a result of non-deposition or subsequent erosion (Baars, 1966).

Four Leadville depositional lithofacies were identified based on cores from Lisbon field (figure 9.2): open marine, shoal flank, restricted marine, and middle shelf. Open-marine lithofacies are represented by crinoidal banks or shoals and Waulsortian-type buildups (figure 9.3). This lithofacies represents a high-energy environment with well-circulated, normal-marine salinity water at possible depths from 5 to 45 feet (1.5–14 m) in a subtidal setting. Waulsortian buildups or mud mounds developed exclusively during the Mississippian in many parts of the world (Wilson, 1975). They are steep-sloped tabular, knoll, or sheet forms composed of several generations of mud deposited in a subtidal setting (Fouret, 1982, 1996; Lees and Miller, 1995) (figure 9.3). Crinoids and sheet-like fenestrate bryozoans, in the form of thickets, are associated with the deeper parts of the mud mounds and are indicative of well-circulated, normal-marine salinity. This lithofacies represents a low- to moderate-energy environment. Water depths possibly ranged from 60 to 90 feet (20–30 m).

Shoal-flank lithofacies are associated with both crinoid bank/shoal and Waulsortian-type buildup facies (figure 9.3). This lithofacies represents a moderate-energy environment, again with well-circulated, normal-marine salinity water at possible depths from 60 to 90 feet (20–30 m) also in a subtidal setting.

Restricted-marine lithofacies are represented by "hard" peloid and oolitic shoals that developed as a result of regularly agitated, shallow-marine processes on the shelf (figure 9.3). Like crinoidal banks and Waulsortian-type buildups, hard peloid and oolitic shoals are common throughout Leadville deposition, especially on paleotopographic highs. This lithofacies represents a moderate- to high-energy environment, with moderately well-circulated water in an intertidal setting. The water probably had slightly elevated salinity compared to the

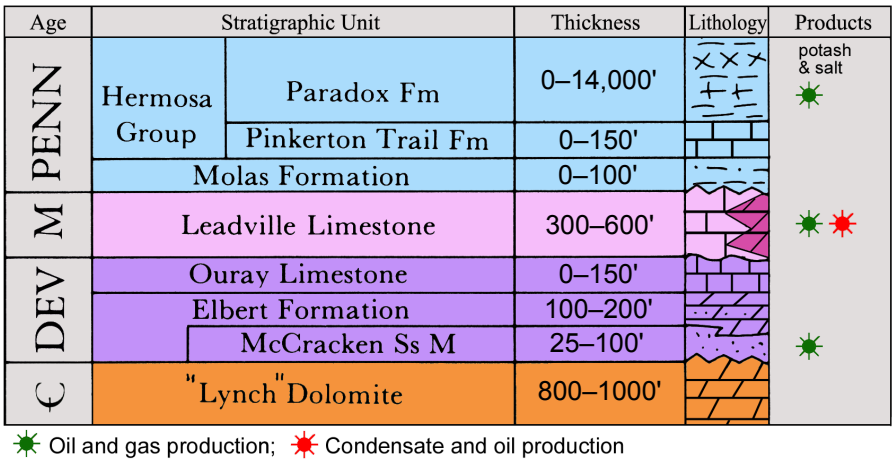

Figure 9.1. *Stratigraphic column of a portion of the Paleozoic section determined from subsurface well data in the Paradox fold and fault belt, Grand and San Juan Counties, Utah. Modified from Hintze and Kowallis (2009).*

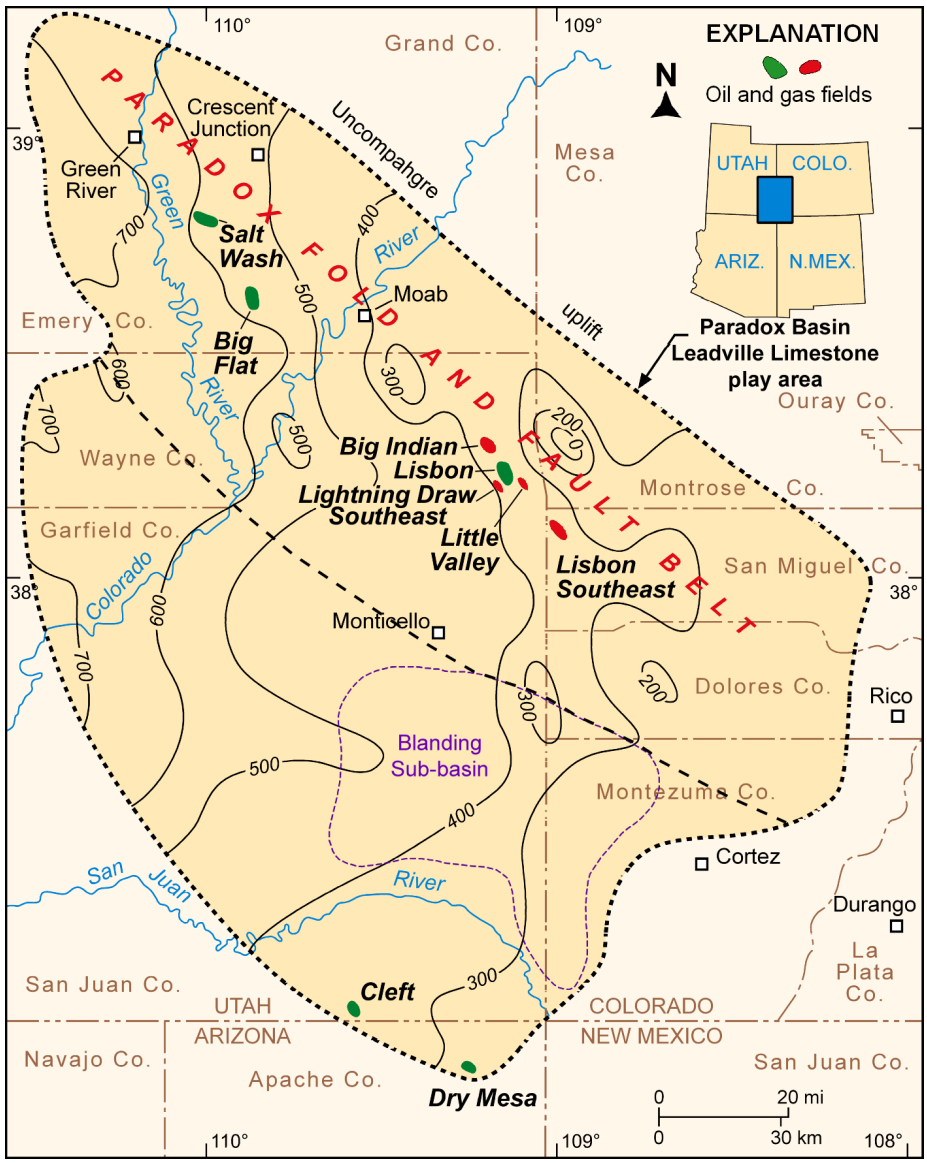

Figure 9.2. *Location of fields that produce from the Mississippian Leadville Limestone, Arizona, Utah, and Colorado. Thickness of the Leadville is shown; contour interval is 100 feet. Modified from Parker and Roberts (1963). The Leadville Limestone Paradox Basin play area is dotted. Modified from Morgan (1993a).*

other lithofacies. Sediment deposition and modification probably occurred in water depths generally ranging from near zero to 20 feet (6 m).

Middle-shelf lithofacies covered extensive areas across the shallow shelf. This lithofacies represents a low-energy, often restricted-marine environment (figure 9.3). Mud and some sand were deposited in a subtidal (burrowed), inter-buildup/shoal setting. Water depths possibly ranged from 60 to 90 feet (20–30 m).

STRATIGRAPHY AND THICKNESS

The Leadville Limestone is typically 300 to 600 feet (100–200 m) thick in the play area (Hintze and Kowallis, 2009). However, the Leadville thins from more than 700 feet (230 m) in the northwest corner of the Paradox Basin to less than 200 feet (70 m) in the southeast corner (Morgan, 1993a) (figure 9.2). Thinning is a result of both depositional onlap onto the Mississippian cratonic shelf and erosion. The Leadville is divided into two informal members, a dolomitic lower member and a limestone and dolomite upper member, separated by an intraformational discomformity (Fouret, 1982, 1996). Each unit has a subtle but distinct characteristic geophysical log response (figure 9.5).

The Leadville Limestone is overlain by the Pennsylvanian Molas Formation and underlain by the Devonian Ouray Limestone (figures 9.1 and 9.5). Average depth to the Leadville in Paradox Basin fields is 8760 feet (2920 m).

LITHOLOGY

The depositional fabrics of open-marine crinoidal banks and shoals include grainstone and packstone (figure 9.6A). Rocks representing crinoidal banks and shoals typically contain the following diagnostic constituents: dominantly crinoids and rugose corals, and lesser amounts of broken fenestrate bryozoans, brachiopods, ostracods, and endothyroid forams as skeletal debris. Low to medium cross-bedding is common. Rock units having this lithofacies constitute a significant reservoir potential, having both effective porosity and permeability when dissolution of skeletal grains, followed by dolomitization, has occurred.

The depositional fabrics of the open-marine Waulsortian-type buildups include mud-supported boundstone, packstone, and wackestone (figure 9.6B). Rocks representing Waulsortian-type buildups typically contain the following diagnostic constituents: peloids, crinoids, bryozoans, and associated skeletal debris, and stromatactis (spar-filled cavities often associated with carbonate mud mounds). Rock units having this lithofacies constitute a significant reservoir potential, having both effective porosity and permeability, especially after dolomitization.

Table 9.1. *Geologic, reservoir, and production data for fields in the Mississippian Leadville Limestone Paradox Basin play. Data compiled from Stowe (1972), Cargile (1978), Clark (1978), Latch (1978a, 1978b), Norton (1978a), Smith (1978b), Parker (1981), Morgan (1993a), Smouse (1993b, 1993c), Utah Division of Oil, Gas, and Mining (2016a), and Colorado Oil and Gas Conservation Commission (2016).*

State	County	Field	Discovery Date	Active Producers	Abandoned Producers	Acres	Spacing (acres)	Pay (feet)	Porosity (%)	Permeability (mD)	Temp. (°F)	Initial Reservoir Pressure (psi)	Average Monthly Production		Cumulative Production	
													Oil (bbl)	Gas (MCF)	Oil (bbl)	Gas (BCF)
Colorado	San Miguel	Lisbon Southeast	1960	4	2	800	640	50	8	10	NA	2340	33	9333	169,892	17.3
Utah	San Juan	Big Flat	1957	0	3	480	80	30	9	variable	125	2450	0	0	83,469	0.05
Utah	San Juan	Big Indian	1961	1	0	640	640	72	6	3–10	148	3240	0	0	178,160	26.4
Utah	San Juan	Lisbon	1960	18	18	5120	320	225	6	22	127	2982	400	87,071*	50,465,801	794.6*
Utah	San Juan	Little Valley	1961	1	2	660	160	100	6	6–10	127	3043	0	0	137,848	17.3
Utah	Grand	Salt Wash	1961	2	8	920	160	19	8	NA	143	4075	1	0	1,651,644	11.7

NA = Not available
*Includes cycled gas

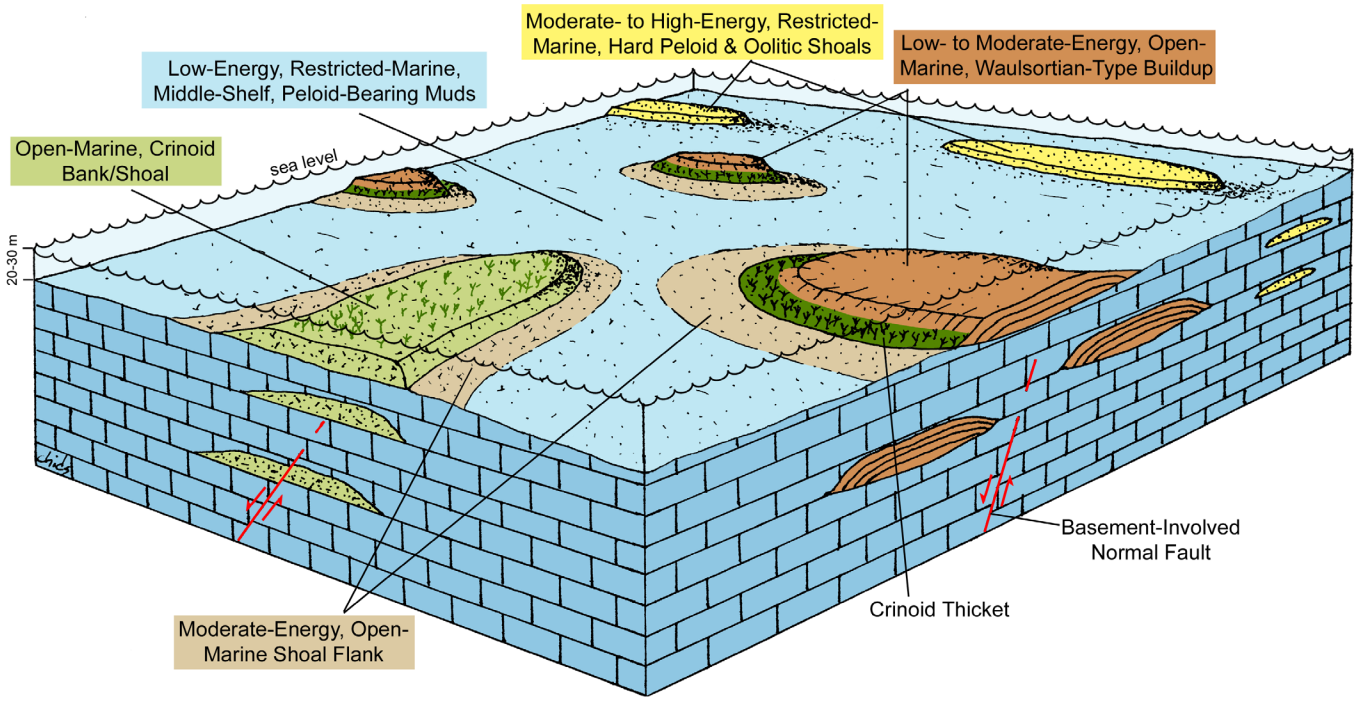

Figure 9.3. *Block diagram displaying major depositional environments/lithofacies, as determined from core, for the Mississippian Leadville Limestone.*

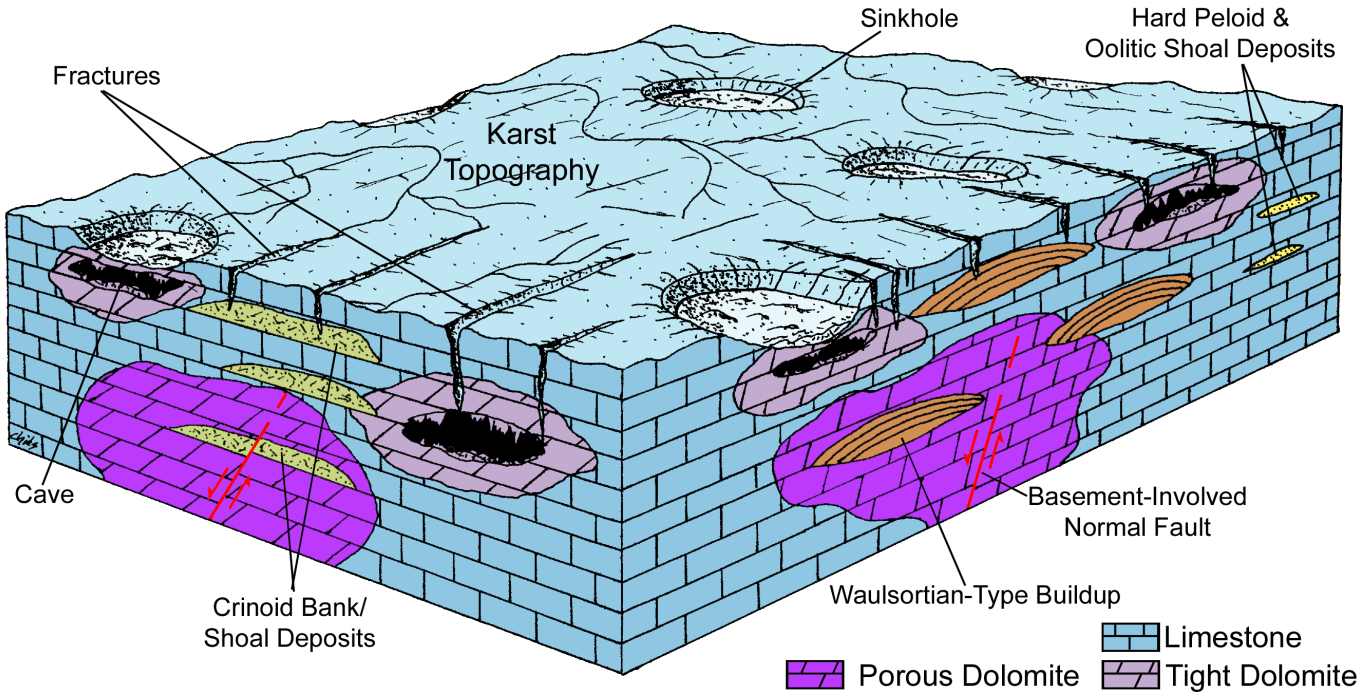

Figure 9.4. *Block diagram displaying post-Leadville karst and fracture overprint.*

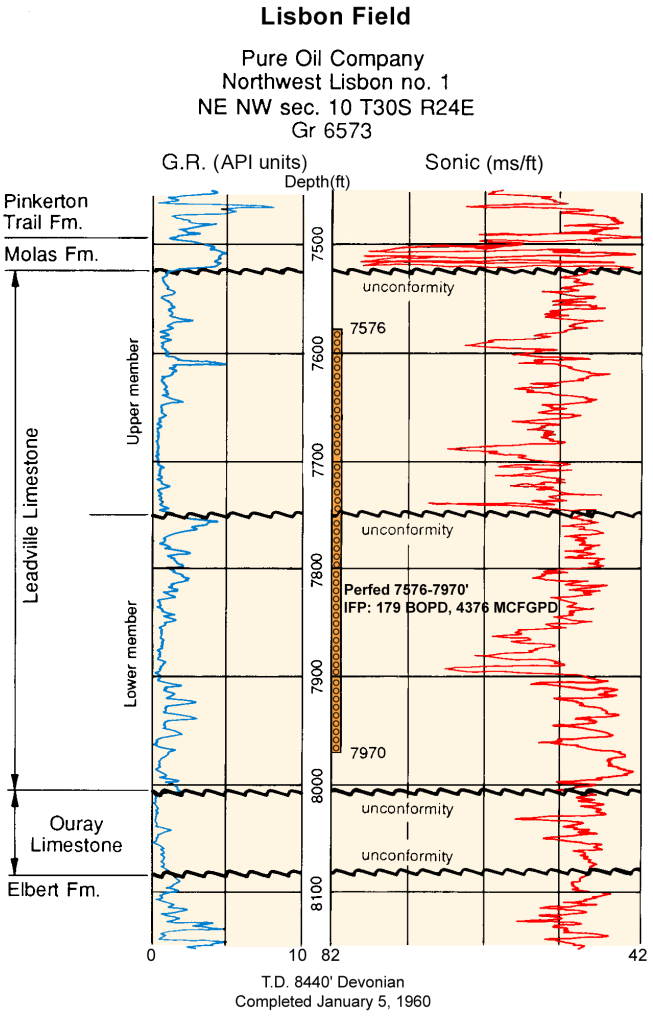

Figure 9.5. *Typical gamma ray-sonic log of the Leadville Limestone, Lisbon field discovery well, San Juan County, Utah. Producing (perforated) interval between depths of 7576 and 7970 feet. See figure 9.2 for location of Lisbon field.*

The depositional fabrics of the shoal-flank lithofacies include peloidal/skeletal packstone and wackestone (figure 9.7A). Bedding is generally absent in cores. Rocks representing this lithofacies typically contain the following diagnostic constituents: peloids, crinoids, bryozoans, brachiopods, and associated skeletal debris, and talus, depositional breccia, and conglomerate (Fouret, 1982, 1996). Rock units having shoal-flank lithofacies constitute a limited reservoir potential, having little effective porosity and permeability.

The depositional fabrics of the restricted-marine lithofacies include grainstone and packstone (figure 9.7B). Rocks representing this lithofacies typically contain the following diagnostic constituents: ooids, coated grains, and hard pelloids. Fossils are relatively rare. Rock units having restricted-marine lithofacies constitute good reservoir potential. Remnants of visible interparticle and moldic porosity may be present in this lithofacies. Dolomitization significantly increases the reservoir quality of this lithofacies.

The depositional fabrics of the middle-shelf lithofacies include wackestone and mudstone (figure 9.7C). The most common is bioturbated lime to dolomitic mudstone with sub-horizontal feeding burrows. Rocks representing this facies typically contain the following diagnostic constituents: soft pellet muds, "soft" peloids, grain aggregates, crinoids and associated skeletal debris, and fusulinids. Rock units having middle-shelf lithofacies generally act as barriers and baffles to fluid flow, having very little effective porosity and permeability. Few megafossils and little visible matrix porosity are present, with the exception of an occasional moldic pore. However, recognizing this lithofacies is important because low-energy carbonates of the middle shelf form the substrate for the development of the higher energy crinoid banks, oolitic/hard peloid shoals, and Waulsortian-type buildups (figure 9.3). The middle-shelf lithofacies can contain reservoir-quality rocks if dolomitized.

Fractures in the Leadville Limestone are an important reservoir component. They are associated with folding and faulting or collapse related to karst processes.

HYDROCARBON SOURCE AND SEALS

Hydrocarbons in Leadville Limestone reservoirs were likely generated from source rocks in the Pennsylvanian Paradox Formation (figure 9.1). Organic-rich units are well established source rocks for oil produced from the Paradox Formation itself (Hite and others, 1984; Nuccio and Condon, 1996). For details on the source rock characteristics of the organic-rich shale zones in the Paradox Formation refer to descriptions in chapter 10.

Hydrocarbon generation in the Paradox Formation occurred during maximum burial in the Late Cretaceous and early Tertiary. Hydrocarbons were then expelled and subsequently migrated, primarily along fault planes, into carrier beds or structures where the Leadville Limestone was juxtaposed directly against Pennsylvanian source rocks. Fracture systems developed along fault systems may have provided secondary migration routes. Oil generated from non-Pennsylvanian source rocks require long-distance migration.

The seals for the Leadville producing zones are the overlying clastic beds of the Pennsylvanian Molas Formation (figure 9.1). Hydrocarbons in the Leadville are further sealed by evaporite (salt and anhydrite) beds within the overlying Pennsylvanian Paradox Formation.

STRUCTURE AND TRAPPING MECHANISMS

Most oil and gas produced from the Leadville Limestone is in basement-involved, northwest-trending structural traps with closure on both anticlines and faults (figure 2.22). Lisbon, Big

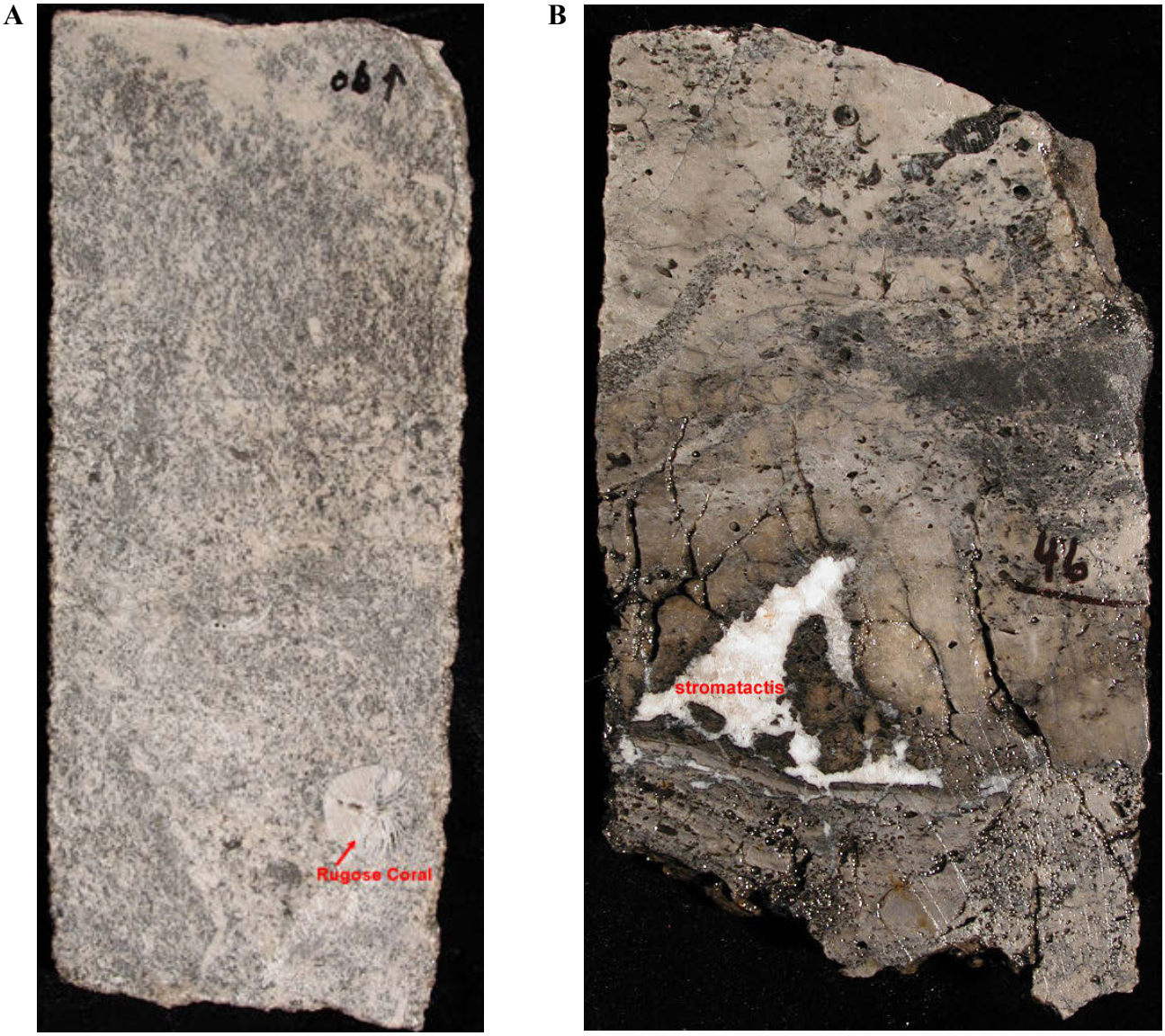

Figure 9.6. *Typical Leadville Limestone depositional fabrics from Lisbon field, San Juan County, Utah.* ***A.*** *Crinoidal/skeletal grainstone/packstones representing high-energy, open-marine shoal lithofacies; slabbed core from 8506.5 feet, Lisbon No. B-816 well.* ***B.*** *Peloidal/skeletal packstone/wackestones representing moderate- to low-energy, open-marine, Waulsortian-type buildup lithofacies; slabbed core from 8646 feet, Lisbon No. B-816 well.*

Indian, Little Valley, and Lisbon Southeast fields (figure 9.2) are on sharply folded anticlines that close against the Lisbon fault zone. Salt Wash and Big Flat fields (figure 9.2), northwest of the Lisbon area, are on unfaulted, east-west- and north-south-trending anticlines, respectively. The unfaulted structures probably developed from movement on deep, basement-involved faults that do not rise to the level of the Leadville. These and other faults affecting the Leadville probably reflect the reactivation of pre-existing, Precambrian-age faults during the Laramide orogeny or later. As examples of both types of structural traps, Big Flat and Lisbon fields are briefly described below.

Big Flat Field

Big Flat field, Grand County, Utah, was the first Mississippian discovery in the Paradox Basin (figure 9.2). The trap is a doubly plunging anticline with 276 feet (84 m) of structural closure (figure 9.8) that produced from Leadville limestone and dolomite (Smith, 1978b). The net reservoir thickness is 30 feet (10 m), which extends over a 480-acre (190 ha) area. The field now produces oil from horizontal wells in the Cane Creek shale of the Paradox Formation, on a separate structure north of the original, abandoned Leadville feature.

Lisbon Field

Lisbon field, San Juan County, Utah, (figure 9.2) accounts for most of the Leadville oil production in the Paradox Basin. The trap is an elongate, asymmetric, northwest-trending anticline, with nearly 2000 feet (600 m) of structural closure and bounded on the northeast flank by a major, basement-involved normal fault with over 2500 feet (760 m) of displacement (Smith

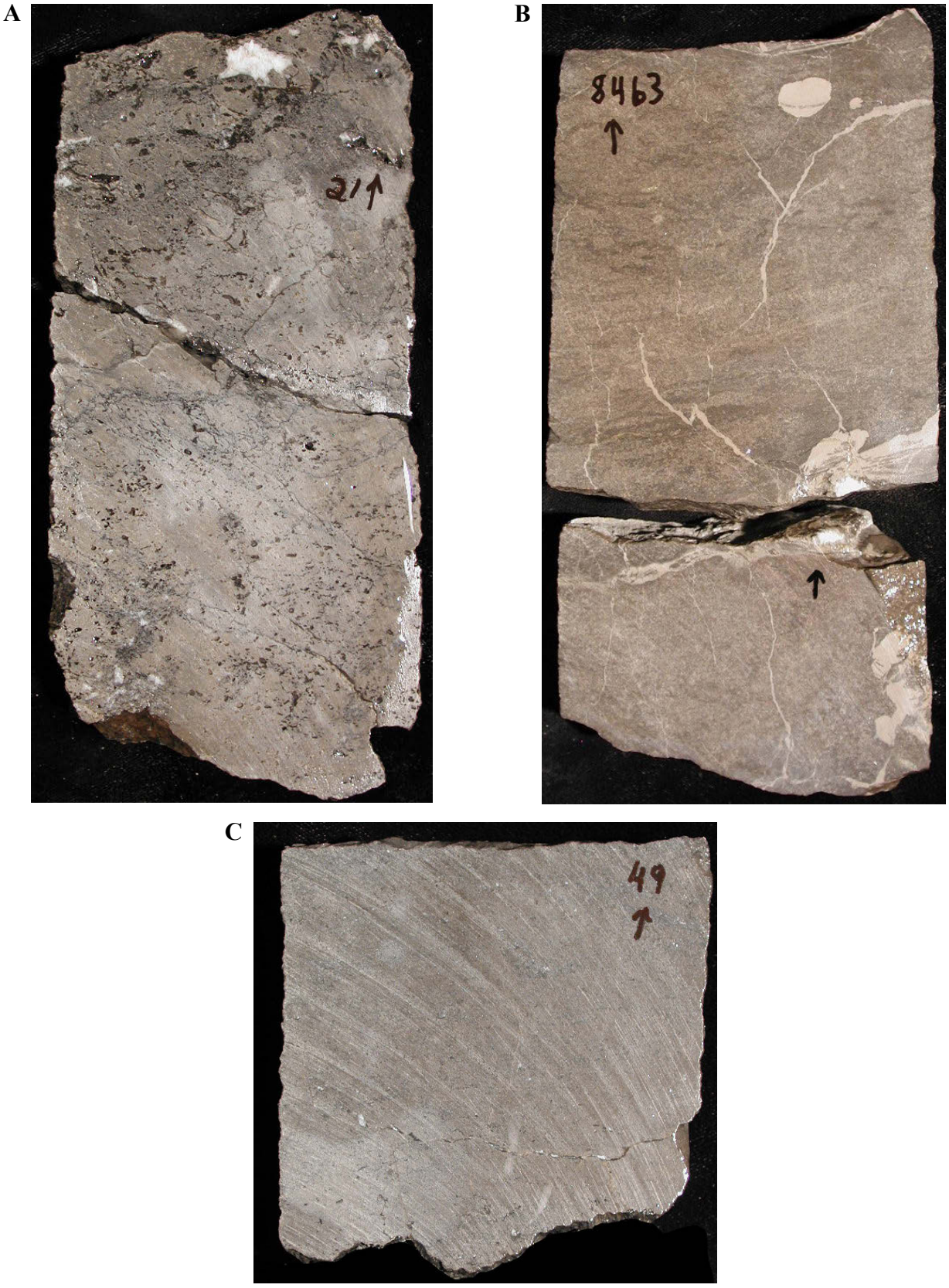

Figure 9.7. *Typical Leadville Limestone depositional fabrics from Lisbon field, San Juan County, Utah.* ***A.*** *Peloidal/skeletal packstone/wackestone representing moderate-energy, open-marine, shoal-flank lithofacies; slabbed core from 8521 feet, Lisbon No. B-816 well.* ***B.*** *Peloidal grainstone/packstone representing moderate-energy, restricted-marine, "hard" peloid shoal lithofacies; slabbed core from 8463 feet, Lisbon No. B-816 well.* ***C.*** *Skeletal/"soft" peloidal wackestone/mudstone representing low-energy, restricted-marine, middle-shelf lithofacies; slabbed core from 8549 feet, Lisbon No. B-816 well.*

and Prather, 1981) (figures 9.9 and 9.10). Several minor, northeast-trending normal faults dissect the Leadville reservoir into segments. The net reservoir thickness is 225 feet (69 m) over a 5120-acre (2100 ha) area (Clark, 1978; Smouse, 1993b).

RESERVOIR PROPERTIES

The Leadville Limestone has heterogeneous reservoir properties because of (1) depositional lithofacies with varying porosity and permeability, (2) early and late diagenetic effects, and (3) fracturing. Identification and correlation of depositional lithofacies in individual Leadville reservoirs is important to determine their effect on production rates and paths of petroleum movement. Natural fractures also affect permeability, and control hydrocarbon production and injection fluid pathways. Leadville reservoir porosity ranges from 4 to 21% and typical porosity averages 6 to 8% (Morgan, 1993a). Permeability is variable, generally ranging from 3 to 10 mD. At Lisbon field, San Juan County, Utah (figure 9.2), the permeability ranges from less than 1 to 1100 mD, averaging 22 mD (Smouse, 1993b).

The early diagenetic history of the Leadville sediments, including some dolomitization (finely crystalline) and leaching of skeletal grains (figure 9.11A), resulted in low-porosity and/or low-permeablility rocks. Most of the porosity and permeability associated with hydrocarbon production at Lisbon field, for example, was developed during later, deep subsurface dolomitization (coarsely crystalline replacement and saddle [hydrothermal?] dolomite) and dissolution (figures 9.4 and 9.11B). Predating or concomitant with saddle dolomite formation are pervasive leaching episodes that cross-cut the carbonate host rocks with dissolution resulting in late vugs as well as extensive microporosity. Pyrobitumen appears to coat most intercrystalline dolomite as well as dissolution pores associated with the late dolomite. Extensive solution-enlarged fractures and autobreccias are also common (figure 9.12A). Sediment-filled cavities are relatively common throughout the upper third of the Leadville in Lisbon field (figure 9.12B). These cavities or cracks were related to karstification of the exposed Leadville (figure 9.4). Infilling of the cavities by detrital carbonate and siliciclastic sediments occurred before the deposition of the Pennsylvanian Molas Formation.

Leadville net-pay thickness is also variable, depending on diagenesis and fracturing, and ranges from 19 to 225 feet (6–75 m). The average Leadville reservoir temperature is 134°F 57°C). Water saturations range from 25 to 50%, salinities range from 1830 to 20,000 ppm, and resistivities (R_w) range from 0.059 to 0.103 ohm-m at 68°F (20°C). Initial reservoir pressures average about 3022 psi (20,840 kPa). The reservoir drive mechanisms include gas expansion, water drive, and gravity drainage.

Reservoir data for individual fields in the Mississippian Leadville Limestone Paradox Basin play are summarized in table 9.1. For details see Stowe (1972), Cargile (1978), Clark (1978),

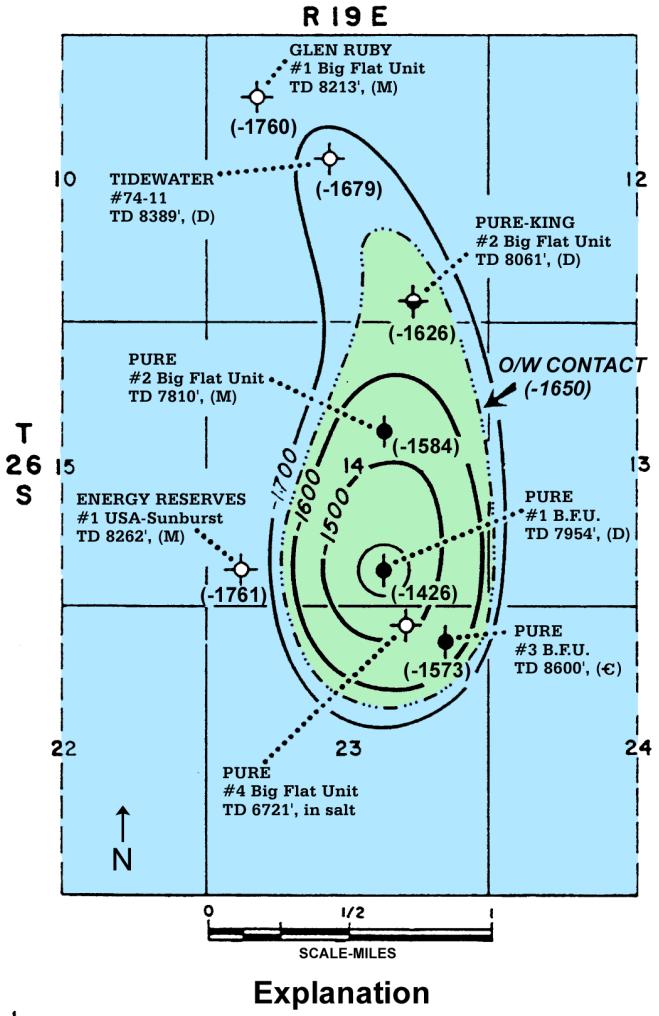

Figure 9.8. *Top of structure of the Leadville Limestone, Big Flat field, Grand County, Utah. Contour interval = 100 feet, datum = mean sea level. Modified from Smith (1978a).*

Latch (1978a, 1978b), Norton (1978a), Smith (1978b), Parker (1981), Morgan (1993a), Smouse (1993b, 1993c), Gwynn (1995), Utah Division of Oil, Gas, and Mining (2016), and Colorado Oil and Gas Conservation Commission (2016).

OIL AND GAS CHARACTERISTICS

In major reservoirs, the produced Leadville oil and condensate are rich, volatile crudes. The API gravity of the oil ranges from 41 to 54°; the GOR ranges between 50 and 3150 cubic feet/bbl. The API gravity of the condensate ranges from 60 to 66°. Oil colors vary from brownish green to yellow/amber to red, and condensate can be light green to yellow to red. The

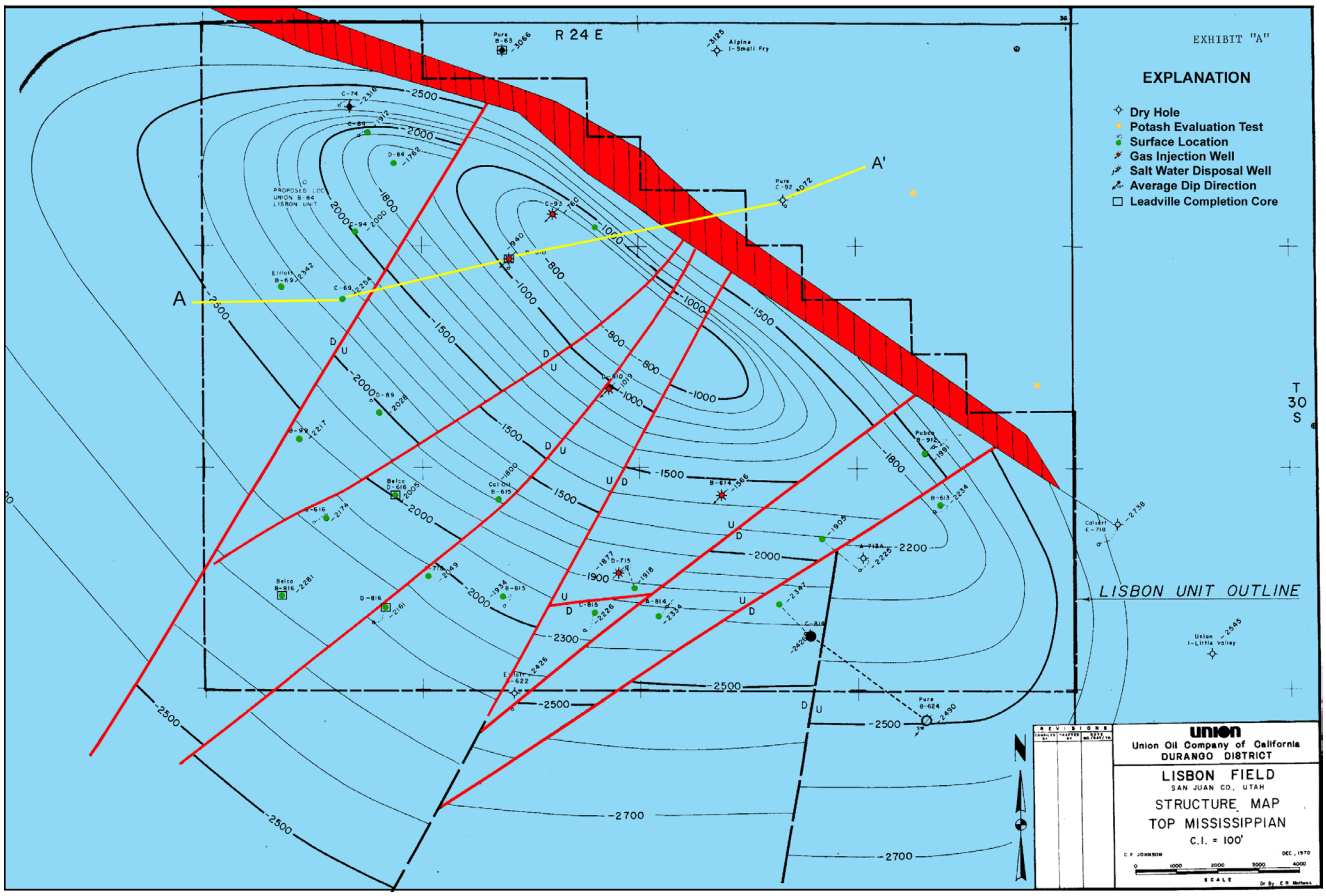

Figure 9.9. *Top of structure of the Leadville Limestone, Lisbon field, San Juan County, Utah. Contour interval = 500 feet, datum = mean sea level. The field is bounded on its northeast flank by a major, basement-involved normal fault (in red) with greater than 2500 feet of displacement. Note the multiple, northeast-trending faults that divide the Leadville reservoir into several segments. Some of the best producing wells are located close to these faults. Modified from C.F. Johnson, Union Oil Company of California files (1970); courtesy of Tom Brown, Inc. Cross section A–A' shown on figure 9.10.*

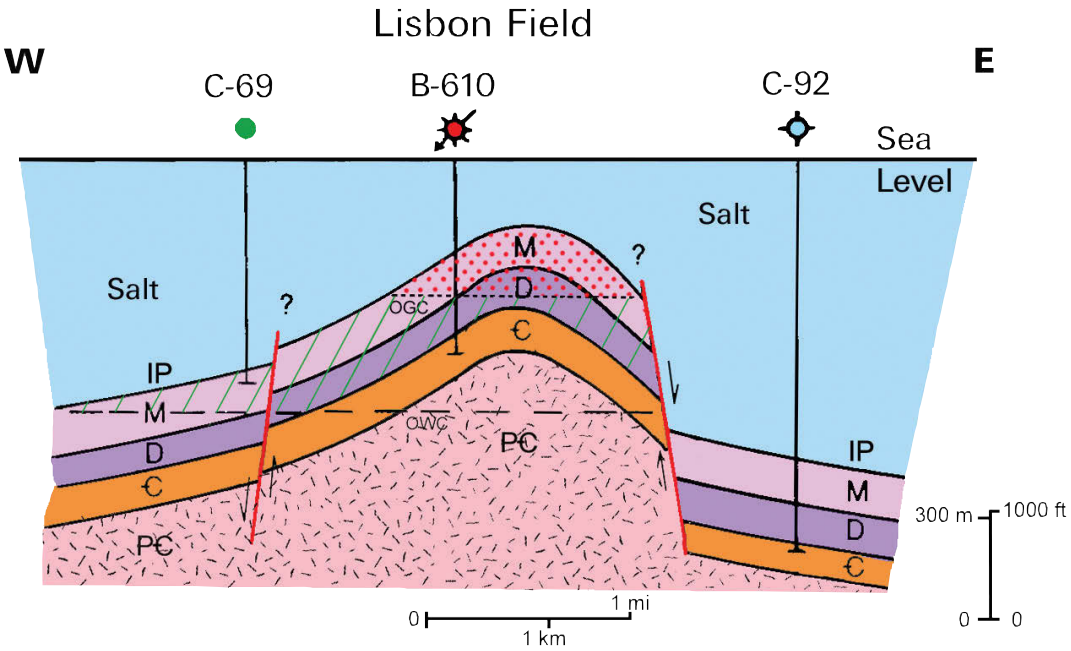

Figure 9.10. *Schematic east-west cross section through Lisbon field. Line of section shown on figure 9.9. Note the juxtaposition of the Mississippian (M) section against the Pennsylvanian (IP) section which includes evaporites (salt) and organic-rich shale. OGC = oil-gas contact, OWC = oil-water contact. Modified from Clark (1978).*

viscosity of the crude oil ranges from 32 to 55 sus at 100°F (38°C); the viscosity of the condensate is less than 32 sus at 100ºF (38°C). The pour point of the crude oil ranges from 40 to 85°F (4–29°C). The average weight percent sulfur and nitrogen of produced Leadville hydrocarbon liquids are 0.13 and 0.005, respectively (Stowe, 1972).

Leadville reservoirs produce associated gas that is variable in composition. Associated gas produced at Lisbon field contains 40% methane, 9% ethane, 7% propane, 2% butane, 1% pentane, 0.5% hexane and higher fractions, 13% N_2, 27% CO_2, and 1% helium. The gas heating value averages 892 Btu/ft^3; the specific gravity averages 1.046. Associated gas produced at Salt Wash field contains 13% methane, 3% ethane, 3% propane, 3% butane, 1% pentane, 0.5% hexane and higher fractions, 71% N_2, 3% CO_2, and 1.5% helium. The gas heating value averages 443 Btu/ft^3; the specific gravity averages 1.005 (Moore and Sigler, 1987).

Leadville reservoirs produce nonassociated gas that is relatively uniform in composition: 64% methane, 5% ethane, 2% propane, 1% butane, 0.3% pentane, 0.4% hexane and higher fractions, 13% N_2, 13% CO_2, and 0.7% helium. The gas heating values average 864 Btu/ft^3; the specific gravity averages 0.813 (Moore and Sigler, 1987). Gas produced from the reservoirs in the Leadville Limestone Paradox Basin play contains only a trace of H_2S.

PRODUCTION

Three fields in the Leadville Limestone Paradox Basin play have produced crude oil and associated gas. Big Flat, Lisbon, and Salt Wash fields (figure 9.2) have combined to produce over 52 million BO (8.3 million m^3) and 806 BCFG (22.8 BCMG) from the Leadville as of January 1, 2016 (Utah Division of Oil, Gas, and Mining, 2016a) (table 9.1). Currently these three fields have 20 active producers and 29 abandoned Leadville producers (table 9.1).

Three fields in the Leadville Limestone Paradox Basin play have produced condensate and nonassociated gas. Big Indian, Lisbon Southeast, and Little Valley fields (figure 9.2) have combined to produce 485,900 BC (77,252 m^3) and 61 BCFG (1.73 BCMG) from the Leadville as of January 1, 2016 (Utah Division of Oil, Gas, and Mining, 2016a; Colorado Oil and Gas Conservation Commission, written communication, July 2016) (table 9.1). Currently these three fields have six active producers and four abandoned producers (table 9.1).

In 2015, the monthly production from the Leadville Limestone averaged 435 BO (and condensate) (69 m^3) and 96 MCFG (2.27 MCMG) (Utah Division of Oil, Gas, and Mining, 2016a; Colorado Oil and Gas Conservation Commission, 2016). Production peaked in the mid to late 1960s, and has generally declined since then.

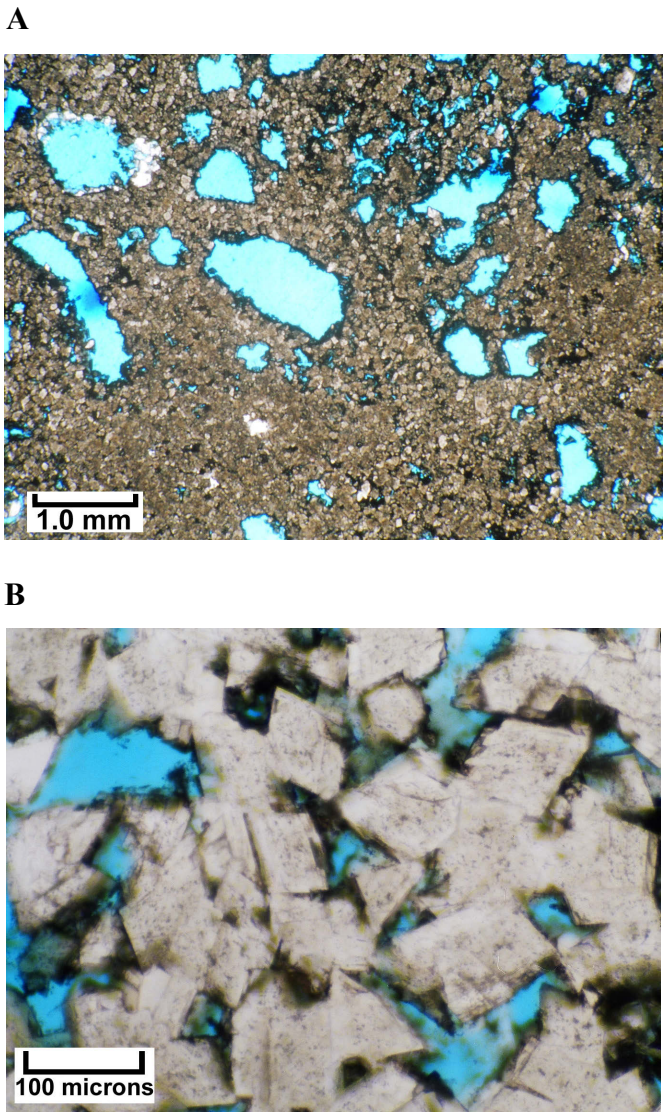

Figure 9.11. *Leadville Limestone diagenetic characteristics from Lisbon field, San Juan County, Utah.* ***A.*** *Representative photomicrograph (plane light) of the tight, finely crystalline dolomite with isolated grain molds. Most of this fabric-selective dolomite formed early in the diagenetic history of the skeletal/peloid sediment.* ***B.*** *Representative photomicrograph (plane light) of the coarser, replacement dolomite (both euhedral rhombs and occasional "saddle" overgrowths). The black (opaque) areas are the result of pyrobitumen films. From Lisbon No. D-816 well, 8433 feet, porosity = 2%, permeability <0.1 mD.*

EXPLORATION POTENTIAL AND TRENDS

The buried fault block has been the most common target for exploration of hydrocarbons in the Leadville Limestone because it has a proven history of success and fault blocks can be identified on gravity, aeromagnetic, and seismic geophysical data. Therefore future exploration will likely continue to focus on fault-related anticlines along existing producing trends. However, regional lithofacies mapping (from studying cores and geophysical well logs) show that stratigraphic oil accumulations may exist to the west and southwest of the fold

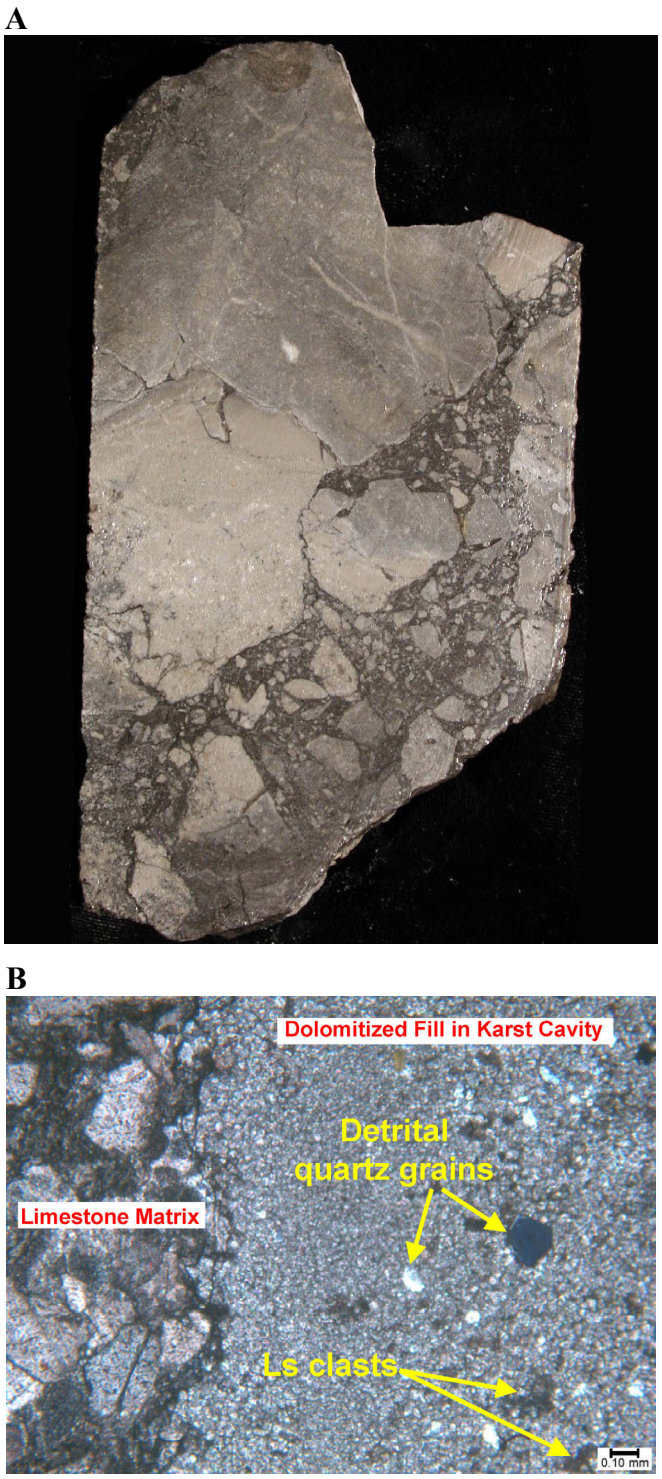

Figure 9.12. *Leadville Limestone diagenetic characteristics from Lisbon field, San Juan County, Utah.* ***A.*** *Conventional core slab showing a dolomite "autobreccia" in which the clasts have moved very little. The black material surrounding the in-place clasts is composed of porous late dolomite coated with pyrobitumen. From Lisbon NW USA No. B-63 well, 9938.3 feet, porosity = 6.4%, permeability = 54 mD.* ***B.*** *Photomicrograph (cross-polarized light) showing contact between limestone matrix and the dolomitized karst cavity filling; note that the dolomitized filling is composed of very fine crystals with detrital quartz grains and small carbonate clasts. From Lisbon No. D-616 well, 8308 to 8309 feet, porosity = 1.2%, permeability = 11.1 mD.*

and fault belt. Traps may be formed by porous Waulsortian mounds, or other carbonate buildups, where porosity is further enhanced by early dolomitzation. Additional traps may also be developed in the regolith deposits, that is collapse breccia associated with karstification of the exposed Leadville during Late Mississippian time. Diagenetic traps formed from late, possibly hydrothermal dolomite may be present especially along major fault trends. Surface geochemical surveys (Seneshen and others, 2009) and high-resolution 3-D seismic are required to improve the ability to identify these subtle stratigraphic and diagenetic traps.

Eby and others (2008) identified potential oil-prone areas for exploration in the northern Paradox Basin based on shows in drill cuttings (using low-cost epifluorescence techniques). The epifluorescence analysis of Leadville oil compared to epifluorescence in the cores and cuttings from Lisbon field created a Leadville epifluorescence standard. The standard can be used to map Leadville oil migration patterns (no hydrocarbons, hydrocarbons passed through, hydrocarbons present but not mobile, hydrocarbons mobile). As expected, productive wells (fields) are distinguished by generally higher epifluorescence ratings. However, a regional southeast-northwest trend of relatively high epifluorescence parallels the southwestern part of the Paradox fold and fault belt while the northeastern part shows a regional trend of low epifluorescence. These trends imply that hydrocarbon migration and dolomitization were associated with regional northwest-trending faults and fracture zones, which created potential oil-prone areas along the southwest trend.

CHAPTER 10:
PENNSYLVANIAN PARADOX FORMATION PARADOX BASIN PLAY

by

Thomas C. Chidsey, Jr., and Craig D. Morgan
Utah Geological Survey

and

David E. Eby
Eby Petrography & Consulting, Inc.

CONTENTS

FIGURES

TABLES

CHAPTER 10:
PENNSYLVANIAN PARADOX FORMATION PARADOX BASIN PLAY

INTRODUCTION

The most prolific oil and gas play in the Paradox Basin is the Pennsylvanian Paradox Formation play (figure 10.1). The Paradox has produced over 549 million BO (87 million m^3) and 627 BCFG (17 BCMG); however, much of the gas included in the production figures is cycled gas, including CO_2, for pressure maintenance (Utah Division of Oil, Gas, and Mining, 2016a; Arizona Geological Survey, 2016; Ken Robertson, Colorado Oil and Gas Conservation Commission, written communication, 2016). Since the early 1920s, the Paradox Basin has been a site for oil exploration drilling. The Cane Creek anticline in the Paradox fold and fault belt was one of the most obvious structural drilling targets and first tested oil in 1924 (figure 1.9). However, the Cane Creek field only produced 1887 BO (300 m^3) and 25 MMCFG (0.7 MMCMG), primarily from the Cane Creek shale (Stowe, 1972). The first commercial production from the Paradox Formation did not begin until the 1950s. Greater Aneth field, Utah's largest oil producer, was discovered in 1956, and it has produced over 479 million BO (76 million m^3) (Utah Division of Oil, Gas, and Mining, 2016a). The remaining 70 million BO of production is from nearly 100 small fields in the basin. Using a minimum production cutoff of 500,000 BO (80,000 m^3), currently 27 significant Paradox fields are in Utah, eight in Colorado, and one in Arizona. Geologic data for 32 individual fields in the play are summarized in table 10.1.

The play outline for the Paradox Formation represents the maximum extent of petroleum potential in the Paradox Basin as defined by lithofacies trends, source rocks, producing reservoirs, and hydrocarbon shows. The attractiveness of the Paradox Formation play (and other Paradox Basin oil and gas plays) to the petroleum industry is basically the same as the Leadville Limestone play: oil and gas prices, risks, reserve potential, pipeline access, drilling costs, and especially environmental issues. When evaluating these criteria, the Paradox Formation play now generally meets the exploration guidelines of small, independent companies. Prospective drilling targets in the Paradox Formation play are delineated using high-quality 2-D and 3-D seismic data, 2-D and 3-D forward modeling/visualization tools, well control, dipmeter information, lithofacies mapping, and detailed analyses of the diagenetic history; the use of cores is critical.

The three main producing zones of the Paradox Formation are informally named the Cane Creek shale zone, Desert Creek zone, and Ismay zone (figure 10.2). Fractured shale beds in the Cane Creek shale are oil productive in the Paradox Basin fold and fault belt. The Ismay mainly produces oil from fields along a trend that crosses the southern Blanding sub-basin. The Desert Creek produces oil in fields along a trend that crosses the central Blanding sub-basin and Aneth platform. Both the Ismay and Desert Creek buildups generally trend northwest-southeast. Various lithofacies changes and extensive diagenesis have created complex reservoir heterogeneity within the diverse Desert Creek and Ismay zones.

The Paradox Formation oil play area includes nearly the entire Paradox Basin (figure 10.1); the formation produces only gas in the southeastern part of the basin in Colorado. The Paradox Formation play is divided into four subplays (figures 10.3 and 10.4): (1) fractured shale, (2) Blanding sub-basin Desert Creek zone, (3) Blanding sub-basin Ismay zone, and (4) Aneth platform Desert Creek zone.

DEPOSITIONAL ENVIRONMENTS

In Pennsylvanian time, the Paradox Basin was rapidly subsiding along its northeast margin, but with a shallow-water carbonate shelf on the south and southwest margins of the basin that locally contained algal-mound buildups. These carbonate buildups, and the material shed from their flanks, formed petroleum traps where reservoir-quality porosity and permeability have developed. The substrates for these buildups were often black, organic-rich marine muds.

During the Pennsylvanian, the Paradox Basin had subtropical, dry climatic conditions along the trade-wind belt, 10° to 20° north of the paleo-equator. Prevailing winds were from present-day north (Peterson and Hite, 1969; Heckel, 1977; Parrish, 1982). During transgressions, open-marine waters flowed across a shallow cratonic shelf into the basin through up to four postulated normal marine access ways. The Cabezon accessway, located to the southeast, is generally accepted as the most likely normal marine-water conduit to maintain circulation on the shallow shelf (Fetzner, 1960; Ohlen and McIntyre, 1965; Hite, 1970). Periodic decreased circulation in the basin resulted in deposition of thick salts (halite with sporadic thinner beds of potash and magnesium salts) and anhydrite. The deeper interior of the basin to the north and northeast consists almost entirely of salt deposits and is referred to as the evaporite salt basin (figure 10.5).

Cyclicity during Paradox Basin deposition was primarily controlled by glacio-eustatic fluctuations. The shape of the Penn-

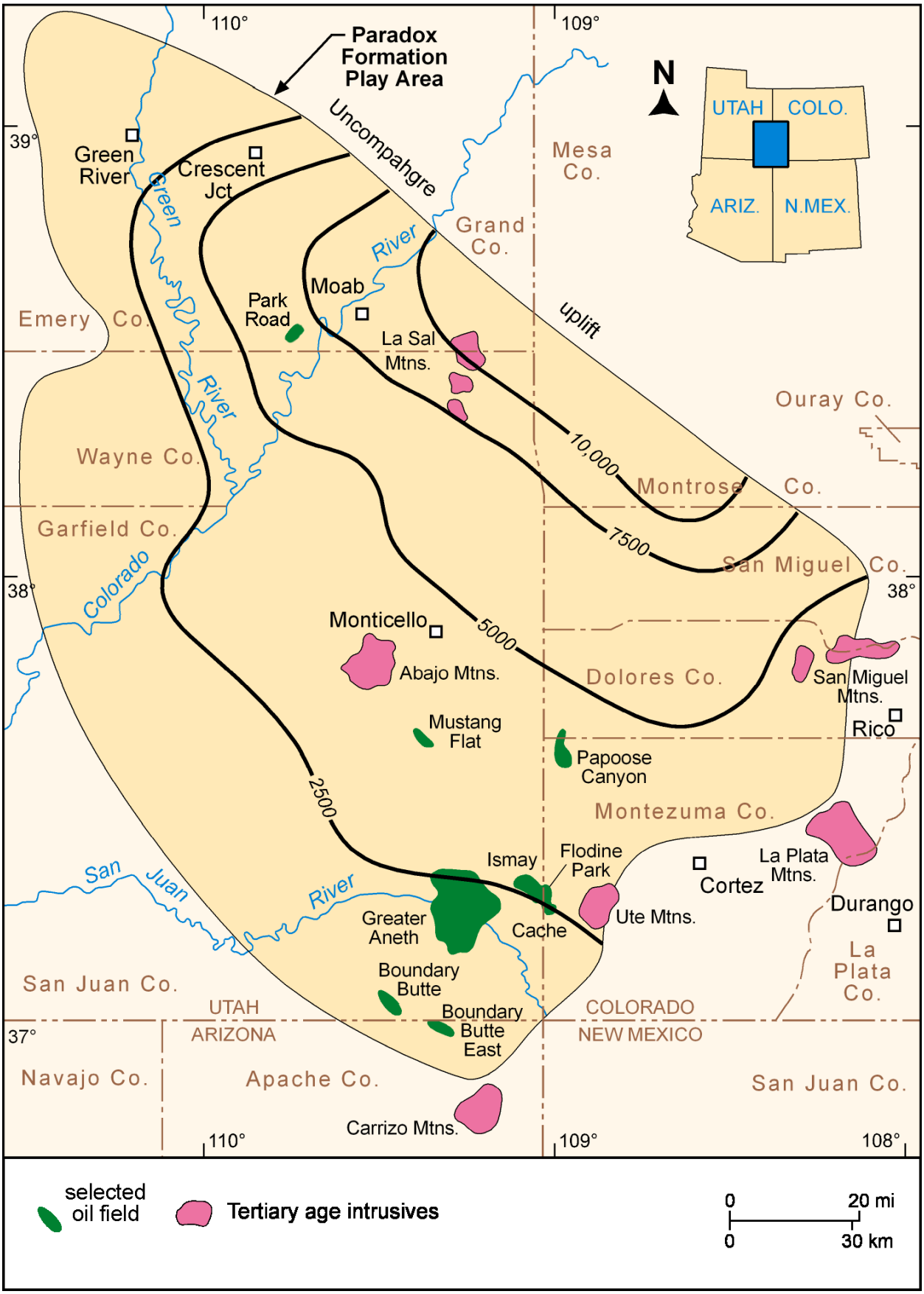

Figure 10.1. *Pennsylvanian Paradox Formation play area and selected fields, Utah, Colorado, and Arizona. Thickness of the Pennsylvanian rocks shown in feet. Modified from Choquette (1983).*

Table 10.1. *Well and production data for fields in the Blanding sub-basin Desert Creek zone, Blanding sub-basin Ismay-zone, and Aneth platform Desert Creek zone subplays, Pennsylvanian Paradox Formation play. Data from Colorado Oil and Gas Conservation Commission (2016), Utah Division of Oil, Gas, and Mining (2016a), Arizona Geological Survey (2016); Ken Robertson, Colorado Oil and Gas Conservation Commission, written communication (2016).*

State	County	Field	Zone	Discovery Date	Active Producers	Abandoned Producers	Acres	Spacing (acres)	Average Monthly Production		Cumulative Production	
									Oil (bbl)	Gas (MCF)	Oil (bbl)	Gas (BCF)
Blanding sub-basin Desert Creek zone subplay												
Colorado	Montezuma	Island Butte	Desert Creek	1991	5	1	NA	NA	1504	2663	2,181,271	5.7
Colorado	Montezuma	McClean	Desert Creek	1974	8	5	NA	NA	4258	11,814	5,996,337	19.7
Colorado	Dolores/Montezuma	Papoose Canyon	Desert Creek	1970	38	2	1920	160	2007	31,185	6,750,905	41.7
Utah	San Juan	Bug	Desert Creek	1980	8	6	600	160	269	3742	1,659,728	5.2
Blanding sub-basin Ismay zone subplay												
Colorado	Montezuma	Cache	Ismay	1964	0	17	1040	40	0	0	4,712,100	7.8
Colorado	Montezuma	Flodine Park	Ismay	1959	2	7	1440	80	511	2165	2,746,902	10.5
Colorado	Montezuma	Marble Wash	Ismay	1958	3	4	400	80	144	396	1,017,727	1.8
Colorado	Montezuma	Roadrunner	Ismay	1984	7	6	NA	40	136	0	2,213,916	4.6
Colorado	Montezuma	Towaoc	Ismay	1959	1	4	160	80	331	513	847,744	1.3
Utah	San Juan	Cave Canyon	Ismay	1984	9	2	30	20	49	437	2,505,822	4.1
Utah	San Juan	Deadman-Ismay	Ismay	1986	4	0	120	40	197	1760	825,370	12.8
Utah	San Juan	Ismay	Ismay	1956	8	40	4370	80	1009	827	10,998,320	17.6
Utah	San Juan	Kachina	Ismay	1986	3	4	400	80	259	240	2,703,232	2.4
Utah	San Juan	Kiva	Ismay	1984	5	2	350	80	0	0	2,739,300	4.0
Utah	San Juan	McElmo Mesa	Ismay	1960	0	8	2240	80	0	0	2,219,175	2.9
Utah	San Juan	Mustang Flat	Ismay	1982	8	1	320	160	120	5176	798,070	17.7
Utah	San Juan	Patterson Canyon	Ismay	1974	9	2	320	none	1554	2757	1,343,791	3.0
Utah	San Juan	Tin Cup Mesa	Ismay	1980	10	0	880	80	134	186	2,504,268	3.8
Aneth platform Desert Creek zone subplay												
Arizona	Apache	Boundary Butte East	Ismay-Desert Creek-Akah	1954	0	10	2800	80	0	0	890,705	9.8
Utah	San Juan	Akah	Ismay-Desert Creek-Akah	1955	1	1	240	80	40	32	546,999	0.5
Utah	San Juan	Anido Creek	Ismay-Desert Creek	1960	0	3	375	80	0	0	612,082	0.4
Utah	San Juan	Bluff	Desert Creek	1951	7	11	1040	none	243	854	1,708,500	3.9
Utah	San Juan	Clay Hill	Desert Creek	1977	3	1	200	none	95	189	1,038,565	1.5
Utah	San Juan	Desert Creek	Desert Creek	1954	6	2	300	80	1758	1634	2,331,072	2.0
Utah	San Juan	Gothic Mesa	Desert Creek	1956	3	14	1520	80	4	0	1,965,268	1.3
Utah	San Juan	Greater Aneth	Desert Creek	1956	445	215	48,260	40	343,449	592,309	479,088,740	432.8
Utah	San Juan	Recapture Creek	Ismay-Desert Creek	1956	5	5	1350	80	518	1085	2,302,927	4.0
Utah	San Juan	Runway	Desert Creek	1990	3	0	193	40	768	979	939,813	3.2
Utah	San Juan	Tohonadla	Ismay-Desert Creek-Akah	1957	9	7	1200	80	4811	4072	2,708,322	1.2
Utah	San Juan	Turner Bluff	Desert Creek	1957	3	13	720	80	30	31	945,504	0.8

NA = Not available

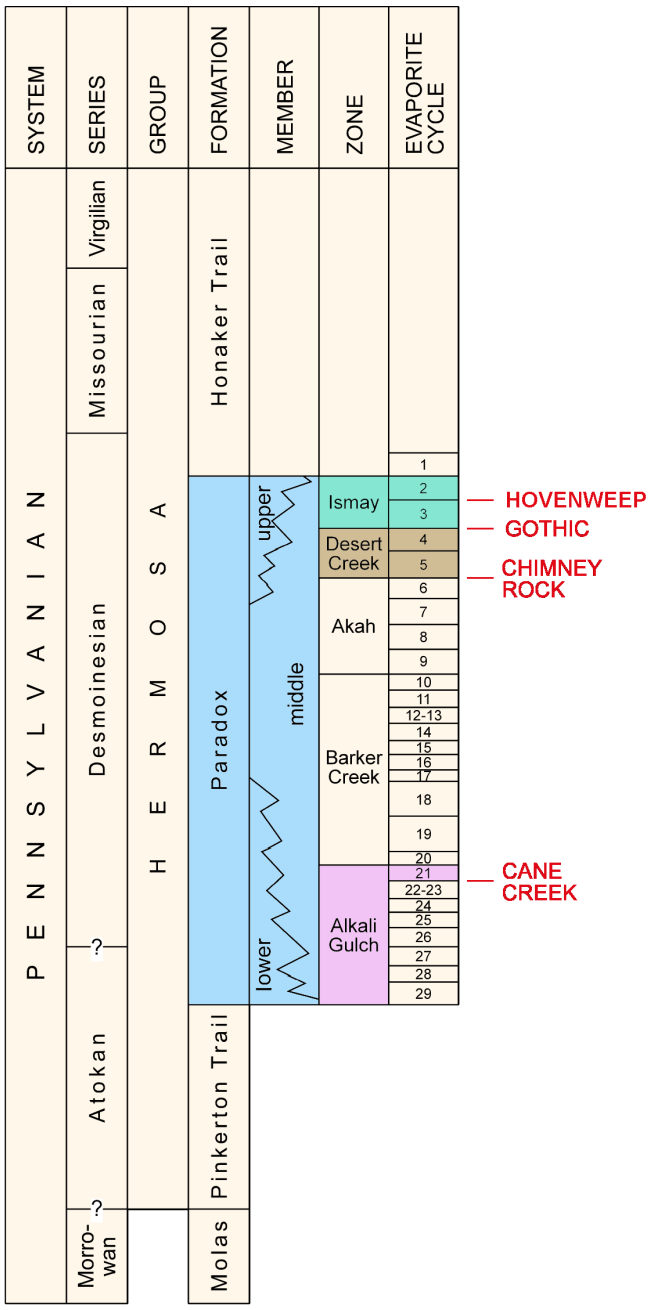

Figure 10.2. *Pennsylvanian stratigraphic chart for the Paradox Basin; informal zones and cycles with significant production are highlighted with colors. Red text represents organic-rich shale intervals; the Cane Creek shale zone is a significant oil producer as well in the Paradox fold and fault belt. Modified from Hite (1960), Hite and Cater (1972), and Reid and Berghorn (1981).*

sylvanian sea-level curve reflects rapid marine transgressions (rapid melting of ice caps) and slow, interrupted regression (slow ice cap buildup) (Imbrie and Imbrie, 1980; Denton and Hughes, 1983; Heckel, 1986, 2008). Irregular patterns within the transgressive-regressive cycles are thought to be a response to interference of orbital parameters (Imbrie and Imbrie, 1980). These sea-level cycles were also influenced by (1) regional tectonic activity and basin subsidence (Baars, 1966; Baars and Stevenson, 1982), (2) proximity to basin margin and evaporites (Hite, 1960; Hite and Buckner, 1981), (3) climatic variation and episodic blockage of open marine-water access ways, and (4) fluctuations in water depth and water energy (Peterson and Ohlen, 1963; Peterson, 1966; Hite and Buckner, 1981; Heckel, 1983).

Fractured Shale Subplay

Shale generally records an open- to restricted-marine, low-energy environment varying between aerobic to dysaerobic and occasionally anoxic conditions (for thin, organic-rich black mud). Deposition included (1) black to dark gray, non-calcareous, non-fossiliferous mud and silty mud, (2) spiculitic lime mud, (3) pelagic lime mud with microfossils, and (4) dolomitic mud. Water depths were variable, ranging from below fair-weather and storm wave base to relatively shallow to near exposure for silt, sand, lime mud, microbialites, primary dolomite, and evaporites.

Blanding Sub-Basin Ismay and Desert Creek Zones Subplays

Ismay and Desert Creek zone depositional environments that trend across the Blanding sub-basin are shown schematically on figure 10.6. Reservoirs within the Utah portion of the upper Ismay zone of the Paradox Formation are dominantly limestones composed of small, phylloid-algal buildups; locally variable, inner-shelf, skeletal calcarenites; and rarely, open-marine, bryozoan mounds (figure 10.6A). The Desert Creek zone is dominantly dolomite, comprising regional, nearshore, shoreline trends with highly aligned, linear facies tracts (figure 10.6B).

The controls on the sedimentation of each depositional environment were water depth (which was primarily controlled by glacio-eustatic fluctuations), water temperature and salinity, oxygenation, prevailing wave energy, and paleostructural position. In the Ismay zone, the following depositional environments are recognized: open-marine shelf; organic (carbonate) buildups and calcarenites at the platform edge; middle shelf or open platform interior; and restricted inner shelf or platform interior. In the Desert Creek zone, the following depositional environments are recognized: basinal; calcarenites (carbonate islands) at the platform edge; middle shelf or open platform interior; restricted inner shelf or platform interior; platform interior salinas (evaporites); and shoreline and terrestrial.

The basinal environment represents deep water (at possible depths of 90 to 120 feet [30–40 m]) and euxinic conditions. Deposition included (1) black to dark gray, non-calcareous, non-fossiliferous mud and silty mud, (2) spiculitic lime mud, (3) pelagic lime mud with microfossils and occasional thin-shelled bivalves such as *Halobia*, and (4) thick, deep-water siliciclastic sand. The open-marine deposition was below wave base under normal-marine salinity and low-energy conditions.

The middle shelf or open platform interior represents a well-circulated, low- to moderate-energy, normal salinity, shallow-

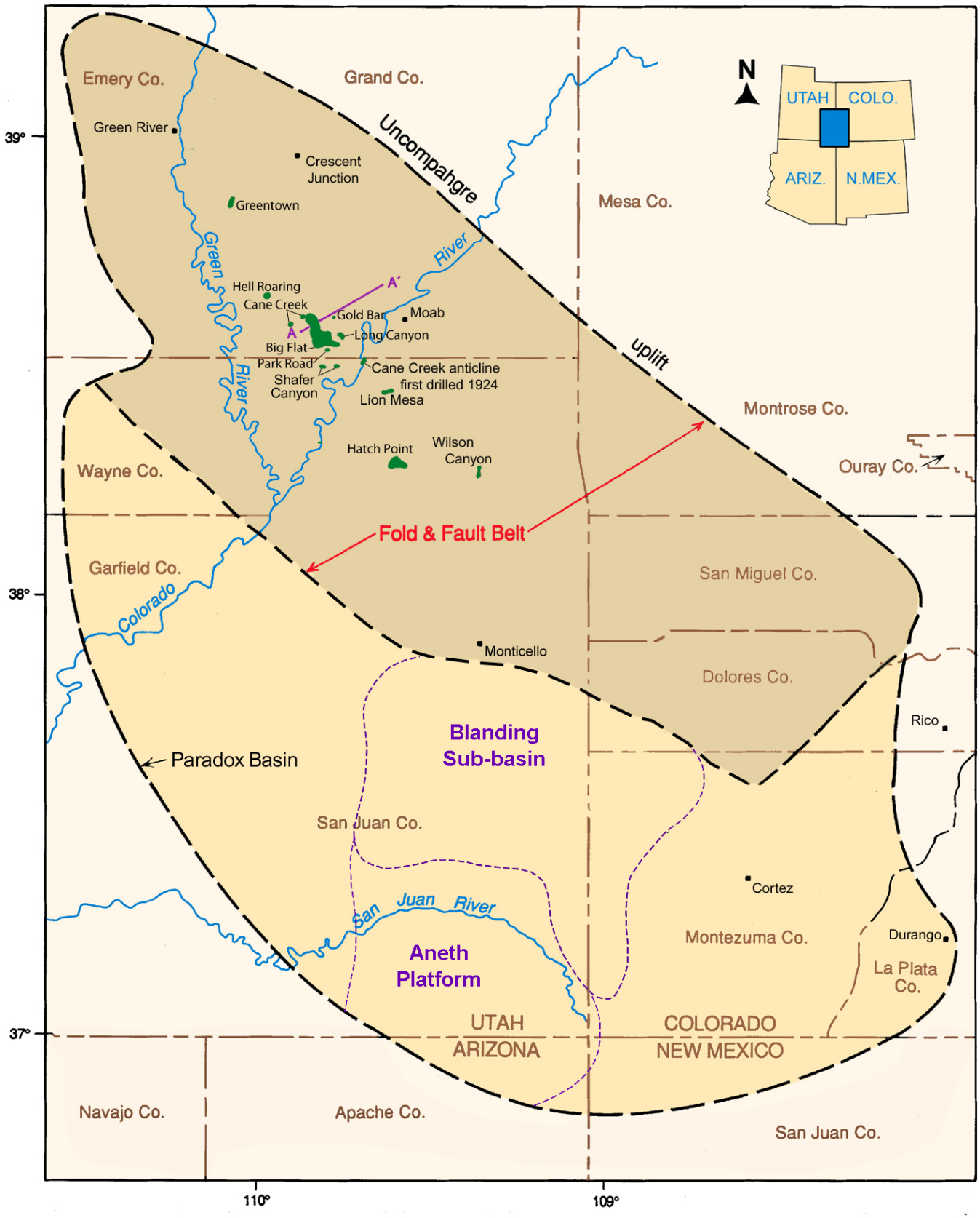

Figure 10.3. *Location map of the Paradox Basin showing the fold and fault belt which approximately matches the fractured shale subplay. Fields shown in solid green areas are productive from the Cane Creek shale of the Pennsylvanian Paradox Formation. Line A–A' is figure 10.35.*

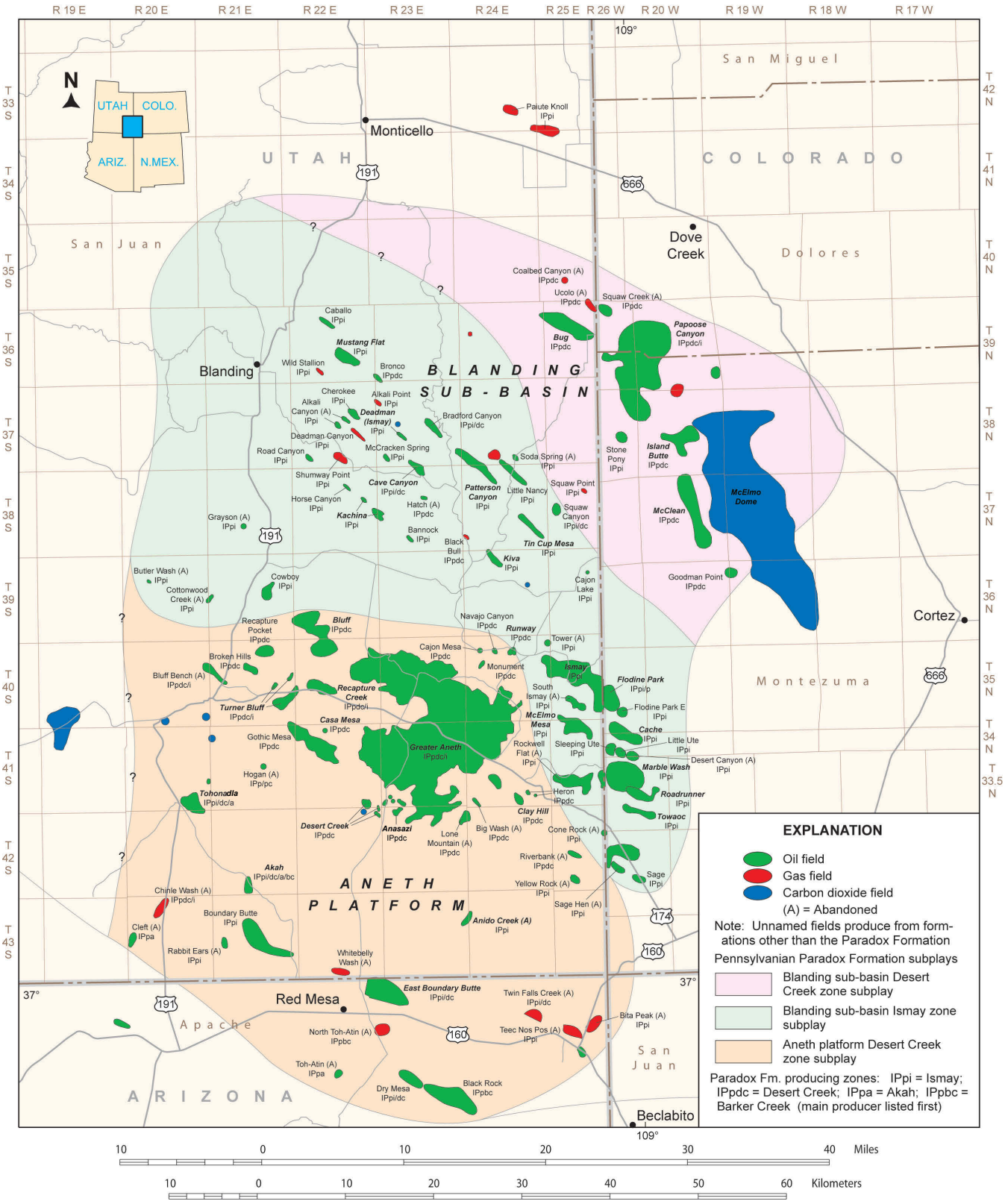

Figure 10.4. *Location of the Paradox Formation Blanding sub-basin Desert Creek zone, Blanding sub-basin Ismay zone, and Aneth platform Desert Creek zone subplays, southeastern Utah, southwestern Colorado, and northeastern Arizona. The fractured shale subplay includes the entire Paradox Basin as shown on figure 10.1. Fields in italics have produced over 500,000 BO as of January 1, 2016. Modified from Wray and others (2002); Wood and Chidsey (2015).*

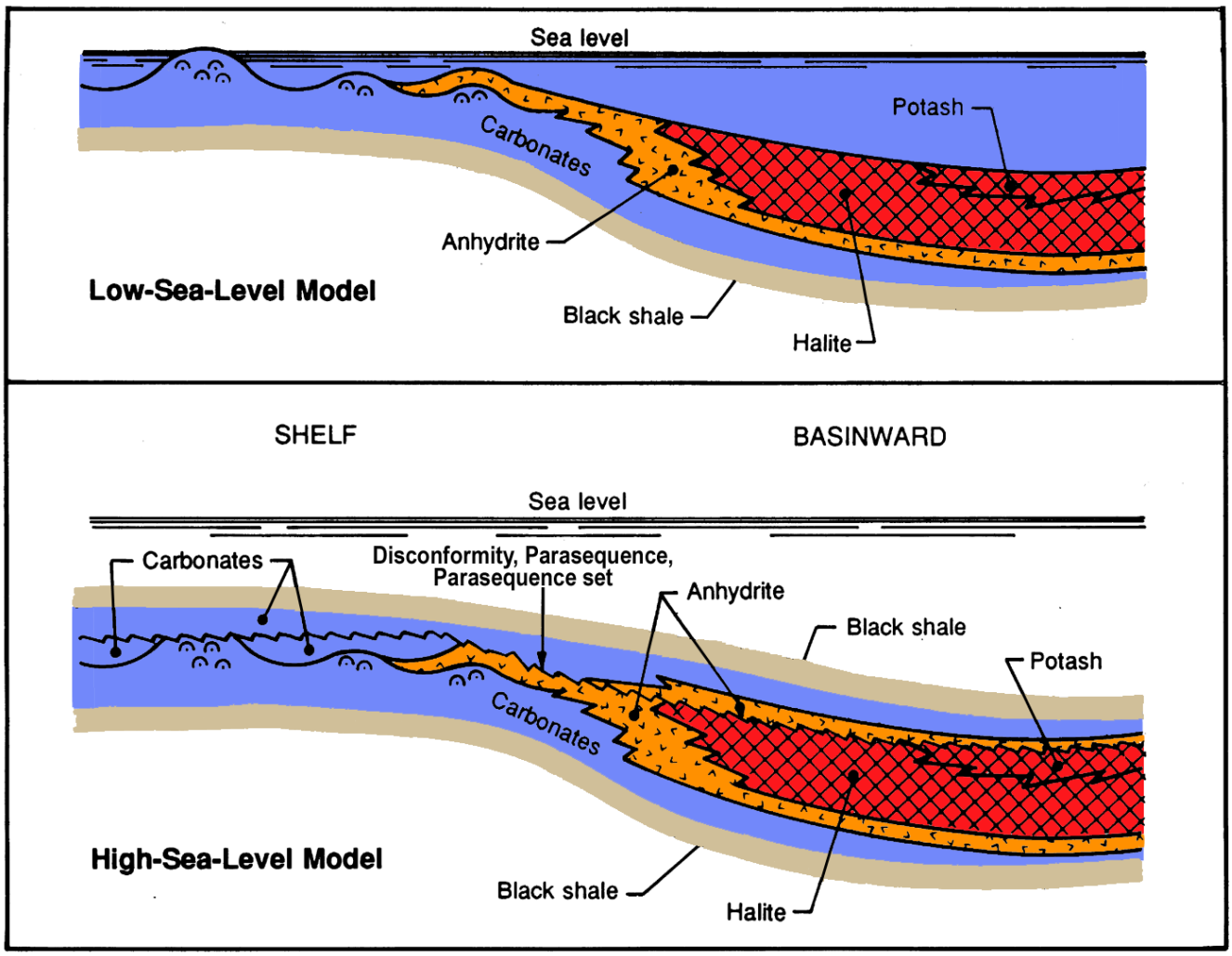

Figure 10.5. *Diagram of the depositional sequence during Paradox time and the relationships of various basin and shelf facies. Wavy line represents disconformity, parasequence, or parasequence set. Symbol in the shelf carbonate represents algal-mound development. Modified from Hite and Cater (1972).*

water (between nothing and 90 feet [0–30 m]) environment. Lithofacies from this environment form the dominant producing reservoirs in the Ismay and Desert Creek zones that trend across the Blanding sub-basin. Benthic forams, bivalve molluscs, and codiacean green algae (*Ivanovia* and *Kansasphyllum*) are common. Bryozoan mounds developed in the relatively quiet, deeper water of the middle shelf. Echinoderms are rare and open-marine cephalopods are generally absent. The principal buildup process, phylloid-algal growth, occurred during sea-level highstands. Paleotopography from Mississippian-aged normal faulting (reactivation of Precambrian faults [Baars, 1966; Baars and Stevenson, 1982]) produced the best marine conditions for initial algal growth.

Calcarenites are recognized in both the Desert Creek and Ismay zones and represent moderate- to high-energy, regularly agitated, marine environments where shoals and/or islands developed. Sediment deposition and modification probably occurred from 5 feet (1.5 m) above sea level to 45 feet (14 m) below sea level. These platform-edge deposits include (1) oolitic and coated grain sands, (2) crinoid, foram, algal, and fusilinid sands, (3) small, benthic foram and hard peloid sands representing stabilized peloid grain flats, and (4) shoreline carbonate islands of shell hash.

The restricted inner shelf or platform interior represents shallow water (nothing to 45 feet [0–14 m]), and generally low-energy and poor circulation conditions. Fauna are limited mainly to stromatolitic algae, gastropods, certain benthic forams, and ostracods. Deposits included (1) bioclastic lagoonal to bay lime mud, (2) tidal-flat muds often with early dolomite, and (3) shoreline carbonate islands with birdseye fenestrae, stromatolites, cryptoalgal laminations, and dolomitic crusts. Platform-interior evaporites, usually anhydrite, were deposited in salinity-restricted areas.

Shoreline and terrestrial siliciclastic deposits represent beach, fluvial, and flood-plain environments. These siliciclastic deposits include argillaceous to dolomitic silt with rip-up clasts, scour surfaces, or mudcracks.

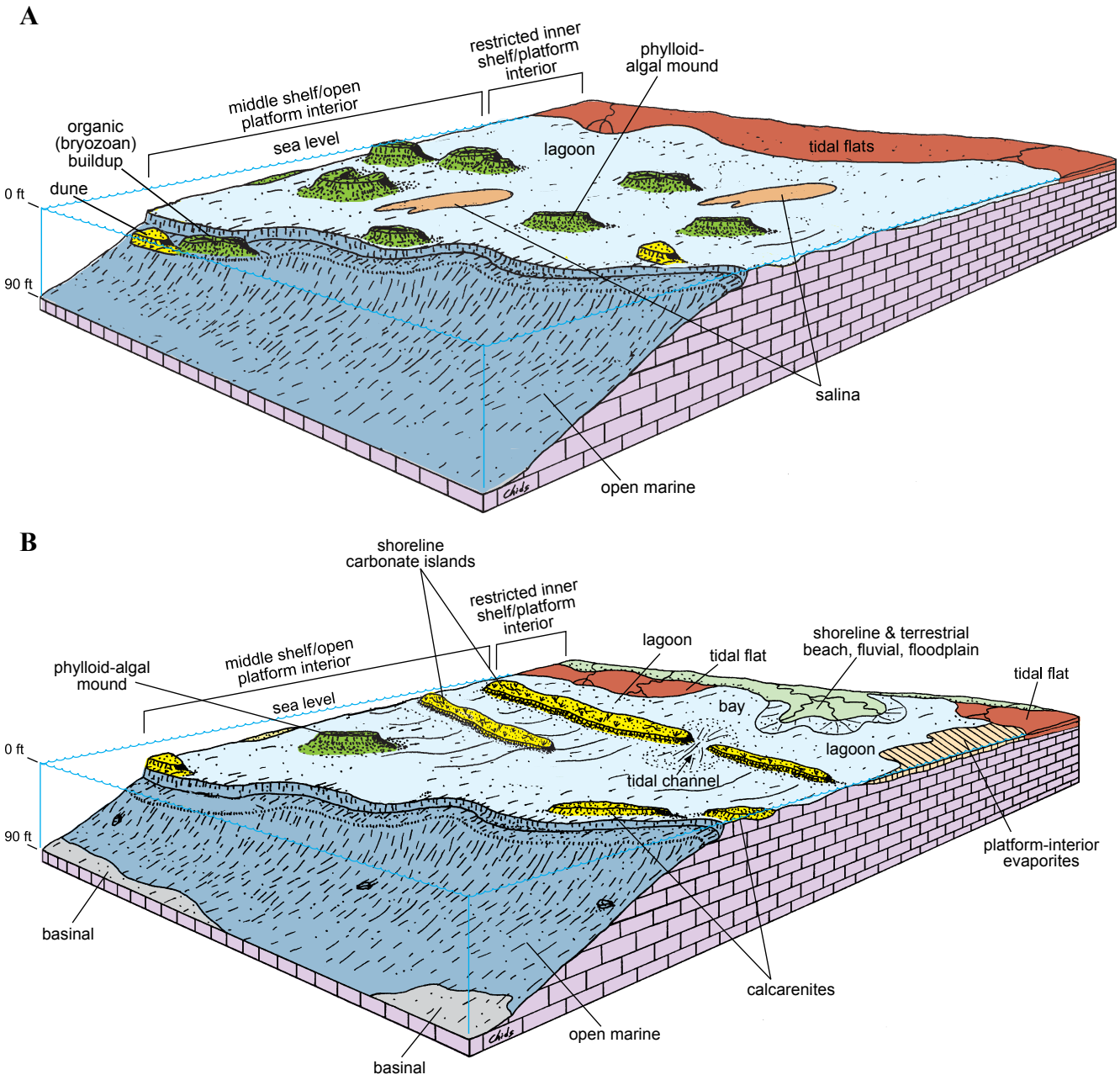

Figure 10.6. *Block diagrams displaying major depositional environments, as determined from core, for the Ismay (A) and Desert Creek (B) zones, Pennsylvanian Paradox Formation, Utah and Colorado.*

Within these depositional environments, several major Ismay and Desert Creek lithofacies are recognized and mapped across the Blanding sub-basin (figures 10.7 through 10.9). Mapping of these lithofacies delineates prospective reservoir trends containing porous and productive buildups. Ismay lithofacies include open marine, middle shelf, inner shelf/tidal flat, bryozoan mound, phylloid-algal mound, quartz sand dune, and anhydritic salina. Desert Creek lithofacies include open marine, middle shelf, proto-mound/collapse breccia, and phylloid-algal mound.

Open-marine lithofacies dominates the lower Desert Creek zone in the Blanding sub-basin where there is very little hydrocarbon potential (figure 10.9). However, this lithofacies developed in different areas for both the upper part (northeastern and southern regions [figure 10.7]) and lower part (western to north-central regions [figure 10.8]) of the upper Ismay zone. Middle-shelf lithofacies of the upper Ismay zone covers extensive areas and surround important intra-shelf basins described later. Bryozoan mounds, quartz sand dunes, proto-mounds and some phylloid-algal mounds, and inner shelf/tidal flats developed on the low-energy carbonates of the middle-shelf environment (figures 10.7 through 10.9).

Inner shelf/tidal flat lithofacies represent relatively small areas in geographical extent, especially in the upper part of the upper Ismay zone. However, recognizing this facies is important because inner shelf/tidal flats often form the sub-

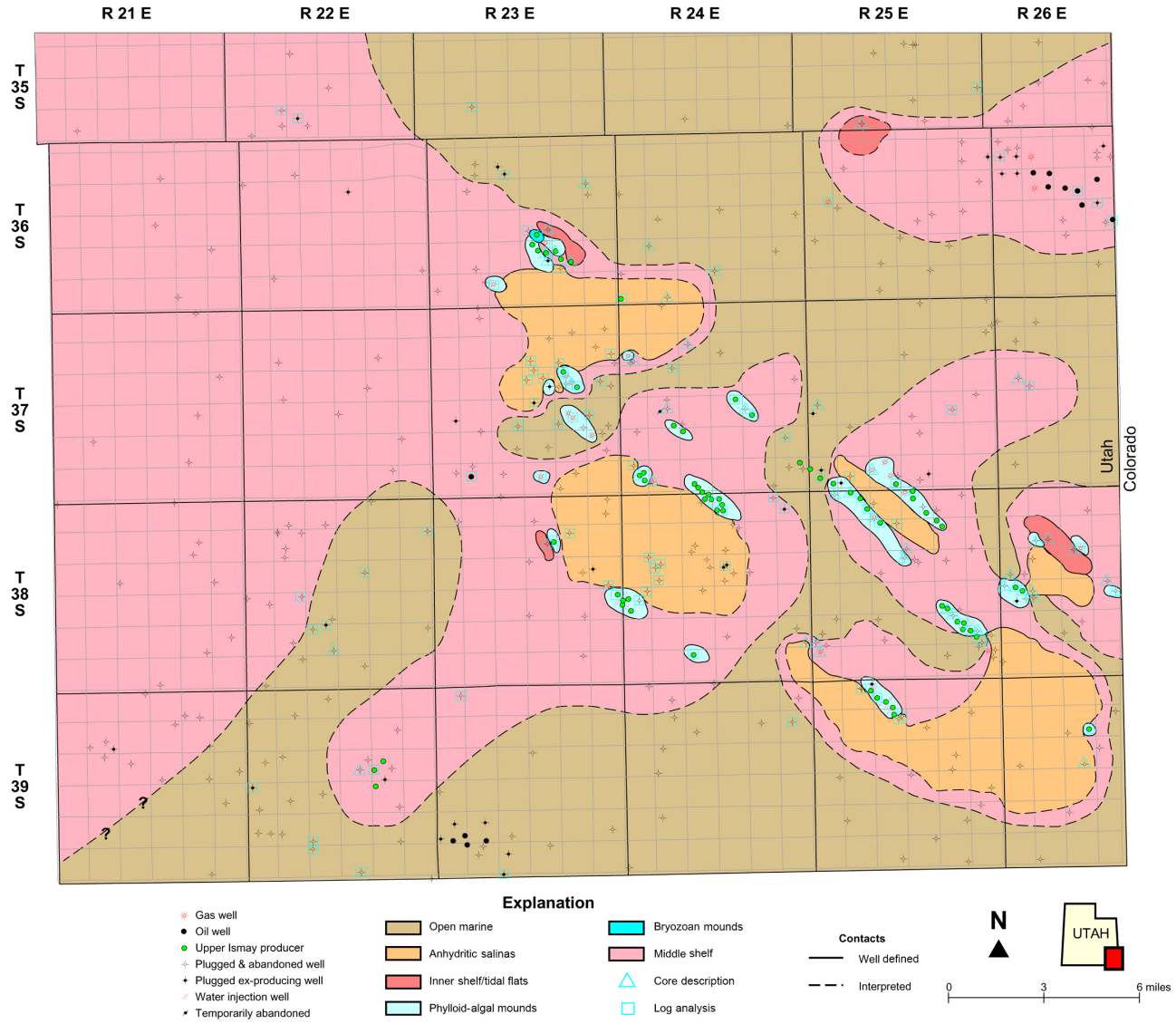

Figure 10.7. *Regional lithofacies map of the upper part of the upper Ismay zone, Paradox Formation, in the Blanding sub-basin, Utah.*

strate for phylloid-algal mound development. Proto-mound/collapse breccia lithofacies is found in the Desert Creek zone and represent the initial stage of a mound buildup or one that never fully developed. This lithofacies contains dolomitized and brecciated algal plates, marine cements, and internal sediments suggesting subaerial exposure. Proto-mound/collapse breccia lithofacies are usually near phylloid-algal mound lithofacies, but generally lack any significant porosity. They may appear as promising buildups on seismic, but in actuality have little potential other than as guides to nearby fully developed mounds (figure 10.9). In the upper Ismay zone, most phylloid-algal mounds developed adjacent to widespread intra-shelf (anhydrite-filled) basins (figures 10.7 and 10.8). Porous Desert Creek mound lithofacies, such as the reservoir for Bug field, occurs in linear bands that appear to be shorelines (carbonate islands) that developed on the middle shelf (figure 10.9). Regional lithofacies mapping clearly defines anhydrite-filled, intra-shelf basins. Inner shelf/tidal flat and associated productive, phylloid-algal mound lithofacies trends of the Ismay are present around the anhydritic salinas of intra-shelf basins (figures 10.7 and 10.8).

Aneth Platform Desert Creek Zone Subplay

Three generalized, regional depositional environments (lithofacies) are identified in the Aneth platform Desert Creek zone subplay (figures 10.10 and 10.11): (1) open-marine, (2) shallow-shelf/shelf-margin, and (3) intra-shelf, salinity-restricted (Chidsey and others, 1996c). The open-marine lithofacies includes open-marine buildups (typically crinoid-rich mounds), open-marine crinoidal- and brachiopod-bearing carbonate muds, euxinic black shales, wall complexes, and detrital fans. Sediments in the open-marine environment were deposited at water depths between possibly 45 and 120 feet (14–37 m). This depositional environment is the most extensive and surrounds the shallow-shelf/shelf-margin depositional environment.

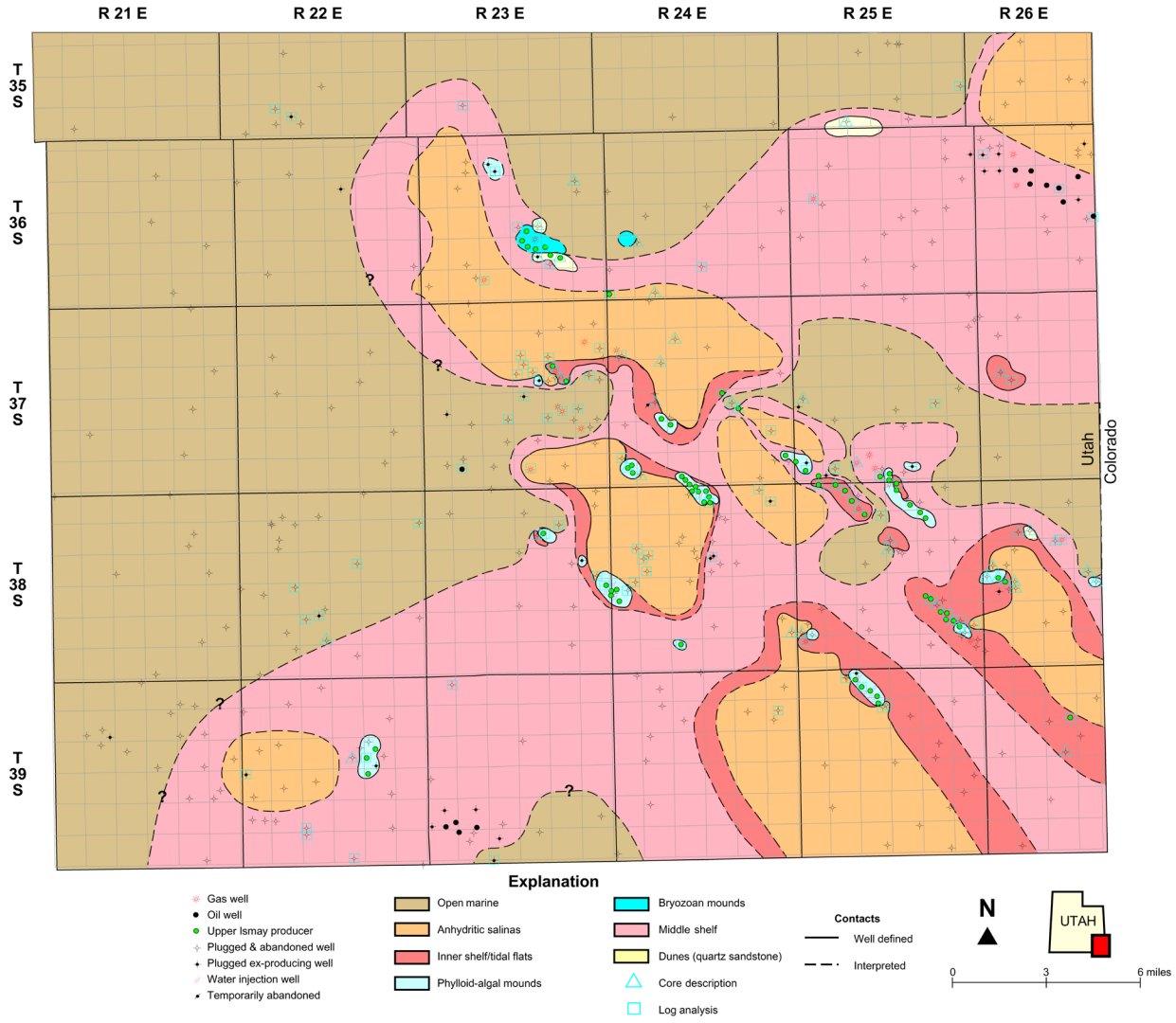

Figure 10.8. *Regional lithofacies map of the lower part of the upper Ismay zone, Paradox Formation, in the Blanding sub-basin, Utah.*

The shallow-shelf/shelf-margin depositional environment includes shallow-shelf buildups (phylloid algal, coralline algal, bryozoan, and marine-cemented buildups [mounds]), calcarenites (beach, dune, and stabilized grain flats, and oolite banks), and platform-interior carbonate muds and sands. Sediments were deposited at water depths between 0 and 40 feet (0–12 m). Karst characteristics are occasionally present over mounds. Tubular tempestites (burrows filled with coarse sand as a result of storm pumping) are found in some carbonate muds and sands. Most oil fields in the Aneth platform Desert Creek zone subplay are located within lithofacies representing this depositional environment, including the giant Greater Aneth field (figures 10.10 and 10.11).

The intra-shelf, salinity-restricted depositional environment represents small sub-basins within the shallow-shelf/shelf-margin depositional environment. The water had slightly elevated salinity compared to the other depositional environments. This depositional environment includes platform-interior evaporites, dolomitized tidal-flat muds, bioclastic lagoonal muds, tidal-channel carbonate sands and stromatolites, and euxinic dolomites. Sediments were deposited at water depths generally between 20 and 45 feet (6–14 m). Euxinic dolomites often display karst characteristics. Two intra-shelf sub-basins have been identified in the southeastern part of the Paradox Basin in Utah; each is separated from the open-marine by a fringe of the shallow-shelf/shelf-margin (figure 10.10).

Within the depositional environments described above and shown on figure 10.6, three local Desert Creek lithofacies are common: platform-interior carbonate sands and muds, platform-margin calcarenites, and carbonate buildups (figure 10.11) (Chidsey and others, 1996c). The platform-interior carbonate mud and sand lithofacies are widespread across the shallow shelf. This lithofacies represents a low- to moderate-energy environment. Mud and sand were deposited in subtidal (burrowed), inter-buildup, and stabilized grain-flat (pellet shoals) settings intermixed with tubular and bedded tempestites. Water depths generally ranged from 5 feet to 45 feet (1.5–14 m). The platform-margin calcarenite lithofacies is located along the margins of the larger shallow shelf or the rims of phylloid-algal buildup complexes. This lithofacies represents

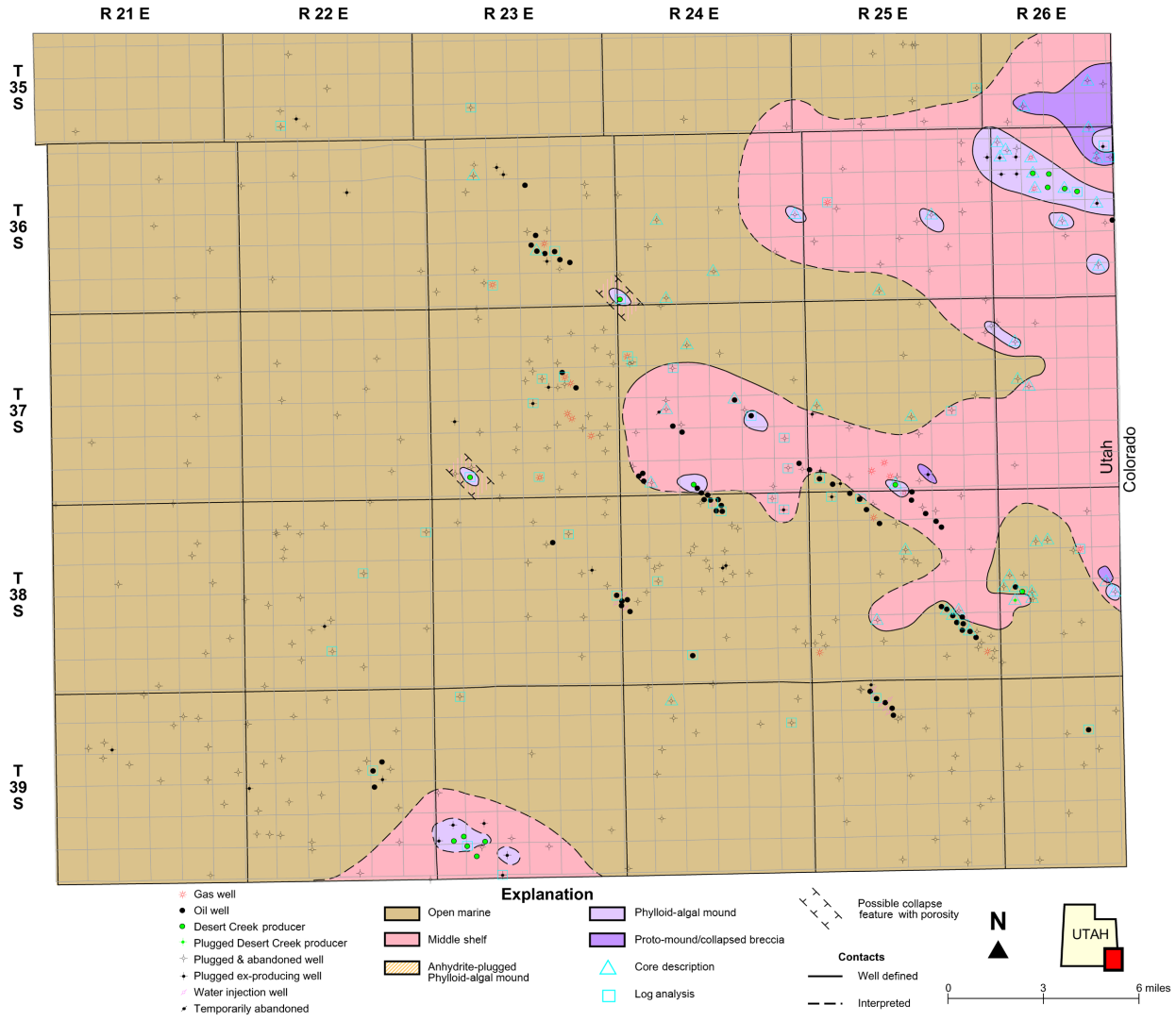

Figure 10.9. *Regional lithofacies map of the lower Desert Creek zone, Paradox Formation, in the Blanding sub-basin, Utah.*

a high-energy environment where shoals and/or islands developed as a result of regularly agitated, shallow-marine processes on the shelf. Characteristic features of this lithofacies include medium-scale cross-bedding and bar-type, carbonate, sandbody morphologies. Water depth likely ranged from nothing to 20 feet (6 m). Stabilized calcarenites occasionally developed subaerial features (up to 5 feet [1.5 m] above sea level) such as beach rock, hard grounds, and soil zones.

Productive carbonate buildups are located in the shallow-shelf/shelf-margin areas. These buildups can be divided into three lithofacies types: (1) phylloid algal, (2) coralline algal, and (3) bryozoan (Eby and others, 1993; Chidsey and others, 1996c). The controls on the development of each buildup type were again water depth, water temperature and salinity, oxygenation, prevailing wave energy, and paleostructural position. The phylloid-algal buildup, the dominant producing reservoir lithofacies, represents a moderate-energy environment with well-circulated water at possible depths from 10 to 50 feet (3–13 m). Mapping of seismic anomalies and reservoir thicknesses indicates that carbonate phylloid-algal buildups, or mounds, were doughnut or horseshoe shaped, or a composite of the two shapes (figures 10.12 and 10.13). Many of the phylloid-algal buildups were large enough to enclose interior lagoons. The Desert Creek at Greater Aneth field was deposited as a horseshoe-shaped buildup of numerous coalescing mounds capped by banks of oolitic sands, similar to the present-day Bahamas open-marine, carbonate-shelf system. The coralline-algal buildup lithofacies is located along shallow-shelf margins facing open-marine waters or within the intra-shelf, salinity-restricted lithofacies belt (where they are non-productive). On the shallow shelf, this lithofacies represents a low- to high-energy environment with well-circulated water at possible depths ranging from 25 to 45 feet (8–14 m). These buildups are a component of the wall complex (figure 10.11) in association with early marine cementation and are stacked vertically. They may surround other types of buildup complexes. Bryozoan buildup lithofacies is located on the deeper flanks of phylloid-algal buildup complexes (figure 10.14A). This lithofacies represents a low-energy environment with well-circulated water. Water depths may have ranged from 25 to 45 feet (8–14 m). This lithofacies is prevalent on the shallow shelf where winds

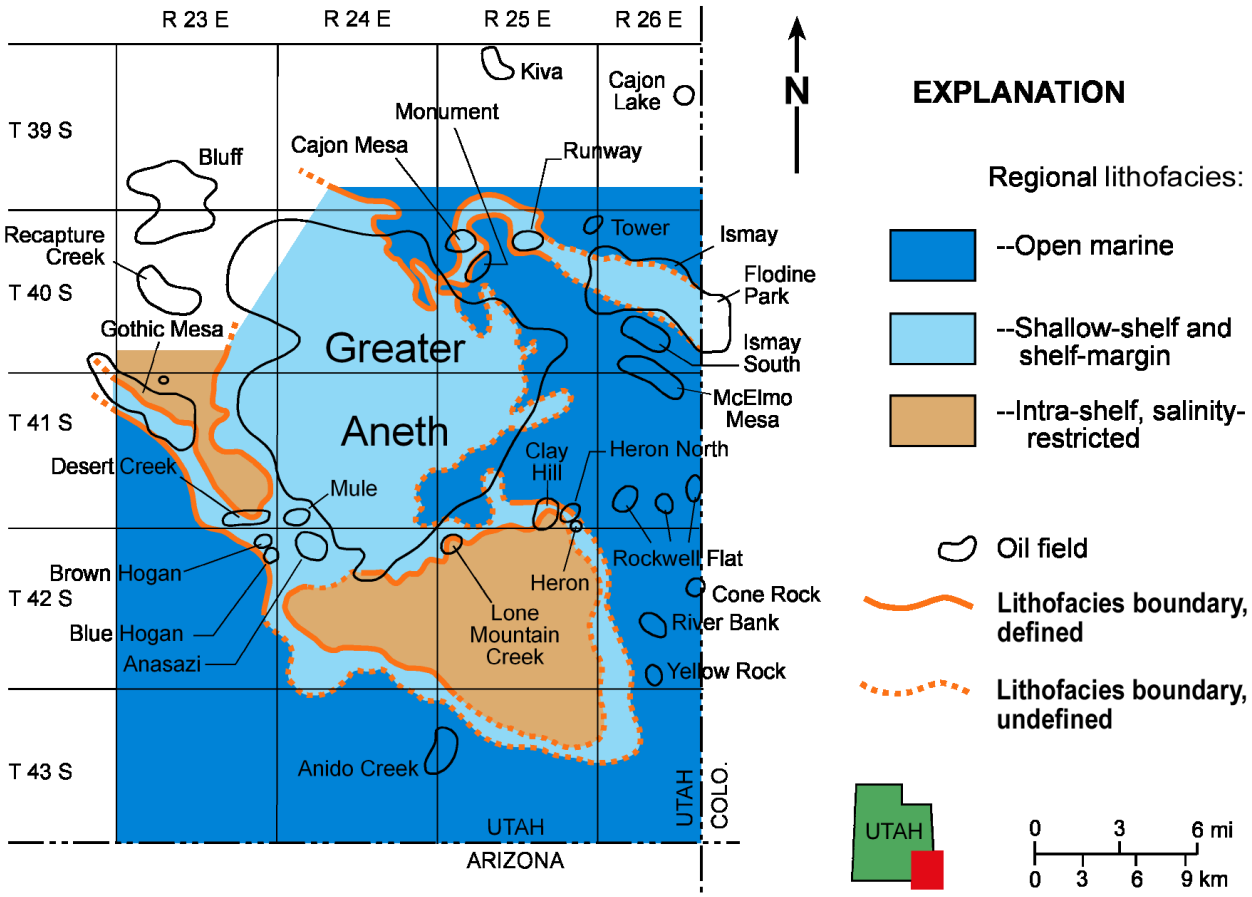

Figure 10.10. *Map of major depositional environments/lithofacies for the Aneth platform Desert Creek zone subplay. After Chidsey and others (1996c).*

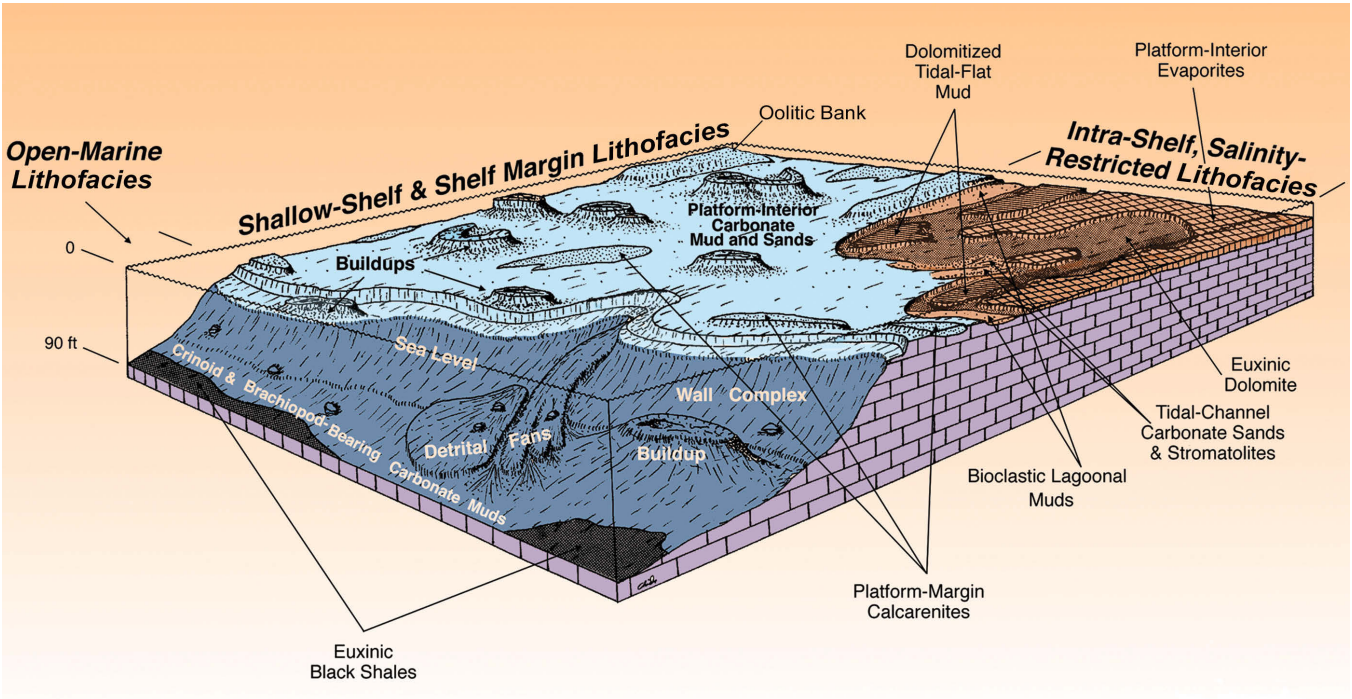

Figure 10.11. *Block diagram displaying depositional environments within the Aneth platform Desert Creek zone subplay. After Chidsey and others (1996c).*

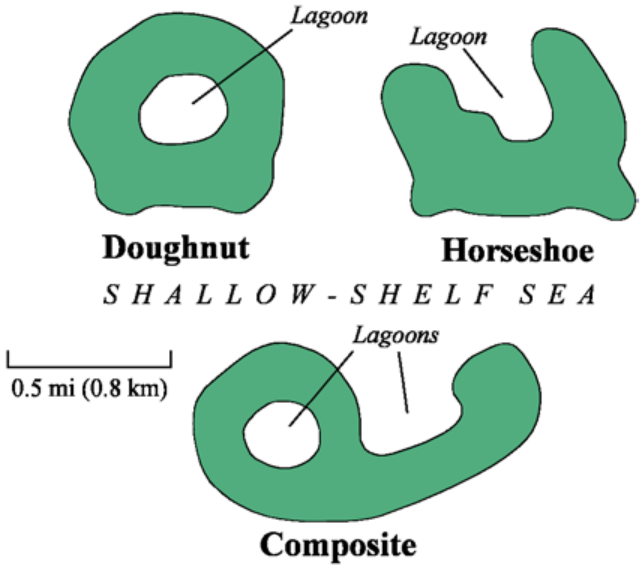

Figure 10.12. *Map view of typical carbonate buildup shapes (most often phylloid algal in composition) on the shallow carbonate shelf during Desert Creek time. After Chidsey and others (1996c).*

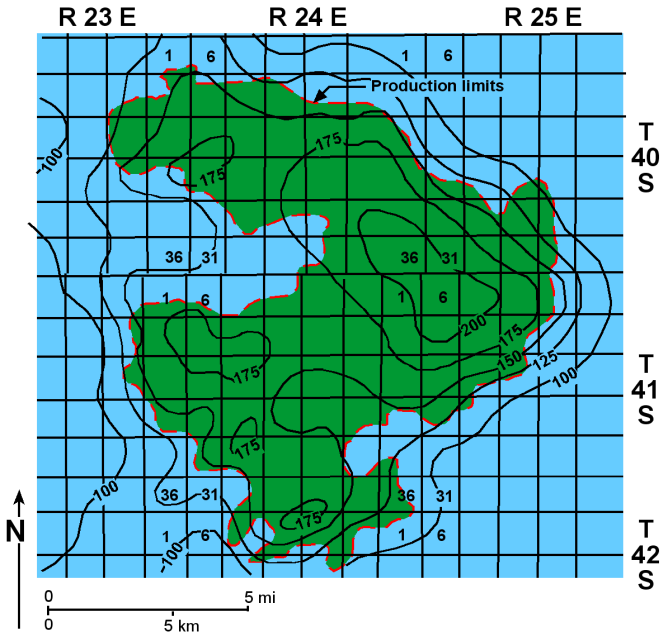

Figure 10.13. *Generalized thickness map of the Desert Creek zone, Greater Aneth field, San Juan County, Utah; contour interval = 25 feet. Modified from Peterson and Ohlen (1963).*

from the east, and paleotopography from Mississippian-aged normal faulting, produced better marine conditions for bryozoan colony development.

The principal buildup process for phylloid-algal growth occurred during sea-level highstands (figure 10.14A) (Chidsey and others, 1996c). Phylloid-algal mounds generally developed on platform-interior carbonate mud and sand. The mound substrate of platform-interior carbonates is referred to as the platform interval. Calcified phylloid-algal plates sheltered abundant primary "vugs," with mounds of phylloid algae building upward within the available accommodation space. As mounds grew, detrital skeletal material was shed and deposited as dipping beds along the exterior flanks and within interior lagoons. The floors of the interior lagoons consisted of muddy, marine limestone with fossils. Early marine cementation commonly occurred along mound walls facing open-marine environments. Bryozoan-dominated buildups developed in deeper water along the flanks of phylloid-algal mounds. Coralline-algal buildups developed in association with marine-cemented walls and detrital-fan complexes.

During sea-level lowstands, these buildups experienced considerable porosity modification (figure 10.14B). Leached cavities, vugs, and seepage-reflux dolomites developed in the mound core and flank sediments. Evaporitic dolomite and anhydrite filled the interior lagoons. Islands consisting of high-depositional-energy calcarenites and low-depositional-energy stromatolites, as well as troughs representing tidal channels, formed on the top of buildups during times of subaerial exposure (figures 10.14B and 10.14C). These high-energy portions of buildups are referred to as supra-mound intervals.

STRATIGRAPHY AND THICKNESS

The Paradox Formation is part of the Pennsylvanian Hermosa Group (Baker and others, 1933) (figure 10.2). The 500- to 5000-foot-thick (150–1500 m) Paradox is overlain by the Honaker Trail Formation and underlain by the Pinkerton Trail Formation (Wengerd and Matheny, 1958). The Paradox is divided into (1) a lower member consisting of interbedded black shale, siltstone, dolomite, and anhydrite, (2) a middle (saline) member consisting of thick halite interbedded with dolomite, dolomitic siltstone and shale, and anhydrite, and (3) an upper member of interbedded dolomite, dolomitic shale, and anhydrite.

Hite (1960), Hite and Cater (1972), and Hite and Buckner (1981) divided the middle (saline) member of the Paradox Formation in the evaporite basin into 29 salt cycles that onlap onto the basin shelf to the west and southwest (figure 10.2); Rasmussen (2010) recognizes as many as 35 cycles. Each cycle consists of a clastic-carbonate interval/salt couplet. The clastic-carbonate intervals are typically interbedded dolomite, dolomitic siltstone, silty limestone, black organic-rich shale, and anhydrite. The clastic-carbonate intervals typically range in thickness from 10 to 200 feet (3–60 m) and are generally overlain and underlain by 200 to 400 feet (60–120 m) of halite beds. Within the interior of the basin, a typical cycle consists of a clastic-carbonate interval or zone overlain almost entirely by salt, whereas on the shelf, a cycle consists of a black shale lithofacies overlain primarily by carbonates. The regionally extensive black shale lithofacies within clastic-carbonate intervals allows correlation of salt cycles in the interior of the basin with carbonate cycles on the shelf.

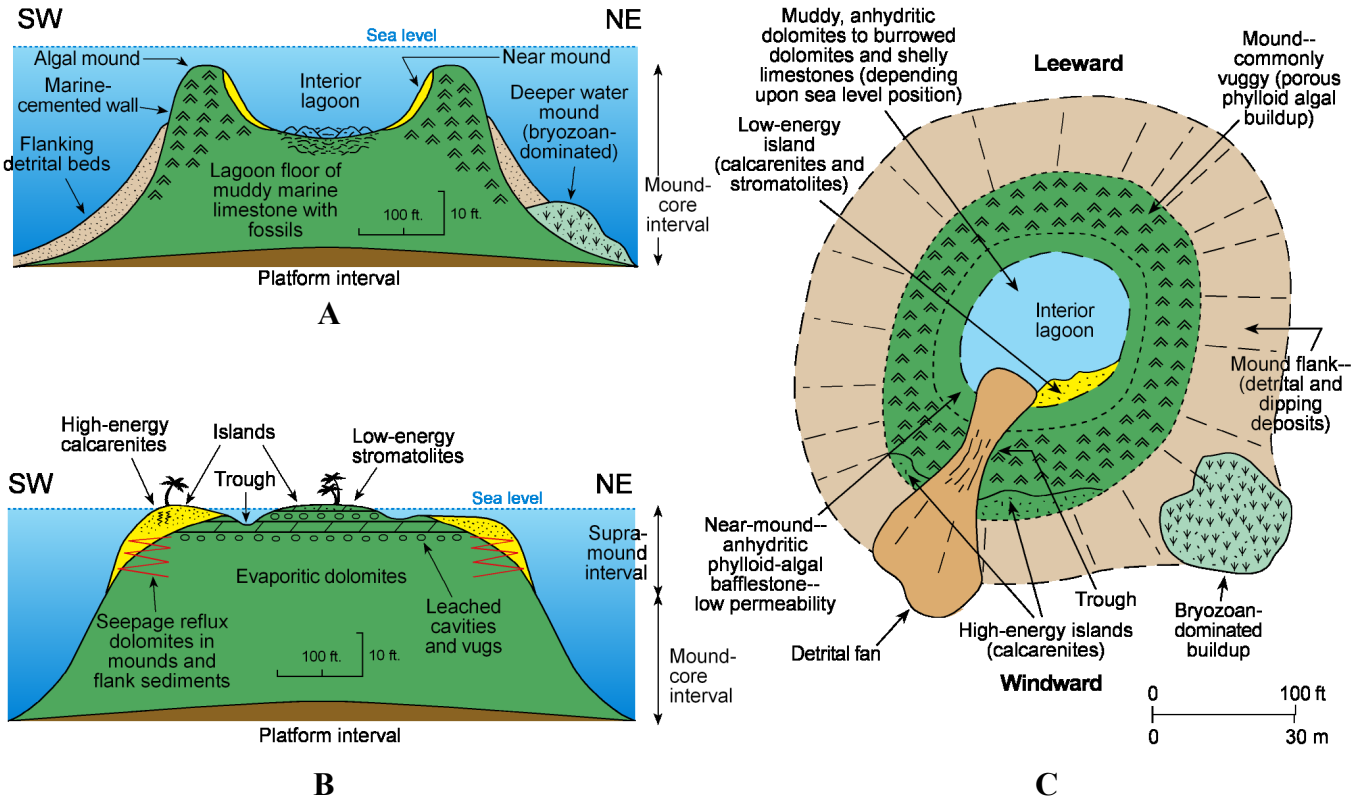

Figure 10.14. *Detailed environmental setting of Desert Creek algal buildup features surrounding the Greater Aneth field.* ***A.*** *Cross section during sea-level highstands when the mound was actively growing.* ***B.*** *Cross section during sea-level lowstands when the mound experienced porosity modification, erosion of the mound margins, evaporite dolomites filled in the lagoon, and troughs (tidal channels) and islands developed on the top.* ***C.*** *Map view of idealized algal buildup. After Chidsey and others (1996c).*

Hite and Cater (1972) and Reid and Berghorn (1981) divided the Paradox Formation into informal zones, in ascending order: Alkali Gulch, Barker Creek, Akah, Desert Creek, and Ismay (figure 10.2). This terminology is currently the most common in the literature, as well as in completion and production reports.

The Cane Creek shale zone, the only current oil-producing unit in the fractured shale subplay, is the basal part of cycle 21 and the targeted shale generally ranges from 0 to about 200 feet (60 m) thick (figure 10.15). The depositional strike of the Cane Creek is northwest to southeast, and it thins to the southwest where it laps onto the lower Paradox member or the Pinkerton Trail Formation. Thickness variations are the results of diapiric salt movement, depositional thickening on the downthrown side of faults, or depositional thinning on the upthrown side of faults (figure 10.15). The Cane Creek is divided into three units in descending order: A, B, and C. The Cane Creek is overlain and generally underlain by anhydrite and halite (figure 10.16). The thickness of the A unit averages 31 feet (10 m), ranging 10 and 84 feet (3–26 m); it is generally thicker to the north. The average thickness of the B unit is 26 feet (8 m), ranging from 4 to 72 feet (1.2–22 m). Unit B forms a thick band east-west across the subplay area. The average thickness of the C unit is 36 feet (11 m), ranging from 10 to 81 feet (3–25 m); it is generally thicker to the south.

In the Blanding sub-basin (figures 10.3 and 10.4), the Desert Creek and Ismay zones are relatively easy to correlate because they are bounded by persistant shale or other units that have distinctive geophysical log responses (figures 10.17 and 10.18). The Desert Creek zone is typically dolomite, while the Ismay is mainly limestone with some dolomite units. The average thickness of the Desert Creek zone is 85 feet (24 m), and the zone is overlain by the Gothic shale and underlain by the Chimney Rock shale, both informal units of the Paradox Formation (figure 10.17). The average depth to the Desert Creek in Blanding sub-basin fields is 5920 feet (1800 m). The average thickness of the Ismay zone is 230 feet (70 m), and the zone is overlain by the Honaker Trail Formation and underlain by the Gothic shale (figure 10.18). The Ismay zone is subdivided into an upper interval and a lower interval separated by a 30- to 45-foot-thick (10–15 m) unit informally called the Hovenweep shale (figure 10.18). The average depth to the Ismay in Blanding sub-basin fields is 5630 feet (1880 m).

On the Aneth platform (figures 10.3 and 10.4), the Desert Creek and Ismay zones are predominately limestone, with local dolomitic units, and are the major producers in the area; the Akah and Barker Creek zones are minor producers in comparison. Like in the Blanding sub-basin, the Desert Creek is again overlain by the Gothic shale and underlain by the Chimney Rock shale. The geophysical log response has varia-

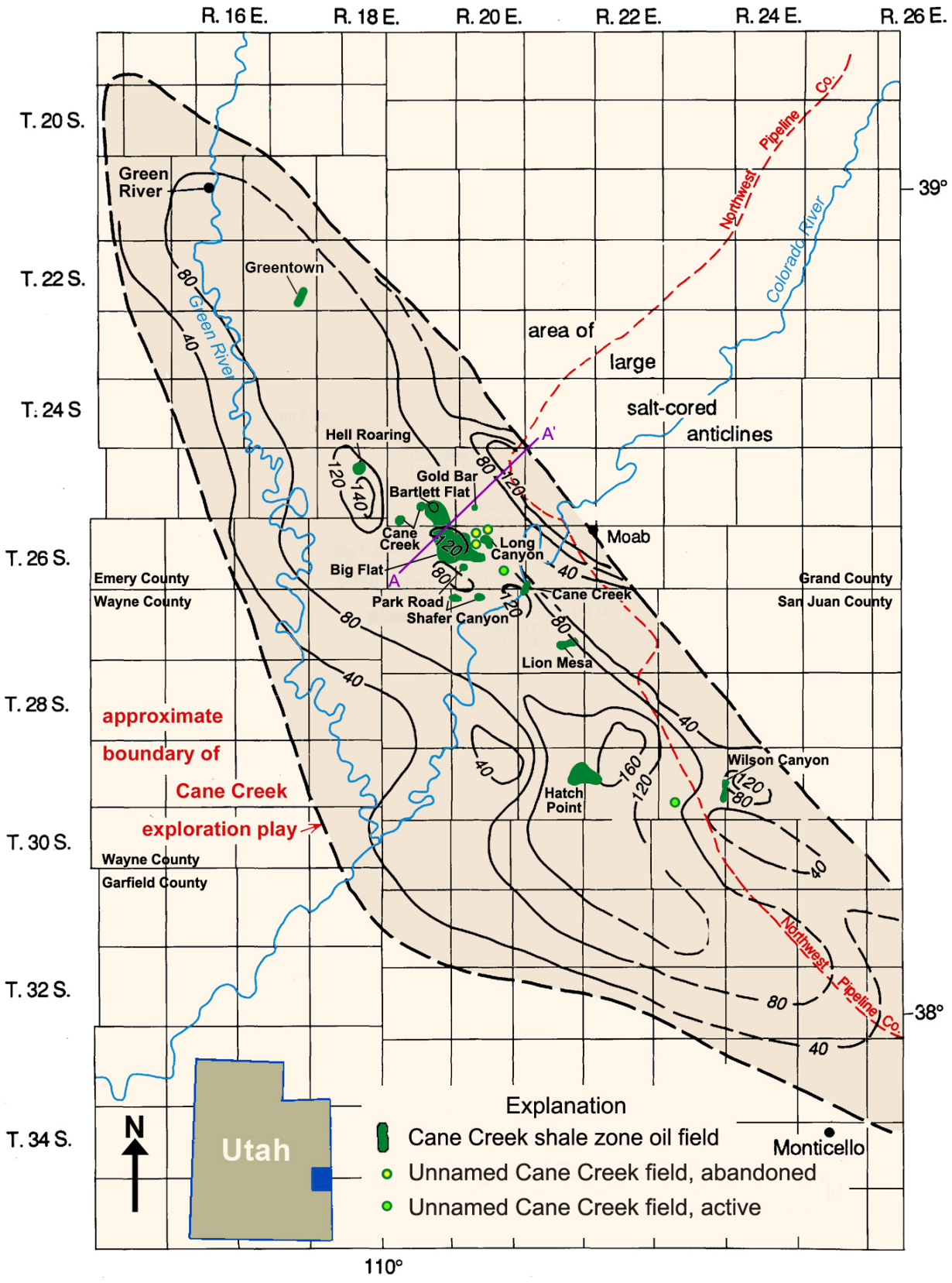

Figure 10.15. *Thickness map of the Cane Creek shale zone of the Paradox Formation, northern Paradox Basin. The shale onlaps to the west and southwest. Thickness of the Cane Creek shale in the area of large salt-cored anticlines is unknown. Local thickness varies due to salt flowages over anticlines and fault blocks. Contour interval = 40 feet. Line A–A' is figure 10.35, see tables 10.5 and 10.6 for field status, unnamed field locations, etc.*

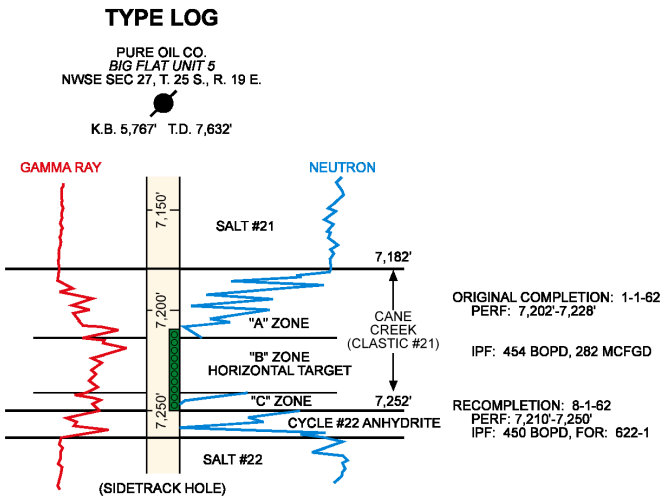

Figure 10.16. *Log section of the Cane Creek shale zone of the Paradox Formation from the Big Flat No. 5 well (section 27, T. 25 S., R. 19 E., SLBL&M), Big Flat field, Grand County, Utah. The Cane Creek is divided into units A, B, and C. The B zone is the primary fractured oil reservoir. See figure 10.15 for location of Big Flat field. After Grove and others (1993).*

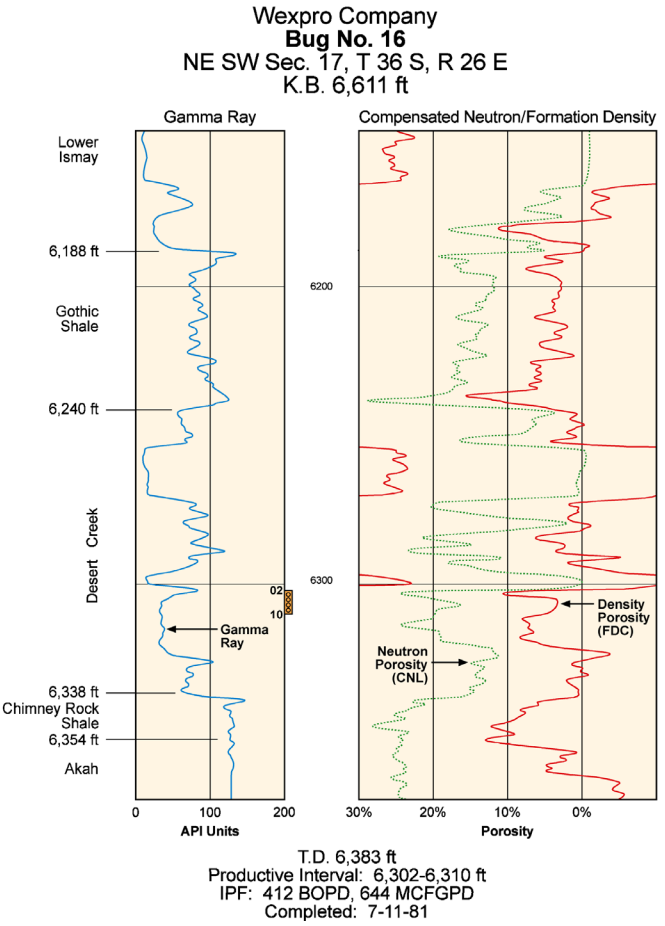

Figure 10.17. *Typical gamma ray-compensated neutron/formation density log for the Desert Creek zone in the Blanding sub-basin, from the Bug No. 16 well (section 17, T. 36 S., R. 26 E., SLBL&M), Bug field, San Juan County, Utah. Producing (perforated) interval between depths of 6302 and 6310 feet. See figure 10.4 for location of Bug field.*

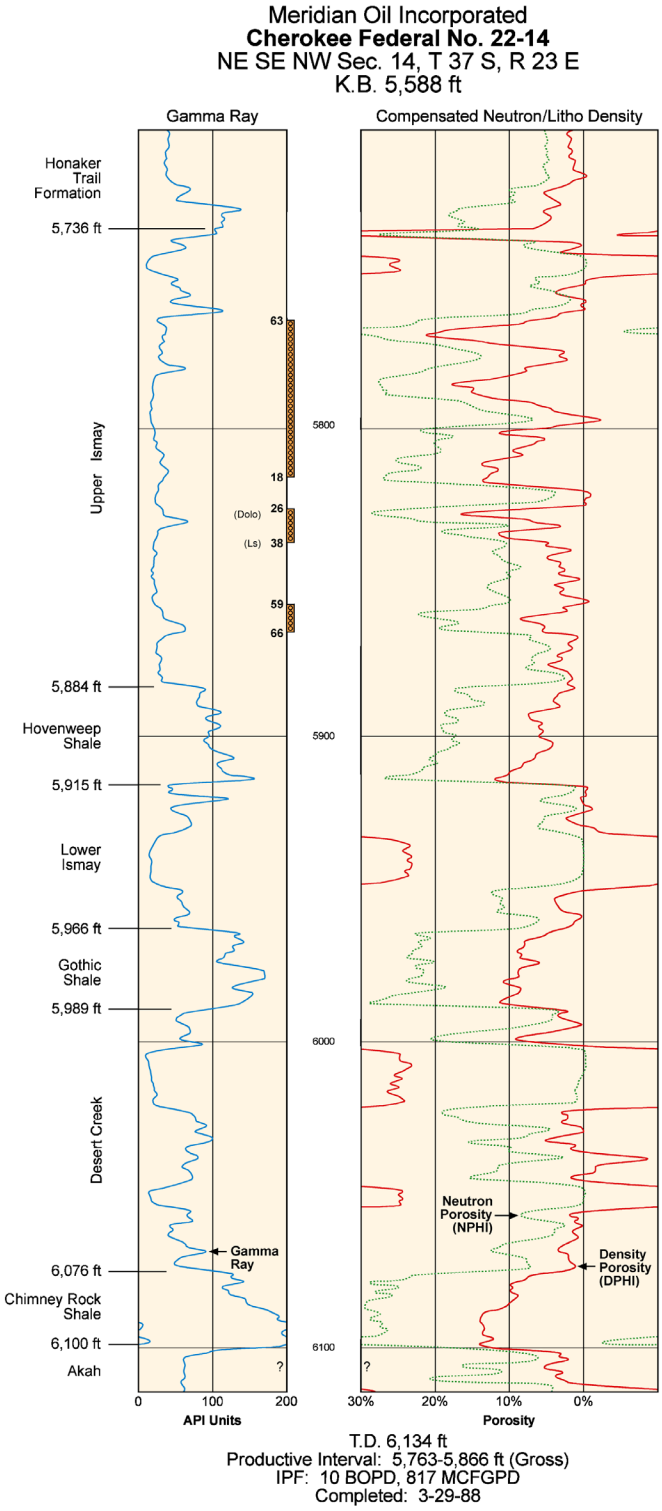

Figure 10.18. *Typical gamma ray-compensated neutron/litho density log for the Ismay zone in the Blanding sub-basin, from the Cherokee Federal No. 22-14 well (section 14, T. 37 S., R. 23 E., SLBL&M), Cherokee field, San Juan County, Utah. Producing (perforated) interval between depths of 5763 and 5866 feet. See figure 10.4 for location of Cherokee field.*

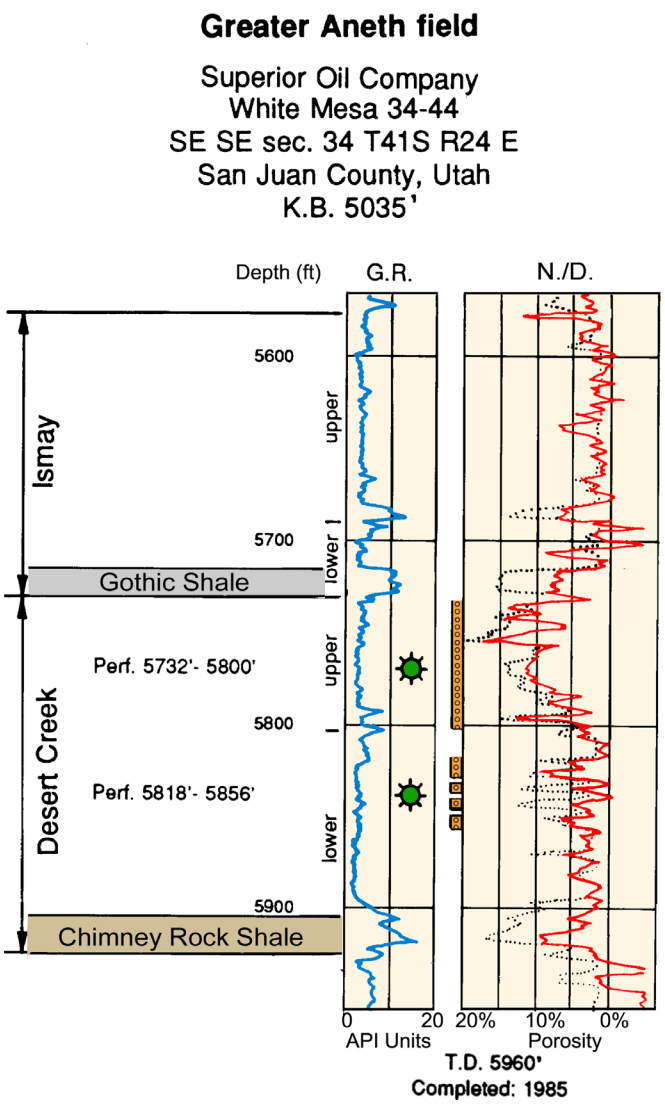

Figure 10.19. *Typical gamma ray-compensated neutron/density log for the Desert Creek zone in the Aneth platform, from the White Mesa No. 33-44 well (section 34, T. 41 S., R. 24 E., SLBL&M), Greater Aneth field, San Juan County, Utah. Producing (perforated) interval between depths of 5732 and 5856 feet. See figure 10.4 for location of Greater Aneth field.*

tions that correspond to changes in lithofacies (figure 10.19). As a result, the Desert Creek is often subdivided into informally named sub-intervals in the larger fields. Thickness of the Desert Creek zone averages 140 feet (45 m). The average depth to the Desert Creek in Aneth platform fields is 5530 feet (1840 m). The Ismay zone is again overlain by the Honaker Trail Formation and underlain by the Gothic shale. The Ismay geophysical log response also has variations that correspond to changes in lithofacies; however, the Hovenweep shale is not well developed in this part of the Paradox Basin (figure 10.20). Thickness of the Ismay zone averages 160 feet (50 m). The average depth to the Ismay in Aneth platform fields is 5320 feet (1770 m).

LITHOLOGY

Fractured Shale Subplay

In the Cane Creek shale zone (figure 10.16), unit A is composed of alternating thin beds (1 to 4 feet [0.3–1.2 m] thick) of silty to shaly carbonate (both limestone and dolomite) with interbedded, gray to black organic-rich shale and laminated to nodular anhydrite. Unit B, the primary fractured oil reservoir unit, is composed of interbedded, gray and black organic-rich shale, silty to sandy laminated dolomite, dolomitic mudstone, limestone, thin dolomitic siltstone, and dolomitic sandstone (figures 10.21 and 10.22). Some beds appear to be bioturbated or contain minor mottled anhydrite. Fractures are commonly sealed with halite, anhydrite, clay, and calcite. Unit C is composed of interbedded shaly to silty dolomite, dolomitic sandstone to siltstone, anhydrite, and minor black, organic-rich shale beds.

Blanding Sub-Basin Ismay and Desert Creek Zones Subplays

Open-marine lithofacies is in both the Ismay and Desert Creek zones of the Blanding sub-basin (figures 10.7 through 10.9, and 10.23). Rock representing this lithofacies consists of lime mudstone containing well-preserved rugose corals, crinoids, brachiopods, bryozoans, articulated thin-shelled bivalves, and benthic forams indicative of normal-marine salinity and low-energy conditions. Rock units of this lithofacies have very little effective porosity and permeability, and act as barriers and baffles to fluid flow.

Middle-shelf lithofacies is also in both the Ismay and Desert Creek zones (figure 10.24). The most common depositional fabrics of this lithofacies are bioturbated lime to dolomitic mudstone with ubiquitous sub-horizontal feeding burrows, and fossiliferous peloidal wackestone. Few megafossils and little visible matrix porosity exist. However, some fusulinid-rich lime wackestone to packstone is also present in very tight, biogenically graded limestone.

Inner shelf/tidal flat lithofacies is in the Ismay zone as dolomitized packstone and grainstone (figure 10.25). Clotted, lumpy, and poorly laminated microbial structures resembling small thrombolites and intraclasts are common. Megafossils and visible porosity are very rare in the inner shelf/tidal flat setting. Non-skeletal grainstone (calcarenite) composed of ooids, coated grains, and "hard peloids" occurs as high-energy deposits in some inner shelf/tidal flat settings. Remnants of interparticle and moldic pores may be present in this lithofacies.

Bryozoan mound lithofacies is in the Ismay zone as mesh-like networks of tubular and sheet-type (fenestrate) bryozoans (figure 10.26). These bryozoans provide the binding agent for lime mud-rich mounds. Crinoids and other open-marine fossils are common. Large, tubular bryozoans and marine cement are also

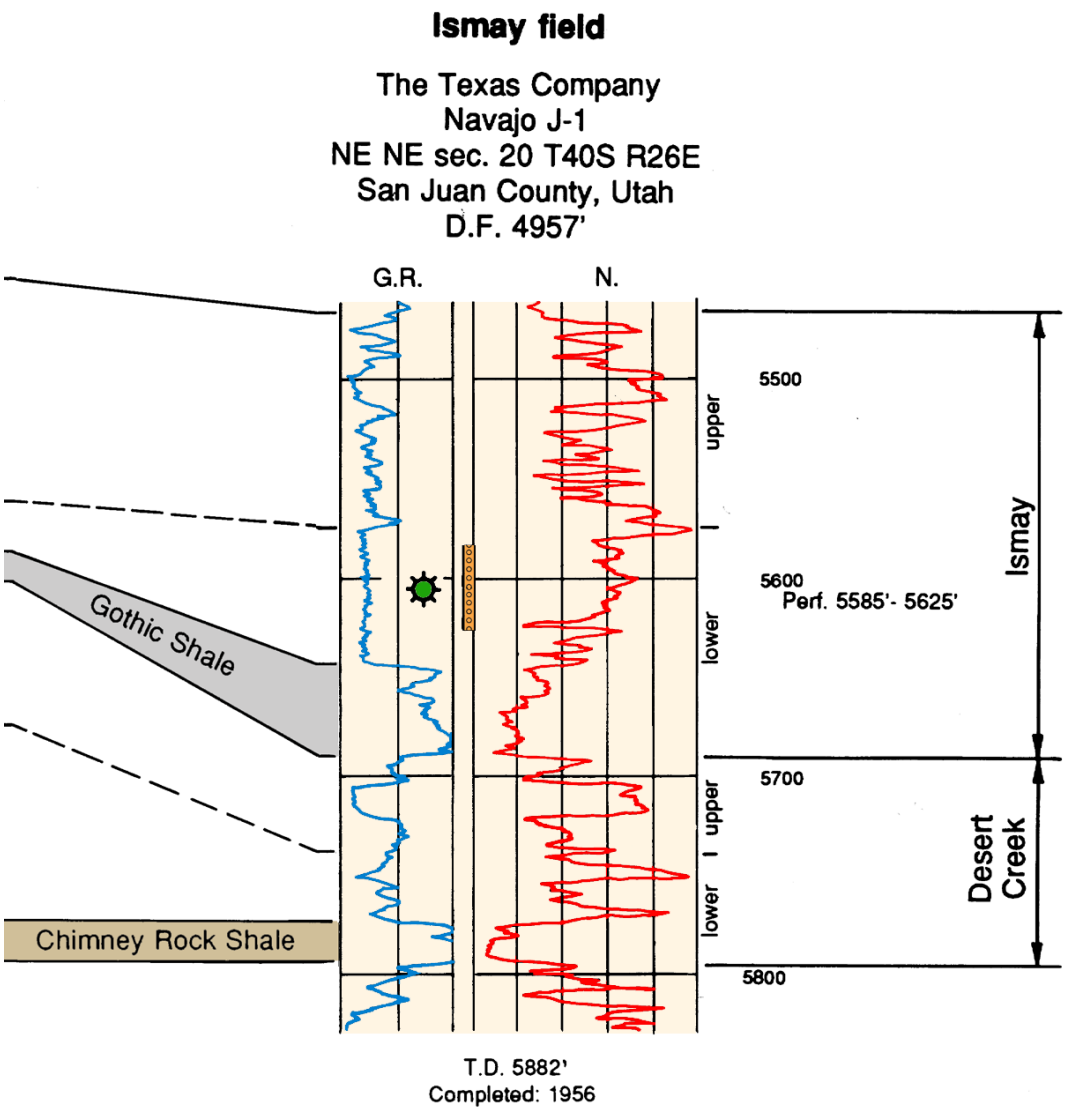

Figure 10.20. *Typical gamma ray-compensated neutron log for the Ismay zone in the Aneth platform, from the Navajo No. J-1 well, Ismay field (section 20, T. 40 S., R. 26 E., SLBL&M), San Juan County, Utah. Producing (perforated) interval between depths of 5585 and 5625 feet. See figure 10.4 for location of Ismay field.*

common in areas of high-energy, and possibly shallow, water. Porosity is mostly confined to preserved intraparticle spaces.

Phylloid-algal mound lithofacies is in both the Ismay and Desert Creek zones (figures 10.7 through 10.9, and 10.27). Very large phylloid-algal plates of *Ivanovia* (the dominant genus in the Ismay zone) and skeletal grains create bafflestone or bindstone fabrics. In mound interiors, algal plates are commonly found in near-growth positions surrounded by lime mud (figure 10.27A). On the high-energy margins of algal mounds, algal plates and skeletal grains serve as substrates for substantial amounts of botryoids and other early-marine cements, and internal sediments (figure 10.27B). Desert Creek mounds are dolomitized, contain plates of the *Kansasphyllum* (figure 10.27C), and show evidence of subaerial exposure (breccia or beach rock). Pore types include primary shelter pores preserved between phylloid-algal plates and secondary moldic pores.

Anhydrite salina lithofacies is within locally thick accumulations in upper Ismay (upper and lower parts) intra-shelf basins (figures 10.7 and 10.8). Anhydrite growth forms include nodular-mosaic ("chicken-wire"), palmate, and banded anhydrite (figure 10.28). Large palmate crystals probably grew in a gypsum aggregate indicative of subaqueous deposition. Detrital and chemical evaporites (anhydrite) fill in the relief around palmate structures. Thin, banded couplets of pure anhydrite and dolomitic anhydrite are products of very regular chemical changes in the evaporite intra-shelf basins. These varve-like couplets are probably indicative of relatively "deep-water" evaporite precipitation.

Aneth Platform Desert Creek Zone Subplay

Platform-interior carbonate mud and sand lithofacies include a diverse assortment of grainstone, packstone, bindstone, wackestone, and mudstone fabrics. Rocks representing this

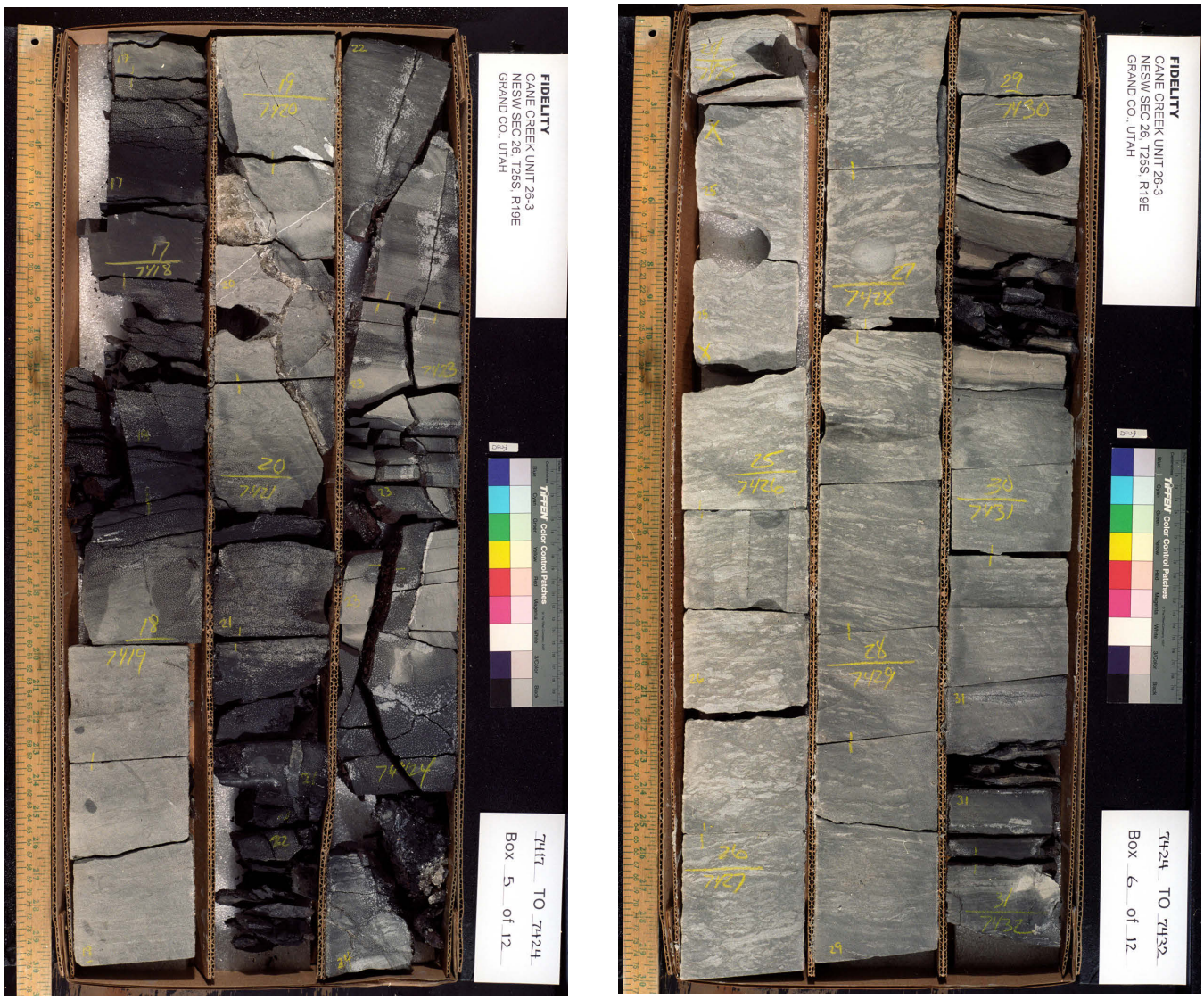

Figure 10.21. *Typical fractured, silty to muddy dolomite with thin siltstone and black organic-rich shale beds in the deep water, open marine of unit B in the Cane Creek shale zone; Cane Creek Unit No. 26-3 well (section 26, T. 25 S., R. 19 E., SLBL&M), Big Flat field, San Juan County, Utah, slabbed core from 7418 to 7432 feet. Core photography by Triple O Slabbing, Denver, Colorado, provided courtesy of Fidelity Exploration & Production Company.*

lithofacies typically contain the following diagnostic constituents: soft-pellet muds, hard peloids, grain aggregates, crinoids, fusulinids, and associated skeletal debris. The platform-interior carbonate mud and sand lithofacies can contain reservoir-quality rocks if dolomitized. However, effective porosity and permeability are highly variable.

Calcarenite lithofacies include grainstone (figures 10.29 and 10.30) and packstone fabrics. Rocks representing this facies typically contain the following diagnostic constituents: oolites, coated grains, hard peloids, bioclastic grains, shell lags, and intraclasts.

Phylloid-algal buildup lithofacies can be subdivided into shelter, mud-rich, and solution breccia lithofacies. Rocks representing shelter, phylloid-algal buildup lithofacies contain in-situ phylloid-algal plates (*Ivanovia*, *Kansasphyllum*, and *Eugonophyllum*), encrusting forams (for example *Tetrataxis*), soft peloidal mud, and minor amounts of internal sediment (mud or grains deposited after storms [suspended load]). The depositional fabric is predominantly bafflestone (figure 10.31). The mud-rich, phylloid-algal buildup lithofacies is represented by bafflestone and wackestone depositional fabrics. These rocks contain in-situ algal plates surrounded by lime mud, fine skeletal debris, and microfossils. The solution breccia, phylloid-algal buildup lithofacies includes disturbed rudstone and floatstone with some packstone depositional fabrics. Rocks of this lithofacies contain chaotic phylloid-algal and exotic clasts, peloids, and internal sediments (muds).

Coralline-algal buildup lithofacies consists of selectively dolomitized bindstone, boundstone, and framestone depositional fabrics. Rocks representing this lithofacies contain calcareous,

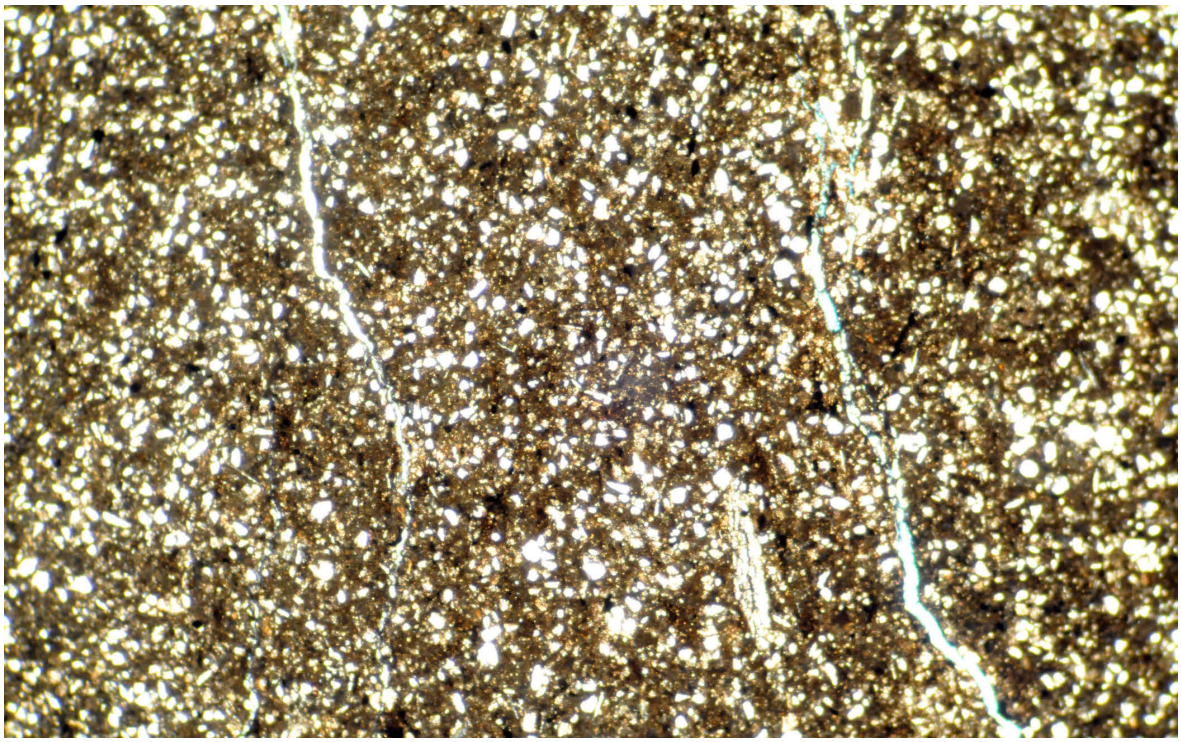

Figure 10.22. *Fractured silty dolomite in unit B in the Cane Creek shale zone. Remington No. 21-1H wildcat well (section 21, T. 31 S., R. 23 E., SLBL&M), San Juan County, Utah, photomicrograph (plane light) from 7450 feet. From Nielsen and others (2013).*

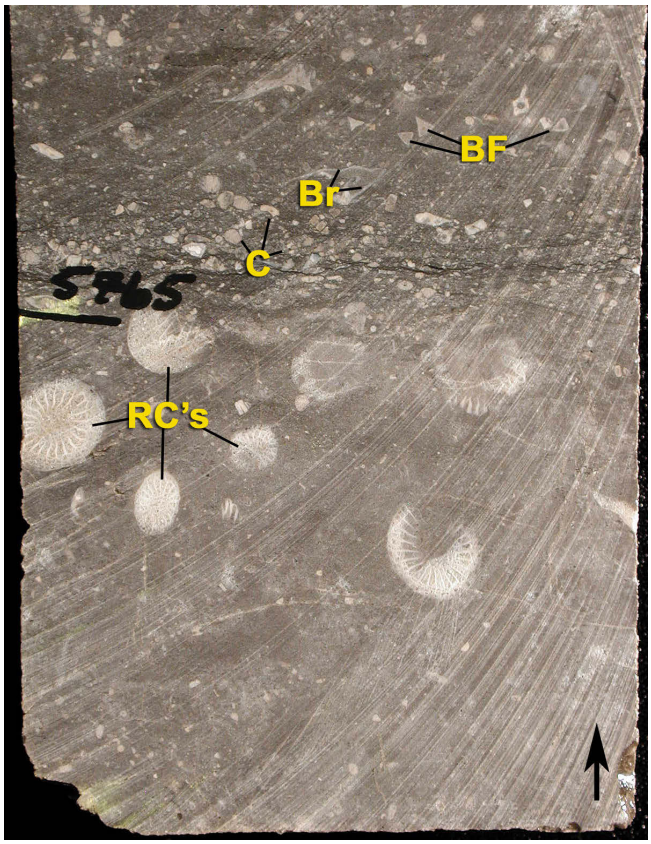

Figure 10.23. *Typical Ismay zone open-marine lithofacies showing well-preserved rugose corals (RC), crinoids (C), brachiopods (Br), and benthic forams (BF); No. 1-28 Cuthair wildcat well (section 28, T. 38 S., R. 22 E., SLBL&M), San Juan County, Utah, slabbed core from 5765 feet.*

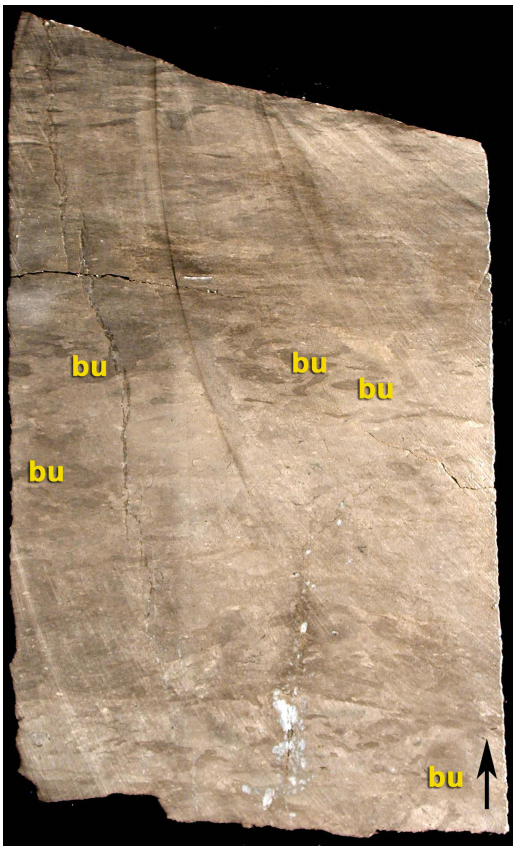

Figure 10.24. *Typical Ismay zone middle-shelf lithofacies showing bioturbated lime mudstone containing compacted sub-horizontal feeding burrows (bu); Tank Canyon No. 1-9 wildcat well (section 9, T. 37 S., R. 24 E., SLBL&M), San Juan County, Utah, slabbed core from 5412.5 feet.*

Figure 10.25. *Typical Ismay zone inner shelf/tidal flat lithofacies showing dolomitized lumpy microbial structures resembling small thrombolites (th) and intraclasts (in) composed of desiccated and redeposited thrombolitic fragments; Tin Cup Mesa No. 2-23 well (section 23, T. 38 S., R. 25 E., SLBL&M), Tin Cup Mesa field, San Juan County, Utah, slabbed core from 5460.5 feet.*

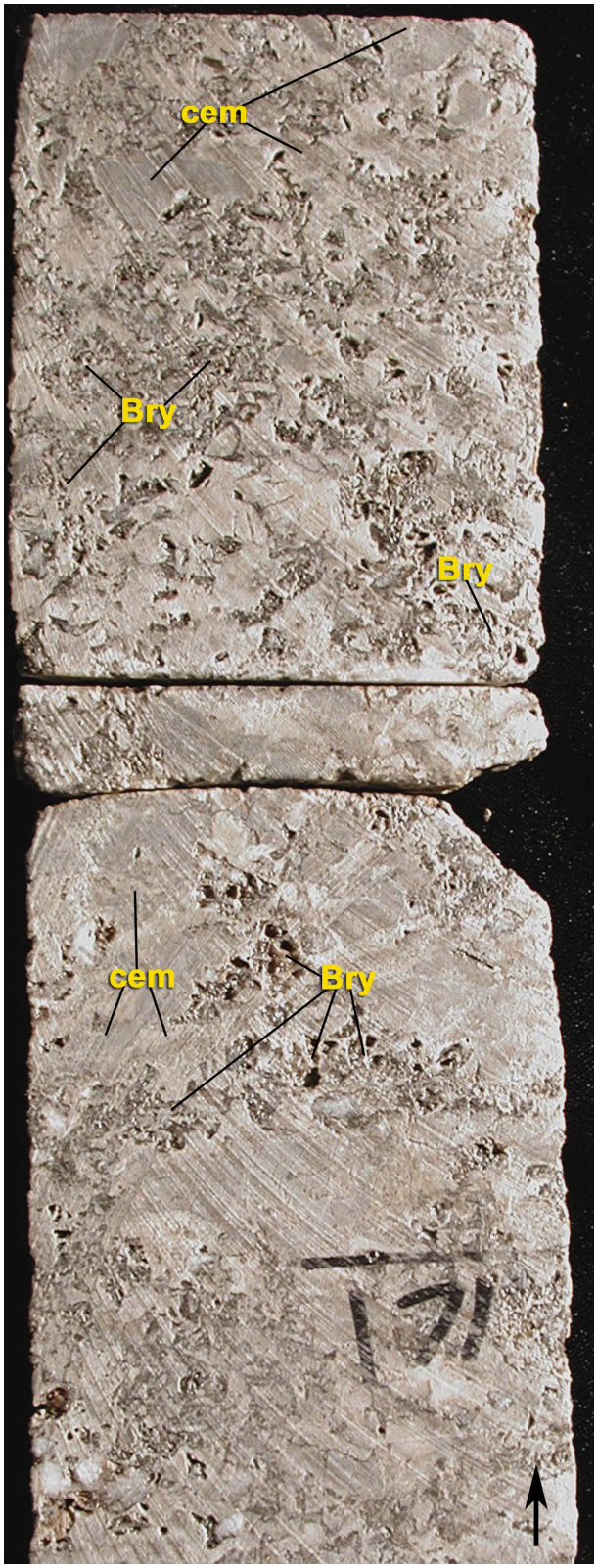

Figure 10.26. *Typical Ismay zone bryozoan-mound lithofacies showing large tubular bryozoans (Bry) and "lumps" of marine cement (cem). Scattered phylloid-algal plates are also present. This mound fabric is typical of higher energy, and possibly shallower water than the mud-dominated fabrics. Mustang No. 3 well (section 26, T. 36 S., R. 25 E., SLBL&M), Mustang Flat field, San Juan County, Utah, slabbed core from 6171 feet.*

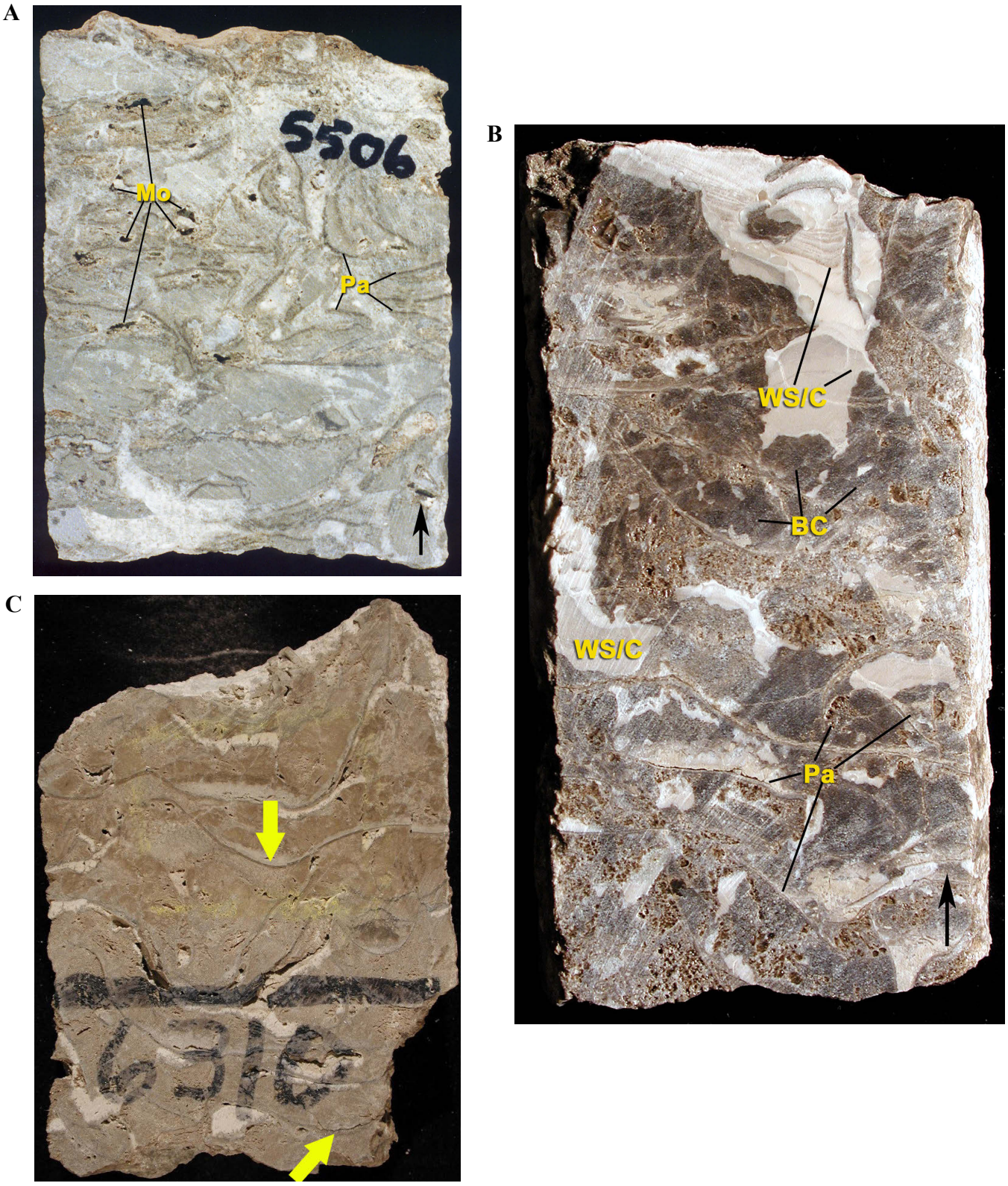

Figure 10.27. *Typical Ismay and Desert Creek phylloid-algal mound facies.* ***A.*** *Ismay bafflestone fabric showing large phylloid-algal plates (Pa) in near-growth positions surrounded by light gray lime muds; note the scattered moldic pores (Mo) that appear black here. Tin Cup Mesa No. 3-26 well (section 26, T. 38 S., R. 25 E., SLBL&M), Tin Cup Mesa field, San Juan County, Utah, slabbed core from 5506 feet.* ***B.*** *Ismay bindstone (cementstone) showing very large phylloid-algal plates (Pa), loose skeletal grains, and black marine botryoids (BC) as well as light brown, banded, internal sediments and marine cements (WS/C); note the patches of preserved porosity within coarse skeletal sediments between algal plates. Bonito No. 41-6-85 wildcat well (section 6, T. 38 S., R. 25 E., SLBL&M), San Juan County, Utah, slabbed core from 5590.5 feet.* ***C.*** *Desert Creek mound composed of dolomitized algal plates of the genus* Kansasphyllum *(arrows); May Bug No. 2 well (section 7, T. 36 S., R. 26 E., SLBL&M), Bug field, San Juan County, Utah, slabbed core from 6310 feet.*

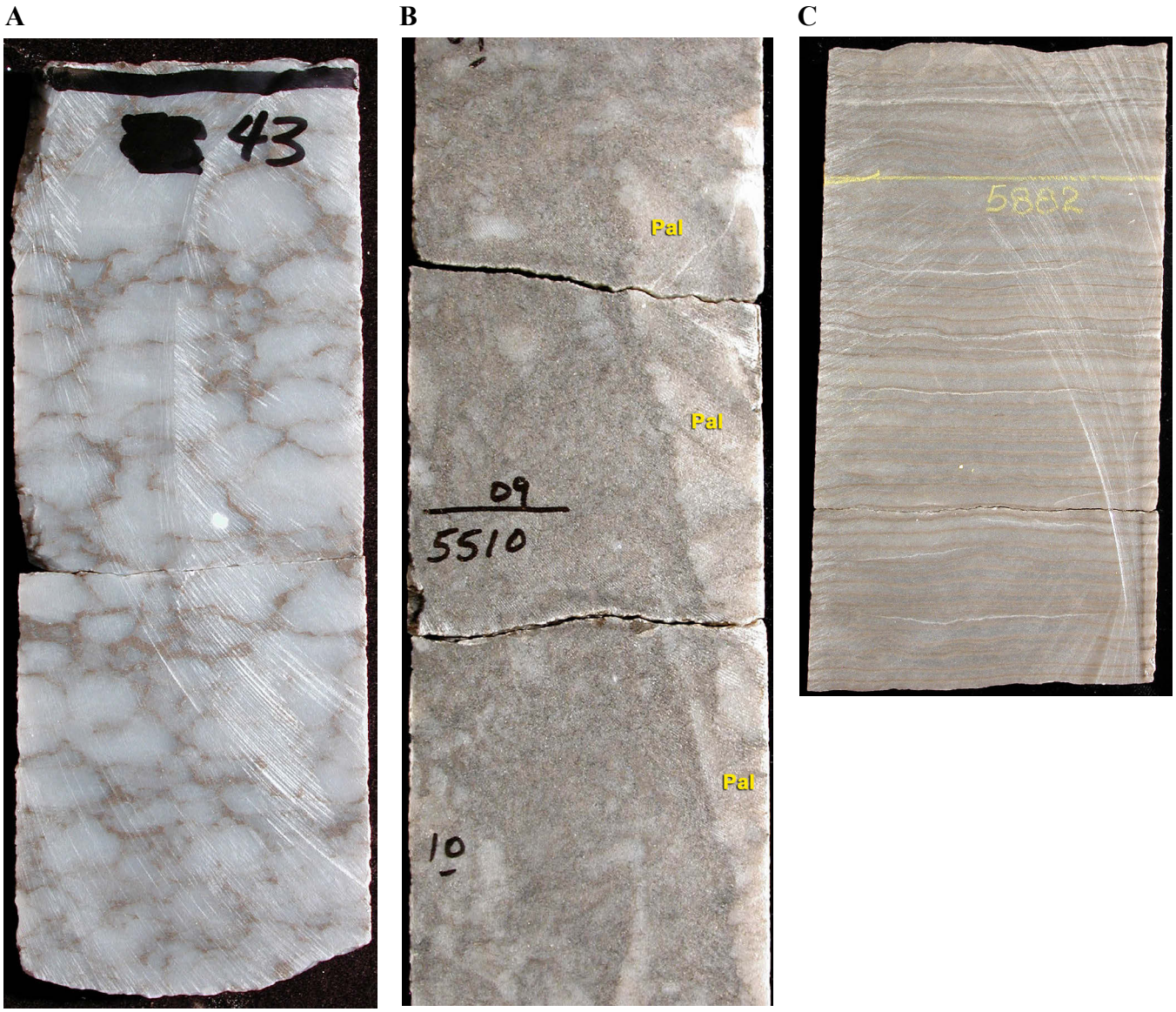

Figure 10.28. *Anhydrite growth forms typically found in anhydrite salina facies of upper Ismay intra-shelf basins.* ***A.*** *Nodular-mosaic ("chicken-wire") anhydrite; Tank Canyon No. 1-9 wildcat well (section 9, T. 37 S., R. 24 E. SLBL&M), San Juan County, Utah, slabbed core from 5343 feet.* ***B.*** *Large palmate crystals of anhydrite (Pal) along the right margin of this core segment probably grew in a gypsum aggregate that resembled an inverted candelabra while the remainder of the core segment consists of detrital and chemical anhydrite that filled in the relief around the palmate structure; Sioux Federal No. 30-1 wildcat well (section 30, T. 38 S., R. 25 E., SLBL&M), San Juan County, Utah, slabbed core from 5510 feet.* ***C.*** *Thin (cm-scale), banded couplets of pure anhydrite (white to light gray) and dolomitic anhydrite (brown); Montezuma No. 41-17-74 wildcat well (section 17, T. 37 S., R. 24 E., SLBL&M), San Juan County, Utah, slabbed core from 5882 feet.*

encrusting and bulbous coralline (red) algae, variable amounts of lime mud, microfossils, and calcispheres.

Bryozoan buildup lithofacies is represented by bindstone, bafflestone, and packstone depositional fabrics that are rarely dolomitized. Rocks of this lithofacies contain the following diagnostic constituents: bryozoan colonies (*Chaetetes*), small rugose corals, scattered small calcareous sponges and phylloid-algal plates, microfossils, and lime muds.

Greater Aneth field (figure 10.4), Utah's largest oil producer, was discovered in 1956 and has produced over 479 million BO (76 million m^3) (Utah Division of Oil, Gas, and Mining, 2016a). The primary reservoir at Greater Aneth field consists of limestone (algal boundstone/bafflestone and oolitic, peloidal, and skeletal grainstone and packstone) and finely crystalline dolomite. The Desert Creek zone in the unit is divided into two subzones: a lower interval composed predominantly of phylloid-algal buildup lithofacies, and an upper interval composed of oolitic-peloidal calcarenite lithofacies (figures 10.30 through 10.32) (Peterson and Ohlen, 1963; Babcock, 1978a, 1978b, 1978c, 1978d; Peterson, 1992; Moore and Hawks, 1993; Chidsey and Eby, 2014). These subzones create a west-northwest-trending reservoir buildup (figure 10.13).

Figure 10.29. *Typical Desert Creek zone dolomitized grainstone, calcarenite lithofacies; North Heron No. 35-C well (section 35, T. 41 S., R. 25 E., SLBL&M), Heron field, San Juan County, Utah, slabbed core from 5589 feet.*

Figure 10.30. *Typical Desert Creek zone oolitic grainstone; Aneth No. 27-D-4 well (section 27, T. 40 S., R. 24 E., SLBL&M), Greater Aneth field, San Juan County, Utah, slabbed core from 5620 feet. Note excellent moldic porosity development.*

HYDROCARBON SOURCE AND SEALS

Hydrocarbons in Paradox Formation reservoirs were generated from source rocks within the formation itself. Organic-rich informal units, such as the Cane Creek, Hovenweep, Chimney Rock, and Gothic shales (figure 10.2), are well-established source rocks (Hite and others, 1984; Nuccio and Condon, 1996). These rocks are composed of black, sapropelic shale and shaley dolomite (Morgan, 1993b). The average TOC content of the black shale in the Cane Creek shale is 15% with some samples containing up to 28% (Grummon, 1993; Morgan and others, 2014). Unit B is both the primary source and reservoir for oil and gas in the Cane Creek (figure 10.16). The Chimney Rock shale has from 1 to 3% TOC and a mean vitrinite reflectance (R_o mean) of 1.3 to 2.5% (Hite and others, 1984; Peterson, 1992). The Gothic shale has from 1.5 to near 4% TOC and an R_o mean of 0.8 to 1.2% (Hite and others, 1984; Peterson, 1992). Other, deeper shale facies in the Paradox Formation contain as much as 13% TOC (Hite and others, 1984). Peterson (1992) calculated a cumulative thickness of more than 1000 feet (330 m) of organic-rich rocks in the Paradox.

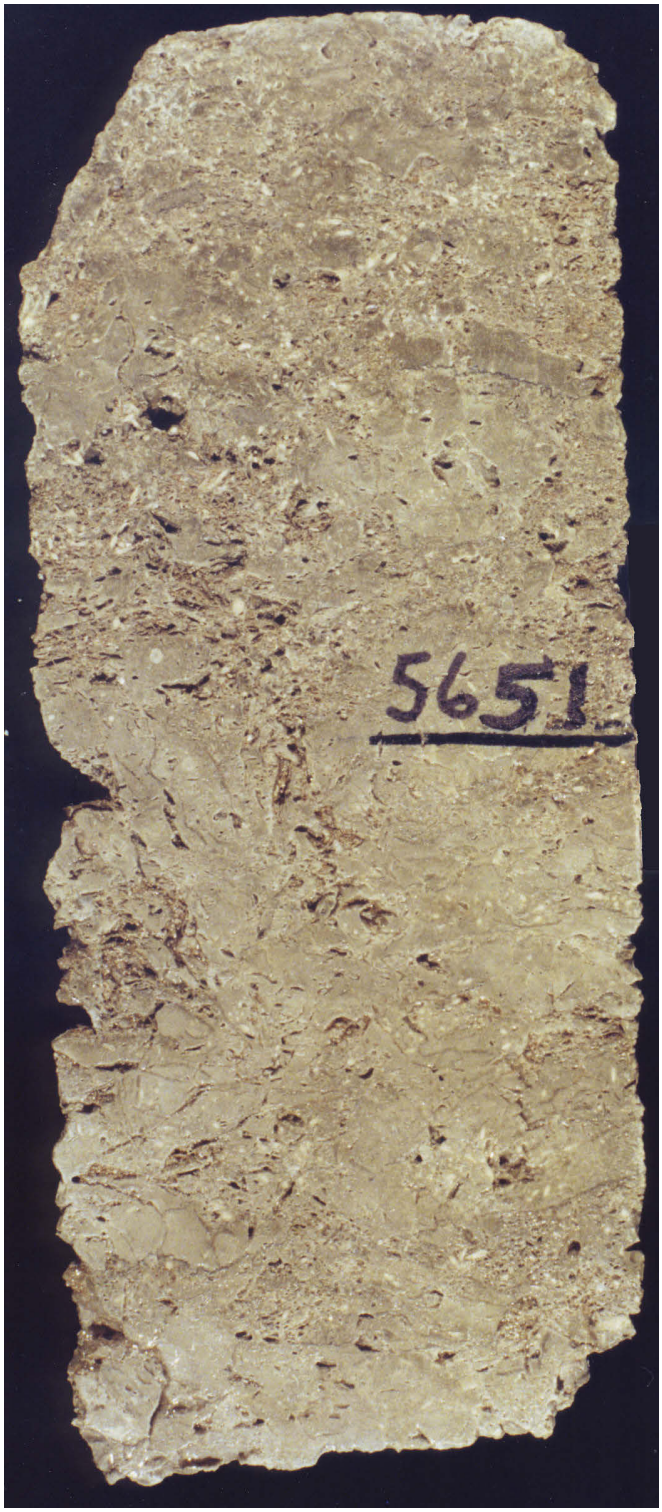

Figure 10.31. *Typical highly productive Desert Creek zone phylloid-algal plate bafflestone; Anasazi No. 1 well (section 5, T. 42 S., R. 24 E., SLBL&M), Greater Aneth field, San Juan County, Utah, slabbed core from 5651 feet. Note good visual shelter porosity.*

Hydrocarbon generation occurred during maximum burial in the Late Cretaceous and early Tertiary. Hydrocarbons were then expelled and subsequently migrated through carrier beds to carbonate buildups (stratigraphic traps) or structures.

Vertical reservoir seals for the Paradox producing zones are shale, halite, and anhydrite within the formation; lateral seals are permeability barriers created by unfractured, off-mound (non-buildup) mudstone, wackestone, and anhydrite. In the fractured shale subplay, upper and lower seals are provided by anhydrite and halite. Lateral seals are permeability barriers in unfractured rock. In the Cane Creek shale zone, the A and C units are also anhydrite rich and provide upper and lower seals to the productive B unit.

STRUCTURE AND TRAPPING MECHANISMS

The structural top of the Cane Creek shale zone is deepest in northern part of the Paradox fold and fault belt and shallows near the western edge shelf of the basin (figure 10.33). Oil is trapped in the Cane Creek (and possibly in other fractured units) on anticlines and along structural noses (figures 10.34). The northern Paradox Formation is mostly salt which can be highly deformed (figure 10.35). Second-order folds due to salt flowage have amplitudes of 15 to 100 feet (5–30 m) and apparent wavelengths of 300 to 1000 feet (90–300 m). The folds are aligned directly over local budges of Paradox salt rather than the massive salt walls described by Doelling (1988, 2003). The overlying rocks were fractured and extended by minor faults just off the crests of the anticlines. Salt movement progresses along zones of weakness or areas of low confining pressure, forming large folds such as the Cane Creek and Shafer anticlines. The weak zones likely developed above and along the northwest-trending basement faults in the region which experienced periodic movement during both the Laramide and earlier Cretaceous Sevier (to the west) orogenies. Salt-cored anticline development has been active intermittently from the Pennsylvanian to the present day (Shoemaker and others, 1958; Cater, 1970; Case and Joesting, 1973; Baars and Doelling, 1987; Doelling, 1988; Oviatt, 1988; Friedman and others, 1994). Fracture data from oriented cores in the Cane Creek shale show regional, northwest to southeast and northeast to southwest, near-vertical, open, extensional fracture systems that are not significantly affected by orientations of localized folds (figure 10.36) (Grove and Rawlins, 1997). Hydrocarbon production from the Cane Creek is not limited strictly to the tops of anticlines. Production also has been established from structurally high positions on upthrown fault blocks and on the downthrown side of faults. Plunging noses without apparent four-way closure produce from the Cane Creek as well. Individual traps may exist in any structural position where fracturing of the self-sourced Cane Creek has occurred.

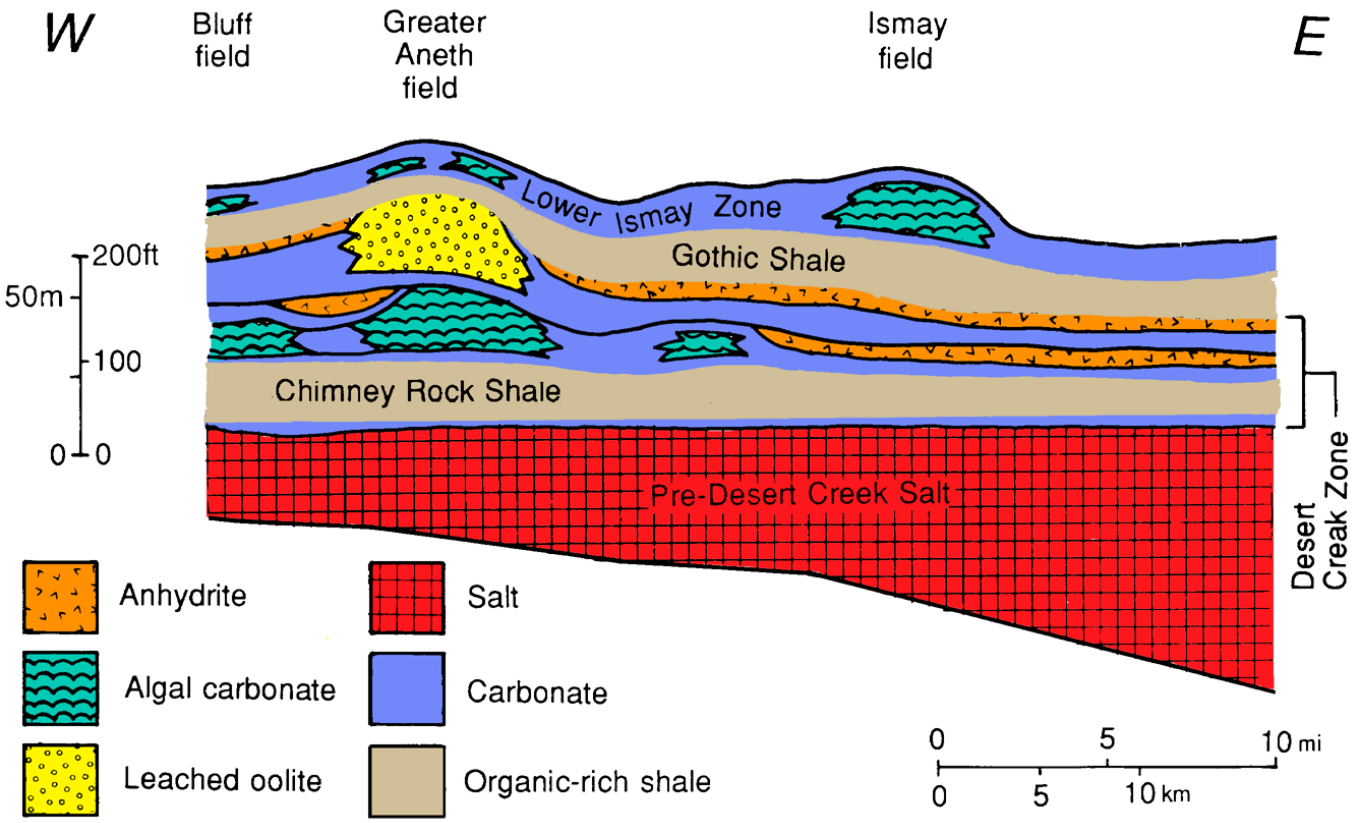

Figure 10.32. *Diagrammatic lithofacies cross section, Greater Aneth field, southeastern Utah. Datum is base of the Desert Creek zone of the Paradox Formation. Modified from Peterson (1992).*

Trap types in the Blanding sub-basin and Aneth platform regions include stratigraphic, combination stratigraphic/structural, and diagenetic. Regional dip is gently to the north-northeast towards the center of the basin. Hydrocarbons are most often stratigraphically trapped in porous and permeable rocks within Ismay and Desert Creek carbonate buildups described earlier. The trap is formed as these buildups rapidly thin and grade laterally into impermeable mudstone, wackestone, and anhydrite. The traps are effectively sealed by impermeable platform intervals at the base and a relatively thick layer of anhydrite (20 feet [6 m]) or shale (for example, the 50-foot-thick [15 m] Gothic shale above the Desert Creek zone) at the top. The best stratigraphic traps in the region are associated with phylloid-algal buildup and associated calcarenite lithofacies. These traps are widely distributed, generally small to moderate in size (200 to 2000 acres [80–800 ha]), and can be readily identified on seismic records. However, Greater Aneth field is the exception in terms of size (figures 10.1 and 10.4), and is Utah's largest oil producer. Structural relief is often shown on top of structure maps for the Desert Creek zone (or the Ismay zone) at Greater Aneth (figure 10.37) and numerous other fields in the region. However, this relief is created by the variations between the thick mound, or carbonate buildup, and thinner off-mound lithofacies (figure 10.13) (Babcock, 1978a). Overlying units are generally thin and drape over the buildup; however, usually no surface expression of these features in evident.

Many carbonate buildups appear to have developed on subtle anticlinal noses or structural closures (figure 10.38). These structures may represent paleobathymetric highs formed by pre-Pennsylvanian reactivation of basement faults, or simply longshore current-formed mudbars on the Paradox shallow-marine shelf (Babcock, 1978a). These "highs" provided the substrate for algal growth and mound buildup. An opposing origin is presented by Matheny and Longman (1996); Matheny and others (2009). They contend that fields such as Bug (figure 10.39), Cutthroat, Island Butte, and Spargo (figure 10.4) produce from phylloid-algal buildups deposited in sea-floor lows resulting from dissolution of halite in the underlying Akah zone (figure 10.2). Phylloid-algal lithofacies thickness was dictated by the timing and amount of halite dissolution—the greater the halite dissolution during algal growth, the thicker the potential reservoir (Matheny and Longman, 1996).

In some instances, stratigraphic traps have been enhanced by true structural relief, fracturing, and minor normal faults. Other traps include carbonate buildups located directly on anticlines. For example, Desert Creek field (figure 10.4) produces from a carbonate-buildup reservoir located directly on the crest of a north-northwest to south-southeast-trending anticline with 300 feet (100 m) of four-way closure (figure 10.40). A 500-foot (150 m), down-to-the-east normal fault parallels the west flank of the structure. Production from other

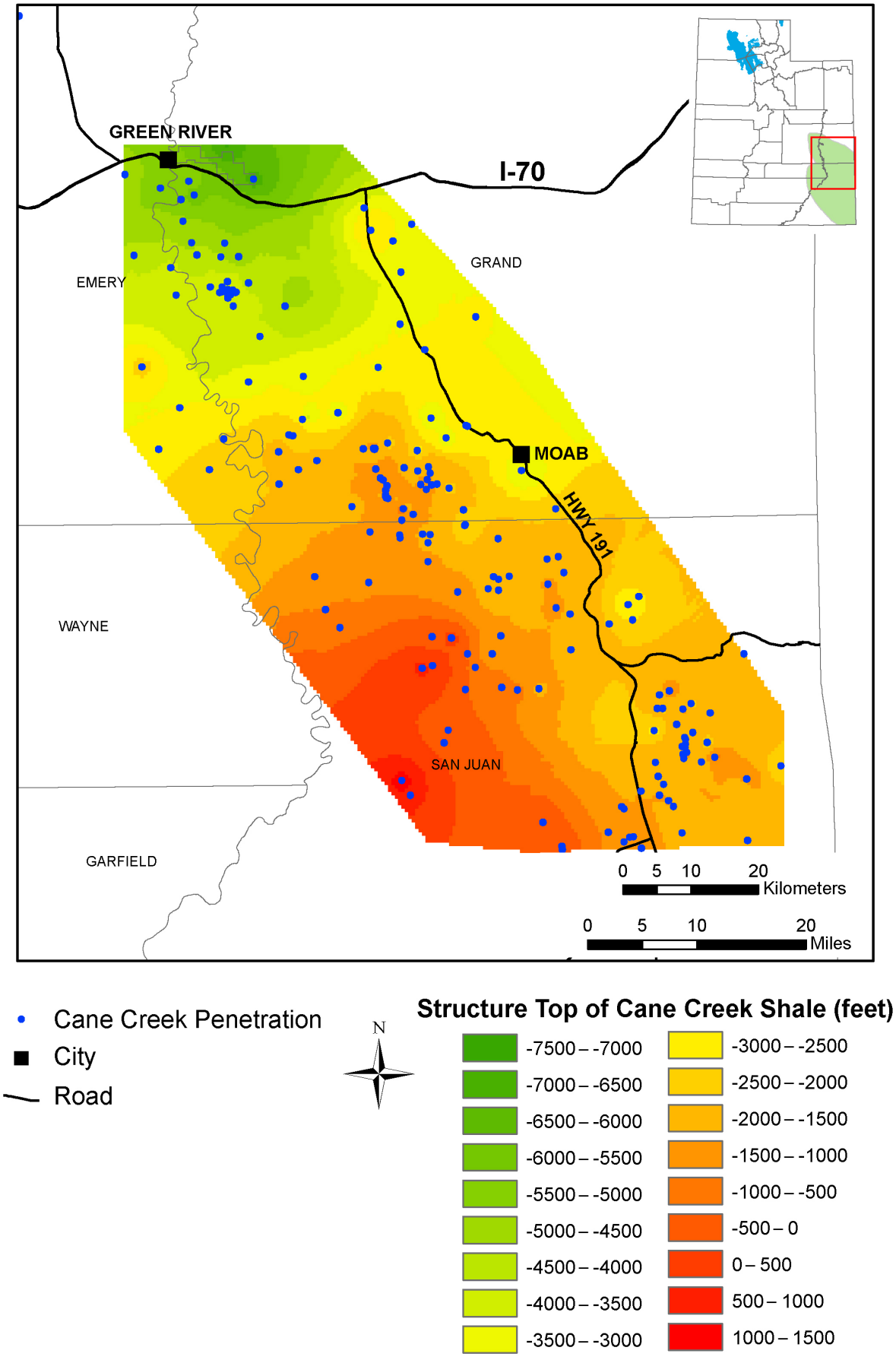

Figure 10.33. *Cane Creek shale zone structure map, northern Paradox Basin, Utah. After Carney and others (2014).*

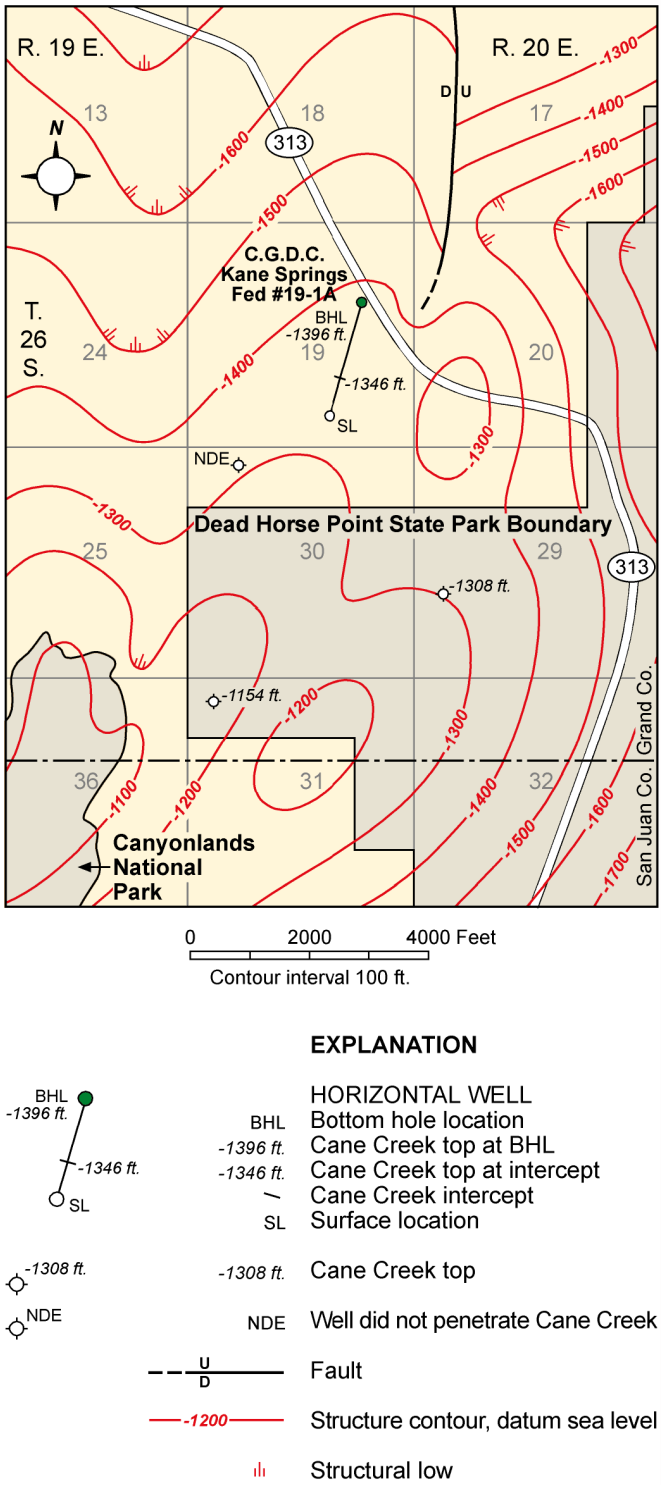

Figure 10.34. *Cane Creek shale zone structure map, Park Road oil field, Grand County. Surface location, direction, and length of horizontal well shown. After Grove and others (1993). See figure 10.1 for location of Park Road field.*

anticlinal traps on the Aneth platform is at Tohonadla in San Juan County, Utah (Norton, 1978b), and Boundary Butte East in Apache County, Arizona (Dunn, 1978) (figure 10.4).

Diagenesis is commonly a major component of trap development and reservoir heterogeneity in the carbonate buildups of Blanding sub-basin and Aneth platform fields. Dolomitzation and the creation of microporosity can yield reservoir quality in carbonate fabrics that are typically non-productive, such as wackestone and packstone (Chidsey and others, 1996c; Eby and Chidsey, 2001; Chidsey, 2002; Chidsey and Eby, 2002). The reservoir at Bug field (figure 10.4) is an elongate, northwest-trending, dolomitized carbonate buildup in the lower Desert Creek zone. The trapping mechanism is primarily an updip porosity pinchout (figure 10.39).

RESERVOIR PROPERTIES

The Paradox Formation has heterogeneous reservoir properties, similar to the Leadville Limestone, because of (1) depositional lithofacies with varying porosity and permeability, (2) carbonate buildup (mound) relief and flooding surfaces (parasequence boundaries), and (3) a range of diagenetic effects. Analysis of these characteristics are used to predict lithofacies patterns, determine reservoir quality and compartmentalization, and provide data input for modeling and simulation studies. Identification and correlation of depositional lithofacies and parasequences in individual Paradox reservoirs is critical (1) to understand their effect on water/CO_2 injection programs, (2) determine the direction and target zones for horizontal wells, and (3) estimate reserves.

Porosity and Permeability

Paradox Formation porosity in carbonate reservoirs ranges from 7 to 16% with typical porosity averaging 11%. Permeability is highly variable, generally ranging from less than 1 up to 55 mD with an average of 14 mD. At Greater Aneth field (figure 10.4), the porosity averages 10.2% (averaging 16.5% in selected intervals) and permeability ranges from less than 3 up to 30 mD, averaging 10 mD (Moore and Hawks, 1993). Dolomites and sandstones have been the main targets of horizontal drilling in the Cane Creek shale zone. In the Big Flat field area, the Cane Creek has an average fractured shale porosity (matrix and fractures) up to 15%; permeability ranges from 39 to 400 mD from Horner plots (Grove and others, 1993; Morgan and others, 2014). The oriented cores from the Cane Creek show two types of fracture sets: (1) the large-scale northwest- to southeast- and northeast- to southwest-oriented fractures described previously (figure 10.36) related to regional tectonics and salt movement, and (2) microfractures that resulted from internal hydrocarbon generation (Fritz, 1991). The larger tectonic fractures may account for most of the permeability, but the microfractures probably provide most of the fracture porosity in the reservoir.

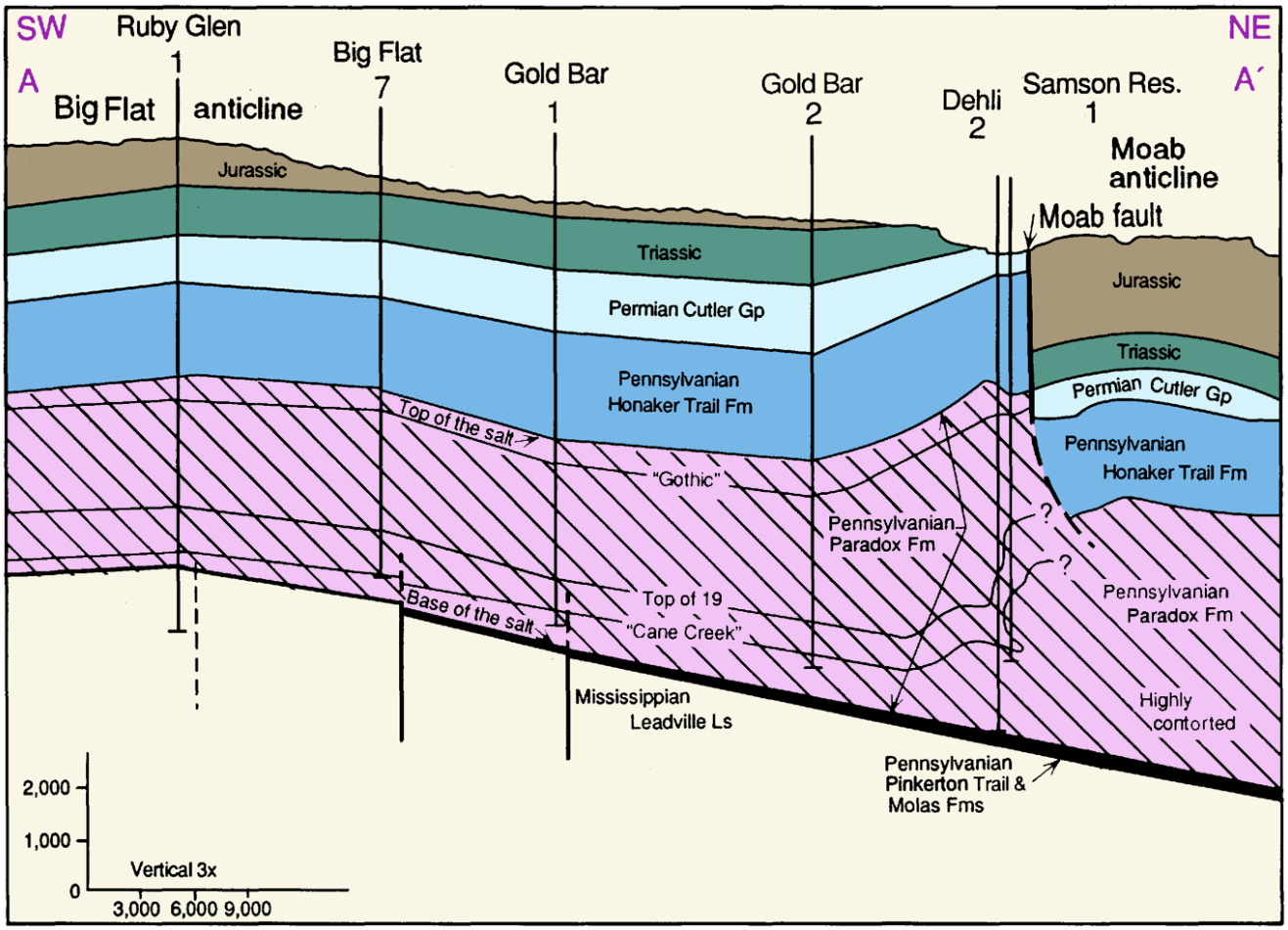

Figure 10.35. *Cross section, A–A', from the Moab anticline to the Big Flat anticline. Location of cross section is shown in figure 10.3. The interbeds in the Paradox Formation are organic-rich shales, dolomite, and clastics that are both source and reservoir for oil. The Cane Creek shale zone is the most prolific producer and is in the basal portion of the Paradox.*

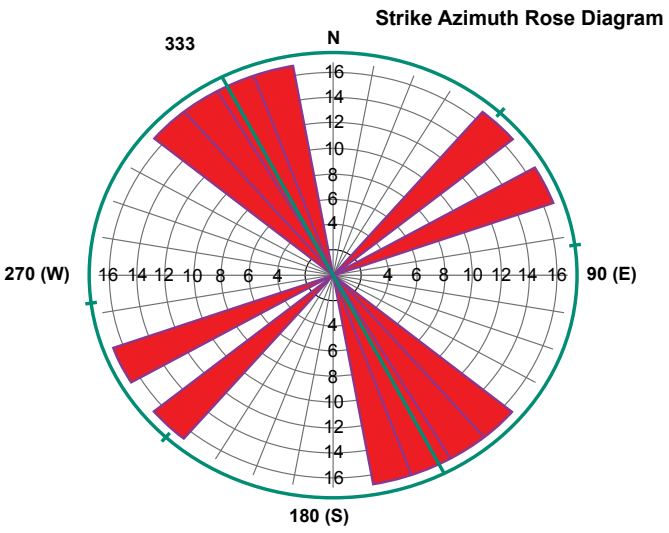

Figure 10.36. *Predominant northwest-southeast open fracture system in Cane Creek Shale zone from oriented core, Cane Creek Unit No. 26-3 well, Big Flat field, Grand County, Utah. Courtesy of Fidelity Exploration & Production Company.*

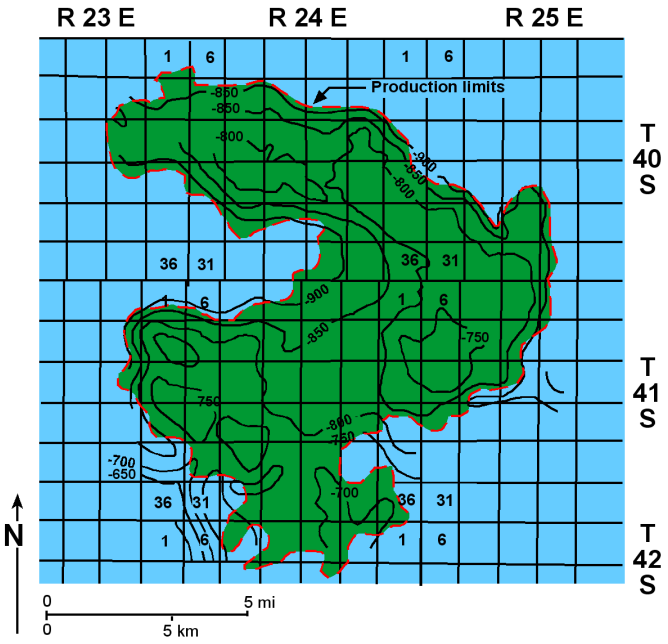

Figure 10.37. *Structure contour map of the top of the Desert Creek zone, Greater Aneth field, San Juan County, Utah; contour interval = 50 feet, datum = sea level. Modified from Peterson (1992).*

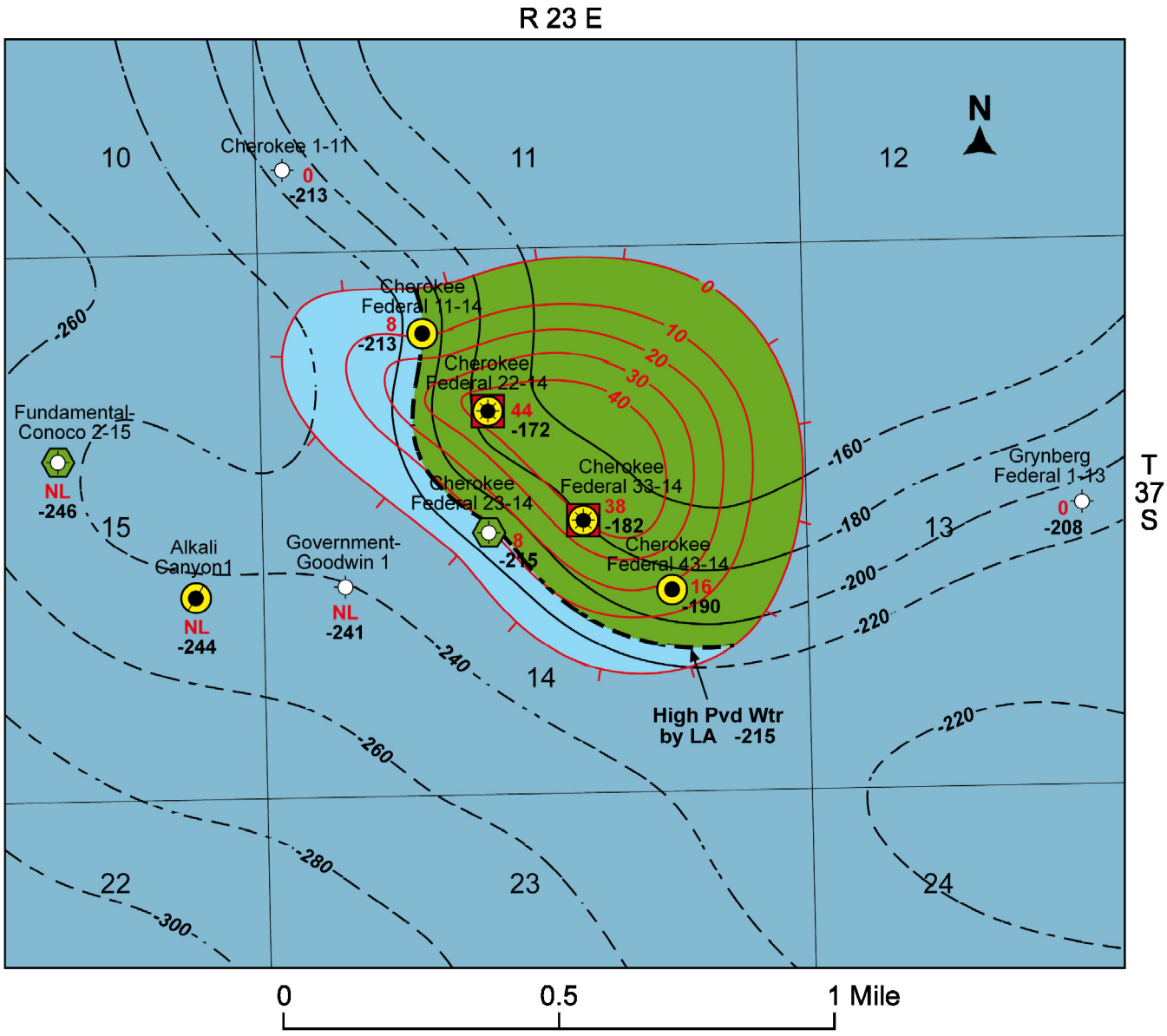

Upper Ismay Isochore
Porosity Units 1–5
Contour Interval = 10 ft

Structure Contour
Top of Upper Ismay
Clean Carbonate
Contour Interval = 20 ft
Datum = Sea Level

Explanation
- Plugged and abandoned
- Ismay drill-stem test
- Ismay completion
- Abandoned Ismay producer
- Ismay completion/core
- NL — No neutron/density log
- Oil
- Off-mound
- Mound/clean carbonate

Figure 10.38. *Map of combined top of structure and isochore of porosity, upper Ismay zone mound, Cherokee field, San Juan County, Utah.*

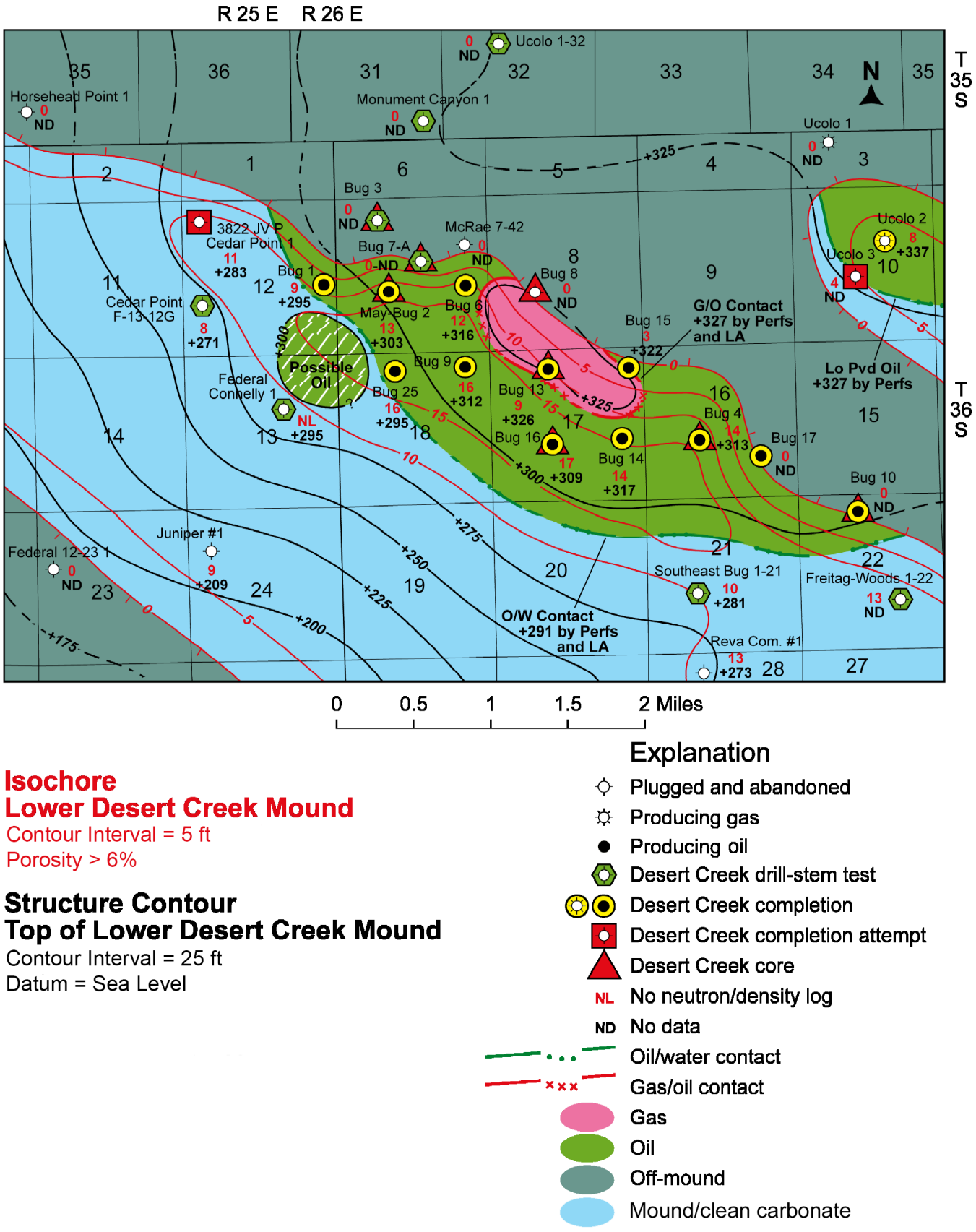

Figure 10.39. *Map of combined top of structure and isochore of lower Desert Creek zone mound, Bug field, San Juan County, Utah.*

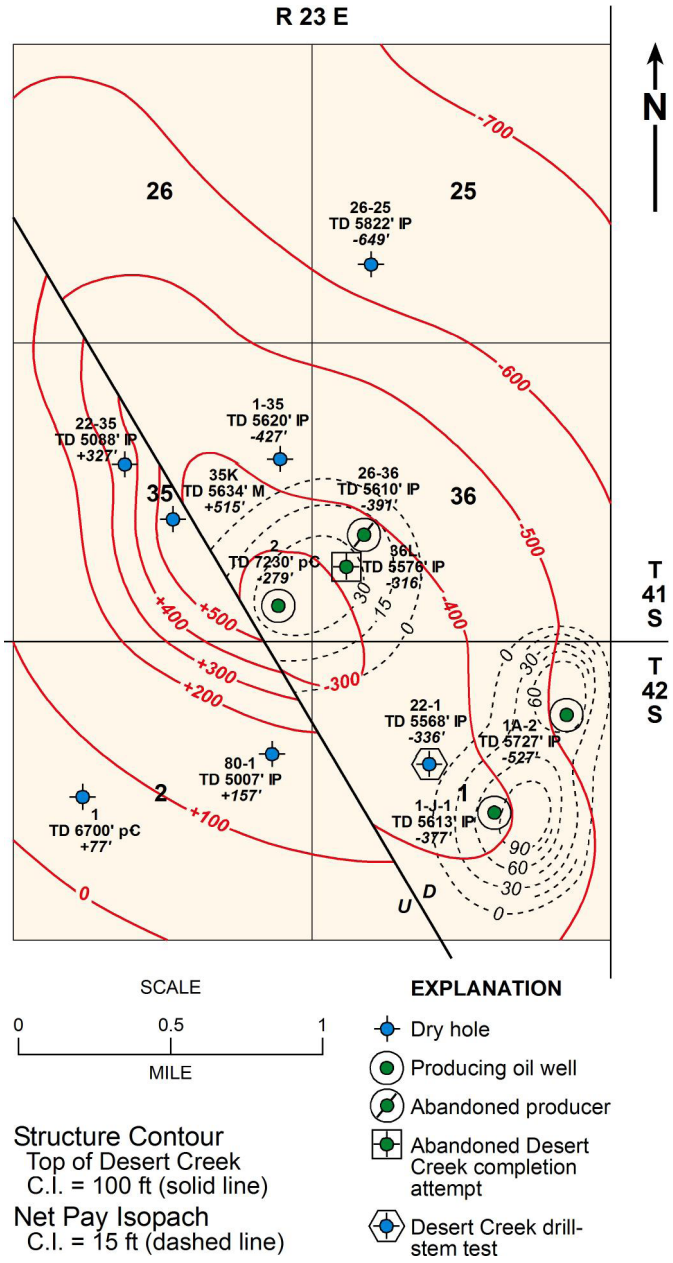

Figure 10.40. *Map of combined top of structure and isochore of the Desert Creek zone mound, Desert Creek field, San Juan County, Utah. Modified from Lauth (1978b).*

Diagenesis and Pore Types

The diagenetic fabrics and porosity types found in the Cane Creek shale and various hydrocarbon-bearing carbonate rocks of the Desert Creek and Ismay zones are indicators of reservoir flow capacity, storage capacity, potential for water- and/or CO_2-flooding, and horizontal drilling. Pore types in the Cane Creek dolomites include intercrystalline, microbial constructional pores, microporosity, and minor interparticle porosity. Sandstones and siltstones exhibit intergranular porosity. These lithologies also can contain significant microporosity and fracture porosity. The framework grains of carbonate buildups consist predominantly of phylloid-algal plates, with lesser amounts of brachiopods, bryozoans, pelloids, oolites, ostracods, and forams. They yield primary porosity such as shelter (figure 10.41), interparticle (figure 10.42), and intraparticle (particularly in bryozoan-dominated buildups) (figure 10.43) pore types. Where these pore types are well developed, the reservoirs have excellent hydrocarbon storage and fluid-flow capacity, and are good candidates for CO_2 flooding.

Most shallow-shelf/shelf-margin carbonate buildups, or mounds, had relief with exposure occurring when sea level fell. This setting produced four major, generally early, diagenetic environments (figure 10.44): (1) fresh-water (meteoric) vadose zone (above the water table, generally at or near sea level), (2) meteoric phreatic zone (below the water table), (3) marine phreatic zone, and (4) mixing zone (Longman, 1980). The "iceberg" principle (the Ghyben-Herzberg theory)—which is that for every foot the water table rises above sea level there may be 20 feet (6 m) of fresh water below the water table, a 1:20 ratio—can generally be applied to both carbonate-mound and island buildups (Friedman and Sanders, 1978). The typical early diagenetic events occurred in the following order (figure 10.45): (1) early marine cementation which may include first-generation micrite and fibrous isopachous cementation, second-generation botryoidal cementation, and third-generation radiaxial cementation (note: early-marine cements are not always present), (2) post-burial, replacement, rhombic dolomite cementation due to seepage reflux, (3) vadose and meteoric phreatic diagenesis including leaching/dissolution, neomorphism, and fresh-water cementation (dogtooth, stubby, and small equant calcite), (4) mixing-zone dolomitization, (5) syntaxial cementation, (6) anhydrite cementation/replacement, and (7) minor silica replacement.

That portion of the carbonate buildup facing the open-marine environment was generally a steep-wall complex where early-marine cements (such as fibrous isopachous, botryoidal, and radiaxial cements) were deposited from invading sea water flowing through the system and filled most original pore space (figures 10.44, 10.46, and 10.47). Locally, cemented zones can have a major impact on reservoir flow and storage capacity. The opposite side of the mound typically bordered a hypersaline lagoon filled with dense brine that seeped into the phreatic zone (seepage reflux) to form a wedge-shaped zone of early, low-temperature dolomite—both early replacement dolomite and dolomite cement. Seepage reflux dolomization is usually complete dolomitization. Little original fabric/matrix remains. Crystals are fine to medium grained, often sucrosic; intercrystalline porosity dominates (figure 10.48). Seepage reflux overprints the fresh-water phreatic, marine phreatic, and mixing zones across the entire extent of the mound buildup. Thick seepage reflux dolomites are often proximal to evaporite-plugged lagoonal sediments. Locally, seepage reflux dolomitization can enhance both reservoir flow and storage capacity. Those reservoirs with excellent storage capacity may be considered candidates for CO_2 flooding projects.

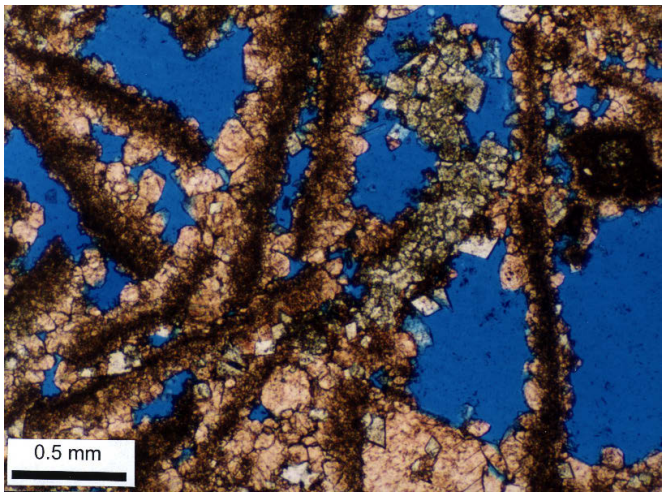

Figure 10.41. *Typical Desert Creek zone primary shelter and early solution porosity within a phylloid-algal bafflestone partially occluded by stubby to equant to dogtooth spar cements of probably meteoric phreatic origin; porosity = 12.5%, permeability 53.8 mD by core-plug analysis. These types of cements have degraded the permeability of these solution-enhanced pore systems. Runway No. 10-C-5A well (section 10, T. 40 S., R. 25 E., SLBL&M), photomicrograph (plane light) from 6127.4 feet, Runway field, San Juan County, Utah.*

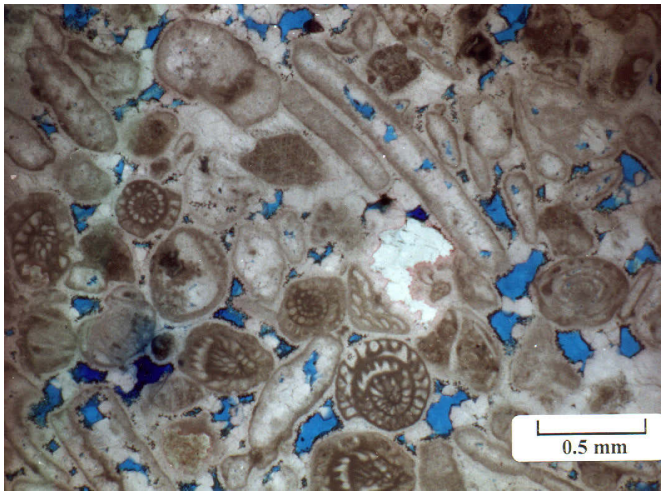

Figure 10.42. *Typical Ismay zone interparticle porosity developed in a high-energy calcarenite skeletal and aggregate grainstone; porosity = 4.6%, permeability = 0.018 mD by core-plug analysis. Among the typical grains of this facies are benthic forams (including fusulinids), phylloid-algal plates, "hard" peloids or micritized skeletal grains, and grain aggregates. The scattered pores (in blue) visible in this image are principally the remnants of primary interparticle space between the skeletal components of this grainstone. Early marine isopachous cements, followed by probable meteoric dogtooth calcite spar and minor anhydrite (in white) have occluded most of the original interparticle porosity. Little Ute No. 1 well (section 11, T. 34 S., R. 20 W.), photomicrograph (plane light with white card technique [diffused light using a piece of paper on the stage of the microscope]) from 5940.5 feet, Little Ute field, Montezuma County, Colorado.*

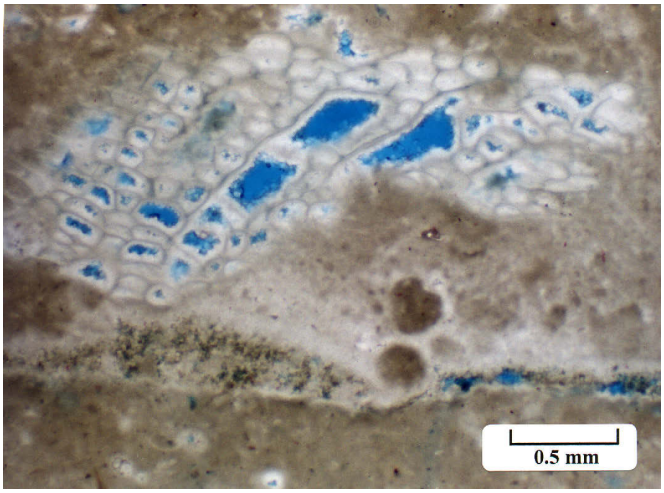

Figure 10.43. *Ismay zone intraparticle porosity; porosity = 9.8%, permeability = 12.2 mD by core-plug analysis. Open pores (in blue) are shown here within the uncemented chambers of encrusting organisms surrounded by lime muds. This sample is from within a phylloid-algal mound core. Little Ute No. 1 well (section 11, T. 34 S., R. 20 W.), photomicrograph (plane light with white card technique) from 5870.9 feet, Little Ute field, Montezuma County, Colorado.*

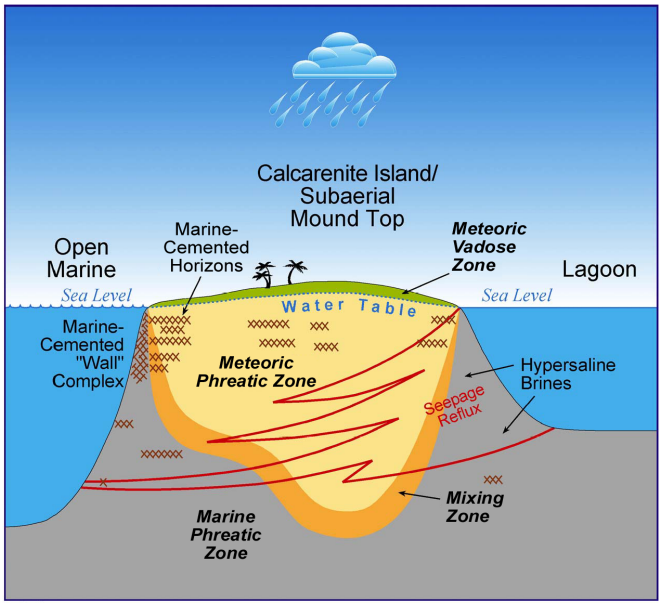

Figure 10.44. *Model of early diagenetic environments found in the Desert Creek zone of the Paradox Formation, southern Paradox Basin. Modified from Longman (1980).*

The meteoric and marine phreatic zones were separated by a mixing zone (fresh and sea water), all of which changed with sea-level fluctuation. Most carbonate buildups have both a mixing-zone and fresh-water overprint. Some early dolomitization took place in the mixing zone (figure 10.49). Dissolution was the dominant porosity-enhancing process of meteoric diagenesis and created molds, vugs, and channels (figures 10.50 and 10.51). Much of the original fabric remains or can be determined. However, some grainstone, packstone, and calcarenite have only non-connected moldic

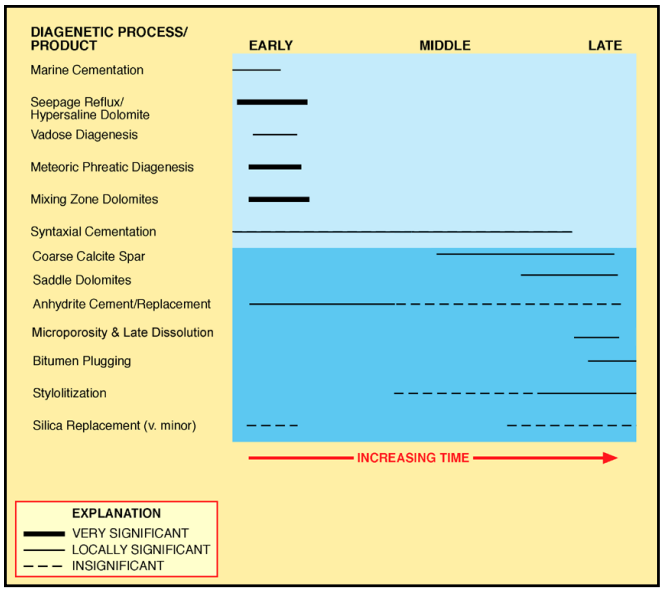

Figure 10.45. *Typical diagenetic sequence through time based on thin section analysis, Ismay and Desert Creek zones.*

Figure 10.46. *Typical pattern of marine cementation within the well-lithified Desert Creek zone "wall" complex. Blue Hogan No. 1-J-1 well (section 1, T. 42 S., R. 23 E., SLBL&M), slabbed core from 5415.5 to 5416.1 feet, Desert Creek field, San Juan County, Utah.*

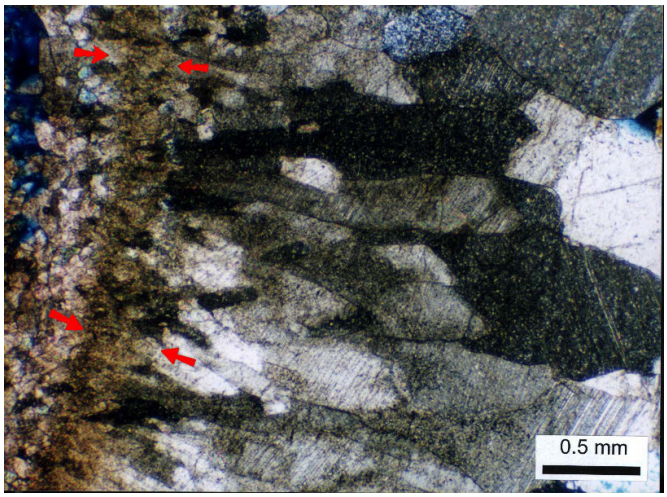

Figure 10.47. *Two generations of probable early-marine cements. The earlier generation was a brown micritic to microfibrous cement (between arrows) which was followed by a bladed radiaxial generation. Filling of most original pore space was by the radiaxial cements. Blue Hogan No. 1-J-1 well (section 1, T. 42 S., R. 23 E., SLBL&M), photomicrograph (crossed nicols) from 5420.3 feet, Desert Creek field, San Juan County, Utah.*

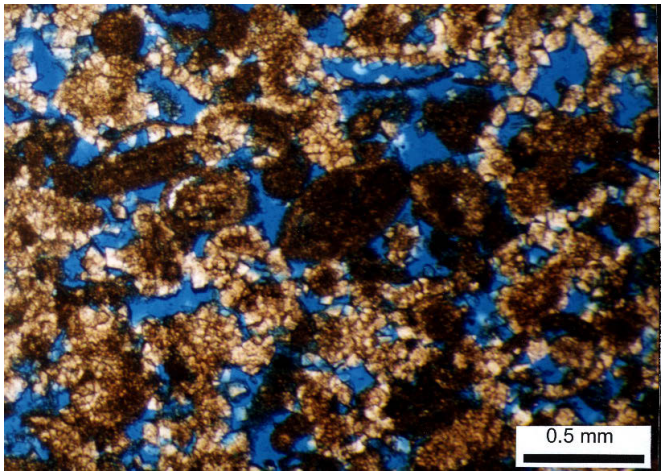

Figure 10.48. *Typical Desert Creek zone dolomitized, well-sorted, pelloidal/oolitic/bioclastic grainstone; porosity = 13.4%, permeability = 33.9 mD by core-plug analysis. Note the very fine crystalline dolomite formed by seepage reflux processes followed by partial dissolution and other meteoric overprints. The combination of both processes has led to good storage potential and excellent flow capacity. North Heron No. 35-C well (section 35, T. 41 S., R. 25 E., SLBL&M), photomicrograph (plane light) from 5569.2 feet, Heron field, San Juan County, Utah.*

pores that result in classic "heart break" reservoirs. Early dissolution of lime muds also created microporosity. Indicative cements include stubby to equant calcite and dogtooth calcite spars that sporadically line pores (figure 10.41). Vadose zones generally have less cement than the fresh-water phreatic zones. The depth/thickness of the meteoric vadose and fresh-water phreatic zones is dependent on the extent and duration of subaerial exposure as well as the amount of meteoric water influx. Locally, meteoric diagenesis enhances reservoir

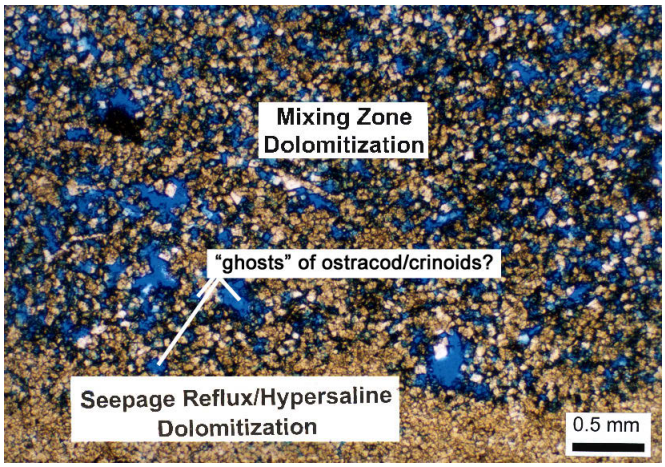

Figure 10.49. *Desert Creek zone dolomitized wackestone/packstone showing the contrast between probable seepage reflux/hypersaline dolomitization toward the base and more porous mixing-zone dolomitization above; porosity = 20.3%, permeability = 39.8 mD by core-plug analysis. Note "ghosts" of probable ostracods and crinoids. Runway No. 10-C-5A well (section 10, T. 40 S., R. 25 E., SLBL&M), photomicrograph (plane light) from 6120.2 feet, Runway field, San Juan County, Utah.*

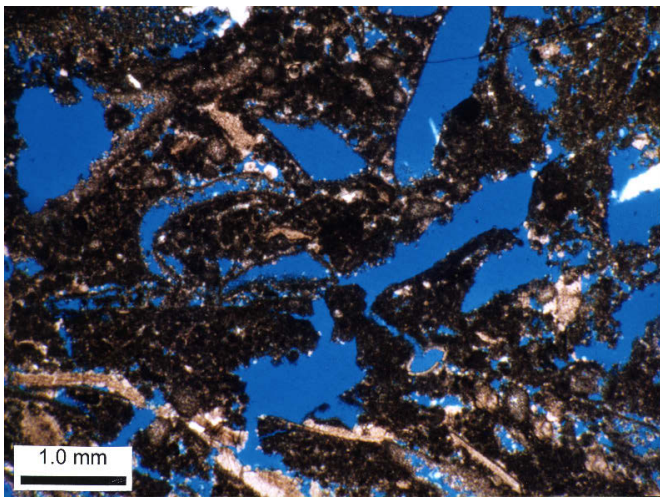

Figure 10.50. *Desert Creek zone grainstone/packstone showing interconnected solution-channel and moldic porosity with very little visible meteoric cements; porosity = 13.2%, permeablility = 20.4 mD by core-plug analysis. Mule No. 31-M well (section 31, T. 41 S., R. 24 E., SLBL&M), photomicrograph (plane light) from 5729.8 feet, Greater Aneth field, San Juan County, Utah.*

performance. Subaerial exposure of carbonate buildups, for example the Desert Creek zone at Bug field (figure 10.4), occasionally produced intense, early micro-box-work porosity. Figure 10.52 shows the pattern of patchy dolomite dissolution which includes a micro-box-work pattern of pores. Some of the pores in this view occur between elongate, rectilinear networks of dolomite laths. Micro-box-work porosity represents an important site for exploiting untapped hydrocarbons using horizontal drilling. Extensively leached intervals may have both excellent storage and flow capacity, and should be considered candidates for CO_2 flooding projects.

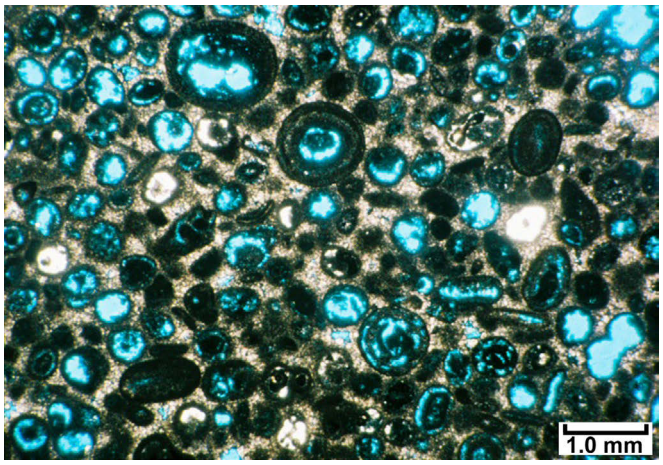

Figure 10.51. *Desert Creek zone grainstone showing oomoldic porosity with very little interconnection between pores; porosity = 10.3%, permeablility = 0.1 mD by core-plug analysis. Aneth Unit No. E-313 well (section 13, T. 4 S., R. 24 E., SLBL&M), photomicrograph (plane light) from 5767.6 feet, Greater Aneth field, San Juan County, Utah.*

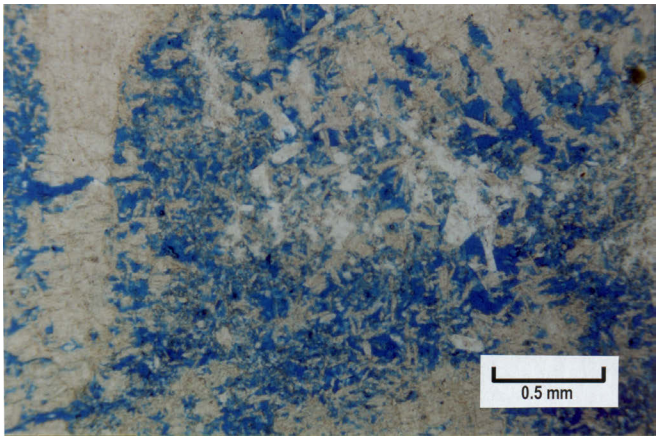

Figure 10.52. *Desert Creek zone dolomitized, phylloid-algal bafflestone showing a pattern of patchy dolomite dissolution which includes a "micro-box-work" pattern of pores (in blue); porosity = 10.5%, permeability = 7.5 mD by core-plug analysis. Bug No. 10 well (section 22, T. 36 S., R. 26 E., SLBL&M), photomicrograph (plane light with white card technique) from 6327.5 feet, Bug field, San Juan County, Utah.*

Post-burial diagenesis included additional syntaxial cementation, silicification, late coarse calcite spar formation, saddle dolomite cementation, stylolitization, additional anhydrite replacement, late dissolution (microporosity development), bitumen plugging (figure 10.45), and fracturing. Progression from least to most important is observed (syntaxial cementation to anhydrite replacement) and relates to increased reservoir heterogeneity in Paradox reservoirs. Some of these diagenetic products create barriers and baffles to fluid flow, such as the case where anhydrite and bitumen (or solid hydrocarbons) plug pores and pore throats. They are not observed on seismic records, are difficult to predict, and locally influence reservoir performance, storage capacity, and drainage. Some reservoirs, the Ismay zone in Cherokee field for example (figure 10.4), display intense microporosity (figures 10.53 and 10.54) that developed late, along

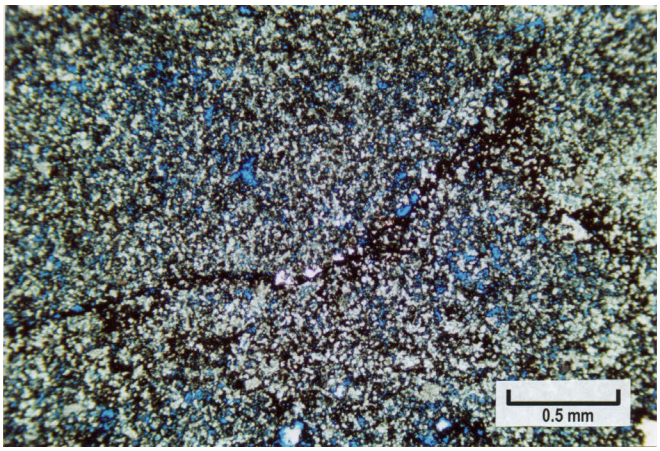

Figure 10.53. *Ismay zone peloidal packstone/grainstone dominated by microporosity and bitumen plugging; porosity = 22.9%, permeability = 215 mD. Cherokee No. 22-14 well (section 14, T. 37 S., R. 23 E., SLBL&M), photomicrograph (plane light) from 5768.7 feet, Cherokee field, San Juan County, Utah.*

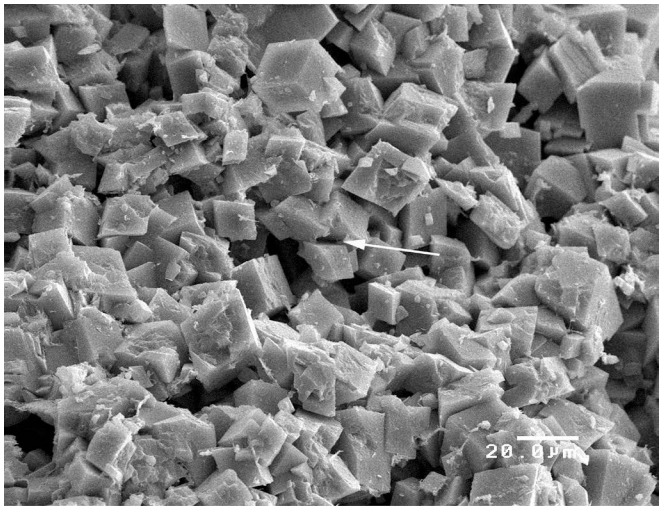

Figure 10.54. *Ismay zone packstone/grainstone displaying well-developed dolomite rhombs exhibiting abundant intercrystalline microporosity (arrow); porosity = 23.6%; permeability = 103 mD by core-plug analysis. Cherokee No. 33-14 well (section 14, T. 37 S., R. 23 E., SLBL&M), scanning electron microscope photomicrograph (scale represents 20 microns [0.02 mm]) of a core plug from 5781.2 feet, Cherokee field, San Juan County, Utah. Photomicrograph by Louis H. Taylor, Standard Geological Services, Inc.*

solution fronts by the action of aggressive hydrothermal solutions from depth (CO_2 escaping from Mississippian Leadville Limestone or from deep decarboxylation of organic matter). Microporosity increases storage capacity, but limits fluid recovery. Microporosity represents an important site for untapped hydrocarbons and possible targets for horizontal drilling.

Engineering Data

Paradox net-pay thickness is also variable, depending primarily on diagenesis, and ranges from 9 to 100 feet (3–30 m), averaging 35 feet (11 m). The average Paradox reservoir temperature is 126°F (52°C). Initial water saturations range from 25 to 50% (averaging 34%) (estimated at 10% for the fractured Cane Creek shale zone), salinities range from 80,000 to 349,000 ppm, and resistivities (R_w) range from 0.045 to 0.07 ohm-m at 68°F (20°C). Initial reservoir pressures average about 2200 psi (15,000 kPa). The Cane Creek is highly overpressured with fluid gradients exceeding 0.85 psi/ft (19.23 kPa/m); the initial reservoir pressures average 6650 psi (45,850 kPa). The reservoir drive mechanisms for Paradox reservoirs are predominantly solution gas but include gas-cap expansion, water drive, gas/pressure depletion, fluid expansion, and gravity drainage.

Well, production, and reservoir data for individual fields that have produced over 500,000 BO (80,000 m^3) in the Paradox Formation play are summarized in tables 10.1 and 10.2. For detailed summaries of these fields see Stowe (1972), Babcock (1978a, 1978b, 1978c, 1978d), Brown (1978, 1983), Campbell (1978a), Dunn (1978), Krivanek (1978, 1981, 1993), Lauth (1978a, 1978b), Mecham (1978a, 1978b), Mickel (1978a, 1978b, 1978c), Miesner (1978), Norton (1978b), Reid and Stevenson (1978), Riggs (1978d), Smith (1978a, 1978b, 1978c, 1978d, 1978e), Spencer (1978), Wold (1978), Martin (1981, 1983), Lehman (1983), Ott and Roylance (1983), Scanlon and Wendling (1983), Matheny and Martin (1987), Dawson (1988), Herrod and Gardner (1988), Peterson (1992), Baars (1993), Crawley-Stewart and Riley (1993a, 1993b), Grove and others (1993), Lentz (1993), Moore and Hawks (1993), Ross and Handley (1993), Steele and White (1993), Chidsey and others (1996a), Oline (1996), Scott (2003), Colorado Oil and Gas Conservation Commission (2016), Utah Division of Oil, Gas, and Mining (2016a), and the Arizona Oil and Gas Conservation Commission (2016).

OIL AND GAS CHARACTERISTICS

The produced Paradox oils are commonly sweet, paraffinic crudes. The API gravity of the oil ranges from 36° to 53° (averaging 43°); the GOR ranges between 250 and 76,500 cubic feet/bbl. Oil colors are predominantly green, but can be dark to light green, brownish green, dark to yellowish to light reddish brown, straw yellow, or black. The viscosity of the crude oil averages 0.46 sus at 104°F (40°C). The pour point of the crude oil ranges from 0 to 50°F (0–10°C). The average weight percent sulfur and nitrogen of produced Paradox hydrocarbon liquids are 0.07 and 0.037, respectively (Stowe, 1972).

Paradox reservoirs produce associated gas that is fairly uniform in composition, averaging 66% methane, 16% ethane, 9% propane, 4% butane, 2% pentane, 1% hexane and higher fractions, 1% N_2, and 0.2% CO_2, and occasionally a trace of H2S and helium (Moore and Sigler, 1987). The gas heating value averages 1400 Btu/ft^3; the specific gravity averages 0.794. One exception to the typical gas compositions in the

Table 10.2. *Reservoir data for fields in the Blanding sub-basin Desert Creek zone, Blanding sub-basin Ismay zone, and Aneth platform Desert Creek zone subplays, Pennsylvanian Paradox Formation play.*

State	County	Field	Zone	Pay (feet)	Porosity (%)	Perm. (mD)	Temp. (°F)	Initial Reservoir Pressure (psi)	Water Saturation	Resistivity of Formation Water	Salinity	Drive
Blanding Sub-Basin Desert Creek Zone Subplay												
Colorado	Montezuma	Island Butte [1]	Desert Creek	NA	NA	NA	NA	NA	NA	NA	NA	NA
Colorado	Montezuma	McClean [1, 2, 3]	Desert Creek	30	14	250	130	3595	69	0.045@68°F	348,534	solution gas/water drive
Colorado	Dolores/Montezuma	Papoose Canyon [1, 4]	Desert Creek	9	12.2	4.4	NA	3416	53	NA	NA	gas cap expansion
Utah	San Juan	Bug [5, 6, 7]	Desert Creek	15	11	27.5	170	3550	32	0.03@BHT	331,831	gas cap expansion/solution gas/limited water drive
Blanding Sub-Basin Ismay Zone Subplay												
Colorado	Montezuma	Cache [1, 8]	Ismay	57	10.4	12.3	NA	2170	35	0.11@68°F	62,700	solution gas/part water drive
Colorado	Montezuma	Flodine Park [1, 9]	Ismay	41	11	13	NA	2212	41	NA	NA	solution gas
Colorado	Montezuma	Marble Wash [1, 10]	Ismay	15	10	2	NA	2250	NA	0.051@68°F	234,685	solution gas
Colorado	Montezuma	Roadrunner [1]	Ismay	NA	NA	NA	NA	NA	NA	NA	NA	NA
Colorado	Montezuma	Towaoc [1, 11]	Ismay	16	10	25	NA	2290	44	NA	NA	solution gas/water drive
Utah	San Juan	Cave Canyon [12]	Ismay	75	14	55	132	2121	11	0.02@BHT	NA	fluid expansion/solution gas
Utah	San Juan	Deadman-Ismay [13]	Ismay	62	13	0.9	132	2441	18-46	0.047@68°F	NA	gas expansion/depletion
Utah	San Juan	Ismay [14, 15]	Ismay	24	11.2	16.5	131	2205	41	NA	NA	solution gas
Utah	San Juan	Kachina [16]	Ismay	100	13	8	132	2108	23	NA	NA	solution gas
Utah	San Juan	Kiva [17]	Ismay	38	16	21.9	135	1862	24	NA	NA	solution gas
Utah	San Juan	McElmo Mesa [18]	Ismay	29	9	NA	119	2176	37	NA	NA	water drive
Utah	San Juan	Mustang Flat [19]	Ismay	30	9	4	126	2642	34	NA	NA	gas expansion/water drive
Utah	San Juan	Patterson Canyon [20, 21]	Ismay	17	13	10	128	2572	41	0.054@68°F	222,554	solution gas/water drive
Utah	San Juan	Tin Cup Mesa [22, 23, 24]	Ismay	50	14.3	8.3	121	2080	31	0.065@77°F	256,894	solution gas
Aneth Platform Desert Creek Zone Subplay												
Arizona	Apache	Boundary Butte East [25]	Ismay-Desert Creek-Akah	20	8	2.3	NA	1550	20	NA	62,000	gas expansion/solution gas
Utah	San Juan	Akah [26]	Ismay-Desert Creek-Akah	NA	NA	NA	112	1875	NA	NA	NA	water drive/gas expansion
Utah	San Juan	Anido Creek [27]	Ismay-Desert Creek	19	8	24	105	1974	28	NA	80,000-100,000	solution gas/fluid expansion
Utah	San Juan	Bluff [28, 29]	Desert Creek	33	7.5	0.3	140	1800	NA	NA	NA	solution gas
Utah	San Juan	Clay Hill [30]	Desert Creek	40	14	30	115	2000	25	0.03@130°F	191,000	solution gas
Utah	San Juan	Desert Creek [31]	Desert Creek	26	13	5	126	2005	28	NA	NA	solution gas/fluid expansion
Utah	San Juan	Gothic Mesa [32]	Desert Creek	10	8.8	1.6	124	2150	45	NA	NA	pressure depletion
Utah	San Juan	Greater Aneth [33, 34, 35]	Desert Creek	50	12	20	125	2170	24	NA	150,000	solution gas/fluid expansion
Utah	San Juan	Recapture Creek [36]	Ismay-Desert Creek	19	10.9	1.6	130	2175	23	NA	160,000	solution gas/weak water drive
Utah	San Juan	Runway [37]	Desert Creek	50	11.9	17.3	126	2162	10-63	0.07@67°F	199,709	gas expansion
Utah	San Juan	Tohonadla [38]	Ismay-Desert Creek-Akah	25	6.5	12.5	126	1895	24	NA	82,000	solution gas
Utah	San Juan	Turner Bluff [39, 40]	Desert Creek	15	9	2	124	1637	28	0.07@68°F	120,000	solution gas

NA = not available

[1] Scott (2003), [2] Matheny and Martin (1987), [3] Mickel (1978a), [4] Miesner (1978), [5] Martin (1983), [6] Oline (1996), [7] Krivanek (1981), [8] Wold (1978), [9] Mecham (1978a), [10] Brown (1978), [11] Spencer (1978), [12] Lentz (1993), [13] Ross and Handley (1993), [14] Mecham (1978b), [15] Dawson (1988), [16] Crawley-Stewart and Riley (1993a), [17] Crawley-Stewart and Riley (1993b), [18] Mickel (1978b), [19] Brown (1983), [20] Martin (1981), [21] Krivanek (1978), [22] Ott and Roylance (1983), [23] Herrod and Gardner (1988), [24] Steele and White (1993), [25] Dunn (1978), [26] Riggs (1978), [27] Lauth (1978a), [28] Campbell (1978), [29] Baars (1993), [30] Lehman (1983), [31] Lauth (1978b), [32] Reid and Stevenson (1978), [33] Babcock (1978a, 1978b, 1978c, 1978d), [34] Peterson (1992), [35] Moore and Hawks (1993), [36] Scanlon and Wendling (1983), [37] Chidsey and others (1996a), [38] Norton (1978), [39] Mickel (1978c), [40] Krivanek (1993).

Table 10.3. *Oil properties for fields in the Blanding sub-basin Desert Creek zone, Blanding sub-basin Ismay zone, and Aneth platform Desert Creek zone subplays, Pennsylvanian Paradox Formation play.*

State	County	Field	Zone	Gas/Oil Ratio	Oil Characteristics					
					API Gravity	Color	Viscosity	Pour Point (°F)	Sulfur (%)	Nitrogen (%)
Blanding Sub-Basin Desert Creek Zone Subplay										
Colorado	Montezuma	Island Butte	Desert Creek	NA	NA	NA	NA	NA	NA	NA
Colorado	Montezuma	McClean [1, 2]	Desert Creek	2200	46°	light reddish brown	NA	0.09	NA	NA
Colorado	Dolores/Montezuma	Papoose Canyon [3]	Desert Creek	NA	50°	light green/straw yellow	NA	NA	NA	NA
Utah	San Juan	Bug [4, 5]	Desert Creek	1900	47°	light reddish brown	NA	0	NA	NA
Blanding Sub-Basin Ismay Zone Subplay										
Colorado	Montezuma	Cache [6]	Ismay	918	45°	NA	0.35 sus	NA	NA	NA
Colorado	Montezuma	Flodine Park [7]	Ismay	NA	45°	green	NA	NA	NA	NA
Colorado	Montezuma	Marble Wash [8]	Ismay	2200	42°	NA	NA	NA	NA	NA
Colorado	Montezuma	Roadrunner	Ismay	NA	NA	NA	NA	NA	NA	NA
Colorado	Montezuma	Towaoc [9]	Ismay	754	42°	NA	NA	NA	NA	NA
Utah	San Juan	Cave Canyon [10]	Ismay	529	44°	black	NA	NA	0	NA
Utah	San Juan	Deadman-Ismay [11]	Ismay	5556	40-47°	NA	NA	5-10	NA	NA
Utah	San Juan	Ismay [12, 13]	Ismay	NA	46°	brownish green	33 sec@100°F	10	0.05	0.02
Utah	San Juan	Kachina [14]	Ismay	745	39°	NA	0.443 sus	55	NA	NA
Utah	San Juan	Kiva [15]	Ismay	645	41°	NA	0.64 sus	35	NA	NA
Utah	San Juan	McElmo Mesa	Ismay	NA	NA	NA	NA	NA	NA	NA
Utah	San Juan	Mustang Flat [16]	Ismay	76,508	53°	NA	NA	NA	NA	NA
Utah	San Juan	Patterson Canyon [17]	Ismay	NA	42°	yellow brown	NA	>0	NA	NA
Utah	San Juan	Tin Cup Mesa [18]	Ismay	1390	44°	yellow brown	NA	15	NA	NA
Aneth Platform Desert Creek Zone Subplay										
Arizona	Apache	Boundary Butte East [19]	Ismay-Desert Creek-Akah	NA	41°	NA	NA	NA	NA	NA
Utah	San Juan	Akah [20]	Ismay	NA	39°	dark green	NA	25	0.2	0.06
Utah	San Juan	Anido Creek [21]	Ismay-Desert Creek	NA	43°	green	NA	NA	NA	NA
Utah	San Juan	Bluff [12, 22, 23]	Desert Creek	NA	41.4°	green	38 sec@100°F	25	0.05	0.019
Utah	San Juan	Clay Hill [24]	Desert Creek	NA	41°	NA	NA	NA	NA	NA
Utah	San Juan	Desert Creek [12, 25]	Desert Creek	NA	39°	green	40 sec @100°F	50	0.11	0.04
Utah	San Juan	Gothic Mesa [12, 26]	Desert Creek	NA	42°	green	37 sec@100°F	25	0.05	0.03
Utah	San Juan	Greater Aneth [12, 27]	Desert Creek	665	38-42°	green	0.53 sus	10	0.07	0.04
Utah	San Juan	Recapture Creek [12, 28]	Ismay-Desert Creek	NA	40°	green	35 sec@100°F	20	0.1	0.03
Utah	San Juan	Runway [29]	Desert Creek	967	40.5°	dark green	0.314 sus	NA	0	NA
Utah	San Juan	Tohonadla [12, 30]	Ismay	NA	38°	brownish green	40 sec@100°F	20	0.09	0.07
Utah	San Juan	Turner Bluff [31]	Desert Creek	259	43°	dark brown	NA	NA	0.1	NA

NA = not available, sus = Saybolt Univeral Seconds, sec = seconds

[1] Matheny and Martin (1987), [2] Mickel (1978a), [3] Miesner (1978), [4] Martin (1983), [5] Oline (1996), [6] Wold (1978), [7] Mecham (1978a), [8] Brown (1978), [9] Spencer (1978), [10] Lentz (1993), [11] Ross and Handley (1993), [12] Stowe (1972), [13] Mecham (1978b), [14] Crawley-Stewart and Riley (1993a), [15] Crawley-Stewart and Riley (1993b), [16] Brown (1983), [17] Krivanek (1978), [18] Steele and White (1993), [19] Dunn (1978), [20] Riggs (1978), [21] Lauth (1978a), [22] Campbell (1978), [23] Baars (1993), [24] Lehman (1983), [25] Lauth (1978b), [26] Reid and Stevenson (1978), [27] Moore and Hawks (1993), [28] Scanlon and Wendling (1983), [29] Chidsey and others (1996a), [30] Norton (1978), [31] Krivanek (1993).

Paradox is Akah field, San Juan County, Utah, where the reservoir contains 13% N_2 and 18% CO_2; the gas heating value is 863 Btu/ft^3 (Stowe, 1972; Moore and Sigler, 1987).

Oil and gas properties for individual fields that have produced over 500,000 BO (80,000 m^3) in the Paradox Formation play are summarized in tables 10.3 and 10.4.

PRODUCTION

Eighteen fields in the fractured shale (Cane Creek shale zone) subplay have produced crude oil and associated gas (tables 10.5 and 10.6). Three fields have produced over 500,000 BO (80,000 m^3) (figure 10.15 and table 10.1). Prior to 1991, oil had been produced from 11 vertical wells perforated in the Cane Creek (table 10.5). All wells drilled and completed in the Cane Creek since 1991 have used horizontal drilling technology with the exception of one vertical well in Greentown field (figures 10.3 and 10.15, tables 10.5 and 10.6). The development history of the subplay has been described by Fritz (1991), Morgan and others (1991), Morgan (1992a, 1992b), Montgomery (1992), Grove and others (1993), Grummon (1993), Grove and Rawlins (1997), and Doelling and others (2003). Many vertical wells have been completed in the Cane Creek shale, but only the Long Canyon No. 1 well (section 8, T. 26 S., R. 20 E., SLBL&M, Grand County, Utah) has been an economic success. The Long Canyon No. 1 well in Long Canyon field (figure 10.3) was drilled in 1962 and has produced more than 1 million BO (173,000 m^3). The well is estimated to have produced more than 1 BCFG (0.03 BCMG), but is not gauged due to a lack of a gas pipeline. In 1991, Columbia Gas Development Corporation drilled the first commercial horizontal well in the abandoned Bartlett Flat field, the Kane Springs No. 27-1 well (section 27, T. 25 S., R. 19 E., SLBL&M, Grand County) which included a 1012-foot (308 m) horizontal leg in the Cane Creek shale zone. The well was completed with an initial production rate flowing 914 BOPD (145 m^3/d) and 290 MCFGPD (8200 m^3/d) from 7438 to 8240 feet (2267–2512 m) (7248 feet [2209 m] total true vertical depth). The discovery was designated Big Flat field (figure 10.3). Exploration in the area has resulted in numerous new field discoveries as horizontal drilling techniques have improved and the geology of the Cane Creek has become better understood. Horizontal drilling has not resulted in wells that produce more oil than the Long Canyon well, but has greatly improved the success rate of new economical discoveries.

Eight fields in the Blanding sub-basin Desert Creek zone subplay have produced crude oil and associated gas. These fields have combined to produce over 16.7 million BO (2.7 million m^3) and 74.5 BCFG (2.1 BCMG) from the Desert Creek zone (Scott, 2003; Colorado Oil and Gas Conservation Commission, 2016; Utah Division of Oil, Gas, and Mining, 2016a). About 50 active Desert Creek producers are currently in these fields. Four fields have produced over 500,000 BO (80,000 m^3) (figure 10.4 and table 10.1).

Forty-five fields in the Blanding sub-basin Ismay zone subplay have produced crude oil and associated gas. These fields have combined to produce over 42.5 million BO (6.8 million m^3) and 114.9 BCFG (3.3 BCMG) from the Ismay zone (Scott, 2003; Colorado Oil and Gas Conservation Commission, 2016; Utah Division of Oil, Gas, and Mining, 2016a). About 130 active Ismay producers are currently in these fields. A few scattered fields produce or are now abandoned in the Desert Creek zone. Sixteen fields have produced over 500,000 BO (80,000 m^3) from the Ismay zone (figure 10.4 and table 10.1).

Thirty-two fields—six in Arizona and the rest in Utah (figure 10.4)—in the Aneth platform Desert Creek zone subplay have produced crude oil and associated gas. These fields have combined to produce nearly 500 million BO (79.4 million m^3) and 478.5 BCFG (13.5 BCMG) (including cycled gas) from the Desert Creek zone; of this total over 479 million BO (76.2 million m^3) and 432.8 BCFG (12.3 BCMG) have been produced from Greater Aneth field (Utah Division of Oil, Gas, and Mining, 2016a). About 485 active Desert Creek producers are currently in these fields; over 445 wells are in Greater Aneth field. Thirteen fields have produced over 500,000 BO (80,000 m^3) (figure 10.4 and table 10.1). Several fields on the Aneth platform have also produced from the Ismay zone, from commingled Ismay and Desert Creek zones, or the Akah and Barker Creek zones (several Arizona fields). However, most of these fields are abandoned: Anido Creek, Cleft, Rabbit Ears, Toh-Atin, Twin Falls, and Bita Creek fields, for example (figure 10.4).

In 2015, the monthly production from the Paradox Formation averaged 364,000 BO (57,900 m^3) and 0.76 BCFG (0.02 BCMG) (Colorado Oil and Gas Conservation Commission, 2016; Utah Division of Oil, Gas, and Mining, 2016a; Arizona Geological Survey, 2016). Production peaks in the Paradox play have been strongly influenced by production at Greater Aneth field: in the late 1950s and early 1960s as the field was being developed, the onset of water and CO_2 floods in 1962 and 1985, respectively, and an extensive horizontal drilling program in the 1990s. Production also increased from a number of significant discoveries during the 1980s in the Blanding sub-basin Desert Creek and Ismay zones subplays (table 10.1). Production received boosts again in the 1990s with a series of discoveries in satellite mounds around Greater Aneth field. Production in the Blanding sub-basin Desert Creek and Ismay zones subplays has declined since 2000 due to maturing fields where no new enhanced oil recovery programs have been initiated. Also, no significant discoveries have been made since the early 1990s due to limited exploratory drilling.

Table 10.4. *Gas properties for fields in the Blanding sub-basin Desert Creek zone, Blanding sub-basin Ismay zone, and Aneth platform Desert Creek zone subplays, Pennsylvanian Paradox Formation play.*

State	County	Field	Zone	Gas Characteristics											
				Methane (%)	Ethane (%)	Propane (%)	Butane (%)	Pentaine (%)	Hexane + (%)	Nitrogen (%)	CO_2 (%)	Helium (%)	Hydrogen Sulfide (%)	BTU	Specific Gravity
Blanding Sub-Basin Desert Creek Zone Subplay															
Colorado	Montezuma	Island Butte	Desert Creek	NA	NA	NA	NA	NA	NA	NA	NA	NA	NA	NA	NA
Colorado	Montezuma	McClean [1, 2, 3]	Desert Creek	78	14	5	2	0.5	0.4	0.5	0.05	0.01	0	1254	0.715
Colorado	Dolores/ Montezuma	Papoose Canyon [4]	Desert Creek	63	18	10	5	2	0.5	2	0.3	0.1	0	1475	0.870
Utah	San Juan	Bug [5, 6]	Desert Creek	78	13	5	2	0.5	0.3	0.63	0.08	0	0	1232	0.717
Blanding Sub-Basin Ismay Zone Subplay															
Colorado	Montezuma	Cache [7]	Ismay	66	16	9	3	NA	1	NA	0.6	NA	NA	1436	0.851
Colorado	Montezuma	Flodine Park [4]	Ismay	75	13	6	3	1	0.2	2	0.5	0.1	0	1247	0.763
Colorado	Montezuma	Marble Wash	Ismay	NA	NA	NA	NA	NA	NA	NA	NA	NA	NA	NA	NA
Colorado	Montezuma	Roadrunner	Ismay	NA	NA	NA	NA	NA	NA	NA	NA	NA	NA	NA	NA
Colorado	Montezuma	Towaoc [8]	Ismay	56	18	13	7	3	0.5	2	0.1	.02	0	1607	NA
Utah	San Juan	Cave Canyon	Ismay	NA	NA	NA	NA	NA	NA	NA	NA	NA	NA	NA	NA
Utah	San Juan	Deadman-Ismay [9]	Ismay	74	15	7	2	0	0	1.3	0.05	0	0	1294	NA
Utah	San Juan	Ismay	Ismay	NA	NA	NA	NA	NA	NA	NA	NA	NA	NA	NA	NA
Utah	San Juan	Kachina [10]	Ismay	65	17	10	NA	NA	NA	NA	NA	NA	Tr	1464	0.909
Utah	San Juan	Kiva [11]	Ismay	65	15	10	NA	NA	NA	NA	NA	NA	Tr	1515	0.9
Utah	San Juan	McElmo Mesa [12]	Ismay	61	19	11	5	2	1	1.8	0.1	Tr	0	NA	NA
Utah	San Juan	Mustang Flat	Ismay	NA	NA	NA	NA	NA	NA	NA	NA	NA	NA	NA	0.6
Utah	San Juan	Patterson Canyon [13]	Ismay	57	22	12	5	2	2	0.2	0.2	NA	NA	1568	0.937
Utah	San Juan	Tin Cup Mesa [14]	Ismay	69	15	9	3	1	0.5	1	0.4	NA	NA	1400	0.68
Aneth Platform Desert Creek Zone Subplay															
Arizona	Apache	Boundary Butte East [15]	Ismay-Desert Creek-Akah	70	4	2	0.8	0.3	0.2	8.2	13.8	1.0	0.1	871	0.778
Utah	San Juan	Akah [16]	Ismay-Desert Creek-Akah	57	6	NA	NA	NA	NA	13	18	NA	NA	863	NA
Utah	San Juan	Anido Creek	Ismay-Desert Creek	NA	NA	NA	NA	NA	NA	NA	NA	NA	NA	NA	NA
Utah	San Juan	Bluff [4]	Desert Creek	75	14	5	2	1	0.5	2	0.4	Tr	0	1640	0.954
Utah	San Juan	Clay Hill [17]	Desert Creek	54	23	13	6	2	2	1	0.3	0	Tr	1636	0.970
Utah	San Juan	Desert Creek [4]	Desert Creek	65	18	9	4	2	0.6	3	0.1	Tr	0	1412	0.836
Utah	San Juan	Gothic Mesa	Desert Creek	NA	NA	NA	NA	NA	NA	NA	NA	NA	NA	1150	NA
Utah	San Juan	Greater Aneth [4, 18, 19]	Desert Creek	62	18	11	5.5	2.5	<1	0	0.1	0	0	1450	NA
Utah	San Juan	Recapture Creek [19, 20]	Ismay-Desert Creek	NA	NA	NA	NA	NA	NA	NA	NA	NA	NA	1425	0.834
Utah	San Juan	Runway [21]	Desert Creek	72	15	7	3	1	0.6	1.1	0.6	0	0	1366	0.779
Utah	San Juan	Tohonadla [4]	Ismay-Desert Creek-Akah	60	22	9	4	1	0.3	3	0.2	0.1	0	1449	0.861
Utah	San Juan	Turner Bluff	Desert Creek	NA	NA	NA	NA	NA	NA	NA	NA	NA	NA	NA	NA

NA = not available.

[1] Scott (2003), [2] Matheny and Martin (1987), [3] Mickel (1978a), [4] Moore and Sigler (1987), [5] Martin (1983), [6] Oline (1996), [7] Wold (1978), [8] Spencer (1978), [9] Ross and Handley (1993), [10] Crawley-Stewart and Riley (1993a), [11] Crawley-Stewart and Riley (1993b), [12] Mickel (1978b), [13] Krivanek (1978), [14] Steele and White (1993), [15] Dunn (1978), [16] Riggs (1978), [17] Lehman (1983), [18] Moore and Hawks (1993), [19] Stowe (1972), [20] Scanlon and Wendling (1983), [21] Chidsey and others (1996a).

Table 10.5. *Cumulative oil and gas production from vertical wells completed in the Cane Creek shale zone. Data from Stowe (1972) and the Utah Division of Oil, Gas, and Mining as of January 1, 2016. All locations are SLBL&M.*

Field Name Well Name Location	Completion Date	Current Status	Cumulative Production Oil* Gas†
Greentown Federal 28-11 Section 28, T. 28 S., R. 17 E.	2008	Producing	71,535 BO 266,462 MCFG
Bartlett Flat Big Flat 5 Section 27, T. 25 S., R. 19 E.	1961	Abandoned 1965	39,393 BO 22,051 MCFG
Gold Bar Gold Bar 1 Section 29, T. 25 S., R. 20 E.	1982	Abandoned 1984	13,393 BO 14,800 MCFG
Unnamed Mathew Federal 1 Section 4, T. 26 S., R. 20 E.	1981	Abandoned 1982	1343 BO 0 MCFG
Unnamed Skyline 1 Section 5, T. 26 S., R. 20 E.	1982	Abandoned 1982	675 BO 1430 MCFG
Unnamed Skyline 8-44 Section 8, T. 26 S., R. 20 E.	1976	Abandoned 1976	507 BO 0 MCFG
Long Canyon Long Canyon 1 Section 9, T. 26 S., R. 20 E.	1962	Shut-in	1,087,375 BO 1,128,167 MCFG
Cane Creek MGM 2 Section 36, T. 26 S., R. 20 E.	1959	Abandoned 1969	1887 BO 25,000 MCFG
Shafer Canyon Shafer 3 Section 4, T. 27 S., R. 20 E.	1963	Abandoned 1963	1325 BO 0 MCFG
USA 1 Section 6, T. 27 S., R. 20 E.	1962	Abandoned 1967	66,231 BO 63,807 MCFG
Lion Mesa Lion Mesa 27-1A Section 27, T. 27 S., R. 21 E.	1980	Shut-in	1608 BO 0 MCFG
Wilson Canyon Chevron Federal 1 Section 24, T. 29 S., R. 23 E.	1968	Shut-in	98,544 BO 129,713 MCFG
TOTAL			1,383,816 BO 1,651,430 MCFG

*BO = barrels of oil
† MCFG = thousand cubic feet of gas

EXPLORATION POTENTIAL AND TRENDS

Fractured Shale Subplay

An important consideration in defining the exploration limits of the Cane Creek shale zone in fractured shale subplay may be the depositional limits of the underlying salt beds of cycles 22 through 29 (figure 10.2). Where it is not encased by thick, plastic salts that provide the reservoir seal, the Cane Creek may not be overpressured. In addition, fracturing of the Cane Creek by diapiric salt movement will not occur where the underlying salts were never present; the density of fracturing may thus be greatly reduced. If subsequent drilling supports this interpretation, then stratigraphic traps (pinchout or updip reduction of fractures) may occur where the underlying salt pinches out.

Exploration activity has been concentrated in areas where the Cane Creek shale zone has a history of production. Many of the earlier wells drilled in the area (figure 10.15) had excellent shows in the Cane Creek but were not completed in the shale because of poor production history, lower prices, and the lack of modern fractured shale completion technology. Horizontal drilling might also be used to test other fractured shale zones in the basin. Clastic intervals are associated with all of the 30 plus cycles in the Paradox Formation. Many of these units contain organic-rich black shales, some with TOC values of nearly 13%. In addition, oil or gas has been recovered from cycles 2 through 22 in the mapped area (figure 10.15). The Gothic, Chimney Rock, and Hovenweep shales (figure 10.2) also are excellent candidates for horizontal drilling. These shales are more than 40 feet (12 m) thick, are regionally extensive, and have numer-

Table 10.6. *Cumulative oil and gas production from horizontal wells completed in the Cane Creek shale zone. Data from the Utah Division of Oil, Gas, and Mining as of January 1, 2016. All locations are SLBL&M.*

Field Name or Well Name and Location	Completion Date	Active Horizontal Wells	Current Status	Cumulative Production Oil Gas
Big Flat	1991	21	Producing	5,034,861 BO 3.4 BCFG
Park Road	1991	2	Producing	489,564 BO 0.2 BCFG
Hell Roaring Field	1992	1	Producing	659,883 BO 0.6 BCFG
Hatch Point	2009	2	Producing	71,836 BO 0.04 BCFG
Wildcat Two Fer 26-30 Section 26, T. 26 S., R. 20 E.	2009	1	Producing	11,028 BO 0 BCFG
Wildcat La Sal 29-28 Section 29, T. 29 S., R. 23 E.	2011	1	Producing	5458 BO 0.01 BCFG
Cane Creek	2014	2	Producing	57,582 BO 0.03 BCFG
Wildcat Cane Creek 36-1-25-18 Section 36, T. 25 S., R. 18 E.	2014	1	Shut-in	No production
TOTAL		31		6,330,212 BO 4.28 BCFG

ous oil shows. Hite and others (1984) calculated that the Gothic shale has generated at least 4970 BO/acre (1950 m^3/ha). The Gothic, Chimney Rock, and Hovenweep Shale Oil and Gas Assessment Unit estimated to contain a mean of 256 million bbls of oil (40.7 MMCM) (U.S. Geological Survey, 2012).

Blanding Sub-Basin Ismay and Desert Creek Zones Subplays

Mapping the upper Ismay zone lithofacies as two intervals (upper and lower parts) delineates very prospective reservoir trends that contain porous, productive carbonate buildups (figures 10.7 and 10.8). The mapped lithofacies trends clearly define anhydrite-filled, intra-shelf basins. Lithofacies and reservoir controls imposed by the anhydritic, intra-shelf basins should be considered when selecting the optimal location and orientation of any horizontal drilling for undrained reserves, as well as identifying new exploration trends. Projections of the inner shelf/tidal flat and mound trends around the intra-shelf basins identify potential exploration targets, which could be developed using horizontal drilling techniques (figures 10.55 and 10.56). Drilling horizontally from known phylloid-algal reservoirs along the inner shelf/tidal flat trend could encounter previously undrilled porous buildups. Intra-shelf basins are not present in the lower Desert Creek zone of the Blanding sub-basin (figure 10.9). However, drilling horizontally from productive mound lithofacies along linear shoreline trends could also encounter previously undrilled porous Desert Creek intervals and buildups.

Aneth Platform Desert Creek Zone Subplay

The shallow-shelf/shelf-margin depositional environment includes shallow-shelf carbonate buildups, platform-margin calcarenites, and platform-interior carbonate muds and sands (described earlier). Pervasive marine cement may be indicative of "wall" complexes suggesting potential nearby carbonate buildups, particularly phylloid-algal mounds (figure 10.44). Carbonate buildups, tidal-channel carbonate sands, and other features often appear promising on seismic records. However, if these carbonate buildups are located within the open-marine and intra-shelf, salinity-restricted depositional environments/lithofacies (figures 10.10 and 10.57), the reservoir quality is typically poor. Porosity and permeability development, if present, is limited or plugged with anhydrite, respectively in these depositional environments.

Platform-margin calcarenites are located along the margins of the larger shallow shelf or the rims of phylloid-algal buildup complexes. Mapping indicates a relatively untested lithofacies belt of shallow-shelf, calcarenite carbonate deposits (figure 10.57). This narrow, but long, belt of calcarenites is between the open-marine and margins of intra-shelf, salinity-restricted depositional environments. Calcarenite buildups represent high-energy environments where shoals and/or islands developed. However, algal meadows, phylloid-algal buildups, and stromatolite mats were also present in this lithofacies belt (figure 10.58) (Chidsey and Eby, 1997).

Heron field (figures 10.10 and 10.57) is an excellent example of the type of traps which potentially lie within the 20-mile-long (32 km) lithofacies belt described above. The trap for the field is a lenticular, northwest- to southeast-trending linear mound/beach complex, 0.8 mile (1.3 km) long and 0.5 mile (0.8 km) wide (Chidsey and others, 1996b). The reservoir consists of five units: (1) a basal, dolomitized, phylloid-algal (bafflestone) buildup, (2) an anhydrite-plugged, phylloid-algal (bafflestone) limestone buildup, (3) a fusilinid-bearing, lime-wackestone interval, (4) a dolomitized packstone interval with anhydrite nodules, and (5) a porous (15%), sucrosic, dolomitized grainstone and packstone interval. This last unit is the main reservoir, and consists of alternating 2- to 4-foot-thick (0.6–1.2 m) packages of uniform beach calcarenite and poorly sorted foreshore and storm-lag rudstone or breccia deposits.

Platform-margin calcarenite traps have both negative and positive characteristics for hydrocarbon production. Negative characteristics include (1) small reservoir size and storage capacity, (2) poor definition on seismic records, (3) limited distribution, (4) common bitumen plugging, and (5) rapid production declines. Positive characteristics include (1) excellent overall reservoir properties, (2) a common association with phylloid-algal buildups, (3) good potential for water/CO_2 floods, and (4) an extensive untested trend (Chidsey and Eby, 1997).

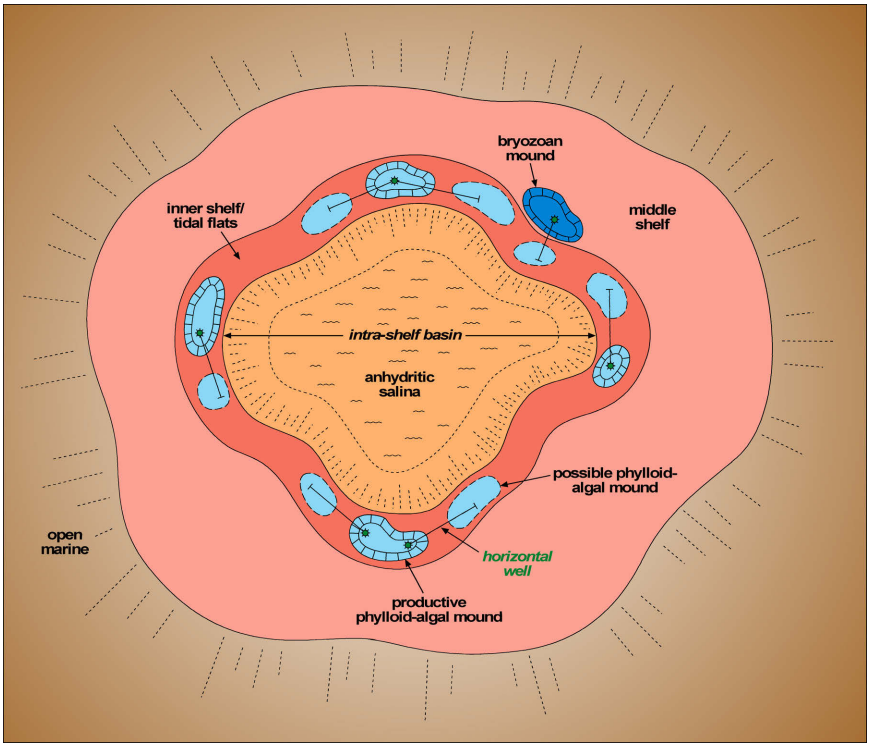

Figure 10.55. *Map view of an ideal upper Ismay intra-shelf basin surrounded by a ring of inner shelf/tidal flat sediments (shown in dark salmon) which encase phylloid-algal mound clusters (in light blue). The central portion of the intra-shelf basin is the location of thick anhydrite (in orange) accumulation. Outboard from the inner shelf/tidal flat and mound fairway are low-energy middle-shelf and open-marine carbonates.*

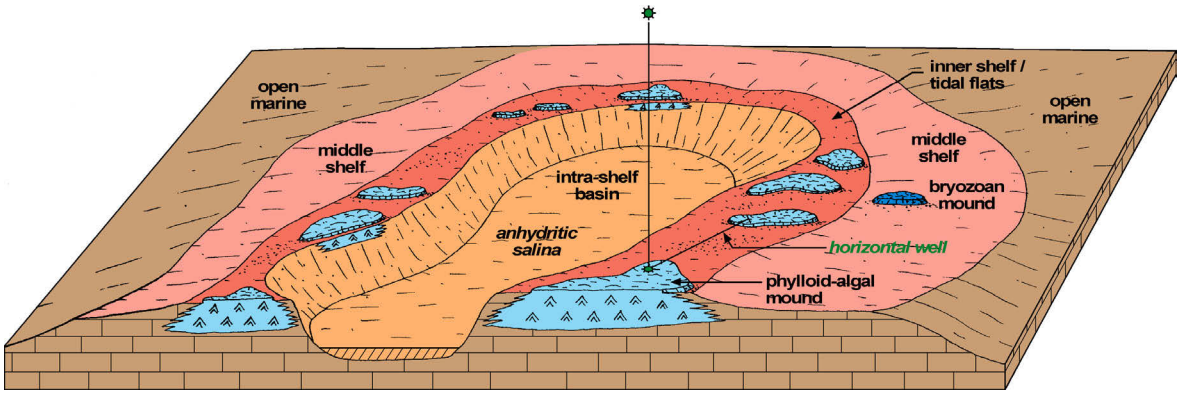

Figure 10.56. *Cut-away block diagram showing the possible spatial relationships of upper Ismay facies types controlled by an intra-shelf basin. Phylloid-algal mounds (in light blue) are the principal reservoir within a curvilinear band that rims the intra-shelf basin. A hypothetical vertical well into a known mound reservoir is used as a kick-off location for horizontal drilling into previously undrained mounds.*

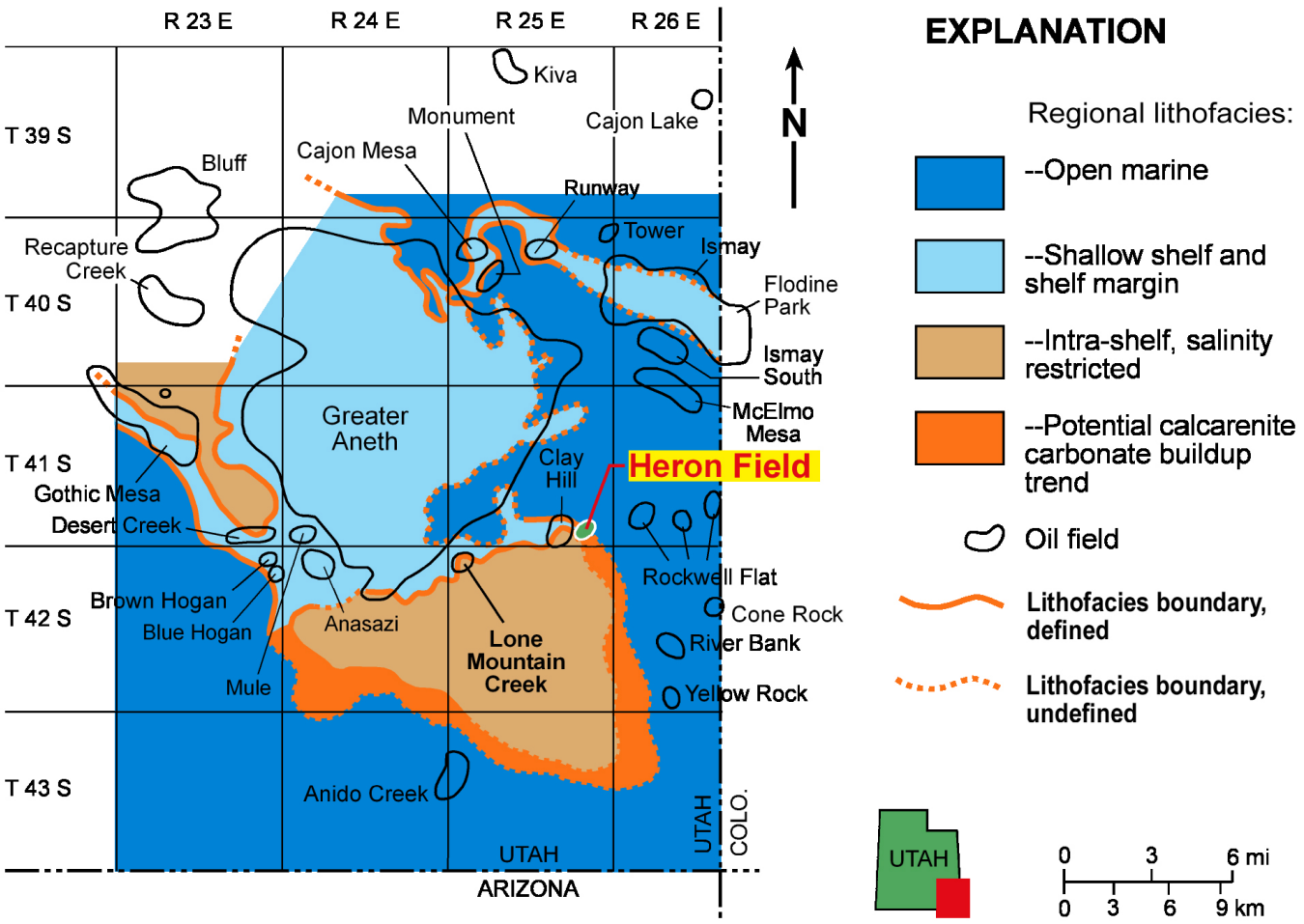

Figure 10.57. *Potential calcarenite buildup trend (orange) within the regional lithofacies belts of the Desert Creek zone, southeastern Utah. Heron field (highlighted) is an excellent example of a lenticular, mound/beach complex hydrocarbon trap in this trend.*

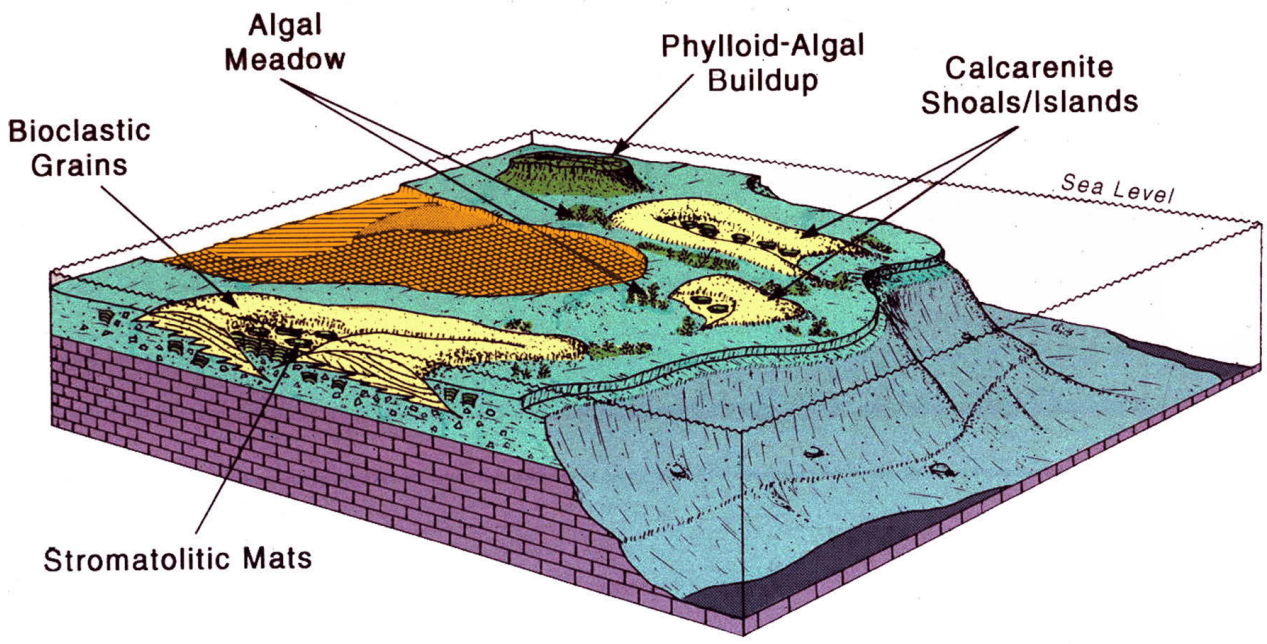

Figure 10.58. *Depositional environments of the calcarenite lithofacies along the narrow shelf margin between the open-marine and intra-shelf, salinity-restricted lithofacies belts.*

CHAPTER 11:
OUTCROP ANALOGS FOR MAJOR RESERVOIRS

by

Thomas C. Chidsey, Jr., Hellmut H. Doelling (retired), Craig D. Morgan, Douglas A. Sprinkel, and Grant C. Willis
Utah Geological Survey

and

David E. Eby
Eby Petrography & Consulting, Inc.

CONTENTS

FIGURES

TABLE

CHAPTER 11:
OUTCROP ANALOGS FOR MAJOR RESERVOIRS

INTRODUCTION

Utah is unique in that representative outcrop analogs (depositional or structural) for each major oil play are present in or near the thrust belt, Paradox Basin, and Uinta Basin. Production-scale analogs provide an excellent view, often in 3-D, of reservoir-facies characteristics, geometry, distribution, and nature of boundaries contributing to the overall heterogeneity of reservoir rocks. The specific objectives of this project are to: (1) increase understanding of vertical and lateral facies variations and relationships within major reservoirs; (2) describe the lithologic characteristics; (3) determine the morphology, internal geometries, and possible permeability and porosity distributions; and (4) identify potential impediments and barriers to fluid flow.

An outcrop-analog model, combined with the details of internal lithofacies characteristics, can be used as a "template" for evaluating data from conventional core, geophysical and petrophysical logs, and seismic surveys. When combined with subsurface geological and production data, the analog model will improve development drilling and production strategies, reservoir-simulation models, reserve calculations, and design and implementation of secondary/tertiary oil recovery programs and other best practices used in the oil fields of Utah and vicinity. Outcrop analogs for the major oil reservoirs in the thrust belt, Uinta Basin, and Paradox Basin are presented in the following sections.

THRUST BELT

Triassic-Jurassic Nugget and Jurassic Navajo Sandstone

Some of the best outcrop analogs to the Upper Triassic-Lower Jurassic Nugget Sandstone reservoirs in the southwest Wyoming and northern Utah thrust belt and the Lower Jurassic Navajo Sandstone (stratigraphically equivalent to the upper Nugget) reservoir in the central Utah thrust belt are in southern Utah. The Navajo Sandstone is famous for its exposures in Zion National Park and Glen Canyon National Recreation Area in southern Utah (figure 11.1). Navajo dunes were straight-crested to sinuous, coalescing, transverse barchanoid ridges with slipfaces dipping toward the downwind direction (Picard, 1975). Regional analyses indicate paleocurrent and paleowind directions were dominantly from the north and northwest (Chidsey and others, 2000a; Anderson and others, 2003). Outcrops along the shores of Lake Powell in Glen Canyon National Recreation Area display classic eolian bedforms (Ahlbrandt and Frybreger, 1982) such as tabular planar, wedge planar, and large-scale trough cross-strata (figure 11.2), which occur in sets up to 25 feet (8 m) thick. Dips of cross-beds between set boundaries vary as much as 40 degrees from the nearly horizontal structural attitude of the formation in Glen Canyon National Recreation Area. Dune sand-flow toes often form tangential contacts of cross-beds with the lower bounding surfaces (Ahlbrandt and Frybreger, 1982). Dune lithofacies from the brink to the toe of the dune slipface consist of (1) thin, reverse graded, tabular, pinstriped grainfall laminae, (2) thick, subgraded avalanche laminae, and (3) thin, tightly packed, reworked ripple strata at the dune toe (Lindquist, 1983). Wind ripples or high-index ripples are occasionally preserved on topset deposits. The south shore of Antelope Island in Lake Powell contains some of the best examples of soft-sediment deformation or contorted bedding in the Navajo. The contorted bedding is the result of slumping on the slopes of sand dunes before the sediments were lithified, possibly during earthquakes. Many of the tortuous and twisted beds have weathered in relief, forming eerie-looking outcrops (figure 11.3).

In addition to "seas" of wind-blown sand dunes, large deserts such as the Sahara and Gobi contain depositional interdune lithofacies, including playas and oases. An oasis is a vegetated area in desert regions where springs or lakes are present for relatively long periods because the water table is close to the surface. A playa is a flat-floored bottom of an undrained desert valley that is only occasionally the site of shallow lakes. Many thin-bedded, lenticular limestone beds are within the Navajo Sandstone around Lake Powell in Glen Canyon National Recreation Area and interpreted as interdune oasis deposits (Chidsey and others, 2000a, 2000b; Anderson and others, 2003). Shallow lacustrine limestone seems to be the most common. Oasis deposits are typically represented by light-gray, 5- to 10-foot-thick (2–3 m), thin and horizontally bedded limestone that commonly contains oscillation ripples and mudcracks (figure 11.4A and B). The limestone beds generally pinch out over very short distances (tens of feet) (figure 11.4C), and can be observed on both sides of the narrower canyons (figure 11.5). Limestone beds in several Navajo outcrops have yielded fossil plants and invertebrates (Stokes, 1991; Santucci, 2000). Many limestone beds also contain cryptalgalaminites (algal laminae) most likely created by coccoid blue-green algal or cyanobacterial processes as organic mats and thrombolites (figures 11.4D and 11.6). Playas or mudflats (some with evaporite minerals)

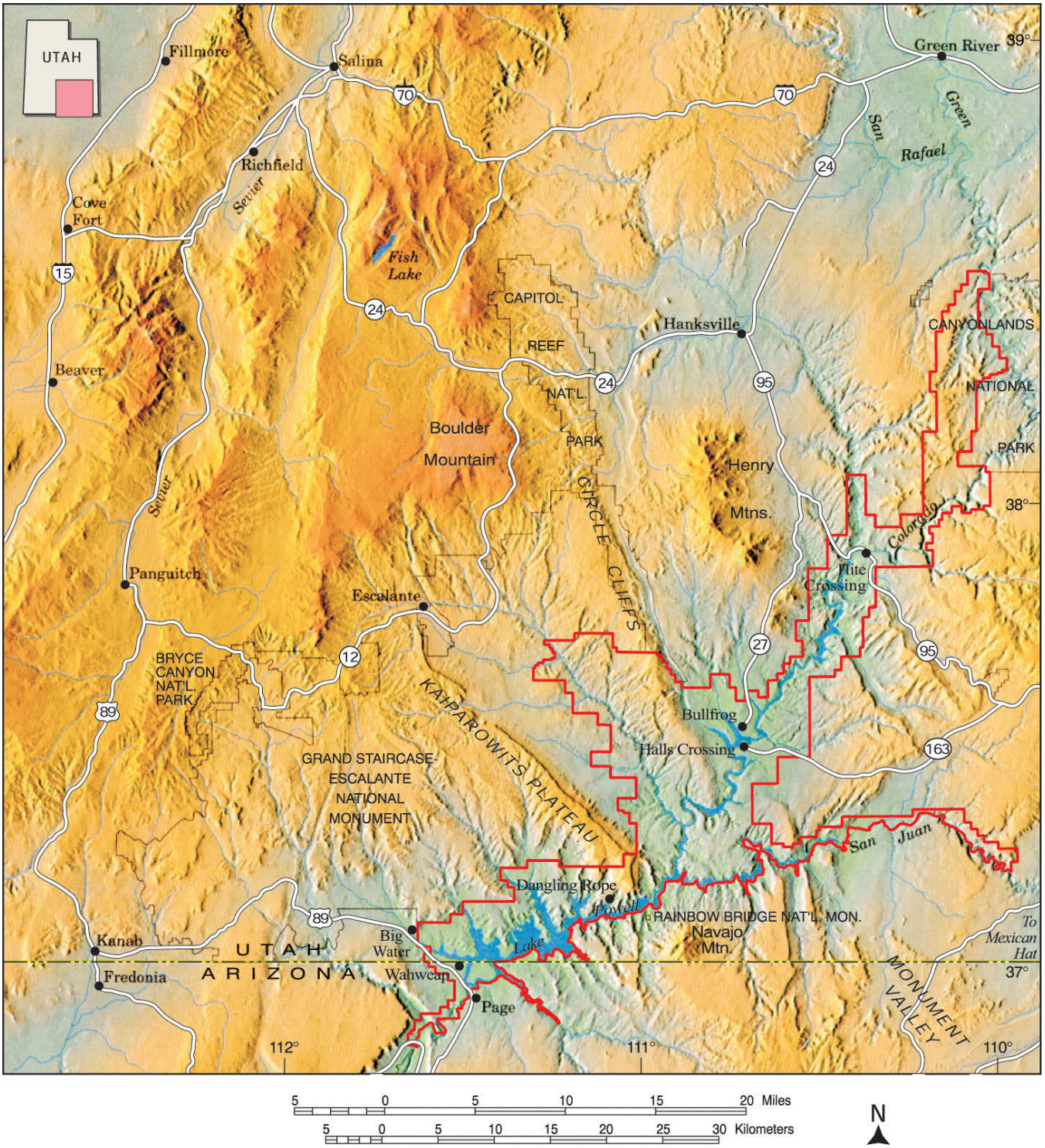

Figure 11.1. *Index map to Glen Canyon National Recreation Area, Utah and Arizona (red outline). Modified from Hintze (1997); topographic relief base map modified with permission, courtesy of Chalk Butte, Inc., Boulder, Wyoming.*

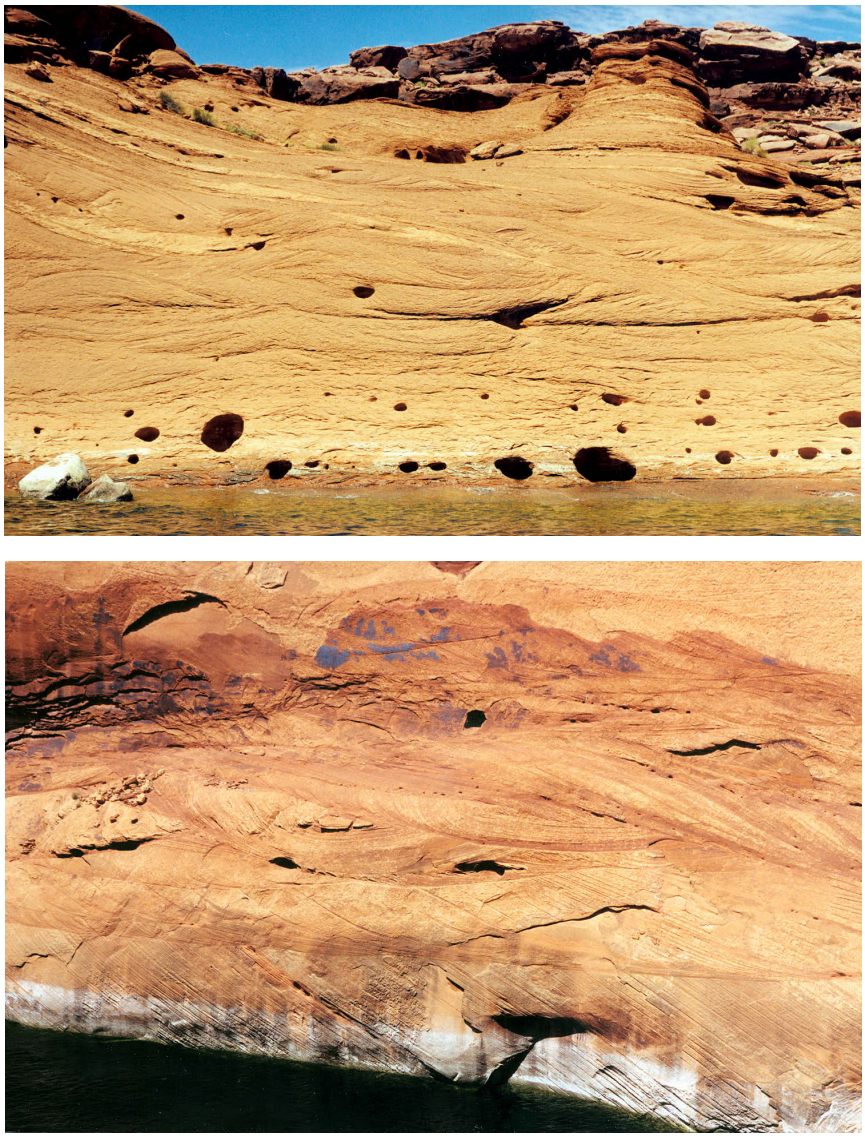

Figure 11.2. *Navajo Sandstone beds display pronounced trough cross-bedding which indicates the paleowinds were from the north and northwest, Lake Powell, Glen Canyon National Recreation Area, Utah.*

Figure 11.3. *Spectacular contorted bedding in Navajo Sandstone; south side of Antelope Island in Lake Powell, Glen Canyon National Recreation Area, Arizona.*

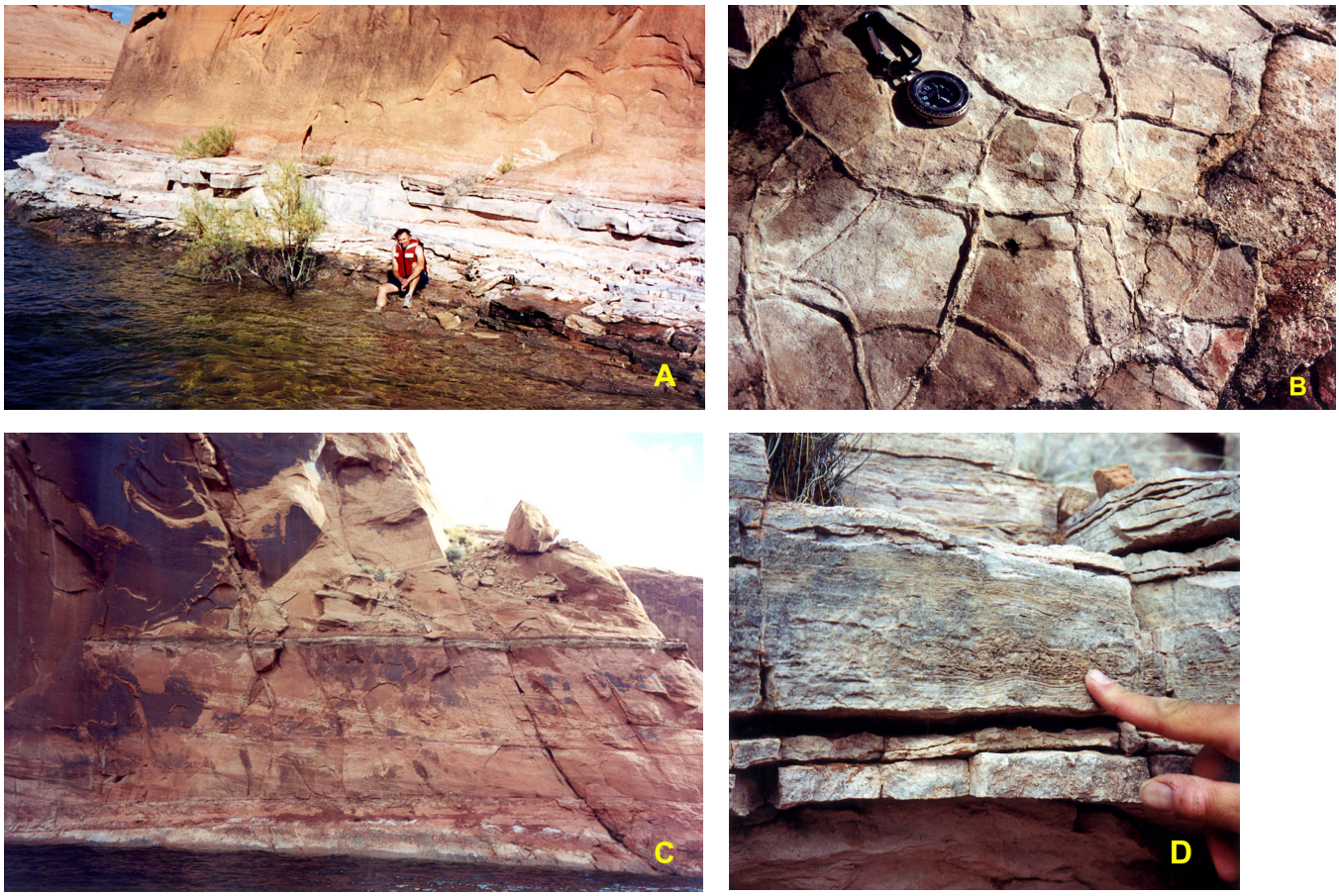

Figure 11.4. *Oasis deposits in the Navajo Sandstone, Lake Powell, Glen Canyon National Recreation Area, Utah.* ***A.*** *Typical limestone oasis deposit near the top of the Navajo Sandstone, Forgotten Canyon.* ***B.*** *Mudcracks in oasis limestone mud above bed containing ripple marks, Forgotten Canyon.* ***C.*** *Rapid pinch out of thin limestone bed, Moki Canyon.* ***D.*** *Algal laminae within the limestone oasis beds in the Navajo Sandstone, Moki Canyon.*

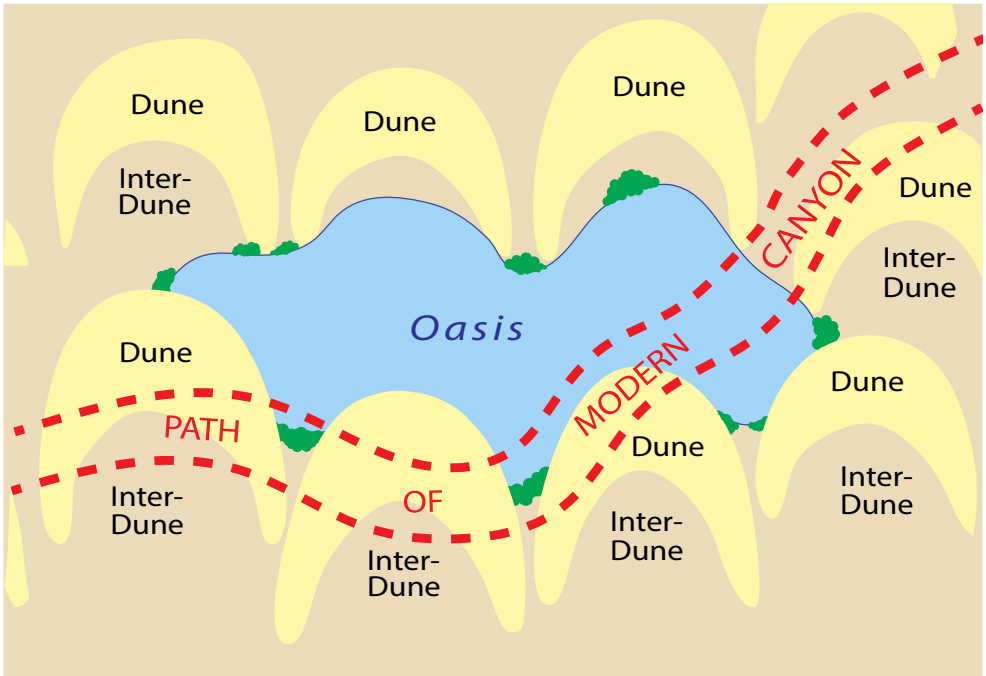

Figure 11.5. *Schematic interpretation, map view, of a Navajo oasis pond surrounded by large dunes. The path of a modern canyon is superimposed to demonstrate the rapid pinch outs of limestones observed along the canyon walls; many of the limestones probably belong to the same oasis deposits.*

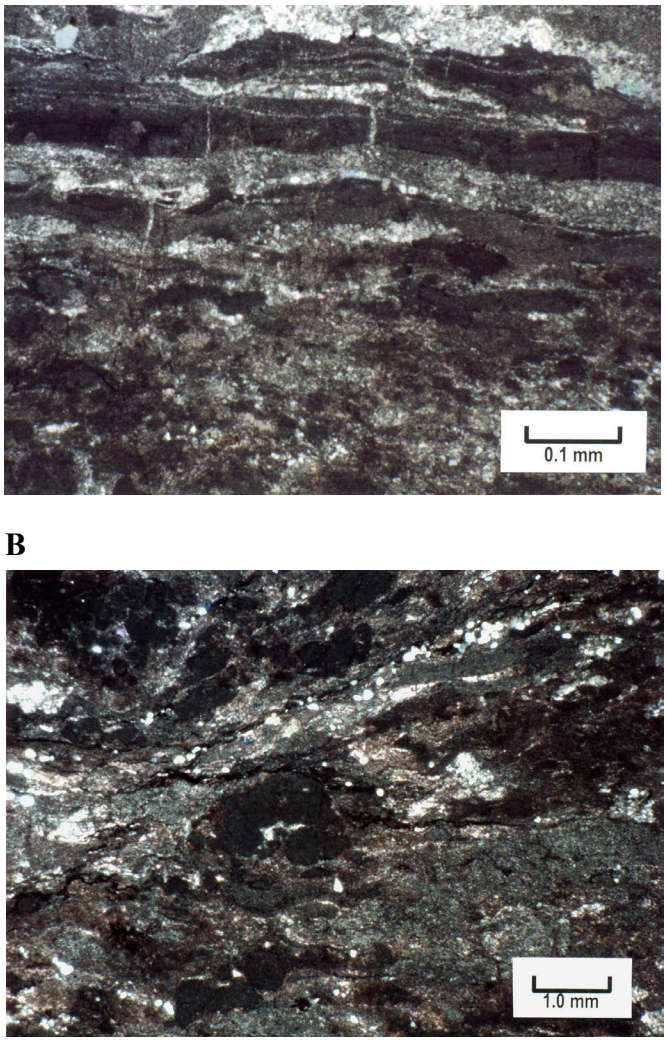

Figure 11.6. *Photomicrographs (crossed nicols) of oasis deposits, Navajo Sandstone, Glen Canyon National Recreation Area, Utah.* ***A.*** *Couplets of alternating cryptalgalaminites and massive microcrystalline layers dominate the upper half of this micrograph. The laminated bands are mostly calcitic (limestones) while the lighter-colored microcrystalline bands are mostly dolomites. These mm-scale couplets are typical of organic blue-green algal or cyanobacterial mats. The lighter-colored, massive or microcrystalline bands are probably the result of dolomitized storm deposits while the microlaminated layers are the result of normal microbial mat trapping and binding activities. The lower half of this image shows a greater concentration of dark-colored rip-up intraclasts.* ***B.*** *Dark-colored clots and pin cushion-like patches of micrite are surrounded by lighter-colored, partially dolomitized detrital sediments and small, white quartz grains. Several of these lumpy clots can be termed "thrombolites" and were most likely created by coccoid blue-green algal or cyanobacterial processes. Such microbial structures could have easily formed in stressed environments that were intermittently desiccated. Salinity stresses, ranging from fresh to hypersaline waters, can promote these types of microbial mini-structures.*

are also present in the Navajo around Lake Powell, represented by planar beds composed of mud, silt, and very fine grained sand.

Similar Navajo limestone beds along the Colorado River near Canyonlands National Park represent small freshwater lakes based on geochemical analysis (Gilland, 1979). Fresh ground water at a shallow depth had to persist for prolonged periods of time, perhaps many thousands of years, to allow the lake or pond deposits of these oases to develop (Stokes, 1991). The continuous supply of fresh water provided favorable environments for life and the deposition of carbonate rocks (figure 11.5). The Alashan area of the Gobi Desert contains a high water table producing similar lakes between massive dunes today (Webster, 2002).

Some Navajo interdunes were erosional (deflation) areas associated with running water, such as a wadi or desert wash (Chidsey and others, 2000a, 2000b). An ancient wadi deposit can be observed in the Navajo Sandstone in Rainbow Bridge National Monument, Utah (figure 11.1) and is represented by several dark, iron-stained channel-form features present on the south side of Rainbow Bridge Canyon (figure 11.7A), a tributary canyon to Glen Canyon and the Colorado River. A wadi is a usually dry streambed or channel in a desert region. A few large blocks of a wadi deposit fell to the terrace bench, near the Rainbow Bridge viewing area, from a channel bed about 3 feet (1 m) thick about 50 feet (15 m) up the cliff. The deposit is a "pudding stone" consisting of tan to reddish-orange, rounded sandstone fragments or clasts, and gray to dark gray, subangular to subrounded dolomitic limestone clasts (figure 11.7B). Clasts vary from pea to small boulder sized. The matrix is medium- to coarse-grained sandstone cemented with iron-bearing quartz and minor calcite. The fallen blocks are horizontally stratified and have some small-scale crossbeds. They contain rip-up clasts of lime muds; some imbricated rip-up clasts are inclined in the downstream direction. Additional wadi deposits are located in other parts of Rainbow Bridge Canyon and nearby Forbidding Canyon, and possibly belonged to the same ancient wadi system (figure 11.7C).

Navajo interdune lithofacies have significantly poorer reservoir characteristics than the dune lithofacies. Although interdune lithofacies are generally not as aerially extensive as the dune reservoir lithofacies above and below, they can compartmentalize a reservoir as observed in outcrops along the west flank of the San Rafael Swell (figure 11.8) (Dalrymple and Morris, 2007). Poorly developed interdune or wadi interdune lithofacies are not laterally extensive and are not effective barriers. These lithofacies have low permeability, giving them the potential to create baffles within a reservoir. Low porosity and permeable limestone of oasis deposits can create a significant barrier to fluid flow. From outcrop observations, oasis lithofacies form barriers if their lateral extent is within the limits of the structural closure of an oil field; the reservoir will be partitioned. If the interdune lithofacies only partially covers the structure, then the interdune will act as a baffle and fluids can move around the impermeable layers (Dalrymple and Morris, 2007).

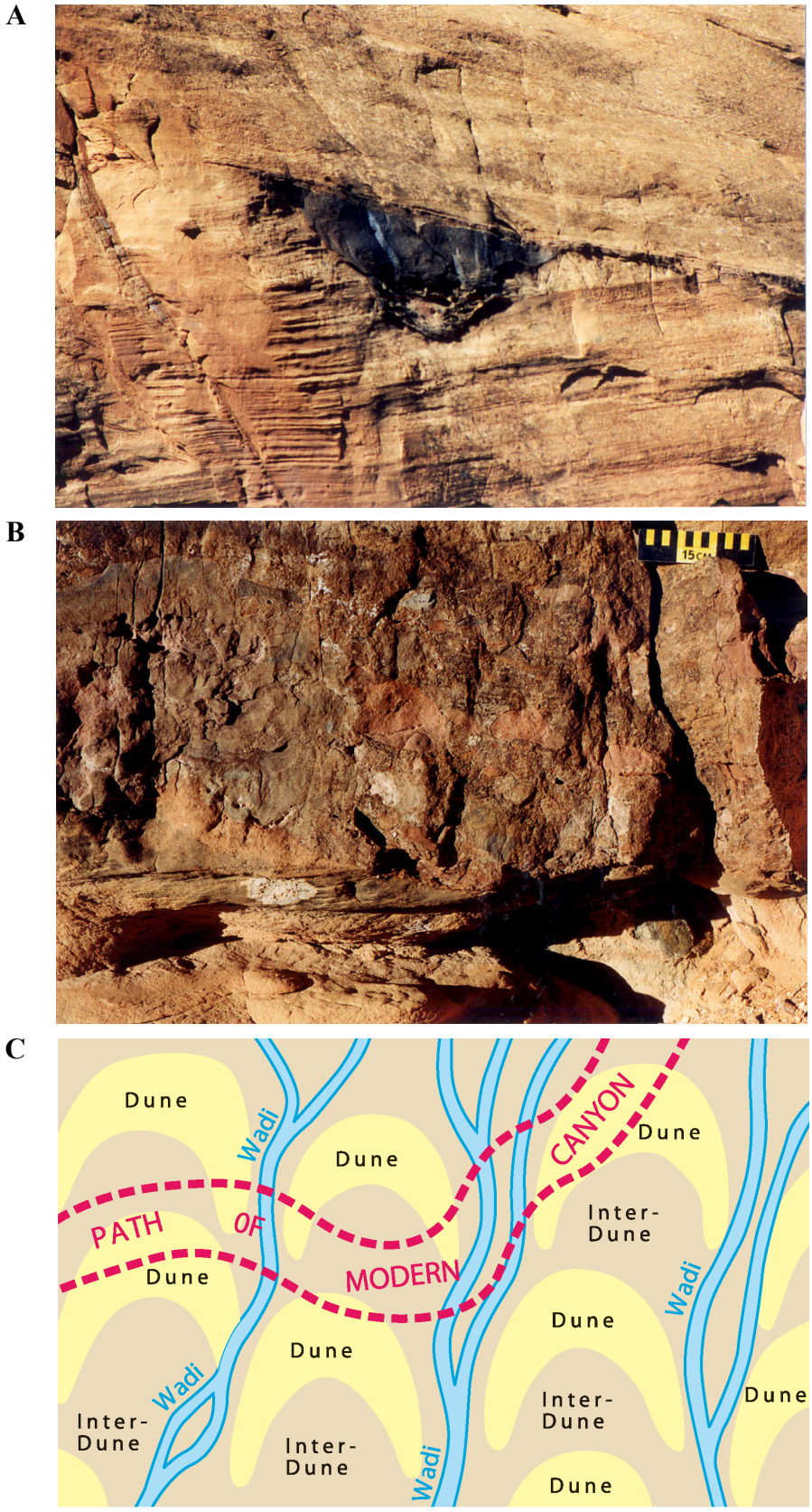

Figure 11.7. *Wadi deposits in the Navajo Sandstone at Rainbow Bridge National Monument, Utah.* ***A.*** *Wadi channel, filled with strongly cemented sand, on the cliff face of the south side of the canyon; channel deposit is about 5 feet (2 m) thick (taken with a telephoto lens).* ***B.*** *Wadi "pudding stone" consisting of sandstone and dolomitic limestone rip-up clasts in a medium- to coarse-grained sandstone matrix. Note horizontal stratification and small-scale cross-beds at base of photo.* ***C.*** *Schematic interpretation, map view, of a Navajo wadi system between large dunes with the path of a modern canyon superimposed.*

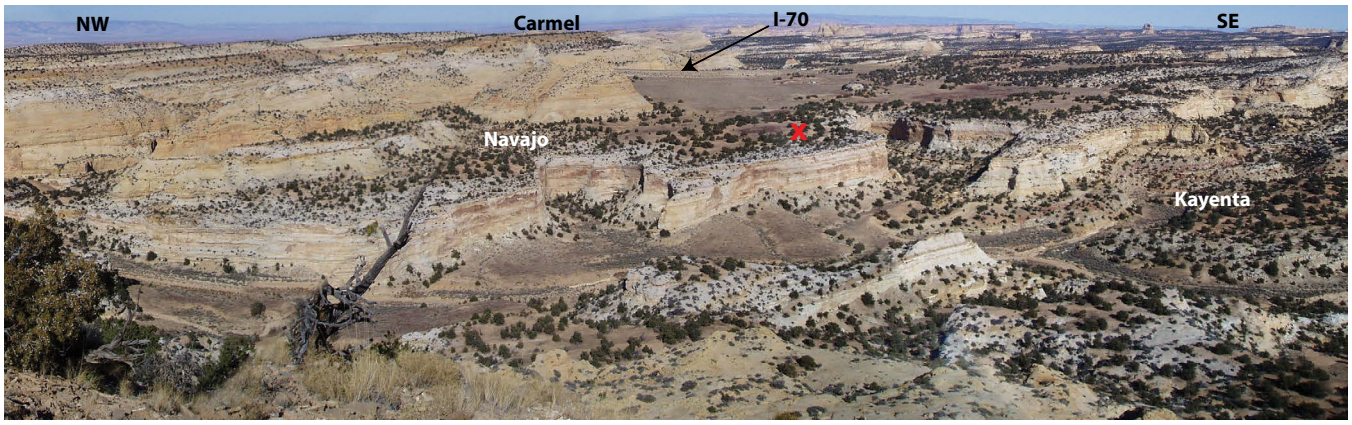

Figure 11.8. *Panorama of the Devils Canyon area, west flank of the San Rafael Swell, central Utah, showing the Navajo Sandstone. A prevalent surface within the Navajo Sandstone (red X on juniper-covered surface) represents a laterally extensive interdune deposit with low permeabilities making this facies likely a barrier to fluid flow if it were in a reservoir. Juniper trees for scale. After Dalrymple and Morris (2007).*

Identification and correlation of dune/interdune lithofacies in individual Nugget reservoirs in the thrust belt is critical to understanding their effects on production rates and paths of petroleum movement (Lindquist, 1983; Hartwick, 2010). Avalanche laminae, soft-sediment deformation, and other depositional features can also result in significant reservoir heterogeneity, even within the dune lithofacies.

Jurassic Temple Cap Formation

The Middle Jurassic Temple Cap Formation exposed near the eastern entrance to Zion National Park (and elsewhere in the park) in southwestern Utah (figures 11.9 and 11.10) is almost a perfect match to both the core and geophysical well logs from Covenant field in the Hingeline area (figures 5.3). All three members are present (figures 11.10 and 11.11): the basal Sinawava, White Throne, and the upper Esplin Point Member (Sprinkel and others, 2009; Biek and others, 2010). The Temple Cap is separated from the underlying Navajo Sandstone by the J-1 unconformity (Pipiringos and O'Sullivan, 1978). This surface is incredibly flat with little apparent relief over short distances. However, over a few miles the relief of the surface may be several hundred feet due to total Navajo thickness differences below, ranging from 1800 to 2200 feet (550–670 m) (Biek and others, 2010). In addition, the thickness of the Temples Cap and its members vary suggesting the presence of pre-Temple Cap topographic highs (Sprinkel and others, 2009; Biek and others, 2010).

In the eastern part of the park, outcrops of the Sinawava Member are 49 feet (15 m) thick and are composed of reddish-brown mudstone, siltstone, and fine-grained sandstone. The member forms a narrow, vegetated slope above the Navajo Sandstone (figure 11.10). The top of the white subunit of the upper Navajo is locally stained red by runoff from the overlying Sinawava mudstone and siltstone units (figure 11.10) (Biek and others, 2010). Siltstone units are planar to horizontal laminated. Sandstone units consist of planar beds and small-scale, low-angle cross-beds. No significant eolian units are found. The Sinawava was deposited in a coastal sabkha and tidal flat environment (Blakey, 1994; Peterson, 1994).

The White Throne Member is 164 feet (50 m) thick composed of yellowish-brown, fine-to medium-grained sandstone with interbeds of planar siltstone (Biek and others, 2010). This member forms a vertical cliff above the Sinawava Member (figure 11.10). The sandtone contains large-scale, high-angle cross-beds representing coastal eolian dunes (Blakey, 1994; Peterson, 1994).

The Esplin Point Member is 23 feet (7 m) thick composed of thin, planar to horizontal laminated beds of tan to brown siltstone and fine-grained sandstone. This unit forms a vegetated ledgey slope above the White Throne Member (figure 11.10). Radiometric age dates of ash beds yield an age of 170.2 ± 0.54 Ma; marine palynomorphs also indicate a Middle Jurassic (Bajocian) age and a return to marginal marine conditions (Sprinkel and others, 2009).

Jurassic Twin Creek Limestone

The best outcrop analogs of the Middle Jurassic Twin Creek Limestone reservoir are about 20 miles (32 km) west of Anschutz Ranch field at Devils Slide on the Crawford thrust plate (figures 11.12 and 11.13), and 9 miles (15 km) southwest of Lodgepole field near the town of Peoa, Utah, on the Absaroka thrust plate (?) (figures 11.12 and 11.14). Both sites are located along highways; however, the Devils Slide outcrop is within a large cement quarry operated by Holcim (U.S.) Inc. and permission must be obtained to gain access; also note that the configuration of the quarry wall changes. All seven formal members are recognized in these outcrops (figure 11.15).

Although the sections are faulted and display some bed repetition, portions, or the entire thickness, of all seven Twin Creek members are exposed at the Devils Slide and Peoa sites. Sections at both sites were measured and described. The Twin Creek at Devils Slide strikes generally parallel to the leading

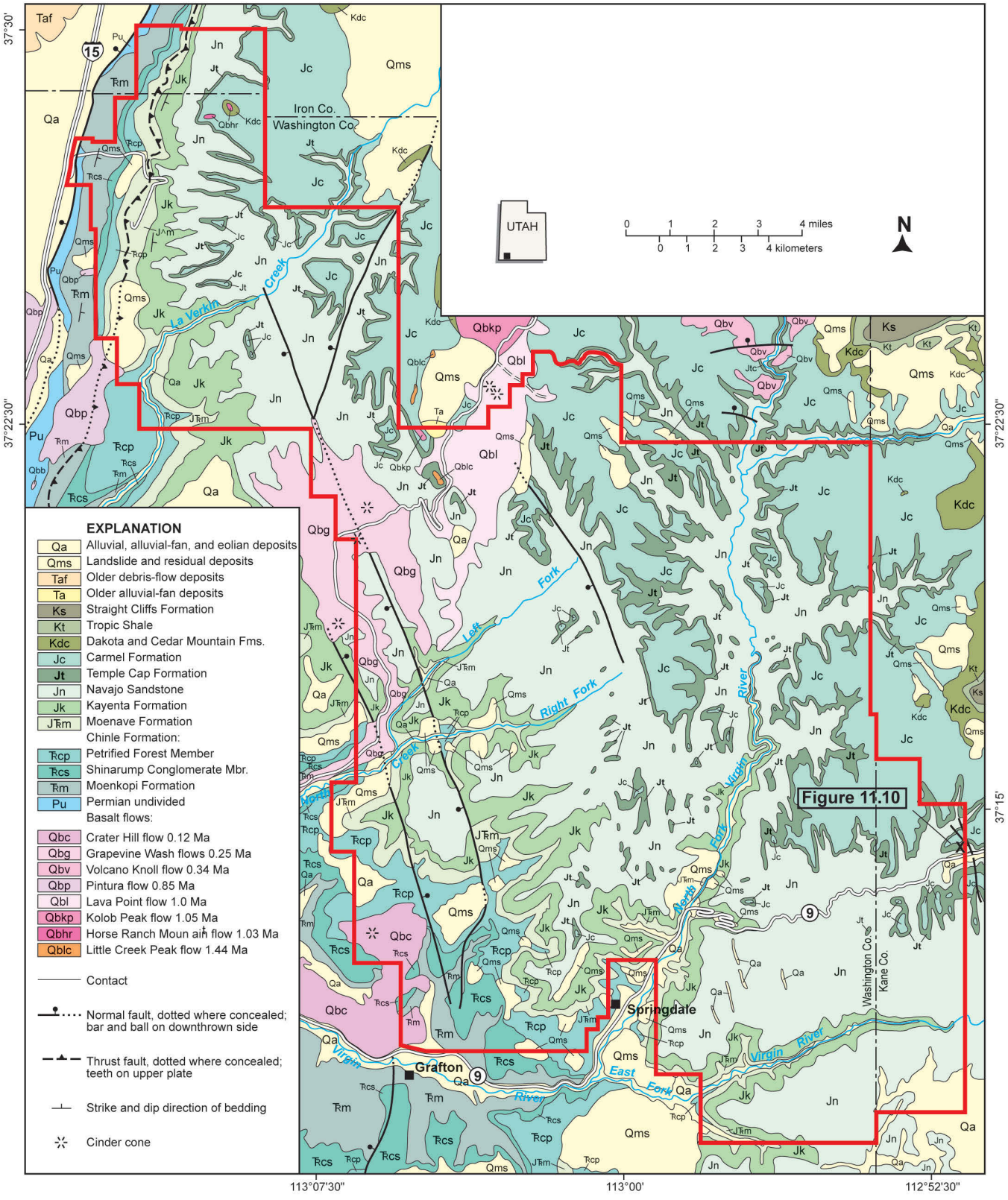

Figure 11.9. *Simplified geologic map of Zion National Park (from Biek and others, 2010). The Middle Jurassic Temple Cap Formation (Jt) is exposed throughout the park. The location of the Temple Cap outcrop is also shown on figure 11.10.*

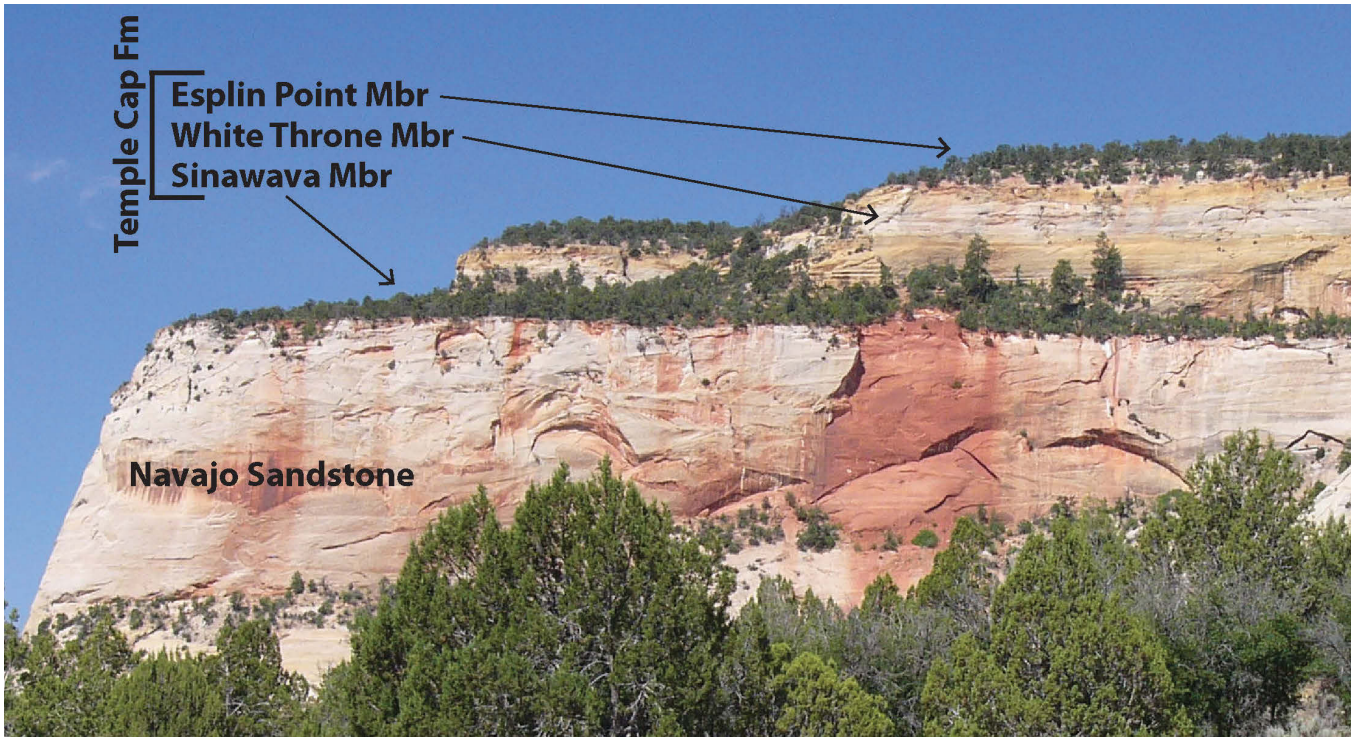

Figure 11.10. *Navajo Sandstone and Temple Cap Formation (view west) at the east gate of Zion National Park. This outcrop serves as an excellent analog to the Covenant field reservoir in the central Utah thrust belt.*

SYSTEM	SERIES	FORMATION	MEMBER	SYMBOL	THICKNESS feet	LITHOLOGY
JURASSIC	MIDDLE	CARMEL FM.	Co-op Creek Limestone Member — Upper unit	Jc	100–110	
			Co-op Creek Limestone Member — Lower unit		150–170	*Isocrinus* J-2? unconformity
		TEMPLE CAP FM.	Esplin Point Member	Jt	3–25	
			White Throne Member		0–190	
			Sinawava Member		3–60	Red marker J-1 unconformity
	LOWER	NAVAJO SANDSTONE	white subunit	Jn	0–800	Highly jointed massive vertical cliffs
			pink subunit		600–1500	Local ironstone High-angle eolian cross-beds
			brown subunit		400–600	Vertical cliffs

Figure 11.11. *Stratigraphic column of a portion of the Jurassic section in Zion National Park. Modified from Biek and others (2010).*

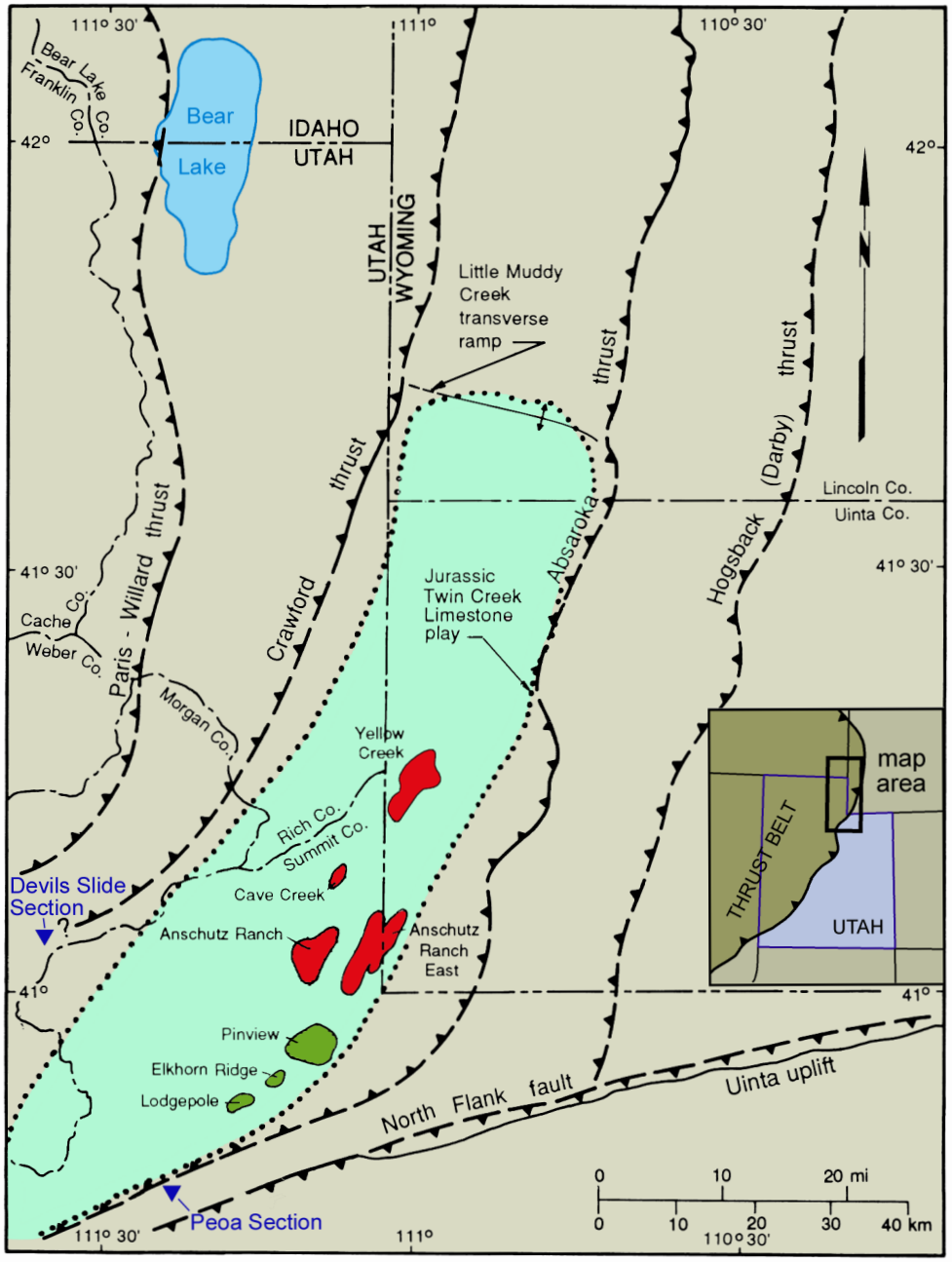

Figure 11.12. *Location of outcrop analogs for reservoirs that produce oil (green) and gas and condensate (red) from the Jurassic Twin Creek Limestone, Utah and Wyoming; major thrust faults are dashed where approximate (teeth indicate hanging wall). The Twin Creek Limestone play area is dotted. Modified from Sprinkel and Chidsey (1993).*

edge of the Crawford thrust (north-northeast) and has beds dipping greater than 65° east to overturned to the west; several small back thrusts are present (figure 11.13). The Twin Creek at Peoa strikes generally parallel to the leading edge of the Absaroka thrust (east-northeast) and the North Flank fault of the Uinta uplift, beds dip more than 70° north-northwest (figure 11.14).

These sections display the same reservoir heterogeneity characteristics that affect production or provide horizontal drilling targets in the Twin Creek Limestone productive fields. This heterogeneity, created by fracturing (or the lack thereof), and lithologic variation provide both the reservoir storage capacity and/or seals (barriers) within the traps. Fractures in the Twin Creek, as is the case with other sedimentary rocks, generally have a consistent geometry with respect to the three principal stresses (σ_1 = greatest, σ_2 = intermediate, σ_3 = least principal compressive effective stress) at the time of the fracture development (Stearns, 1984). Fractures near faults depict the stress field responsible for the fault. Fractures in folds are genetically related to the folding process itself, not a consequence of the regional stress field that produced the folding. Parallel fracture sets are commonly present, and their geometry results from compression and extension (when σ_2 is either parallel or

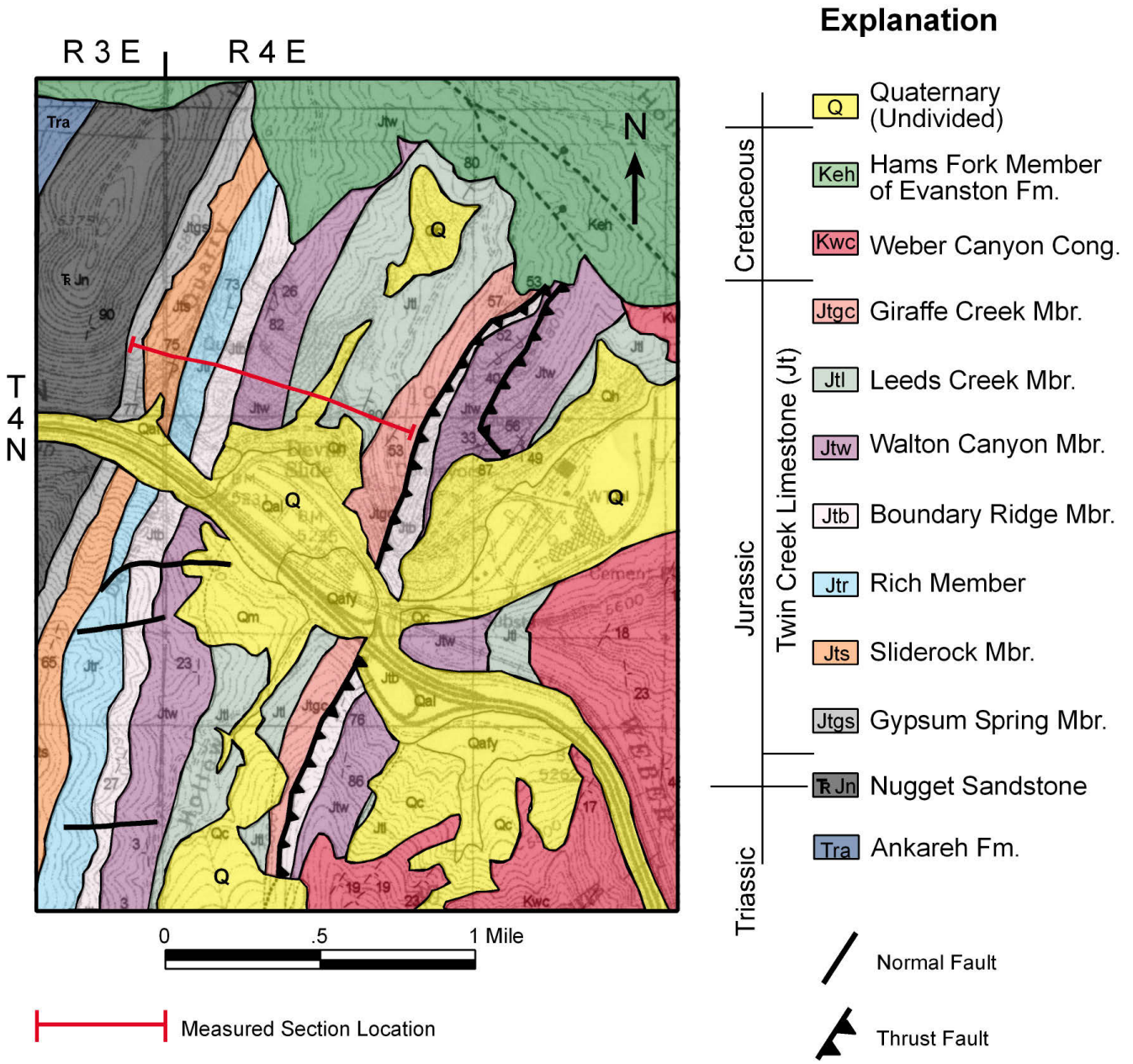

Figure 11.13. *Geologic map of the Devils Slide area, Morgan and Summit Counties, Utah, showing the location of the stratigraphic measured section through the Twin Creek Limestone. Modified from Coogan (1999). See figure 11.12 for location of Devils Slide area.*

normal to bedding) associated with the fold development as well as the type of sedimentary rock involved (Stearns, 1984). Four different orientations of the three principal stresses are recognized in folds (figure 11.16): (1) σ_1 and σ_3 in the bedding plane, σ_1 parallel to the dip direction, (2) σ_1 and σ_3 in the bedding plane, σ_1 parallel to the strike direction, (3) σ_2 parallel to bedding strike, σ_1 normal to bedding, and (4) σ_2 parallel to bedding strike, σ_3 normal to bedding. These four orientations produce 12 possible fracture planes—two shear and one extension for each orientation (Stearns, 1984).

Both faulting and folding account for outcrop orientations at the Devils Slide and Peoa sites. Thus, fractures as described above have likely been generated by these structural events. The general fracture pattern observed in the rocks at these locations can be applied to planning directions of horizontal wells proposed in the Twin Creek Limestone play.

The following sections are general outcrop descriptions of the lithology, sedimentary structures, and fracture patterns in each member of the Twin Creek Limestone, in ascending order, compiled from the Devils Slide and Peoa field observations and measured stratigraphic sections. Detailed descriptions, regional correlation, fossils, and depositional environments of these members are included in Imlay (1967).

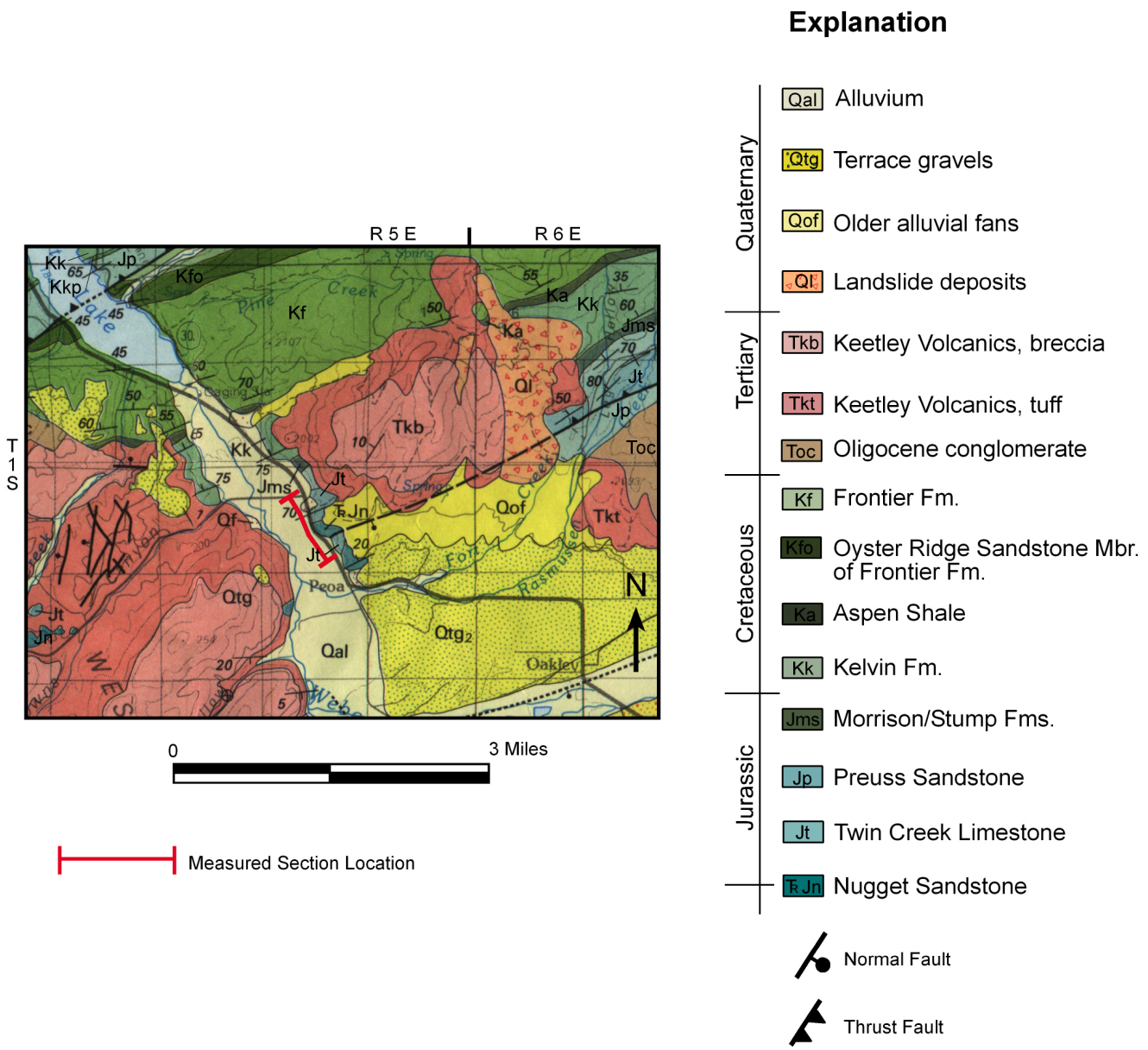

Figure 11.14. *Geologic map of the Peoa area, Summit County, Utah, showing the location of the stratigraphic measured section through the Twin Creek Limestone. Modified from Bryant (1990). See figure 11.12 for location of Peoa area.*

Gypsum Spring Member

The Gypsum Spring Member consists of shale (covered) and a basal pebble-rich to coarse-grained sandstone. Bedding is thick to medium and tabular. The sandstone is composed of rounded to subrounded frosted grains derived from the underlying Nugget Sandstone.

Sliderock Member

The Sliderock Member is composed of dark gray, micritic limestone. The unit is medium to thick bedded, often forming a resistant ledge with some thin laminations and silt partings. Fractures are abundant and commonly closely spaced. Some less resistant (highly fractured) units weather into slopes littered with plates, chips, and pencils.

Rich Member

The Rich Member is composed of light to medium gray, argillaceous to dense micritic limestone that typically forms a barren scree-covered slope (Coogan and others, in review). The lower part generally consists of lime wackestone whereas the upper part is clay-rich micritic limestone. Laminated siltstone partings and sandy limestone are also found in several units of the Rich. Bedding is thick to thin with occasional planar cross-beds and current ripples (figure 11.17A).

Rhombic fracture patterns are developed on bedding planes (figures 11.17B and 11.17C), likely the result of σ_1 and σ_3 in the bedding plane, with σ_1 parallel to the dip direction (set 1 on figure 11.16). Weathering along closely spaced rectilinear fractures within dense homogeneous limestone beds yields

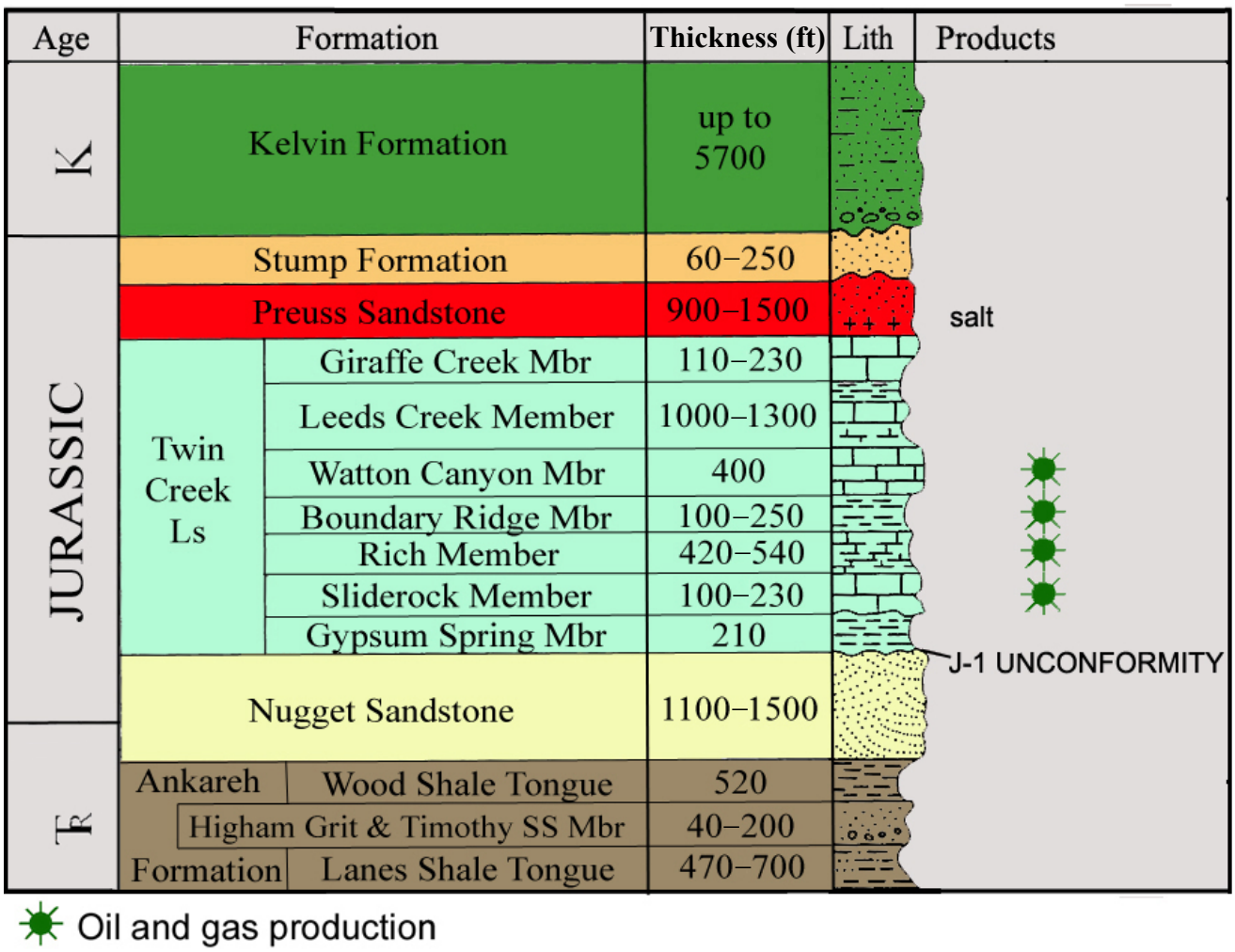

Figure 11.15. *Stratigraphic column of a portion of the Mesozoic section, including members of the Jurassic Twin Creek Limestone, exposed in Weber Canyon near Devils Slide, Morgan and Summit Counties, Utah. Modified from Hintze and Kowallis (2009).*

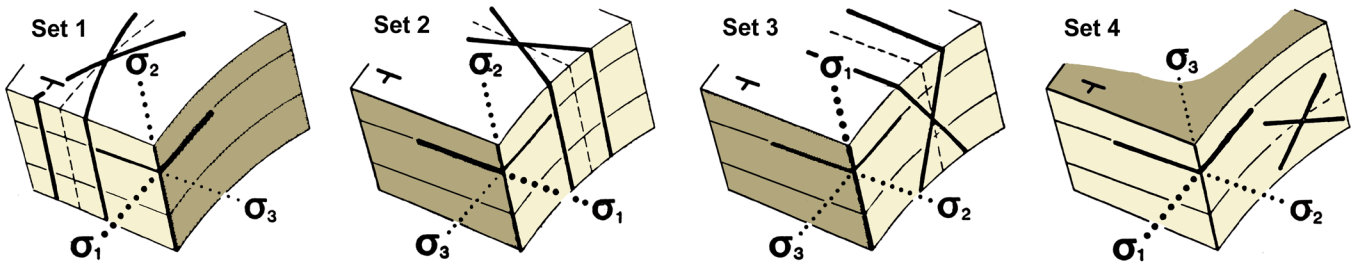

Figure 11.16. *Fracture planes generated by four orientations of the three principal stresses during folding of sedimentary rocks. After unpublished course notes, American Association of Petroleum Geologists fractured reservoir analysis school by D.W. Stearns, 1984.*

abundant pencils and plates (figures 11.17D and 11.17E). Two sets of rhombic fractures, low angle and high angle in relationship to bedding, and another set parallel to bedding are apparent in the outcrop shown on figure 11.17D. As shown on figure 11.16, these fractures correspond to both set 3, where σ_2 is parallel to bedding strike and σ_1 is normal to bedding, and set 4, where σ_2 is parallel to bedding strike and σ_3 is normal to bedding.

The crystalline to micritic limestone units of the Rich Member have little to no primary porosity. However, the contact with the basal siltstone unit (where fractures are sealed) of the overlying Boundary Ridge Member sets up the Rich for hydrocarbon trapping and production (figure 11.17F).

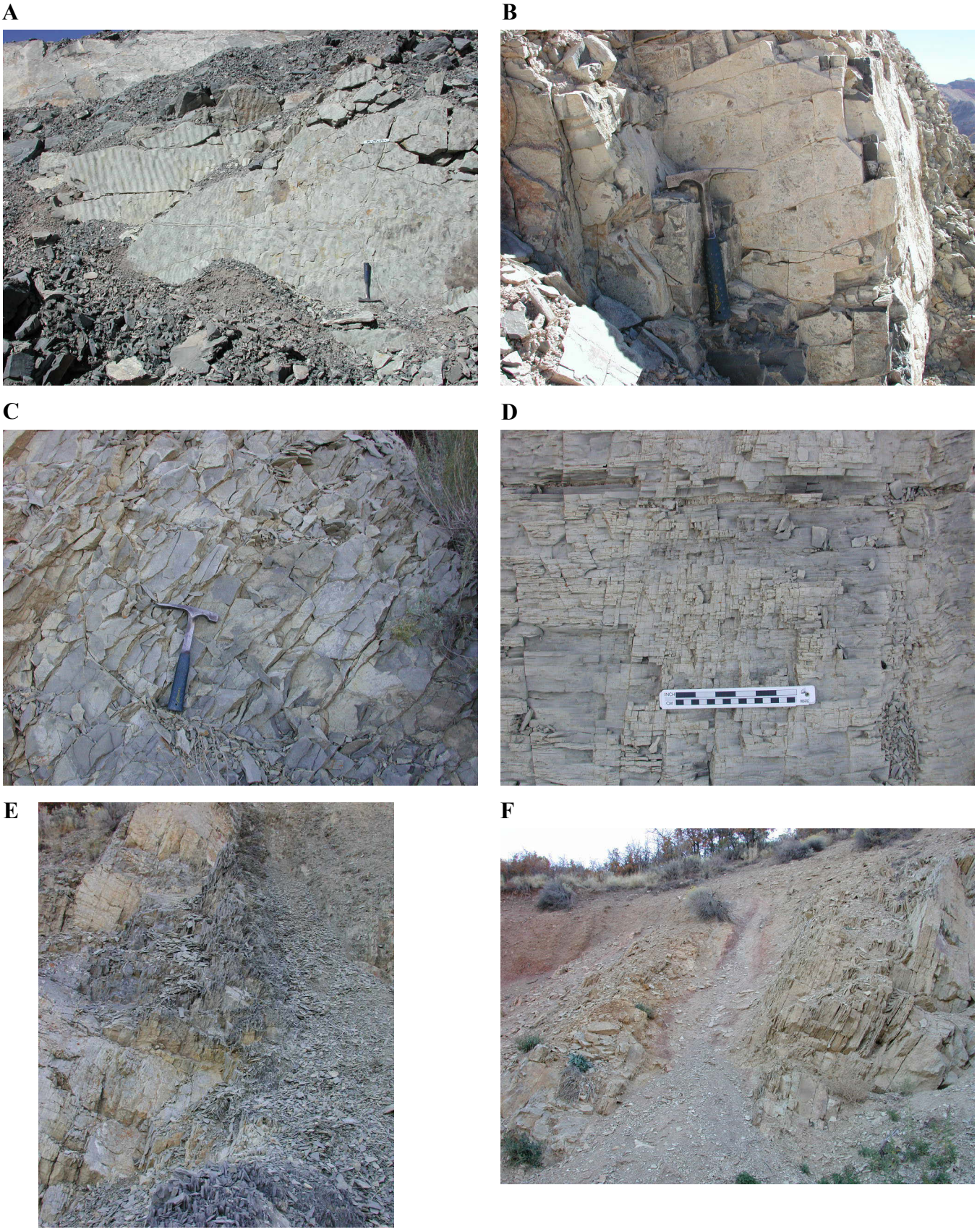

Figure 11.17. *Characteristics of the Rich Member of the Twin Creek Limestone.* ***A.*** *Well-developed current ripples on bedding surface with silt-filled fractures, Devils Slide section.* ***B.*** *and* ***C.*** *Rhombic fracture patterns on bedding planes, Devils Slide and Peoa sections, respectively.* ***D.*** *Closely spaced rectilinear fracturing, Peoa section.* ***E.*** *Pencil weathering, Peoa section.* ***F.*** *Contact between fractured Rich Member limestone and basal siltstone with sealed fractures of the overlying Boundary Ridge Member, Peoa section.*

Figure 11.18. *Devils Slide, a famous landmark along Interstate 84 in Weber Canyon, composed of resistant and non-resistant units of the Boundary Ridge Member of the Twin Creek Limestone.*

Boundary Ridge Member

The Boundary Ridge Member is composed of dark, red-brown siltstone to claystone, gray-green, micritic limestone, and very fine to fine-grained, well-sorted, gray sandstone and calcarenite. Bedding is thin to thick, with some contorted bedding (within lensoidal-shaped bodies), cross-bedding, parallel lamina, and occasional ripples. Some units contain peloids and possible fossil hash. Devils Slide is composed of resistant and non-resistant units of the Boundary Ridge Member. Dense, finely crystalline to micritic limestone with some sandy to calcarenite units form the lower and upper resistant ledges of Devils Slide, respectively (figure 11.18). Red-brown, calcareous siltstone forms the non-resistant center of Devils Slide.

Watton Canyon Member

The Watton Canyon Member is composed of dark to medium gray, dense, resistant, finely crystalline to micritic limestone. Bedding is thin to thick, with large-scale current ripples and silty lamina that exhibit cross-bedding in some units. Limestones occasionally contain stylolites, oolites, peloids, and fossils (primarily pelecypods).

Rectilinear fracturing is pervasive and includes both open and calcite-filled fractures (figure 11.19A through 11.19D); calcite-filled vugs are also present in some beds. Rhombic fracture patterns on bedding planes (figures 11.19A through 11.19D) formed from stresses with σ_1 and σ_3 in the bedding plane and with σ_1 parallel to the dip direction (set 1 on figure 11.16), and/or from σ_1 and σ_3 in the bedding plane, and σ_1 parallel to the strike direction (set 2 on figure 11.16). Fractures also occur parallel to strike on the bedding planes as shown in figures 11.19A and 11.19D, and correspond to set 3 on figure 11.16, where σ_2 is parallel to bedding strike and σ_1 is normal to bedding. The differing fracture patterns formed as the stress fields changed with folding and faulting of the stratigraphic sections over time.

Like the Rich Member, the uppermost fractured limestone unit of the Watton Canyon Member is sealed, in this case by the argillaceous basal unit of the overlying Leeds Creek Member (figure 11.19E). Reservoir heterogeneity within the Watton Canyon itself is observed in outcrop, where thin-bedded siltstones create additional barriers or baffles to fluid flow (figure 11.19F).

Leeds Creek Member

The Leeds Creek Member is composed of interbedded gray, laminated, fissile to dense, microcrystalline limestone, red-brown siltstone to gray-green calcareous mudstone, and very fine grained, well-sorted sandstone and calcarenite. Bedding is thin to thick, weathering into small chips, thick pencils, and plates. Some limestone units contain peloids or coated grains. Argillaceous or clay-rich units may contain sandy interference ripples and cross-beds. Fractures and vugs tend to be calcite filled; calcite veinlets may also be present.

Giraffe Creek Member

The Giraffe Creek Member is composed of interbedded moderately resistant, gray, medium crystalline limestone, calcareous siltstone, and fine- to medium-grained calcarenite. Some units contain oolites, and coated and lithic grains. Cross-bedding and current and interference ripples are also common; a few silty beds are lensoid. At the Devils Slide section, a rectilinear fracture pattern at the top of the Giraffe Creek is marked by a bedding-parallel back thrust (figure 11.13).

UINTA BASIN

Deep Uinta Basin Overpressured Continuous Play

The depositional environments of the Tertiary Green River and Colton reservoirs in the Altamont-Bluebell-Cedar Rim field area of the DUBOC play are, from north to south (proximal to distal): alluvial fans to fan deltas, and marginal lacustrine to open lacustrine. Sediment source was the Uinta uplift north of the field area. The Green River and Colton do not crop out north of the field area, therefore a similar tectonic

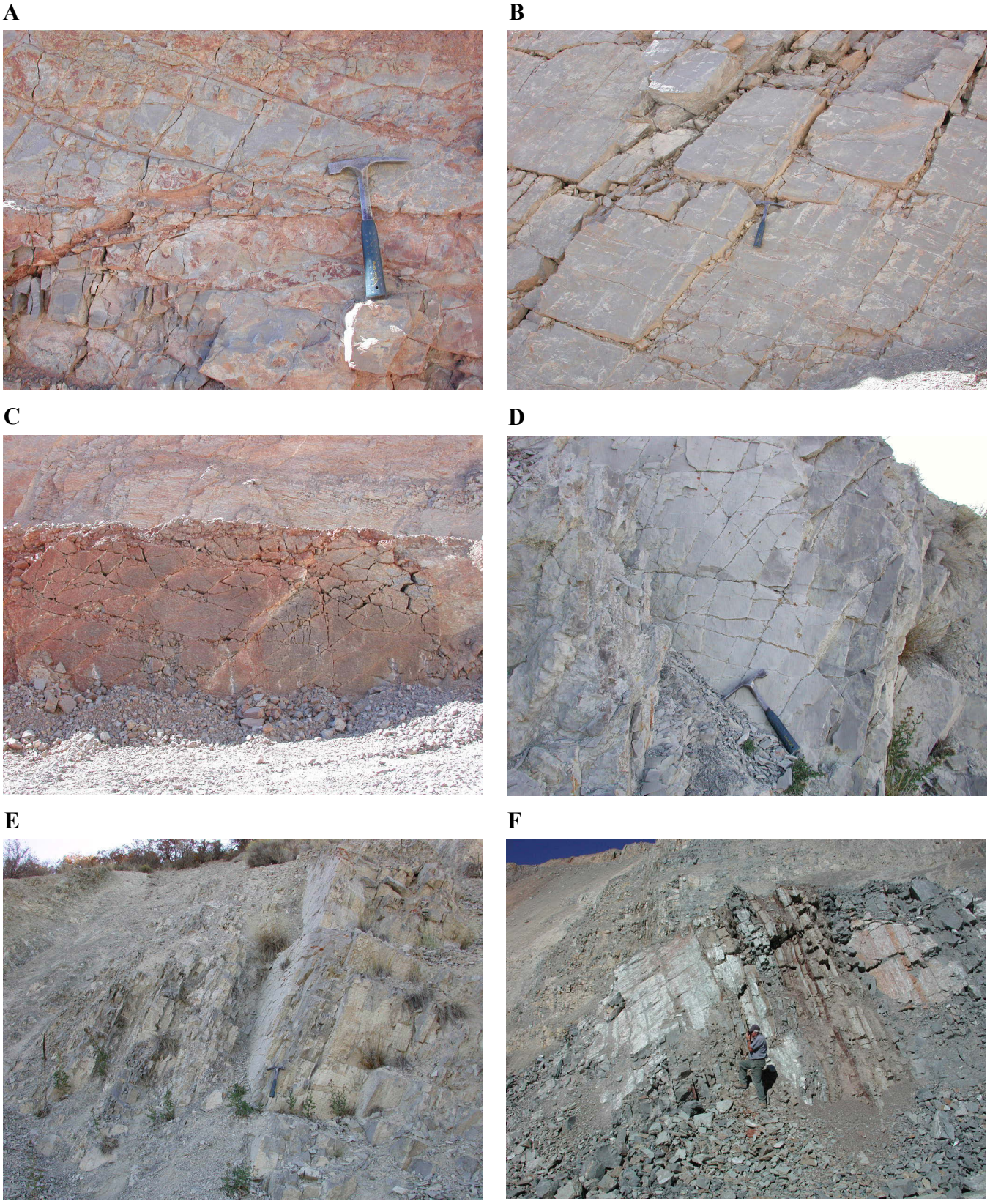

Figure 11.19. *Characteristics of the Watton Canyon Member of the Twin Creek Limestone.* ***A.*** *Closely spaced rectilinear fracturing in dense, micritic limestone, Devils Slide section.* ***B.*** *Large-scale, well-displayed rectilinear fracturing in steeply dipping limestone, Devils Slide section.* ***C.*** *Large-scale, open fractures on bedding plane surface, Devils Slide section.* ***D.*** *Well-displayed rectilinear fracturing on top of the Watton Canyon, Peoa section.* ***E.*** *Contact between fractured Watton Canyon Member limestone and basal argillaceous unit of the overlying Leeds Creek Member, Peoa section.* ***F.*** *Heterogeneity within the Watton Canyon Member caused by thin-bedded siltstone, Devils Slide section.*

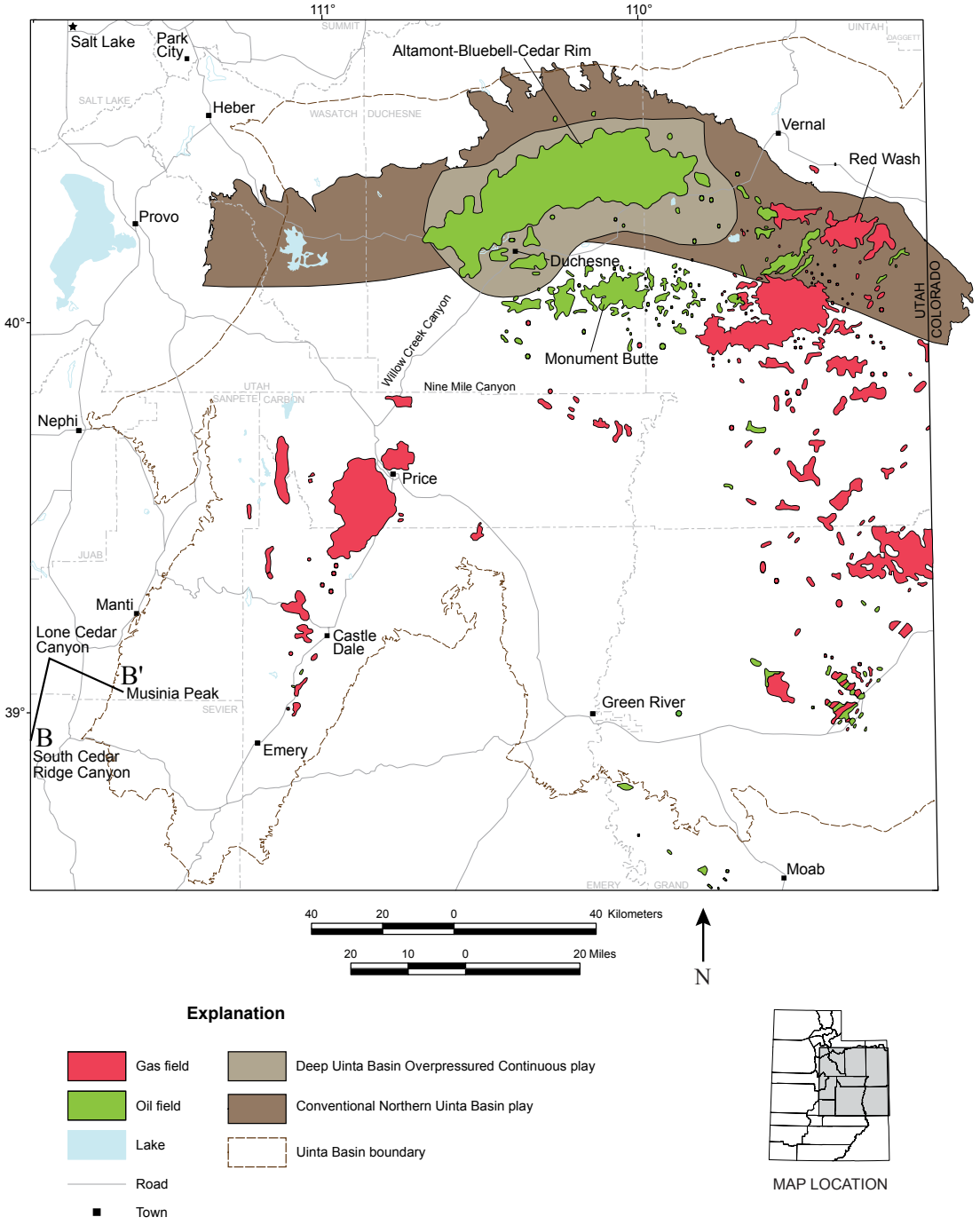

Figure 11.20. *Location map showing the outline of the Uinta Basin and major oil and gas fields. The Conventional Uinta Basin Northern play area and the Deep Uinta Basin Overpressured Continuous play area are shown. Cross section B–B' (figure 11.21) is a series of outcrops in the Flagstaff Limestone demonstrating the proximal to distal facies change that is typical of the two plays.*

setting along the western arm of Lake Uinta is presented as a reservoir analog (figure 11.20).

No single outcrop or outcrop belt provides a view of the complete proximal to distal facies changes in the Flagstaff Limestone (equivalent to the Flagstaff Member of the Green River Formation) as the depositional environment of this unit changes from fan deltas to open lacustrine. Three different locations in Sevier and Sanpete Counties provide good outcrop examples of the various facies shed off the western highlands into Lake Uinta (figure 11.21). South Cedar Ridge Canyon contains exposures of proximal facies consisting of interbedded conglomerate, sandstone, and siltstone that were commonly deposited in water as fan deltas extending into Lake Uinta (figures 11.22 and 11.23). Exposures of medial facies in Lone Cedar Canyon have been described as interbedded shale, sandstone, and limestone deposited in a marginal-lacustrine environment. Another good exposure of the Flagstaff that is more accessible is in Price River Canyon (figure 11.24); here the medial facies of the Flagstaff is composed of open-

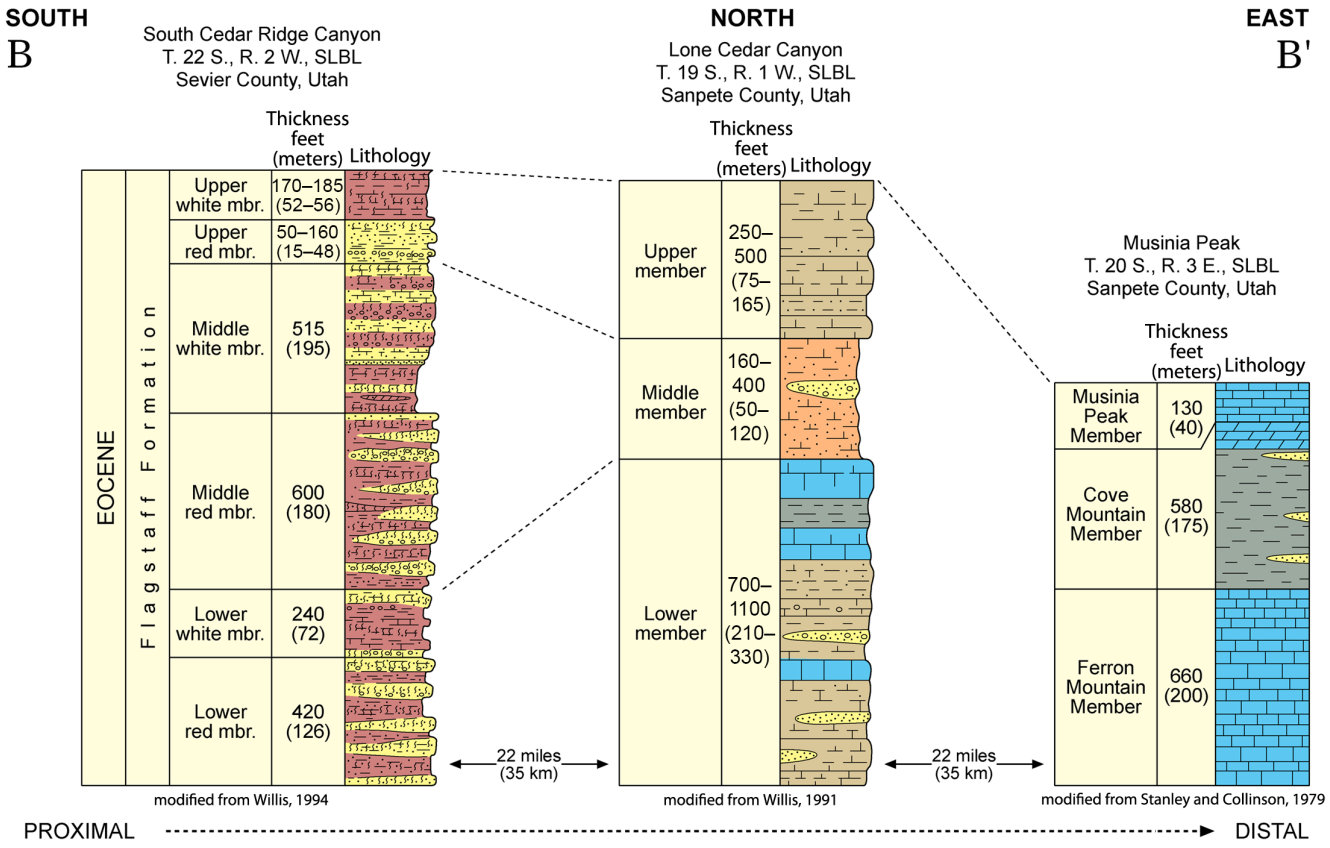

Figure 11.21. *Cross section of measured stratigraphic sections showing transition from proximal to distal facies in the Flagstaff Limestone, similar to the north-south facies change in the Altamont-Bluebell-Cedar Rim field area. Line of section shown on figure 11.20.*

Figure 11.22. *Proximal facies of the Flagstaff Limestone exposed along the east face of the Gunnison Plateau. At this location the Flagstaff is composed of sandstone and siltstone deposited as alluvial fans from the highlands to the southwest. View to the west.*

Figure 11.23. *Sandstone and conglomerate beds in the proximal facies of the Flagstaff Limestone in South Cedar Ridge Canyon. Some of these beds appear to have been deposited in shallow lake water as fan deltas. View to the north.*

Figure 11.24. *Marginal-lacustrine medial facies of the Flagstaff Member of the Green River Formation in Price River Canyon. The outcrop is composed of interbedded red and gray shale, sandstone, and some carbonate. View to the west.*

Figure 11.25. *Distal facies of the Flagstaff Limestone exposed in Manti Canyon on the Wasatch Plateau. The outcrop is composed of open-lacustrine limestone and shale overlying the North Horn Formation (red beds). View to the north.*

lacustrine shale and limestone. Distal Flagstaff facies are also exposed on the Gunnison Plateau and in Manti Canyon (figure 11.25) on the Wasatch Plateau.

Conventional Northern Uinta Basin Play

An outcrop analog for the major oil reservoirs in the Green River Formation in the CNUB play is available along Raven Ridge in the northeastern Uinta Basin (figure 11.26). The Raven Ridge outcrop belt is a 20-mile-long (32 km), dip-oblique transect. Shoreline trends in the Green River are generally east-west and therefore the northwest to southeast outcrop exhibits about 14 miles (23 km) of landward to lakeward facies transitions (Borer, 2003). Several locations offer excellent exposures of shoreline deposits (figure 11.27) that serve as reservoirs, and bay-fill deposits (figure 11.28) that provide organic-rich source rocks for the play. Borer and McPherson (1998), and Borer (2003) have done extensive work on the Raven Ridge outcrops and presented their results in two unpublished field trip guidebooks. Oil Gully is just one of their measured sections, although there are numerous other excellent exposures along Raven Ridge described by Borer and McPherson (1998), and Borer (2003). The following description of Oil Gully is taken largely from their work.

Oil Gully, named for the many tar sands in the exposed rocks, is a good outcrop analog for the reservoirs at Red Wash field. Borer (2003) measured 300 feet (100 m) of section in Oil Gully, which contains numerous depositional rise-to-fall cycles (figure 11.29). Some of the features that Borer describes at Oil Gully include landward-migrating bar forms that develop transgressive caps, gravity flow cycles, and lagoonal and high-energy, upper shoreface facies.

Conventional Southern Uinta Basin Play

Outcrop analogs for the major oil reservoirs in the Green River Formation in the CSUB play are presented in the following sections. The Green River Formation is well exposed in Willow Creek, Indian, and Nine Mile Canyons in the south-central Uinta Basin (figure 11.30). Morgan (2003a) presented road logs describing the exposures in these canyons. The exposures in Willow Creek Canyon are generally limited to road cuts, which provide easy access but limited lateral extent. Indian Canyon provides an excellent view of the upper and saline members of the Green River. Nine Mile Canyon has more than 30 miles (50 km) of continuous exposures of the Green River Formation.

Uteland Butte Interval

The Uteland Butte interval is exposed in Nine Mile Canyon (figure 11.31). At this location, the Uteland Butte interval overlies the Colton Formation and is overlain by a tongue of the Colton (figure 11.32). Little (1988) described the interval as dolomitized ostracod and pellet grainstone and packstone

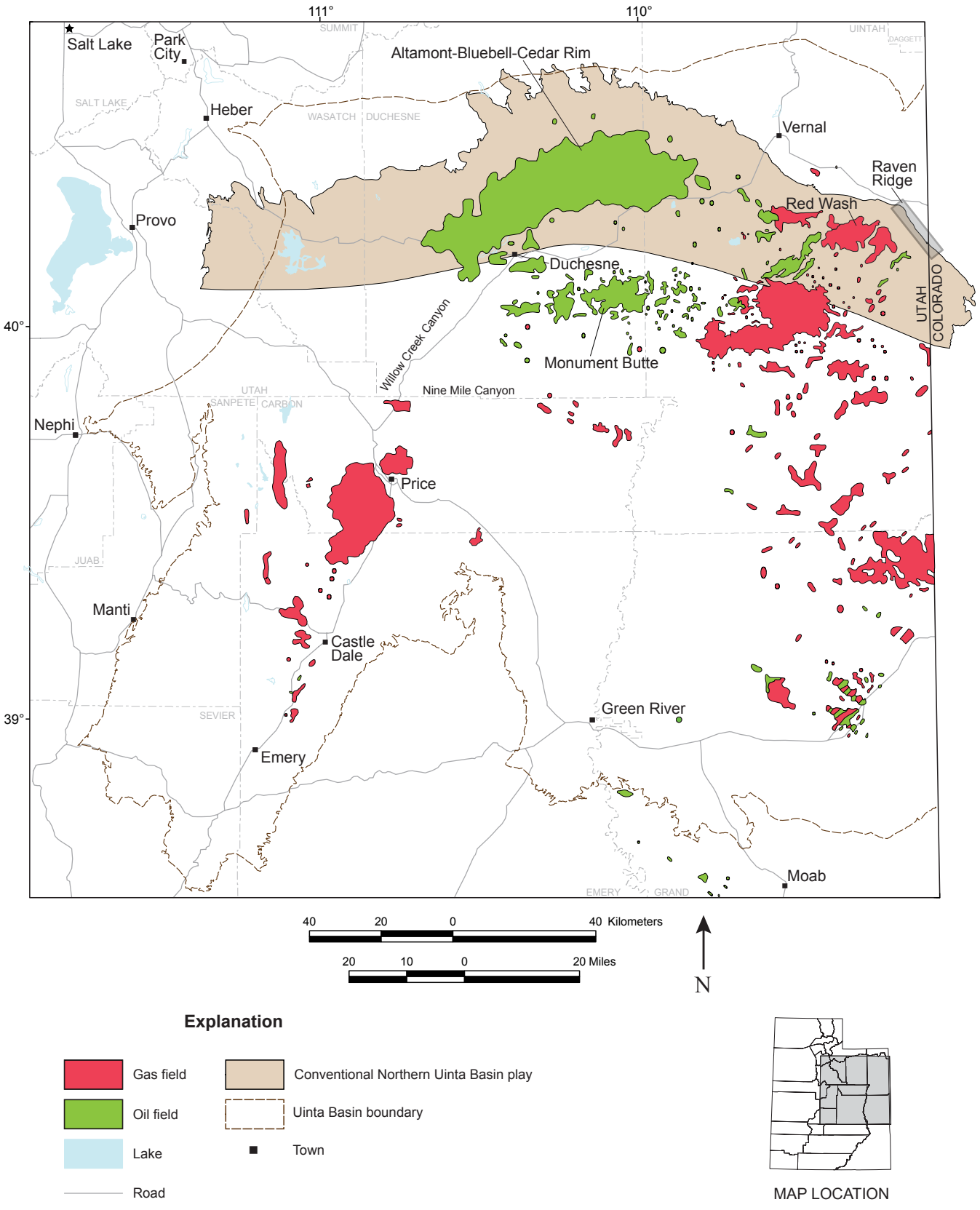

Figure 11.26. *Location map showing the outline of the Uinta Basin and major oil and gas fields. The Conventional Northern Uinta Basin play area is colored tan and the location of Raven Ridge where the Green River Formation is exposed is indicated.*

Figure 11.27. *Douglas Creek Member of the Green River Formation and underlying Wasatch Formation exposed along Raven Ridge. The outcrop is a good analog to sandstone reservoirs in Red Wash field of the Conventional Northern Uinta Basin play. View to the north.*

Figure 11.28. *Organic-rich shale representing good oil source rock in the Douglas Creek Member of the Green River Formation at Raven Ridge of the Conventional Northern Uinta Basin play.*

deposited in shallow-water mudflats; pelecypod-gastropod sandy grainstone, including coquina, commonly interbedded with silty claystone or carbonate mudstone (dolomite) that was deposited in shallow nearshore to open-lacustrine environments; and dark-gray kerogen-rich carbonates that were deposited in deeper offshore environments (figures 11.33 and 11.34). The reservoir rocks are thin fractured dolomites and grainstones (Vanden Berg and others, 2013).

Castle Peak Interval

The Castle Peak interval is exposed in the western portion of Nine Mile Canyon (figure 11.35). At this location, the interval overlies the previously mentioned Colton tongue and is overlain by the Travis interval. The top of the Castle Peak is picked at the top of the carbonate marker bed of Ryder and others (1976). At this location, Remy (1992) measured 443 feet (135 m) of interbedded carbonate, shale, and sandstone (figure 11.36). The primary reservoir rocks are channel sandstone beds described as generally having a sharp base with some rip-up clasts and trough cross-beds, fining upwards from medium to fine grained, and having low-angle to planar bedding. The sandstone beds are typically isolated channel deposits (figure 11.37).

Travis, Monument Butte, and Beluga Intervals

The primary reservoirs for the Travis interval are turbidite and gravity-flow deposits, which have not been identified in outcrop. The secondary reservoirs in the Travis interval and the primary reservoirs in the Monument Butte and Beluga intervals are distributary-channel deposits. The Monument Butte interval typically contains amalgamated stacked channel deposits, whereas in the Travis and Beluga intervals, the distributary channels are generally isolated individual channels. Although the volume of reservoir rock varies between the intervals, the depositional and petrophysical properties are similar. Therefore, one location is described as an outcrop analog for the Travis (secondary reservoir), Monument Butte, and Beluga intervals.

We studied the outcrops from Petes Canyon to Gate Canyon in Nine Mile Canyon (figure 11.38) as an analog to the oil reservoirs in the Monument Butte and adjacent oil fields (Morgan and others, 2003). These outcrops, termed the Nutter's Ranch study site because of its proximity to the historical Nutter Ranch house, lie within section 32, T. 11 S., R. 15 E. (SLBL&M), in Duchesne County, and contain a well-exposed, large-scale depositional cycle (table 11.1). The complete sequence exposed at the Nutter's Ranch study site was described by Remy (1992).

Detailed examination of the outcrop identified the potential heterogeneity that can exist between wells in two dimensions (as well as over a square mile), as an analogy to a typical water-flood unit in the Monument Butte area to the north. Wells in the Monument Butte area are drilled on 40-acre (16.2 ha) spacing resulting in about 1320 feet (400 m) between wells. The typical water-flood unit in the Monument Butte area is a square mile (one section) or larger, with wells in the center of every 40-acre (16.2 ha) lot, or 16 wells per section. The wells are initially completed as oil wells, but after they have all been drilled and the primary production drops below a minimum level, every other well is converted to a water injection well, resulting in eight producing and eight injection wells per section.

The Nutter's Ranch study site includes portions of Petes Canyon and Gate Canyon, and the portion of Nine Mile Canyon between these canyons. The exposure is about 2000 feet (600 m) in the east-to-west direction in Nine Mile Canyon and in the north-to-south direction in Gate Canyon, and about 4200 feet (1300 m) in the north-to-south direction in Petes Canyon. The stratigraphic interval studied is slightly more than 100

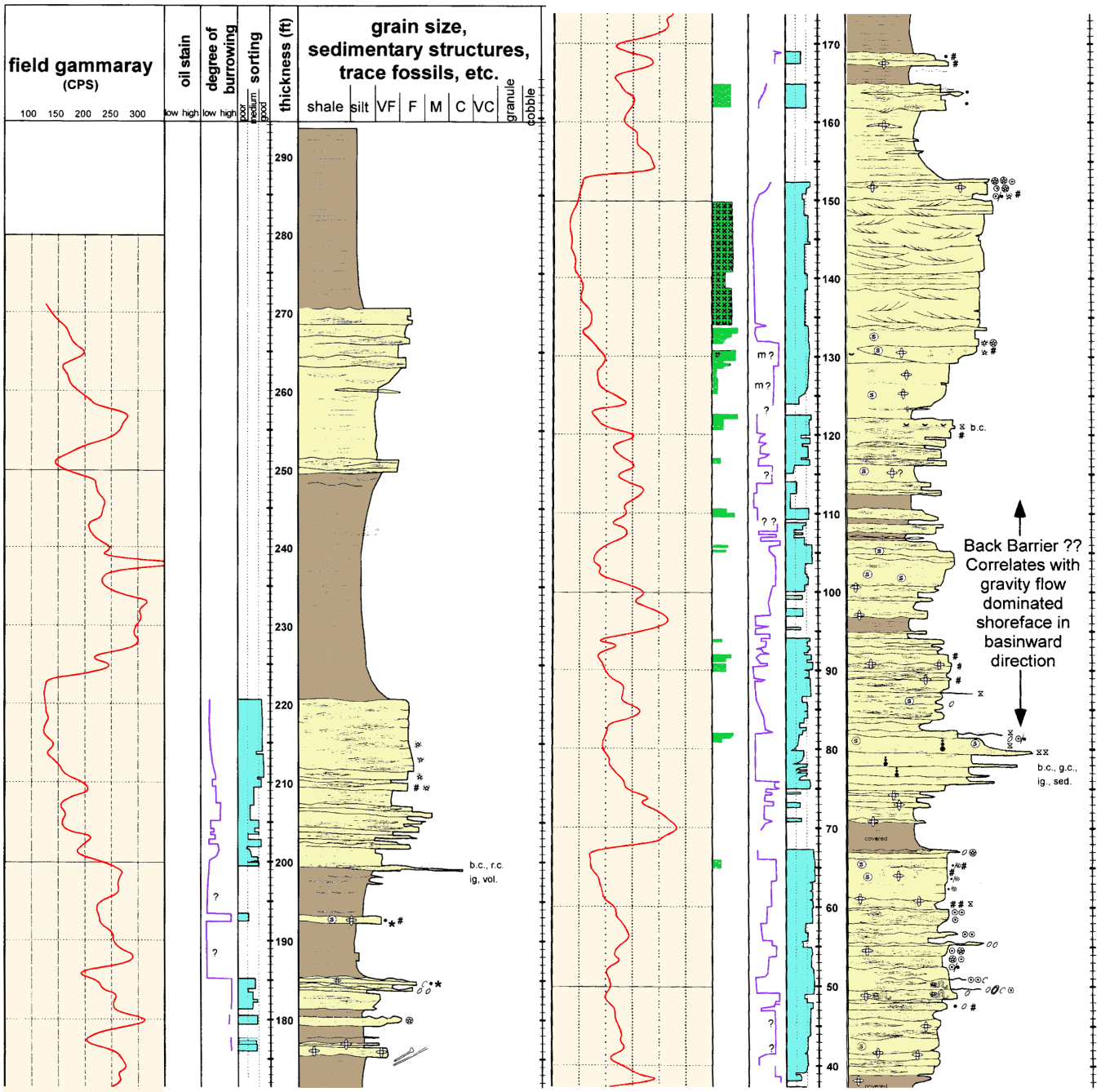

Figure 11.29. *Stratigraphic measured section of Douglas Creek Member, Green River Formation at Oil Gully, Raven Ridge, Uintah County, Utah. From Borer (2003).*

feet (30 m) thick, and is bounded by carbonate beds at the base (M8) and at the top (M9) (figure 11.39). Eight sections were measured and described, and gamma-ray data were gathered from five of the sections. To aid in the stratigraphic interpretation, the site was photographed from the canyon walls opposite the study site, and photomontages were compiled. The photomontages were used to map out individual beds and their relationships (Morgan and others, 1999, 2003).

Two imaginary wells along the Nine Mile Canyon portion of the Nutter's Ranch study site are shown 1320 feet (400 m) apart to illustrate the type of reservoir heterogeneity that could exist between two wells drilled on 40-acre (16.2 ha) spacing units (figures 11.40 and 11.41). Both of the imaginary wells encounter a carbonate bed above (M9) and below (M8), and two reservoir-quality sandstone beds. Well logs could be interpreted to show excellent correlation of the carbonate and sandstone beds (figure 11.40). As a result, good lateral continuity of the sandstone beds would be expected. However, contrary to the interpretation in figure 11.40, the upper sandstone in the two wells is actually two separate deposits (Ss-e and Ss-f) that would probably have very poor to no fluid flow

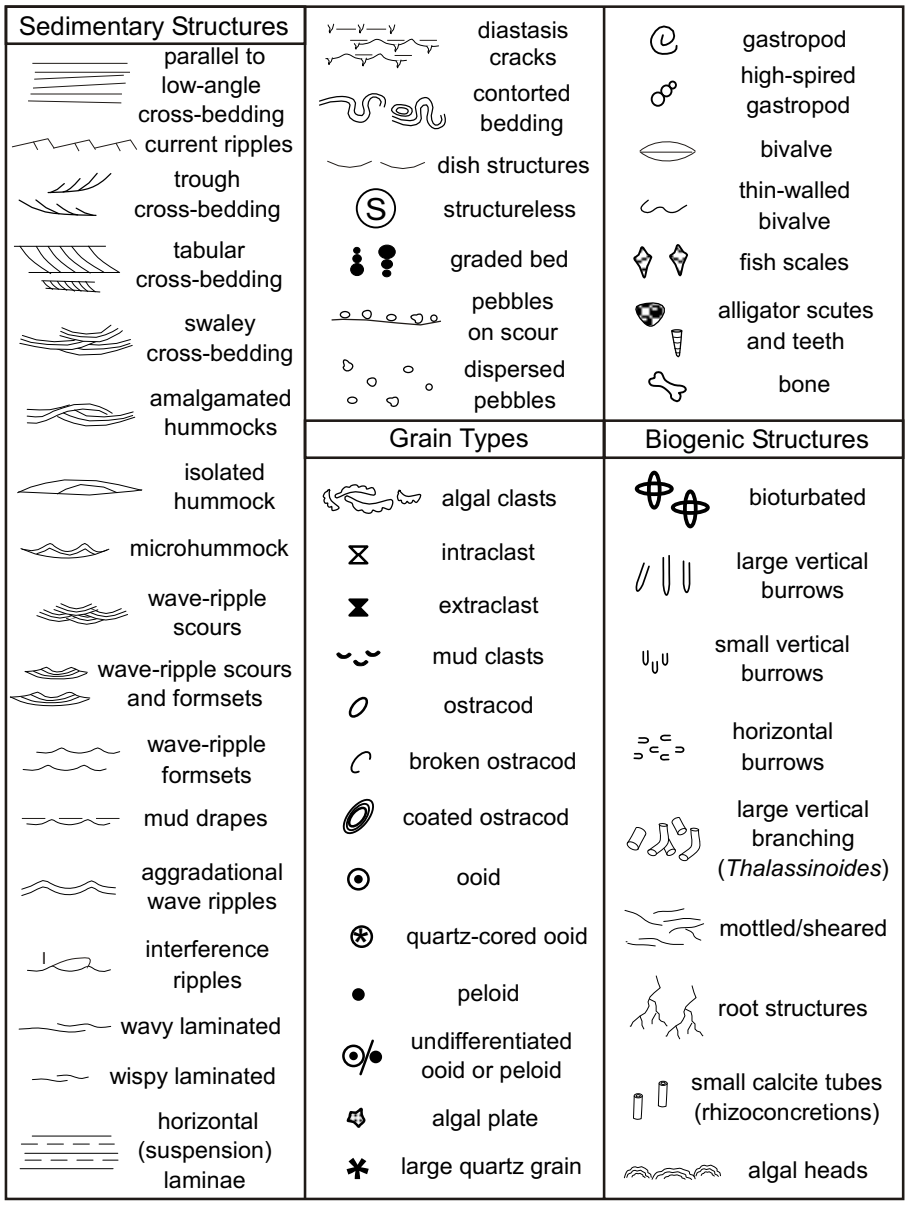

Figure 11.29. *Continued.*

between them (figure 11.41). Ss-e is an amalgamated channel deposit that has good reservoir potential, but Ss-f is a crevasse splay deposit that has complex internal heterogeneity in the proximal channel facies and high clay content in the distal bar facies. As seen on outcrop, the lower sandstone (Ss-c) is the same bed in both of the wells, but has been locally cut out by the overlying channel sandstone (Ss-d). In some places Ss-e has incised down to Ss-c, creating a potential for fluid-flow communication between the two sandstone beds. Ss-d nearly cuts out Ss-c and is a potential reservoir that is not penetrated by either of the imaginary wells. Ss-a is laterally continuous but thin and has poor porosity and permeability due to abundant clay. Ss-b is a very narrow bed that would rarely be penetrated by a well with 40-acre (16.2 ha) spacing and would probably not have sufficient storage capacity to be an economical oil reservoir.

The thickness of the three potential reservoir sandstone beds (Ss-c, Ss-d, and Ss-e) was determined by direct measurement and by extrapolating between the measured sections using photomontages. The sandstone thickness values and associated Universal Transverse Mercator (UTM) coordinates were entered into an Arcview® database. The section that contains the study site (section 32, T. 11 S., R. 15 E., SLBL) was divided into 40-acre (16.2 ha) lots, and the UTM coordinates for the center of each lot were determined and entered into the database as an oil well location with a well number (figure 11.42). Every other well was designated as a water injection well, the typical pattern for a water flood in the Monument Butte area. The imaginary wells in the 2-D model were located directly along the outcrop. The imaginary well locations for the 3-D model are the centers of 40-acre (16.2 ha) lots, and are not the same as the 2-D model imaginary well locations.

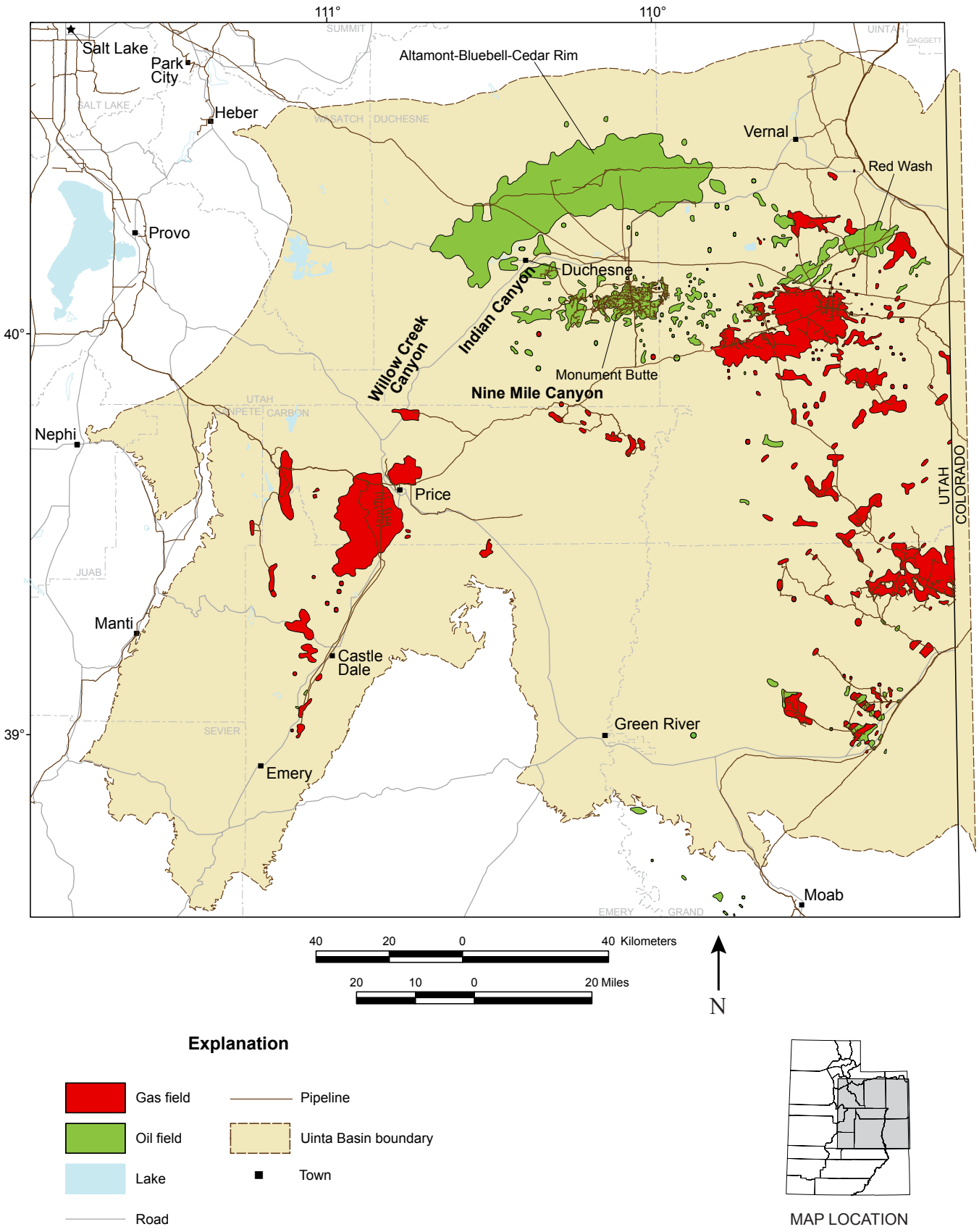

Figure 11.30. *Map showing the location of the Uinta Basin (as defined by Dubiel [2003]), outcrop analogs (Willow Creek, Indian, and Nine Mile Canyons), and the oil and gas fields in and around the basin.*

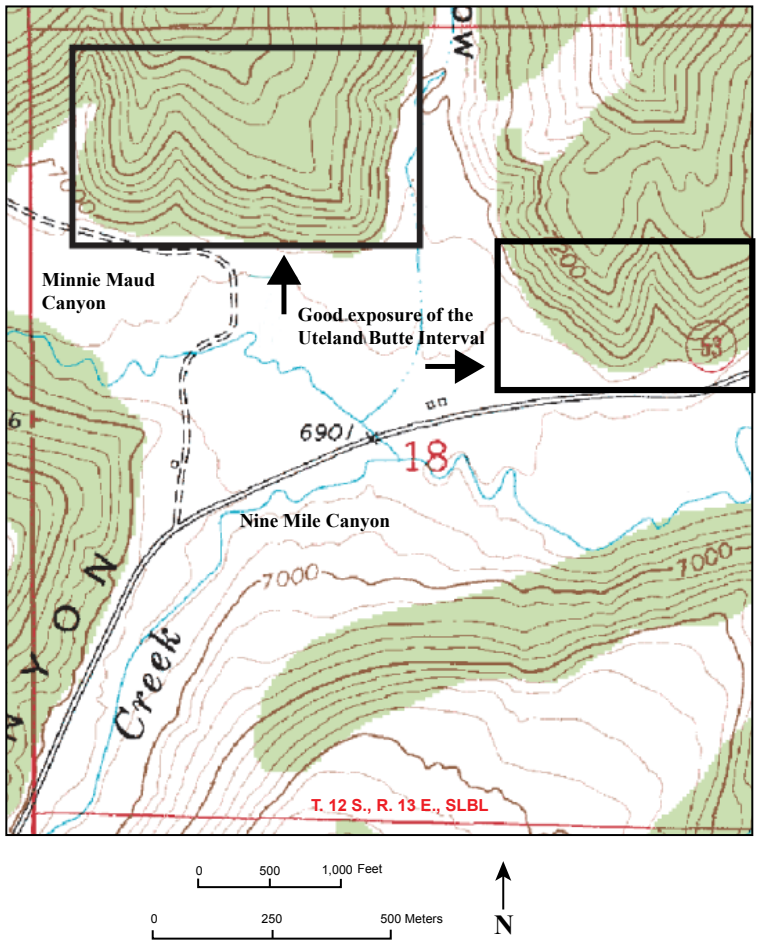

Figure 11.31. *Map showing the location of exposures of the Uteland Butte interval in the lower Green River Formation, described by Little (1988) and Vanden Berg and others (2013) at the junction of Minnie Maud and Nine Mile Canyons. Base map modified from the USGS Minnie Maud Creek East 7.5 minute quadrangle.*

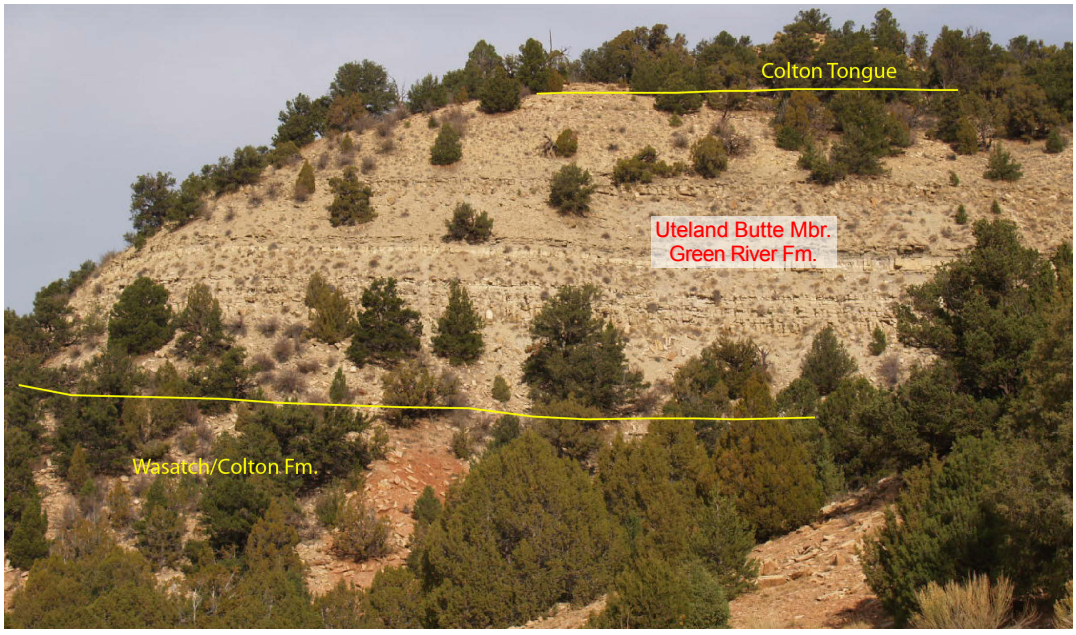

Figure 11.32. *Outcrop of the Uteland Butte interval of the lower Green River Formation and overlying and underlying formations, Nine Mile Canyon, central Utah; see figure 11.31 for location. View to the north.*

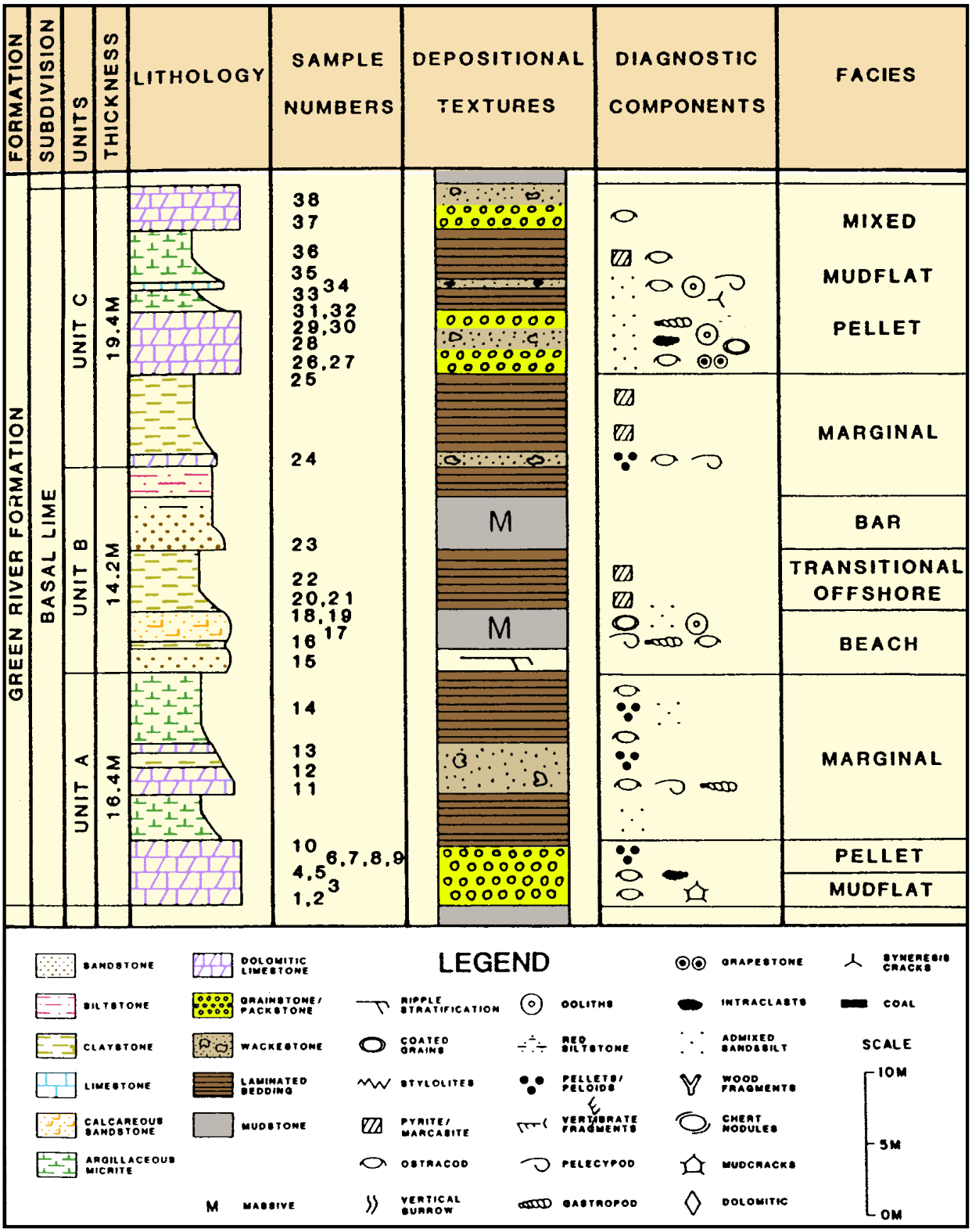

Figure 11.33. *Stratigraphic measured section by Little (1988) of the Uteland Butte interval of the Green River Formation (Little's basal limestone facies) at the junction of Minnie Maud and Nine Mile Canyons.*

Figure 11.34. *Fresh road cut exposing the Uteland Butte interval of the lower Green River Formation consisting of interbedded dolomite, mudstone, and ostracod-bearing limestone, Nine Mile Canyon.*

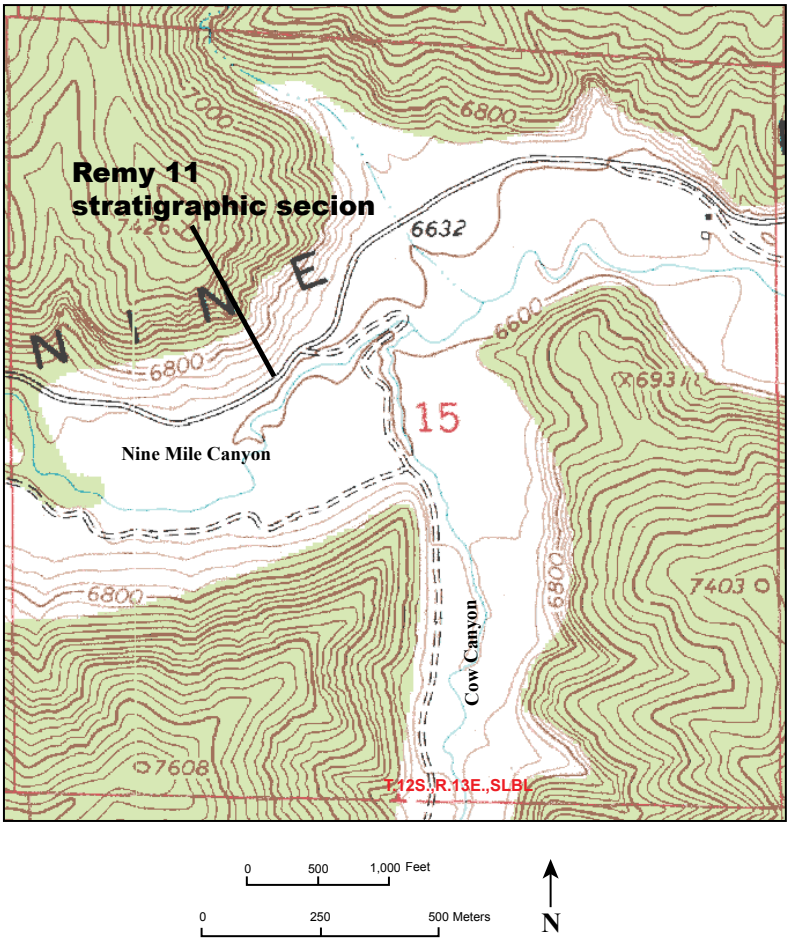

Figure 11.35. *Map showing the location of the stratigraphic measured section of the Castle Peak interval and lower part of the Travis interval of the Green River Formation, by Remy (1992). Base map modified from the USGS Wood Canyon 7.5-minute quadrangle.*

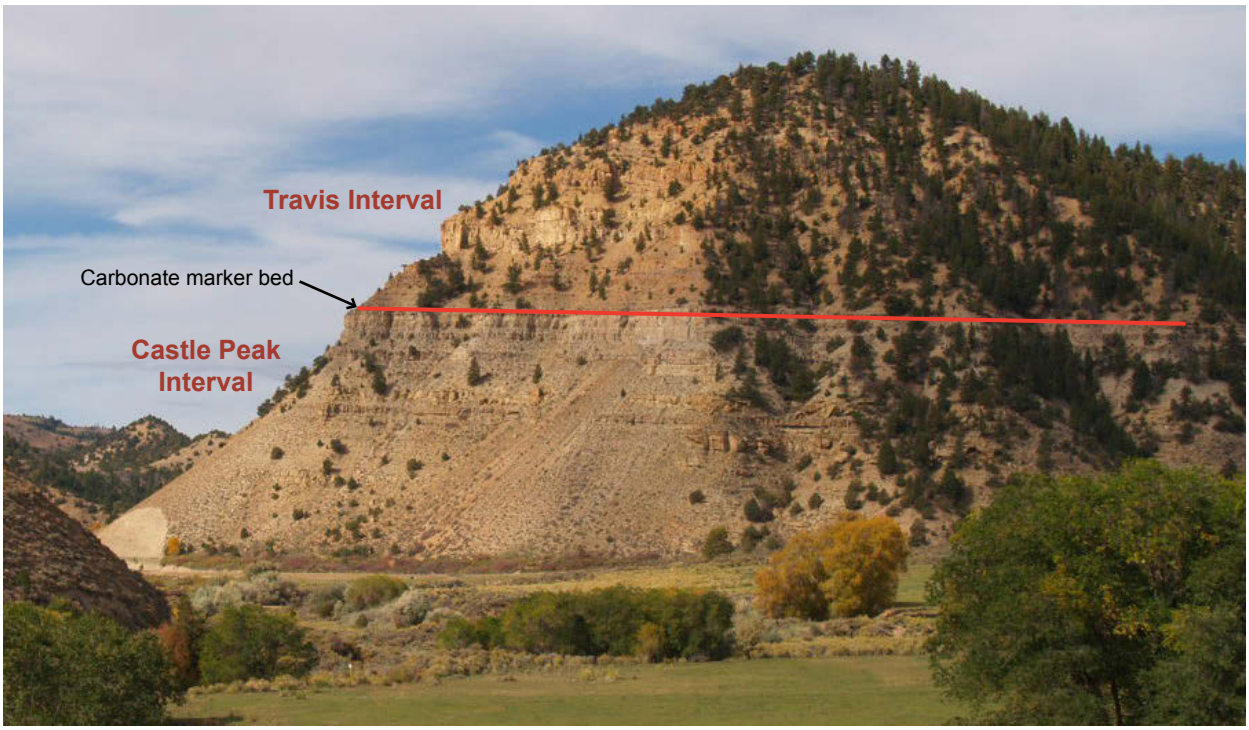

Figure 11.36. *Photograph showing the location (figure 11.35) of Remy's (1992) stratigraphic measured section of the Castle Peak interval and lower part of the Travis interval of the Green River Formation. View to the west. The Castle Peak and Travis intervals are now referred to as the Sunnyside delta interval and carbonate marker unit, respectively, in most current outcrop studies. Photo by Michael Vanden Berg, UGS.*

Figure 11.37. *Photograph of a carbonate bed and overlying channel sandstone deposit in the Castle Peak interval (also called the carbonate marker unit in more recent outcrop studies) of the Green River Formation, Nine Mile Canyon. Photo by Michael Vanden Berg, UGS.*

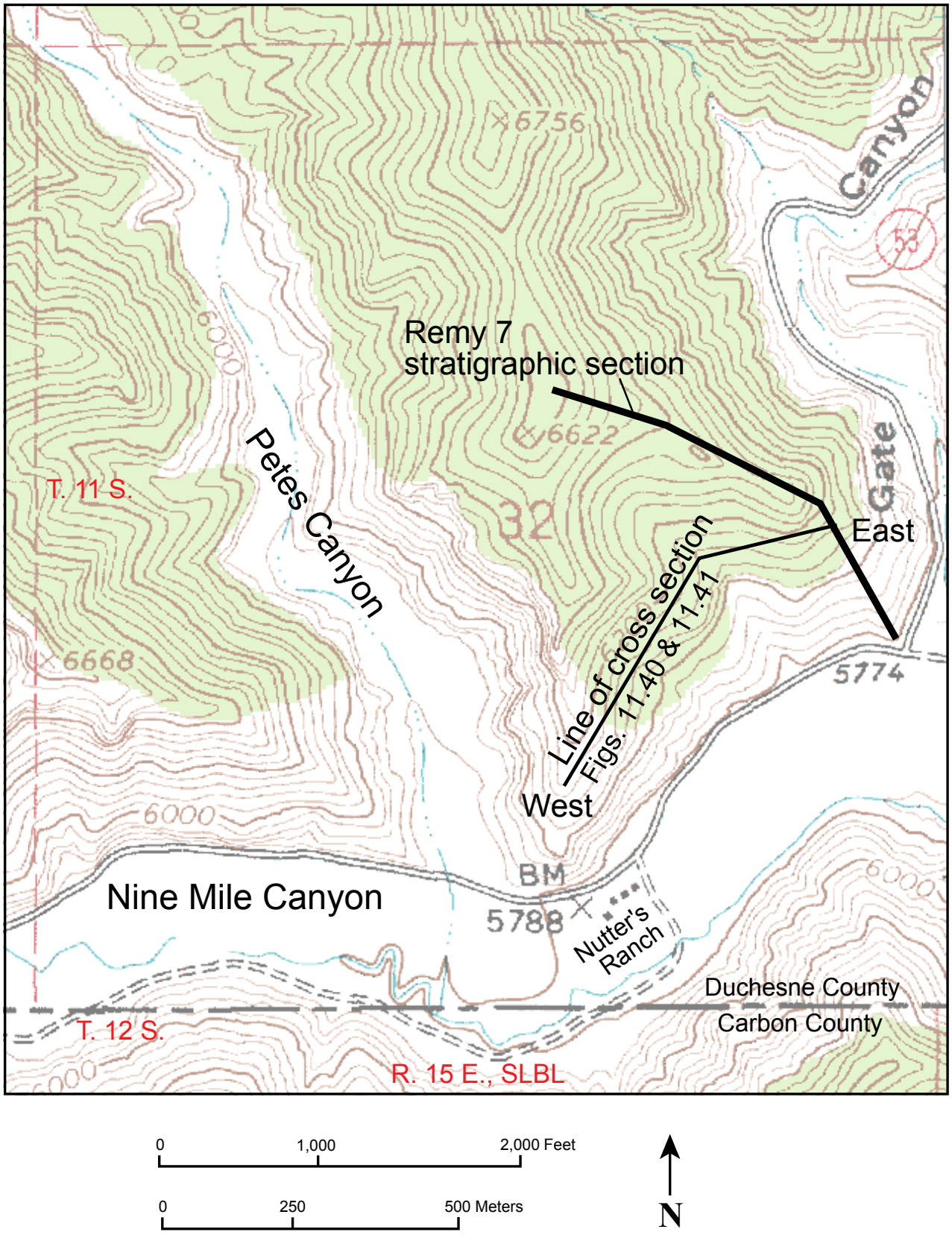

Figure 11.38. *Map showing the location of the stratigraphic measured section of the Monument Butte and Beluga intervals of the middle Green River Formation, by Remy (1992), and the Nutter's Ranch study site between Petes and Gate Canyons in Nine Mile Canyon. Base map modified from the USGS Current Canyon 7.5-minute quadrangle.*

Table 11.1. *Lithology, description, and depositional interpretations from the Nutter's Ranch study site.*

Lithology (bed designations)	Description	Depositional Environment
Carbonate (C)	Oolitic/ostracodal grainstone and micrite, typically contains fossil hash. The beds weather orange.	Lagoonal, beach to shallow nearshore.
Sandstone (Ss-a)	Fine grain, rippled, tabular, thin (<3 feet), laterally continuous except where it is cut by channel sandstone body.	Flood-plain sheet flow.
Sandstone (Ss-b)	Fine grain, deeply incised channel-form bed, trough cross-beds, rip-up clasts and ooids common in lower portion, upper portion some ripples and soft-sediment deformation.	Nonsinuous streams on the upper delta plain.
Sandstone (Ss-c)	Fine grain, channel-form bed, laterally extensive amalgamated channels, planar base due to restrictive carbonate bed preventing downward cutting, promoting lateral migration. Fining upwards with upward decrease in scale of sedimentary structures from trough and low angle cross-beds to planar and rippled. Szantat (1990) Type I sandstone body.	High sinuosity, anastomosing channel deposit in the lower delta plain.
Sandstone (Sd-d)	Fine grain, channel-form bed, laterally limited, incised, individual channel deposit, concave upward lower bounding surface, fining upwards with upward decrease in scale of sedimentary features from lateral accretion beds, trough and low angle cross-bedding to planar and rippled.	Meandering distributary channel.
Sandstone (Ss-e)	Fine grain, channel-form bed, laterally extensive amalgamated channel deposits, concave upward lower bounding surface, fining upwards with upward decrease in scale of sedimentary features from lateral accretion beds, trough and low angle cross-bedding to planar and rippled. Szantat (1990) Type II sandstone body.	High sinuosity, anastomosing channel deposit in the lower delta plain.
Sandstone (Ss-f)	Fine grain, incised channel-form bed, laterally limited, typically inclined trough sets with shale drapes.	Proximal crevasse splay.
Sandstone (Ss-f)	Fine grain, coarsening upward with generally flat top, rippled, thin 1 to 3 feet thick, laterally extensive.	Distal crevasse splay.
Shale and siltstone	Green to gray-green shale and siltstone, typically thinly covered, highly weathered. Some thick covered slopes interpreted to be underlain by shale and siltstone.	Upper and lower delta plain, flood plain to mudflat, to swamp, possibly abandoned channel and overbank deposit.

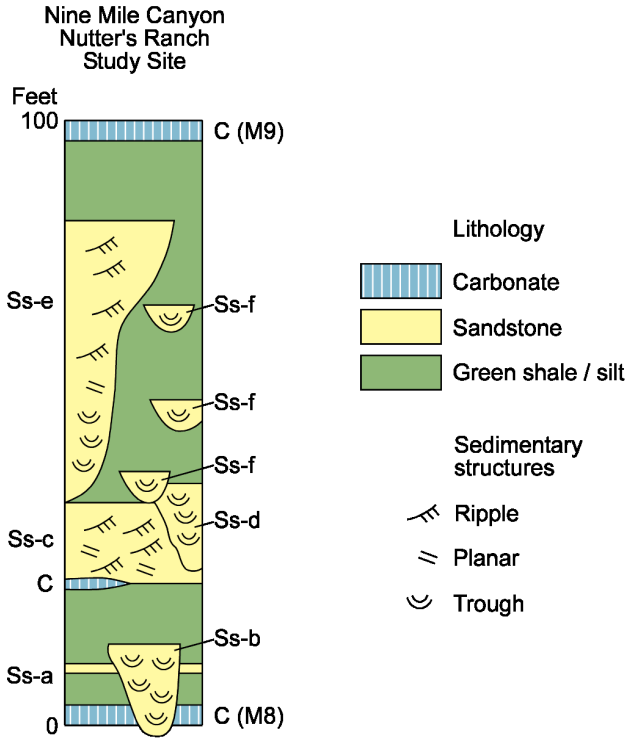

Figure 11.39. *Composite vertical stratigraphic section of the middle Green River Formation, 100-foot depositional cycle in the Nutter's Ranch study site in Nine Mile Canyon. C = carbonate, Ss = sandstone.*

Sandstone thickness maps, based on the outcrop values, were constructed using Arcview Spatial Analyst® and by hand contouring. Sandstone thickness for each of the three beds was assigned to the imaginary wells based on the draft thickness maps and entered into the database. Final sandstone thickness maps for the three beds were generated using Arcview Spatial Analyst®. Ss-c (figure 11.43) is the most laterally extensive of the three potential reservoir beds and ranges from less than 5 feet to more than 55 feet thick (16–180 m). The bed is laterally extensive because it overlies a muddy limestone that it could not cut through, causing the channel to migrate back and forth resulting in laterally extensive deposits. The alternating pattern of producer well and injector well locations would have some success in this bed. However, the thickest portion of this bed, located in the northwest quarter of the section, is not penetrated and would be produced by wells on the flanks of the sandstone trend. Ss-d, which was shown in the 2-D model to nearly cut out Ss-c, isolates a portion of Ss-c in the center of the easternmost portion of the section. While up to 30 feet thick (98 m), Ss-d is narrow (a few meters), has a very limited extent in the study area (figure 11.44), and would contain a very limited volume of oil. The 8-32 production well and the 9-32 injection well penetrate Ss-d, but not along the axis of the sandstone bed. As a result, only a small portion of the limited oil volume of Ss-d would be produced. Ss-e has moderate lateral extent (up to 2500 feet [8202 m]) across in the study site but is generally thicker (up to 55 feet thick

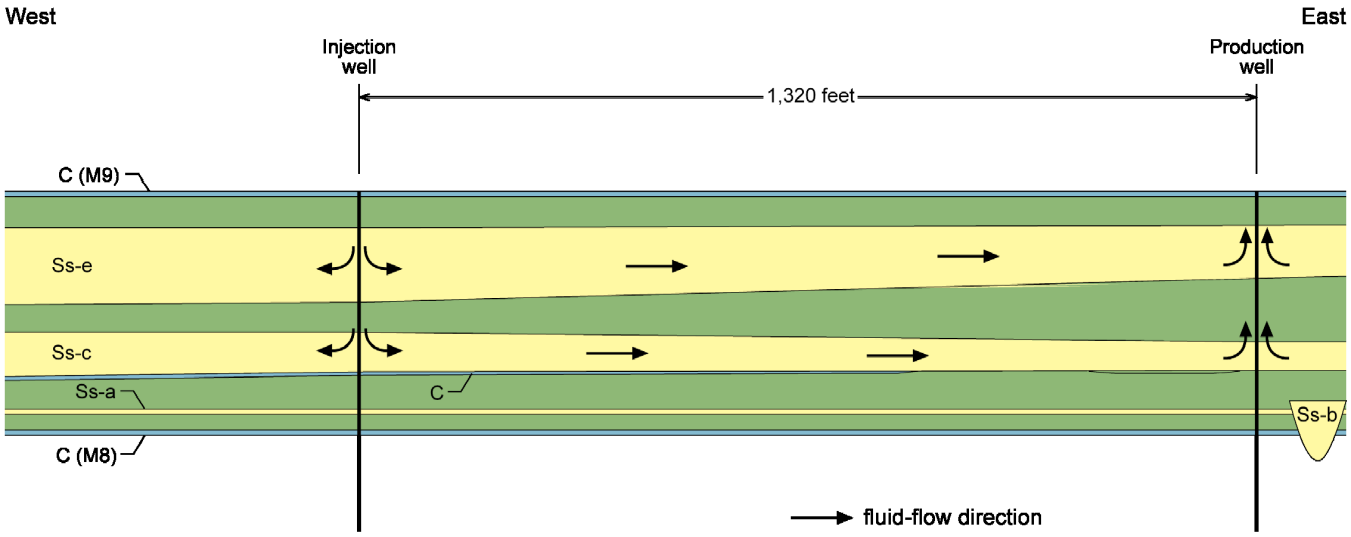

Figure 11.40. *Hypothetical 2-D correlation and potential fluid-flow pattern between two imaginary wells "drilled" at the Nutter's Ranch study site. See figure 11.38 for location of cross section.*

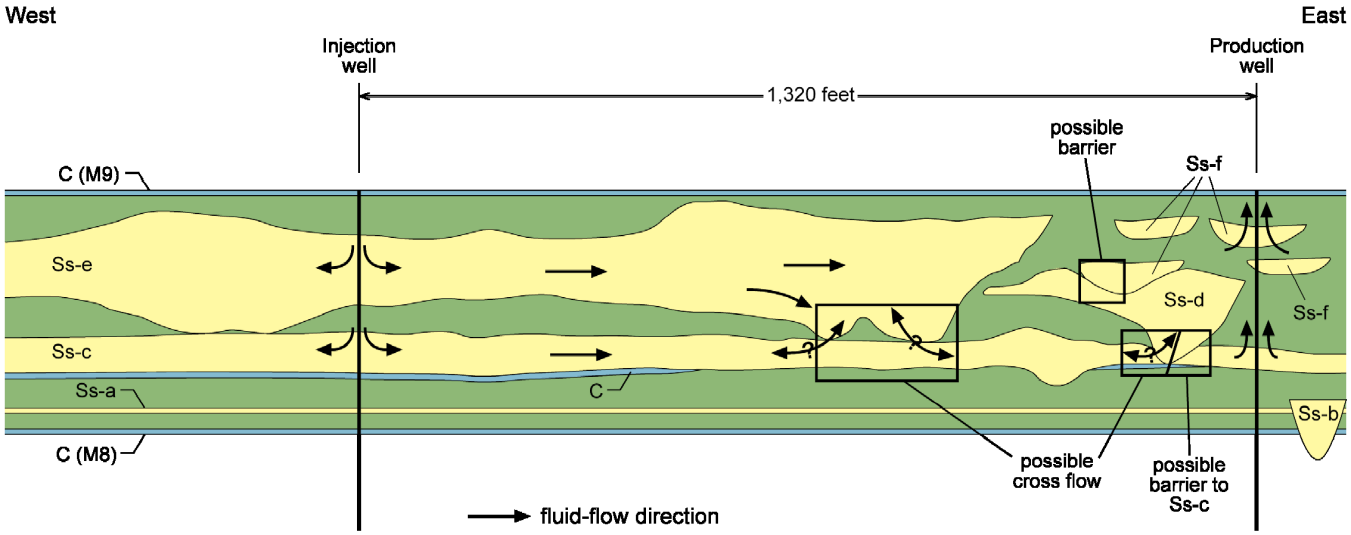

Figure 11.41. *Actual 2-D correlation and potential fluid-flow pattern between the same two imaginary wells "drilled" at the Nutter's Ranch study site as in figure 11.40. The water-flood effectiveness and the "total oil produced" are much less than in the hypothetical model due to the reservoir heterogeneity. If a barrier exists between Ss-f and Ss-e, and a barrier exists between Ss-d and Ss-c, then oil in Ss-e and most of the oil in Ss-c will not be produced. Oil in Ss-d will also probably not be produced. The production "well" will only produce oil from Ss-f and a very limited amount of oil from Ss-c. See figure 11.38 for location of cross section.*

[180 m]), where present, than Ss-c (figure 11.45). The alternating pattern of production and injection wells appears to be moderately effective in draining Ss-e. Some of the thickest sandstone is between injection well 7-32 and production well 8-32. Production well 8-32 penetrates only 4 feet (1.2 m) of Ss-e and as a result would probably be a very poor producer because most of the oil contained in the thick sandstone between the two wells would remain in the ground.

Duchesne Interval Fractured Shale/Marlstone

The Duchesne interval is defined as from MGR 18 to the top of the Green River Formation, and includes the upper portion of the middle member and all of the upper and saline members. The interval represents the maximum rise and eventual waning stages of ancient Lake Uinta and is well exposed in Indian Canyon south of the town of Duchesne (figure 11.30). Fractures can be observed in the Green River Formation in Indian Canyon and throughout the surface exposures in the Duchesne field along the Duchesne fault zone. Any fractured outcrop (sandstones, shale, and marlstones) in the upper and saline members can be considered a reservoir analog, but a person can take a hike to the abandoned wurtzillite mine in Indian Canyon to observe fractures containing hydrocarbons. Wurtzillite is a solid hydrocarbon that was mined from the saline member (?). The trail begins 16.1 miles (25.9 km) south on U.S. Highway 33 from the junction of U.S. Highway 33 and U.S. Highway 40 in the town of Duchesne, 0.4 miles (0.6 km) past the U.S. Forest Service sign.

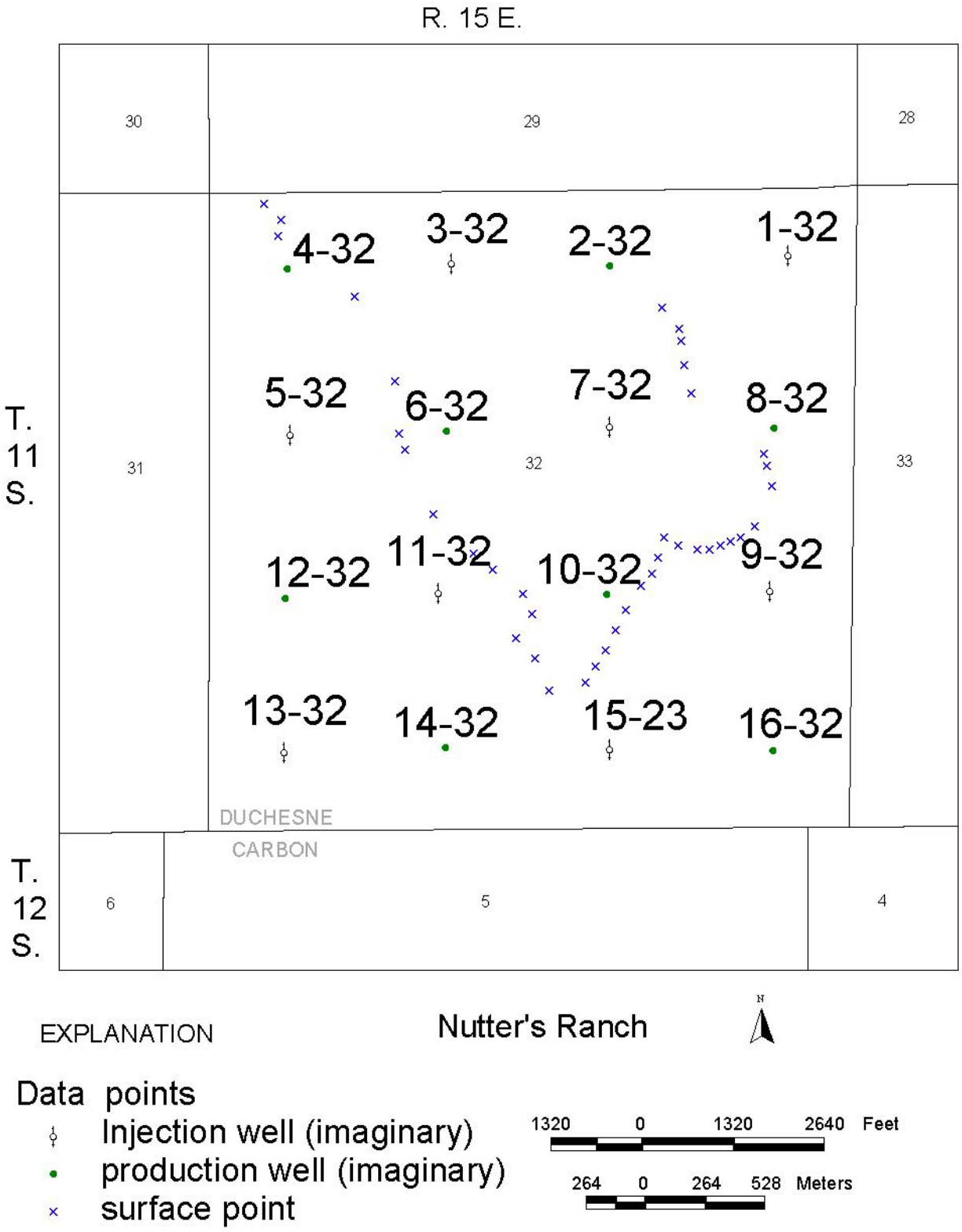

Figure 11.42. *Map of the Nutter's Ranch study site with imaginary well locations in the center of 40-acre lots.*

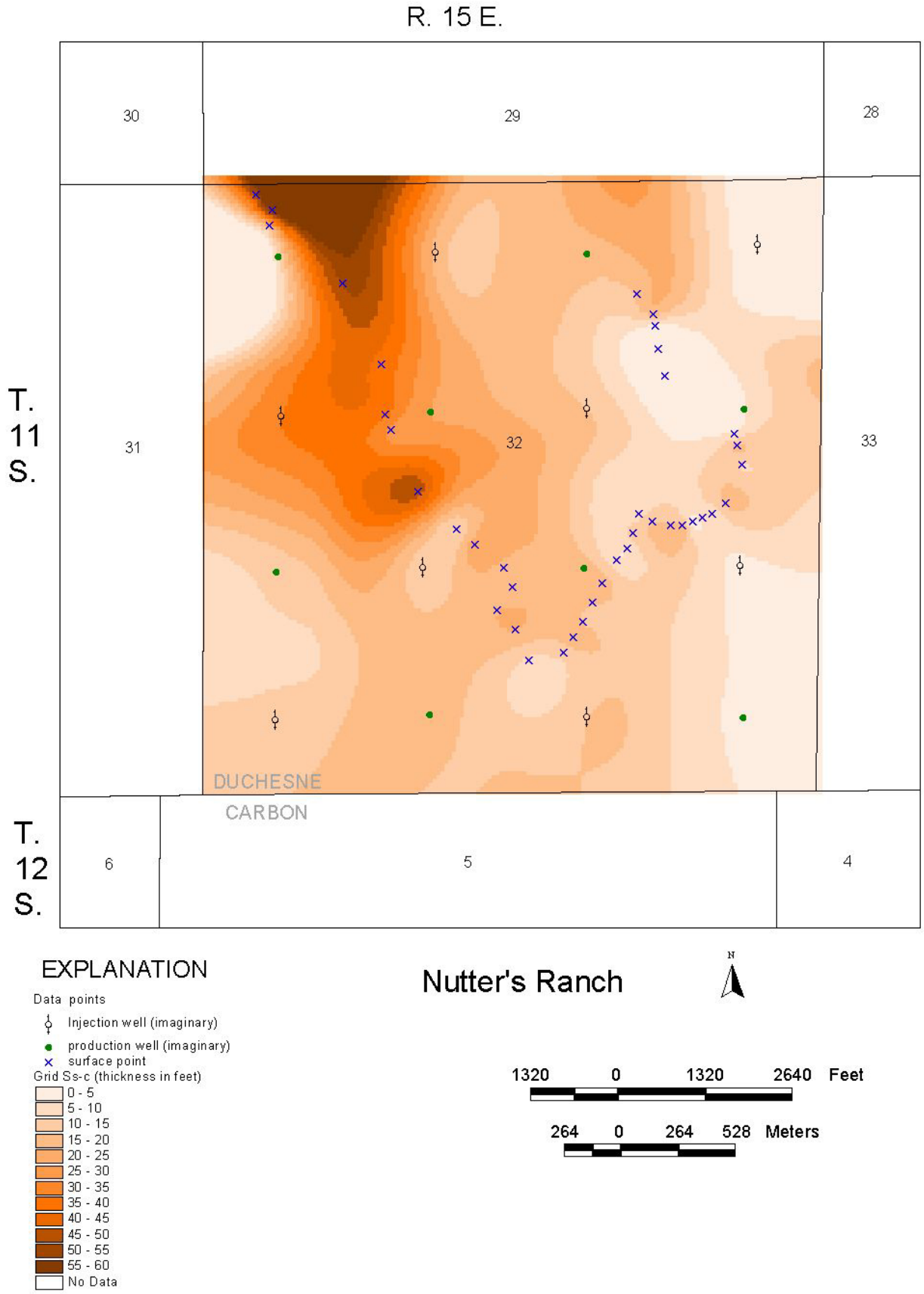

Figure 11.43. *Thickness map of Ss-c bed in the Nutter's Ranch study site. Grid interval is 5 feet. See figure 11.42 for imaginary production and injection well numbers.*

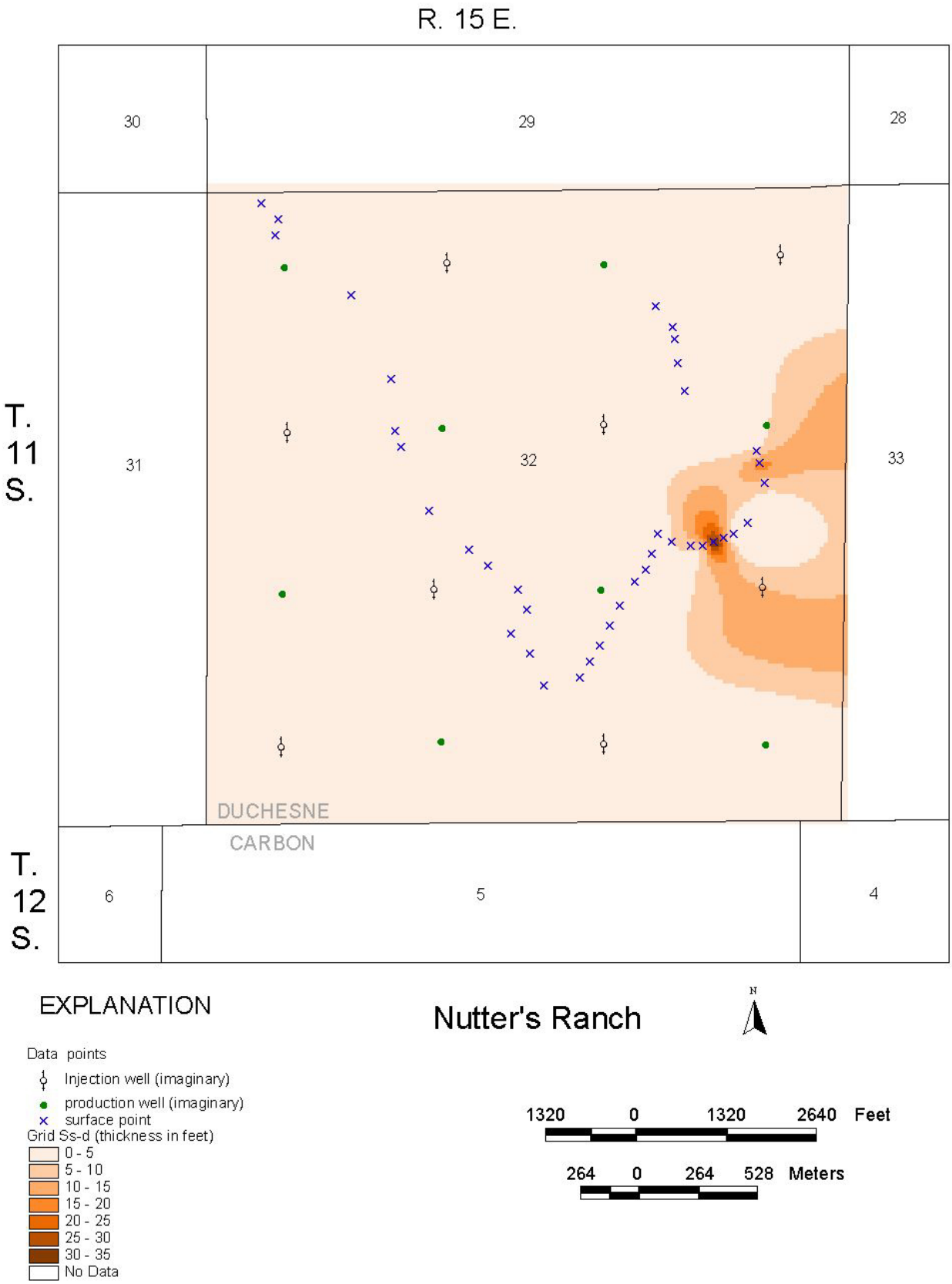

Figure 11.44. *Thickness map of Ss-d bed in the Nutter's Ranch study site. Grid interval is 5 feet. See figure 11.42 for imaginary production and injection well numbers.*

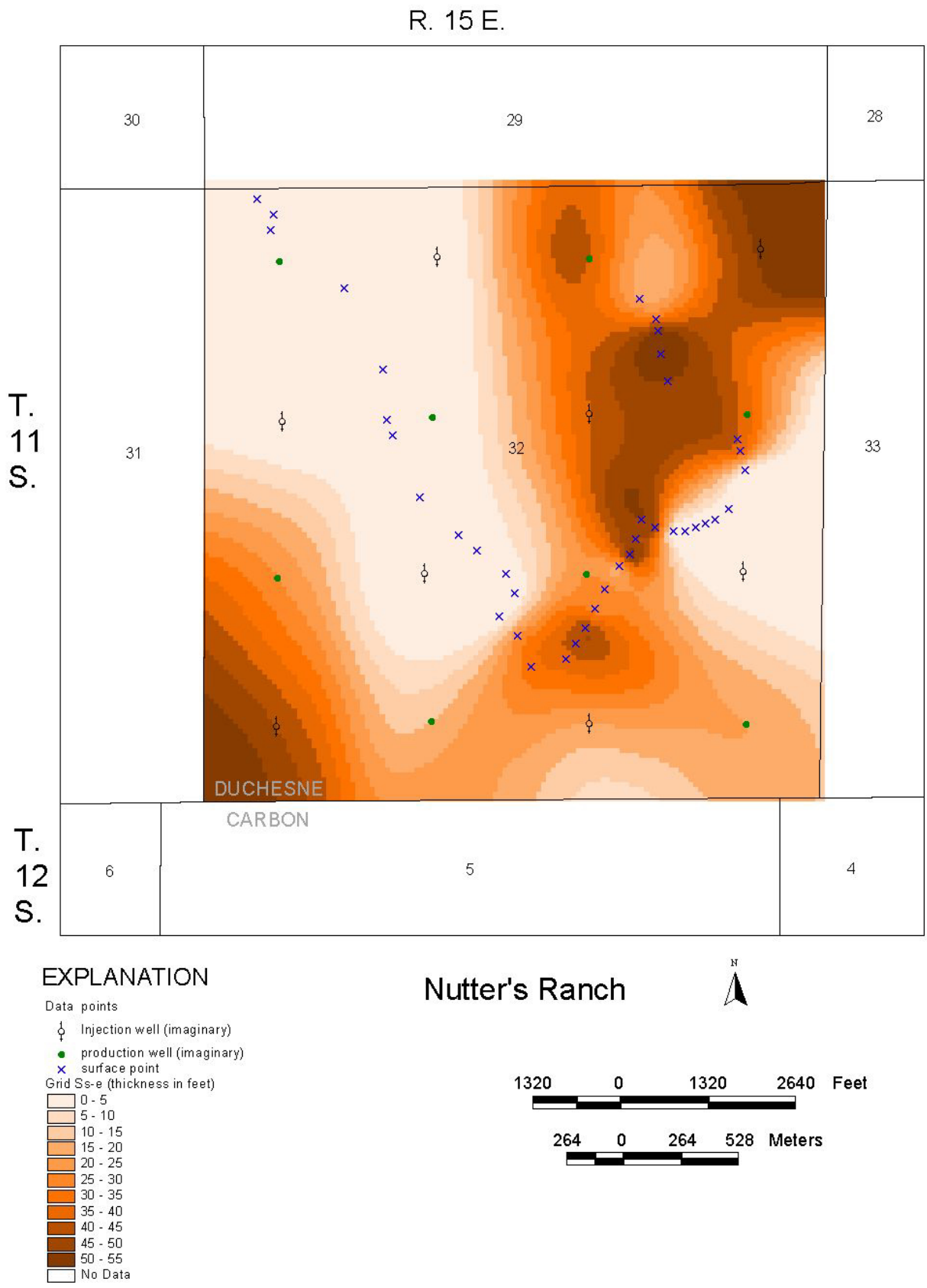

Figure 11.45. *Thickness map of Ss-e bed in the Nutter's Ranch study site. Grid interval is 5 feet. See figure 11.42 for imaginary production and injection well numbers.*

PARADOX BASIN

Mississippian Leadville Limestone

South Flank of the Uinta Mountains, Utah

Although not exposed in southeastern Utah, Mississippian rocks equivalent to the Leadville Limestone outcrop in the northern and western parts of the state (figure 11.46A). These formations include the Madison (figure 11.46B), Deseret (figure 11.47), Gardison, and Little Flat Formations, and have generally the same characteristics as the Leadville. They provide production-scale analogs of the facies characteristics, geometry, distribution, and the nature of boundaries contributing to the overall heterogeneity of Leadville reservoir rocks. Excellent examples of Leadville-equivalent rocks (Madison Limestone) are along the south flank of the Uinta Mountains where they are up to 600 feet (200 m) thick (figure 11.46).

The Madison Limestone is mostly light- to dark-gray, fine- to coarse-crystalline, cherty limestone (figure 11.48A). Dolomitic units are gray to tan, sucrosic to crystalline, and medium bedded with occasional silty partings; both limestone and dolomite are the prime reservoir lithologies for the Leadville Limestone. The Madison is generally thick to massive and unevenly bedded, forming vertical cliffs and dip slopes. Fossils include corals, brachiopods, crinoids, pelecypods, and gastropods (Rowley and Hansen, 1979); however, fossils are relatively rare in some areas. Chert is typically light gray, forming lenses and nodules. In the Whiterocks Canyon area (figure 11.46), the Madison contains some thin-bedded, tan, calcareous, fine- to medium-grained sandstone (Kinney, 1955).

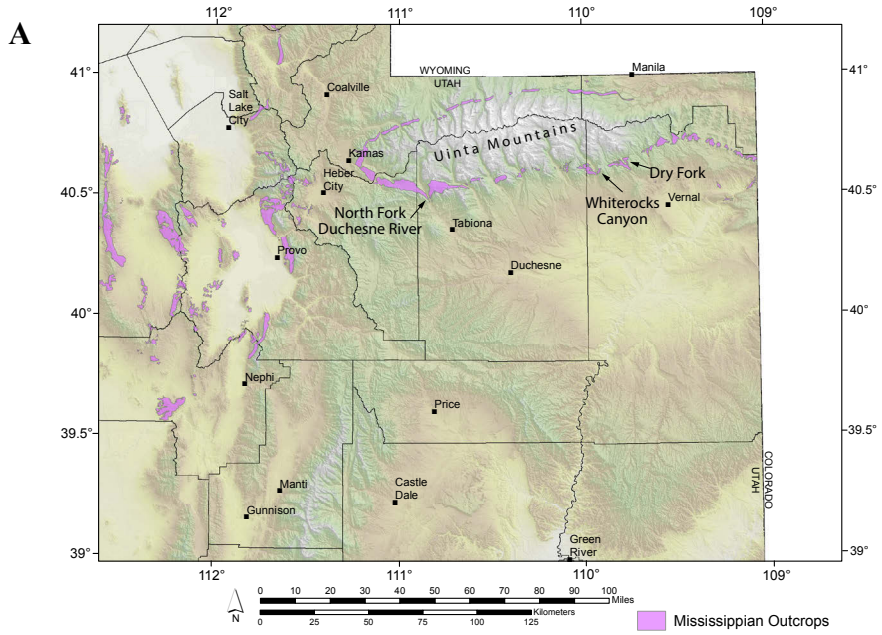

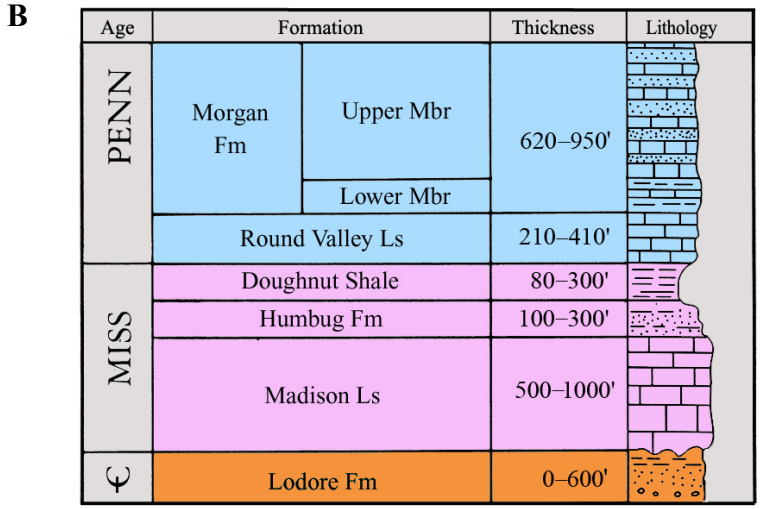

Figure 11.46. *Mississippian outcrop reservoir analogs in Utah.* ***A.*** *Location of Mississippian rock outcrops in Utah equivalent to the Leadville Limestone.* ***B.*** *Stratigraphic column of a portion of the Paleozoic section along the south flank of the Uinta Mountains. Modified from Hintze and Kowallis (2009).*

Figure 11.47. *Mississippian Deseret Limestone forming a jagged, vertical cliff, North Fork of the Duchesne River, Duchesne County, Utah. Note the cavernous nature of the outcrop. See figure 11.46A for location of North Fork of the Duchesne River area. View to the east.*

The Madison, Gardison, and Deseret Limestones commonly contain numerous caverns, sinkholes, and local zones of breccia (due to either collapse associated with karstification or natural hydrofracturing) and vugs (figures 11.47, 11.48B, and 11.48C). Stylolites, jointing, and fractures are also present creating rock sections with high heterogeneity (figures 11.48A, 11.48B, 11.48D, and 11.48E). Possible buildups or oolitic shoals are found in the Madison Limestone in Dry Fork Canyon (figures 11.46 and 11.48F). Brecciation associated with hydrothermal events, fracturing, and dissolution enhance reservoir quality in the Leadville Limestone.

Marble Canyon, Grand Canyon National Park, Arizona

The Mississippian (upper Kinderhookian through lower Meramecian) Redwall Limestone in Grand Canyon National Park forms a prominent and spectacular cliff over 500 feet (170 m) in height (figures 11.49 and 11.50). The Redwall is stratigraphically equivalent to the Leadville Limestone reservoir and provides an excellent outcrop analog. The Marble Canyon area is the best place in the park to observe the stratigraphy, depositional environments, fracturing, and karst-type features of the Redwall as the Colorado River cuts down section through the entire formation (figures 11.49 and 11.50). However, access requires either guided river trips or special scientific permits from the National Park Service.

The Redwall Limestone is divided into four members based on distinct lithologic variations (McKee, 1969; McKee and Gutschick, 1969) in ascending order: the Whitmore Wash, Thunder Springs, Mooney Falls, and Horseshoe Mesa Members (figure 11.51). The Whitmore Wash is a fine-grained dolomite in Marble Canyon with a thickness up to 100 feet (30 m). The Thunder Springs contains thin beds of dolomite and elongate lenses of chert; the member is nearly 90 feet (27 m) thick. The Mooney Falls is nearly 220 feet (67 m) thick with massive bedding (3 to 20 feet [1–6 m] in thickness) composed of pure limestone that is free of terrigenous material (less than 1%) and locally dolomitic. The Horseshoe Mesa is the thinnest member, about 35 to 125 feet (11–38 m), containing thin limestone beds and chert lenses that form receding ledges (Hamblin and Rigby, 1968; McKee, 1969). The Whitmore Wash and Horseshoe Mesa represent the best reservoir analog units while the Thunder Springs represents the worst reservoir analog unit.

The most common lithology of the Redwall Limestone consists of peloidal, skeletal, and oolitic grainstone, packstone, and wackestone; rudstone and floatstone are also present. An

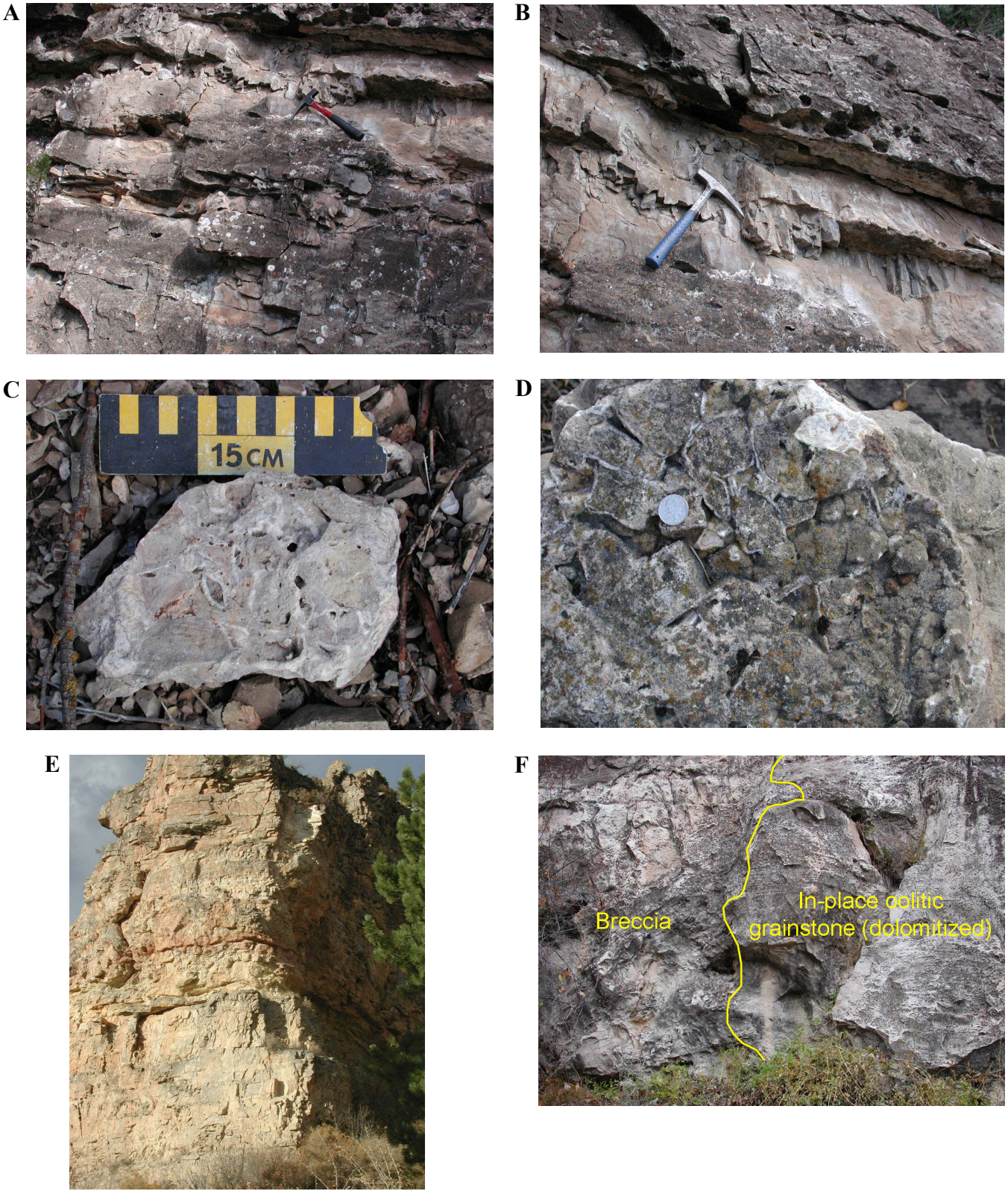

Figure 11.48. *Characteristics of the Mississippian Madison Limestone along the south flank of the Uinta Mountains, Uintah County, Utah.* ***A.*** *Typical exposure of light to dark gray, medium bedded, fine to coarse crystalline, limestone and dolomite containing fractures, stylolites, and crinoid hash, Whiterocks Canyon.* ***B.*** *Vugs and fractures in limestone and dolomitic units, Whiterocks Canyon.* ***C.*** *Close up of open and calcite-filled vugs in limestone matrix, Whiterocks Canyon.* ***D.*** *Close up of small-scale, calcite-filled rectilinear fractures in limestone matrix, Whiterocks Canyon.* ***E.*** *A combination of interbedded limestone and dolomite, containing fractures and zones of solution breccia and vugs, results in a heterogeneous stratigraphic section, Dry Fork Canyon.* ***F.*** *Small-scale oolitic shoal and collapse breccia (outcrop is approximately 10 feet [3 m] high), Dry Fork Canyon. See figure 11.46A for locations of Whiterocks and Dry Fork Canyons.*

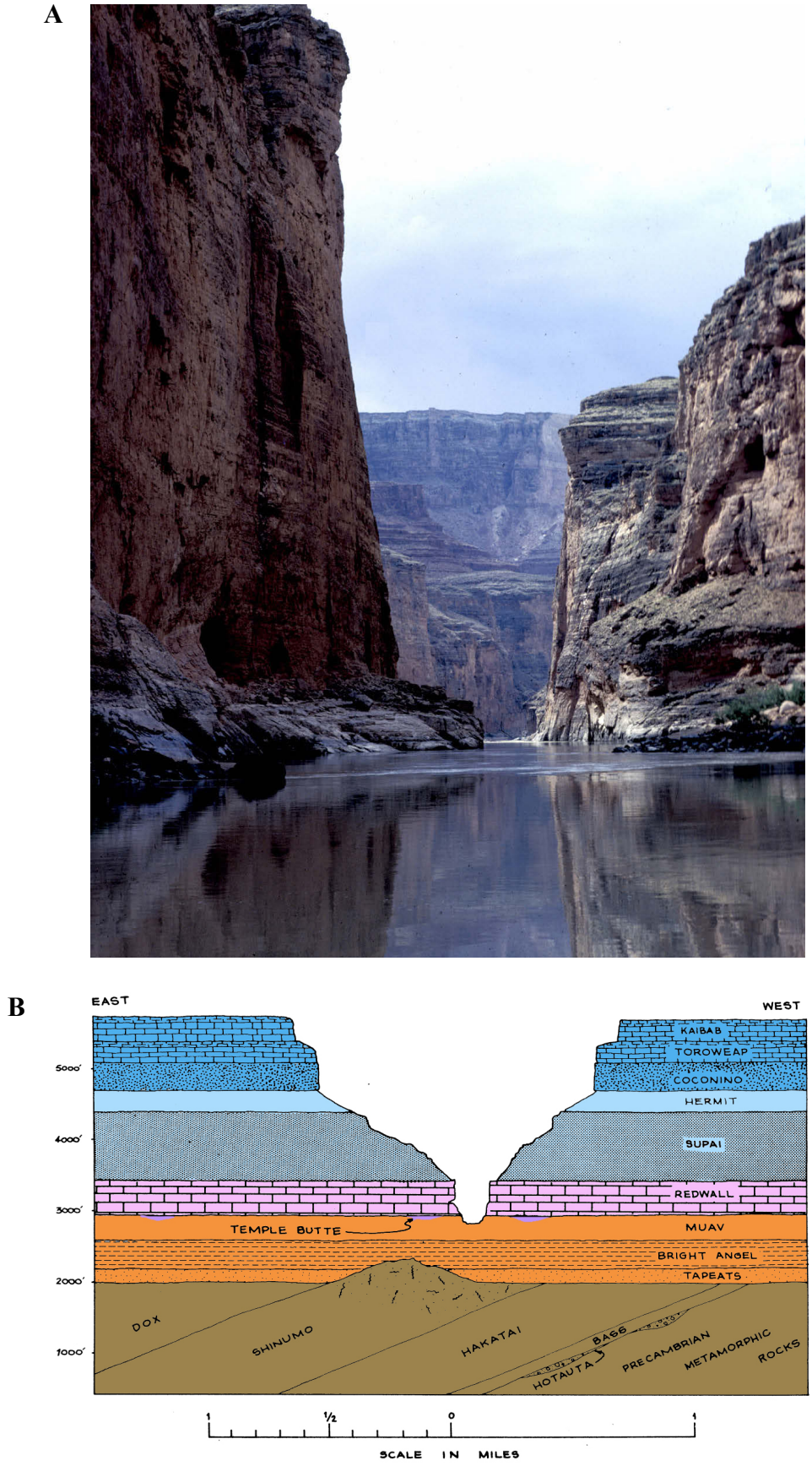

Figure 11.49. *River mile 40, Colorado River, Grand Canyon National Park.* ***A.*** *Mississippian Redwall Limestone spectacularly exposed in Marble Canyon, Grand Canyon National Park, Arizona.* ***B.*** *Generalized cross section showing basic stratigraphy and canyon profile in Marble Canyon. After Hamblin and Rigby (1968).*

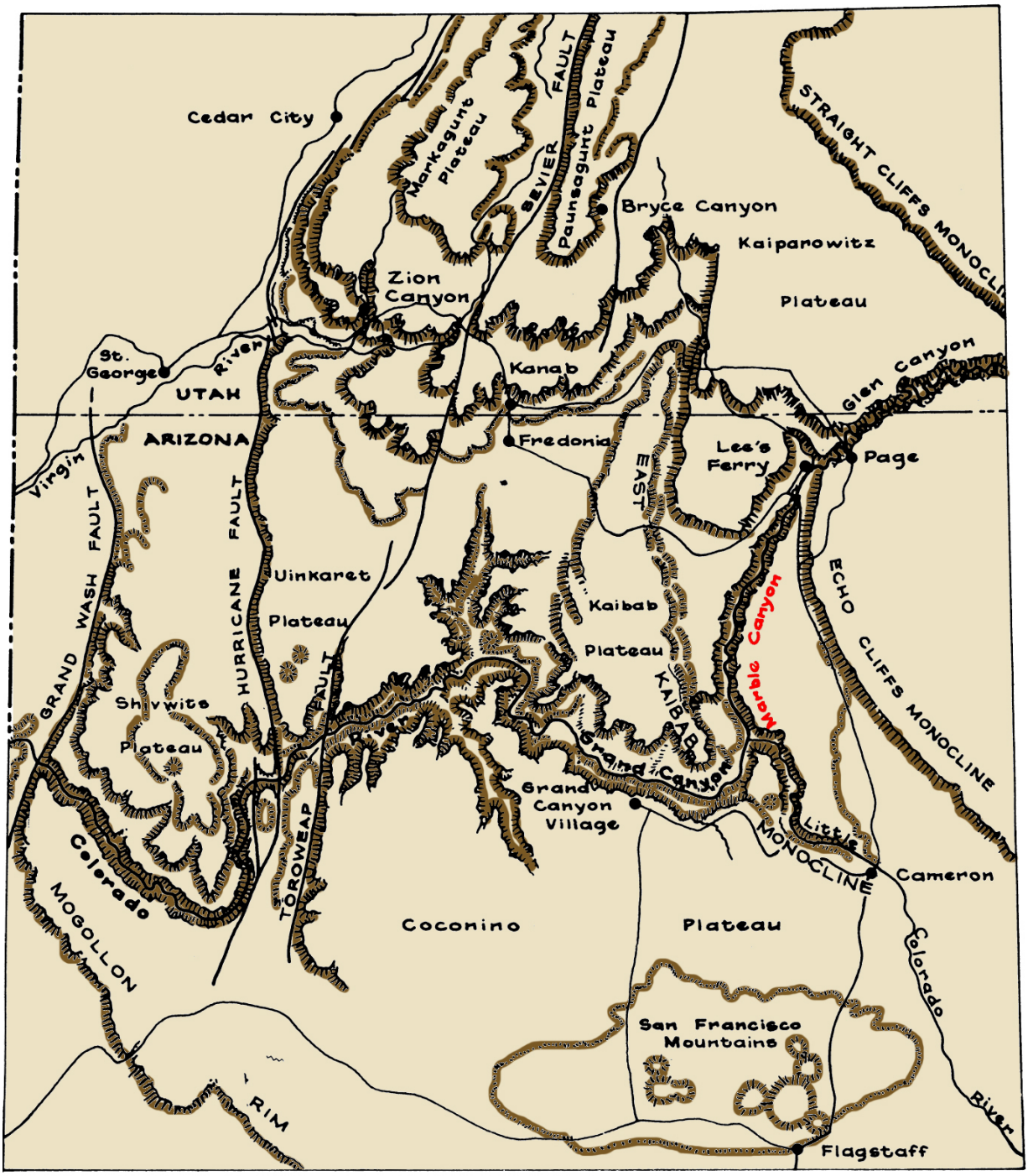

Figure 11.50. *Location of Marble Canyon in Grand Canyon National Park, Arizona, and major physiographic features. After Hamblin and Rigby (1968).*

open-marine facies is represented by corals, brachiopods, foraminifers, and crinoids (figure 11.52A). Other common fauna include bryozoans, pelecypods, cephalopods, and gastropods. Algae, trilobites, ostracods, and fish are present in some Redwall zones (McKee, 1969; McKee and Gutschick, 1969). Several carbonate buildups are observed in the lower half of the Redwall such as shoals or banks of cross-bedded crinoid debris (encrinites) (figure 11.52B). Other buildups may indicate a Waulsortian-type facies (figure 11.52C) consisting of bands of encrinite, containing fenestrate bryozoans, interbedded with chert. With good porosity/permeability development encrinites and Waulsortian buildups represent the best reservoir analog units while low porosity/permeability open marine packstone and wackestone represent the worst reservoir analog units.

Mudstones appear as microcrystalline and cryptocrystalline limestone. Most dolomite zones form early as sedimentary dolomite in nearshore environments (McKee, 1969; MeKee and Gutschick, 1969). The pure limestone of the Mooney

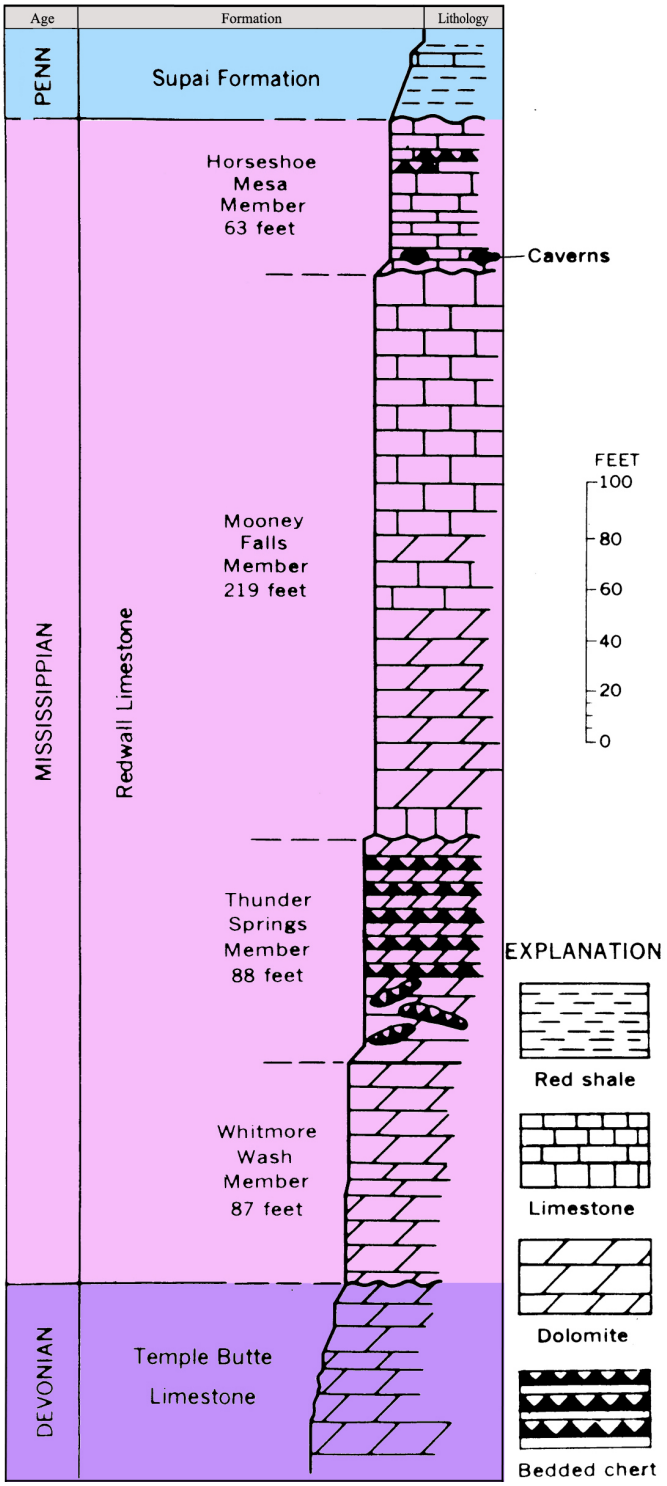

Figure 11.51. *Generalized stratigraphic column for the Mississippian Redwall Limestone, Grand Canyon. After McKee (1969).*

Falls Member likely formed in a broad, shallow, quiet sea far from terrigenous deposition associated with distant shorelines (Hamblin and Rigby, 1968).

Fracturing is present in the Redwall Limestone, especially in the upper members, and is best expressed as closely spaced, vertical fractures throughout thin to medium thick beds or as swarms associated with large and small faults (figure 11.52D) and collapse features. Possible breccia pipes are also observed in the Redwall and may be related to past hydrothermal activity (figure 11.52E). These features enhance reservoir quality.

The contact between the Redwall Limestone and overlying Pennsylvanian (Morrowan) Supai Group is marked by a major unconformity—upper Meramecian and Chesterian rocks are absent (McKee, 1969; Hintze and Kowallis, 2009). This unconformity formed karst topography which has many expressions in Marble Canyon. These include a surface with relief up to 40 feet (12 m) along the top of the Redwall, carbonate breccia-filled sinkholes (figure 11.53A) and solution channels, transported gravel within channels, and abundant caverns and springs. Terra rosa (cave fill) (figure 11.53B), in-place cave pearls (figure 11.53C), and collapse features also provide evidence for filled-in caves and karst topography near the top of the Redwall. However, hundreds of caves, filled or partially filled with collapse debris (figure 11.53D), and springs (figure 11.53E) are exposed throughout the Redwall cliffs. Controls on these features are vertical joints, fractures, and selected bedding planes rather than the unconformity at the top of the Redwall (Hamblin and Rigby, 1968). Karst features also can enhance reservoir quality.

Pennsylvanian Paradox Formation

Carbonate buildups exposed in outcrops of the Paradox Formation along the San Juan River of southeastern Utah provide production-scale analogs of reservoir-facies characteristics, geometry, distribution, and the nature of boundaries contributing to the overall heterogeneity of these rocks. Algal buildups in the Ismay zone are exposed at river level 10 river miles (16 km) east of Mexican Hat, Utah, with some of the best examples in the Eight-Foot Rapid area (figure 11.54). High-resolution, outcrop-based sequence-stratigraphic analysis has been conducted on these rocks by Goldhammer and others (1991, 1994), Simo and others (1994), Best and others (1995), Weber and others (1995a, 1995b), Gianniny and Simo (1996), and Grammar and others (1996). Ten river miles (16 km) west of Mexican Hat, over 1300 feet (400 m) of Pennsylvanian rocks, including almost the entire Paradox Formation, is exposed through the famous Goosenecks of the San Juan River (figures 11.54 and 11.55A) and along the Honaker Trail, which provides access to the river from the canyon rim (figures 11.54 and 11.55B). The Honaker Trail section has been extensively studied by Pray and Wray (1963), Wengerd (1963), Weber and others (1995a), Stevenson (2010), Ritter and others (2002), and many other workers.

Eight-Foot Rapid Area, San Juan River

Phylloid-algal buildups of the Ismay zone exposed in the Eight-Foot Rapid area were deposited in northwest-trending elongate banks on a shallow carbonate shelf. The Ismay zone is divided into two intervals: the lower Ismay, which consists of a single, thick, shoaling-upward carbonate sequence, and

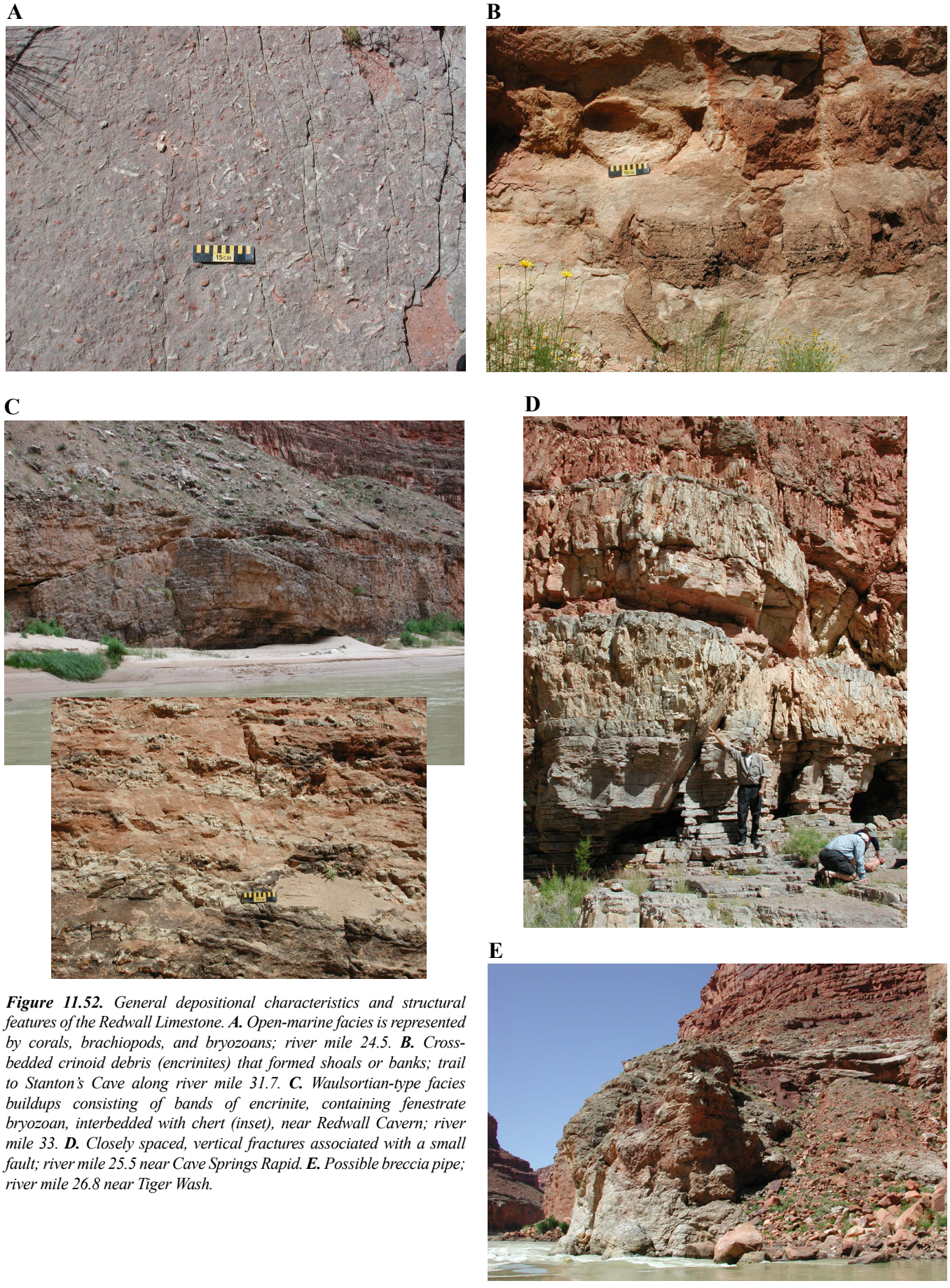

Figure 11.52. *General depositional characteristics and structural features of the Redwall Limestone.* ***A.*** *Open-marine facies is represented by corals, brachiopods, and bryozoans; river mile 24.5.* ***B.*** *Cross-bedded crinoid debris (encrinites) that formed shoals or banks; trail to Stanton's Cave along river mile 31.7.* ***C.*** *Waulsortian-type facies buildups consisting of bands of encrinite, containing fenestrate bryozoan, interbedded with chert (inset), near Redwall Cavern; river mile 33.* ***D.*** *Closely spaced, vertical fractures associated with a small fault; river mile 25.5 near Cave Springs Rapid.* ***E.*** *Possible breccia pipe; river mile 26.8 near Tiger Wash.*

Figure 11.53. *Selected karst features of the Redwall Limestone.* ***A.*** *Debris-filled collapse feature near the top of the Redwall; river mile 24.5.* ***B.*** *Terra rosa and cave-fill breccia deposits near the top of the Redwall; river mile 23.* ***C.*** *In-place cave pearls near the top of the Redwall; river mile 23.* ***D.*** *Numerous partially debris-filled caves; river mile 35 south of Nautaloid Canyon.* ***E.*** *Vasey's Paradise where springs issue several thousand gallons of water per minute from the Redwall cave system (the amount of water varies with the seasons and annual precipitation) (Hamblin and Rigby, 1968); river mile 31.7.*

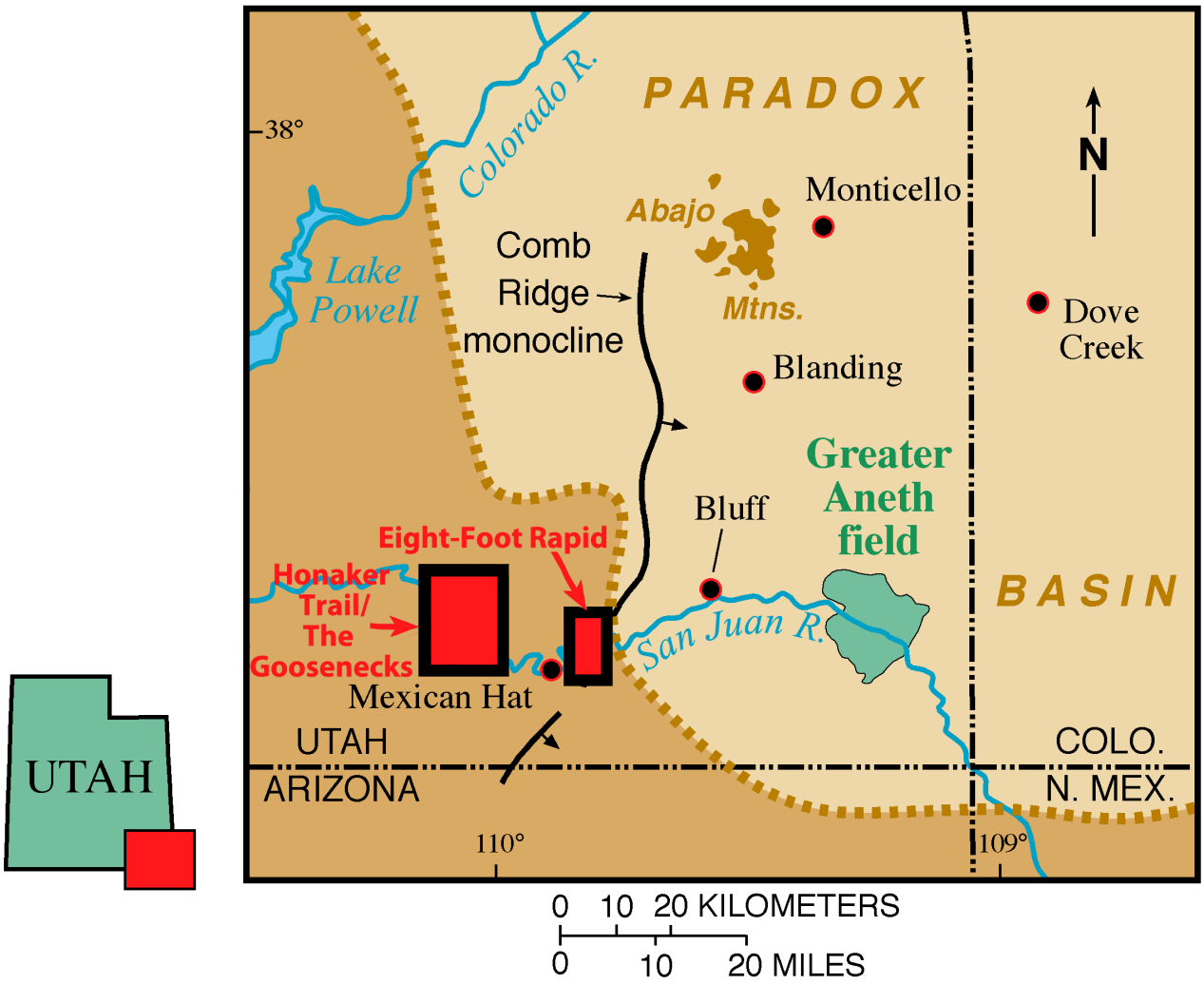

Figure 11.54. *Location of Paradox Formation outcrops in the Eight-Foot Rapid area and The Goosenecks/Honaker Trail, San Juan River, southeastern Utah.*

the upper Ismay, which consists of three or more thinner, shoaling-upward, carbonate and carbonate-evaporite cycles.

Recognizing the morphologic variations in this area is critical to understanding controls on deposition. The following terms distinguish buildup geometry (Brinton, 1986) and are shown schematically in figures 11.56 and 11.57.

Algal bank: The massive, lenticular, biostromal algal buildups, 30 to 40 feet (10–13 m) thick, exposed for several miles along the walls of San Juan Canyon.

Interbank: The channel-like feature that separates, or bisects, algal banks.

Algal mound: Secondary, ridge-and-swale or wave-form-like features that define the upper surfaces of the algal banks and impart the wavy topography that characterizes outcrops.

Intermound: The shallow trough region between algal-mound crests.

The lower Ismay zone algal banks or buildups exposed along the San Juan River appear as flat-bottomed, convex-upward lenticular bioherms with undulating, wave-like upper surfaces and relief as great as 50 feet (15 m) (figure 11.58). The most distinctive feature of buildups and adjacent facies is the undulatory or ridge-and-swale upper surface of the algal banks. The wavy topographic features (mounds and intermounds) extend for miles along the walls of the canyon, displaying regular wavelengths (150 to 200 feet [46–61 m]) and amplitudes (10 to 20 feet [3–6 m]). Mounds appear to be superimposed on the larger-scale algal banks whose length/width ratios are more characteristic of biostromes (Brinton, 1986).

Cyclic sedimentation is recorded by four dominant lithofacies recognized in a single, shoaling-upward sequence (figure 11.59): (1) substrate carbonate, (2) phylloid algal, (3) intermound, and (4) skeletal capping (Brinton, 1986; Grammar and others, 1996). An outcrop in the Eight-Foot Rapid area displaying these and additional lithofacies was selected for detailed

A

B

Figure 11.55. *San Juan River, southeastern Utah.* ***A.*** *Goosenecks of the San Juan River. Photograph by Tom Till, courtesy of the Utah Travel Council. View to the south.* ***B.*** *Pennsylvanian section along Honaker Trail, view to the west.*

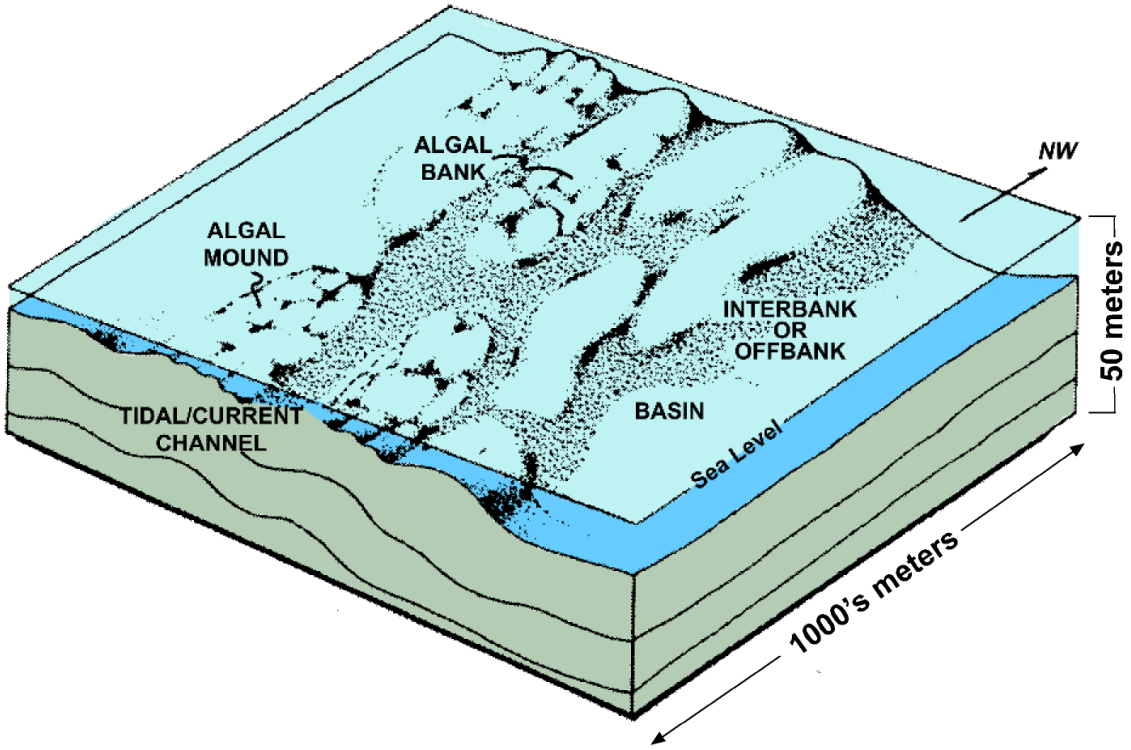

Figure 11.56. *Schematic diagram of Paradox Formation algal banks. From Brinton (1986).*

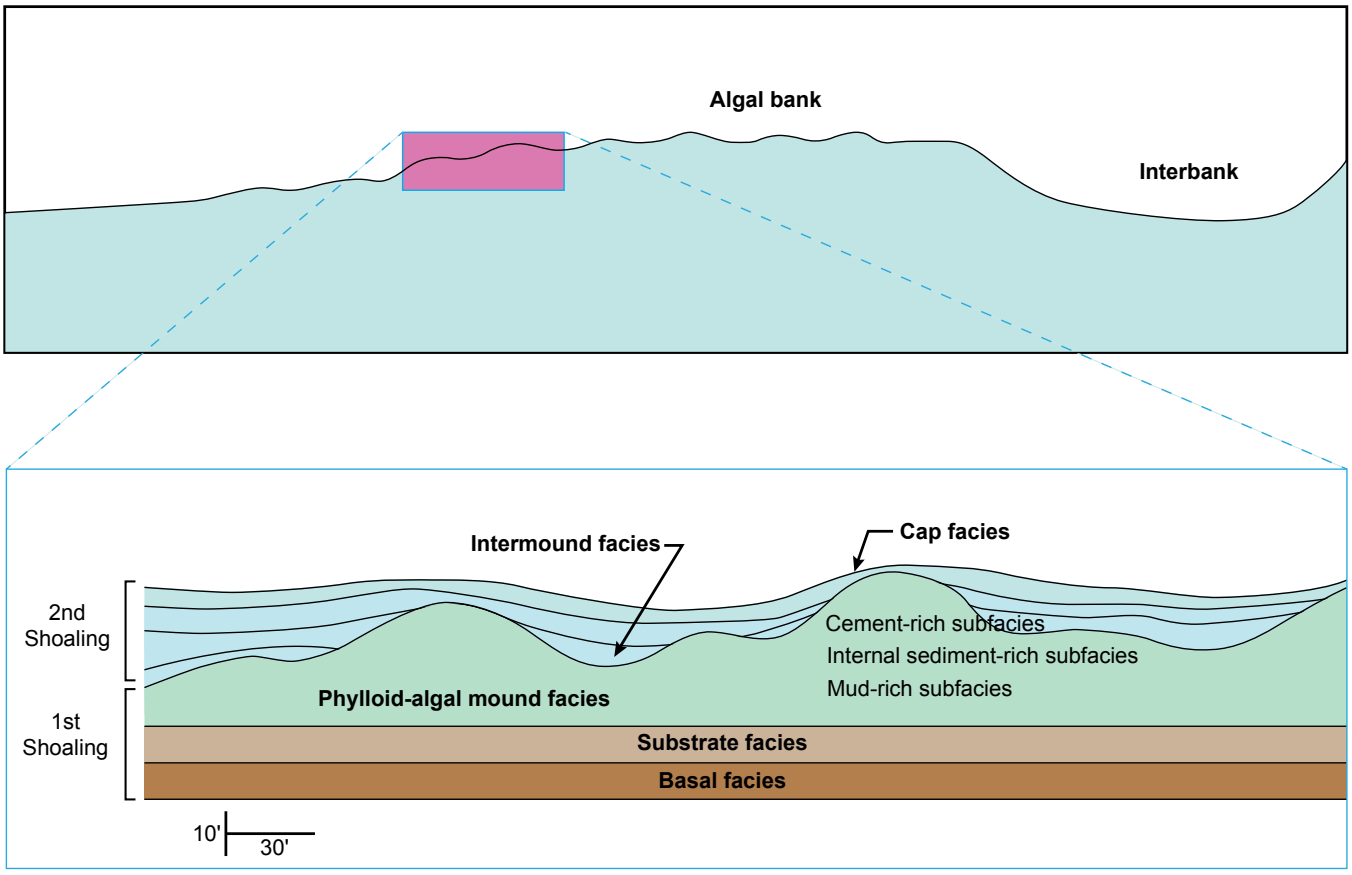

Figure 11.57. *Paradox Formation algal bank/mound topography, morphology, and facies relationships as seen along the San Juan River, Utah. From Brinton (1986).*

Figure 11.58. *Ismay zone algal banks near Eight-Foot Rapid as illustrated in figures 11.56 and 11.57. View to the north.*

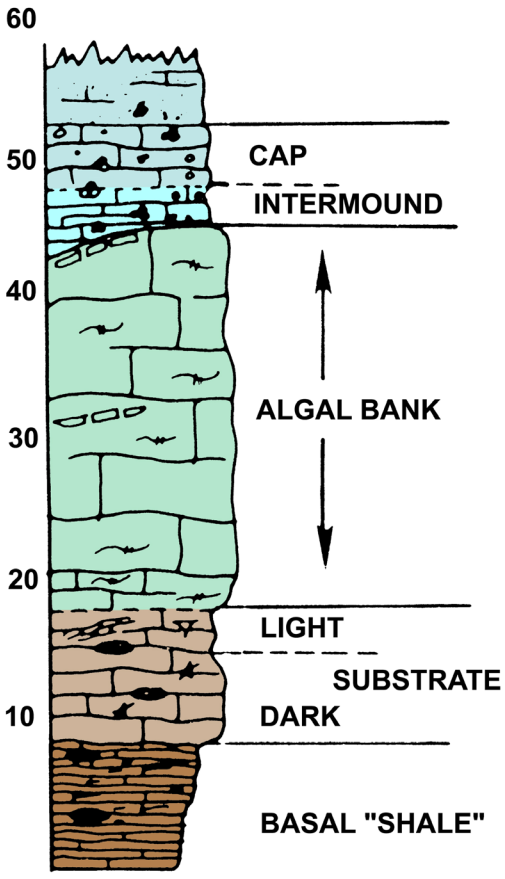

Figure 11.59. *Typical vertical facies succession preserved in the Ismay zone at Eight-Foot Rapid. From Brinton (1986).*

study (figure 11.60A) (Chidsey and others, 1996d). The phylloid algal and skeletal capping lithofacies represent the best reservoir analog units while the substrate carbonate and intermound lithofacies represent the worst reservoir analog units.

The Eight-Foot Rapid study site is interpreted as consisting of three principal reservoir features: (1) a phylloid-algal mound with grainstone buildups deposited at or near sea level, (2) a "reef wall" that formed in a higher energy, more marginal setting than the mound, and (3) a carbonate detrital wedge and fan consisting of shelf debris. Figure 11.61 is a schematic block diagram illustrating hypothetical lithofacies relationships. This interpretation is not only based on observations made at the outcrop, but also incorporates subsurface core data that are discussed in Chidsey and others (1996b).

Bafflestone and *Chaetetes*- and rugose-coral-bearing grainstone and packstone textures observed in the northern part of the Eight-Foot Rapid complex comprise the main phylloid-algal mound (figure 11.60B). A flooding surface recognized on top of the buildup and probable low-permeability lithotypes (packstone and cementstone) within the buildup might act as barriers or baffles to fluid flow in the subsurface. The Eight-Foot Rapid outcrop appears to be only a portion of a larger algal-bank complex, or one of a series observed in San Juan Canyon. Although not documented at this outcrop, observations from cores in other areas in the subsurface suggest an interior-lagoon and other associated lithofacies likely formed to the west as part of this complex (Chidsey and others, 1996b).

A

B

Figure 11.60. *Outcrops in the Ismay zone of the Paradox Formation, Eight-Foot Rapid area near the San Juan River, southeastern Utah.* ***A.*** *Typical phylloid-algal mound composed of algal bafflestone, skeletal grainstone, and packstone. A flooding surface is present at the top of the mound.* ***B.*** *Cement-rich algal bafflestone exposed in a phylloid-algal mound. Original sheltered pore spaces were filled with mud; cement rinds are developed around algal plates.*

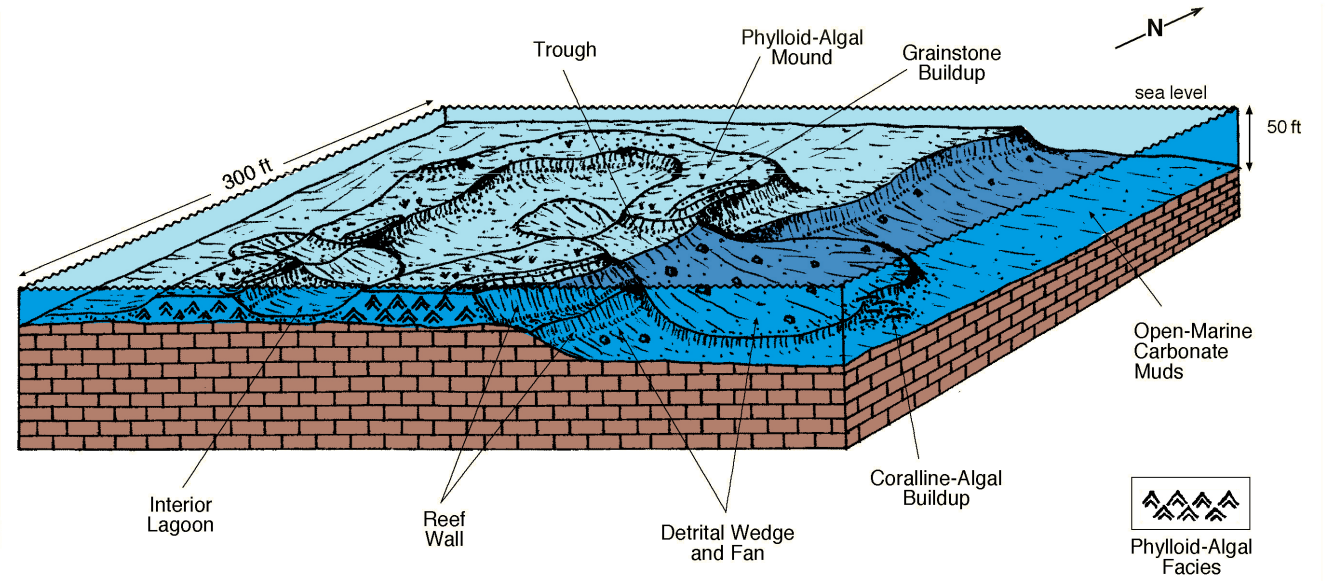

Figure 11.61. *Block diagram displaying depositional interpretation of a mound complex and associated features in the Eight-Foot Rapid area. From Chidsey and others (1996a). This interpretation is a composite of inferences made from outcrop and subsurface data.*

The rudstone, cementstone, and lumpstone depositional textures represent deposits that were part of, or near, what might be interpreted as a "reef wall" (figure 11.61). The presence of internal sediments in these rocks indicates an influx of mud pumped into pores during storms, or mud routinely distributed by stronger currents. The reef wall records deposition and intense sea-floor cementation as a result of reflux of large pore volumes of water through sediments occupying a high-energy setting that is marginal between shallow-shelf and deeper, open-marine conditions. The reef wall may have served as a barrier behind which algal buildups could develop and thrive in a more protected setting that facilitated preservation of primary shelter porosity. The presence of reef-wall lithofacies in a well core might serve as a proximity indicator for a more prospective algal-buildup drilling target. Examples of this relationship have been observed in the Blue Hogan and Brown Hogan fields to the southwest of the Greater Aneth field (figure 10.4) (Chidsey and others, 1996b).

An intermound trough in the center of a mound could represent a tidal channel flowing across the reef wall (figure 11.61). Material shed from the mound and reef wall was subsequently carried through the tidal channel and might have been deposited as a detrital wedge or fan on open-marine carbonate muds. These features are recorded by the grainstone and transported material observed on the east side of the outcrop complex. Coralline-algal buildups may have also developed near the carbonate detrital fan but were not observed at this locality in the canyon.

Reservoir-quality porosity may have developed in troughs, detrital wedges, and fans identified from core and facies mapping. If these types of deposits are in communication with mound-reservoir lithofacies in the subsurface, they could serve as conduits facilitating sweep efficiency in secondary/tertiary recovery projects. However, the relatively small size and the abundance of intermound troughs over short distances, as observed along the river, suggests caution should be used when correlating these lithofacies between development wells. Lithofacies that appear correlative and connected from one well to another may actually be separated by low-permeability lithofacies which inhibit flow and decrease production potential.

Honaker Trail and The Goosenecks

The Paradox Formation section along the Honaker Trail includes both the Ismay and Desert Creek zones, and the Akah and Barker Creek (at river level) zones as well. The Horn Point marker bed defines the top of the lower Ismay zone. Ritter and others (2002) and Ritter and Gianniny (2012) have identified 30 high-frequency cycles or 5th-order parasequences (Goldhammer and others, 1991) from the Horn Point to the bottom of the section based on conodont sequence biostratigraphy. These cycles are 6 to 21 feet (2–7 m) thick and grade from deeper-water sediments at the base to subtidal and shoaling carbonates at the top (Ritter and others, 2002).

The top of the Horn Point is a flooding surface (figure 11.62) representing a 4th-order sequence boundary indicated here by (1) evidence of subaerial exposure, (2) regionally traceable surfaces, and (3) the presence of deeper-water black shales at the contact, in this case the Hovenweep shale above the Horn Point (Goldhammer and others, 1991). This type of surface or sequence boundary, as well as parasequence boundaries (also flooding surfaces [figure 11.63]), is a time-correlative marker in the subsurface. If these surfaces are not recognized and the intervals erroneously correlated lithostratigraphically, the result might be failure to recognize significant fluid-flow barriers, and misinterpretation of reservoir facies geometries and distributions. These surfaces must be recognized in conventional core and/or geophysical logs in order to accurately

Figure 11.62. *Flooding surface (4th-order sequence boundary) at the top of the Horn Point marker bed, lower Ismay zone of the Paradox Formation along the Honaker Trail. Note abundant intact and fragmented productid brachiopods in the medium gray limestone matrix.*

Figure 11.63. *Flooding surface (5th-order parasequence boundary?) at the top of the Barker Creek zone of the Paradox Formation along the Honaker Trail. Note abundant rip-up clasts and sharp contact with the overlying unit.*

predict the distribution and continuity of reservoirs (Weber and others, 1995a, 1995b).

The Paradox Formation along the Honaker Trail (Horn Point marker bed of the lower Ismay zone to the base of the section in the Barker Creek zone) displays most of the major lithofacies associated with carbonate buildups observed in the formation at Eight-Foot Rapid. Carbonate fabrics, from deepest to shallowest, include shaley lime mudstone, sponge spicule-bearing wackestone, skeletal (mainly crinoidal and phylloid-algal) and peloidal wackestone to packstone, and oolitic grainstone (Ritter and others, 2002; Ritter and Gianinny, 2012). An unusual cross-bedded, 5-foot-thick (2 m) quartz sandstone unit (figure 11.64) is present near the top of the lower Ismay above a fossiliferous wackestone. Similar cross-bedded sandstone units have been recognized by Eby and others (2003) in core from wells in the Blanding sub-basin. Large chert nodules, presumably derived from sponge spicules, are common in laminated, deeper-water limestone (figure 11.65). *Chaetetes* are also commonly associated with fossiliferous wackestone in the skeletal-capping facies above the phylloid-algal facies (figure 11.66). Peloidal and oolitic grainstone in the cap and intermound facies display well-developed cross-bedding (figure 11.67).

Distinct phylloid-algal mounds, the primary reservoir lithology, are exposed in the Barker Creek and Akah zones throughout The Goosenecks section of the San Juan River. These mounds vary in length from a few tens of feet to several hundred feet, often rapidly pinching out into non-mound lithofacies (figures 11.68, 11.69, and 11.70). The thickness is also variable from a few tens of feet to well over 50 feet (16 m). Mounds are occasionally stacked but separated by either mound-cap or substrate facies (figure 11.71). Mound flanks are well exposed and consist of angular, poorly sorted clasts of mound material (figure 11.72), whereas intermound channel grainstone deposits show excellent cross-bedding (figure 11.73).

Horizontal drilling has only been conducted in a few typical fields in the Paradox Basin with no commercial success; the exception is within the atypical Greater Aneth field where horizontal drilling has become a significant best practice (see chapter 14). Phylloid-algal mounds in The Goosenecks demonstrate that there are various targets and risks when considering potential horizontal drilling in small, heterogeneous reservoirs in the Paradox Basin. Before selecting the optimal location, orientation, and type of horizontal well (for example single or multiple horizontal laterals, radially stacked laterals, splays or branches), the distribution, both laterally and vertically, of the mound or mounds, mound flanks, and other associated lithofacies must be carefully evaluated.

Figure 11.64. *Very fine grained, cross-bedded quartz sandstone near the top of the lower Ismay zone of the Paradox Formation along the Honaker Trail.*

Figure 11.65. *Large chert nodules in laminated lime mudstone, Akah zone of the Paradox Formation along the Honaker Trail.*

Figure 11.66. Chaetetes *in fossiliferous wackestone of a skeletal-capping facies, lower Ismay zone of the Paradox Formation along the Honaker Trail.*

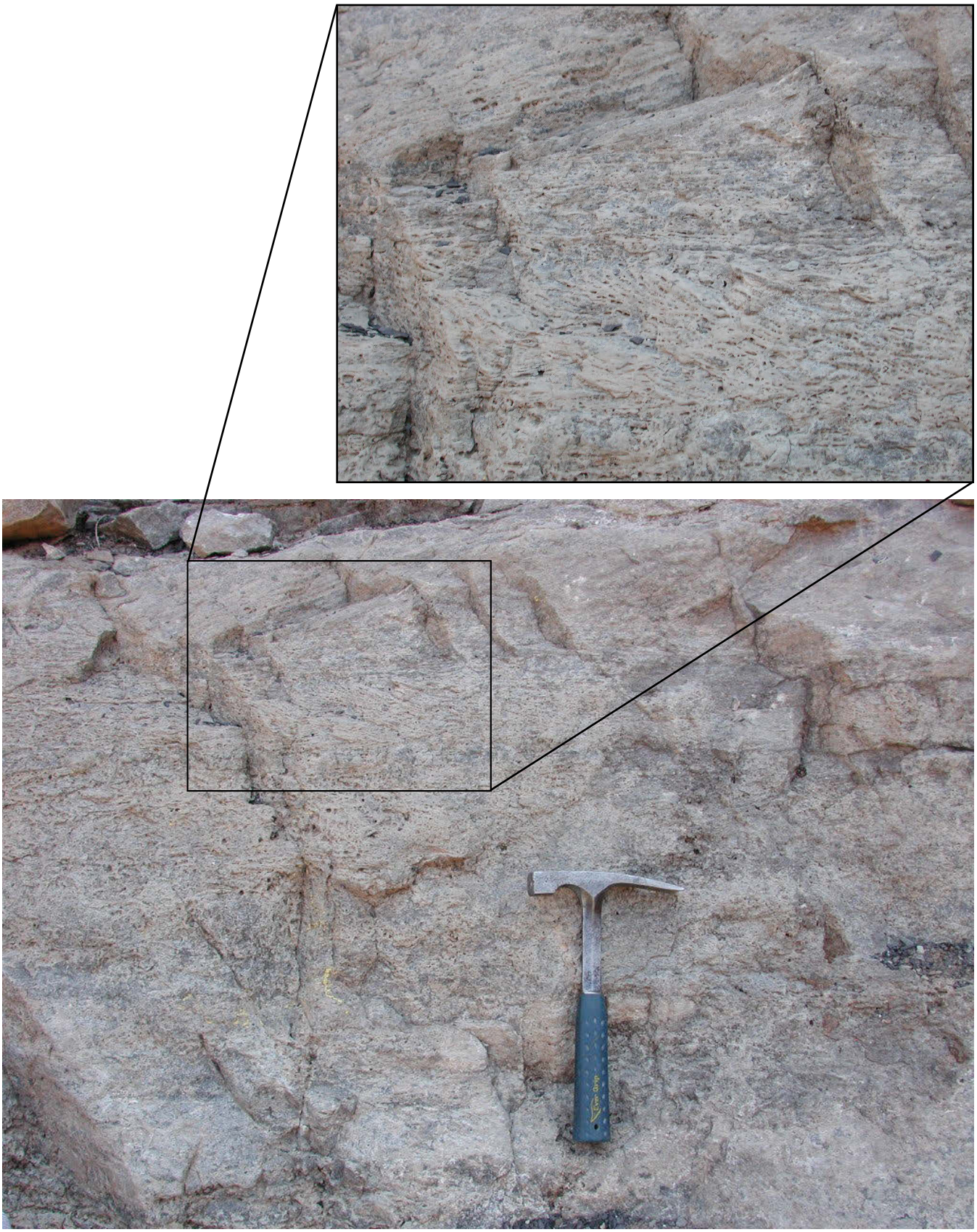

Figure 11.67. *Well-developed cross-bedding in peloidal and oolitic grainstone in the cap and intermound facies of the Barker Creek zone of the Paradox Formation along the Honaker Trail. Close up shown in inset photo.*

Figure 11.68. *Small phylloid-algal mound in the Barker Creek zone of the Paradox Formation, river mile 44.3, San Juan River. View to the south.*

Figure 11.69. *Medium-sized phylloid-algal mound in the Akah zone of the Paradox Formation, river mile 38.5, San Juan River.*

Figure 11.70. *Photomosaic of a large phylloid-algal mound complex in the Barker Creek zone of the Paradox Formation, river mile 40.5, San Juan River. View to the north.*

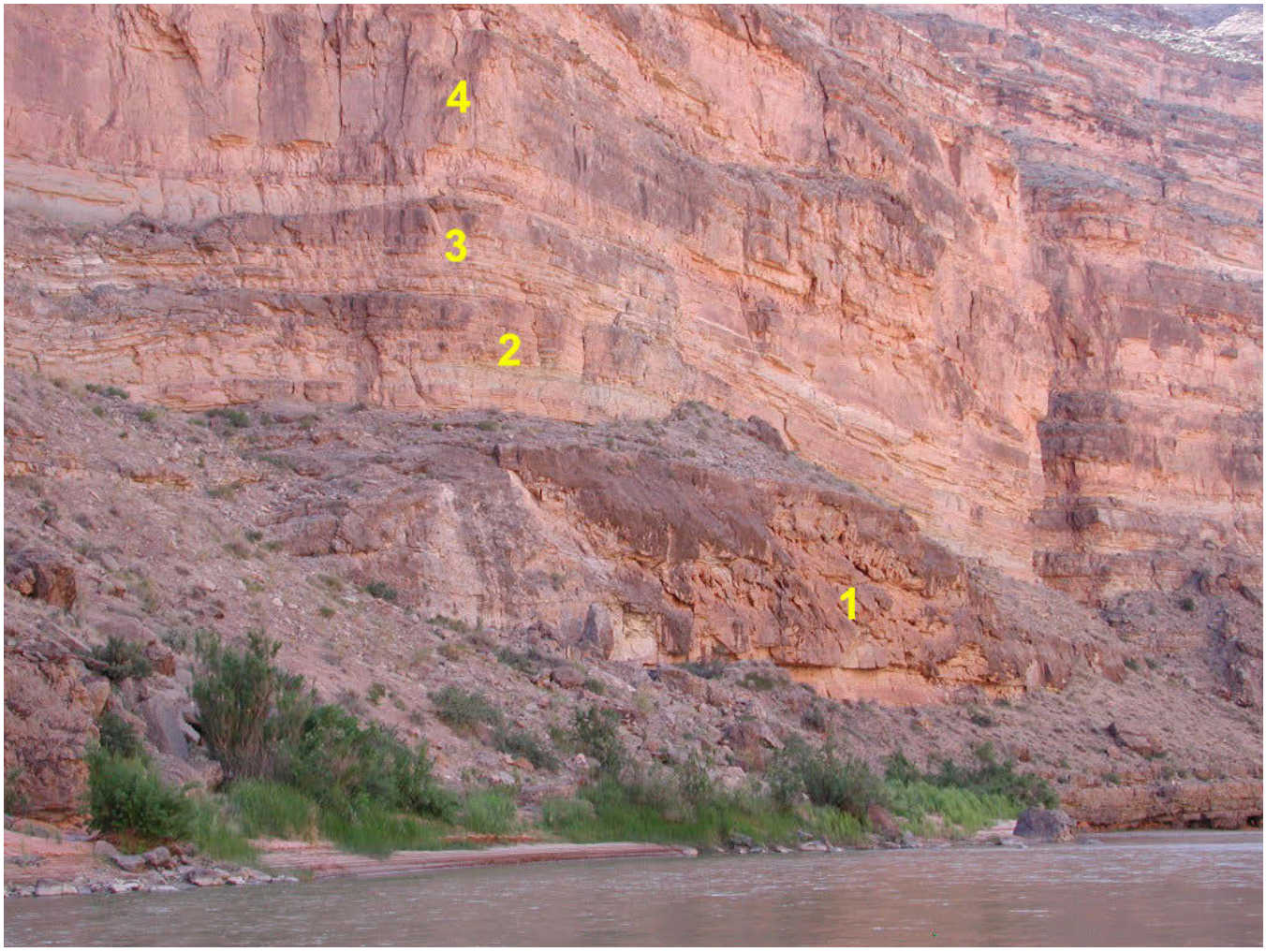

Figure 11.71. *Stacked complex of four phylloid-algal mounds in the Akah and Barker Creek zones of the Paradox Formation, river mile 39.8, San Juan River. View to the south.*

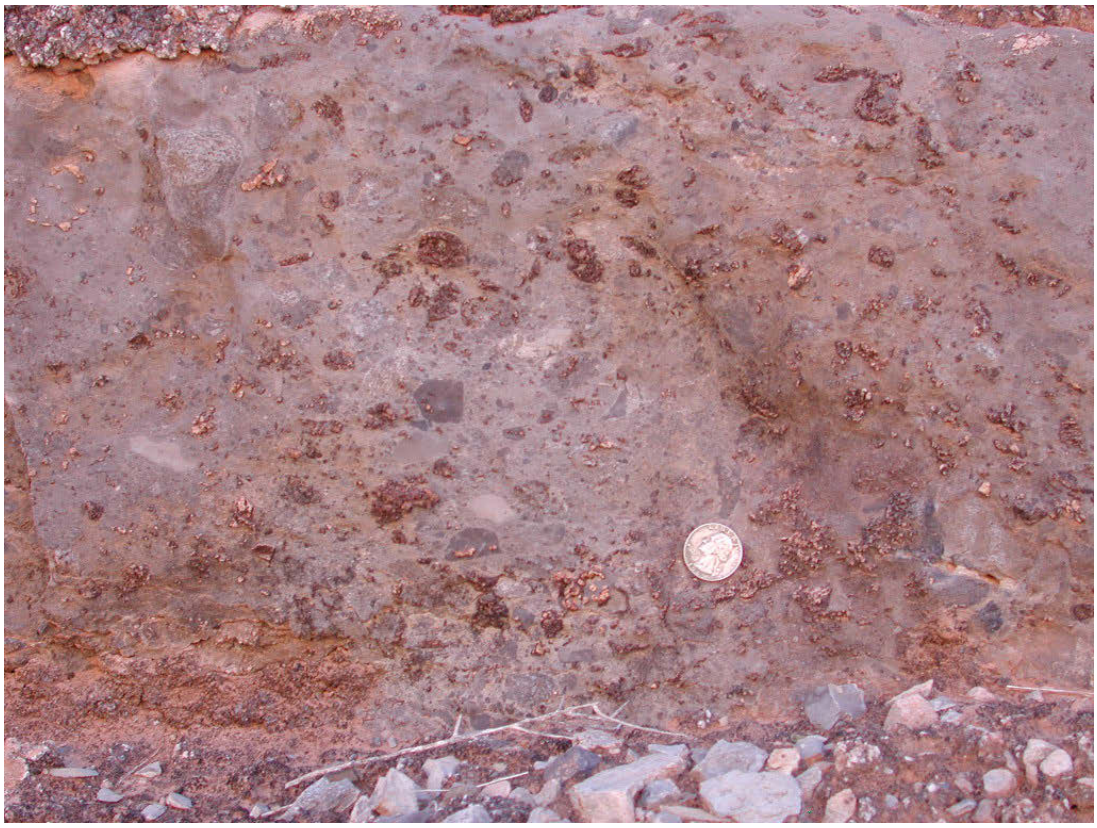

Figure 11.72. *Mound flank material—part of the large phylloid-algal mound complex in the Barker Creek zone shown on figure 11.67, river mile 40.5, San Juan River.*

Figure 11.73. *Cross-bedding in an intermound channel grainstone deposit in the Akah zone of the Paradox Formation, river mile 35.3, San Juan River.*

CHAPTER 12:
SUMMARY AND CONCLUSIONS

by

Thomas C. Chidsey, Jr.
Utah Geological Survey

CONTENTS

CHAPTER 12:
SUMMARY AND CONCLUSIONS

Utah contains large areas that are still virtually unexplored. Significant potential for increased recovery from existing fields remains by employing improved reservoir characterization and the latest drilling, completion, and enhanced-oil-recovery technologies. A combination of depositional and structural events created the right conditions for oil generation and trapping in the major oil-producing provinces (thrust belt, Uinta Basin, and Paradox Basin) in Utah and adjacent areas in Colorado, Wyoming, and Arizona. Oil plays are specific geographic areas having petroleum potential due to favorable source rock, migration paths, reservoir characteristics, and other factors.

MAJOR OIL PLAYS

Triassic-Jurassic Nugget Sandstone Thrust Belt Play

1. The most prolific oil play in the Utah/Wyoming thrust belt province is the Triassic-Jurassic Nugget Sandstone thrust belt play, having produced nearly 292 million BO (46 million m^3) and 6.0 TCFG (0.17 TCMG). The Nugget Sandstone was deposited in an extensive dune field that extended from Wyoming to Arizona. Playas or oases developed in interdune areas. Traps form on discrete subsidiary closures along major ramp anticlines. The seals for the producing horizons are overlying argillaceous and gypsiferous beds within the Middle Jurassic Twin Creek Limestone, or a low-permeability zone at the top of the Nugget Sandstone.

2. Hydrocarbons in Nugget Sandstone reservoirs were generated from subthrust Cretaceous source rocks. The source rocks began to mature after being overridden by thrust plates. Hydrocarbons were then generated, expelled, and subsequently migrated into overlying traps, primarily along fault planes.

3. The Nugget Sandstone has heterogeneous reservoir properties because of (1) cyclic dune/interdune lithofacies with better porosity and permeability that developed in certain dune morphologies, (2) diagenetic effects, and (3) fracturing.

4. The Nugget Sandstone thrust belt play is divided into three subplays: (1) Absaroka thrust–Mesozoic-cored shallow structures, (2) Absaroka thrust–Mesozoic-cored deep structures, and (3) Absaroka thrust–Paleozoic-cored shallow structures. Mesozoic-cored structures subplays both represent a linear, hanging-wall, ramp anticline parallel to the leading edge of the Absaroka thrust. This ramp anticline is divided into a broad, shallow structural high (culmination) and a deep, structural low (depression). Fields in the shallow subplay produce crude oil and associated gas. Fields in the deep subplay produce retrograde condensate. The Paleozoic-cored shallow structures subplay is located immediately west of the Mesozoic-cored structures subplays. This subplay represents a very continuous and linear, hanging-wall, ramp anticline that is also parallel to the leading edge of the Absaroka thrust. The eastern boundary of the subplay is defined by the truncation of the Nugget against a thrust splay. Fields in this subplay produce nonassociated gas and condensate. Traps in these subplays consist of long, narrow, doubly plunging anticlines.

5. Prospective drilling targets in the Nugget Sandstone thrust belt play are delineated using high-quality 2-D and 3-D seismic data, 2-D and 3-D forward modeling/visualization tools, well control, dipmeter information, surface geologic maps, surface geochemical surveys, and incremental restoration of balanced cross sections to access trap geometry. Determination of the timing of structural development, petroleum migration, entrapment, and fill and spill histories is critical to successful exploration.

6. Future Nugget Sandstone exploration could focus on more structurally complex and subtle, thrust-related traps. Nugget structures may be present beneath the leading edge of the Hogsback thrust and North Flank fault of the Uinta uplift.

Jurassic Twin Creek Limestone Thrust Belt Play

1. The Jurassic Twin Creek Limestone thrust belt play in the Utah/Wyoming thrust belt province has produced over 20 million BO (3.2 million m^3) and 186 BCFG (5.3 million m^3). The Twin Creek was deposited in a shallow-water embayment south of the main body of a Middle Jurassic sea that extended from Canada to southern Utah. Traps form on same structures as the underlying Nugget Sandstone where the low-porosity Twin Creek is extensively fractured. The seals for the producing horizons are overlying argillaceous and clastic beds, and non-fractured units within the Twin Creek and the overlying salt beds of the Jurassic Preuss Formation. Hydrocarbons in Twin Creek reservoirs were also generated from subthrust Cretaceous source rocks.

2. Most oil and gas production is from perforated intervals in the Watton Canyon, upper Rich, and Sliderock Members of the Twin Creek Limestone. These members have little to no primary porosity in the producing horizons, but exhibit secondary porosity in the form of fractures. Identification and correlation of barriers and baffles to fluid flow, and recognizing fracture set orientations in individual Twin Creek reservoirs in the thrust belt is critical to understanding their effects on production rates, petroleum movement pathways, and horizontal well plans.

3. The Twin Creek Limestone thrust belt play is divided into two subplays that correspond structurally with Nugget subplays described above except shallower: (1) Absaroka thrust–Mesozoic-cored structures and (2) Absaroka thrust–Paleozoic-cored structures. Fields in these subplays produce crude oil and associated gas and non-associated gas and condenste, respectively. The eastern boundaries of the subplays are defined by the truncation of the Twin Creek against a thrust splay.

4. Future Twin Creek Limestone exploration could target the same structurally complex and subtle, thrust-related traps as the Nugget Sandstone, but using horizontal drilling. Unrecognized microbial carbonates containing porosity represent untested reservoir potential.

Jurassic Navajo Sandstone/Temple Cap Formation Hingeline Play

1. The only play in the central Utah thrust belt is called the Jurassic Navajo/Temple Cap Hingeline play and to date contains two discoveries: Covenant and Providence fields. The Early Jurassic Navajo Sandstone was deposited in the same extensive dune field, which extended from Wyoming to Arizona, as the Nugget Sandstone. The White Throne Member of the Middle Jurassic Temple Cap Formation was deposited as coastal dunes. Traps include fault-bend anticlines associated with thrust imbricate and duplex structures, positioned near Jurassic extension faults. The principal seals for the Navajo/White Throne producing zones consist of salt, gypsum, mudstone, limestone, and shale in the Sinawava and Esplin Point Members of the Temple Cap Formation, Twin Creek Limestone, and Arapien Shale.

2. Hydrocarbons in Navajo and Temple Cap reservoirs were likely generated from Mississippian source rocks. The source rocks began to mature after loading or overridding by thrust plates. When the current Covenant trap formed 70 to 80 million Ma, remigration stripped the original gas-saturated oil of volatiles. No stripping of volatiles occurred at Providence field. The presence of significant amounts of carbon dioxide and nitrogen with hydrocarbon gases at Providence field likely represents a mixing event from sources separate from those responsible for the hydrocarbon charge.

3. The Navajo Sandstone and Temple Cap Formation at Covenant field has 424 feet (139 m) of net pay, an average of 12% porosity, up to 100 mD of permeability, an average water saturation of 38%, and a strong water drive. The First Navajo Sandstone at Providence field has 134 feet (41 m) of net pay, an average of 10.7% porosity, 8 mD of permeability, an average water saturation of 49%, and a reservoir drive mechanism of gas expansion with water drive. The Second Navajo Sandstone at has 96 feet (29 m) of net pay, an average of 5.5% porosity, 3.6 mD of permeability, an average water saturation of 33%, and a reservoir drive mechanism of gas expansion with limited water drive.

4. The OOIP for Covenent field is estimated at 100 million bbls (15.9 million m^3); the estimated recovery factor is 40 to 50%. Although the productive area for Providence field has not been fully defined, OOIP reserves are estimated at 10.7 million bbls (1.7 million m^3). Estimated in place gas reserves are 31.6 BCF (0.89 BCM) based GORs from pressure/volume/temperature analysis. Estimated ultimate recovery for Providence field has not been determined.

5. Future exploration in the central Utah thrust belt should focus on Paleozoic-cored, blind, thrust structures east of the exposed Charleston-Nebo and Pahvant thrusts. The lack of associated gas at Covenant field suggests the possibility that gas-charged traps may be present in the play area.

Uinta Basin Plays

1. Oil and gas production in the Laramide-age Uinta Basin is mostly from the Paleocene and Eocene Green River and Colton/Wasatch Formations. In early late Paleocene time, a large lake, known as ancestral Lake Uinta, developed in the basin. Deposition in and around Lake Uinta consisted of open- to marginal-lacustrine sediments that make up the Green River Formation. Alluvial redbed and floodplain deposits that are laterally equivalent to, and intertongue with, the Green River form the Colton/Wasatch.

2. The USGS defines two assessment units within the Green River Total Petroleum System in the Uinta Basin: the Deep Uinta Overpressured Continuous Oil Assessment Unit (Deep Uinta Basin Overpressured Continuous play in this report) and the Uinta Green River Conventional Oil and Gas Assessment Unit. The Conventional Oil and Gas Assessment Unit can be divided into plays having a dominantly southern sediment source (Conventional Southern Uinta Basin play) and

plays having a dominantly northern sediment source (Conventional Northern Uinta Basin play).

3. The Conventional Northern Uinta Basin and Deep Uinta Basin Overpressured Continuous plays cover the northern Uinta Basin. The Conventional Northern Uinta Basin play typically has drill depths ranging from 5000 feet (1500 m) to a maximum of 10,000 feet (3000 m). The play is divided into two subplays: (1) Conventional Bluebell subplay, and (2) Conventional Red Wash subplay. The Deep Uinta Basin Overpressured Continuous play is delineated where the lower 2500 to 3000 feet (750–900 m) of the Green River and intertonguing Colton Formations are overpressured (gradient >0.5 psi/ft [11.3 kPa/m]). The most rapid increase in reservoir pressure and most of the high-volume, overpressured oil production typically occurs at depths ranging from 11,000 to 14,000 feet (3400–4300 m).

4. In the Conventional Bluebell subplay, sandstone reservoirs typically have low porosity (8 to 12%) and low matrix permeability (0.01 to 10 mD). Sandstone reservoirs in the Conventional Red Wash subplay have higher porosities (8 to 20%) and significantly higher matrix permeabilities, commonly 50 to 500 mD. In the Deep Uinta Basin Overpressured Continuous play, production is fracture controlled in reservoir rocks, which typically have very low (< 0.1 mD) matrix permeability. The reservoirs are fractured lenticular sandstone, shale, and marlstone deposited in the lacustrine and alluvial environments of Lake Uinta.

5. Fields in the Conventional Northern Uinta Basin play and Deep Uinta Basin Overpressured Continuous play produce crude oil with associated gas. Production from the Conventional Bluebell subplay cannot be accurately separated from the Deep Uinta Basin Overpressured Continuous play. The largest fields in the Conventional Red Wash subplay have produced 169.7 million BO (27.0 million m^3) and 605.6 BCFG (17.1 BCMG). The Deep Uinta Basin Overpressured Continuous play has produced nearly 345 million BO (54.8 million m^3) and 620 BCFG (17.6 BCM) primarily from three large fields—Altamont, Bluebell, and Cedar Rim.

6. The Conventional Northern Uinta Basin play and Deep Uinta Basin Overpressured Continuous play areas are also being explored for Mesaverde Group and Mancos Shale gas, when prices are high. The deeper drilling for gas could result in the discovery of new oil fields in the overlying Green River Formation.

7. The Conventional Southern Uinta Basin play is divided into six subplays: (a) Conventional Uteland Butte interval, (b) Conventional Castle Peak interval, (c) Conventional Travis interval, (d) Conventional Monument Butte interval, (e) Conventional Beluga interval, and (f) Conventional Duchesne interval fractured shale/marlstone.

8. The source rocks for the crude oil produced from the Uinta Basin plays are also found in the Green River Formation and consist of kerogen-rich shale and marlstone, which were deposited in nearshore and offshore open-lacustrine environments. Most of these oils are characterized as yellow or black wax. Production from the Deep Uinta Basin Overpressured Continuous play is dominantly yellow wax, while most of the oil production from the Conventional Northern Uinta Basin play and Conventional Southern Uinta Basin play is black wax.

9. Future exploration in the Green River Formation of the Uinta Basin should consist of extending the productive limits of existing fields by step-out drilling and wildcat drilling along producing trends. Ostracodal/oolitic grainstone reservoirs in the lower Green River in the northern Uinta Basin and thin dolomites in the Uteland Butte interval in the central part of the basin represent the greatest potential for new discoveries and reserves using horizontal drilling.

Mississippian Leadville Limestone Paradox Basin Play

1. The Mississippian Leadville Limestone is a major oil and gas play in the Paradox Basin, having produced over 52 million BO (8.3 million m^3) and 867 BCFG (24.6 BCMG). Most Leadville production is from the Paradox fold and fault belt. The Leadville is a shallow, open marine, carbonate-shelf deposit. Local depositional environments included shallow-marine, subtidal, supratidal, and intertidal. Solution breccia and karstified surfaces are common. Most oil and gas produced from the Leadville is in basement-involved structural traps with closure on both anticlines and faults. Lisbon, Big Indian, Little Valley, and Lisbon Southeast fields are on sharply folded anticlines that close against the Lisbon fault zone. Salt Wash and Big Flat fields, northwest of the Lisbon area, are on unfaulted, east-west- and north-south-trending anticlines, respectively. The unfaulted structures probably developed from movement on deep, basement-involved faults that do not rise to the level of the Leadville. These and other faults affecting the Leadville probably reflect the reactivation of preexisting, Precambrian-age faults during the Laramide orogeny or later.

2. Hydrocarbons in Leadville Limestone reservoirs were likely generated from source rocks in the Pennsylvanian Paradox Formation. Hydrocarbon generation occurred during maximum burial in the Late Cretaceous and early Tertiary. The seals for the Leadville producing zones

are the overlying clastic beds of the Pennsylvanian Molas Formation and evaporite (salt and anhydrite) beds within the Pennsylvanian Paradox Formation.

3. The Leadville Limestone has heterogeneous reservoir properties because of lithofacies with varying porosity and permeability, diagenetic effects (dolomitization), and fracturing. The early diagenetic history of the Leadville sediments, including some dolomitization (finely crystalline) and leaching of skeletal grains, resulted in low-porosity and/or low-permeablility rocks. Most of the porosity and permeability associated with hydrocarbon production at Lisbon field was developed during later, deep subsurface dolomitization (coarsely crystalline replacement and saddle [hydrothermal?] dolomite) and dissolution.

4. In major reservoirs, the produced Leadville oil and condensate are rich, volatile crudes. Leadville reservoirs produce associated gas that is variable in composition; nonassociated gas is relatively uniform in composition.

5. New prospective drilling targets in the Leadville Limestone Paradox Basin play are delineated using high-quality 2-D and 3-D seismic data, 2-D and 3-D forward modeling/visualization tools, well control, dipmeter information, and surface geologic maps to assess trap geometry. Relatively low-cost surface geochemical surveys, hydrodynamic analysis, and epifluorescence techniques may identify potential Leadville hydrocarbon migration patterns and oil-prone areas. Diagenetic traps (hydrothermal dolomite) represent difficult to identifiy but significant untested hydrocarbon targets.

Pennsylvanian Paradox Formation Paradox Basin Play

1. The most prolific oil and gas play in the Paradox Basin is the Pennsylvanian Paradox Formation play. The Paradox Formation has produced over 549 million bbls (87 million m^3) of sweet, paraffinic oil and 627 BCFG (17 BCMG) from more than 70 fields. The main producing zones are referred to as the Desert Creek, Ismay, and Cane Creek shale. The Paradox Formation oil play area includes nearly the entire Paradox Basin. The Paradox Formation Play is divided into four subplays: (1) fractured shale, (2) Blanding sub-basin Desert Creek zone, (3) Blanding sub-basin Ismay zone, and (4) Aneth platform Desert Creek zone.

2. In Pennsylvanian time, the Paradox Basin was rapidly subsiding in a subtropical arid environment with a shallow-water carbonate shelf (often restricted) on the south and southwest margins of the basin that locally contained carbonate buildups. In the Blanding sub-basin, Ismay zone reservoirs are dominantly limestones composed of small, phylloid-algal buildups; locally variable, inner-shelf, skeletal calcarenites; and rarely, open-marine, bryozoan mounds. Desert Creek zone reservoirs are dominantly dolomite and have regional, nearshore, shoreline trends with highly aligned, linear facies tracts. On the Aneth platform, Desert Creek reservoirs include shallow-shelf buildups (phylloid algal, coralline algal, and bryozoan buildups [mounds]) and calcarenites (beach, dune, and oolite banks). Here, the Desert Creek and Ismay zones are predominately limestone, with local dolomitic units. The Cane Creek shale zone represents a basinal open-marine environment composed of dolomite (the main reservoir rock), silty limestone, anhydrite, and organic-rich shale.

3. Phylloid-algal mound lithofacies in both the Ismay and Desert Creek zones contain large phylloid-algal plates of *Ivanovia*, *Kansasphyllum*, or *Eugonophyllum*, and skeletal grains create bafflestone or bindstone fabrics. Bryozoan buildup lithofacies are represented by bindstone, bafflestone, and packstone fabrics that are rarely dolomitized. Calcarenite lithofacies include grainstone and packstone fabrics containing oolites, coated grains, hard peloids, bioclastic grains, shell lags, and intraclasts.

4. Hydrocarbons in Paradox Formation reservoirs were generated from source rocks within the formation itself during maximum burial in the Late Cretaceous and early Tertiary. Organic-rich units, informally named the Hovenweep, Chimney Rock, and Gothic shales (as well as the productive Cane Creek shale), are composed of black, sapropelic shale and shaley dolomite. Vertical reservoir seals for the Paradox producing zones are shale, halite, and anhydrite within the formation; lateral seals are permeability barriers created by unfractured, off-mound (non-buildup) mudstone, wackestone, and anhydrite.

5. Trap types in the Blanding sub-basin and Aneth platform regions include stratigraphic, stratigraphic with some structural influence, combination stratigraphic/structural, and diagenetic involving carbonate buildups encased by either evaporites or organic-rich shale. Many carbonate buildups appear to have developed on subtle cored anticlinal noses or structural closures.

6. The Ismay and Desert Creek zones have heterogeneous reservoir properties because of depositional lithofacies with varying porosity and permeability, carbonate buildup (mound) relief and flooding surfaces (parasequence boundaries), and a wide range of both positive and negative diagenetic effects. The extent of these factors, and how they are combined, affect the degree to which they create barriers to fluid flow. Identification and correlation of depositional lithofacies and parasequences in individual Paradox reservoirs is critical to understanding their effect on water/CO_2 injection pro-

grams, production rates, and paths of petroleum movement. The typical early diagenetic events occurred in the following order: (1) early marine cementation, (2) post-burial, replacement, rhombic dolomite cementation due to seepage reflux, (3) vadose and meteoric phreatic diagenesis including leaching/dissolution, neomorphism, and fresh-water cementation, (4) mixing zone dolomitization, (5) syntaxial cementation, and (6) anhydrite cementation/replacement. Post-burial diagenesis included additional syntaxial cementation, silicification, late coarse calcite spar formation, saddle dolomite cementation, stylolitization, additional anhydrite replacement, late dissolution (microporosity development), and bitumen plugging.

7. Mapping the Ismay zone lithofacies delineates very prospective reservoir trends that contain productive carbonate buildups around anhydrite-filled intra-shelf basins. Lithofacies and reservoir controls imposed by the anhydritic intra-shelf basins should be considered when selecting the optimal location and orientation of any horizontal drilling for undrained reserves. Projections of the inner shelf/tidal flat and mound trends around the intra-shelf basins identify potential exploration targets. Pervasive marine cement may be indicative of "wall" complexes of shallow-shelf carbonate buildups suggesting potential nearby carbonate buildups, particularly phylloid-algal mounds. Platform-margin calcarenites in the Desert Creek zone are located along the margins of the larger shallow shelf or the rims of phylloid-algal buildup complexes. Mapping indicates a relatively untested lithofacies belt of calcarenite carbonate deposits south and southeast of Greater Aneth field.

8. Fractured-shale beds in the Pennsylvanian Paradox Formation are oil productive in the Paradox Basin fold and fault belt of southwest Utah. Jointing and fractures are controlled by regional tectonics and more localized salt movement, dissolution, and collapse. Traps in the Cane Creek shale developed on salt-cored structures where fracture intensity is greatest. Thus, the Cane Creek is a fractured, self-sourced oil reservoir that is highly overpressured—an ideal target for horizontal drilling. Fracture data from oriented cores in the Cane Creek show a regional, northeast to southwest, near-vertical, open, extensional fracture system that is not significantly affected by orientations of localized folds.

OUTCROP ANALOGS FOR MAJOR RESERVOIRS

Utah is unique in that representative outcrop analogs for each major oil play are present in or near the thrust belt, Uinta Basin, and Paradox Basin. Production-scale analogs provide an excellent view, often in 3-D, of reservoir-facies characteristics (geometry, distribution, and so forth) and the nature of boundaries contributing to the overall heterogeneity of reservoir rocks. Outcrop analogs can be used as a "template" for evaluation of data from conventional core, geophysical and petrophysical logs, and seismic surveys. When combined with subsurface geological and production data, analog models improve development drilling and production strategies, reservoir-simulation models, reserve calculations, and design and implementation of secondary/tertiary oil recovery programs and other best practices used in the oil fields of Utah and vicinity.

Thrust Belt

Triassic-Jurassic Nugget and Jurassic Navajo Sandstone

The most prolific oil reservoir in the thrust belt is the Triassic-Jurassic Nugget Sandstone and Lower Jurassic Navajo Sandstone. The best outcrop analogs to these reservoirs are found in exposures of the Navajo Sandstone of southern Utah. Outcrops along the shores of Lake Powell and in the San Rafael Swell display classic eolian bedforms such as large-scale dunal cross-strata, and interdunal features such as oases, wadi, and playa lithofacies. Navajo interdune lithofacies have significantly poorer reservoir characteristics than the dune lithofacies and in a reservoir represent potential barriers to flow. Identification and correlation of dune/interdune lithofacies in individual Nugget/Navajo reservoirs in the thrust belt is critical to understanding their effects on production rates and paths of petroleum movement.

Jurassic Temple Cap Formation

The Middle Jurassic Temple Cap Formation exposed near the eastern entrance to Zion National Park in southwestern Utah is almost a perfect match to both the core and geophysical well logs from Covenant field in the Hingeline area. All three members are present: the basal Sinawava, White Throne, and the Esplin Point Members. In the eastern part of the park, outcrops of the Sinawava Member are composed of mudstone, siltstone, and fine-grained sandstone deposited in a coastal sabkha and tidal flat environment. The White Throne Member is a vertical cliff composed of fine-to medium-grained sandstone with large-scale, high-angle cross-beds that represent coastal eolian dunes. The Esplin Point Member is composed of thin, planar to horizontal laminated beds of siltstone and fine-grained marginal marine sandstone. Radiometric age dates of ash beds and marine palynomorphs indicate a Middle Jurassic (Bajocian) age.

Jurassic Twin Creek Limestone

The best outcrop analogs for the Middle Jurassic Twin Creek Limestone reservoir are found west of Anschutz Ranch field at Devils Slide on the Crawford thrust plate and southwest of Lodgepole field near the town of Peoa, Utah, on the Ab-

saroka thrust plate (?). Closely spaced rhombic and rectilinear fracture patterns developed on bedding planes and within dense, homogeneous non-porous (in terms of primary porosity) limestone beds of the Rich and Watton Canyon Members. The contact with the basal siltstone units (where fractures are sealed) of the overlying members set up the Rich and Watton Canyon for hydrocarbon trapping and production. Thin-bedded siltstone within the Rich and Watton Canyon Members, also observed in outcrop, creates additional reservoir heterogeneity. Identification and correlation of these barriers and baffles to fluid flow, and recognizing fracture set orientations in individual Twin Creek reservoirs in the thrust belt is critical to understanding their effects on production and horizontal well plans.

Uinta Basin

Deep Uinta Basin Overpressured Continuous Play

Outcrop analogs for the Deep Uinta Basin Overpressured Continuous play in Sevier and Sanpete Counties, central Utah, provide examples of deposits shed off the western highlands into Lake Uinta. Many of the proximal conglomerates were deposited in water by fan deltas extending into the lake. Other exposures of medial facies include interbedded shale, sandstone, and limestone deposited in a marginal-lacustrine environment. The distal facies of the Flagstaff Limestone is composed of open-lacustrine shale and limestone.

Conventional Northern Uinta Basin Play

An outcrop analog for the major oil reservoirs in the Conventional Northern Uinta Basin play is exposed along Raven Ridge in the northeastern Uinta Basin; these exposures display landward to lakeward facies transitions in the Green River Formation. Several locations offer excellent exposures of shoreline deposits that serve as reservoirs, and bay-fill deposits that provide organic-rich source rock for the play.

Conventional Southern Uinta Basin Play

Outcrop analogs for the major oil reservoirs in the Green River Formation in the Conventional Southern Uinta Basin play are well exposed in Willow Creek, Indian, and Nine Mile Canyons in the south-central Uinta Basin. The Uteland Butte interval is exposed in Nine Mile Canyon as dolomitized ostracod and pellet grainstone and packstone deposited in shallow-water mudflats; pelecypod-gastropod sandy grainstone, commonly interbedded with silty claystone or carbonate mudstone (dolomite) deposited in shallow nearshore to open-lacustrine environments; and dark-gray kerogen-rich carbonates deposited in deeper offshore environments. The Castle Peak interval is exposed in the western portion of Nine Mile Canyon as interbedded carbonate, shale, and sandstone. The primary reservoir rocks are isolated channel deposits. The secondary reservoirs in the Travis interval and the primary reservoirs in the Monument Butte and Beluga intervals are distributary-channel deposits. The Monument Butte interval typically contains amalgamated stacked channel deposits, whereas in the Travis and Beluga intervals, the distributary channels are generally isolated individual channels. One location in Nine Mile Canyon, termed the Nutter's Ranch study site, is an outcrop analog for the Travis (secondary reservoir), Monument Butte, and Beluga intervals. Examination of the outcrop identified the potential heterogeneity that can exist between wells in two dimensions (as well as over a square mile), as an analogy to a typical waterflood unit in the Monument Butte field area to the north. The Duchesne interval represents the maximum rise and eventual waning stages of ancient Lake Uinta and is well exposed in Indian Canyon south of the town of Duchesne.

Fractures can be observed in the Green River Formation in Indian Canyon and throughout the surface exposures in the Duchesne field along the Duchesne fault zone. Any fractured outcrop in the upper and saline members can be considered a reservoir analog.

Paradox Basin

Mississippian Leadville Limestone

Excellent outcrops of Leadville-equivalent rocks are found in the Madison Limestone along the south flank of the Uinta Mountains, Utah, and in the Redwall Limestone in the Marble Canyon area of Grand Canyon National Park, Arizona. These outcrops provide production-scale analogs of facies characteristics, geometry, distribution, and the nature of boundaries contributing to the overall heterogeneity of Leadville reservoir rocks. The Madison and Redwall are fine- to coarse-crystalline, cherty limestone with some dolomite. Limestone units commonly contain numerous caverns, sinkholes, and local zones of solution breccia and vugs. Sections can have high heterogeneity due to stylolites, jointing, and fractures. Possible buildups, shoals or banks, and mud mounds comparable to Waulsortian facies are also found in these formations.

Pennsylvanian Paradox Formation

In the Paradox Basin, hydrocarbons are stratigraphically trapped in heterogeneous reservoirs within carbonate buildups (or phylloid-algal mounds) of the Pennsylvanian Paradox Formation. Carbonate buildups exposed in the Paradox Formation at Eight-Foot Rapid, Honaker Trail, and The Goosenecks along the San Juan River of southeastern Utah provide excellent outcrop analogs of these reservoir rocks. Reservoir-quality porosity may develop in the types of lithofacies associated with buildups, such as troughs, detrital wedges, and fans, identified from these outcrops. If these lithofacies are in communication with mound-reservoir lithofacies in actual reservoirs, they could serve as conduits facilitating sweep efficiency in secondary/tertiary recovery projects. However,

the relatively small size and the abundance of intermound troughs over short distances, as observed along the river, suggests caution should be used when correlating these lithofacies between development wells. Lithofacies that appear correlative and connected from one well to another may actually be separated by low-permeability lithofacies which inhibit flow and decrease production potential. These outcrop analogs also demonstrate that there are various targets and risks when considering potential horizontal drilling in the Paradox Basin. Before selecting the optimal location, orientation, and type of horizontal well, the distribution both laterally and vertically of phylloid-algal mounds and other associated lithofacies must be carefully evaluated.

ACKNOWLEDGMENTS

This Bulletin was supported and encouraged by Richard G. Allis, State Geologist and Director of the Utah Geological Survey (UGS), and David E. Tabet (retired), Program Manager of the UGS Energy and Minerals Program. The research was performed under the Preferred Upstream Management Program (PUMPII) of the U.S. Department of Energy (DOE), National Energy Technology Laboratory (NETL), Tulsa, Oklahoma, contract number DE-FC26-02NT15133. The Contracting Officer's Representatives were Rhonda Jacobs and Virginia Weyland, both formerly with DOE. Additional funding was provided by the UGS.

Numerous professional geological and engineering societies, state regulatory agencies, and universities permitted the use of figures from their publications. We thank the American Association of Petroleum Geologists (AAPG) for use of the following figures obtained from various AAPG publications as identified in the figure captions and cited in the references: figure 2.10, modified from Villien and Kligfield, AAPG©1986; figure 3.5, modified from White and others, AAPG©1990; figure 6.3, from Bredehoeft and others, AAPG©1994; figure 10.1, Choquette, AAPG©1983; figures 10.32 and 10.37, modified from Peterson, AAPG©1992; figure 10.44, modified from Longman, AAPG©1980; figure 11.16, after Stearns, AAPG©1984; and figure 11.29, from Borer, AAPG©2003; reprinted by permission of the AAPG whose permission is required for further use.

We thank Wolverine Gas & Oil Corporation for providing core descriptions, photomicrographs, petrophysical data, and other reservoir analyses from Covenant field; field cores were described by L.F. Krystinik, geologic consultant. We thank Paul G. Lillis, U.S. Geological Survey, for assisting with the interpretation of geochemical data from Covenant field oil. Ken Robertson, Colorado Oil and Gas Conservation Commission, provided production data for Colorado fields. Oil analyses were provided by Humble Geochemical Services and Amoco Oil Company, Salt Lake Business Unit (now operated by Tesoro Corporation). We thank the Monticello Field Office, Bureau of Land Management, for providing the river permit, and our volunteer boatmen, Tom Yeager (deceased), Jim Yeager, and Blake Hopkins, who safely guided us down the San Juan River. We also thank John Warme, Colorado School of Mines, Golden, Colorado, and the Michigan Basin Geological Society for allowing us to visit Redwall Limestone sites during their 2005 Grand Canyon field trip down the Colorado River.

Vicky Clarke, Thomas Dempster, Cheryl Gustin, Sharon Hamre (retired), Jim Parker (deceased), Kevin McClure (formerly with the UGS), Liz Paton (formerly with the UGS), Jay Hill, Lori Steadman, and John Good (UGS) drafted figures and assisted with data compilation. Thomas Dempster, Carolyn Olsen (retired), Michael D. Laine (retired), Peter Nielsen, and Ammon McDonald (now with the Utah Division of Oil, Gas, and Mining) of the Utah Core Research Center photographed core. Kevin McClure assisted with fieldwork. Rebekah Stimpson (UGS) compiled production data. Geographic information systems support was provided by Sharon Wakefield (retired) of the UGS.

This Bulletin, or portions of it, was carefully reviewed by Paul B. Anderson, geological consultant; Stephanie Carney, David Tabet (retired), Mike Hylland, Robert Ressetar (retired), Bryce Tripp (retired), Kimm Harty (retired), and Richard G. Allis, UGS; and Virginia Weyland, NTEL. Their careful reviews and constructive criticism greatly improved the manuscript. Finally, Vicky Clarke, John Good, and the UGS editorial production team are thanked for producing a very high quality publication.

REFERENCES

Abbott, W.O., 1957, Tertiary of the Uinta Basin, *in* Seal, O.G., editor, Guidebook to the geology of the Uinta Basin: Intermountain Association of Petroleum Geologists Eighth Annual Field Conference, p. 102–109.

Ahlbrandt, T.S., and Fryberger, S.G., 1982, Introduction to eolian deposits, *in* Scholle, P.A., and Speraring, D., editors, Sandstone depositional environments: American Association of Petroleum Geologists Memoir 31, p. 11–47.

Ahr, W.M., 1989, Mississippian reef facies in the Southwest—a spectrum of variations in depositional style and reservoir characteristics, *in* Mear, C.E., McNulty, C.L., and McNulty, M.E., editors: Fort Worth Geological Society and Texas Christian University, Symposium on the Petroleum Geology of Mississippian Carbonates in North Central Texas, November 18, 1989, p. 1–19.

Allen, P.A., Verlander, J.E., Burgess, P.M., and Audet, D.M., 2000, Jurassic giant erg deposits, flexure of the United States continental interior, and timing of the onset of Cordilleran shortening: Geology, v. 28, no. 2, p. 159–162.

Allin, D.L., 1990, Colorado Plateau sub-surface water flow key: Oil and Gas Journal, v. 88, no. 30, p. 52–54.

Allin, D.L., 1993, Upper Valley, Garfield County, Utah, *in* Hill, B.G., and Bereskin, S.R., editors, Oil and gas fields of Utah: Utah Geological Association Publication 22, nonpaginated.

Allison, M.L., 1995, Increased oil production and reserves from improved completion techniques in the Bluebell field, Uinta Basin, Utah—annual report for the period September 30, 1993, to September 30, 1994: U.S. Department of Energy, DOE/BC/14953-10, 123 p.

Allison, M.L., 1997, A preliminary assessment of energy and mineral resources within the Grand Staircase–Escalante National Monument: Utah Geological Survey Circular 93, p. 13–25.

Allison, M.L., and Morgan, C.D., 1996, Increased oil production and reserves from improved completion techniques in the Bluebell field, Uinta Basin, Utah—annual report for the period October 1, 1994, to September 30, 1995: U.S. Department of Energy, DOE/BC/14953-14, 118 p.

Anders, D.E., Palacas, J.G., and Johnson, R.C., 1992, Thermal maturity of rocks and hydrocarbon deposits, Uinta Basin, Utah, *in* Fouch, T.D., Nuccio, V.F., and Chidsey, T.C., Jr., editors, Hydrocarbon and mineral resources of the Uinta Basin, Utah and Colorado: Utah Geological Association Publication 20, p. 53–76.

Anderson, P.B., Chidsey, T.C., Jr., Sprinkel, D.A, and Willis, G.C., 2003, Geology of Glen Canyon National Recreation Area, Utah-Arizona, *in* Sprinkel, D.A., Chidsey, T.C., Jr., and Anderson, P.B., editors, Geology of Utah's Parks and Monuments (second edition): Utah Geological Association Publication 28, p. 301–335.

Arizona Oil and Gas Conservation Commission, 2016, Oil, gas, helium report: Online, <azogcc.az.gov/sites/azogcc.az.gov/files/monthly_production/2015_12.pdf>, accessed July 2016.

Armstrong, R.L., 1968, Sevier orogenic belt in Nevada and Utah: Geological Society of America Bulletin, v. 79, p. 429–458.

Baars, D.L., 1966, Pre-Pennsylvanian paleotectonics—key to basin evolution and petroleum occurrences in the Paradox Basin, Utah and Colorado: American Association of Petroleum Geologists Bulletin, v. 50, no. 10, p. 2082–2111.

Baars, D.L., 1993, Bluff, San Juan County, Utah, *in* Hill, B.G., and Bereskin, S.R., editors, Oil and gas fields of Utah: Utah Geological Association Publication 22, non-paginated.

Baars, D.L., and Doelling, H.H., 1987, Moab salt-intruded anticline, east-central Utah, *in* Beus, S.S., editor, Decade of North American geology project: Boulder, Colorado, Geological Society of America, Rocky Mountain Section, Centennial Field Guide, v. II, p. 275–280.

Baars, D.L., and Stevenson, G.M., 1981, Tectonic evolution of the Paradox Basin, Utah and Colorado, *in* Wiegand, D.L., editor, Geology of the Paradox Basin: Rocky Mountain Association of Geologists Guidebook, p. 23–31.

Baars, D.L., and Stevenson, G.M., 1982, Subtle stratigraphic traps in Paleozoic rocks of Paradox Basin, *in* Halbouty, M.T., editor, The deliberate search for the subtle trap: American Association of Petroleum Geologists Memoir 32, p. 131–158.

Babcock, P.A., 1978a, Aneth (Aneth Unit), San Juan County, Utah, *in* Fassett, J.E., editor, Oil and gas fields of the Four Corners area: Four Corners Geological Society Guidebook, v. II, p. 577–579.

Babcock, P.A., 1978b, Aneth (McElmo Creek Unit), San Juan County, Utah, *in* Fassett, J.E., editor, Oil and gas fields of the Four Corners area: Four Corners Geological Society Guidebook, v. II, p. 580–583.

Babcock, P.A., 1978c, Aneth (Ratherford Unit), San Juan County, Utah, *in* Fassett, J.E., editor, Oil and gas fields of the Four Corners area: Four Corners Geological Society Guidebook, v. II, p. 584–586.

Babcock, P.A., 1978d, Aneth (White Mesa Unit), San Juan County, Utah, *in* Fassett, J.E., editor, Oil and gas fields of the Four Corners area: Four Corners Geological Society Guidebook, v. II, p. 587–590.

Baclawski, P., South, J., Lorenz, J., and Cooper, S., 2013, Bluebell-Altamont field—core from the fractured Green River-Wasatch reservoir, Uinta Basin, Utah [abs.]: American Association of Petroleum Geologists Rocky Mountain Section Meeting Program with Abstracts, p. 40.

Baker, A.A., Dane, C.H., and Reeside, J.B., Jr., 1933, Paradox Formation of eastern Utah and western Colorado: American Association of Petroleum Geologists Bulletin, v. 17, p. 963–980.

Baseline DGSI, 2005, Basic crude oil characteristics and biomarker analysis from the Kings Meadow Ranches No. 17-1 well, Covenant field, Sevier County, Utah: Utah Geological Survey Open-file Report 467, 15 p.

Benson, A.K., 1993a, Lodgepole, Summit County, Utah, *in* Hill, B.G., and Bereskin, S.R., editors, Oil and gas fields of Utah: Utah Geological Association Publication 22, non-paginated.

Benson, A.K., 1993b, Elkhorn Ridge, Summit County, Utah, *in* Hill, B.G., and Bereskin, S.R., editors, Oil and gas fields of Utah: Utah Geological Association Publication 22, non-paginated.

Bereskin, S.R., and Morgan, C.D., 2001, Fluvial-lacustrine oil reservoirs in the Middle Member of the Eocene Green River Formation, south-central, Uinta Basin, Utah [abs.]: American Association of Petroleum Geologists Annual Convention, Search and Discovery Article #90906.

Bereskin, S.R., Morgan, C.D., and McClure, K.P., 2004, Descriptions, petrology, photographs, and photomicrographs of core from the Green River Formation, south-central Uinta Basin, Utah: Utah Geological Survey Miscellaneous Publication 04-2, 203 p., CD-ROM.

Bergosh, J.L., Good, J.R., Hillman, J.T., and Kolodzie, S., 1982, Geological characterization of the Nugget Sandstone, Anschutz Ranch East, *in* Nielson, D.L., editor, Overthrust belt of Utah: Utah Geological Association Publication 10, p. 253–265.

Best, D.A., Wright, F.M., III, Sagar, R., and Weber, J.J., 1995, Contribution of outcrop data to improve understanding of field performance—rock exposures at Eight Foot Rapids tied to the Aneth field, *in* Stoudt, E.L., and Harris, P.M., editors, Hydrocarbon reservoir characterization—geologic framework and flow unit modeling: SEPM (Society for Sedimentary Geology) Short Course No. 34, p. 31–50.

Biek, R.F., Willis, G.C., Hylland, M.D., and Doelling, H.H., 2010, Geology of Zion National Park, Utah, *in* Sprinkel,

D.A., Chidsey, T.C., Jr., and Anderson, P.B., editors, Geology of Utah's parks and monuments (third edition): Utah Geological Association Publication 28, p. 109–143.

Blakey, R.C., 1994, Paleogeographic and tectonic controls on some Lower and Middle Jurassic erg deposits, Colorado Plateau, *in* Caputo, M.V., Peterson, J.A., and Franczyk, K.J., editors, Mesozoic systems of the Rocky Mountain region, USA: Denver, Colorado, Rocky Mountain Section of the Society for Sedimentary Geology, p. 273–298.

Blakey, R., and Ranney, W., 2008, Ancient landscapes of the Colorado Plateau: Grand Canyon, Grand Canyon Association, 156 p.

Blazzard, 1979a, Pineview, Summit County, Utah, *in* Cardinal, D.F., and Steward, W.W., editors, Wyoming oil and gas fields symposium, Greater Green River Basin: Wyoming Geological Association, p. 286-288.

Blazzard, 1979b, Lodgepole, Summit County, Utah, *in* Cardinal, D.F., and Steward, W.W., editors, Wyoming oil and gas fields symposium, Greater Green River Basin: Wyoming Geological Association, p. 227-228.

Blazzard, 1979c, Elkhorn, Summit County, Utah, *in* Cardinal, D.F., and Steward, W.W., editors, Wyoming oil and gas fields symposium, Greater Green River Basin: Wyoming Geological Association, p. 138-139.

Borer, J., 2003, High-resolution stratigraphy of the Green River Formation at Raven Ridge and Red Wash field, NE Uinta Basin—facies and stratigraphic patterns in a high-gradient, high-energy lacustrine system: unpublished American Association of Petroleum Geologists field trip guidebook, 101 p.

Borer, J., and McPherson, M., 1998, High-resolution stratigraphy of the Green River Formation, Raven Ridge, northeast Uinta Basin—facies, cycle stacking patterns and petroleum systems in a high-gradient, high-energy lacustrine system: unpublished American Association of Petroleum Geologists field trip guidebook, pt. I, 115 p., pt. II, 10 p.

Boyer, S.E., and Elliott, D., 1982, Thrust systems: American Association of Petroleum Geologists Bulletin, v. 66, no. 9, p. 1196–1230.

Bradley, W.H., 1931, Origin and microfossils of the oil shale of the Green River Formation of Colorado and Utah: U.S. Geological Survey Professional Paper 168, 56 p.

Bredehoeft, J.D., Wesley, J.B., and Fouch, T.D., 1994, Simulations of the origin of fluid pressure, fracture generation, and the movement of fluids in the Uinta Basin, Utah: American Association of Petroleum Geologists Bulletin, v. 78, no. 11, p. 1729–1747.

Brinton, L., 1986, Deposition and diagenesis of middle Pennsylvanian (Desmoinesian) phylloid algal banks, Paradox Formation, Ismay zone, Ismay field and San Juan Canyon, Paradox Basin, Utah and Colorado: Golden, Colorado School of Mines, M.S. thesis, 315 p.

Brown, H.H., 1978, Marble Wash, Montezuma County, Colorado, *in* Fassett, J.E., editor, Oil and gas fields of the Four Corners area: Four Corners Geological Society Guidebook, v. I, p. 143–145.

Brown, H.H., 1983, Mustang, San Juan County, Utah, *in* Fassett, J.E., editor, Oil and gas fields of the Four Corners area: Four Corners Geological Society Guidebook, v. III, p. 1095–1096.

Bruce, C.L., 1988, Jurassic Twin Creek Formation—a fractured limestone reservoir in the overthrust belt, Wyoming and Utah, *in* Goolsby, S.M., and Longman, M.W., editors, Occurrence and petrophysical properties of carbonate reservoirs in the Rocky Mountain region: Rocky Mountain Association of Geologists Guidebook, p. 105–120.

Bryant, B., 1990, Geologic map of the Salt Lake City 30′ x 60′ quadrangle, north-central Utah, and Uinta County, Wyoming: U.S. Geological Survey Miscellaneous Investigation Series Map I-1944, 1:100,000.

Burtner, R.L., and Warner, M.A., 1984, Hydrocarbon generation in the Lower Cretaceous Mowry and Skull Creek Shales of the northern Rocky Mountain area, *in* Woodward, J., Meissner, F.F., and Clayton, J.L., editors, Hydrocarbon source rocks of the greater Rocky Mountain region: Rocky Mountain Association of Geologists Guidebook, p. 449–467.

Campbell, J.A., 1969, The Upper Valley oil field, Garfield County, Utah, *in* Geology and natural history of the Grand Canyon region: Four Corners Geological Society 5th Field Conference Guidebook, p. 195–200.

Campbell, J.A., 1978a, Bluff, San Juan County, Utah, *in* Fassett, J.E., editor, Oil and gas fields of the Four Corners area: Four Corners Geological Society Guidebook, v. II, p. 605–609.

Campbell, J.A., 1978b, Bluff Bench, San Juan County, Utah, *in* Fassett, J.E., editor, Oil and gas fields of the Four Corners area: Four Corners Geological Society Guidebook, v. II, p. 610–614.

Cargile, L.L., 1978, Lisbon, Southeast, San Miguel County, Colorado, *in* Fassett, J.E., editor, Oil and gas fields of the Four Corners area: Four Corners Geological Society Guidebook, v. I, p. 140–142.

Carney, S.M., Nielsen, P., and Vanden Berg, M.D., 2014, Geological evaluation of the Cane Creek shale, Pennsylvanian Paradox Formation, Paradox Basin, southeastern Utah [abs.]: American Association of Petroleum Geologists, Annual Convention and Exhibition (1838157).

Case, J.E., and Joesting, H.R., 1973, Regional geophysical investigations in the central Colorado Plateau: U.S. Geological Survey Professional Paper 736, 31 p.

Cashion, W.B., 1967, Geology and fuel resources of the Green River Formation, southeastern Uinta Basin, Utah and Colorado: U.S. Geological Survey Professional Paper 548, 48 p.

Castle, J.W., 1990, Sedimentation in Eocene Lake Uinta (Lower Green River Formation), northeastern Uinta Basin, Utah, *in* Katz, B.J., editor, Lacustrine basin exploration—case studies and modern analogs: American Association of Petroleum Geologists Memoir 50, p. 243–264.

Cater, F.W., 1970, Geology of the salt anticline region in southwestern Colorado: U.S. Geological Survey Professional Paper 637, 80 p.

Chase, J.D., Stilwell, D.P., and Bentley, R.D., 1992a, Anschutz Ranch East, Uinta County, Wyoming, and Summit County, Utah, *in* Miller, S.M., Crockett, F.J., and Hollis, S.H., editors, Greater Green River Basin and overthrust belt: Wyoming Geological Association, Wyoming Oil and Gas Fields Symposium, p. 20–21.

Chase, J.D., Stilwell, D.P., and Bentley, R.D., 1992b, Bessie Bottom, Uinta County, Wyoming, *in* Miller, S.M., Crockett, F.J., and Hollis, S.H., editors, Greater Green River Basin and overthrust belt: Wyoming Geological Association, Wyoming Oil and Gas Fields Symposium, p. 34–35.

Chidsey, T.C., Jr., 1993, Jurassic-Triassic Nugget Sandstone, *in* Hjellming, C.A., editor, Atlas of major Rocky Mountain gas reservoirs: New Mexico Bureau of Mines and Mineral Resources, p. 77–79.

Chidsey, T.C., Jr., 1999, Petroleum plays in Summit County, Utah, *in* Spangler, L.E., editor, Geology of northern Utah and vicinity: Utah Geological Association Publication 27, p. 233–256.

Chidsey, T.C., Jr., compiler and editor, 2002, Increased oil production and reserves utilizing secondary/tertiary recovery techniques on small reservoirs in the Paradox Basin, Utah—final report: U.S. Department of Energy (NETL/NPTO) Oil Recovery, Field Demonstrations, Program Class II, compact disc, p. 5-2–5-6.

Chidsey, T.C., Jr., Brinton, L., Eby, D.E., and Hartmann, K., 1996d, Carbonate mound reservoirs in the Paradox Formation—an outcrop analogue along the San Juan River, southeastern Utah, *in* Huffman, A.C., Jr., Lund, W.R., and Godwin, L.H., editors, Geology and resources of the Paradox Basin: Utah Geological Association Publication 25, p. 139–156.

Chidsey, T.C., Jr., Hartwick, E.E., Johnson, K.R., Schelling, D.D., Sbarra, Rossella, Sprinkel, D.A., Vrona, J.P., and Wavrek, D.A., 2011, Petroleum geology of Providence oil field, central Utah thrust belt, *in* Sprinkel, D.A., Yonkee, W.A., and Chidsey, T.C., Jr., editors, Sevier thrust belt: northern and central Utah and adjacent areas: Utah Geological Association Publication 40, p. 213–231.

Chidsey, T.C., Jr., DeHamer, J.S., Hartwick, E.E., Johnson, K.R., Schelling, D.D., Sprinkel, D.A., Strickland, D.K., Vrona, J.P., and Wavrek, D.A., 2007, Petroleum geology of Covenant oil field, central Utah thrust belt, *in* Willis, G.C., Hylland, M.D., Clark, D.L., and Chidsey, T.C., Jr., editors, Central Utah—diverse geology of a dynamic landscape: Utah Geological Association Publication 36, p. 273–296.

Chidsey, T.C., Jr., and Eby, D.E., 1997, Heron North field, Navajo Nation, San Juan County, Utah—a case study for small calcarenite carbonate buildups [abs.]: American Association of Petroleum Geologists Bulletin, v. 81, no. 7, p. 1220.

Chidsey, T.C., Jr., and Eby, D.E., 2002, Reservoir diagenesis and porosity development in the upper Ismay zone, Pennsylvanian Paradox Formation, Cherokee field, southeastern Utah [abs.]: American Association of Petroleum Geologists Rocky Mountain Section Meeting Official Program Book, p. 20–21.

Chidsey, T.C., Jr., and Eby, D.E., 2014, Reservoir properties and carbonate petrography of the Aneth Unit, Greater Aneth field, Paradox Basin, southeastern Utah, *in* MacLean, J.S., Biek, R.F., and Huntoon, J.E., editors, Geology of Utah's far south: Utah Geological Association Publication 43, p. 153–197, 2 appendices, 6 plates.

Chidsey, T.C., Jr., Eby, D.E., Groen, W.G., Hartmann, K., and Watson, M.C., 1996a, Runway, San Juan County, Utah, *in* Hill, B.G., and Bereskin, S.R., editors, Oil and gas fields of Utah: Utah Geological Association 22 (Addendum), non-paginated.

Chidsey, T.C., Jr., Eby, D.E., Groen, W.G., Hartmann, K., and Watson, M.C., 1996b, Heron North, San Juan County, Utah, *in* Hill, B.G., and Bereskin, S.R., editors, Oil and gas fields of Utah: Utah Geological Association 22 (Addendum), non-paginated.

Chidsey, T.C., Jr., Eby, D.E., and Lorenz, D.M., 1996c, Geological and reservoir characterization of small shallow-shelf fields, southern Paradox Basin, Utah, *in* Huffman, A.C., Jr., Lund, W.R., and Godwin, L.H., editors, Geology and resources of the Paradox Basin: Utah Geological Association Publication 25, p. 39–56.

Chidsey, T.C., Jr., and Sprinkel, D.A., 2005, Petroleum geology of Ashley Valley oil field and hydrocarbon potential of the surrounding area, Uintah County, Utah, *in* Dehler, C.M., Pederson, J.L., Sprinkel, D.A., and Kowallis, B.J., editors, Uinta Mountain geology: Utah Geological Association Publication 33, p. 347–368.

Chidsey, T.C., Jr., Sprinkel, D.A., Willis, G.C., and Anderson, P.B., 2000a, Geologic guide along Lake Powell, Glen Canyon National Recreation Area and Rainbow Bridge National Monument, Utah-Arizona, *in* Anderson, P.B., and Sprinkel, D.A., editors, Geologic road, trail, and lake guides to Utah's parks and monuments: Utah Geological Association Publication 29, 76 p.

Chidsey, T.C., Jr., Vanden Berg, M.D., and Eby, D.E., 2015, Petrography and characterization of microbial carbonates and associated facies from modern Great Salt Lake and Uinta Basin's Eocene Green River Formation in Utah, USA, *in* Bosence, D.W.J., Gibbon, K.A., Le Heron, D.P., Morgan, W.A., Pritchard, T., and Vining, B.A., editors, Microbial carbonates in space and time—implications for global exploration and production: The Geological Society, London, Special Publication 418, http://dx.dio.org/10.1144/SP418.6.

Chidsey, T.C., Jr., Willis, G.C., Sprinkel, D.A., and Anderson, P.B., 2000b, Geology of Rainbow Bridge National Monument, *in* Sprinkel, D.A., Chidsey, T.C., Jr., and Anderson, P.B., editors, Geology of Utah's parks and monuments: Utah Geological Association Publication 28, p. 251–262.

Choquette, P.W., 1983, Platy algal reef mounds, Paradox Basin, *in* Scholle, P.A., Bebout, D.G., and Moore, C.H., editors, Carbonate depositional environments: American Association of Petroleum Geologists Memoir 33, p. 454–462.

Clark, C.R., 1978, Lisbon, San Juan County, Utah, *in* Fassett, J.E., editor, Oil and gas fields of the Four Corners area: Four Corners Geological Society Guidebook, v. II, p. 662–665.

Claypool, G.E., Love, A.H., and Maughan, E.K., 1978, Organic geochemistry, incipient metamorphism, and oil generation in black shale members of the Phosphoria Formation, western interior United States: American Association of Petroleum Geologists Bulletin, v. 62, no. 1, p. 98–120.

Colburn, J.A., Bereskin, S.R., McGinley, D.C., and Schiller, D.M., 1985, Lower Green River Formation in the Pleasant Valley producing area, Duchesne and Uintah Counties, Utah, *in* Picard, M.D., editor, Geology and energy resources, Uinta Basin, Utah: Utah Geological Association Publication 12, p. 177–186.

Colorado Oil and Gas Conservation Commission, 2016, Colorado oil and gas information system (COGIS)—production data inquiry: Online, <http://cogcc.state.co.us/cogis/ProductionSearch.asp>, accessed July 2016.

Conlon, M.F., 1978, Teec Nos Pos Ismay, Apache County, Arizona, *in* Fassett, J.E., editor, Oil and gas fields of the Four Corners area: Four Corners Geological Society Guidebook, v. I, p. 90–91.

Conner, D.C., and Covlin, R.J., 1977, Development geology of Pineview field, Summit County Utah, *in* Heisey, E.L., Lawson, D.E., Norwood, E.R., Wach, P.H., and Hale, L.A., editors, Rocky Mountain thrust belt geology and resources: Wyoming Geological Association 29th Annual Field Conference, p. 639–650.

Constenius, K.M., Esser, R.P., and Layer, P.W., 2003, Extensional collapse of the Charleston-Nebo salient and its relationship to space-time in Cordilleran orogenic belt tectonism and continental stratigraphy, *in* Reynolds, R.G., and Flores, R.M., editors, Cenozoic systems of the Rocky Mountain region: Society for Sedimentary Geology (SEPM), Rocky Mountain Section, p. 303–354.

Coogan, J.C., 1992, Thrust systems and displacement transfer in the Wyoming-Idaho-Utah thrust belt: Laramie, University of Wyoming, Ph.D. dissertation 239 p.

Coogan, J.C., 1999, Progress report geologic map of the Devils Slide quadrangle, Morgan and Summit Counties, Utah: unpublished 1:24,000 map used to compile the Ogden 30′ x 60′ quadrangle, Utah Geological Survey Open-File Report 380, scale 1:100,000.

Coogan, J.C., and DeCelles, P.G., 1998, Coupled structure and sedimentation through 100 million years of thrust wedge evolution, Sevier thrust belt, northern Utah, western Wyoming, and southeastern Idaho: American Association of Petroleum Geologists Annual Meeting Field Trip Guide, no. 24, 42 p.

Coogan, J.C., King, J.K., and McDonald, G.N., in review, Interim geologic map of the Devils Slide 7.5-minute quadrangle, Morgan and Summit County, Utah: Utah Geological Survey Open-File Report, scale 1:24,000.

Cook, C.W., and Dunleavy, J.R., 1996, Pineview, Summit County, Utah, *in* Hill, B.G., and Bereskin, S.R., editors, Oil and gas fields of Utah: Utah Geological Association Publication 22 (Addendum), non-paginated.

Crawley-Stewart, C.L., and Riley, K.F., 1993a, Kiva, San Juan County, Utah, *in* Hill, B.G., and Bereskin, S.R., editors, Oil and gas fields of Utah: Utah Geological Association Publication 22, non-paginated.

Crawley-Stewart, C.L., and Riley, K.F., 1993b, Kachina, San Juan County, Utah, *in* Hill, B.G., and Bereskin, S.R., editors, Oil and gas fields of Utah: Utah Geological Association Publication 22, non-paginated.

Crouch, B.W., Hackney, M.L., and Johnson, B.J., 2000, Sequence stratigraphy and reservoir character of lacustrine carbonates in the basal limestone member—lower Green River Formation (Eocene), Duchesne and Antelope Creek fields, Duchesne Co., Utah [abs.]: American Association of Petroleum Geologists Annual Convention, Official Program with Abstracts, v. 10, p. A34.

Dahlstrom, C.D.A., 1970, Structural geology in the eastern margin of the Canadian Rocky Mountains: Bulletin of Canadian Petroleum Geology, v. 18, no. 3, p. 332–406.

Dalrymple, A., and Morris, T.H., 2007, Facies analysis and reservoir characterization of outcrop analogs to the Navajo Sandstone in the central Utah thrust belt exploration play, *in* Willis, G.C., Hylland, M.D., Clark, D.L., and Chidsey, T.C., Jr., editors, 2007, Central Utah—diverse geology of a dynamic landscape: Utah Geological Association Publication 36, p. 311–322.

Dawson, W.C., 1988, Ismay reservoirs, Paradox Basin—diagenesis and porosity development, *in* Goolsby, S.M., and Longman, M.W., editors, Occurrence and petrophysical properties of carbonate reservoirs in the Rocky Mountain region: Rocky Mountain Association of Geologists Guidebook, p. 163–174.

DeCelles, P.G., 1994, Late Cretaceous-Paleocene synorogenic sedimentation and kinematic history of the Sevier thrust belt, northeast Utah and southwest Wyoming: Geological Society of America Bulletin, v. 106, p. 32–56.

DeCelles, P.G., 2004, Late Jurassic to Eocene evolution of the Cordilleran thrust belt and foreland basin system, western USA: American Journal of Science, v. 304, p. 105–168.

DeCelles, P.G., and Coogan, J.C., 2006, Regional structure and kinematic history of the Sevier fold-and-thrust belt, central Utah: Geological Society of America Bulletin, v. 118, no. 7/8, p. 841–864.

Decelles, P.G., Lawton, T.F., and Mitra, G., 1995, Thrust timing, growth of structural culminations, and synorogenic sedimentation in the type Sevier orogenic belt, western United States: Geology, v. 23 p. 699–702.

Denton, G.H., and Hughes, T.J., 1983, Milankovitch theory of ice ages—hypothesis of ice-sheet linkage between regional insolation and global climate: Quaternary Research, v. 20, p. 125–144.

Dickinson, W.R., and Gehrels, G.E., 2003, U-Pb ages of detrital zircons from Permian and Jurassic eolian sandstones of the Colorado Plateau, USA—paleogeographic implications: Sedimentary Geology, v. 163, issues 1-2, p. 29–66.

Dickinson, W.R., and Gehrels, G.E., 2010, Synoptic record in space and time of provenance relations for Mesozoic strata in south-central Utah from U-Pb ages of detrital zircons, *in* Carney, S.M., Tabet, D.E., and Johnson, C.L., editors, Geology of south-central Utah: Utah Geological Association Publication 39, p. 178–193.

Dixon, J.S., 1982, Regional structural synthesis, Wyoming salient of western overthrust belt: American Association of Petroleum Geologists Bulletin, v. 66, no. 10, p. 1560–1580.

Doe, T.W., and Dott, R.H., 1980, Genetic significance of deformed cross-bedding—with examples from the Navajo and Weber Sandstones of Utah: Journal of Sedimentary Petrology, v. 50, p. 793–812.

Doelling, H.H., 1980, Geology and mineral resources of Box Elder County, Utah: Utah Geological and Mineral Survey Bulletin 115, p. 209–214.

Doelling, H.H., 1988, Geology of the Salt Valley anticline and Arches National Park, Grand County, Utah, *in* Salt deformation in the Paradox region: Utah Geological and Mineral Survey Bulletin 122, p. 1–60.

Doelling, H.H., 2003, Geology of Arches National Park, Grand County, Utah, *in* Sprinkel, D.A., Chidsey, T.C., Jr., and Anderson, P.B., editors, Geology of Utah's parks and monuments: Utah Geological Association Publication 28, p. 11–36.

Doelling, H.H., Chidsey, T.C., Jr., and Benson, B.J., 2003, Geology of Dead Horse Point State Park, Grand and San Juan Counties, Utah, *in* Sprinkel, D.A., Chidsey, T.C., Jr., and Anderson, P.B., editors, Geology of Utah's parks and monuments (second edition): Utah Geological Association Publication 28, p. 391–409.

Doelling, H.H., and Davis, F.D., 1989, The geology of Kane County, Utah: Utah Geological and Mineral Survey Bulletin 124, 192 p., 10 plates.

Doelling, H.H., Sprinkel, D.A., Kowallis, B.J., and Kuehne, P.A., 2013, Temple Cap and Carmel Formations in the Henry Mountains Basin, Wayne and Garfield Counties, Utah, *in* Morris, T.H., and Ressetar, R., editors, The San Rafael Swell and Henry Mountains Basin—geologic centerpiece of Utah: Utah Geological Association Publication 42, p. 279–318.

Dubiel, R.F., 2003, Geology, depositional models, and oil and gas assessment of the Green River total petroleum system, Uinta-Piceance Province, eastern Utah and western Colorado, *in* U.S. Geological Survey Uinta-Piceance Assessment Team, compilers, Petroleum systems and geologic assessment of oil and gas in the Uinta-Piceance Province, Utah and Colorado: U.S. Geological Survey Digital Data Series DDS-69-B.

Dunn, S.S., 1978, Boundary Butte, East, Apache County, Arizona, *in* Fassett, J.E., editor, Oil and gas fields of the Four Corners area: Four Corners Geological Society Guidebook, v. I, p. 70–72.

Eardley, A.J., 1939, Structure of the Wasatch-Great Basin region: Geological Society of America Bulletin, v. 50, p. 1277–1310.

Eby, D.E., and Chidsey, T.C., Jr., 2001, Heterogeneous carbonate buildups in the Blanding sub-basin of the Paradox Basin, Utah and Colorado—targets for increased oil production using horizontal drilling techniques [abs.]: American Association of Petroleum Geologists Annual Convention, Official Program with Abstracts, v. 10, p. A55.

Eby, D.E., Chidsey, T.C., Jr., and Morgan, C.D., 2008, The use of epifluorescence techniques to determine potential oil-prone areas in the Mississippian Leadville Limestone, northern Paradox Basin, Utah [abs.]: Rocky Mountain Natural Gas Geology and Resource Conference, Rocky Mountain Section of the American Association of Petroleum Geologists and Colorado Oil & Gas Association Official Program with Abstracts, p. 88–89.

Eby, D.E., Chidsey, T.C., Jr., Morgan, C.D., and McClure, K., 2003, Regional facies trends in the upper Ismay zone of the Blanding sub-basin of the Paradox Basin, Utah—aids for identifying possible targets for horizontal drilling [abs.]: American Association of Petroleum Geologists, Annual Convention Program with Abstracts, v. 12, p. A48.

Eby, D.E., Groen, W.G., and Johnson, J.F., 1993, Composition of seismically identified satellite mounds surrounding Greater Aneth field, southeast Utah [abs.]: American Association of Petroleum Geologists Bulletin, v. 77, no. 8, p. 1446–1447.

Energy Information Administration, 2015, U.S. crude oil and natural gas proved reserves, 2014: Online, <http://www.eia.gov/naturalgas/crudeoilreserves/index.cfm>, accessed August 2016.

Fetzner, R.W., 1960, Pennsylvanian paleotectonics of the Colorado Plateau: American Association of Petroleum Geologists Bulletin, v. 44, no. 8, p. 1371–1413.

Forsman, J.P., and Hunt, J.M., 1958, Insoluble organic matter (kerogen) in sedimentary rocks of marine origin, *in* Weeks, L.G., editor, Habitat of oil—a symposium: American Association of Petroleum Geologists, symposium publication, p. 747–778.

Fouch, T.D., 1975, Lithofacies and related hydrocarbon accumulations in Tertiary strata of the western and central Uinta Basin, Utah, *in* Bolyard, D.W., editor, Symposium on deep drilling frontiers in the central Rocky Mountains: Rocky Mountain Association of Geologists Guidebook, p. 163–173.

Fouch, T.D., 1976, Revision of the lower part of the Tertiary system in the central and western Uinta Basin, Utah: U.S. Geological Survey Bulletin 1405-C, 7 p.

Fouch, T.D., 1981, Distribution of rock types, lithologic groups, and interpreted depositional environments for some lower Tertiary and Upper Cretaceous rocks from outcrops at Willow Creek–Indian Canyon through the subsurface of Duchesne and Altamont oil fields, southwest to north-central parts of the Uinta Basin, Utah: U.S. Geological Survey Oil and Gas Investigations Map, Chart OC-81, 2 sheets.

Fouch, T.D., Nuccio, V.F., Anders, D.E., Rice, D.D., Pitman, J.K., and Mast, R.F., 1994, Green River petroleum system, Uinta Basin, Utah, U.S.A., *in* Magoon, L.B., and Dow, W.G., editors, The petroleum system—from source to trap: American Association of Petroleum Geologists Memoir 60, p. 399–421.

Fouch, T.D., Nuccio, V.F., Osmond, J.C., MacMillan, L., Cashion, W.B., and Wandrey, C.J., 1992, Oil and gas in uppermost Cretaceous and Tertiary rock, Uinta Basin, Utah, *in* Fouch, T.D., Nuccio, V.F., and Chidsey, T.C., Jr., editors, Hydrocarbon and mineral resources of the Uinta Basin, Utah and Colorado: Utah Geological Association Publication 20, p. 9–47.

Fouch, T.D., and Pitman, J.K., 1991, Tectonic and climate changes expressed as sedimentary cycles and stratigraphic sequences in the Paleogene Lake Uinta system, central Rocky Mountains, Utah and Colorado [abs.]: American Association of Petroleum Geologists Bulletin, v. 75, no. 3, p. 575.

Fouch, T.D., and Pitman, J.K., 1992, Tectonic and climate changes expressed as sedimentary and geochemical cycles, Paleogene lake systems, Utah and Colorado—implications for petroleum source and reservoir rocks, *in* Carter, L.J., editor, U.S. Geological Survey research on energy resources, 1992 McKelvey Forum program and abstracts [abs.]: U.S. Geological Survey Circular 1074, p. 29–30.

Fouret, K.L., 1982, Depositional and diagenetic environment of the Mississippian Leadville Formation at Lisbon field, Utah: College Station, Texas A&M University, M.S. thesis, 119 p.

Fouret, K.L., 1996, Depositional and diagenetic environment of the Mississippian Leadville Limestone at Lisbon field, Utah, *in* Huffman, A.C., Jr., Lund, W.R., and Godwin, L.H., editors, Geology and resources of the Paradox Basin: Utah Geological Association Publication 25, p. 129–138.

Frahme, C.W., and Vaughn, E.B., 1983, Paleozoic geology and seismic stratigraphy of the northern Uncompahgre front, Grand County, Utah, *in* Lowell, J.D., editor, Rocky Mountain foreland basins and uplifts: Rocky Mountain Association of Geologists Guidebook, p. 201–211.

Franczyk, K.J., Fouch, T.D., Johnson, R.C., Molenaar, C.M., and Cobban, W.A., 1992, Cretaceous and Tertiary paleogeographic reconstructions for the Uinta-Piceance Basin study area, Colorado and Utah: U.S. Geological Survey Bulletin 1787-Q, 37 p.

Frank, J.R., Cluff, S., and Bauman, J.M., 1982, Painter Reservoir and Clear Creek fields, Uinta County, Wyoming, *in* Powers, R.B., editor, Geologic studies of the Cordilleran thrust belt: Rocky Mountain Association of Petroleum Geologists, v. 2, p. 601–611.

Frank, J.R., and Gavlin, S., 1981, Painter Reservoir, East Painter Reservoir, and Clear Creek fields, Uinta County, Wyoming, *in* Reid, S.G., and Miller, D.D., editors, Energy Resources of Wyoming: Wyoming Geological Association 32th Annual Field Conference, p. 83–97.

Friedman, G.M., and Sanders, J.E., 1978, Principles of sedimentology: New York, John Wiley and Sons, p. 149.

Friedman, J.D., Case, J.E., and Simpson, S.L., 1994, Tectonic trends of the northern part of the Paradox Basin, southeastern Utah and southwestern Colorado, as derived from LANDSAT multispectral scanner imaging and geophysical and geological mapping: U.S. Geological Survey Bulletin 2000-C, 30 p.

Fritz, M., 1991, Horizontal drilling comes full circle—seismic, technology triumphs in Utah find: American Association of Petroleum Geologists Explorer, v. 12, p. 1 and 18.

Fryberger, S.G., 1990, Ancient eolian deposits of the Navajo and Weber Sandstones, northeast Utah and Colorado, *in* Fryberger, S.G., Krystinik, L.F., and Schenk, C.J., editors, Modern and ancient eolian deposits—petroleum exploration and production: Society for Sedimentary Geology (SEPM), Rocky Mountain Section Publication, Chapter 19, 12 p.

Gautier, D.L., Dolton, G.L., Takahashi, K.I., and Varnes, K.L., editors, 1996, 1995 National assessment of United States oil and gas resources—results, methodology, and supporting data: U.S. Geological Survey Digital Data Series DDS-30, release 2.

Gianniny, G.L., and Simo, J.A.T., 1996, Implications of unfilled accommodation space for sequence stratigraphy on mixed carbonate-siliciclastic platforms—an example from the lower Desmoinesian (Middle Pennsylvanian), southwestern Paradox Basin, Utah, *in* Longman, M.W., and Sonnenfeld, M.D., editors, Paleozoic systems of the Rocky Mountain region: Rocky Mountain Section, SEPM (Society for Sedimentary Geology), p. 213–234.

Gibson, R.I., 1987, Basement tectonic controls on structural style of the Laramide thrust belt interpreted from gravity and magnetic data, *in* Miller, W.R., editor, The thrust belt revisited: Wyoming Geological Association 38th Field Conference Guidebook, p. 27–35.

Gilland, J.K., 1979, Paleoenvironment of a carbonate lens in the lower Navajo Sandstone near Moab, Utah: Utah Geological and Mineral Survey, Utah Geology, v. 6, no. 1, p. 29–38.

Goldhammer, R.K., Oswald, E.J., and Dunn, P.A., 1991, Hierarchy of stratigraphic forcing—example from Middle Pennsylvanian shelf carbonates of the Paradox Basin, *in* Franseen, E.K., Watney, W.L., Kendall, C.G., and Ross, W., editors, Sedimentary modeling: Kansas Geological Survey Bulletin 233, p. 361–413.

Goldhammer, R.K., Oswald, E.J., and Dunn, P.A., 1994, High frequency, glacio-eustatic cyclicity in Middle Pennsylvanian of the Paradox Basin—an evaluation of Milankovitch forcing, *in* deBoer, P.L., and Smith, D.G., editors, Orbital forcing and cyclic sequences: Special Publication of the International Association of Sedimentologists 19, p. 243–283.

Goolsby, S.M.L., Dwyff, L., and Fryt, M.S., 1988, Trapping mechanisms and petrophysical properties of the Permian Kaibab Formation, south-central Utah, *in* Goolsby, S.M.L., and Longman, M.W., editors, Occurrence and petro-physical properties of carbonate reservoirs in the Rocky Mountain region: Rocky Mountain Association of Geologists Guidebook, p. 193–210.

Grammar, G.M., Eberli, G.P., Van Buchem, F.S.P., Stevenson, G.M., and Homewood, P., 1996, Application of high-resolution sequence stratigraphy to evaluate lateral variability in outcrop and subsurface—Desert Creek and Ismay intervals, Paradox Basin, *in* Longman, M.W., and Sonnenfeld, M.D., editors, Paleozoic systems of the Rocky Mountain region: Rocky Mountain Section, SEPM (Society for Sedimentary Geology), p. 235–266.

Grammer, G.M., Harris, P.M., and Eberli, G.P., 2004, Integration of outcrop and modern analogs in reservoir modeling—overview of examples from the Bahamas, *in* Grammer, G.M., Harris, P.M., and Eberli, G.P., editors, Integration of outcrop and modern analogs in reservoir modeling: American Association of Petroleum Geologists Memoir 80, 394 p.

Grove, K.W., Horgan, C.C., Flores, F.E., and Bayne, R.C., 1993, Bartlett Flat Big Flat (Kane Springs Unit), Grand and San Juan Counties, Utah, *in* Hill, B.G., and Bereskin, S.R., editors, Oil and gas fields of Utah: Utah Geological Association Publication 22, non-paginated.

Grove, K.W., and Rawlins, D.M., 1997, Horizontal exploration of oil and gas-bearing natural fracture systems in the Cane Creek clastic interval of the Pennsylvanian Paradox Formation, Grand and San Juan Counties, Utah, *in* Close, J., and Casey, T., editors, Natural fracture systems in the southern Rockies: Four Corners Geological Society Guidebook, p. 133–134.

Grummon, M.L., 1993, Exploiting the self-sourced Cane Creek zone of the Paradox Formation with horizontal well bores [abs.]: American Association of Petroleum Geologists Bulletin, v. 77, no. 8, p. 1449–1450.

Gwynn, J.W., 1995, Resistivities and chemical analyses of selected oil and gas field, water well, and spring waters, Utah: Utah Geological Survey Circular 87, 142 p.

Hamblin, W.K., and Rigby, J.K., 1968, Guidebook to the Colorado River, Part 1—Lee's Ferry to Phantom Ranch in Grand Canyon National Park (Studies for Students No. 4): Brigham Young University Geology Studies, v. 15, pt. 5, 84 p.

Harr, C.L., 1996, Paradox oil and gas potential of the Ute Mountain Ute Indian Reservation, *in* Huffman, A.C., Jr., Lund, W.R., and Godwin, L.H., editors, Geology and resources of the Paradox Basin: Utah Geological Association Publication 25, p. 13–28.

Harry, D.L., and Mickus, K.L., 1998, Gravity constraints on lithospheric flexure and the structure of the late Paleozoic Ouachita orogen in Arkansas and Oklahoma, south-central North America: Tectonics, v. 17, no. 2, p. 187–202.

Harthill, N., and Bates, C.R., 1996, Fracture definition in the Rocky Mountain foreland: Rocky Mountain Association of Geologists, The Outcrop, v. 45, no. 2, p. 4 and 9.

Harthill, N., Bates, C.R., Lynn, H.B., and Simon, K.M., 1997, Fracture definition by surface seismic at the Bluebell-Altamont field, Uinta Basin, Utah, *in* Hoak, T.E., Klawitter, A.L., and Blomquist, P.K., editors, Fractured reservoirs—characterization and modeling: Rocky Mountain Association of Geologists Guidebook, p. 155–163.

Hartwick, E.E., 2010, Eolian architecture of sandstone reservoirs in the Covenant field, Sevier County, Utah [abs]: American Association of Petroleum Geologists, Rocky Mountain Section Meeting Program with Abstracts, p. 49.

Heckel, P.H., 1977, Origin of phosphatic black shale facies in Pennsylvanian cyclothems of mid-continent North America: American Association of Petroleum Geologists Bulletin, v. 61, no. 7, p. 1045–1068.

Heckel, P.H., 1983, Diagenetic model for carbonate rocks in midcontinent Pennsylvanian eustatic cyclothems: Journal of Sedimentary Petrology, v. 53, p. 733–759.

Heckel, P.H., 1986, Sea-level curve for Pennsylvanian eustatic marine transgressive-regressive depositional cycles along midcontinent outcrop belt, North America: Geology, v. 14, p. 330–334.

Heckel, P.H., 2008, Carboniferous Period, *in* Ogg, J.G., Ogg, G., and Gradstein, F.M., editors, The concise geologic time scale: New York, Cambridge University Press, p. 73–83.

Hefner, T.A., and Barrow, K.T., 1992, Rangely field—U.S.A., Uinta/Piceance Basins, Colorado, *in* Beaumont, E.A., and Foster, N.H., editors, Structural traps III, tectonic

fold and fault trap: American Association of Petroleum Geologists Treatise of Petroleum Geology, Atlas of Oil and Gas Fields, v. A-25, p. 29–56.

Hemborg, H.T., 1993, Weber Sandstone, *in* Hjellming, C.A., editor, Atlas of major Rocky Mountain gas reservoirs: New Mexico Bureau of Mines and Mineral Resources, p. 104.

Herrod, W.H., and Gardner, P.S., 1988, Upper Ismay reservoir at Tin Cup Mesa field, *in* Goolsby, S.M., and Longman, M.W., editors, Occurrence and petrophysical properties of carbonate reservoirs in the Rocky Mountain region: Rocky Mountain Association of Geologists Guidebook, p. 175–191.

Hill, B.G., and Bereskin, S.R., editors, 1993, Oil and gas fields of Utah: Utah Geological Association Publication 22, non-paginated.

Hintze, L.F., 1980, Geologic map of Utah: Utah Geological Survey Map M-A-1, 2 sheets, scale 1:500,000.

Hintze, L.F., 1997, Geologic highway map of Utah: Brigham Young University Geology Studies Special Publication 3, scale 1:1,000,000.

Hintze, L.F., 2005, Utah's spectacular geology—how it came to be: Provo, Brigham Young University Geology Studies Special Publication 8, p. 60–67.

Hintze, L.F., and Kowallis, B.J., 2009, Geologic history of Utah: Brigham Young University Geology Studies Special Publication 9, 225 p.

Hite, R.J., 1960, Stratigraphy of the saline facies of the Paradox Member of the Hermosa Formation of southeastern Utah and southwestern Colorado, *in* Smith, K.G., editor, Geology of the Paradox Basin fold and fault belt: Four Corners Geological Society, Third Field Conference Guidebook, p. 86–89.

Hite, R.J., 1970, Shelf carbonate sedimentation controlled by salinity in the Paradox Basin, southeast Utah, *in* Ran, J.L., and Dellwig, L.F., editors, Third symposium on salt: Northern Ohio Geological Society, v. 1, p. 48–66.

Hite, R.J., Anders, D.E., and Ging, T.G., 1984, Organic-rich source rocks of Pennsylvanian age in the Paradox Basin of Utah and Colorado, *in* Woodward, J., Meissner, F.F, and Clayton, J.L., editors, Hydrocarbon source rocks of the greater Rocky Mountain region: Rocky Mountain Association of Geologists Guidebook, p. 255–274.

Hite, R.J., and Buckner, D.H., 1981, Stratigraphic correlation, facies concepts and cyclicity in Pennsylvanian rocks of the Paradox Basin, *in* Wiegand, D.L., editor, Geology of the Paradox Basin: Rocky Mountain Association of Geologists 1981 Field Conference, p. 147–159.

Hite, R.J., and Cater, F.W., 1972, Pennsylvanian rocks and salt anticlines, Paradox Basin, Utah and Colorado, *in* Mallory, W.W., editor, Geologic atlas of the Rocky Mountain region: Rocky Mountain Association of Geologists Guidebook, p. 133–138.

Holm, M.R., 1992, Chicken Creek, Uinta County, Wyoming, *in* Miller, S.M., Crockett, F.J., and Hollis, S.H., editors, Greater Green River Basin and overthrust belt: Wyoming Geological Association, Wyoming Oil and Gas Fields Symposium, p. 96–97.

Hunt, J.M., Stewart, F., and Dickey, P.A., 1954, Origin of the hydrocarbons of the Uinta Basin, Utah: American Association of Petroleum Geologists Bulletin, v. 38, no. 8, p. 1671–1698.

Hunter, R.E., 1977, Basic types of stratification in small eolian dunes: Sedimentology, v. 24, p. 361–387.

Imbrie, J., and Imbrie, J.Z., 1980, Modeling the climatic response to orbital variations: Science, v. 207, p. 943–953.

Imlay, R.W., 1967, Twin Creek Limestone (Jurassic) in the Western Interior of the United States: U.S. Geological Survey Professional Paper 540, 105 p.

Imlay, R.W., 1980, Jurassic paleobiogeography of the conterminous United States in its continental setting: U.S. Geological Survey Professional Paper 1062, 134 p.

Johnson, C.E., 1964, Ashley Valley oil field, Uintah County, Utah, *in* Sabatka, E.F., editor, Guidebook to the geology and mineral resources of the Uinta Basin—Utah's hydrocarbon storehouse: Intermountain Association of Petroleum Geologists 13th Annual Field Conference, p. 187–189.

Johnson, C.F., 1970, Structure map, top Mississippian, Lisbon field, San Juan County, Utah: Union Oil of California files, scale: 1 inch = 4000 feet.

Johnson, E.A., 2003, Geologic assessment of the Phosphoria total petroleum system, Uinta-Piceance Province, Utah and Colorado, *in* Petroleum systems and geologic assessment of oil and gas in the Uinta-Piceance province, Utah and Colorado: U.S. Geological Survey Digital Data Series DDS-69-B, Chapter 9, 37 p.

Jones, E.V., Jr., 1979, Painter Reservoir, Uinta County, Wyoming, *in* Cardinal, D.F., and Steward, W.W., editors, Greater Green River Basin and overthrust belt: Wyoming Geological Association, Wyoming Oil and Gas Fields Symposium, p. 272–273.

Kay, M., 1951, North American geosynclines: Geological Society of America Memoir 48, 143 p.

Keele, D., and Evans, J., 2008, Analysis of reservoir properties of faulted and fractured eolian thrust-belt reservoirs: Utah Geological Survey Open-File Report 529, 50 p., 3 plates.

Kelly, J.M., and Hine, F.O., 1977, Ryckman Creek field, Uinta County, Wyoming, *in* Heisey, E.L., Lawson, D.E., Norwood, E.R., Wach, P.H., and Hale, L.A., editors, Rocky Mountain thrust belt geology and resources: Wyoming Geological Association 29th Annual Field Conference, p. 619–628.

Kelso, B.S., and Ehrenzeller, J.L., 2008, Petroleum geology of the Brundage Canyon oil field, southern Tertiary oil trend, Uinta Basin, *in* Longman, M.W., and Morgan, C.D., editors,

Hydrocarbon systems and production in the Uinta Basin, Utah: Rocky Mountain Association of Geologists and Utah Geological Association Publication 37, p. 283–302.

Kinney, D.M., 1955, Geology of the Uinta River-Brush Creek area, Duchesne and Uintah Counties, Utah: U.S. Geological Survey Bulletin 1007, 185 p.

Kluth, C.F., 1986, Plate tectonics of the Ancestral Rocky Mountains: American Association of Petroleum Geologists Memoir 41, p. 353–369.

Kluth, C.F., and Coney, P.J., 1981, Plate tectonics of the Ancestral Rocky Mountains: Geology, v. 9, p. 10–15.

Kocurek, G., and Dott, R.H., Jr., 1983, Jurassic paleogeography and paleoclimate of the central and southern Rocky Mountains region, *in* Reynolds, M.W., and Dolly, E.D., editors, Symposium on Mesozoic paleogeography of west-central U.S.: Society for Sedimentary Geology (SEPM), Rocky Mountain Section, p. 101–116.

Krivanek, C.M., 1978, Patterson, San Juan County, Utah, *in* Fassett, J.E., editor, Oil and gas fields of the Four Corners area: Four Corners Geological Society Guidebook, v. II, p. 688–690.

Krivanek, C.M., 1981, Bug field, T. 36 S., R. 25 & 26 E., San Juan County, Utah, *in* Wiegand, D.L., editor, Geology of the Paradox Basin: Rocky Mountain Association of Geologists Guidebook, p. 47–54.

Lamb, C.F., 1980, Painter Reservoir field, giant in Wyoming thrust belt: American Association of Petroleum Geologists Bulletin, v. 64, no. 4, p. 638–644.

Krivanek, C.M., 1993, Turner Bluff, San Juan County, Utah, *in* Hill, B.G., and Bereskin, S.R., editors, Oil and gas fields of Utah: Utah Geological Association Publication 22, non-paginated.

Lamerson, P.R., 1982, The Fossil Basin area and its relationship to the Absaroka thrust fault system, *in* Powers, R.B., editor, Geologic studies of the Cordilleran thrust belt: Rocky Mountain Association of Geologists Guidebook, v. 1, p. 279–340.

Larson, J.B., 1993, Ashley Valley, Uintah County, Utah, *in* Hill, B.G., and Bereskin, S.R., editors, Oil and gas fields of Utah: Utah Geological Association Publication 22, non-paginated.

Latch, B.F., 1978a, Big Indian Mississippian, San Juan County, Utah, *in* Fassett, J.E., editor, Oil and gas fields of the Four Corners area: Four Corners Geological Society Guidebook, v. II, p. 602–604.

Latch, B.F., 1978b, Little Valley, San Juan County, Utah, *in* Fassett, J.E., editor, Oil and gas fields of the Four Corners area: Four Corners Geological Society Guidebook, v. II, p. 602–604.

Lauth, R.E., 1978a, Anido Creek, San Juan County, Utah, *in* Fassett, J.E., editor, Oil and gas fields of the Four Corners area: Four Corners Geological Society Guidebook, v. II, p. 591–593.

Lauth, R.E., 1978b, Desert Creek, San Juan County, Utah, *in* Fassett, J.E., editor, Oil and gas fields of the Four Corners area: Four Corners Geological Society Guidebook, v. II, p. 639–641.

Lawton, T.F., 1985, Style and timing of frontal structures, thrust belt, central Utah: American Association of Petroleum Geologists Bulletin, v. 69, p. 1145–1159.

Lawton, T.F., Sprinkel, D.A., DeCelles, P.G., Mitra, G., Sussman, A.J., and Weiss, M.P., 1997, Stratigraphy and structure of the Sevier thrust belt and proximal foreland-basin system in central Utah—a transect from the Sevier Desert to the Wasatch Plateau, *in* Link, P.K., and Kowallis, B.J., editors, Mesozoic to Recent geology of Utah: Brigham Young University Geology Studies, v. 42, part II, p. 33–67.

Lees, A., and Miller, J., 1995, Waulsortian banks, *in* Monty, C.L.V., Bosencce, D.W.J., Bridges, P.H., and Pratt, B.R., editors, Carbonate mud-mounds—their origin and evolution: International Association of Sedimentologists Special Publication No. 23, p. 191–271.

Lehman, D.D., 1983, Rockwell Springs, San Juan County, Utah, *in* Fassett, J.E., editor, Oil and gas fields of the Four Corners area: Four Corners Geological Society Guidebook, v. III, p. 1114–1116.

Lelek, J.J., 1982, Anschutz Ranch East field, northeast Utah and southwest Wyoming, *in* Powers, R.B., editor, Geologic studies of the Cordilleran thrust belt: Rocky Mountain Association of Geologists Guidebook, v. 2, p. 619–631.

Lentz, R., 1993, Cave Canyon, San Juan County, Utah, *in* Hill, B.G., and Bereskin, S.R., editors, Oil and gas fields of Utah: Utah Geological Association Publication 22, non-paginated.

Lindquist, S.J., 1983, Nugget formation reservoir characteristics affecting production in the overthrust belt of southwestern Wyoming: Journal of Petroleum Technology, v. 35, p. 1355–1365.

Lindquist, S.J., 1988, Practical characterization of eolian reservoirs for development—Nugget Sandstone, Utah-Wyoming thrust belt: Sedimentary Geology, v. 56, p. 315–339.

Lindquist, S.J., and Ross, R.A., 1993, Anschutz Ranch East, Summit County, Utah, *in* Hill, B.G., and Bereskin, S.R., editors, Oil and gas fields of Utah: Utah Geological Association Publication 22, non-paginated.

Lillis, P.G., Warden, A., and King, J.D., 2003, Petroleum systems of the Uinta and Piceance Basins—geochemical characteristics of oil types, *in* Petroleum systems and geologic assessment of oil and gas in the Uinta-Piceance province, Utah and Colorado: U.S. Geological Survey Digital Data Series DDS-69-B, Chapter 3, 25 p.

Little, T.M., 1988, Depositional environments, petrology, and diagenesis of the basal limestone facies, Green River Formation (Eocene), Uinta Basin, Utah: Salt Lake City, University of Utah, M.S. thesis, 154 p.

Lomax, J.D., 1993, Monument Butte, Duchesne County, Utah, *in* Hill, B.G., and Bereskin, S.R., editors, Oil and gas fields of Utah: Utah Geological Association Publication 22, non-paginated.

Longman, M.W., 1980, Carbonate diagenetic textures from nearshore diagenetic environments: American Association of Petroleum Geologists Bulletin, v. 64, no. 4, p. 461–487.

Loucks, G.G., 1975, The search for Pineview field, Summit County, Utah, *in* Bolyard, D.W., editor, Symposium on deep drilling frontiers of the central Rocky Mountains: Rocky Mountain Association of Geologists Guidebook, p. 255–264.

Lucas, P.T., and Drexler, J.M., 1975, Altamont-Bluebell—a major naturally fractured and overpressured stratigraphic trap, Uinta Basin, Utah, *in* Bolyard, D.W., editor, Symposium on deep drilling frontiers in the central Rocky Mountains: Rocky Mountain Association of Geologists Guidebook, p. 265–273.

Lutz, S.J., Nielson, D.L., and Lomax, J.D., 1994, Lacustrine turbidite deposits in the lower portion of the Green River Formation, Monument Butte field, Uinta Basin, Utah [abs.]: American Association of Petroleum Geologists Annual Convention, Official Program with Abstracts, v. 3, p. 203.

Lynn, H.B., Bates, C.R., Layman, M., and Jones, M., 1995, Natural fracture characterization using P-wave reflection seismic data, VSP, borehole imaging logs, and in-situ stress field determination: Society of Petroleum Engineers Proceedings of the Joint Rocky Mountain Meeting—Low-Permeability Reservoirs Symposium, SPE 29595, p. 493–506.

Lynn, H.B., Beckham, W.E., Simon, K.M., Bates, C.R., Layman, M., and Jones, M., 1999, P-wave and S-wave azimuthal anisotropy at a naturally fractured gas reservoir, Bluebell-Altamont field, Utah: Geophysics, v. 64, no. 4, p. 1312–1328.

Maher, P.D., 1976, The geology of the Pineview field area, Summit County, Utah, *in* Hill, J.G., editor, Geology of the Cordilleran Hingeline: Rocky Mountain Association of Geologists, p. 345–350.

Martin, G.W., 1981, Patterson field, San Juan County, Utah, *in* Wiegand, D.L., editor, Geology of the Paradox Basin: Rocky Mountain Association of Geologists Guidebook, p. 61–69.

Martin, G.W., 1983, Bug, San Juan County, Utah, *in* Fassett, J.E., editor, Oil and gas fields of the Four Corners area: Four Corners Geological Society Guidebook, v. III, p. 1073–1077.

Matheny, J.P., 1978, Beta Peak, Apache County, Arizona, *in* Fassett, J.E., editor, Oil and gas fields of the Four Corners area: Four Corners Geological Society Guidebook, v. I, p. 65–67.

Matheny, J.P., and Longman, M.W., 1996, Lower Desert Creek reservoirs in the Paradox Basin—examples of phylloid algae filling depositional lows related to salt dissolution, *in* Longman, M.W., and Sonnenfeld, M.D., editors, Paleozoic systems of the Rocky Mountain region: Society for Sedimentary Geology (SEPM) Rocky Mountain Section Guidebook, p. 267–282.

Matheny, J.P., and Martin, G.W., 1987, McClean field, T37N, R19W, Montezuma County, Colorado, *in* Campbell, J.A., editor, Geology of Cataract Canyon and vicinity: Four Corners Geological Society Tenth Annual Field Conference Guidebook, p. 145–150.

Matheny, J.P., Rigatti, V.G., Longman, M.W., 2009, Island Butte field, Dolores and Montezuma Counties, Colorado—a Desmoinesian salt-solution sag filled with phylloid algae, *in* Houston, W.S., Wray, L.L., and Moreland, P.G., editors, The Paradox Basin revisited—new developments in petroleum systems and basin analysis: Rocky Mountain Association of Geologists 2009 Special Publication—The Paradox Basin, p. 534–566.

McDonald, R.E., 1972, Eocene and Paleocene rocks of the southern and central basins, *in* Mallory, W.W., editor, Geologic atlas of the Rocky Mountain region: Rocky Mountain Association of Geologists, p. 243–256.

McKee, E.D., 1969, Paleozoic rocks of the Grand Canyon, *in* Baars, D.L., editor, Geology and natural history of the Grand Canyon region: Four Corners Geological Society, 5th Field Conference, Powell Centennial River Expedition, p. 78–90.

McKee, E.D., and Gutschick, R.C., 1969, History of the Redwall Limestone of northern Arizona: Geological Society of America Memoir 114, 726 p.

McPherson, B.J., 1996, A three-dimensional model of the geologic and hydrodynamic history of the Uinta Basin, Utah—analysis of overpressures and oil migration: Salt Lake City, University of Utah, Ph.D. dissertation, 119 p.

Mecham, D.F., 1978a, Flodine Park, Montezuma County, Colorado, *in* Fassett, J.E., editor, Oil and gas fields of the Four Corners area: Four Corners Geological Society Guidebook, v. I, p. 121–123.

Mecham, D.F., 1978b, Ismay, San Juan County, Utah, *in* Fassett, J.E., editor, Oil and gas fields of the Four Corners area: Four Corners Geological Society Guidebook, v. II, p. 654–657.

Meneses-Rocha, J., and Yurewicz, D.A., 1999, Petroleum exploration and production in fold and thrust belts—ideas from a Hedberg research symposium: American Association of Petroleum Geologists Bulletin, v. 83, no. 6, p. 889–897.

Mickel, E.G., 1978a, McClean, Montezuma County, Colorado, *in* Fassett, J.E., editor, Oil and gas fields of the Four Corners area: Four Corners Geological Society Guidebook, v. I, p. 146–147.

Mickel, E.G., 1978b, McElmo Mesa, San Juan County, Utah, *in* Fassett, J.E., editor, Oil and gas fields of the Four Cor-

ners area: Four Corners Geological Society Guidebook, v. II, p. 679–681.

Mickel, E.G., 1978c, Turner Bluff, San Juan County, Utah, *in* Fassett, J.E., editor, Oil and gas fields of the Four Corners area: Four Corners Geological Society Guidebook, v. II, p. 706–708.

Miesner, J.F., 1978, Papoose Canyon, Delores County, Colorado, *in* Fassett, J.E., editor, Oil and gas fields of the Four Corners area: Four Corners Geological Society Guidebook, v. I, p. 154–156.

Mitra, S., 1986, Duplex structures and imbricate thrust systems—geometry, structural position, and hydrocarbon potential: American Association of Petroleum Geologists Bulletin, v. 70, no. 9, p. 1087–1112.

Mitra, S., 1990, Fault-propagation folds—geometry, kinematics, and hydrocarbon traps: American Association of Petroleum Geologists Bulletin, v. 74, no. 6, p. 921–945.

Moklestad, T.C., 1979, Yellow Creek, Uinta County, Wyoming, *in* Cardinal, D.F., and Steward, W.W., editors, Greater Green River Basin and overthrust belt: Wyoming Geological Association, Wyoming Oil and Gas Fields Symposium, p. 426–427.

Montgomery, S.L., 1984, Kaiparowits Basin—an old frontier with new potential: Petroleum Frontiers, v. 1, no. 2, p. 4–25.

Montgomery, S., 1992, Paradox Basin Cane Creek play: Petroleum Frontiers, 66 p.

Moore, B.J., and Sigler, S., 1987, Analyses of natural gases, 1917–1985: U.S. Bureau of Mines, Information Circular 9129, 1197 p.

Moore, T.R., and Hawks, R.L., 1993, Greater Aneth, San Juan County, Utah, *in* Hill, B.G., and Bereskin, S.R., editors, Oil and gas fields of Utah: Utah Geological Association Publication 22 (Addendum), non-pagenated.

Morgan, C.D., 1992a, Horizontal drilling potential of the Cane Creek shale, Paradox Formation, Utah, *in* Schmoker, J.W., Coalson, E.B., and Brown, C.A., editors, Geological studies relevant to horizontal drilling in western North America: Rocky Mountain Association of Geologists Guidebook, p. 257–265.

Morgan, C.D., 1992b, Cane Creek exploration play area, Emery, Grand, and San Juan Counties, Utah: Utah Geological Survey Open-File Report 232, 5 p., 9 plates, scale 1:500,000.

Morgan, C.D., 1993a, Mississippian Leadville Limestone, *in* Hjellming, C.A., editor, Atlas of major Rocky Mountain gas reservoirs: New Mexico Bureau of Mines and Mineral Resources, p. 94.

Morgan, C.D., 1993b, Paradox Formation, *in* Hjellming, C.A., editor, Atlas of major Rocky Mountain gas reservoirs: New Mexico Bureau of Mines and Mineral Resources, p. 92–93.

Morgan, C.D., 1997, Increased oil production and reserves from improved completion techniques in the Bluebell field, Uinta Basin, Utah—annual report for the period October 1, 1995, to September 30, 1996: U.S. Department of Energy, DOE/BC/14953-19, 34 p.

Morgan, C.D., 2003a, Geologic guide and road logs of the Willow Creek, Indian, Soldier Creek, Nine Mile, Gate, and Desolation Canyons, Uinta Basin, Utah: Utah Geological Survey Open-File Report 407, 57 p.

Morgan, C.D., editor, 2003b, The Bluebell oil field, Uinta Basin, Duchesne and Uintah Counties, Utah—characterization and oil well demonstration: Utah Geological Survey Special Study 106, 95 p.

Morgan, C.D., 2008, Greater Monument Butte oil field—infill drilling results and potential CO_2 enhanced oil recovery, *in* Longman, M.W., and Morgan, C.D., editors, Hydrocarbon systems and production in the Uinta Basin, Utah: Rocky Mountain Association of Geologists and Utah Geological Association Publication 37, p. 303–318.

Morgan, C.D., and Bereskin, S.R., 2003, Characterization of petroleum reservoirs in the Eocene Green River Formation, central Uinta Basin, Utah: Rocky Mountain Association of Geologists, Mountain Geologist, v. 40, no. 4, p. 111–127.

Morgan, C.D., Carney, S., Nielsen, P., Vanden Berg, M.D., and Wood, R.E., 2014, Play analysis of the Cane Creek shale, Pennsylvanian Paradox Formation, Paradox Basin, southeast Utah [abs.]: American Association of Petroleum Geologists, Rocky Mountain Section Meeting Official Program, p. 36.

Morgan, C.D., Chidsey, T.C., Jr., Hanson, J.A., McClure, K.P., Weller, K., Bereskin, S.R., Deo, M.D., and Yeager, R., 1999, Reservoir characterization of the lower Green River Formation, southwest Uinta Basin, Utah: Utah Geological Survey, unpublished biannual technical progress report to the U.S. Department of Energy for the period 10/1/98 through 3/31/99, 11 p.

Morgan, C.D., Chidsey, T.C., Jr., McClure, K.P., Bereskin, S.R., and Deo, M.D., 2003, Reservoir characterization of the lower Green River Formation, southwest Uinta Basin, Utah: Utah Geological Survey Open-File Report 411, 140 p., CD-ROM.

Morgan, C.D., Yonkee, W.A., and Tripp, B.T., 1991, Geological considerations for oil and gas drilling on state potash leases at Cane Creek anticline, Grand and San Juan Counties, Utah: Utah Geological Survey Circular 84, 24 p.

Morris, T.H., McBride, J.H., and Monn, W.D., 2005, A multidisciplinary approach to reservoir characterization of the coastal Entrada erg-margin gas play: Utah Geological Survey Open-File Report 459, 52 p.

Moulton, F.C., 1976, Lower Mesozoic and upper Paleozoic petroleum potential of the Hingeline area, central Utah, *in* Hill, J.G., editor, Symposium on geology of the Cordilleran Hingeline: Rocky Mountain Association of Geologists Guidebook, p. 219–229.

Moyle, R.W., 1958, Paleoecology of the Manning Canyon

Shale in central Utah: Brigham Young University Research Studies, v. 5, no. 7, 86 p., 7 plates.

Mueller, E., 1998, Temporal and spatial source rock variation and the consequence on crude oil composition in the Tertiary petroleum system of the Uinta Basin, Utah, U.S.A.: Norman, University of Oklahoma, Ph.D. dissertation, 170 p.

Mueller, E., and Philp, R.P., 1998, Extraction of high molecular weight hydrocarbons from source rocks—an example from the Green River Formation, Uinta Basin, Utah: Organic Geochemistry, v. 28, p. 625–631.

Mullen, D., 1992a, Clear Creek, Uinta County, Wyoming, *in* Miller, S.M., Crockett, F.J., and Hollis, S.H., editors, Greater Green River Basin and overthrust belt: Wyoming Geological Association, Wyoming Oil and Gas Fields Symposium, p. 104–105.

Mullen, D., 1992b, Ryckman Creek, Uinta County, Wyoming, *in* Miller, S.M., Crockett, F.J., and Hollis, S.H., editors, Greater Green River Basin and overthrust belt: Wyoming Geological Association, Wyoming Oil and Gas Fields Symposium, p. 266–267.

Narr, W.N., and Currie, J.B., 1982, Origin of fracture porosity—example from Altamont field, Utah: American Association of Petroleum Geologists Bulletin, v. 66, no. 9, p. 1231–1247.

Nielsen, P.J., Morgan, C.D., and Vanden Berg, M.V., 2013, Detailed sedimentology and stratigraphy of the Remington 21-1H Cane Creek shale core, Pennsylvanian Paradox Formation, southeastern Utah—implications for unconventional hydrocarbon recovery [abs.]: American Association of Petroleum Geologists Rocky Mountain Section Meeting Program with Abstracts, p. 61.

Neuhauser, K.R., 1988, Sevier-age ramp-style thrust faults at Cedar Mountain, northwestern San Rafael Swell (Colorado Plateau), Emery County, Utah: Geology, v. 16, p. 299–302.

Nixon, R.P., 1973, Oil source beds in the Cretaceous Mowry Shale of northwestern interior United States: American Association of Petroleum Geologists Bulletin, v. 57, no. 1, p. 136–157.

Norton, J.A., 1978a, Salt Wash, Grand County, Utah, *in* Fassett, J.E., editor, Oil and gas fields of the Four Corners area: Four Corners Geological Society Guidebook, v. II, p. 697–699.

Norton, J.A., 1978b, Tohonadla, San Juan County, Utah, *in* Fassett, J.E., editor, Oil and gas fields of the Four Corners area: Four Corners Geological Society Guidebook, v. II, p. 1061–1063.

Nuccio, V.F., and Condon, S.M., 1996, Burial and thermal history of the Paradox Basin, Utah and Colorado, and petroleum potential of the Middle Pennsylvanian Paradox Formation, *in* Huffman, A.C., Jr., Lund, W.R., and Godwin, L.H., editors, Geology of the Paradox Basin: Utah Geological Association Publication 25, p. 57–76.

Ohlen, H.R., and McIntyre, L.B., 1965, Stratigraphy and tectonic features of Paradox Basin, Four Corners area: American Association of Petroleum Geologists Bulletin, v. 49, no. 11, p. 2020–2040.

Oline, W.F., 1996, Bug, San Juan County, Utah, *in* Hill, B.G., and Bereskin, S.R., editors, Oil and gas fields of Utah: Utah Geological Association Publication 22 (Addendum), non-paginated.

Osmond, J.C., 1992, Greater Natural Buttes gas field, Uintah County, Utah, *in* Fouch, T.D., Nuccio, V.F., and Chidsey, T.C., Jr., editors, Hydrocarbon and mineral resources of the Uinta Basin, Utah and Colorado: Utah Geological Association Publication 20, p. 143–163.

Osmond, J.C., 2000, West Willow Creek field—first productive lacustrine stromatolite mound in the Eocene Green River Formation, Uinta Basin, Utah: The Mountain Geologist, v. 37, no. 3, p. 157–170.

Ott, V.D., and Roylance, M.H., 1983, Tin Cup Mesa, San Juan County, Utah, *in* Fassett, J.E., editor, Oil and gas fields of the Four Corners area: Four Corners Geological Society Guidebook, v. III, p. 1134–1135.

Oviatt, C.G., 1988, Evidence for Quaternary deformation in the Salt Valley anticline, southeastern Utah, *in* Salt deformation in the Paradox region: Utah Geological and Mineral Survey Bulletin 122, p. 61–76.

Parker, J.M., 1981, Lisbon field area, San Juan County, Utah, *in* Wiegand, D.L., Geology of the Paradox Basin: Rocky Mountain Association of Geologists Guidebook, p. 89–100.

Parker, J.W., and Roberts, J.W., 1963, Devonian and Mississippian stratigraphy of the central part of the Colorado Plateau, *in* Bass, R.O., and Sharps, S.L., editors, Shelf carbonates of the Paradox Basin: Four Corners Geological Society, 4th Field Conference Guidebook, p. 31–60.

Parra, J.O., and Collier, H.A., 2000, Characterization of fractured zones in the Twin Creek reservoir, Lodgepole field, Utah-Wyoming overthrust belt: Petrophysics, v. 41, no. 5, p. 351–362.

Parrish, J.T., 1982, Upwelling and petroleum source beds, with reference to the Paleozoic: American Association of Petroleum Geologists Bulletin, v. 66, no. 6, p. 750–774.

Pennington, B.I., Dyer, J.E., Lomax, J.D., and Deo, M.D., 1996, Green River Formation water flood demonstration project, final technical progress report: U.S. Department of Energy DOE/BC/14958-15 (DE96001264), 150 p.

Peterson, F., 1988, Pennsylvanian to Jurassic eolian transportation systems in the western United States, *in* Kocurek, G., editor, Late Paleozoic and Mesozoic eolian deposits of the western interior of the United States: Sedimentary Geology, v. 56, p. 207–260.

Peterson, F., 1994, Sand dunes, sabkhas, streams, and shallow seas—Jurassic paleogeography in the southern part of the Western Interior Basin, *in* Caputo, M.V., Peterson, J.A., and Franczyk, K.J., editors, Mesozoic systems of the

Rocky Mountain region, USA: Denver, Colorado, Rocky Mountain Section of the Society for Sedimentary Geology, p. 233–272.

Peterson, J.A., 1966, Stratigraphic vs. structural controls on carbonate-mound accumulation, Aneth area, Paradox Basin: American Association of Petroleum Geologists Bulletin, v. 50, no. 10, p. 2068–2081.

Peterson, J.A., 1992, Aneth field—U.S.A., Paradox Basin, Utah, *in* Foster, N.H., and Beaumont, E.A., editors, Stratigraphic traps III: American Association of Petroleum Geologists Treatise of Petroleum Geology and Atlas of Oil and Gas Fields, p. 41–82.

Peterson, J.A., 2000, Carboniferous-Permian (late Paleozoic) hydrocarbon system, Rocky Mountains and Great Basin U.S. region—major historic exploration objective [abs.]: American Association of Petroleum Geologists Bulletin, v. 84, no. 8, p. 1244.

Peterson, J.A., 2001 (updated 2003), Carboniferous-Permian (late Paleozoic) hydrocarbon system, Rocky Mountains and Great Basin U.S. region—major historic exploration objective: Rocky Mountain Association of Geologists Open-File Report, 54 p.

Peterson, J.A., and Hite, R.J., 1969, Pennsylvanian evaporite-carbonate cycles and their relation to petroleum occurrence, southern Rocky Mountains: American Association of Petroleum Geologists Bulletin, v. 53, p. 884–908.

Peterson, J.A., and Ohlen, H.R., 1963, Pennsylvanian shelf carbonates, Paradox Basin, *in* Bass, R.O., editor, Shelf carbonates of the Paradox basin: Four Corners, Geological Society Symposium, 4th Field Conference, p. 65–79.

Peterson, P.R., 1973, Upper Valley field, Garfield County, Utah: Utah Geological and Mineralogical Survey Oil and Gas Field Studies, no. 7, 4 p.

Peterson, V.E., 1950, Ashley Valley oil field, Uintah County, Utah, *in* Eardley, A.J., editor, Guidebook to the geology of Utah: Utah Geological Society Publication 5, p. 135–138.

Peterson, V.E., 1957, Ashley Valley oil field, Uintah County, Utah, *in* Seal, O.G., editor, Guidebook to the geology of the Uinta Basin: Intermountain Association of Petroleum Geologists 8th Annual Field Conference, p. 191–192.

Peterson, V.E., 1961, Ashley Valley oil field, Uintah County, Utah, *in* Preston, D., editor, A symposium of the oil and gas fields of Utah: Intermountain Association of Petroleum Geologists Guidebook, non-paginated.

Petroleum Information, 1981, The overthrust belt—1981: Petroleum Information Corporation, Denver, Colorado, 251 p.

Petroleum Information, 1984a, Paradox Basin—unravelling the mystery: Petroleum Frontiers, v. 1, no. 4, p. 22.

Petroleum Information, 1984b, Overthrust belt field summaries: Petroleum Information Corporation, Denver, Colorado, 99 p.

Peyton, S.L., Constenius, K.N., and DeCelles, P.G., 2011, Early eastward translation of shortening in the Sevier thrust belt, northeast Utah and southwest Wyoming, U.S.A., *in* Sprinkel, D.A., Yonkee, W.A., and Chidsey, T.C., Jr., editors, Sevier thrust belt—northern and central Utah and adjacent areas: Utah Geological Association Publication 40, p. 57–72.

Picard, M.D., 1955, Subsurface stratigraphy and lithology of the Green River Formation in Uinta Basin, Utah: American Association of Petroleum Geologists Bulletin, v. 39, no. 1, p. 75–102.

Picard, M.D., 1957, Green shale facies, lower Green River Formation, Utah: American Association of Petroleum Geologists Bulletin, v. 41, p. 2373–2376.

Picard, M.D., 1975, Facies, petrography and petroleum potential of Nugget Sandstone (Jurassic), southwestern Wyoming and northeastern Utah, *in* Bolyard, D.W., editor, Symposium on deep drilling frontiers of the central Rocky Mountains: Rocky Mountain Association of Petroleum Geologists Guidebook, p. 109–127.

Pipiringos, G.N., and O'Sullivan, R.B., 1978, Principal unconformities in Triassic and Jurassic rocks, western Interior United States—a preliminary survey: U.S. Geological Survey Professional Paper 1035-A, 29 p.

Pitman, J.K., Fouch, T.D., and Goldhaber, M.B., 1982, Depositional setting and diagenetic evolution of some Tertiary unconventional reservoir rocks, Uinta Basin, Utah: American Association of Petroleum Geologists Bulletin, v. 66, no. 10, p. 1581–1596.

Poole, F.G., and Claypool, G.E., 1984, Petroleum source-rock potential and crude oil correlation in the Great Basin, *in* Woodward, J., Meissner, F.F., Clayton, J.L., editors, Hydrocarbon source rocks of the greater Rocky Mountain region: Rocky Mountain Association of Geologists Guidebook, p. 179–229.

Powers, R.B., 1992, Glasscock Hollow, Uinta County, Wyoming, *in* Miller, S.M., Crockett, F.J., and Hollis, S.H., editors, Greater Green River Basin and overthrust belt: Wyoming Geological Association, Wyoming Oil and Gas Fields Symposium, p. 156–157.

Pray, L.C., and Wray, J.L., 1963, Porous algal facies (Pennsylvanian) Honaker Trail, San Juan Canyon, Utah, *in* Bass, R.O., editor, Shelf carbonates of the Paradox Basin: Four Corners Geological Society, 4th Field Conference Guidebook, p. 204–234.

Rahl, J.M., Reiners, P.W., Campbell, I.H., Nicolescu, S., and Allen, C.M., 2003, Combined single-grain (U-Th)/He and U/Pb dating detrital zircons from the Navajo Sandstone, Utah: Geology, v. 31, no. 9, p. 761–764.

Rasmussen, D.L., 2010, Halokinesis features related to flowage and dissolution of Pennsylvanian Hermosa salt in the Paradox Basin, Colorado and Utah [abs]: American Association of Petroleum Geologists, Rocky Mountain Section Meeting Program with Abstracts, p. 59.

Reid, F.S., and Berghorn, C.E., 1981, Facies recognition and hydrocarbon potential of the Pennsylvanian Paradox Formation, *in* Wiegand, D.L., editor, Geology of the Paradox Basin: Rocky Mountain Association of Geologists Guidebook, p. 111–117.

Reid, F.S., and Stevenson, G., 1978, Gothic Mesa, San Juan County, Utah, *in* Fassett, J.E., editor, Oil and gas fields of the Four Corners area: Four Corners Geological Society Guidebook, v. II, p. 591–593.

Remy, R.R., 1992, Stratigraphy of the Eocene part of the Green River Formation in the south-central part of the Uinta Basin, Utah: U.S. Geological Survey Bulletin 1787-BB, 79 p.

Riggs, E.A., 1978a, Toh Atin, Apache County, Arizona, *in* Fassett, J.E., editor, Oil and gas fields of the Four Corners area: Four Corners Geological Society Guidebook, v. I, p. 94–95.

Riggs, E.A., 1978b, Toh Atin, North, Apache County, Arizona, *in* Fassett, J.E., editor, Oil and gas fields of the Four Corners area: Four Corners Geological Society Guidebook, v. I, p. 96–97.

Riggs, E.A., 1978c, Twin Falls Creek, Apache County, Arizona, *in* Fassett, J.E., editor, Oil and gas fields of the Four Corners area: Four Corners Geological Society Guidebook, v. I, p. 98–99.

Riggs, E.A., 1978d, Akah, San Juan County, Utah, *in* Fassett, J.E., editor, Oil and gas fields of the Four Corners area: Four Corners Geological Society Guidebook, v. II, p. 569–571.

Ritter, S.M., and Gianniny, G.L., 2012, Geological guide to Honaker Trail, San Juan River gorge (near Goosenecks State Park), southeastern Utah, *in* Anderson, P.B., and Sprinkel, D.A., editors, Geologic road, trail, and lake guides to Utah's parks and monuments (3rd edition): Utah Geological Association Publication 29, 32 p.

Ritter, S.M., Barrick, J.E., and Skinner, M.R., 2002, Conodont sequence biostratigraphy of the Hermosa Group (Pennsylvanian) at Honaker Trail, Paradox Basin, Utah: Journal of Paleontology, v. 76, no. 3, p. 495–517.

Roberts, L.N.R., 2003, Structure contour map of the Dakota Sandstone, Uinta-Piceance Province, Utah and Colorado, *in* U.S. Geological Survey Uinta-Piceance Assessment Team, compilers, Petroleum systems and geologic assessment of oil and gas in the Uinta-Piceance Province, Utah and Colorado: U.S. Geological Survey Digital Data Series DDS-69-B.

Robertson, J.M., and Broadhead, R.F., 1993, editors, Atlas of major Rocky Mountain gas reservoirs: New Mexico Bureau of Mines & Mineral Resources, 206 p.

Ross, J., and Handley, G., 1993, Deadman (Ismay pool), San Juan County, Utah, *in* Hill, B.G., and Bereskin, S.R., editors, Oil and gas fields of Utah: Utah Geological Association Publication 22, non-paginated.

Rowley, P.D., and Hansen, W.R., 1979, Geologic map of the Split Mountain quadrangle, Uintah County, Utah: U.S. Geological Survey Map GQ-1515, scale 1:24,000.

Royse, F., Jr., 1993, Case of the phantom foredeep—Early Cretaceous in west-central Utah: Geology, v. 21, no. 2, p. 133–136.

Royse, F., Jr., Warner, M.A., and Reese, D.L., 1975, Thrust belt structural geometry and related stratigraphic problems, Wyoming-Idaho-Northern Utah, *in* Bolyard, D.W., editor, Symposium on deep drilling frontiers of the central Rocky Mountains: Denver, Colorado, Rocky Mountain Association of Geologists, p. 41–54.

Ruble, T.E., 1996, Geochemical investigations of the mechanisms of hydrocarbon generation and accumulation in the Uinta Basin, Utah: Norman, University of Oklahoma, Ph.D dissertation, 333 p.

Ruble, T.E., and Philp, R.P., 1998, Stratigraphy, depositional environments, and organic geochemistry of source-rocks in the Green River petroleum system, Uinta Basin, Utah, *in* Pitman, J.K., and Carroll, A.R., editors, Modern and ancient lake systems; new problems and perspectives: Utah Geological Association Guidebook 26, p. 289–328.

Ruble, T.E., Philp, R.P., Lewan, M.D., and Mueller, E., 1998, Organic geochemical characterization of key source facies in the Green River petroleum system, Uinta Basin, Utah [abs.]: American Association of Petroleum Geologists Annual Convention, Abstract on CD ROM.

Ryder, R.T., Fouch, T.D., and Elison, J.H., 1976, Early Tertiary sedimentation in the western Uinta Basin, Utah: Geological Society of America Bulletin, v. 87, p. 496–512.

Sandberg, C.A., and Gutschick, R.C., 1984, Distribution, microfauna, and source-rock potential of the Mississippian Delle Phosphatic Member of Woodman Formation and equivalents, Utah and adjacent states, *in* Woodward, J., Meissner, F.F., and Clayton, J.L., editors, Hydrocarbon source rocks of the greater Rocky Mountain region: Rocky Mountain Association of Geologists Guidebook, p. 135–178.

Sanderson, I.D., 1974, Sedimentary structures and their environmental significance in the Navajo Sandstone, San Rafael Swell, Utah: Brigham Young University Geology Studies, v. 21, pt. 1, p. 215–246.

Santucci, V.L., 2000, A survey of the paleontological resources from the national parks and monuments in Utah, *in* Sprinkel, D.A., Chidsey, T.C., Jr., and Anderson, P.B., editors, Geology of Utah's parks and monuments: Utah Geological Association Publication 28, p. 535–556.

Scanlon, D.S., and Wendling, M.J., 1983, Recapture Creek, *in* Fassett, J.E., editor, Oil and gas fields of the Four Corners area: Four Corners Geological Society Guidebook, v. III, p. 1073–1077.

Schelling, D.D., Strickland, D.K., Johnson, K.R., and Vrona, J.P., 2007, Structural geology of the central Utah thrust belt, *in* Willis, G.C., Hylland, M.D., Clark, D.L., and

Chidsey, T.C., Jr., editors, Central Utah—diverse geology of a dynamic landscape: Utah Geological Association Publication 36, p. 1–29.

Schelling, D.D., Strickland, D.K., Johnson, K.R., Vrona, J.P., Wavrek, D.A., and Reuter, J., 2005, Structural architecture and evolution of the central Utah thrust belt—implications for hydrocarbon exploration [abs.]: American Association of Petroleum Geologists Annual Convention, Official Program with Abstracts, v. 14, non-paginated.

Schenk, C.J., 1981, Porosity and textural characteristics of eolian stratification [abs.]: American Association of Petroleum Geologists Bulletin, v. 65, no. 5, p. 986.

Schuh, M.L., 1993a, Red Wash, Uintah County, Utah, *in* Hill, B.G., and Bereskin, S.R., editors, Oil and gas fields of Utah: Utah Geological Association Publication 22, non-paginated.

Schuh, M.L., 1993b, Wonsits Valley, Uintah County, Utah, *in* Hill, B.G., and Bereskin, S.R., editors, Oil and gas fields of Utah: Utah Geological Association Publication 22, non-paginated.

Schumn, S.A., and Ethridge, F.G., 1994, Origin, evolution and morphology of fluvial valleys, *in* Dalrymple, R.W., and Zaitlin, B.A., editors, Incised-valley systems—origin and sedimentary sequences: Society of Sedimentary Geology Special Publication no. 51, p. 11–27.

Scott, P.K., 2003, Paradox Basin, Colorado—maps, cross sections, and database for oil, gas, and CO_2 fields: Colorado Geological Survey Resource Series 43, CD-ROM.

Seneshen, D.M., Chidsey, T.C., Jr., Morgan, C.D., and Vanden Berg, M.D., 2009, New techniques for new discoveries—results from the Lisbon field area, Paradox Basin, Utah, *in* Houston, W.S., Wray, L.L., and Moreland, P.G., editors, The Paradox Basin revisited—new developments in petroleum systems and basin analysis: Rocky Mountain Association of Geologists Special Publication, p. 604–633.

Sercombe, W.J., 1989, Performance of lower-porosity Nugget reservoirs, Anschutz Ranch East, Bessie Bottom, and North Pineview fields, Utah and Wyoming, *in* Coalson, E.B., editor, Petrogenesis and petrophysics of selected sandstone reservoirs of the Rocky Mountains: Rocky Mountain Association of Geologists Guidebook, p. 109–116.

Sharp, G.C., 1976, Reservoir variations at Upper Valley field, Garfield County, Utah, *in* Hill, J.G., editor, Symposium on the geology of the Cordilleran Hingeline: Rocky Mountain Association of Geologists Guidebook, p. 325–344.

Sharp, G.C., 1978, Upper Valley, Garfield County, Utah, *in* Fassett, J.E., editor, Oil and gas fields of the Four Corners area: Four Corners Geological Society Guidebook, v. II, p.709–711.

Shoemaker, E.M., Case, J.E., and Elston, D.P., 1958, Salt antinclines of the Paradox Basin: Intermountain Association of Petroleum Geologists 9th Annual Field Conference, p. 39–59.

Silverman, S.R., and Epstein, S., 1958, Carbon isotope compositions of petroleum and other sedimentary organic materials: American Association of Petroleum Geologists Bulletin, v. 42, p. 998–1012.

Simo, J.A., Gianniny, G.L., and De Miranda, D.R., 1994, Contrasting facies successions in cyclic Pennsylvanian and Cretaceous mixed carbonate-siliciclastic shelves [abs]: American Association of Petroleum Geologists, Annual Convention Program with Abstracts, v. 3, p. 259.

Smith, A.G., Hurley, A.M., and Briden, J.C., 1981, Phanerozoic paleocontinental world maps: Cambridge University Press, Cambridge Earth Science Series, 102 p.

Smith, K.T., 1978a, Big Flat, Grand County, Utah, *in* Fassett, J.E., editor, Oil and gas fields of the Four Corners area: Four Corners Geological Society Guidebook, v. II, p. 596–598.

Smith, K.T., 1978b, Bartlett Flat, Grand County, Utah, *in* Fassett, J.E., editor, Oil and gas fields of the Four Corners area: Four Corners Geological Society Guidebook, v. II, p. 1061–1063.

Smith, K.T., 1978c, Cane Creek, San Juan County, Utah, *in* Fassett, J.E., editor, Oil and gas fields of the Four Corners area: Four Corners Geological Society Guidebook, v. II, p. 624–626.

Smith, K.T., 1978d, Long Canyon, Grand County, Utah, *in* Fassett, J.E., editor, Oil and gas fields of the Four Corners area: Four Corners Geological Society Guidebook, v. II, p. 676–678.

Smith, K.T., 1978e, Shafer Canyon, San Juan County, Utah, *in* Fassett, J.E., editor, Oil and gas fields of the Four Corners area: Four Corners Geological Society Guidebook, v. II, p. 700–702.

Smith, K.T., and Prather, O.E., 1981, Lisbon field—lessons in exploration, *in* Wiegand, D.L., editor, Geology of the Paradox Basin: Rocky Mountain Association of Geologists Guidebook, p. 55–59.

Smouse, D., 1993a, Altamont-Bluebell, Duchesne and Uintah Counties, Utah, *in* Hill, B.G., and Bereskin, S.R., editors, Oil and gas fields of Utah: Utah Geological Association Publication 22, non-paginated.

Smouse, D., 1993b, Lisbon, San Juan County, Utah, *in* Hill, B.G., and Bereskin, S.R., editors, Oil and gas fields of Utah: Utah Geological Association Publication 22, non-paginated.

Smouse, D., 1993c, Salt Wash, Grand County, Utah, *in* Hill, B.G., and Bereskin, S.R., editors, Oil and gas fields of Utah: Utah Geological Association Publication 22, non-paginated.

Sofer, Z., 1984, Stable carbon isotope compositions of crude oils—application to source depositional environments and petroleum alteration: American Association of Petroleum Geologists Bulletin, v. 68, no. 1, p. 31–49.

Spencer, C.W., 1978, Towaoc, Montezuma County, Colorado, *in* Fassett, J.E., editor, Oil and gas fields of the Four Corners area: Four Corners Geological Society Guidebook, v. I, p. 164–167.

Sprinkel, D.A., Castaño, J.R., and Roth, G.W., 1997, Emerging plays in central Utah based on a regional geochemical, structural, and stratigraphic evaluation [abs.]: American Association of Petroleum Geologists Bulletin Annual Convention, Official Program with Abstracts, v. 6, p. A110.

Sprinkel, D.A., and Chidsey, T.C., Jr., 1993, Jurassic Twin Creek Limestone, *in* Hjellming, C.A., editor, Atlas of major Rocky Mountain gas reservoirs: New Mexico Bureau of Mines and Mineral Resources, p. 76.

Sprinkel, D.A., Doelling, H.H., Kowallis, B.J., Waanders, G., and Kuehne, P.A., 2011, Early results of a study of Middle Jurassic strata in the Sevier fold and thrust belt, Utah, *in* Sprinkel, D.A., Yonkee, W.A., and Chidsey, T.C., Jr., editors, Sevier thrust belt—northern and central Utah and adjacent area: Utah Geological Association Publication 40, p. 151–172.

Sprinkel, D.A., Kowallis, B.J., and Jensen, P.H., 2011, Correlation and age of the Nugget Sandstone and Glen Canyon Group, Utah, *in* Sprinkel, D.A., Yonkee, W.A., and Chidsey, T.C., Jr., editors, Sevier thrust belt—northern and central Utah and adjacent areas: Utah Geological Association Publication 40, p. 131–149.

Stanley, K.O., and Collinson, J.W., 1979, Depositional history of Paleocene—lower Flagstaff Limestone and coeval rocks, central Utah: American Association of Petroleum Geologists Bulletin, v. 63, no. 3, p. 311–323.

Steele, D.D., and White, R.G., 1993, Tin Cup Mesa, San Juan County, Utah, *in* Hill, B.G., and Bereskin, S.R., editors, Oil and gas fields of Utah: Utah Geological Association Publication 22, non-paginated.

Stevenson, G.M., 2010, Geology of Goosenecks State Park, San Juan County, Utah, *in* Sprinkel, D.A., Chidsey, T.C., Jr., and Anderson, P.B., editors, Geology of Utah's parks and monuments (third edition): Utah Geological Association Publication 28, p. 451–465.

Stevenson, G.M., and Baars, D.L., 1986, The Paradox—a pull-apart basin of Pennsylvanian age, *in* Peterson, J.A., editor, Paleotectonics and sedimentation in the Rocky Mountain region: American Association of Petroleum Geologists Memoir 41, p. 513–539.

Stevenson, G.M., and Baars, D.L., 1987, The Paradox—a pull-apart basin of Pennsylvanian age, *in* Campbell, J.A., editor, Geology of Cataract Canyon and vicinity: Four Corners Geological Society, 10th Field Conference, p. 31–55.

Stokes, W.L., 1976, What is the Wasatch Line?, *in* Hill, J.G., editor, Symposium on geology of the Cordilleran Hingeline: Rocky Mountain Association of Geologists Guidebook, p. 11–25.

Stokes, W.L., 1991, Petrified mini-forests of the Navajo Sandstone, east-central Utah: Utah Geological Survey, Survey Notes, v. 25, no. 1, p. 14–19.

Stowe, C., 1972, Oil and gas production in Utah to 1970: Utah Geological and Mineral Survey Bulletin 94, p. 170.

Strickland, D., Johnson, K.R., Vrona, J.P., Schelling, D.D., and Wavrek, D.A., 2005, Structural architecture, petroleum systems, and geological implications for the Covenant field discovery, Sevier County, Utah: Online, American Association of Petroleum Geologists, Search and Discovery Article #110014, http://www.searchanddiscovery.com/documents/2005/av/strickland/softvnetplayer.htm, posted August 30, 2005.

Swetland, P.J., Clayton, J.L., and Sable, E.G., 1978, Petroleum source-bed potential of Mississippian-Pennsylvanian rocks in parts of Montana, Idaho, Utah, and Colorado: The Mountain Geologist, v. 14, p. 79–87.

Tillman, L.E., 1989, Sedimentary facies and reservoir characteristics of the Nugget Sandstone (Jurassic), Painter Reservoir field, Uinta County, Wyoming, *in* Coalson, E.B., editor, Petrogenesis and petrophysics of selected sandstone reservoirs of the Rocky Mountains: Rocky Mountain Association of Geologists Guidebook, p. 97–108.

Tissot, B., Deroo, G., and Hood, A., 1978, Geochemical study of the Uinta Basin—formation of petroleum from the Green River Formation: Geochimica et Cosmochimica Acta, v. 42, p. 1469–1485.

U.S. Geological Survey, 2012, Assessment of undiscovered oil and gas resources in the Paradox Basin province, Utah, Colorado, New Mexico, and Arizona, 2011: U.S. Geological Survey Fact Sheet 2012-3021, March 2012, 4 p., online, http://pubs.usgs.gov/fs/2012/3031/FS12-3031.pdf, accessed July 25, 2012.

Utah Division of Oil, Gas, and Mining, 1978, Pineview field, Nugget structure map: Cause No. 160-10, Exhibit No. 5, 1 inch = 1500 feet.

Utah Division of Oil, Gas, and Mining, 1980a, Anschutz Ranch field, Nugget structure map: Cause No. 183-4, Exhibit No. 4, 1 inch = 2000 feet.

Utah Division of Oil, Gas, and Mining, 1980b, Anschutz Ranch field, Twin Creek structure map: Cause No. 183-4, Exhibit No. 2, 1 inch = 2000 feet.

Utah Division of Oil, Gas, and Mining, 1980c, Anschutz Ranch field, structural cross section: Cause No. 183-4, Exhibit No. C.

Utah Division of Oil, Gas, and Mining, 2010, Structural configuration, Providence field: Cause No. 269-01, Docket 2010-010, Exhibit No. F.

Utah Division of Oil, Gas, and Mining, 2016a, Oil and gas production report, December 2015: Online, <http://www.ogm.utah.gov/oilgas/PUBLICATIONS/Reports/PROD_book_list.htm>, accessed April 2016.

Utah Division of Oil, Gas, and Mining, 2016b, Drilling commenced (wells spudded)—by year: Online, <http://oilgas.ogm.utah.gov/Statistics/SPUD_annual.cfm>, accessed April 2016.

Utah Division of Oil, Gas, and Mining, 2016c, Applications for permit to drill (APD)—by year: Online, <http://oilgas.ogm.utah.gov/Statistics/APD_annual.cfm>, accessed April 2016.

Vanden Berg, M.D., Morgan, C.D., Chidsey, T.C., Jr., and Nielsen, P., 2013, The Uteland Butte Member of the Eocene Green River Formation—an emerging unconventional carbonate tight oil play in the Uinta Basin, Utah [abs.]: American Association of Petroleum Geologists Annual Convention Abstracts Volume (1555982).

Ver Ploeg, A.J., and De Bruin, R.H., 1982, The search for oil and gas in the Idaho-Wyoming-Utah salient of the overthrust belt: Geological Survey of Wyoming Report of Investigations no. 21, 116 p., 1 plate.

Villien, A., and Kligfield, R.M., 1986, Thrusting and synorogenic sedimentation in central Utah, *in* Peterson, J.A., editor, Paleotectonics and sedimentation in the Rocky Mountain region: American Association of Petroleum Geologists Memoir 41, p. 281–306.

Walters, R.R., 1992, Elkhorn Ridge, Summit County, Utah, *in* Miller, S.M., Crockett, F.J., and Hollis, S.H., editors, Wyoming oil and gas fields symposium, Greater Green River Basin and overthrust belt: Wyoming Geological Association, p. 135.

Warner, M.A., 1982, Source and time of generation of hydrocarbons in the Fossil basin, western Wyoming thrust belt, *in* Powers, R.B., editor, Geologic studies of the Cordilleran thrust belt: Denver, Colorado, Rocky Mountain Association of Geologists, v. 2, p. 805–815.

Wavrek, D.A., Ali-Adeeb, J., Chao, J.C., Santon, L.E., Hardwick, E.A., Strickland, D.K., and Schelling, D.D., 2007, Paleozoic source rocks in the central Utah thrust belt—organic facies response to tectonic and paleoclimatic variables: American Association of Petroleum Geologists, Rocky Mountain Section Meeting Official Program, p. 58–59.

Wavrek, D.A., Schelling, D.D., Sbarra, R., Vrona, J.P., and Johnson, K.R., 2010, Central Utah thrust belt discoveries—a tale of two hydrocarbon charges [abs.]: American Association of Petroleum Geologists, Rocky Mountain Section Meeting, Official Program with Abstracts, p. 72–73.

Wavrek, D.A., Strickland, D., Schelling, D.D., Johnson, K.R., and Vrona, J.P., 2005, A major paradigm shift—Carboniferous versus Permian petroleum systems in the central Rocky Mountains, U.S.A. [abs.]: American Association of Petroleum Geologists Annual Convention, Official Program with Abstracts, v. 14, non-paginated.

Weber, L.J., Sarg, J.F., and Wright, F.M., 1995a, Sequence stratigraphy and reservoir delineation of the Middle Pennsylvanian (Desmoinesian), Paradox Basin and Aneth field, Milankovitch sea-level changes, cycles, and reservoirs on carbonate platforms in greenhouse and ice-house worlds: SEPM (Society for Sedimentary Geology) Short Course No. 35, p. 1–81.

Weber, L.J., Wright F.M., Sarg, J.F., Shaw, E., Harman, L.P., Vanderhill, J.B., and Best, D.A., 1995b, Reservoir delineation and performance—application of sequence stratigraphy and integration of petrophysics and engineering data, Aneth field, southeast Utah, U.S.A., *in* Stoudt, E.L., and Harris, P.M., editors, Hydrocarbon reservoir characterization—geologic framework and flow unit modeling: SEPM (Society for Sedimentary Geology) Short Course No. 34, p. 1–29.

Webster, D., 2002, Alashan—China's unknown Gobi: National Geographic, v. 201, no. 1, p. 48–76.

Wegner, M., 1996, Core analysis and description as an aid to hydrocarbon production enhancement—lower Green River and Wasatch Formations, Bluebell field, Uinta Basin, Utah: Provo, Utah, Brigham Young University, M.S. thesis, 233 p.

Wegner, M., and Morris, T.H., 1996, Core analyses and description as an aid to hydrocarbon production enhancement—lower Green River and Wasatch Formations, *in* Allison, M.L., and Morgan, C.D., editors, Increased oil production and reserves from improved completion techniques in the Bluebell field, Uinta Basin, Utah, annual report for the period October 1, 1994, to September 30, 1995: U.S. National Technical Information Service DE96001227, p. 35–47.

Weiss, M.P., Witkind, I.J., and Cashion, W.B., 1990, Geologic map of the Price 30′ x 60′ quadrangle, Carbon, Duchesne, Uintah, Utah, and Wasatch Counties, Utah: U.S. Geological Survey Miscellaneous Investigations Series Map I-1981, scale 1:100,000.

Welsh, J.E., and Bissell, H.J., 1979, The Mississippian and Pennsylvanian (Carboniferous) Systems in the United States—Utah: U.S. Geological Survey Professional Paper 1110-Y, 35 p.

Wengerd, S.A., 1963, Stratigraphic section at Honaker Trail, San Juan Canyon, San Juan County, Utah, *in* Bass, R.O., editor, Shelf carbonates of the Paradox Basin: Four Corners Geological Society, 4th Field Conference Guidebook, p. 205–243.

Wengerd, S.A., and Matheny, M.L., 1958, Pennsylvanian system of the Four Corners region: American Association of Petroleum Geologists Bulletin, v. 42, p. 2048–2106.

West, J., and Lewis, H., 1982, Structure and palinspastic reconstruction of the Absaroka thrust, Anschutz Ranch area, Utah and Wyoming, *in* Powers, R.B., editor, Geologic studies of the Cordilleran thrust belt: Rocky Mountain Association of Geologists Guidebook, v. 2, p. 633–639.

White, R.R., Alcock, T.J., and Nelson, R.A., 1990, Anschutz Ranch East field—U.S.A., Utah-Wyoming thrust belt,

in Beaumont, E.A., and Foster, N.H., editors, Structural traps III, tectonic fold and fault traps: American Association of Petroleum Geologists Treatise of Petroleum Geology, Atlas of Oil and Gas Fields, v. A-25, p. 31–55.

Wiggins, W.D., and Harris, P.M., 1994, Lithofacies, depositional cycles, and stratigraphy of the lower Green River Formation, southwestern Uinta Basin, Utah, *in* Lomando, A.J., Schreiber, B.C., and Harris, P.M., editors, Lacustrine reservoirs and depositional systems: Society for Sedimentary Geology (SEPM) Core Workshop No. 19, p. 105–141.

Willis, G.C., 1991, Geologic map of the Redmond Canyon quadrangle, Sanpete and Sevier Counties, Utah: Utah Geological Survey Map 138, 17 p., 2 pl., scale 1:24,000.

Willis, G.C., 1994, Geologic map of the Richfield quadrangle, Sevier County, Utah: Utah Geological Survey Open-File Report 309, 105 p., 2 pl., scale 1:24,000.

Willis, G.C., 1999, The Utah thrust system—an overview, *in* Spangler, L.E., editor, Geology of northern Utah and vicinity: Utah Geological Association Publication 27, p. 1–9.

Wilson, J.L., 1975, Carbonate facies in geologic history: New York, Springer-Verlag, 471 p.

Witkind, I.J., 1982, Salt diapirism in central Utah, *in* Nielson, D.L., editor, Overthrust belt of central Utah: Utah Geological Association Publication 10, p. 13–30.

Wold, J.T., 1978, Cache, Montezuma County, Colorado, *in* Fassett, J.E., editor, Oil and gas fields of the Four Corners area: Four Corners Geological Society Guidebook, v. I, p. 108–110.

Wood, R.E., and Chidsey, T.C., Jr., 2015, Oil and gas fields map of Utah: Utah Geological Survey Circular 119, scale 1:700,000.

Wray, L.L., Apeland, A.D., Hemborg, H.T., and Brchan, C., 2002, Oil and gas fields map of Colorado: Colorado Geological Survey Map Series 33, scale 1:500,000.

Wyoming Oil and Gas Conservation Commission, 1998, Chevron USA Inc. engineering review, lateral and multilateral extensions, Painter Reservoir unit—Painter and East Painter fields: Docket No. 239-98, Exhibit No. 3.

Wyoming Oil and Gas Conservation Commission, 2016, Anschutz Ranch East, Bessie Bottom, Chicken Creek, Clear Creek, East Painter Reservoir, Glasscock Hollow, Ryckman Creek, and Yellow Creek fields: Online, http://wogcc.state.wy.us/, accessed July 2016.

Yonkee, W.A. 1992, Basement-cover relations, Sevier orogenic belt, northern Utah: Geological Society of America Bulletin, v. 104, p. 280–302.

Yonkee, W.A., and Weil, A.B., 2011, Evolution of the Wyoming salient of the Sevier fold-thrust belt, northern Utah to western Wyoming, *in* Sprinkel, D.A., Yonkee, W.A., and Chidsey, T.C., Jr., editors, Sevier thrust belt—northern and central Utah and adjacent areas: Utah Geological Association Publication 40, p. 1–56.